The role of miR-23a~24~27a cluster in the pathogenesis of treatment resistant Rheumatoid Arthritis

Marina Frleta Gilchrist
MD

Submitted in fulfilment of the requirements for the degree of Doctor of Philosophy

College of Medical, Veterinary and Life Sciences
Institute of Infection, Immunity and Inflammation
University of Glasgow

November 2016

Abstract

Background: Rheumatoid arthritis (RA) is a symmetric polyarthritis arising from autoimmune dysregulation leading to severe disability and increased risk of co-morbidities and death. A chronic disproportionate inflammatory process lies at the heart of disease pathogenesis. Breach of self-tolerance, subsequent immune effector cell activation in the context of abundant expression of effector cytokines all contribute to uncontrolled inflammation. Molecular safeguards that normally operate to promote immune regulation appear defective in RA. Intensive basic and translational research over the last 30 years have contributed the emergence of an array of new therapeutics for the treatment of RA, which has transformed patient outcomes. The identity of the cytokine targeting treatments that have been most successful elucidates a functional hierarchy that implicates elements of both innate and adaptive immunity. In particular, dysregulation of TNFα and IL-6 biology are at the core of effector pathways and as such unravelling their detailed regulation is of critical importance. Moreover their primary synthesis places myeloid cells, and, in particular, blood-derived monocytes at the heart of pathogenic circuitry.

Best current clinical practice is to treat early disease and deploy aggressive treatments directed towards restoration of immune balance in virtually all patients. However only a proportion of such patients will actually have poor prognosis disease and in reality merit such aggressive interventions - the identification of such clinical endotypes is a major challenge for the next decade. The field of epigenetics and consequent regulatory control of inflammatory cells offers rich potential in this regard. Examples of such regulatory elements are small RNA species – microRNAs (miRs), which serve as negative regulators of cellular transcription and thereby repress protein translation. Importantly they do so across functionally integrated pathways, operating beyond individual moieties. A growing body of evidence implicates a significant role of miRs in the regulation of inflammatory processes in the context of RA.

Objectives: To identify miR species that are differentially regulated in patients with poor response to therapeutic intervention, compared to patients with well-controlled disease and healthy controls. Thereafter, to characterise candidate

miRs arising from these investigations to thereby determine their functional significance. Together these studies will shed light on a substantially ignored area of RA biology, namely the underlying mechanisms that subserve drug resistance in RA.

Key Results: Microarray profiling of $CD14^+$ monocytes derived from patients with drug resistance upon receipt of DMARDs or biologic treatments, compared with good responders or matched healthy controls identified the miR-23a~24-2~27a cluster to be significantly repressed in monocytes from resistant RA. Further analysis identified that two members of the cluster, miR-23a and miR-27a are implicated in a feedback loop regulating the IL-6 pathway. Thus IL-6 stimulation of primary monocytes suppresses the expression of this miR cluster, permitting expression of their direct molecular target, namely IL-6R, thus sensitising cells to further IL-6 signalling. I also observed that cells lacking miR-23a and miR-27a express higher levels of the pro-inflammatory cytokines TNFα and IL-6 when stimulated with LPS, further confirming that lack of these miRs has direct implications for chronic inflammatory processes.

The remaining member of this miR cluster, miR-24, was shown to directly target methylene tetrahydrofolate reductase but not dihydrofolate reductase enzymes, implicating it in the target pathway of methotrexate (MTX), the most commonly used anchor DMARD. Although this is unlikely to confer disease resistance, this interaction suggests that miR-24 levels could be predictive of tolerability of methotrexate use. The potential biomarker capabilities of miR-24 in relation to MTX use, or miR-23a and miR-27 with regards to responsiveness to anti-IL-6 or JAK signalling inhibition therapeutics will be evaluated in my future work.

Conclusion: This series of studies has elucidated highly novel pathways that mediate amplification of inflammatory responses in blood-derived monocytes through feedback pathways operating via regulatory miRs. Furthermore, analysis of a distinct cohort of RA patients allowed identification of miR species that have the potential to be utilised as clinical biomarkers for treatment efficacy or tolerability evaluation. Although a separate validation study is required, the detailed investigation of the role of these miRs performed here provides a clear mechanistic insight into their function and will certainly support future discovery.

Table of Contents

List of Tables

List of Figures

Acknowledgment

First of all, I would like to thank my supervisor Iain McInnes for the continuous inspiration, support and guidance. I believe that neither of us knew that day, five years ago when we first met at the fellowship interview in Amsterdam, that Glasgow will be the place where I will find my personal and professional happiness, and my true home. I cannot thank him enough for supporting me through this period of my life, and I look forward to mastering new heights of clinical arthritis with his support in the near future.

I would like to thank Mariola for always being willing to discuss data, suggest experiments and help. Your passion for science is truly admirable.

Now I understand why people say that completing PhD will challenge you in more ways than you ever suspected and I would like to express my sincere gratitude to all my friends, without whom completing my thesis would not be possible. Thank you to Ashleigh and Claire for paving the way in miR PhDs, I know that it was not easy. To Lynn for processing endless amount of patient samples with a smile. Thank you to Ashley G for teaching me every little thing I needed to know when I just started, and to Donna for simply being the best. My sincere thanks to Aziza are for the help with transfection experiments but also for her kind words and moral support; and to Pamela for great tissue culture chats and for always doing experiments that were much more complicated than mine, it made me feel so much better. A huge thank you is also due to Jim, Shauna and Robin for knowing everything and fixing anything that no one else could, especially when it came to finding freezer space or, even worse, later remembering where that space was.

I also thank Susan, Moeed and Brian for always being there and helping me with everything they could, I really appreciated that, almost as much as the endless amount of sweets you kept in your drawer. There were more times than I care to remember when those were my breakfast, lunch and dinner if days got busy. I would like to thank Neal, Jagtar and Jamie for helping me understand how the NHS works and also making me believe that doing science and clinical work is possible as a junior doctor, their advice was always welcome. To James-a, Florian and Julia I can only say that I miss you greatly and the moments shared

with you guys were some of the happiest of my life. Finally, I think you all for making my wedding an absolutely wonderful and unforgettable party, and I will be looking for an excuse so that Immunology can do Croatia again soon.

My special thanks are devoted to patients suffering from rheumatoid arthritis for their incredible bravery in dealing with this disease but also in helping our research efforts, you are truly inspirational.

I would also like to thank my family for support, love and appreciation they always have for me and for knowing when to ask and when not to ask: “how is writing going?”. My parent's commitment to my cause also means that by now they know what miRNAs are and how they work, I only wish I could say the same. I am grateful for my Grandpa setting an example and would be proud to put a copy of my thesis next to his books. I also thank my brother, who amongst his many talents writes me a song when I am feeling blue. I have to say that it is an excellent life skill to have.

Finally, I would like to thank my husband for being my all and everything. I had my suspicions that you loved me, but I could never have imagined that it would be as much as this. I cannot thank you enough for changing my life for the better and I promise that yours will too, as soon as I graduate.

Author's Declaration

I declare that, unless otherwise stated, this thesis is the result of my own work and has not been submitted for any other degree at the University of Glasgow or any other Institution.

Signature: ..... Printed name: Marina Frleta-Gilchrist

Abbreviations

ACPA	Anti-Citrullinated Protein Antibody
ACR	American College of Rheumatology
ADACTA	Tocilizumab monotherapy versus adalimumab monotherapy for treatment of rheumatoid arthritis
ADAMTS-4	metallopeptidase with thrombospondin type 1 motif 4
ADCC	antibody dependent cytotoxicity
AUGUST III	Atacicept for Reduction of Signs and Symptoms in Rheumatoid Arthritis Trial III
AP1	Activator protein 1
APC	Antigen presenting cell
APRIL	A proliferation-inducing ligand
ARA	American Rheumatology Association
ARRISE	Assessment of Rituximab's immunomodulatory synovial effects
ASSURE	The Abatacept Study of Safety in Use with Other Therapies
BAFF	B cell activating factor of the TNF family
BCL-6	B-cell lymphoma protein 6
BCR	B cell receptor
BLIMP1	PR domain zinc finger protein 1
BlyS	B lymphocyte stimulator
bp	base pair
B reg	Regulatory B cell
cAMP	cyclic adenosine monophosphate
CAGE	Cap Analysis of Gene Expression
CCL	Chemokine (C-C motif) ligand
CCR	C-C chemokine receptor
CD39	cluster of differentiation 39
CDAI	Clinical disease activity index
cDC	classical cendritic cell
CDK	Cyclin dependent kinase
cDNA	Complimentary DNA
CIA	Collagen induced arthritis
CHARISMA	Chugai Humanized Anti-Human Recombinant Interleukin-6 Monoclonal Antibody
ChIP	Chromatin Immunoprecipitation
CLASH	crosslinking, ligation, and sequencing of hybrids
CRP	c-reactive protein
CRT	cell surface calriticulin
CSF1R	Colony stimulating factor one receptor
CSR	class switch recombination
Ct	Cycle threshold
CTLA	cytotoxic T-lymphocyte-associated protein
DAMPs	Damage associated molecular patterns
DAS	Disease activity score
DC	Dendritic cells
DGR8	DiGeorge syndrome critical region gene 8
DHFR	Dihydrofolate reductase
DKK-1	Dickkopf-related protein
dPBS	Dulbeccos Phospate Buffered Saline
DMARD	disease modifying anti-rheumatic drug
DNA	Deoxyribonucelic acid

E. coli	Escherichia coli
EF1α	Elongation factor 1 alpha
ELISA	Enzyme linked immunosorbent assay
ER	Endotoxin removal
ERAP-1	endoplasmic reticulum aminopeptidase 1
ESR	erythrocyte sedimentation rate
ETS-1	V-Ets Avian Erythroblastosis Virus E26 Oncogene Homolog
EULAR	European League Against Rheumatism
EXP5	Exportin 5
FACS	Fluorescence-activated cell sorting
FAF1	Fas associated factor 1
FGF	fibroblast growth factor
FLS	fibroblast like synoviocytes
FMO	fluorescence minus one
FOXP3	forkhead box P3
GBRC	Glasgow Biomedical Research Centre
GM-CSF	Granulocyte-macrophage colony-stimulating factor
GWAS	Genome wide association study
HAQ	Health assessment questionnaire
HC	Healthy Control
HCQ	Hdroxychloroquine
HDAC	Histone deacetylase
HDL	high density lipoprotein
HERA	hydroxychloroquine in early rheumatoid arthritis
HIF1	Hypoxia inducible factor 1
HITS-CLIP	High-throughput sequencing of RNA isolated by crosslinking immunoprecipitation
HMGB1	high mobility group box 1
HSCs	haematopoetic stem cells
Hsp	Heat shock protein
iDC	inflammatory DCs
IFN	interferon
IGFR-1	Insulin like growth factor 1
Ig	immunoglobulin
IKK	IKappa B kinase
IL	interleukin
im	intramuscular
IRAK	Interleukin-1 receptor associated kinase
IRG	Interferon regulated genes
IRF4	interferon regulatory factor 4
JAK	Janus kinase
kb	kilobase
LB	Luria Bertani
LDL	low density lipoprotein
LPS	Lipopolysachride
LXRα	Liver X receptor alpha
MAGENTA	meta-analysis gene-set enrichment of variant associations
MBS	MicroRNA Binding Site
MCP-1	monocyte chemotactic protein 1
M-CSF	macrophage-colony stimulating factor
mDC	Myeloid dendritic cell
MHC	Major Histocompatibility Complex

miR	microRNA
MMP	matrix metalloproteinase
mRNA	Messenger RNA
MTHFR	Methylene tetrahydrofolate reductase
mTOR	Mammalian target of rapamycin
MTX	methotrexate
Mut	mutated
NFκB	Nuclear Factor Kappa Beta
NICE	National Institute of Health and Care Excellence
NKT	Natural Killer T cells
NLRP3	Nod-like receptor protein 3
NSAIDs	non-steroidal anti-inflammatory drugs
OA	osteoarthritis
ORBIT	The Optimal Management of patients with rheumatoid arthritis who Require Biologics
ORF	Open reading frame
PAD	peptidylargenine deaminase
PAMP	pathogen associated molecular pattern
PAR-CLIP	Photoactivatable Ribonucleoside-Enhanced Crosslinking and Immunoprecipitation
PB	Peripheral blood
PBMCs	peripheral blood mononuclear cells
PC	Principal component
PD-1	Programmed cell death gene 1
pDC	Plasmacytoid dendritic cell
PDE4	phosphodiesterase 4
PFA	paraformaldehyde
PGK	Phospho glycerate kinase
PIP	proximal interphalangeal joints
PPARγ	Peroxisome proliferator-activated receptor gamma
PMA	Phorbol Myristate Acetate
PU.1	Spi-1 proto-oncogene
qPCR	Quantitative polymerase chain reaction
RA	Rheumatoid Arthritis
RACE	Rapid extension of cDNA ends
RANK	receptor activator of NF-κB
RASF	Rheumatoid arthritis synovial fibroblast
RE	Restriction enzyme
REFLEX	Randomized Evaluation of Long-Term Efficacy of RTX
RF	Rheumatoid factor
RISC	RNA induced silencing complex
RNA	Ribonucleic Acid
RORC	RAR-related orphan receptor C
RT	Reverse Transcriptase
RTX	Rituximab
SERENE	Study evaluating rituximab's efficacy in MTX inadequate responders
SCID	Severe combined immunodeficiency
SDAI	Simple disease activity index
SE	Shared epitope
SF	Synovial fluid
SHIP-1	inflammation Phosphatidylinositol-3,4,5-trisphosphate 5-phosphatase 1

SJC	swollen joint count
SLE	Systemic lupus erythematosus
SNBTS	Scottish national blood transfusion service
SNPs	single nucleotide polymorphisms
SOCS	suppressor of cytokine signalling
STAT	Signal transducer and activator of transcription
SSZ	Sulfasalazine
TA375	technology appraisal guidance 375
TAE	Tris Acetate EDTA
TAB1	TAK1-binding protein 2
TE	Tris EDTA
TCR	T cell receptor
TCZ	Tocilizumab
TEAR	Triple Therapy in Early RA
TF	Transcription Factor
TGF	transforming growth factor
T_H	T helper cells
TICORA	Tight Control of RA
TIMP	Tissue Inhibitors of Metalloproteinases
TJC	Tender joint count
TLR	Toll like receptor
TLR4	Toll like receptor 4
TNF	Tumour necrosis factor
TNFAIP3	Tumour necrosis factor, alpha-induced protein 3
TNFR2	TNF receptor 2
TOWARD	Tocilizumab in Combination With Traditional DMARD Therapy
TSS	Transcriptional Start Site
TYMS	Thymidylate synthetase
tolDC	Tolerogenic dendritic cell
TRAF2	TNF receptor-associated factor 2
TRAF6	TNF receptor-associated factor 6
TRAP	Tartrate-resistant acid phosphatase
Treg	Regulatory T cell
TTP	Tristraprolin
Tyk2	Tyrosine kinase 2
UTR	Untranslated region
VAS	visual analogue scale
VEGF	vascular endothelial growth factor
WT	Wild type

1 General Introduction

Rheumatoid arthritis (RA) is a symmetric inflammatory polyarthritis considered to be a systemic autoimmune disease with as yet unknown aetiology. The progressive chronic nature of this condition ultimately leads to deformity through erosive destruction of the cartilage and bone in the affected joints. Up to 1% of the general population suffers from RA. If left untreated or unresponsive to the treatment, RA leads to a severe disability, difficulties with tasks of daily living and unemployment [1]. The systemic nature of the disease involves multiple extra articular manifestations and increased risk for cardiovascular events, metabolic disorder and depression [2,3]. More importantly, RA is associated with an independently increased risk of premature death, a troubling prospect for the patient and responsible physician [4,5]. RA management has been transformed through the implementation of translational research in rheumatology: herein I will highlight new frontiers of scientific discovery in RA and thereafter focus upon my own question of particular interest.

1.1 Historical understanding and approach to treatment of RA

One common thing between historical and current approaches to RA is the importance of deep understanding of the pathogenesis and the wealth of clinical experience in the diagnosis and management of this disease. Clinical heterogeneity at the time of presentation and throughout the natural course of the disease requires a truly holistic approach. The area in which this specialty has struggled the most over the last few decades is how to objectively capture and apply the deep understanding of RA that every experienced rheumatologist has and to apply this to new pathway discovery. To this end, several attempts were made to develop diagnostic and classification criteria, disease activity scores with disease and treatment biomarkers. But firstly, I will review the historical development of thinking about RA and improvements in all aspects of treatment, made through the years.

1.1.1 Diagnostic classification criteria

Traditionally, the diagnosis of RA was based entirely on clinical criteria. These have been implemented in 1958 by American Rheumatism Association (ARA) and were revised every 10 to 20 years [6]. The most influential criteria were developed in 1987 and included 5 clinical parameters, measurement of rheumatoid factor (RF) and radiographic changes, shown in Table 1.1 [7]. For the diagnosis of RA four of these criteria had to be present for at least 6 weeks. With this, 93.5% sensitivity and 89.3% specificity was achieved. Although this classification defines the staple principles of clinical diagnosis and for the first time includes an objective biomarker, it had multiple issues. Firstly, no other condition was excluded. Secondly, it included rheumatoid nodules and radiographic erosive changes that are features of established disease, therefore significantly limiting the early diagnosis. It is important to understand that these criteria, and their limitations, were used for diagnostic and classification purposes, and were included in virtually all clinical trials conducted from 1987 until 2010.

Criterion	Definition
1. Morning stiffness	Morning stiffness in and around the joints, lasting at least 1 hour before maximal improvement
2. Arthritis of 3 or more joint areas	Soft tissue swelling in at least 3 joints, assessed simultaneously by a physician.
3. Arthritis of hand joints	At least one swollen area in a wrist, MCP or PIP joint.
4. Symmetric arthritis	Simultaneous involvement of the same areas from both sides
5. Rheumatoid nodules	Subcutaneous nodules, over bony prominences or extensor surfaces, or in juxtaarticular regions
6. Serum rheumatoid factor	Abnormal amounts of serum rheumatoid factor
7. Radiographic changes	Typical radiographic changes on posteroanterior hand and wrist radiographs

Table 1.1 The 1987 revised criteria for the classification of rheumatoid arthritis.
Adopted from Arnett at al., A&R 1988 **[7].**

1.1.2 Historic Treatments

Early definition of RA as an autoimmune inflammatory disease consequentially led to the use of immune suppressants and anti-inflammatory agents. Since the introduction of corticosteroids, there has been an ongoing search for more efficient and less toxic treatments. Non-steroidal inflammatory drugs (NSAIDs), such as aspirin and indomethacin, have shown some efficacy in addition to a regular steroid use and were introduced in order to improve functional outcome and pain relief in RA patients [8,9]. NSAIDs remained a first line treatment for inflammatory arthritis, alongside physiotherapy and splints, until the 1990's. Interestingly, measurable functional outcomes at the time included inflammatory index, measurement of the PIP swelling with steel jewellers tape, walking time and shoe-tie time in attempt to objectify trial outcomes [9]. Joint injections with steroids or aspirin were also popular [10-12]. These early studies demonstrated that achieving reduced inflammation state is not enough to control the disease and cross over to placebo would result in symptom flare.

Since the 1950's there was a growing body of cases that claimed successful use of cytotoxic drugs in treatment of difficult cases of RA, including methotrexate [13]. This prompted a double-blind placebo controlled studies of the efficacy of azathioprine, cyclophosphamide, chloroquine, and gold preparations [14-18]. The placebo controlled gold preparation study included patients meeting early ARA criteria for at least 6 months. This trial showed 'slight but definite improvement in the measured parameters' which was acceptable rate of response at the time [18]. It also demonstrated the shift towards induction and maintenance therapy, that proved beneficial during 2 year follow-up, with significant difference in active joint count, grip strength and erythrocyte sedimentation rate (ESR) compared to symptom triggered bolus treatment [18]. Sharp et al. comprehensively reviewed the effects of chrysotherapy after 2 year follow-up study, during which 1/3 of the patients achieved remission, 1/3 had a partial response and 1/3 were classified as treatment failures [19]. Most importantly, this study noted that the only valuable prognostic factor of long term benefit was initial good clinical response to treatment after 3 months, similar to that now observed with modern agents. Authors also clearly defined the need for a satisfactory method to analyse treatment response, lack of which was additionally confusing the way trials were reported and implemented.

A head-to-head comparison of the efficacy of azathioprine, cyclophosphamide and gold was carried out in a double blind randomised trial lasting 18 moths and involving 121 patients with ‘relatively early’ RA (under 3 years of duration) [16]. Here, two ‘immunosuppressive’ agents produced clinical improvement compared to gold containing agents, facilitated reduction in the background steroid dose and hindered radiographic joint damage. Despite this, severe side effects of the used at the time immunosuppressants forbad people to stay on the medications long term and maintenance therapy with non-steroidal anti inflammatory agents (NSAIDs) was given, with increased risk of repeat flares.

Patients with progressive treatment resistant disease constituted 1/3 of all patients with RA and were subjected to a variety of extremely invasive procedures like chemical or radiation synovectomy, total lymphoid irradiation, lymphocytic apheresis and thoracic duct drainage [20-23]. Alternatively, early attempts at combination therapy were made. To this effect, a small open study was conducted on 15 seropositive, treatment refractory patients that were given cyclophosphamide, azathioprine and hydroxychloroquine for an average of 27 months [24]. Treatment benefit onset was observed from 3 to 16 month, during which 5 patients achieved remission, 9 patients had a partial response and three patients had no improvement. This was the first demonstration that small dose triple therapy could be better tolerated and more efficacious in the long-term disease control when compared to a single high dose agent. Additionally, this has demonstrated the benefit of the use of ‘disease-modifying antirheumatic drugs’ (DMARDs) over NSAIDs, which were extremely popular due to the quick analgesic, antipyretic and anti-inflammatory effects. On the contrary, available DMARDs were slow to act and provided less symptomatic relief, therefore were still considered a second line treatment after physiotherapy, rest and NSAIDs [25].

These early studies demonstrate how slow unravelling of the magnitude of the inflammatory process behind clinical arthritis clearly defined a need for the continuous immunosuppression over periodic flare treatment. A growing body of data on the long term radiographic and functional outcomes confirmed that therapy with gold and cyclophosphamide can retard radiographic progression of the disease, setting a new therapeutic goal [26]. Necessities for clinical response

criteria and long term safety data were clearly defined. More importantly, the discovery of more tolerable drugs was a matter of urgency.

1.1.3 Modern DMARDs

A vast array of drugs were screened for their anti rheumatic properties. Different approaches, from new anti-inflammatory and cytotoxic agents to antibiotics including antimalarial agents were tested. Clear need for randomized controlled studies was appreciated, however poorly controlled disease and ineffective therapy were major confounding factors for early controlled studies, that could not manage treatment compliance beyond 2 years duration [19]. From late 1970's until the 1990's a series of well designed, placebo controlled, double blind randomized clinical trials showed efficacy of a variety of DMARDs, including methotrexate (MTX), sulfasalazine (SSZ), auranofin, hydroxychloroquine (HCQ), D-penicillamine and cyclosporine A [27-31]. Here, I will review the clinical trials and mechanism of action behind DMARDs currently in use in the clinical practice.

1.1.3.1 Sulfasalazine

Nanna Svartz from Sweden introduced SSZ for the treatment of rheumatoid arthritis in 1941. She believed that the core rheumatoid lesions were in the connective tissue and inflammatory in nature, therefore the higher tissue affinity of the combination of salicylic acid and sulphapiridine would have improved tissue penetration. Her initial positive experiences with sulfasalazine were diminished by the open label study conducted by Sinclair and Duthie in 1949 [32]. After a significant period of neglect, the first rigorous randomized double-blind placebo controlled study of SSZ and intramuscular sodium aurothiomalate was conducted in Glasgow in 1983 [28]. This study clearly demonstrated non-inferiority of SSZ compared to gold preparation as a second line agent that was meant to reduce laboratory inflammatory variables. Both treatment groups differed significantly from placebo group. Additionally, SSZ in the 3g daily dose had a better safety profile (predominantly gastrointestinal disturbance) that allowed completion of the 24 weeks trial in the majority of participants [28]. Following this, other controlled studies proved clinical effectiveness of SSZ compared to placebo, despite the slow onset of the effect.

Thereafter, SSZ was successfully used in the clinical practice, although initially still reserved for NSAIDs and gold failures. Direct comparison of SSZ to HCQ in a double blind randomized trial on DMARDs naïve patients showed that those treated with SSZ developed less joint erosions and had lower joint damage scores after 24 and 48 weeks of treatment [33]. The 3 year follow-up of this study showed persistent benefit from the treatment in 38% of patients in SSZ group and 24% in HCQ group with sustained retardation of radiographic progression [34]. Other studies in 'early' pre-erosion RA patients treated with SSZ confirmed positive radiographic outcome, however noted that SSZ is not excellent in inducing clinical remission in a substantial proportion of patients were still symptomatic [35].

Despite obvious clinical benefits and wide use, the mode of action of SSZ is still not fully explored. Earlier work implicated SSZ in the regulation of nuclear factor kappa B (NFκB) transcription factor (TF) and production of proinflammatory cytokines [36]. However, a recent large genome wide association study (GWAS) connected SSZ to the functioning of mediator of RNA polymerase II transcription subunit 1 (MED1) gene, serving as a co-factor of peroxisome proliferator activated receptor gamma (PPARγ) TF, crucial to the polarization of anti-inflammatory macrophages [37,38]. Both of these pathways, NFκB and PPARγ, are critical for osteoclastogenesis and can impact the formation of bone erosions [39,40]. PPARγ is also in the centre of adipogenesis as it regulates the fatty acid storage and glucose metabolism, evident from the gene knock out mouse model, which failed to generate fat tissue [41]. Use of SSZ could therefore influence adipogenesis and insulin-resistance in RA patients who are already at a higher risk of metabolic disease, although these studies have not been done. On the other hand, SSZ was shown to inhibit platelet aggregation and exhibit cardioprotective effect in patients with inflammatory arthritis, similar to that of aspirin [42].

These data suggest a relevant pathophysiologic and clinical rationale for the use of SSZ in subjects with RA. Further clinical studies evaluating full potential and combinational use of this DMARD will be reviewed below.

1.1.3.2 Methotrexate

Methotrexate is the most established and most beneficial DMARD to date. It was first successfully used in the treatment of psoriasis before introduction to the rheumatic field. MTX is designed as a folic acid antagonist that inhibits de novo purine and deoxyribonucleic acid (DNA) synthesis by inhibiting dihydrofolate reductase (DHFR) enzyme in cells. The initial rational behind its use in autoimmune conditions was the high rate of division of immune cells during active inflammation, which is inhibited by MTX. Indeed, MTX treatment of THP-1 human monocytic cell line leads to increase apoptosis of these cells [43]. Alternatively, MTX potentiates the expression of adenosine and leads to the increased intracellular cAMP (cyclic adenosine monophosphate) levels that have anti-inflammatory properties and reduce cytokine expression [43]. More recently, it was shown that CD39 (cluster of differentiation 39) generates adenosine upon toll-like receptor (TLR) stimulation of the cells to maintain the balance of the macrophage response [44]. Lack of CD39 or adenosine sustained the inflammation and cytokine production by myeloid cells [44]. Adenosine receptor agonists are now being tested in clinical trials for their antirheumatic and analgesic properties [45]. It would certainly be intriguing to compare these data with the efficacy of MTX alone.

Nevertheless, historically MTX was classified as a cytotoxic drug and despite early uses in 1950s, it is not until 1980s that controlled clinical trails with low doses of drug were conducted in RA. In the meantime, it was used sporadically in difficult cases and for intraarticular injections with some minor benefits [46].

The first convincing 24 weeks double-blind randomized cross-over placebo controlled trial demonstrated significant efficacy of the low dose MTX in RA patients with refractory disease treated for 12 weeks or in placebo cross over patients at 24 weeks [27]. At the time, 2.5 mg to 5 mg dose were used every 12 hours three times per week and it was well tolerated. 3 year follow up of the patients that chose to continue with MTX treatment showed that 62% of cases reported some side effects, predominantly nausea, mild leukopenia, mild thrombocytopenia and transitory liver transaminitis without cirrhosis on the biopsy [47]. This indicated better safety profile of MTX than other cytotoxics like

cyclophosphamide, known for induction of azospermia and bone marrow suppression.

Similar study conducted same year included 12 patients in the placebo controlled double-blind cross over design testing efficacy of once weekly intramuscular (im) MTX in patients with progressive erosive disease that have failed other available treatments [48]. Once weekly MTX dose was titrated from 5 mg to 25 mg in small increments depending on the clinical response of the patient. There was significant improvement in tender and swollen joint counts, duration of the morning stiffness, visual analogue scale (VAS) of the well-being and physicians global score after 13 weeks of MTX treatment. Additionally, this study included extensive laboratory testing that indicated no change in the titre of RF and decrease of previously abundant numbers of monocytes amongst peripheral blood mononuclear cells (PBMCs) of the MTX treated subjects [48]. It was common at the time for clinical trials to include a small and homogeneous group of patients. Nevertheless, these studies have established MTX as an efficacious second line treatment in patients who fail NSAIDs and slow acting conventional DMARDs (gold). Addition of supplemental folic acid has significantly improved the tolerability of long term treatment with MTX [49].

On the contrary, little progress was made in discovery of biomarkers of clinical response to MTX. Early hopes with HLA-DR2 expression were disproved by the multicentre randomized controlled study [50]. Further use of MTX coincided with the understanding that it is necessary to start early treatment to prevent occurrence of the erosions. The field was moving towards the idea of sustained prolonged treatment despite clinical remission, after reports demonstrated severe flares following discontinuation of methotrexate in previously stable patients [51].

1.1.3.3 Hydroxycloroquine

Cloroquine and hydroxycholoquine are anti-malarial drugs that have been successfully used in the treatment of RA for decades. A review from 1983 summarizes a series of open label and double-blind controlled trials concluding a 70% moderate efficacy of HCQ in previous NSAIDs failures or early progressive disease, of which 15% had excellent and 55% had partial clinical response [52].

Safety profile has remained very satisfactory if daily dose is limited to 6.5 mg/kg, with the exception of late stage retinopathy requiring annual clinical review [52]. Low risk and comparable efficacy with gold preparations or D-penicillamine rendered HCQ a first choice among remittive drugs [30,52]. Despite satisfactory clinical responses, later head-to-head comparison of HCQ and SSZ showed a higher rate of erosive disease in HCQ treatment group after 24 and 48 weeks [33]. Methodological difficulties of the earlier studies failed to produce conclusive results. The HERA study, involving 120 patients with RA of less than 2 years duration treated with HCQ or placebo for a period of 36 weeks, unequivocally demonstrated significant benefit on synovitis, pain and disability, but no psychological improvement in patients treated with HCQ [53].

The main mechanism of action was thought to be acidification of the cell cytoplasm and interference with protein processing of the cell resulting in inhibited antigen presentation [54]. This very different mode of action is what rendered HCQ a suitable candidate for the combination treatment with other slow acting DMARDs. This was the crucial step in attempting earlier, more aggressive disease control in 1990's that led to development of modern treatment protocols.

1.1.3.4 Combination treatment

Interest in combination therapy has arisen form the series of published reports suggesting that sequential use of available DMARDs in addition to standard therapy with NSAIDs and corticosteroids prevents joint damage, long term disability and most importantly, increases life span of RA patients [23]. By the 1990's it was not unusual practice to utilise conventional combination therapy with an additional DMARD of preference, even though randomized controlled trials were sparse. Whether this practice was established due to then popular views that RA is a 'non-malignant B-lymphoproliferative disease' where cytotoxics are beneficial or from sheer desperation in cases of unresponsive disease, initial results were satisfactory [55]. There was even a separate session at the 1993 American College of Rheumatology (ACR) meeting in San Antonio devoted to combination therapy in RA [56]. The field was influenced by the seminal paper from Wilske and Healey who formulated goals of RA therapy with crystal clarity: "to supress RA inflammation as completely as possible for the

patient's entire lifetime and, thereby, to prevent the initial, and then progressive, joint damage that leads to eventual disability" [57]. Needless to say that this statement is entirely applicable to current clinical practice.

Clinical trials evaluating combinational treatment of RA followed. An open study on 32 patients treated with combination of SSZ and MTX showed clinical improvement with no additional toxicity compared to therapy with MTX alone [58]. However, it is not until the seminal study from O'Dell et al, published in 1996, that triple DMARD therapy in treatment non responders was tested [59]. 102 patients with RA who previously failed at least one DMARD were divided in three equal groups to receive MTX, a combination of SSZ and HCQ or triple therapy with MTX, SSZ and HCQ for 2 years. 77% of patients in triple treatment group achieved 50% improvement after 9 months, compared to 40% in HCQ and SSZ combination group and 33% in MTX only group, while safety profile was comparable between all groups [60]. Superior efficacy of the triple therapy over either combination of MTX with SSZ or HCQ was once again confirmed in the separate two year double blind placebo controlled trial, conducted by the same group [59]. As a result, superiority of triple therapy use was demonstrated in patients with both early and more established RA [61-63].

Mounting data on the better long-term outcomes, financial benefit and satisfactory safety profile has supported the mainstream use of DMARD treatment as the first line therapy of RA. The next step was to establish how early and how intensive should treatment be. Reviewing the protocols from the treatment of other chronic diseases such as hypertension or type I diabetes raised a possibility that rigorous disease monitoring and tight control would lead to the improved long-term outcomes. Indeed, the Tight Control of RA (TICORA) study was based on the hypothesis that whatever DMARD is initially used, as long as the therapy is adequately escalated it will ultimately lead to the full disease control in a majority of patients, some of which will achieve remission with a single agent whilst other will require triple therapy [64]. Indeed, a striking 65% of patients in the intensive protocol group achieved remission after 18 months of the treatment, compared to 16% in the routine group - possibly due to the ~50% of subjects receiving triple therapy in the intensive group compared to 3% in the routine management group [64].

Lack of biomarkers, aside from acute phase reactants and clinical review, makes it sometimes difficult to gauge if patients are over- or undertreated. Step-up approaches in response to clinical inflammation left many with the feeling that treatment is designed to merely ‘catch up’ rather then to prevent disease progression.The Triple Therapy in Early RA (TEAR) trial was a crucial study designed to explore the benefits of the triple DMARD therapy from the onset compared to the step up treatment in response to clinical need [65]. Study results showed no additional benefit from the parallel triple therapy use above appropriate and timely step up treatment in poorly controlled subjects. Second validation of the MTX-first strategy was demonstrated in the American TEAR study involving 755 participants and randomizing them to receive MTX monotherapy, MTX with SSZ and HCQ triple therapy or MTX and etanercept combination with biologic therapy [66]. Results demonstrated that 30% of the patients will achieve good disease control on MTX monotherapy, while 70% of the patients will require additional treatments. Unfortunately, the later group of patients is not clinically or radiographically distinguishable from the good responders and there is an acute need for appropriate biomarkers to identify such individuals a priori.

In summary, rigorous carefully designed clinical trials have transformed treatment approaches and outcomes of RA. Expectations have significantly changed as well. Disease remission is achievable and can be common with a treat-to-target approach. A wide variety of safer medications are now available and the field is moving forward with remarkable speed. Despite this, early clinical response to treatments is still the most valuable predictor of the long-term outcome. Rigorous clinical monitoring and incremental treatment are still the best ways to improve the rate of clinical remission, reduce physical disability and radiographic progression [67]. The next step to truly personalized and stratified medicine has been slow and difficult.

1.2 Current classification criteria and clinical scores in RA

1.2.1 2010 Classification criteria

A major shortcoming of the 1987 classification criteria for RA was the exclusion of the patients with early RA. This has been recently reviewed by the ACR and EULAR (European League Against Rheumatism) collaboration and new classification criteria were implemented in 2010. These criteria of RA are based on the presence of synovitis in at least 1 joint, absence of the alternative explanation for the synovitis and the minimal score of 6 out of maximum possible 10 for other associated features, summarized in Table 1.2. Although radiographs are not necessary for the diagnosis, people with existing bone erosions or previously diagnosed RA would also be classified as having RA.

Absolute Criteria	
Synovitis (swelling in at least 1 joint)	
No better explanation of synovitis	
Additional Criterion	**Score**
A. Joint involvement	
1 large joint	0
2-10 large joints	1
1-3 small joints	2
4-10 small joints	3
>10 joints (at least 1 small joint)	5
B. Serology	
Negative RF and negative ACPA	0
Low-positive RF or low-positive ACPA	2
High-positive RF or high-positive ACPA	3
C. Acute-phase reactants	
Normal CRP and normal ESR	0
Abnormal CRP or abnormal ESR	1
D. Duration of symptoms	
<6 weeks	0
≥6 weeks	1

Table 1.2 2010 ACR/EULAR classification criteria for RA.

1.2.2 DAS score

Implementation of clinical response criteria significantly improved and simplified clinical practice and clinical trial reporting. Several scores are developed for the assessment of disease severity, progression and effect of treatment. Most frequently used is the disease activity score (DAS). DAS was invented in the 1990s in a search for a clinical composite measure that would closely correlate and reflect predicted clinical outcome while incorporating a minimal amount of meaningful components [68,69]. It has since been evaluated in many large clinical trials and is widely accepted in clinical practise [70-72]. This score produces meaningful and interpretable results at every clinic appointment and allows better implementation of clinical trial results in everyday practice. The score is based on separate counts of swollen and painful joints amongst preselected 28 (or 44) joints assessed by the clinician, visual analogue scale (VAS) for the average weekly pain estimate by the patient and inflammatory marker CRP or ESR, making DAS28-CRP or DAS28-ESR scores. DAS44-CRP and DAS44-ESR are also used. The main drawbacks of this test are variable inter-observer reproducibility of the clinical joint examination and potential underestimation of low-grade arthritis [73]. Although some recent reports would suggest that clinical estimation of disease progression using DAS28 score is just as efficacious as ultrasound (US) at the treatment escalation and achieving remission [74,75]. Therefore, reduction in DAS28 score is an established treatment target and a benchmark for classifying the prescription of biologic agents like anti-TNFα inhibitors in the UK [76].

DAS28 score is a continuous scale, in which a DAS of >5.1 represents high disease activity, DAS28 score between >3.2 and <5.1 results in moderate activity, while DAS28 score in the range of 2.6-3.2 is a mark of low disease activity at the time of assessment. Clinical remission is classified with the DAS28 score of <2.6. A change of 1.2 in the score of the individual patient is considered a clinically significant change.

1.2.3 SDAI and CDAI scores

The Simplified Disease Activity Index (SDAI) [77] and Clinical Disease Activity Index (CDAI) [78] are two other continuous clinically used measures that have served as the most recent tools for the clinical trial outcomes. Similarly to DAS28, the SDAI score involves 28 joint count for tender and swollen joints, acute reactant CRP (mg/dl) and patient's global assessment, however, the additional component is the physician's global assessment also measured on 0-10 Likert scale. High disease activity according to SDAI core is >26, moderate range is 12-26, mild <3.4-11, and remission is suggested with SDAI of <3.3. 22 points represent a major change, while the improvement in 10 to 21 points is considered a minor change.

Given that a CRP result is not always available at the time of the patient's appointment, CDAI score was developed to be interpretable at the clinic and includes the sum of 28 TJC and SJC, patient's global assessment and patient's overall pain score. No acute phase reactant is necessary for the CDAI score [79]. High disease activity is represented by score >22, moderate range lies between 11-22, low disease activity is within the score of 2.9-10, and remission is <2.8. Latest ACR guidelines on evaluation of disease activity in RA suggest that use of DAS28, CDAI and SDAI scores incorporating CRP are all valid discriminative measures and prediction of clinical outcomes correlate with each other [78,80].

1.2.4 Clinical criteria for the trial outcomes

Assessment of drug efficacy during clinical trials requires the measurement of both continuous and categorical outcomes. EULAR response criteria are based on DAS28 score and are the most commonly used measure, which provides results that are easily extrapolated to the daily clinical setting. However, categorical scores are preferable in comparison of study results with other trials of the same or other drugs. For this purpose, ACR criteria based on the reached value principle were developed [81].

The ACR criteria were developed to maximally discriminate effective treatment from the placebo control [82]. This is achieved by setting several progressively more difficult to achieve goals by calculating the number of patients that have shown 20%, 50% or 70% improvement. Much like DAS, these criteria incorporate patient's global assessment, physician's global assessment, VAS for pain, disability and functional questionnaire as well as one of the acute phase reactants (CRP or ESR). In order to classify for ACR20, 20% improvement in at least three from available 5 criteria must be detected. ACR 20 response is considered a clinically relevant improvement, although some investigators have questioned this [83]. With the field moving towards frequent achievement of good clinical response, ACR50 and ACR70 criteria were developed, for these 50% and 70% improvement in three out of five measures must be observed [84]. The performance of EULAR and ACR response criteria has been validated in different clinical trials, and resulting discrepancy was found to as low as 5% [85].

More difficult and yet more crucial was obtaining a consensus on the definition of remission in patients with RA. After much investigation, RA remission in clinical trials can be classified when wither scores of the tender joints, swollen joints, CRP (mg/dl) an patient's global assessment are all ≤1, or when SDAI score is ≤3.3 to ensure minimal chance of further radiographic damage and progression of disability [86,87].

1.3 Current understanding of the pathogenesis of RA

RA is a complex disease and our understanding of the pathogenesis has changed over the years with new discoveries made. Historically, it was believed to be a disease of the adaptive immune system, whether it was called “non-malignant B-cell lymphoproliferative disease” in 1960’s and 70’s for its association with autoantibodies, or a T cell dependent disease as a part of the ‘shared epitope’ (SE) model. The SE model suggests self or similar to self peptide to be presented to T cells by antigen presenting cells (APC) in such a way that autoreactive T cells are selected and breach of self tolerance occurs. This hypothesis is based on the association of RA with MHC class II genes, and in particular, a specific amino acid sequences in HLA-DR1 and HLA-DR4 alleles, responsible for APC-T cell cross talk [88]. Preference of RA T cells for citrulinated peptides, which are more prevalent in smokers, also stems from the way self peptides are processed and presented [88]. In addition, early genetic association studies identified single nucleotide polymorphism in the PTPN22 locus and programmed death gene (PD-1) that inhibits apoptosis in auto-reactive T cells [88]. On the contrary, twin studies have shown that concordance rate of disease is only around 15% and the occurrence of the disease after the age of 40 suggests a weaker genetic component [89]. Overall , thought debated, heritability of RA is probably around 60% at best. This supports a strong environmental component and perhaps epigenetic influences on pathogenesis (see later).

Clinical trials have taught us that more efficacious treatments are those that target broad-spectrum proinflammatory cytokines, pointing towards a significant involvement of the innate immune system as well as the pro-inflammatory aspects of the resident cells, such as fibroblast-like synoviocytes (FLS), together with cells of the adaptive response e.g. via co-stimulatory blockade or B cell depletion. One thing we can agree on is that involvement of the immune system in RA has to be viewed in its entirety, if further therapeutic progress is to be made. Unfortunately, understanding to why RA localises predominantly in joints and not other parts of the body, remains somewhat evasive.

1.3.1 T cells

The importance of T cells in RA pathogenesis was established early, since increased numbers of CD3+ effector T cells were found in synovial histology [90,91]. In mouse models, adoptive transfer of T cells from diseased mice was sufficient to induce the disease in the recipient, further supporting the T cell oriented model of the pathogenesis [91,92]. Since then, several types of effector T cells were identified. Thymic differentiation of T cells generates $CD4^+$ and $CD8^+$ T cells, the former most investigated in RA.

1.3.1.1 $CD4^+$ T cells

From $CD4^+$ T helper cells T_H1, T_H2 and T_H17 subsets are recognised. T_H1 cells deliver a viral response; they differentiate under the guidance of IL-12 and IL-18 and *T-bet* TF and are a major source of IFNγ [93]. T_H2 cells mature with the presence of IL-33, IL-4 cytokines and *gata-3* TF and they produce IL-4, IL-5, IL-9, IL-13, which are effective against parasites, but also mediate allergic responses and manifest clinically for example as asthma [94]. T_H17 cells are crucial in defence against extracellular bacteria and fungi and differentiate under influence of TGFß, IL-1, IL-6, IL-21, and IL-23 to initiate *rorc* TF expression and become mature cells producing IL-17 (IL-17A), IL-17F, TNFα and CCL20 [95]. Recently they have been recognised to be more plastic and some are also noted to express IL-10, GM-CSF and other cytokines. Less investigated types include T_H9 for IL-9 expression and T_H22 for IL-22 expression respectively, however the relation of these cells to other T helper subsets and their functional roles are still unclear [96].

Original data supported the role of T_H1 cells as the main drivers of RA synovitis, due to the raised levels of IFNγ in synovial fluid. With the discovery of T_H17 cells, it is now suggested that synovial IL-17 contributes to the influx of inflammatory cells, activation of pro-inflammatory cytokine production and significant bone and cartilage damage due to the direct effects on osteoclasts and chondrocytes [90,97]. In fact, both hypotheses are likely to be correct as significant plasticity occurs in synovial T cells, as might be expected from commentary above. A high proportion of cells co-express IFNγ with IL-17, driven by the activation of both RORC and T-bet TFs [98-100]. This phenomenon of

superactivation is specific to synovial inflammation, as PB cells remain single positive for either IFNγ or IL-17 [98]. More importantly, double positive T_H1/ T_H17 cells produce GM-CSF and contribute to the chemotaxis and maturation of synovial dendritic cells (DCs), in parallel instructing them to further prime new generations of T_H17 type cells [101,102].

A further major advancement was made with discovery of regulatory T helper cells - T_{REG} cells – that develop in the thymus in the presence of TGFß and IL-2 and express *foxp3* TF [103]. Their role is to suppress other T cells and APCs through secreting anti-inflammatory cytokines such as IL-10 and providing an inhibitory CTLA-4 signal instead of CD80/86 co-stimulation on APCs to induce tolerance [103]. Similarly to other T helper cells, inflammatory monocytes can induce expansion of T_{REG} cells at the site of inflammation and increased numbers are found in arthritic joints [104,105]. It is, therefore, of utmost importance to understand whether it is the inappropriate activation of effector T cells or the failure of the regulatory mechanisms that allow chronicity in RA. Now, there is a considerable amount of evidence suggesting that both occur. Namely, T cells, and in particular T_H17 cells, derived from the site of inflammation are irresponsive to suppression, especially in the presence of TNFα and IL-6 [106-109]. On the other hand, synovial fluid T_{REG} cells are functional *in vitro,* however activation with CD28, IL-6, IFNα and TNFα through an expressed TNF receptor 2 (TNFR2) directly impair their ability for suppression [110-115]. This may explain the enhanced supressing abilities of T_{REG} cells in patients receiving treatment with an anti-TNFα agent [115-117].

1.3.1.2 $CD8^+$ T cells

Increased interest in $CD8^+$ T cells is now elucidating new pathways, involved in RA pathogenesis. Patients with early active RA have increased absolute numbers of PB $CD8^+$ T cells when compared to matched healthy controls [118]. This is followed by a decrease in absolute numbers of cells during remission [119]. Expanded populations of $CD8^+$ T cells are noticed in RA synovial fluid where it negatively correlates with DAS28 clinical scores [120]. Newly defined subtypes of $CD8^+$ T cells, such as CD73+ cells exhibiting anti-inflammatory properties, are likely to transform our view of T cells in RA and give rise to new therapeutic interest in the near future [121].

1.3.1.3 T cell targeted treatment

Accumulating data on the importance of T cells in RA resulted in development of multiple anti-leucocyte, anti-CD4 and TCR compounds, which were amongst the first biologic treatments ever tested [122-124]. Unfortunately, anti-CD4 treatment approach showed no sustained benefit in patients with severe RA despite causing severe leukopenia. With the discovery of T_{REG} cells and co-stimulatory pathway of activation, targeting of CD28-CD80/86 axis was more appealing as it was believed to prevent activation rather than cause full depletion of T cells. This new approach capitalised on a fusion protein of CTLA-4 and a fragment of the Fc domain of human IgG1 named Abatacept. The Abatacept Trial in Treatment of Anti-TNFα Inadequate Responders (ATTAIN) was a phase 3, large randomized placebo controlled study involved 258 patients in the treatment group and 133 patients receiving placebo [125]. Patients had a wash-out period from TNFα agent before the trial, however they continued with a conventional DMARD of choice. Here, ACR 20 improvement was the primary outcome and was achieved by 50.4% of the actively treated patients and by 19.5% of placebo group. Improved rate of ACR 50 and ACR 70 responses, higher rates of low disease activity and remission according to DAS-28 criteria and comparable incidence of side effects with slightly higher rate of mild to moderate infection in the abatacept group rendered it an efficacious treatment in TNFα failures [125].

Further safety data were obtained during the ASSURE trial (The Abatacept Study of Safety in Use with Other Therapies) where recipients of abatacept in combination with DMARDs or other biologics were followed for 1 year [126]. This trial demonstrated similar safety profile of abatacept in the combination with DMARDs as the placebo control group, however a higher rate of significant adverse events were found in the group treated with abatacept in the combination with other biologics (22.3%), most commonly an anti-TNF agent (11.7-12.5% in placebo or DMARDs combination groups, respectively) [126]. Therefore, the use of abatacept in combination with other biologic agents was not advisable in the clinical practice. On the contrary, further evidence was provided for the use of abatacept in the combination with methotrexate, since patients who were initial responders to this treatment maintained efficacy and had reduced radiographic progression after 2 years follow-up [127].

Subsequently, deeper understanding of osteobiology has revealed that CTLA-4 (or abatacept) binding to CD80/86 molecules on the surface of osteoclast precursors prevents further differentiation of the cells despite presence of stimulatory factors such as M-CSF or RANKL, explaining direct influence of abatacept on the bone erosion formation in RA [128,129].

Naturally, the question of efficacy of abatacept in early RA with biologics naive patients has arisen. This was investigated in the AMPLE trial (Abatacept versus Adalimumab Comparison in Biologic-naïve RA Subjects with Background Methotrexate) on 646 patients failing monotherapy with MTX and randomly assigned to receive a weekly subcutaneous (sc) injection of abatacept or twice weekly sc adalimumab (anti-TNFα agent) [130]. Primary outcome – ACR20 score at 1 year was achieved by 64.8% of patients receiving abatacept and 63.4% taking adalimumab. Comparable secondary outcomes in both groups confirmed non-inferiority of the use of abatacept in the primary DMARDs failures.

Most recent NICE (National Institute of Health and Care Excellence) technology appraisal guidance [TA375] from January 2016 allow the use of abatacept in patients with severe RA who have failed treatment with a combination of DMARDs, providing this therapy is not more costly than other available choices.

1.3.1.3.1 Targeting IL-17 and IL-12/23 axis

A broad spectrum of pro-inflammatory and bone remodelling effects are exhibited by IL-17. Higher presence in synovial fluid, association with disease activity and reduced response to treatments comprised the clinical potential of IL-17 targeting in RA [97,131]. Several human monoclonal antibodies were developed. Secukinumab and Ixekizumab are both targeting IL-17A cytokine, while Brodalumab is directed towards its receptor - IL-17RA.

Although showing safety and modest efficacy at phase II clinical trials, large, multicentre placebo controlled phase III trial of Secukinumab in previous non-responders to anti-TNF treatment were terminated due to the lack of effect and insignificant amount of patients achieving ACR 20 compared to placebo after 24 weeks of the study [132,133]. Similarly, trials with Ixekizumab and brodalumab have been withheld after phase II trials, due to the incomparable efficacy when compared to the TNFα inhibitors [134,135]. Instead, targeting of IL-17 pathway has proven significantly more beneficial in psoriasis and psoriatic arthritis [136].

Other approaches were taken with Ustekinumab, a monoclonal antibody inhibiting the p40 subunit of IL-12/IL-23 cytokines and affecting both T_H1 and T_H17 cells. Despite impressive results demonstrated in psoriasis and psoriatic arthritis, ustekinumab failed to achieve ACR20 response in more than 55% of patients in phase II dose range study after 28 weeks of treatment [137].

These findings indicate that although pathogenic, $T_H1/17$ cells are not cells with sufficient hierarchical dominance in RA. Improved outcomes with abatacept but failure of anti-IL-12 and anti-IL-17 treatments questions if abatacept works through inducing tolerance in broader spectrum of immune cells and if balance of T cell subsets is important for the resolution of chronicity. Additionally, inefficacy of full T cell depletion by earlier agents further supports the need for presence and balanced T cells. These data also point towards significant involvement of the innate immune system and, in particular, myeloid cells in RA inflammation.

1.3.2 B cells

Since the discovery of rheumatoid factor (RF), an auto-antibodies against Fc tail region of hosts own immunoglobulins, by Waaler in 1937, B cells were suspected to play a role in the pathogenesis of RA [138]. Low specificity of RF for RA and presence in other autoimmune diseases soon led to the change of hypothesis evolving around T cells and macrophages, which resulted in development of related therapies [139]. Clinical efficacy of B cell depletion therapies in mice and human inspired new research in the role of these cells, beyond autoantibody production [140-142].

B cells originate in the bone marrow from the common haematopoietic progenitor and display unique B cell receptor (BCR) [143]. Lengthy processes of bone marrow and spleen differentiation of B cells ensures that autoreactive clones are deleted, edited or rendered anergic during normal development as they migrate to secondary lymphoid organs [144]. Induction of tolerance requires multiple check points for the BCR but also involves AID (activation-induced cytidine deaminase enzyme) and serum BAFF (B-cell activating factor) levels [144]. Induction of central and peripheral tolerance is defective in RA, leading to accumulation of autoreactive mature naïve B cells [145]. Links between PTPN22 polymorphism and autoreactive B cells has been established, indicating that genetic or epigenetic changes in the bone marrow progenitors could be present in RA [144]. Constant replenishing of autoreactive B cells partially explains why treatment with cytokine neutralizing antibodies and regulation of peripheral inflammation is not a cure for RA [146].

Apart from autoreactivity, naïve B cells in RA are also more resistant to Fas-mediated apoptosis [147]. Systemic support for defective B cells is evident from increased levels of BAFF in the serum and the synovial fluid from RA patients [148]. Toll-like receptor (TLR) stimulation of myeloid cells, but also of resident synovial fibroblasts are main sources of BAFF survival signal in RA [149,150]. Independently, TLR signals can activate B cells and promote immunoglobulin (Ig) isotype switching in T cell independent manner outside of germinal centres (GCs) [151,152].

In RA pathogenesis, B cells are known for their autoantibody production, T cell activation and cytokine secretion. A large number of autoantibodies are detected in patients with RA, however RF and ACPA antibodies are the mainstay of the disease diagnosis. Although regularly utilized in the clinical setting, understanding how these antibodies come to be generated is considerably more difficult. It is believed that autoreactive recognition of self-IgG antibodies (generating RFs) occurs in a T cell independent way outside of GCs through self-antigen activation of intrinsic B cell TLRs [152,153]. Indeed, RFs are predominantly non-switched IgMs. In contrast, ACPA antibodies are believed to arise within the GCs upon encounter with autoreactive T cells, hence its strong association with HLA DR genes and amino acid replacement mutations [154,155]. Involvement of two pathogenic pathways partially explains the worse treatment prognosis in double seropositive patients [156].

Autoreactive, and, in particular, RF^+ B cells have a higher affinity for uptake and cross presentation of immune complexes and self-antigens to T cells, therefore serving as an autoreactive APCs [157,158]. This has also been demonstrated in severe combined immunodeficient (SCID) mice, where anti-CD20 treatment led to disappearance of tertiary follicles in transplanted inflamed synovial tissue [159]. Lastly, B cells are an important source of IL-6, IL-12, IL-23 and TNFα [160,161]. Synovial B cells produce RANKL and support osteoclastogenesis in the arthritic joints [161]. Most recently, $CD19^+$ cells were identified as an additional source of IL-17A, which has wide range of pro-inflammatory effects [162].

1.3.2.1 B cell targeted treatment

The rational behind the first use of B cell depletion therapy in RA was two fold: firstly, RF generating B cells were considered self sufficient and pathogenic, as they further promote autoreactivity through uptake of self-generated immunocomplexes; secondly, RF antibodies and immunocomplexes were shown to activate other cells and facilitate TNFα production [140]. The surface B cell marker CD20 was a suitable, if not ideal target for the purpose. CD20 is exclusively and highly expressed on pre- and mature B cells and is not found on stem cells, plasma cells or any other immune cells, allowing replenishment of B cell population after the removal of autoreactive clones [163-165]. Additional benefits were gained from the stability of this cell marker, since it is not cleaved

from the cell surface, internalised or solubilized at any point [166]. Anti-CD20 chimeric monoclonal antibody, Rituximab (RTX), was previously used for the treatment of non-Hodgkin's lymphoma and was available for testing in RA [167,168].

A first open label, proof of concept trial using B cell depletion therapy was conducted by Edwards and Cambridge and included only 5 patients with uncontrollable RA [140]. All subjects achieved ACR50 and 3 patients achieved ACR70 response after 6 months of treatment. More importantly, investigators witnessed stable levels of serum IgM and IgG antibodies (Ab) and replenishment of B cell populations after completion [140]. Following this, successful use of RTX in RA was demonstrated in the phase II dose ranging DANCER trial (Dose-Ranging Assessment: International Clinical Evaluation of Rituximab in RA) in biologic naïve patients receiving MTX and 2 doses of RTX [169]. Success of the trial was defined by ACR20 score, which was achieved by 55% in lower dose and by 54% in higher dose RTX groups after 24 weeks, meeting primary endpoint [169]. The phase III Randomized Evaluation of Long-Term Efficacy of RTX in RA (REFLEX) Trial was done in patients with active longstanding erosive RA who were inadequate responders to one or more anti-TNFα agents [170]. Here, the primary endpoint was met when significantly higher number of patients (51%) achieved ACR20 in treatment group when compared to 18% in placebo controls. More importantly, there was significant meaningful improvement in ACR response parameters, including fatigue, disability and quality of life scores, while safety profile remained satisfactory [170]. Detailed analysis of patients from REFLEX trial demonstrated sustained benefit in pain relief, functional disability and quality of life indices [171], as well as significant inhibition of radiographic progression of joint damage [172], which was sustained after 2 [173] and 5 years of follow up [174].

Many subsequent studies investigated immunological effects of RTX treatment. Synovial biopsy before and 4 weeks after RTX treatment showed significant decrease in the total number of B cells in the synovial tissue, but only in a part of the patients [175]. The ARISE trial (Assessment of Rituximab's immunomodulatory synovial effects) further clarified that RTX treatment leads to a decrease but not a full depletion of synovial B cells, unlike in the circulation of patients after 8 weeks of treatment [176]. Some authors suggested potential

gain from re-treatment with RTX at a later stage, however this remained controversial [177,178]. Additional use of RTX in combination with MTX and TNFα blocking agent in patients with active disease showed no clinical benefit from triple therapy, while safety profile was comparable to previously seen in MTX only combination during 24 weeks of the trial [179].

The Study Evaluating Rituximab's Efficacy in MTX iNadequate rEsponders (SERENE) was a phase III trial, randomly assigning patients with active disease to receive a course of RTX or placebo in addition to continuous use of MTX [180]. At 24 weeks, non-responders were permitted a second course of RTX or a switch to the active drug from the placebo group. Active treatment group has achieved primary outcome with ACR20 in >50% of patients compared to 23% in placebo group, after 24 and 48 weeks, proving benefit from first line RTX treatment in biologic naïve subjects [180]. McGonagle et al have reported that use RTX is a suitable option when TNFα treatment is inappropriate or unavailable [181]. Indeed, the ORBIT (The Optimal Management of patients with rheumatoid arthritis who Require Biologic Therapy) study recently demonstrated that rituximab is a non-inferior and more affordable first line biologic agent compared to available anti-TNFα options [182].-

Attempts at enhancing efficacy of RTX were made in the AUGUST III study (Atacicept for Reduction of Signs and Symptoms in Rheumatoid Arthritis Trial III) where it was combined with Atacicept, an antagonist of two B cell survival factors BlyS (B lymphocyte stimulator) and APRIL (a proliferation-inducing ligand) [183]. Unfortunately, this combinational treatment was not associated with clinical benefit. Alternative approach to targeting B cells with anti-BAFF agent Tabalumab were tested in the early clinical trials in patients with severe RA but were unsuccessful [184].

1.3.3 Fibroblasts

In RA, fibroblast like synoviocytes (FLS) exhibit some aggressive traits; they increase in number, are resistant to apoptosis and produce cytokines and chemokines, thus aiding chronicity of the inflammation. Interestingly, these cells retain their behavior after removal to in vitro culture, suggesting epigenetic imprinting of certain features [185,186]. If transplanted into SCID immunedeficient mice, FLS originating from RA synovium are capable of causing bone erosions and arthritis [187]. Additionally, RA FLS have a capacity to migrate and sustain inflammation in other joints, away from initial site [188].

Unaffected diarthrodial joints have a thin layer of synovial membrane responsible for the production of synovial fluid and balanced secretion of degrading and protecting enzymes, which are maintaining the extracellular matrix. Intimal lining layer consists of macrophage like synoviocytes (type A cells) and fibroblast like synoviocytes (FLS or type B cells). FLS produce vimentin, adhesion molecules and collagens as well as surface CD90 marker [189]. Additionally they display, CD55 molecule, an enzyme required for the hyaluronic acid synthesis [190]. More importantly, structure of synovial lining is governed by adhesion molecule Cadherin-11, which induces in vitro accumulation of FLS cells and regulates expression of pro-inflammatory cytokines, such as IL-6 by FLS [191,192]. It is possible that therapeutic targeting of Cadherin-11, and therefore FLS cells, could provide beneficial outcome in the treatment of RA [193]

In RA, FLS are implicated in initiation, chronicity and formation of the inflammatory pannus, as well as the destruction of the joint anatomy. Higher numbers of FLS and thickening of synovial membrane is caused by inhibited apoptosis and reduced turnover, rather than increased proliferation of the cells [194,195]. Resistance to apoptosis persists during in vitro cultures and seems independent from RA cytokine milieu [186]. During inflammation, FLS secrete multiple enzymes degrading extracellular matrix, such as matrix metalloproteinases 1 and 13 (MMP1 and MMP13) and cathepsin [196,197]. They further contribute to osteoclastogenesis and formation of bone erosions by secreting RANKL and Dickkopf-related protein 1 (DKK-1) [198,199]. Upon encounter with pro-inflammatory stimuli, such as TNFα, FLS secrete IL-6, IL-18

and GM-CSF [200]. They directly support the influx of new inflammatory cells by secreting migratory chemokine CCL2 and indirectly by promoting angiogenesis through vascular endothelial growth factor (VEGF) [201]. Lastly, RA FLS promote formation of tertiary germinal centers, attract T cells and promote B cell survival by secreting CXCL12 chemokine and BAFF [202].

As to causes leading to transformation of FLS cells, studies have looked at genetic and epigenetic changes. RA FLS were shown to have mutations of p53 apoptosis pathway, similar to the ones found in cancer cells [203,204]. Even if mutation have not existed before the occurrence of inflammation, TNFα stimulation of FLS leads to increased accumulation of mitochondrial DNA mutations [205]. Epigenetically, FLS were seen to have reduced global methylation and altered expression of miRs regulating proliferation and apoptosis, such as miR-124a, miR-203 [206-208].

Despite the central role of FLS cells in the pathogenesis of RA and connections to all aspects that promote and perpetuate chronicity of this disease, therapeutics, targeting these cells are only just emerging. Apremilast, a selective inhibitor of phosphodiesterase 4 (PDE4) was shown to inhibit the spontaneous production of TNFα by synovial FLS and is approved for the clinical use in psoriatic arthritis while currently undergoing clinical evaluation for the use in RA [209]. Also, a new class of Janus kinase (JAK) inhibitors are shown to have a direct effect on RA FLSs, as they inhibit TNF induced type I IFN signatures and break the autoreactive loop [210].

1.3.4 Myeloid cells

1.3.4.1 Monocytes

Monocytes are circulating cells that originate in the bone marrow from an erythromyeloid progenitors expressing c-Myb TF [211]. Two major subsets of circulating monocytes have been identified in mice, according to the expression of Ly6C, a membrane monocytic marker and CCR2 (C-C chemokine receptor type 2) [212]. The subsets include 'classical' Ly6C^{+}CCR2^{+} and alternative Ly6C^{low}CCR2^{-} cells [213]. Classical Ly6C^{+} cells are also termed inflammatory monocytes and are the most abundant population, which requires CCR2 expression in order to enter the circulation and produces inflammatory cytokines upon activation in a GM-CSF dependent manner [214-216]. Ly6C^{+} monocytes are required for the initiation of arthritis in murine models and they differentiate into classically activated macrophages to drive inflammation [213,217]. A number of studies have shown that Ly6C^{+} CCR2^{+} monocytes are responsible for the phenotype in collagen induced arthritis (CIA) in mice [218]. The second subset, Ly6C^{low} monocytes are significantly less prevalent in the circulation and they are believed to be patrolling the endothelium and maintaining vascular integrity [219].

Characterization of human monocytes led to the discovery of three distinctive subsets on the bases of CD14 (the TLR4 co-receptor) and CD16 (the FcγRIII receptor for IgG) expression: classical CD14+CD16- (resembling murine Ly6C^{+}CCR2^{+}), intermediate CD14+CD16+ and non-classical CD14^{low}CD16+ cells [220]. Data on both human and murine subsets are still sparse and any extrapolation should be done with caution, especially since species specific monocyte transcriptomes were defined [221]. Nonetheless, classical human monocytes, CD14+CD16-, comprise ~90% of circulatory monocytes and resemble inflammatory Ly6C^{+} CCR2^{+} murine cells [222]. The non-classical, CD14^{low}CD16+ are considered human endothelial patrolling cells, similar to Ly6C^{low}CCR2^{-} cells in mice. However, it is the intermediate CD14+CD16+ monocytes that proved to be of particular importance in autoimmune disease. This population is significantly expanded in the circulation and synovial fluid of patients with RA and is associated with active disease and poorer treatment response [223-226]. When derived from patients with RA, double positive cells express high levels of CCR1,

CCR5, ICAM-1 and pathogen receptor TLR2 [227,228]. Stimulation of membrane CD16 molecule with specific immune complexes results in TNFα release, suggesting that CD16 expression is pathogenic as well as a marker for inflammatory monocytes [228-230]. Expansion of this intermediate population of monocytes could be explained by activation and increased proliferation of existing cells and/or newly triggered co-expression of CD16 upon activation of classical monocytes. Indeed, CD16 expression was induced in experimental treatment of healthy monocytes with RA synovial fluid or TGFβ [231].

1.3.4.1.1 Tissue migration of monocytes

In order to migrate from the bone marrow, monocytes require the expression of CCR2 chemokine receptor. Two ligands are capable of binding to this receptor and both are required to guide monocytes into inflamed or infected tissues. These ligands are CC-chemokine ligand 2 (CCL2 or MCP1) and CCL7 (MCP3) [232]. Almost all nucleated cells are capable of expressing CCL2 upon stimulation with inflammatory cytokines [232-235]. It is believed that CCL2 is also circulating in the lymph and responsible for attracting patrolling monocytes to the lymph nodes in a gradient dependant manner [236,237]. Deletion of either of these two chemokine genes in mice decreases monocyte recruitment by ~50% [238]. Other ligands, such as CCL8 and CCL12, have an affinity for CCR2 receptor, still deletion of these genes had no significant impact on monocyte trafficking [232].

Monocyte recruitment is thought to occur through stages of rolling, adhesion and endothelial transmigration. These actions are enabled by a series of integrins and other adhesion molecules, as well as non-redundant chemokines CCL3 and CCL5, which ligate CCR1 and CCR5 receptors on the cell surface of monocytes and aid transendothelial chemotaxis towards the higher gradient of CCL5 expression in the tissues [239-241]. Upon tissue entry, monocytes are capable of differentiating into macrophages or inflammatory dendritic cells, still they can also remain as monocytes, upregulate MHC class II genes, acquire antigens and carry them to the lymph nodes [242].

1.3.4.2 Macrophages

Migrated monocytes, exposed to certain stimuli upregulate macrophage-associated genes and differentiate into macrophages [243]. During this period

cells are capable of expressing proliferation-associated genes, yet it is not entirely clear whether proliferation of human inflammatory macrophages occurs [244]. Almost all mononuclear phagocytes and resident macrophages rely on macrophage colony stimulating factor (M-CSF) as the main lineage regulator and driver of differentiation. M-CSF 1 receptor (CSF1R) is expressed on the majority, if not all macrophages and some types of dendritic cells [245]. Csf1r-null mice have taught us that in murine development this receptor is unique, while the role of the ligand is split between M-CSF in bone marrow, spleen or liver macrophages and IL-34 for the more primitive, tissue resident macrophages in brain microglia or skin Langerghans cells [246,247]. Apart from M-CSF, other growth factors like IL-3 and VEGFA can promote development of macrophages in tissue culture. Mice lacking IL-3 and GM-CSF show impaired function of alveolar macrophages, while VEGFA is thought to promote osteoclast development *in vivo* [248-250]. While M-CSF is constitutively expressed to regulate macrophage numbers through negative feedback loop, GM-CSF is produced upon challenge [251] [216]. Despite this, blockade of M-CSF was not successful in RA clinical trials, while GM-CSF shows promising outcomes and will be discussed separately [252].

Diversity of macrophage phenotypes likely stems from diversity of transcriptional regulation, whether it is the regulation of haematopoietic progenitors by c-myb, or crucial myeloid lineage commitment defined by PU.1 [253]. Nevertheless, research in this area has been somewhat limited to the exploration of PU.1 as the most important of these transcription factors since its mutation leads to complete depletion of murine macrophages [253]. Other identified factors, like Gata2 were found crucial for monocyte development but had no role in tissue resident macrophages [254]. Its effects are so profound that a Gata2 SNP is at the heart of several human syndromes evolving around severe monocytopenia. The roles of CEBPα and RUNX1 transcription factors and PU.1 enhancers were recently described [255]. However, it is the role of transcription factor Ets2 to directly target and initiate transcription of CSF1R allowing response to M-CSF [256]. During inflammation, differentiation and activation of cells coincides in the same process, guided by the surrounding milieu of cytokines and growth factors.

1.3.4.2.1 Polarization of macrophages

Many reports have advocated a broad classification of activated macrophages in to two main groups – classically activated with IFNγ and/or LPS (M1) and alternatively activated with IL-4 (M2) [257] [258] [259]. This view of macrophage activation through principle cytokines allowed association of M1/M2 with Th1 and Th2 cells promotion, therefore pointing towards M1 involvement in bacterial defence and antigen presentation with high levels of class II MHC, while M2 are typically relevant in parasitic infections, respiratory and tumour immunity [38]. These differences are reflected in the transcription processes where STAT1 and IRF5 collaborate to promote M1 phenotype, while STAT6 and IRF4 drive to M2 polarisations [38]. The crude nature of M1 and M2 nomenclature runs into difficulty when we consider other important stimuli, such as length and chronicity of activation and exposure to multiple potentially contradictory events. Recently revised nomenclature has called for more detailed description of laboratory generated macrophages in order to promote clear understanding of the cell phenotype as well as to encourage reproducibility of results [260]. Implementation of these guidelines should also ensure understanding of a spectrum of activated macrophages instead of previously binary categorization of M1/M2 type cells. Certainly, single cell analysis would indicate that every individual macrophage has unique gene signature in order to challenge that pathogen in its own unique way [261]. Gaps in our understanding are further deepened by comparison between mouse and human activated macrophages [262].

Nevertheless, several functional properties distinguish these two macrophage phenotypes. M1 polarized macrophages typically express high levels of IL-12, IL-23 and TNFα, chemokines CXCL9 and CXCL10 and miR-155, while M2 cells are known for high IL-10 expression, CCL17 and CCL22 and miR-223 [260,263,264]. It is still unclear what phenotype is prevalent in the arthritic joint, yet high levels of TNFα and IL-1, typically released by M1 macrophages are abundant in RA, while IL-10 expression is relatively low [265].

1.3.4.2.2 The role of macrophages in RA

The role of macrophages is broad. They are involved in early stages of development, maintenance of homeostasis, tissue repair and immune protection from the invading pathogens. Homeostasis is achieved by 'patrolling' tissues on several levels [266]. Firstly, tissue derived macrophages are resident cells responsible for engulfing apoptotic cells, debris clearance and tissue growth support. As such, they appear to have homeostatic properties and act predominantly in an anti-inflammatory manner to achieve that role. Recent investigations of murine parabiosis models indicated that tissue resident macrophages replenish from their tissue progenitor and do not require blood-derived monocytes [266]. In fact they are likely never to go through a monocyte stage in their development, contrary to popular belief. Secondly, they play a role in patrolling for acute invasion by intracellular or extracellular pathogens, which is achieved by monocytes and blood derived macrophages present in organs that are turned outwards – like gut mucosal layer or skin [266]. Difficulty thereof lies in the understanding of the cross talk between newly recruited inflammatory macrophages and resident regulatory cells, especially in chronic conditions like cancer, obesity or in outright inflammatory conditions like RA.

In RA, monocytes and macrophages are one of the main drivers of cytokine production and inflammation [257]. In synovial tissue from RA patients, significantly raised numbers of both inflammatory monocytes and activated macrophages were found [267,268]. Synovial tissue myeloid cells are the principle source of TNFα and IL-6 cytokines [269-271]. Reciprocally, anti-TNF treatment leads to depletion of the total number of synovial myeloid cells and in some cases resolution of inflammation [272,273].

As main cytokine producers, monocytes and differentiated macrophages promote differentiation of T cells [274]. Monocyte to T cell contact is involved in the destruction of cartilage and bone destruction [275]. In fact, deregulated cross talk between T cells and monocytes has substantial implications for perpetuation of chronic inflammation in RA [276,277]. Macrophage accumulation in the synovium is clearly a determinant of the outcome of RA, and probably a useful disease biomarker, although not a practical one [265].

Several proposals for targeting myeloid cells have been made. Unfortunately, targeting of chemokine pathways, such as CCR2, did not show efficacy in reducing synovial inflammation [278]. Furthermore, depletion of tissue resident MHC class II^+ macrophages in serum transfer murine arthritis model had also no effect on the course of disease, while depletion of both circulating and tissue resident cells led to resolution [213]. On the other hand, depleting CD64 expressing synovial macrophages caused an improvement of adjuvant induced arthritis in rats [279]. Immunotoxin targeting of CD64 is was considered for clinical use [280].

A new era of repositioning of the already existing medicines led to re-thinking of the use of FDA approved therapeutic trabectedin, which induces apoptosis of mononuclear phagocytes and is used for the treatment of liposarcoma and leiomyosarcoma [281]. Such treatments could be useful as a myeloid depletion with a possibility of re-setting the way that myeloid cells respond to future insults and should be tested for this purpose [218].

1.3.4.3 Dendritic cells

Historically, dendritic cells (DCs) are known as the main antigen presenting cells (APCs) for their ability to sample surrounding self and foreign antigens and present them to T and B cells. Now it is clearly understood that DCs directly instruct adaptive immune cells towards specific inflammatory or regulatory responses. DCs are a heterogeneous population of cells that includes several distinct phenotypes, summarised in the Table 1.3.

Name	Surface markers	Originate from	Main function
Plasmacytoid DCs (pDCs)	CD123, CD303, CD304, CD11b and CD11c	BM progenitor cells	Major source of type I interferons.
Classical CD141$^+$ DCs	CD141, CD11c^{low}	BM progenitor cells	Preferentially Induce T_H2 phenotype.
Classical CD1c$^+$ DCs	CD1c, CD11b, CD11c, CD172	BM progenitor cells	Preferentially Induce T_H1 phenotype.
Inflammatory DCs (iDCs)	CD1c, CD11b, CD11c, CD1a, CD14, HLA-DR, FcεR1, CD206, CD172a	Blood derived monocytes	Preferentially Induce T_{eff} phenotype.

Table 1.3 Main DCs subsets.
References: pDCs –**[282,283]**; CD141$^+$ DCs –**[283-285]**; CD1c$^+$ DCs –**[286,287]**; iDCs –**[283,288]**.

Predominantly, DCs originate from BM derived progenitor cells, with the exception of inflammatory DCs (iDCs), which are recruited from the circulating blood monocytes and mature at the site of inflammation (Table 1.3). Inflammatory DCs were found in the experimental models of arthritis, as well as in the synovial fluid from RA patients [102,288-290].

During inflammation, monocytes and immature DCs express CXCR1 and CX3CR1 chemokine receptors and are attracted by inflammatory homing chemokines such as CCL1, CCL2, CCL5 and CCL6 [291]. More recent data suggest that TNFα

and IFNγ activated FLS can also guide DC migration through the expression of the adipokine chemerin [292-294]. Once in the tissue, there are two main ways to ensure DC activation. Primarily, DCs recognise pathogen associated molecular patterns (PAMPs) through TLRs, C-type lectin receptors, NOD-like receptors (nucleotide oligomerization domain) and RIG-I-like (retinoic acid-inducible genes) receptors [295]. Alternatively, endogenous activating signals can become available during necrosis of damaged and inflamed tissues. There are many candidates for the role of DAMPs: heat shock proteins, HMGB1 (high mobility group box 1), extracellular matrix proteins like hyaluronic acid and metabolites such as uric acid, all detected in the RA synovium [296].

Activation and maturation of DCs results in the upregulation of class I and II MHC molecules and CD40, CD80 and CD86 T cell co-stimulatory factors. Increased expression of CCR7 chemokine receptor is associated with CCL19 and CCL21 guided homing to secondary lymphoid organs or to ectopic lymphoid structures in the RA synovium [297,298]. This allows formation of tertiary germinal centres in the inflamed synovial tissue, detected in almost half of RA patients [299,300]. It is suspected that the presence of homing markers causes accumulation of iDCs and reduced efflux from RA affected tissues [297,298,301]. High numbers of synovial iDCs certainly contribute to disease chronicity.

The main function of activated DCs is to instruct adaptive immune cells. Although some specificity is suggested in Table 1.3, classical $CD141^+$ and $CD1_c^+$ DCs are capable of antigen cross-presentation and induction of all T_H subtypes depending on the surrounding stimuli [284,302,303]. On the contrary, pDCs are less efficient at T cell priming and contribute more to the induction of tolerogenic T_{reg} cells [304]. Both cDCs and pDCs are decreased in the peripheral blood and increased in the synovial fluid from patients with RA [305]. On the other hand, iDCs are particularly effective in the generation of T_H1, T_H17 and T_{reg} cells through secretion of polarizing cytokines (IL-12, IL-23 and IL-10, respectively) [288]. Expression of surface proteins such as OX40 ligand (TNF ligand superfamily 4) could result in T_H2 polarization [306]. In RA synovium however, mature iDCs predominantly secrete IL-12 and IL-23 cytokines, causing the imbalance between T_H1/T_H17 and T_{reg} cells [288,297,305,307,308]. In fact, purified synovial fluid iDCs induce T_H17 polarisation in previously naïve CD4 T cells [288]. The resulting high levels of IL-17A and GM-CSF are extremely

inflammatory within the synovial tissue, as evident from the growing body of reports and successful clinical targeting of IL-17A cytokine, which will be discussed below [309-311].

pDCs are also present in RA synovium, particularly in patients with raised ACPA antibody titres [307]. As stated previously, pDCs are predominantly tolerogenic under normal conditions. During inflammation, pDCs are a major source of type I interferons to guide monocyte differentiation and of soluble BAFF and April molecules, serving as B cell survival signals [312]. It is therefore suspected that pDCs contribute to the formation of synovial germinal centres and induction of autoreactive B cells [312]. Additionally, type I interferons promote antibody production and isotype switching in activated B cells [313].

Summarizing data above, it is easily appreciated that there have been attempts at utilizing tolerogenic DCs in the therapy of autoimmune conditions. This was supported by the immunomodulaory effect of transferred DCs in animal models of arthritis [314,315]. In humans, a phase I clinical trial was recently completed. Here, 18 patients with RA received subcutaneous transfer of autologous DCs treated with NFκB inhibitor and citrulinated peptide antigens [316]. Treatment resulted in reduction of effector and increase in regulatory T cells, as well as some clinical improvement after 1 month of treatment [316]. A second trial of this sort utilized steroid and vitamin D3 treated DCs, which were subsequently activated by TLR4 and autologous synovial fluid before intraarticular transfer [317]. Results of the latter trial are still awaited. Apart from the cellular therapy, existing and newly developed cytokine targeting agents can also significantly influence the function of iDCs and will be discussed in the section below.

1.3.4.4 Osteobiology

Osteobiology is at the centre of RA pathogenesis with bone erosions as a main disabling feature of untreated arthritis. The human skeleton is composed of trabecular bone enclosing the bone marrow and cortical bone providing the structural support. Both types of bone are prone to erosions in RA and occur as early as 6 months after disease onset in a half of untreated patients [318]. Additionally, the risks of generalised osteopenia and osteoporosis are independently increased in RA.

Bone erosion is a radiological term. This feature is visible on the plain radiograph as a break in the cortical bone surface, and it should not be confused with bone cysts typically found inside of the trabecular bone. Radiographic bone erosions are included in the diagnostic criteria for RA and are used for treatment and monitoring purposes. Moreover, all currently used antirheumatic agents were shown to prevent structural joint damage during clinical trials.

Osteobiology has seen increasing advancements in understanding the function of bone making osteoblast and bone eroding osteoclast cells. Osteoclasts are giant multinucleated cells derived from the monocyte lineage and are the only cells capable of bone absorption [319]. They form tight junctions with the surface of the bone along the entire perimeter of the cells in a way that secreted acidic components are sealed and dissolve the calcium from the bone below. Osteoclasts also secrete matrix enzymes like cathepsin K and matrix metalloproteinases (MMPs) to degrade residual bone matrix [320].

Osteoclastogenesis occurs from blood derived monocytes and is mediated by M-CSF and RANKL (receptor activator of nuclear factor kB ligand) [321-323]. It is now known that monocytes can be pre-primed for osteoclast differentiation by TNF exposure, which leads to surface expression of osteoclast-associated immunoglobulin-like receptors [324]. TLR stimulation of the synovial cells induces RANKL expression and further aids osteoclastogenesis [325]. Similar effects are achieved by synovial pro-inflammatory cytokines like TNF, IL-1, IL-6 and IL-17, which trigger and work together with RANKL expression [90,326,327]. Final differentiation into osteoclasts occurs upon contact with bone.

In RA, presence of autoimmune antibodies is the strongest prognostic factor of erosive process, more so than any other measure of inflammation [328]. One study suggests that ACPA antibodies bind to citrulinated vimentin on the surface of differentiating cells and promote maturation of osteoclasts [329]. These cells also express PADI2 (peptidyl-arginine deaminize type 2) enzyme that is dependent on the calcium flux to induce protein citrullination, likely utilised in protein breakdown during bone resorption [329].

Blockade of differentiating molecules M-CSF, RANKL, or both prevents bone erosion in all tested animal models of experimental arthritis [330-332]. Attempts were made to utilise this in the clinical setting with denosumab, an antibody against RANKL [333]. Phase II dose finding clinical trial has shown that use of denosumab slowed the progression of the erosions but it did not influence the inflammation [333]. This suggests that there is no positive feedback loop in which synovial inflammation is perpetuated by the underlying bone pathology. In contrast, inhibition of TNFα or IL-6 cytokines are amongst the most effective approaches to control the inflammation, slow erosive process and systemic bone loss [334].

Less successful was the search for agents capable of repairing already existing bone damage and at present erosions are considered irreversible. It is not due to the lack of osteoblasts, as they are seen to repopulate the surface of the eroded bone upon resolution of the inflammation in animal arthritis models [335]. Wnt signalling is crucial for the function of osteoblasts [336]. It is suspected that Wnt signalling and bone formation pathways are permanently suppressed during inflammation by Dkk-1 and sclerostin, as examples [335-337]. This is a developing topic that requires further testing, hopefully resulting in new bone supporting therapeutics.

1.3.4.5 Neutrophils

The contribution of neutrophils to pathogenesis of RA is somewhat less explored than other leukocytes, despite their abundance in the circulation and in synovial fluid [338]. Indeed, neutrophils constitute 60% of all leucocytes in the circulation and are attracted to synovium by L-selectins, granulocyte and macrophage colony stimulating factors (G-CSF, GM-CSF, M-CSF) and cytokines such as IFNγ and IL-17A [339-341]. Inflammatory neutrophils exhibit similar function to activated macrophages and even dendritic cells, by expressing a variety of cytokines, including membrane bound TNFα and RANKL to promote osteoclastogenesis and BLyS and BAFF B cell survival factors [342,343]. Activated neutrophils are also a major source of IL-6 [344].

By upregulating MHC class II molecules, neutrophils are capable of cross presenting antigens to T cells [345]. This ability to act as an APC might be more relevant to RA pathology, than initially assumed. Citrullination of proteins is one of the strategies of neutrophils to modify and disarm foreign peptides. In the context of RA, this leads to the accumulation of hypercitrullinated proteins in synovial fluid neutrophils, which are a potential source of anti-ACPA antibodies [346].

The synovial inflammatory environment promotes neutrophil survival through key proteins, such as MCL-1 (myeloid cell leukemia sequence 1) [347]. During their short life span, neutrophils contribute to perpetuation of inflammation, but also directly contribute to bone and cartilage damage through the release of reactive oxygen species and specific enzymes [348]. In fact, a majority of current treatments for RA were shown to aid the onset of apoptosis in activated neutrophils and prevent further joint damage [349].

In 2004, a new way by which neutrophils trap extracellular pathogens was described [350]. Namely, instead of apoptosis, neutrophil death results in release of their chromatin and formation of neutrophil extracellular traps or NETs [350]. At the same time, granules with enzymes are released which help to capture and kill bacteria. This novel process was implicated in the break of self-tolerance in autoimmune diseases, especially in SLE, which is associated with appearance of anti-nuclear and anti-DNA antibodies [351]. In RA, synovial fluid

neutrophils are thought to be a/the source of citrullinated peptides [346]. With enhanced NETosis, it is possible that this is a source of antigen for the formation of ACPA antibodies [352].

1.3.5 Cytokine targeted treatments in RA

1.3.5.1 Targeting TNFα

TNFα is one of the true master regulators of the RA pathogenesis [139]. It is believed to be at the top of the RA cytokine hierarchy as it is capable of inducing a complicated cascade of inflammatory mediators, including IL-1, IL-6, IL-8, GM-CSF as well as directly influencing angiogenesis, pain, cell migration and joint damage [353]. TNFα is predominantly produced by myeloid cells and is classified as an innate immune cytokine [218]. Although all of these effects were not obvious in the late 1980's and early 1990's when it was discovered, TNFα inhibition ameliorated arthritis in CIA murine model and led to development of truly transformative treatments for RA [354]. In fact, the idea that inhibition of a single cytokine could give such clinical improvement was somewhat revolutionary at the time and changed the way RA pathogenesis was viewed [355].

Since than, 5 anti-TNFα agents have been approved and widely used in clinical practice: infliximab, adalimumab, golimumab and certolizumab pegol are monoclonal human antibodies towards the cytokine while etanercept is a circulating receptor fusion protein [356-361]. Although very efficacious on their own, the full potential of anti-TNF agents was discovered when a combination treatment with MTX resulted in a marked long term radiographic benefit [362,363]. Expected outcomes from this mode of treatment is for 60-70% of patients to achieve ACR20 score, while ACR50 and ACR70 are met by ~40% and ~20%, respectively. The percentage of primary non responders varies but is approximately ~30%, comprising a persistent unmet clinical need [355]. Clinical use of TNFα inhibitors is now enriched by the variety of biosimilar molecules, which are expected to make this treatment option more affordable.

Over last 20 years, the combination of basic and clinical research revealed the full scope of benefits from the anti-TNFα treatment. TNFα inhibition leads to a rapid decrease in serum IL-6 levels, followed by reduced numbers of synovial neutrophils, adhesion molecules and chemokines, inhibiting overall recruitment to the synovium [364,365]. Also, reduced expression of VEGF and decreased rates of angiogenesis are noted [366]. Rapid normalization of systemic

inflammatory features such as anaemia and high platelet count extends further to improvement in fatigue, depression, metabolism and insulin resistance in treated patients over time [193,355]. On the cellular level, anti-TNFα treatment leads to abolished numbers of synovial T cells, B cells and inflammatory macrophages, while activating and promoting proliferation of T_{REG} cells [353]. This effect appeared specific to agents targeting cytokine and binding both membrane and soluble forms, rather than to etanercept which captures only soluble TNF. This observed contradiction was explained by the hypothesis that anti-inflammatory role of anti-TNF treatment is mediated by blocking of TNFR1 while T_{REG} activation is, in fact, possible through binding and activation of TNFR2, which is predominantly expressed on the surface of regulatory cells [353]. Indeed, it is accepted that adalimumab, for example, has a superior efficacy compared to etanercept in a range of autoimmune conditions [367]. Additionally, this finding reiterates the importance of immunological balance in restoration of health in patients with RA. Lastly, long-term data on the efficacy of TNFα agents show a distinctive percentage of people maintaining good clinical outcome years after it was initiated, indicating that RA pathogenesis, once established, might be very stable and early stratification of patients is of utmost importance [355].

1.3.5.2 Targeting IL-1

IL-1 and its family of cytokines, including IL-1a, IL-1b, IL-1Ra, IL-18, IL-33 and IL-36, are highly detectable in RA synovial inflammation [368]. It is believed that IL-1 expression is triggering formation of bone erosions in RA synovium [369]. Animal models of inflammatory arthritis have shown that IL-1 mediates cartilage and bone loss during inflammation [370,371]. Even though blockade of IL-1 is not sufficient to contain the inflammation during active RA it provides protection from occurrence of bone erosions [372]. Despite lack of efficacy in RA, IL-1 directed treatment is considered in other inflammatory disease associated with bone deformities such as gout and broader inflammatory conditions, such as juvenile idiopathic arthritis, where benefits are substantial [129,368].

1.3.5.3 Targeting IL-6

IL-6 is another pleotropic cytokine displaying a wide variety of inflammatory but also hormone-like traits [373]. IL-6 was initially discovered as a cytokine promoting T cell (T_H17) and B cell differentiation, while regulating an acute-phase response [374,375]. More recently, new functions were discovered, were IL-6 plays a role in atherosclerosis, lipid metabolism, insulin resistance, mitochondrial metabolism and depression [376-379]. Additionally, transgenic expression of IL-6 in mouse strains led to neurological disorders when cytokine was overexpressed in the brain and pulmonary fibrosis with hypertension when IL-6 was overexpressed in the lungs. Deficiency of IL-6, on the other hand, leads to impaired immune responses to viral, bacterial or parasitic infections, confirming its importance [380]. Some of these functions are very similar to those of TNFα, hence the overlap between these pathways in research and clinical data.

IL-6 cytokine is almost undetectable during homeostasis with rapid increase in its expression during infection, autoimmunity or cancer where it can be used as a better disease activity biomarker than corresponding CRP levels [381,382]. Its receptor (IL-6R) is expressed by leukocytes, megakaryocytes and hepatocytes, yet broad spectrum of IL-6 effects stretches far beyond immune cells by the virtue of trans signalling, where soluble IL-6 and IL-6R form a functional complex which then signals through the membrane bound receptor subunit GP130 (CD130, IL6ST) [383-385]. GP130 is a ubiquitously expressed cytokine receptor shared between IL-6, IL-11, IL-27, oncostatin-M, ciliary neutrotrophic factor, cardiotrophin-1, cardiotropin-like cytokine and leukemia inhibitory factor, all of which belong to type I family of cytokines [386,387]. While deletion of GP130 in murine models leads to embryonic death, mice lacking IL-6 or IL-6R are fully viable and show impairment in defence against infections, wound healing and glucose metabolism [388,389]. Both classical or alternative (trans-) signalling require the formation of IL-6-IL-6R-GP130 complex, where IL-6R is membrane bound or soluble, respectively [390]. When fully formed, IL-6 membrane complex can utilise Ras and Raf signalling effector pathways to control proliferation or differentiation of the cells, although its proinflammatory effects are predominantly mediated by the engagement of Jak tyrosine kinase family (Jak1, Jak2 and Tyk2) that leads to phosphorylation of STAT1, STAT3 and, less

so, of STAT5 [390]. SOCS (suppressors of cytokine signalling), CIS (cytokine inducible SH2 domain containing) inhibitors of cytokine receptors and PIAS (inhibitors of activated STATs) tightly control this signalling pathway [390]. From these, SOCS3 has been recognized as a major regulator of IL-6 signalling [391].

It is believed that classical IL-6 signalling is responsible for haematopoiesis and induction of acute immune response including hyperthermia, while also regulating glucose metabolism, fatigue and loss of appetite [392]. On the contrary, the IL-6 trans signalling is implicated in perpetuating chronic inflammation by the recruitment of leucocytes, activation of effector T cells, proliferation of B cells, survival of plasma cells and involvement of stromal resident cells, like FLS [373]. During inflammation, soluble IL-6R is expressed by activated monocytes and T cells and serves as an alarmin, creating an inflammatory milieu at the site of infection [393,394]. Alternatively, multiple inflammatory mediators, including CRP can induce shedding of the surface IL-6R [395,396]. Additionally, IL-6R can be cleaved from the surface of the cell by aminopeptidases such as ERAP-1 (endoplasmic reticulum aminopeptidase 1, or ARTS-1) and adamolysin proteases such as ADAM10 or ADAM17, also responsible for shedding of TNFR1 [397,398]. Shedding is not the only mechanism that creates a soluble IL-6R, since a distinct transcript lacking the exon of the membrane domain is also expressed and will be discussed in details in chapter 6.

In RA, the IL-6 pathway exhibits a multitude of effects on both innate and adaptive cells. By inhibiting CXCL1, CXCL8 (IL-8) and CX3CL1 chemokines and upregulating expression of CXCL5, CXCL6, CCL2 and CCL8 as well as adhesion molecules ICAM-1 and VCAM-1, IL-6 attracts migration of neutrophils, which in turn promote the shedding of membrane IL-6R and amplify the immune response [399,400]. In myeloid cells, IL-6 regulates the expression of CSF1R to promote differentiation of recruited monocytes into macrophages at the expense of DCs [401,402]. In joint resident FLS cells, IL-6 induces expression of RANKL, MMP1, 3 and 13 to promote osteoclastogenesis and sustain bone resorption [403].

Despite considerable effects on innate cells, IL-6 is still considered to be a link, coordinating T cell and B cell activity, through promotion of follicular T helper cells in the immunological synapse [404]. This was confirmed by the lack of humoral response in IL-$6^{-/-}$ mice immunized with a T cell-dependant antigen

[380]. In models of arthritis, IL-6 deficiency leads to reduced numbers of T_H17 cells and IL-17 cytokine [405]. Its effects on T cell extends further with IL-6 inhibition leading to increased functionality of T_{REG} cells in mice models and human subjects with arthritis [405]. In the absence of IL-6, ever-present TGFβ supports differentiation of T_{REG} cells, while the combination of TGFβ and IL-6 are required for the induction of RORC TF and T_H17 differentiation. Resulting expression of IL-17 has a multitude of inflammatory roles, including B cell differentiation and class-switching, that are discussed above. This provides a mechanism by which, therapeutic targeting of IL-6 causes functional modulation of inflammatory T and B cells, while supporting development of regulatory cells [406].

Nonetheless, the role of IL-6 is not at all straightforward. A recent investigation of T cell plasticity has identified cells, which upon IL-6 stimulation co-express FoxP3, T bet and RORγt, although it is not yet clear if this occurs during synovial inflammation [407]. The anti-inflammatory role of IL-6 was also seen in circumstance when it promotes IL-10 production by T cells [408,409]. Moreover, inhibition of SOCS3 regulator allowed IL-6 to behave in a manner similar to IL-10 and aid the resolution of the inflammation [391,410]. This might be the mechanism by which IL-6 promotes polarization of M2 macrophages associated with wound healing and termination of inflammatory processes [389,410].

Association of IL-6 biology with RA was also confirmed when GWAS studies identified SNP close to the transcriptional start site of IL-6 causing overexpression of the cytokine leading to increased risk of coronary artery disease, idiopathic juvenile arthritis and other arthropathies [411-413].

1.3.5.3.1 IL-6 targeted treatment of RA

This abundance of experimental data resulted in development of IL-6 targeting treatments. It was known from earlier cancer trials that targeting of the IL-6 cytokine leads to its compensatory overexpression and, to overcome this issue, new therapies, directed towards IL-6R were developed [414,415]. Tocilizumab (TCZ), an anti-IL-6R agent was tested for its use in RA. The first large phase II 'CHARISMA' trial (the Chugai Humanized Anti-Human Recombinant Interleukin-6 Monoclonal Antibody) involved 359 patients with active RA and poor response to

MTX treatment [416]. This was a dose ranging, placebo controlled study that included option of combination treatment with MTX. Primary endpoint, an ACR20 improvement after 16 weeks, was met by 63% of patients on higher dose of TCZ treatment alone, compared to 74% in combination group and 41% in methotrexate with placebo group [416]. This study clearly demonstrated the direct effect of IL-6 inhibition on the generation of acute response parameters, CRP and ESR, as well as hepatic transaminases, total cholesterol, triglycerides, high-density lipoprotein levels and total neutrophil count. Rapid normalization of CRP and ESR parameters, independently from disease activity was later recognized as a confounding factor for the use of disease activity scores that incorporate these measures in evaluating IL-6 blocking therapeutics.

A further phase III clinical trial TOWARD (Tocilizumab in Combination With Traditional DMARD Therapy) has confirmed benefits of addition of TCZ treatment to a range of individual DMARDs or triple DMARD therapy with ACR 20 response ranging from 57.7-65.7% in all combination groups, apart from treatment with TCZ and Azathioprine where response was 33.3% [417]. True clinical benefit was reflected in improved quality of life index score (SF-36), disability index (HAQ) and fatigue score (FACIT-F), while the overall incidence of adverse events was also higher in the TCZ treated group, consistent with previously seen [417]. Subsequent trials have shown that combination treatment with TCZ and MTX prevents structural joint damage and reduces systemic bone resorption as well as secretion of bone degrading mediators [418,419].

The most interesting are studies directly comparing TCZ with other modes of biologic treatment. One such example is the ADACTA study comparing tocilizumab with adalimumab monotherapy in 326 patients with severe RA, poorly controlled with MTX over 6 months or longer and who cannot tolerate further DMARD treatment [420]. This study showed superiority of TCZ compared to the anti-TNFα agent, yet the primary clinical endpoint was measured by the mean change in DAS score, which is partially confounded by the inclusion of CRP and ESR measures. Nevertheless, this study allowed direct comparison of serum and synovial samples for the identification of therapy specific signatures in a search for predictive biomarkers [421]. A synovial gene expression signature allowed identification of lymphoid, myeloid, low inflammatory and fibroid synovial phenotypes. Furthermore, serum samples from myeloid type had higher

expression of soluble ICAM1 and low levels of CXCL13 chemokine, associated with a good response from anti-TNFα treatment; while lymphoid type had opposite low serum levels of sICAM1 and raised CXCL13 expression and responded well to TCZ treatment [421]. These results support the broad division between innate control of TNF and adaptive effects of IL-6.

Summaries of previous data resulted in several conclusions about the clinical use of TCZ. Firstly, network meta-analysis suggested similar efficacy of TCZ with MTX combination to that of other biologics with MTX [422]. Secondly, monotherapy of TCZ is superior to monotherapy of anti-TNFα agent, as evidenced above [420,422]. These conclusions were behind the design of the recent U-Act-Early strategy trial recruiting 317 patients with very early (median symptom duration of 25 days) active RA (median DAS28 score was >5.0 for all groups), who were blindly randomized to receive combination of TCZ with MTX, or either agent alone for 2 years [423]. More importantly, primary outcome of this study was sustained clinical remission, which was attained by 86% of patients receiving combination treatment, compared to 84% in the TCZ only arm and 44% in the MTX only arm. These data are impressive since stricter definition of DAS28 remission based on score of <2.6 but also 4 or fewer swollen joints was used. A placebo group was deemed unethical and was not included. Design of this trial did not allow the comparison between medications, but only between treatment strategies, as patients with poorly controlled disease on MTX only treatment received TCZ at a later stage. Interestingly, a treat to target approach resulted in similar rates of achieved remission despite TCZ first or MTX first approaches. This study, although not truly generalizable, indicated that early treatment with effective and quick acting treatments such as TCZ can be beneficial in early induction of remission, in keeping with the early window of treatment opportunity hypothesis [424]. The authors speculate that tapering of TCZ does also work, and maintenance of remission on MTX only would be possible, increasing the cost-effectiveness of this approach. However, long term data on efficacy, dropout rates and radiographic progression will be available after an additional 3-year follow-up is complete in due course. Certainly, if these results are confirmed in other larger and multinational trials, this could provide a precedent for the change of current guidelines, which call for DMARDs first treatment approach, and place IL-6 targeting at the center of management

of RA and its most common co-morbidities. Additionally, direct comparison of TCZ with T cell targeting abatacept and B cell depleting rituximab are needed to evaluate if IL-6 effects are entirely dependent on the regulation of adaptive immune responses, or new pathways could be discovered to explain the differences found.

1.3.5.4 Targeting of common γ chain cytokines

Type I cytokines include a family of factors sharing a common γ chain receptor subunit (γc, or IL-2Rγ subunit). This group includes IL-2, IL-4, IL-7, IL-9, IL-15 and IL-21 [425]. The primary cytokine of this group, IL-2, exhibits a multitude of pro- and anti- inflammatory effects including T cell survival and reduction of cytolytic activity of CD8 T cells and NK cells. Blockade of IL-2R with daclizumab is used to support adherence of transplantation tissue and in treatment of multiple sclerosis [90,426].

IL-4 is known for promoting differentiation of M2 macrophages, but also for its role in allergic disease [427]. Raised levels of IL-4 were found in synovial tissue from patients with established disease, yet not enough evidence was gathered to suggest that targeting of this pathway would be beneficial in treatment of arthritis [427].

Next, IL-7 and IL-15 are considered to be a homeostatic cytokines playing a role in the maintenance of circulating T cell numbers [428]. Links with RA were made when increased expression of IL-15 cytokine was detected in synovial fluid and it was shown to mediate osteoclastogenesis and bone erosions [429]. Demonstration of its ability to support T cell and NK cell activation as well as to lower the T cell activation threshold and mediate T cell-macrophage cross talk in the RA synovium supported the hypothesis for potential targeting in RA [430-432]. More so, a genetic link with RA was provided by the discovery of SNP in the gene encoding IL-15, which correlated with the rate of joint destruction in patients with active disease [433]. Despite this, targeting of neither IL-15 nor IL-21, known for effects on T cell activation and B cell maturation, have not yielded any benefit in the treatment of RA [432].

1.3.5.5 Targeting GM-CSF

GM-CSF is a pluripotent cytokine that regulates a variety of important cellular functions in myeloid cells. It shares its common β chain with cytokines IL-3 and IL-5 and is also considered a type I cytokine. GM-CSF is primarily known for activation, survival and differentiation of blood derived monocytes into inflammatory DCs, while also regulating phagocytosis, expression of MHC class II and pattern recognition receptors and the production of inflammatory cytokines and chemotactic molecules [216,434,435]. Mouse knock-out studies have shown that GM-CSF inhibition does not prevent development of myeloid cells but severely impairs the infection response, rendering GM-CSF more relevant in provoked immune responses. More recently it has been established that GM-CSF also enhances upregulation of MHC class I molecules and cross presentation of antigens to CD8+ T cells by CD103+CD8+ tissue resident DCs [436].

Apart from myeloid cells, T cells and specifically T_H17 cells are a significant source of GM-CSF, while the corresponding RORγt TF directly initiates its expression [437]. Additionally, natural killer (NKT) cells trigger GM-CSF expression to attract neutrophils during antifungal response [438]. In RA models, RF^+ autoreactive B cells were capable of producing GM-CSF in response to TLR stimulations, which, in turn, close the autocrine loop by further promoting IgM production [439].

Severe bone ache is a common side effect during treatment with GM-CSF agents [440]. Indeed, GM-CSF is expressed by sensory neurons of the dorsal root ganglia, while its receptor directly sensitizes pain receptors in these neurons and mediates hyperalgesia [441,442]. This pathway directly mediates pain in mouse models of arthritis in response to prostaglandin activation [443].

Both, immunopathologic and nociceptive roles of GM-CSF are desirable targets for the treatment of RA. Several agents targeting GM-CSF (Namilumab, MOR103) and GM-CSFR (Mavrilumab, MORAb 002) are currently tested in the phase I and II clinical trials (https://clinicaltrials.gov, NCT02354599, NCT01317797, NCT02129777, NCT02393378, NCT02379091, NCT01023256, NCT01517282, NCT01603277, NCT02546284, NCT01357759, NCT00771420, NCT01050998, NCT01715896, NCT01706926).

Most of the currently available data concern Mavrilumab, a fully human anti-GM-CSF receptor alpha monoclonal antibody with high affinity for human protein, yet more data is available on mouse models tested with mouse analog, a CAM-303 antibody [444]. Exposure of mice to very high doses of CAM-303 agent led to microscopic granulomatous changes in the lungs, in keeping with the role of GM-CSF in maintenance of alveolar macrophages. In murine model of collagen-induced arthritis (CIA), administration of CAM-303 inhibited disease progression as effectively as the use of anti-TNF agents.

A double blind, placebo controlled, randomized phase II trial of efficacy and safety of Mavrilumab included 233 patients with active RA on concomitant MTX therapy [445]. The primary end point was described as achieving clinically meaningful improvement in DAS28-CRP score (reduction of >1.2 points) after 12 weeks of treatment and was met by ~55% of active treatment group and 34.7% of placebo group [445]. A second multicenter, randomized double-blind, placebo controlled dose ranging study also met its primary endpoint, set as >1.2 point improvement in baseline DAS28-CRP at 12 weeks and ACR20 score at 24 weeks of the study [446,447]. Here, the highest dose group also demonstrated significant benefit of the treatment with 40.5% in the active treatment group and 12.4% in the placebo group achieving ACR50 response, while ACR70 improvement was seen in 13.9% and 3.7% of patients from respective groups [446,447]. Interestingly, treatment with Mavrilumab had an almost immediate effect with improvement in patient reported parameters after one week and continuous incremental benefit registered until week 12. Results from a phase IIb clinical trial comparing Mavrilumab to anti-TNFα agent golimumab were recently presented at the annual ACR meeting and suggest similar efficacy between the groups [448].

1.3.5.6 Interferons in RA

IFNs are a group of molecules eliciting antiviral responses and together with IL-10 related cytokines comprise the type II cytokine family. There are three main types of IFNs: type I family consists of α, ß, ω, ε, κ, δ and t forms, type II includes one member – IFNγ and type III IFNs involve IFNλ or IL-28 and IL-29. Separation into 3 groups is made according to the corresponding receptors, as type I family signals through ubiquitously expressed type I receptor (subunits

IFNAR1 and IFNAR2), while IFNγ signals through type II receptor (IFNGR1 and IFNGR2) and IFNλ signals through a heterodimer of IL10R2 and IFNLR1 [449,450]. Effects of all three IFN families largely overlap due to the utilization of same intracellular signal transduction pathways, of which JAK kinases and STAT signal transducers are most investigated [451,452]. Downstream interferon response elements or IREs are well characterized in a large number of microarray datasets, which suggest that only 37% of IREs are specific for type I interferons, while 69% of IFNγ IREs can also be induced by type I IFNs [452]. From these, some genes encode antiviral defence programs, while others are responsible for apoptosis, cell proliferation and angiogenesis, with part still unclear [453,454]. Triggering of IREs sets in motion several feedback loops, some of which facilitate type I IFN production genes, such as TLR7 or IRF5, while others are regulating same pathways through SOCS family of inhibitors [454].

Increased expression of interferon regulated genes (IRGs) was detected in a multitude of autoimmune diseases, including systemic lupus erythematosus (SLE) and RA, therefore the term 'Type I IFN signature' was introduced [455,456]. It appears that one quarter of RA patients have a pronounced type I interferon signature and form a specific pathogenic subgroup [457]. From all type I IFNs, IFNα is most commonly studied. In RA, pDCs are the main source of IFNα, while FLS cells were found to secrete high levels of IFNß [282,283,458]. Autoantibodies and immune complexes with nucleic acids can trigger TLR7 and 9 signalling, also resulting in upregulation of IFNα [459]. Upon TNFα stimulation, synovial macrophages express large numbers of IRGs [460].

Overexpression of type I interferons and associated IRGs likely have major impact on the pathogenesis of RA. Primarily they are meant to inhibit viral replication, however they can serve as immune adjuvants [461]. The resulting increase in expression of MHC class I molecules potentiates antigen presentation and enhances engagement of cytotoxic T cells, in keeping with recently emerging data on pathogenicity of CD8 T cells in RA. IFNα is also capable of prolonging survival of T cells and B cells, inducing immunoglobulin switching and potentiating antibody production, while its effects on innate cells include increased uptake of oxidized low-density lipoproteins by activated macrophages and formation of foam cells within atherosclerotic plaques [462]. On the contrary, both type I and type II interferons also display some anti-inflammatory

traits. IFNα is a potent suppressor of osteoclastogenesis and have bone protective effects, while IFNß is effective treatment for the multiple sclerosis [129,425]. In CIA models, mice lacking *Ifnγ* gene are not protected from developing arthritis and IFNγ deficiency can exacerbate the symptoms [425].

In an attempt to utilize this in the clinical setting, three monoclonal anti-IFNα antibodies were developed (Rontalizumab, Sifalimumab and AGS-009). Efficacy of these agents is currently being investigated in SLE, a disease with significantly stronger IFN signature than RA [463,464]. However, transcriptomic studies in RA derived PBMCs have shown that suppression of the type I IFN signature is the only marker for good clinical response to the treatment with current biologic agents [465,466]. In fact, it is proposed that anti-malarial treatments, such as hydroxychloroquine inhibit intracellular TLRs and suppress induction of IRGs and could be of particular clinical benefit in patients with increased IFN signature [467].

1.3.5.7 New DMARDs targeting cytokines – Jakinibs

The Janus kinases (JAKs) are functional intracellular domains of specific extracellular membrane bound receptors of type I and II cytokines. This family of kinases includes JAK1, JAK2, JAK3 and TYK2 (tyrosine kinase) members, different combinations of which are associated with different cytokine receptors (reviewed in [425])[468]. For example, JAK3 signalling is downstream from all γ chain (γc) cytokines and its mutations resemble γc deficiency resulting in severe combined immunodeficiency syndrome (SCID) [469,470].

Upon activation of receptor, JAKs transfer phosphate from ATP (adenosine triphosphate) to the tyrosine residue of their substrates, which are most commonly STAT signalling molecules. JAKs are also capable of autophosphorylating or transferring a phosphate group to other JAKs in the vicinity. Downstream STAT signalling transducers include seven members: STAT1-4, STAT5A, STAT5B and STAT6. Upon phosphorylation, activated STATs translocate into the nucleus and serve as TF for target genes, therefore completing the signalling pathway [468].

As stated above, combinations of JAK-STAT signal transducers are downstream from type I and II family of cytokines. Type I cytokines include common γ chain family (IL-2, IL-4, IL-5, IL-7, IL-9, IL-15, IL-21) targeting of which gave equivocal results in RA; common ß chain cytokines (IL-3, IL-5 and GM-CSF) with promising studies in GM-CSF inhibition; cytokines sharing GP130 receptor subunit (IL-6, IL-11, IL-27) with excellent results in IL-6 targeting; and, additionally, an IL-12 family of cytokines (IL-12, IL-23, IL-35) that have proinflammatory traits and proved much more important for the pathogenesis of psoriatic arthritis. Type II cytokines include all members of the interferon family with specific implication of type I IFNs in RA; and a range of cytokines sharing similarities with IL-10 (IL-10, IL-19, IL-20, IL-22, IL-24 and IL-26) that are believed to contribute to the resolution of inflammation and wound healing [90,471]. It is therefore clear that inhibition of JAK kinases has a potential of combining the effects of successful treatments, such as targeting of IL-6, GM-CSF and type I interferons, while potentially having unwanted effects on anti-inflammatory functions of IL-10, IL-2 and IFNß, as well as some growth factors for example.

Several JAK inhibitors, or Jakinibs, are being tested for clinical use. Although these are considered as new synthetic DMARDS, they essentially prevent cytokine signalling and exhibit efficacy closer to that of biologic agents than of conventional DMARDs. First approved in the treatment of RA was Tofacitinib, a JAK1/3 inhibitor with less affinity for JAK2 [472]. Initial proof of concept trials were very promising [473], and Tofacitinib was than tested in the series of phase II and III trials where it showed efficacy as monotherapy, or in combination with DMARDs (most commonly MTX) and as a first line agent in early disease, or in DMARDs and biologics failures [474-478]. Tofacitinib is considered as effective as adalimumab in patients requiring biologics and superior to MTX in treatment of naïve patients, similarly to that demonstrated by Tocilizumab [423,478,479]. At present, FDA approved Tofacitinib for a single treatment use in inadequate responders to MTX, yet it remains non-licenced in Europe due to safety concerns.

JAK1/2 inhibitor Ruxolitinib was the first FDA approved Jakinib demonstrating efficacy against myeloiproliferative conditions [480]. Its use in RA is now being investigated in phase II clinical trials. However, Baricitinib, also a JAK1/2 inhibitor, has shown efficacy in the treatment of RA in patients with inadequate

response to DMARDs and biologics [481,482]. Moreover, Baricitinib reduces radiographic progression, joint space narrowing and formation of erosions [481,482]. It is expected to be approved for use in RA in early 2017.

So far, clinical experiences with Jakinibs were positive despite specific safety signatures. The most common adverse events are upper respiratory tract infections, urinary tract infections and viral gastroenteritis, which are more common in Tofacitinib treated patients. However, serious cases of tuberculosis, bacterial and pneumocystis pneumonias and fungal infections were reported [483,484]. The overall risk of infections is believed to be comparable with other biologic treatments, with potentially higher incidence of varicella zoster virus recurrence [483,485]. This could be mediated by reduced functioning of NK cells through inhibited IL-15 or inhibited interferon signalling leading to impaired viral responses [486]. Certainly, impaired vaccination responses were also noted in Tofacitinib treated patients [487]. Additionally, all first generation Jakinibs inhibit JAK2 to a certain degree and therefore inhibit effects of erythropoietin, thrombopoietin and colony stimulating factors resulting in anaemia and neutropenia, yet these are usually not a cause for the discontinuation of the treatment.

Of more importance is the metabolic effect of Jakinibs. Treatment with Tofacitinib leads to increased levels of total cholesterol, LDL and HDL cholesterol levels [473,483]. Despite this, Tofacitinib improves arterial stiffness and overall cardiovascular outcomes in RA patients [488]. These effects were also observed with IL-6R blockade by Tocilizumab [489]. In both instances, altering lipoprotein kinetics and improving lipid metabolism seems to be net beneficial for the disease outcome and management of co-morbidities [490,491].

Jakinibs provide a new and improved alternative for the oral treatment of RA, with efficacy comparable to that of biologic agents. More insight will be gained with the testing of new, more selective JAK inhibitors, also referred to as the second generation Jakinibs. Early phase I and II trials suggest that selective JAK1 inhibitor Filgotonib is effective in the treatment of RA [492]. Side effects remain a major focus of the clinical outcomes and long term data as well safety profiles of new selective agents remain to be evaluated. Overall summary of the RA pathogenesis and currently used treatments is depicted below in Figure 1.1.

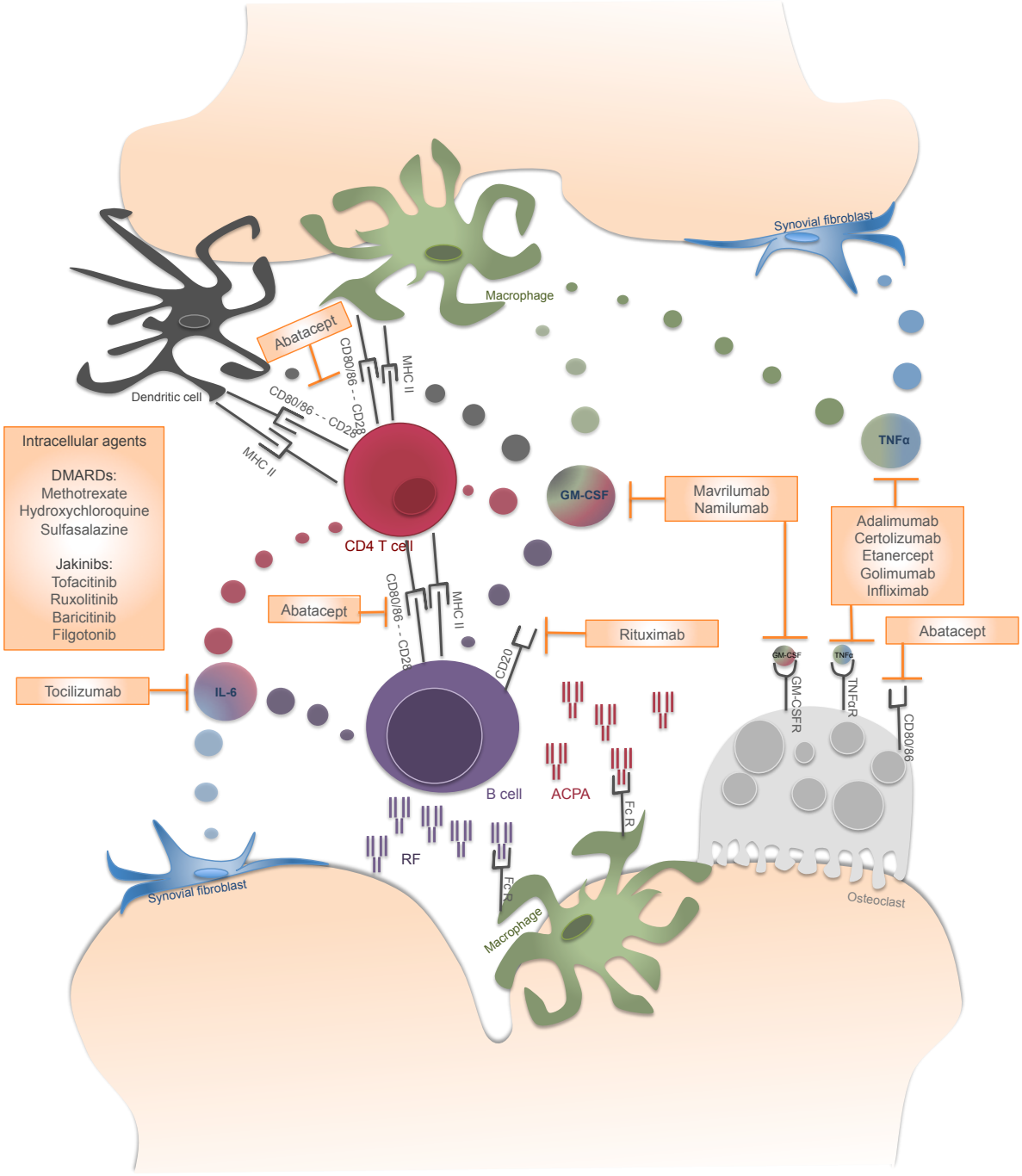

Figure 1.1 Summary of the pathogenesis and currently approved treatments for the treatment of RA.

Schematic of the arthritic joint, illustrating the influx of immune cells. RA pathogenesis revolves around the activation of antigen presenting cells (APCs), such as dendritic cells (in black), macrophages (in green) or even B cells (in purple). The resulting activated T cells (in red) produce cytokines such as IL-6 and GM-CSF, while activated B cells (in purple) secrete cytokines along with autoreactive ACPA and RF antibodies, causing further activation of APCs. Additionally, pro-inflammatory cytokines and co-activation molecules trigger maturation of osteoclasts and promote bone resorption. Orange boxes represent currently used therapeutic agents and their targets.

1.4 Lessons from the Genetics of RA

RA is a partially heritable disease. The largest GWAS study is a meta-analysis that involved 29,880 patients with established, predominantly seropositive RA and 73,758 healthy individuals from European and Asian populations [37]. As a result, genetic susceptibility is thought to comprise around 65% of the total risk for RA and is overwhelmingly associated with the immunological component of the disease [493,494]. Population studies on patients with RA have identified over 100 genetic loci, which collectively account for approximately 15% of the phenotypic variability of RA [37,495]. This is a strong indicator that RA is a highly polygenic disease. Despite significant progress, the analysis of GWAS data is complicated by the fact that single nucleotide polymorphisms (SNPs) that are truly associated with RA are hidden among a multiplicity of sites with little to no importance, and individual analysis of each loci is necessary [496].

1.4.1 Association with MHC loci

Variation in MHC loci account for most (>60%) of the genetic susceptibility of RA [37]. The major histocompatibility region comprises over 250 functional genes, including some complement factors, cytokines, and antigen processing and presentation genes, such as HLAs [497]. Several HLA-DR alleles were identified under the SE hypothesis [498]. Within this hypothesis, certain HLA-DRB1 alleles (*04:01, *04:04, *04:05, *04:08, *10:01, *01:01 and 01:02) directly increase the risk of developing ACPA antibodies and RA in Caucasian population [498]. Changed amino acid residues, encoded by these HLA variants, are positioned within the epitope-binding pockets of HLA molecules on the surface of APCs, and display increased affinity for cross presentation of citrullinated peptides [499]. Moreover, heterozygotes for HLA-DRB1 alleles are found to be at even higher risk of developing RA, possibly due to the cross presentation of a greater variety of autoantigens [495]. Recent logistic regression models of MHC alleles, which include hierarchical dominance models, explained an additional 1.4% of the risk for developing ACPA positive RA, increasing to total to 9.5% explained by these genetic loci.

On the contrary, the association of MHC loci with ACPA negative RA remains largely controversial [500]. Partially, this could be explained by low sensitivity of

commonly used ACPA detection methods, as >10% of patients turn out to be antibody positive on retesting [501]. Otherwise this could be explained by the possibility of other autoimmune diseases masquerading as ACPA-negative RA and introducing more heterogeneity. Some progress was made with a rigorous investigation of a homogeneous ACPA negative RA cohort, which identified distinct HLA-DRβ1 and HLA-B variants associated only with ACPA-negative arthritis, still more work is needed in this field [502].

1.4.2 Association with non-MHC loci

Amongst loci identified by GWAS studies there are 58 previously reported non-MHC loci and 42 newly identified sites, which together account for 5.5% heritability in European and 4.7% in Asian populations [37]. Some authors argue that these 100 loci include up to 377 genes, identified on the basis of prior knowledge of pathways and protein-protein interactions, yet this is still controversial. Although this approach can potentially introduce bias it also identified genes that were previously implicated in the pathogenesis of RA, such as PTPN22, PADI4, STAT4, TNFAIP3 (A20), ANKRD55, CTLA4 and CD40, some of which are shared with other autoimmune disease and used as successful therapeutic targets [37,503].

Of most importance is to dissect which cell types and pathways are associated with genetic susceptibility of RA and how these can be utilized in the search for new or repurposing of available treatments to benefit our patients. Here, platforms utilizing gene ontology networks and biological pathways, such as MAGENTA (meta-analysis gene-set enrichment of variant associations) have identified T cell, B cell and cytokine signalling pathways to respond to identified 100 non-MHC loci [37]. For example, 27 out of 100 RA risk variants are mapped to gene enhancement regions that are specific for $CD4^+$ T cells [504]. As well as the majority of identified long noncoding transcripts, which are crucial to $CD4^+$ T cell functioning [505].

Great examples of association of genetically identified susceptibility genes and successful therapies are Abatacept targeting CTLA4 co-stimulatory pathway and Tocilizumab, or IL-6 inhibition. The most recent published investigation of the possible drug benefits has identified 871 drug-target gene interactions, of which

247 had basis for further investigation in RA [37]. One of the examples of successful implementation of such analysis is identification of a single SNP rs4810485, which accounts for entire susceptibility of CD40 (TNF receptor superfamily member 5) locus and corresponding small molecule inhibitor [506]. In fact, silencing of CD40 expression in human B cell line resulted in decreased NFκB signalling and will be further evaluated for the clinical use [506]. Alternatively, attempts were made at gene editing therapy in RA, however a greater understanding of current data and further investigations are needed before this will become a fruitful approach to treatment [507-509].

Clinical genetic studies in well-defined cohorts are just as important, not only for the discovery of new therapeutics, but also for the investigation of the potential clinical biomarkers. One such example is given by the study that identified HLA-DRβ1 susceptibility loci as a clinical marker for RA severity, mortality and efficacy of anti-TNFα agents [510]. A translational approach and clinical understanding is just as important to genetic studies, as it is to pathogenesis, immunologic or drug discovery investigations.

1.5 MiRs in RA

“Epigenetics is the study of heritable information that is carried by genetic material but is not encoded in the DNA sequence” [511]. According to this definition, epigenetic phenomena include DNA methylation and histone modifications, such as acetylation and small RNA species – micro RNAs (miRs). Epigenetic changes play a significant pathogenic role in RA were they also explain the link between smoking and the increased risk of the disease [511]. While other epigenetic phenomena involve modification of structures supporting DNA, miRs belong to a large family of small RNAs, capable of supressing unwanted genetic materials and transcripts in eukaryotes [512]. Moreover, miRs themselves are also controlled by epigenetic events, such as histone modification and methylation of the DNA, alike all other genes in the genome [513]. Given the expanding body of data implicating miRs in the pathogenesis of RA and regulation of blood or tissue derived immune cells this work will further solely focus on the biogenesis and role of miRs in disease context rather than other epigenetic mechanisms.

1.5.1 Biogenesis of miRs

MicroRNAs are a class of small RNAs ~22 nucleotides long that control gene expression via the translational repression, degradation or destabilisation of the mRNAs they target (Reviewed in [514]). In this role, they act by providing sequence specificity to Argonaute as part of the RNA-induced silencing complex (RISC). Early studies revealed that miRs recognise partially complementary sequences in the 3' untranslated region (3'UTR) of their target mRNAs. Base-pairing between the target sequence and positions 2-7 of the miR, called the seed region, were found to be particularly important for target recognition. This highly conserved class of molecules play fundamental roles in all cellular processes. Individual miR can regulate 100s of genes often coordinating the expression of entire pathways. Their importance is underlined by the fact that dysregulation of miRs is associated with a broad range of human diseases, including cancer, heart disease, neurodevelopmental disorders, and autoimmunity [515,516]. For these reasons, it is not surprising that their biogenesis is tightly regulated.

As the number of miRs identified rapidly increased a numerical nomenclature was adopted in which miRs were numbered sequentially according to the order in which they were discovered (e.g. miR-23). These names also include a prefix describing the species in which they occur (e.g. hsa-miR-23, human miR-23). MiRs that share seed sequences are classed as belonging to the same 'miR family' and are distinguished by lettered suffixes (e.g. hsa-miR-23a and hsa-miR-23b). If two mature miRs arise from different genes but retain identical sequences they are distinguished by number suffixes, such as miR-24-1 and miR-24-2, to indicate their gene of origin. Further complexity arises as each miR locus can produce two mature miRs, one from the 5' strand the other from the 3' strand and are designated accordingly, for example, hsa-miR-23a-5p or hsa-miR-23a-3p. In most cases, one form predominates over the other.

1.5.1.1 Transcription of miR genes.

Primary miR transcripts share many structural features with protein coding genes. Nearly all are synthesised by RNA polymerase II, contain 5' caps and are polyadenylated ([517]. They can be synthesised individually or together with other miR in polycistronic clusters. MiRs can also be co-transcribed in the introns of host genes. MiRs originating from the same cluster are, generally, co-transcribed yet, single miRs can be preferentially expressed at the post-transcriptional level. For example, miR let-7 is post-transcriptionally suppressed in the embryonic stem cells, while other members of the cluster miR-100~let-7~miR-125 are processed into their mature forms [518].

Conventional methods used to characterise mRNA transcripts are ill-suited for the study of primary miR transcripts, which are short-lived due to rapid processing into their mature forms. The identification of transcription start sites (TSS) has proved to be particularly challenging for this reason. Consequently mapping the precise location of miR promoters lags behind that of protein-coding genes. However, recent developments in high-throughput technologies such as RNAseq, ChIPseq (Chromatin Immunoprecipitation followed by sequencing) and mapping of CpG islands, has begun to change this. These approaches revealed that miRs in many cases have multiple promoters, allowing miR genes to be expressed in numerous cell types or respond to a range of different stimuli [519]. miRNA genes like protein-coding genes are regulated

directly by interactions of transcription factor binding to sequences in their promoters. Additional layers of regulation are applied by histone modifications and DNA methylation [520].

Once transcription of pri-miR is complete, it undergoes several maturation steps (Figure 1.2, steps 2-5). Primary miR transcripts contain a 33-35 bp hairpin loop, containing the mature miR sequences is recognised by microprocessor complex containing Drosha and DGCR8 (Pasha). This complex clips the hairpin structure out of the primary transcript producing a ~65 nucleotide precursor-miR (pre-miR) intermediate. This essential step in miR biogenesis pathway is itself tightly regulated. A particularly elegant mechanism involves DGCR8 stabilising Drosha through protein-protein interaction, while Drosha itself destabilised DGCR8 mRNA [521]. In addition, the stability, nuclear localisation and activity of the microprocessor is regulated by post-translation modifications [522]. This first stage in the miR biogenesis pathway takes place in the nucleus and once complete, pre-miR are exported into the cytoplasm by the protein exportin 5 (EXP5) [523]. Here pre-miR is cleaved by Dicer enzyme near the terminal loop, liberating a small double strand RNA, approximately 22 nucleotides in length [524]. This small RNA duplex is loaded onto one of four available Argonaute proteins (AGO1-4) to form the RNA-induced silencing complex (RISC) [525]. From the RNA duplex, one strand will become the effector ‘guide’ strand, while the other, known as the ‘passenger’ strand is quickly degraded upon AGO loading. This explains a strong bias towards the guide strand in the mature miR pool [513]. On rare occasions, passenger stands are also incorporated and have distinct functions.

RNA silencing function of miRs is guided by the complementary base pairing of its sequence with 3' untranslated region (UTR) of the target mRNA, while associated RISC protein complex acts as an effector by instigating translational repression, deadenylation and decay (Figure 1.2, 6)[526]. Although binding is predominantly guided by the complementarity of the ‘seed’ region, pairing is aided if other parts of the miR sequence are also complimentary. Some reports have shown that imperfect base-pairing at positions 8-10 of the miR promotes target repression via sequestration rather than degradation or destabilisation. (Figure 1.2, 7)[513]. Either way protein translation is prevented. The next

section will explain how this principle is utilised in the search for potential miR:mRNA interactions.

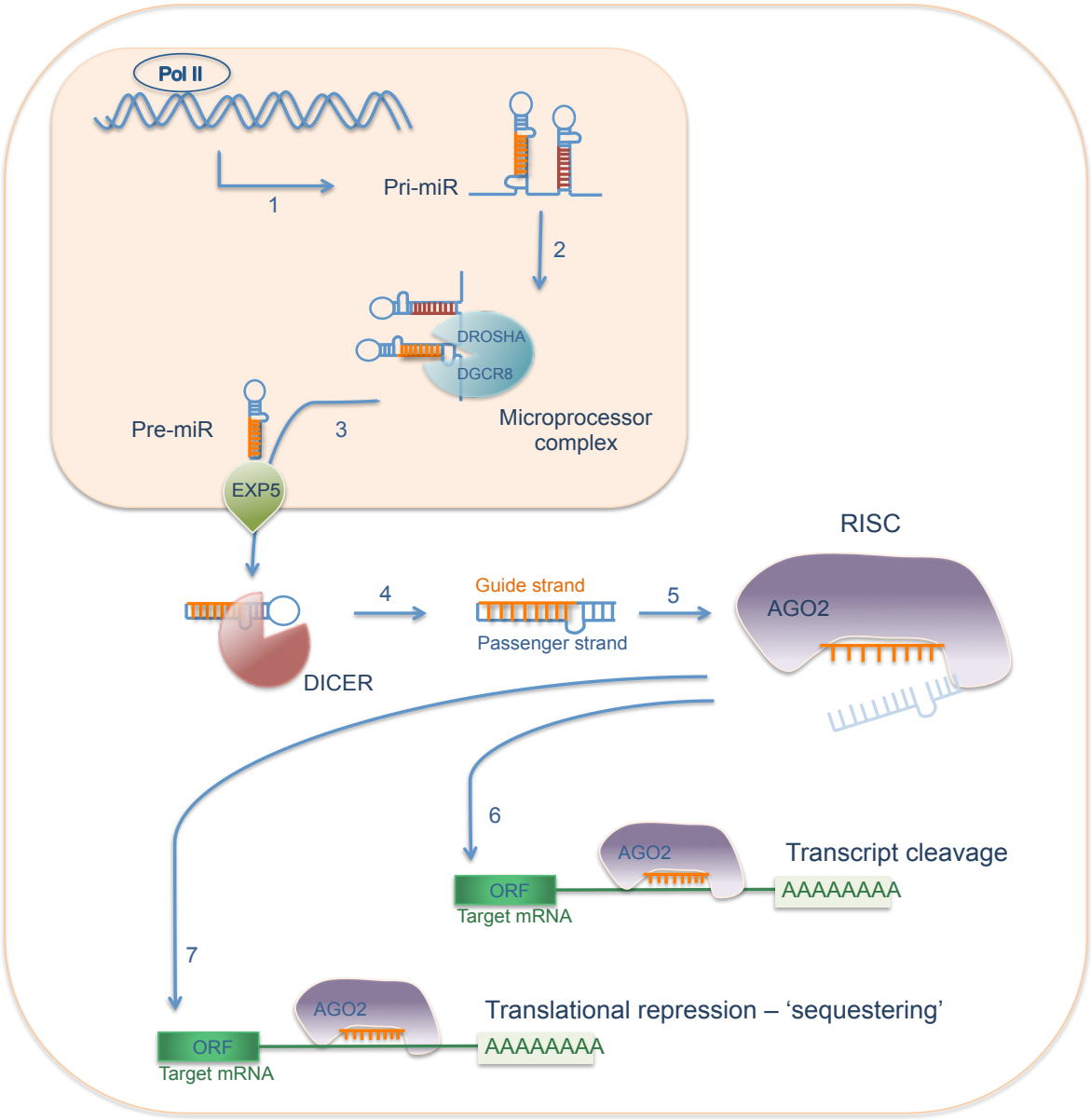

Figure 1.2 Schematic representation of miR biogenesis in mammalian cells.

(**1**). MiR gene is transcribed by polymerase II (Pol II) and forming the hairpin loop structures of the pri-miR (**2**). Next, microprocessor complex containing DROSHA and DGCR8 enzymes cleaves off the loop containing single pre-miR from the rest of the transcript. (**3**). Once the pre-miR is formed it is transported from the nucleus to the cytoplasm by exportin 5 (EXP5) (**4**). In the cytoplasm, DICER enzyme cleaves the 'loop' end of the pre-miR and forming the mature miR duplex. (**5**) The guide strand from the miR duplex is incorporated into the Argonaut protein (AGO) and forms a functional RISC complex which can initiate the degradation of the target mRNA transcript (**6**) or instigate its sequestering (**7**). Further details are in the text.

1.5.2 Methodology of miR research

The foundation of all research into the roles of miRs is the identification of miR:mRNA interactions. Since their discovery in 2001 more than half a million experimentally validated miR:mRNA interactions have been reported [527]. Along with the ever-growing number of interactions, the number of techniques and tools used to predict or identify them has also increased in the last ten years. There are many excellent reviews describing various strategies that have been developed to identify these interactions, ranging from individual miR:mRNA pairings through to techniques that capture pan-cellular miR:mRNA interaction (Reviewed in [528-530]).

The formation of functional miR:mRNA interactions is assumed to require Watson and Crick base pairing between miR, in particular, its ‘seed' region, and its target binding site. Despite intense efforts to understand these interactions at the molecular level no formula or set of rules has been able to explain why a miR selects one target over another. This has led to the development of a variety of approaches to miR target prediction, with the complementarity between the seed region and the miR binding site (MBS) at their heart. On top of these criteria, some programs infer an MBS's importance from its conservation amongst mammalian species, while others analyse secondary structure surrounding the MBS thereby inferring likely accessibility of RISC complex. Currently, target prediction algorithms have false-positive rates between 20 and 50% [531]. Despite this, such programs are invaluable and inexpensive tools enabling researchers to make rapid theoretical assessments of the miRs that have the potential to regulate their genes of interest. Other options include investigation of direct miR:mRNA interactions through complex immunopurification techniques or through sequencing of the manipulated cells and tissues that overexpress or silence the miR of interest. Whichever approach is employed, the interaction must eventually be confirmed by the appropriate validation method. Workflows for identification of miR:mRNA interactions are summarised in Figure 1.3.

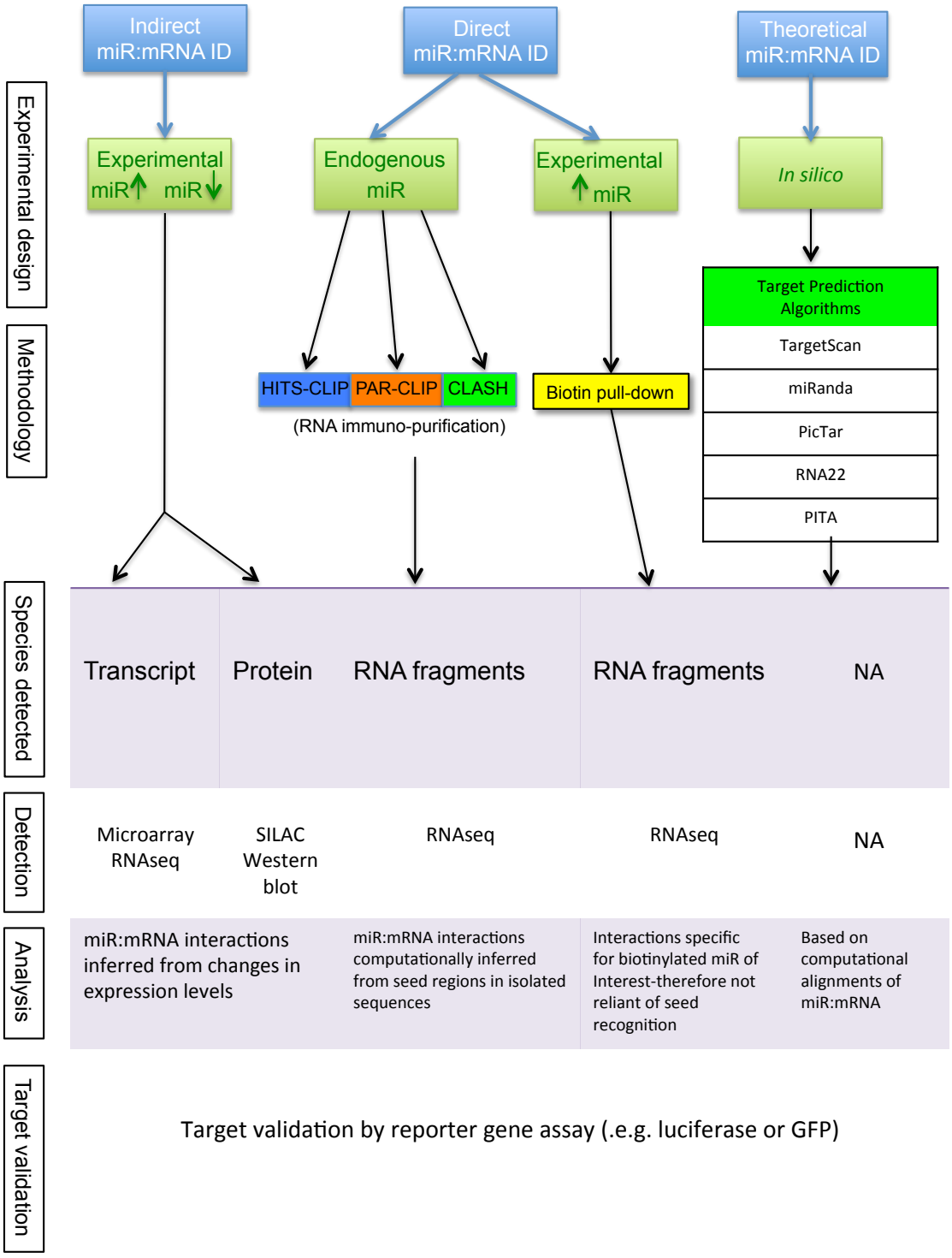

Figure 1.3 Overview of miR:mRNA interaction methodologies.

HITS-CLIP - high-throughput sequencing of RNA isolated by crosslinking immunoprecipitation; PAR-CLIP - photoactivatable ribonucleoside–enhanced crosslinking and immunoprecipitation; CLASH - crosslinking, ligation, and sequencing of hybrids; RNAseq – RNA sequencing; SILAC - Stable Isotope labelling by/with amino acids in cell culture.

1.5.2.1 Theoretical identification of miR targets

1.5.2.1.1 TargetScan (Human)

The algorithm used by Targetscan restricts its predictions to sites found in the 3'UTR of transcripts annotated in the Ensembl human database [532]. Here it searches for sequences that have full complementary to the seed regions of know human miRs. Potential miR:mRNA interactions are ranked according to whether MBSs are evolutionary conserved [533]. An additional score is given for interactions that have an adenosine at position one of the MBS which is thought to be conserved - possibly acting as an anchor for the RISC complex [534]. One of every two predicted targets are considered to represent legitimate targets [535].

1.5.2.1.2 PITA

The algorithm used in PITA is unusual in that it uses the accessibility of miR to potential MBS as a parameter [536]. Like other algorithms PITA initially searches for sequences complementary to miR-seed regions within 3'UTR sequences. Once identified, it then infers miR accessibility to this region by estimating the local secondary structure. The assumption being that a miR cannot regulate a transcript if it is unable to access a potential MBS. PITA predicts correct targets 26% of the time [535].

1.5.2.1.3 PicTar

PicTar searches for seed region matches in conserved 3'UTRs calculating the free energy of miR:MBS duplex [531]. Identified MBSs are then aligned against the homologous sequences from 8 vertebrate species; the degree of conservation is taken into account when scoring the potential interactions. Predictions made by PicTar have an experimental validation rate of 49% [535].

1.5.2.1.4 miRanda

Like Targetscan and PicTar, MiRanda screens 3'UTR regions for sequences complementary to miR, binding energy and evolutionary conservation [537]. Additionally, the location of the MBS in the 3'UTR is also scored, with binding sites at the beginning and the end of the 3'UTR scored highest. Unlike

TargetScan, miRanda recognises complementarity outwith the seed region, taking into account different types of miR:mRNA interactions. miRanda predictions are correct 29% of the time [535].

1.5.2.1.5 RNA22

RNA22 tackles the problem of target prediction in an entirely different way to that of other target prediction algorithms [538]. The premise behinds RNA22's algorithm is that the reverse compliment of miRs, using pattern discovery techniques, should permit the identification of MBS in a provided sequence. Once target MBS has been located a targeting miR can be identified using an algorithm that calculates RNA:RNA duplexes. Unlike the other programs discussed here, RNA22 does not rely on cross-species conservation or base pairing of the seed region. RNA22 has the highest false positive rate, correctly predicting targets in only 24% of the time [535].

With the exception of miRanda and RNA22, most target predictions algorithms identify targets based on seed region complementarity with the MBS sequence in the 3'UTR of the target gene. Recent studies have found that only 40% of miR:mRNA interactions identified using techniques such as HITS-CLIP are located in 3'UTRs, the other 60% are spread amongst sequences in the 5'UTR and ORF [539]. Indeed, these interactions have biological significance. Takagi and colleagues showed that miR-24 down-regulated Hepatocyte Nuclear Factor 4 alpha (HNF4a) via a binding site in the coding region [540]. With this in mind, it is likely that an overreliance on the above mentioned programs for target discovery can cause a large number of highly significant miR:mRNA interactions to be overlooked. Fortunately, more accurate high-throughput techniques have been developed that capture the majority of miR:mRNA interactions within the cell and allow the unprejudiced identification of MBS. These will be discussed below.

1.5.2.2 Indirect identification of miR targets

The limitations of one-to-one miR:mRNA investigation and a desire to obtain a more comprehensive picture of the miR regulatory network led to a flood of studies that employed miR overexpression coupled to a microarray analysis to investigate the miR's role in its totality. This approach has the advantage of

sampling total transcriptomic changes. While this data set will undoubtedly include changes in target genes and related pathways, it, however, cannot differentiate between primary and secondary effects limiting its use as a miR discovery tool. Nor can it detect interactions in which translational repression but not transcript destabilisation is induced. Again this technique relies on supra-physiological over-expression of miR and identified targets do not necessary reflect what is happening in the cell under homeostatic conditions where miR levels are in most cases low [541].

This can be overcome to some extent by adopting a miR-inhibition strategy. The merit of this approach is that only transcripts that are actively being repressed by the miR-inhibited should exhibit changes in expression levels. However, as before, this does not differentiate between primary or secondary effects, nor does it identify targets that have been translationally repressed. This method can be improved by using a proteomic-based approach where changes in protein levels after the modulation of miR levels are measured [542]. This method uses Stable Isotope Labelling with Amino acids in Cell culture (SILAC) followed by mass spectrometry.

1.5.2.3 High-throughput identification of miR targets

One-to-one or overexpression methods have been superseded by high throughput RNA-immuno-purification technologies capable of capturing and characterising the entire miR:mRNA interactome of the cell in a single experiment. The first of these techniques called ‘high-throughput sequencing of RNA isolated by crosslinking immunoprecipitation’ or HITS-CLIP was developed in the laboratory of Robert Darnell [543]. This method involves UV cross-linking of miR-RISC complexes to the mRNAs that they are associated with. Samples are then treated with RNases, which degrades unbound RNA leaving the mRNA regions underlying the miR-RISC complexes protected. The miR-RISC-mRNA complexes are then isolated using an antibody against Ago2. Isolated RNAs are sequenced by RNAseq, generating a map of miR-binding sites. A similar method called PAR-CLIP makes use of photoactivatable nucleosides that reversibly cross-link miR to their mRNA targets when exposed to UV light [539].

These techniques, although powerful, do have some limitations. Firstly, their reliance on anti-Ago2 antibodies to retrieve miR-mRNA complexes means that miR-complexes involving the other Argonaute proteins are ignored. Secondly and perhaps most seriously, both of these techniques require that miRs be disassociated from its target mRNA before analysis. Interactions are then inferred computationally using target prediction algorithms. One technique, known as CLASH (crosslinking, ligation and sequencing of hybrids) ingeniously overcomes this limitation by ligating the miR-mRNA fragments together before sequencing allowing the miR and binding site to be captured together [544]. However, this method is relatively inefficient with less than 2% of reads corresponding to miR:mRNA interactions.

Lastly, Biotin-linked chromatography captures miR:mRNA interactions of a single miR species by introducing synthetic biotinylated miRs into cells [545]. These are then incorporated into the RISC complex, cells lysed and the biotin labelled miR:mRNA complexes purified using streptavidin-linked beads. Finally captured RNAs are then sequenced. The main merit of this technique is that it captures miR along with its target mRNA allowing interactions to be shown directly. While the data collected represents all the potential binding sites of a single miR species, it does not reveal which ones are occurring under physiological conditions.

The techniques described above represent powerful resources for the study of miR-target interactions. While being technically challenging, they will be hugely informative as we move away from the one-miR-one-target studies that make up most of the miR research to date. However, even with these rich data sets, it is important to establish that a particular miR:mRNA interaction does occur. In other words, just because a miR can target an mRNA it does not necessarily mean that it does in a given cell type at a given time. Transcripts can limit or extend the repertoire of miRs that regulate them via the utilisation of alternative polyA signals. The selective use of polyadenylation sites allows a transcript to alter the length of its 3'UTR thereby rendering them sensitive or insensitive to miR that would otherwise target them. It is estimated that 70% of human genes use more than one polyA signal with 50% using 3 or more [546]. This has significant biological consequences and can explain why a miR regulates a target in one cell type and not another [546].

1.5.2.4 Validation of miR:mRNA interaction with reporter gene assay.

Whatever the method used to identify potential miR:mRNA interactions, they must be experimentally challenged, most frequently using reporter gene assay. In these studies, regions containing putative MBS are cloned downstream of a reporter gene (luciferase or GFP) if the interaction is real, the expression of the reporter will be sensitive to the corresponding miR when co-transfected into an appropriate cell line[547]. Loss of inhibition upon mutation of MBS provides the final, conclusive proof of a miR regulation of that target. Although this proves that physical interaction occurs and is functional, whether it occurs in a particular cell under specific conditions has to be inferred from other *in vitro* studies. Additionally, as these studies involve the massive over-expression of both miR and target they can reveal interactions that would never occur under normal physiological conditions. With these caveats in mind, reporter gene assays provide the ultimate evidence of miR:mRNA interactions.

1.5.3 miRs in RA

The functions of miRs are cell and context dependent. With their ability to target many targets at the same time and tendency to regulate many members of the same pathway, differential expression can have significant consequences for the cell. MiRs are implicated in every physiologic process currently known, from embryogenesis to normal immune response to a pathogen (as evidenced by 55614 PubMed citations). They are also involved in many diseases, from cancers, in which they are now being considered for therapeutic targeting, through to dementia. They play a profound role in autoimmune diseases, where they regulate many aspects of immune cells, such as differentiation, activation, apoptosis and cytokine secretion [548]. This is a rapidly evolving field, and new miR-target interactions are discovered every day. Nevertheless, the most studied miRs in the context of RA remain miR-155, miR-146 and miR-223.

1.5.3.1 miR-155

MiR-155 is one of the first recognised pro-inflammatory miRs. MiR-155 transgenic mice have increased serum levels of TNFα and are susceptible to endotoxin shock [549]. Overexpression of miR-155 directly leads to increased production of TNFα through the repression of inflammatory suppressors SHIP-1

(Phosphatidylinositol-3,4,5-trisphosphate 5-phosphatase 1) and SOCS1 [550,551]. Macrophages and dendritic cells upregulate miR-155 upon stimulation with LPS [549] is essential to mounting an adequate inflammatory response since mice lacking miR-155 have defective T- and B-cell functions, as well as impaired antigen presentation capabilities of DCs [549]. Additionally, expression of miR-155 is raised in both, PB and synovium of RA patients [550]. Exposure of healthy PB monocytes to synovial fluid from RA patients triggers expression of miR-155 and increases levels of TNFα, IL-6 and IL-1ß [550]. Conversely, inhibition of miR-155 limits the expression of TNFα, while miR knock-out mice are protected from arthritis in CIA model [550]. More recent work has shown that increased miR-155 in RA monocytes promotes secretion of chemokines and triggers recruitment of inflammatory cells to the joints, while raised expression in PB B cells stimulates antibody secretion and is associated with ACPA+ RA [552,553].

1.5.3.2 miR-146a

MiR-146a is considered to play an anti-inflammatory role in RA, despite the fact that it is raised in PB cells, synovium and synovial fluid and correlates with disease activity score [554,555] [556,557]. Stimulation of FLS and CD4 T cells with LPS induces miR-146a expression [556]. In turn, miR-146a directly disrupts TLR activation by targeting TRAF6 and IRAK1 downstream signalling molecules; however, this feedback loop is not functional in RA cells as high levels of miR-146a does not inversely correlate with that of its targets [554]. Additionally, Zhou et al. have shown that failure of miR-146a to regulate STAT1 expression in T_{REG} cells is at the heart of their impaired ability to control cytokine production in RA [558]. If, however, miR-146a is injected intra-articulately in mice model of arthritis, it ameliorates formation of bone erosions through impairing osteoclastogenesis and regulating targets mentioned above [559]. It is therefore believed that the anti-inflammatory properties of miR-146a are curtailed in the chronic inflammatory setting of RA and contribute to the chronicity of the disease. In this case, overexpression of regulatory miR in a failed attempt to control the immune response exemplifies that function of miRs should not be judged solely on its presence or absence, especially when multiple contradictory events are involved, such as in chronic disease.

1.5.3.3 Other miRs in RA

MiR-223 is considered to play both pro- and anti-inflammatory roles in RA. This miR is abundantly detected in serum and synovium of RA patients and negatively correlates with the tender joint count [557]. MiR-223 promotes T_H1 polarisation and IFNγ expression while reducing the synthesis of pro-inflammatory IL-17 [560]. In keeping with this, it is highly present in naïve CD4 T cells and absent in T_H17 [561]. However, in murine SF myeloid cells, high levels of miR-223 promoted osteoclastogenesis and its inhibition prevented bone erosions, while reducing the severity of arthritis indicating cell and context-dependent functions of miR-223, which is why its association with RA requires further investigation [562].

The exploration of RA FLS cells has identified increased expression of miRs-203, miR-221, miR-222 and miR-323, which are believed to support expansive phenotype of FLS cells and their resistance to apoptosis [208,563]. In contrast, RA FLS were reported to have lower levels of miR-22, miR-34a*, miR-124a, miR-152 and miR-375 [564]. Amongst them, miR-22 was shown to target matrix protein Cyr61, implicated in angiogenesis, inflammation and matrix remodelling, while low levels of miR-22 coincided with overexpression of Cyr61 in RA synovium [564]. Downregulation of two other members, miR-34a* and miR-124a leads to overexpression of anti-apoptotic molecules, such as XIAP (E3 ubiquitin-protein ligase) and CKD2 (cyclin-dependent kinase 2); and migratory chemokine CCL2, respectively [207,565]. Remaining miR-152 and miR-375 were implicated in the control of Wnt signalling and bone remodelling in arthritis models in rats. [566].

1.5.4 MiR-23~24~27 clusters

All three of miRs in this cluster are implicated in a multitude of diseases, including prominent roles in inflammation and bone metabolism [567]. MiRs from this cluster were the first described in myeloid lineage commitment during development [568]. Since then, they have been actively investigated in many cancers for their ability to regulate cell proliferation and apoptotic pathways, while their immunomodulatory role is just emerging.

There are two genes in the mammalian genome expressing miR-23~24~27 cluster. These paralogs have arisen by gene duplication and are highly conserved among vertebrates. Both clusters contain three miRs: miR-23, miR-24 and miR-27. The miR-23a cluster is localised in the intragenic position on the chromosome 19q22 and contains miR-23a, miR-24-2 and miR-27a. This ‘a’ cluster exists as a separate gene and has its own promoter sequence upstream from the transcriptional start site (TSS) (Figure 1.4, A) [569]. In fact, this was the first miR cluster to be investigated for the transcription of consecutive miRs, where it was shown that miR clusters, such as this one, are transcribed by Pol II as a single primary transcript [517,570]. In contrast, its paralog, miR-23b~24-1~27b cluster is located on the chromosome 9 and is placed in intron 14 of the host C9ORF3 (chromosome 9 open reading frame 3) gene, whose function has yet to be determined (Figure 1.4, B). This ‘b' cluster contains miR-23b and miR-27b, which have a single nucleotide difference from their respective ‘a' cluster paralogs, while the sequence of miR-24-1 is identical to the one of miR-24-2. Hence they are distinguished by the numbered suffix. Recently, a new miR-3074 was described on the opposite strand of miR-24, however, it is unknown if this interferes with the expression of miR-24-1. Lastly, a third copy of miR-23c, but not other miRs from the cluster, has been recently discovered on the X chromosome. Unfortunately data on its expression and regulation are still sparse. Interspecies conservation and sequences of all miRs from these clusters are depicted in Table 1.4.

There have been several attempts at investigating the reason for miR gene duplication and conservation. It has been suggested that such events allows miRs to perform redundant functions in different cell types or under different circumstance, guided by distinct transcription factors [571]. Retained similarity

in sequence indicates that their portfolio of target genes are likely shared, and differences in function are guided by differential expression [572]. Co-expressed miRs, derived from the same cluster, were shown to work in synergy to accomplish targeting of designated pathways [573]. Nevertheless, significant posttranscriptional regulation can promote the expression of some miR members over others in a context-dependent manner. For example, overexpression of miR-23a~24-2~27a cluster in HEK293 (human embryonic kidney) cells leads to the accumulation of miR-24-2 and miR-27a, but not miR-23a [574].

miR	Species	Unique ID number	Sequence
miR-23a	human	MIMAT0000078	AUCACAUUGCCAGGGAUUUCC
	mouse	MIMAT0000532	AUCACAUUGCCAGGGAUUUCC
miR-23b	human	MIMAT0000418	AUCACAUUGCCAGGGAUUACC
	mouse	MIMAT0000125	AUCACAUUGCCAGGGAUUACC
miR-23c	human	MIMAT0018000	AUCACAUUGCCAGUGAUUACCC
miR-24-1/2	human	MIMAT0000080	UGGCUCAGUUCAGCAGGAACAG
	mouse	MIMAT0000219	UGGCUCAGUUCAGCAGGAACAG
miR-27a	human	MIMAT0000084	UUCACAGUGGCUAAGUUCCGC
	mouse	MIMAT0000537	UUCACAGUGGCUAAGUUCCGC
miR-27b	human	MIMAT0000419	UUCACAGUGGCUAAGUUCUGC
	mouse	MIMAT0000126	UUCACAGUGGCUAAGUUCUGC

Table 1.4 Interspecies conservation of miR-23~24~27 paralogs.

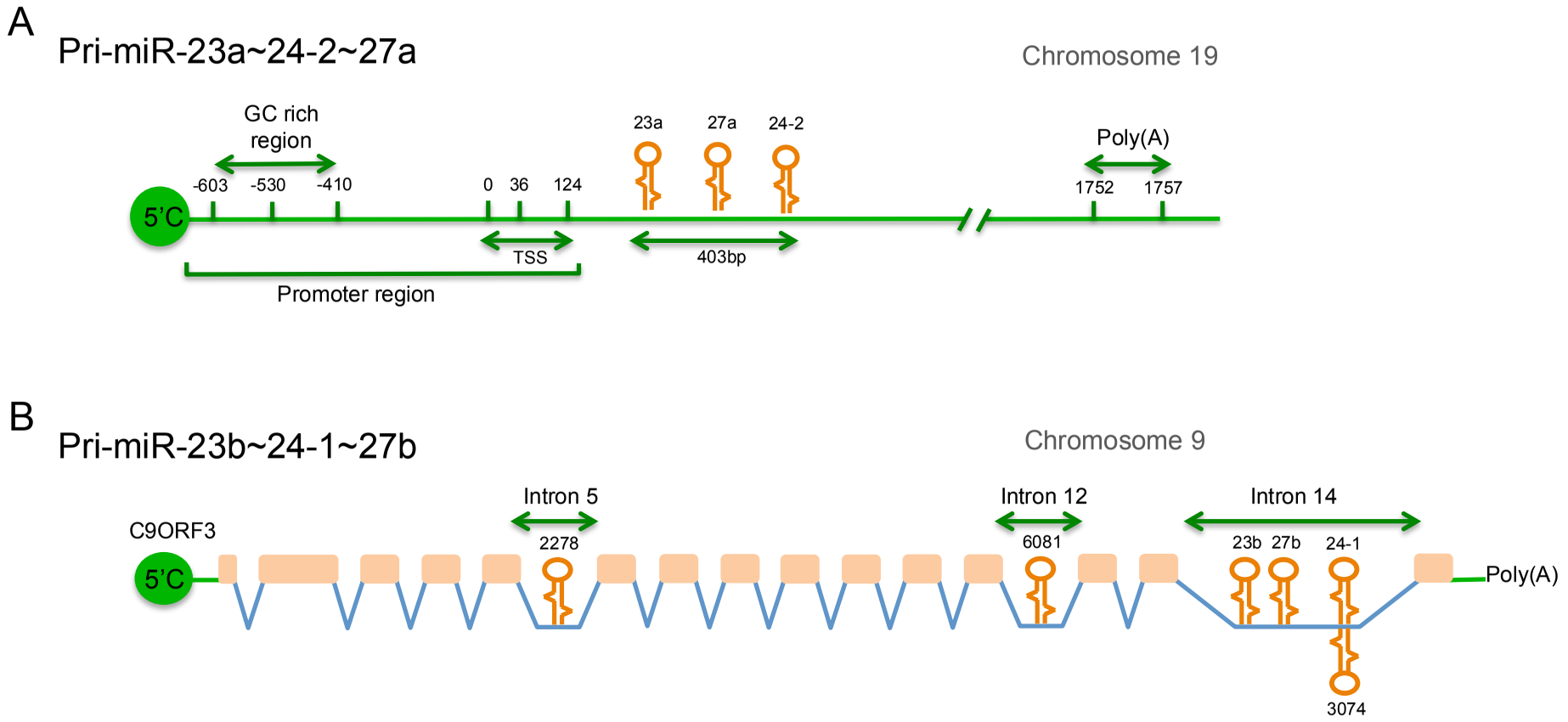

Figure 1.4 Schematic representation of miR-23a~24-2~27a and miR-23b~24-1~27b cluster genes.

(A) Depiction of the primary transcript of miR-23a~24-2~27a cluster, localised on chromosome 19; TSS – transcriptional start site, PolyA – polyadenylation signal. (B) Depiction of the primary transcript of miR-23b~24-1~27b cluster, localised within the intron C9ORF3 gene on Chromosome 19. Promoter region for this miR cluster has not been yet characterized.

1.5.4.1 The role in cancer

Increased expression of all members of miR-23a~24~27a cluster was found in acute lymphoblastic and myeloid leukaemia, chronic lymphocytic leukaemia, breast and gastric cancers, as well as hepatocellular carcinoma cells (HCC) (reviewed in [567]). Although it is not clear if this upregulation is a driver of the underlying pathology or a consequence of it, this miR cluster was implicated in regulating TGFβ driven cell apoptosis with overexpression of entire miRs cluster promoted TGFβ resistance and the growth of HCC cells [575]. Here the effect on apoptosis was mediated by direct targeting of the downstream signalling molecules SMAD 3, 4 and 5 by both miR-23a and miR-23b [542]. A report by Wang et al. showed that miR-24 inhibits type I activin receptor (ALK4) which phosphorylates SMAD2 and SMAD3, further inhibiting TGFβ pathway [576]. Moreover, TGFβ driven upregulation of miR-27a inhibits DC-mediated differentiation of T_H1/T_H17 cells and promotes T_{REG} phenotype through secretion of IL-10, thus securing immune evasiveness of the tumour [577].

Supporting angiogenesis is another way of promoting tumour growth and metastases. Repression of TRIB3 (Tribbles-like protein-3) by miR-24 attenuates the effect of TGFβ and BMP and promotes angiogenesis in response to wound healing [578]. In breast cancer, miR-27a was shown to indirectly increase the activity of Sp1 TF and promote proliferation and angiogenesis by upregulating VEGF and its receptors [579]. Similarly, miR-27b was shown to target Notch ligand Dii4, Sprouty 2, PPARγ and semaphorin 6A to exhibit its pro-angiogenic effects, while its overexpression led to improved tissue revascularization [580-582]. In fact, high constitutive expression of miR-23a by human umbilical vein endothelial cells (HUVECs) suggests an important role of this cluster in vascular homeostasis [583].

Naturally, the most direct way of promoting tumour growth is through the regulation of the cell proliferation and apoptosis pathways. Here, miR-27a together with miR-96 and miR-182 are shown to inhibit FOXO-1 TF involved in apoptosis, cell cycle and metabolism which may be crucial to the maintenance of an aggressive phenotype in breast cancer cells [584]. Inhibition of miR-27a encourages cells to enter G2-M phase through the induction of Myt-1 [585]. In oral squamous cell carcinoma overexpression of miR-24 targeted kinase

inhibitory protein 2 (KIP2 or p57) tumour suppressor and promoted tumorigenesis [586]. In hormone-insensitive prostate cancer miR-24 regulated Fas-associated factor-1 (FAF-1) and displayed significant anti-apoptotic effect [587]. At the same time, miR-24 appears to repress cell proliferation through a repression of MYC, E2F2 cyclins and associated genes [588].

In some cases, loss of miR-23~24~27 clusters also led to disease development. For example, reduced expression of all members of miR-23~24~27a cluster was described in acute promyelocytic leukaemia, while the lack of miR-27a and miR-23b was found in malignant melanoma cells [589,590]. Interestingly, reduced expression of miR-23a and miR-27a was associated with autism disorders and miR-24 with schizophrenia, implicating this miR cluster in a broad range of tissues and pathologies [591,592].

1.5.4.2 The Role in Immunity

Just after the beginning of this project, a seminal paper by Zhu et al unequivocally implicated miR-23b in IL-17 driven inflammation, demonstrating a correlation between low levels of the miR and high levels of the cytokine in the synovial tissue from RA patients [593]. This was mirrored in the CIA murine arthritis model, where miR-23b was downregulated in the synovium after 15 days of the arthritis onset. Moreover, adenoviral delivery of miR-23b prevented the formation of bone erosions, while adenoviral delivery of miR-23b inhibitor-induced dramatic erosive bone loss. The authors have demonstrated that IL-17 inhibited the expression of miR-23b via NFκB in human FLS cells. Reduced expression of miR-23b, in turn, fails to regulate IKKα, TAB2 and TAB3 signalling molecules perpetuating inflammation. Unfortunately, it is unclear to which promoter sequence authors allude to since the given primer sequences do not correspond to any murine genome. Considering the intronic placement of both human and murine miR-23b it is possible that IL-17 also inhibits host gene expression, which was not acknowledged by authors of this work. An additional shortcoming of this study was the lack of consideration given to possible roles that miR-23a play in this process. Nevertheless, this was the first significant demonstration of the critical involvement of a member of the miR-23~24~27 cluster in autoimmune disease and, particularly, RA.

1.5.4.2.1 The role in monocytes and macrophages

Regulated by the TF PU.1, miR-23a~24~27a cluster plays a decisive role in promoting myelopoiesis over lymphopoiesis [568]. This miR cluster is also more abundant in myeloid progenitors and mature myeloid cells than in lymphocytes [568]. On an individual level, all members of the cluster were shown to have an effect on the function of monocytes and macrophages. For example, rapid downregulation of miR-24 is essential for both M-CSF-induced differentiation of monocytes to macrophages and GM-CSF-IL-4 induced differentiation into monocyte-derived DCs [594]. Re-introduction of miR-24 resulted in impaired immune response to LPS stimulation and lower production of TNFα, IL-12 and IL-6 cytokines by mature macrophages [594]. Additionally, overexpression of miR-24 led to impaired antigen presentation capabilities of both macrophages and DCs [595].

In concordance with this, other members of the cluster play roles in myeloid activation. IFNα induced repression of miR-23a relives Blimp-1 (B lymphocyte-induced maturation protein 1) and promotes differentiation of pDCs, aiding anti-viral immune response [451]. In contrast, Zheng et al. have shown that IFNα inhibition of miR-27a forms part of a negative feedback loop, whereby miR-27a targets two negative regulators of type I IFNs – Siglec1 (sialic acid-binding Ig-like lectin) and TRIM27 (E3 ubiquitin ligase tripartite motif-containing protein 27) [596]. In this model, the initial expression of IFNα leads to a reduction in miR-27a and consequential de-repression of IFNα inhibitors, thus safeguarding the extent of inflammatory response providing the mechanism by which mice lacking miR-27a exhibit aggravated viral replication in vivo [596]. In a separate work, miR-27a was shown to inhibit IL-12 production by DCs and, consequently, DC-mediated differentiation of T_H1/T_H17 cells [577]. Anti-inflammatory role of miR-27a was also demonstrated when the overexpression of this miR triggered the release of IL-10 in primary transfected monocytes [597].

Given the profound role of miR-23a~24~27a cluster on the differentiation of monocytes, it is no surprise that it also impacts differentiation of osteoblasts. In bone remodelling, miR-23a cluster expression was directly suppressed by Runx2 TF, an essential regulator of osteoblastogenesis [598]. In turn, each member of the miR cluster targets SATB2, a protein that synergizes with Runx2 to promote

bone formation. The authors believe that this allows a twofold activation of the osteoblastogenesis, by which initially upregulated Runx2 induces the activation of accessory protein by repressing corresponding miRs [598]. Unfortunately, no data is yet available on the function of this pathway during inflammation, where overexpression of paralogue miR-23b exhibited a strong protective role [593]. Certainly, in RA FLS cells miR-27a expression inhibited the invasive phenotype and limited *in vitro* migratory capacity [599]. High levels of miR-27a also reduced the expression of damaging molecules, such as MMP2, MMP9 and MMP13. Understandably, miR-27a levels were low in the serum, synovial tissue and FLS cells from RA patients with active disease [599].

MiR-23~24~27 clusters may play additional roles in the RA co-morbidities beyond the regulation of the inflammation. New data has emerged describing their ability to suppress differentiation of adipocytes, control atherosclerosis and mediate cardiac hypertrophy [600-605]. It would certainly be of interest to investigate these pathways in the context of RA.

1.5.4.2.2 The role in T cells

During last year several significant reports have implicated miR-23a~24~27a cluster in the development and, more importantly, the phenotype of T cells. MiR-23a expression is crucial to the early expansion of CD4 T cells, as it protects the cells from reactive oxygen species (ROS) induced necrosis [606]. In murine CD4 T cells, overexpression of the entire cluster negatively impacted all T_H lineages, mainly affecting T_H2 cells through the inhibition of IL-4 and GATA3 [607]. Although the function of miR appears coordinated, the authors noted that overexpression of miR-24 alone can promote T_H1, T_H17 and induced T_{REG} polarisation [607]. Parallel reports have confirmed that miR-24 and miR-27 suppress allergic response by mediating T_H2 differentiation in murine models [608]. Raised expression of miR-23a was also shown to inhibit cytotoxicity of both CD8 T cells and NK cells [609,610]. The only human study to date showed that miR-27a was increased in the PB CD4 T cells from patients with relapsing multiple sclerosis when compared to the remitting phase, with miR-27a playing a pro-inflammatory role [611]. These studies are technically very challenging and more data is required before the roles of different members of this cluster can be concluded.

1.5.4.2.3 The role in drug resistance

Interestingly, the miR-23~24~27 cluster is implicated in several pathways underlying drug resistance in cancer patients. Since some therapeutics are shared between the treatment of RA and certain cancers, this warrants further discussion.

MiR-27a expression has been described in relation to the multi-drug resistance gene 1 (MDR1) in many human cancer cells, thus conferring resistance to a broad range of treatments [612,613]. It appears that inhibition of miR-27a somehow suppresses MDR1 and P-glycoproteins, thus allowing the intracellular accumulation of cytotoxic drugs. With regards to other cluster members, p53 mediated apoptosis was shown to increase the expression of miR-23a resulting in the direct inhibition DNA topoisomerase I, and promotion of apoptosis [614]. It is this mechanism that miR-23a expression aids the effect of etoposide, a topoisomerase inhibitor often used for its cancer suppression properties [614]. Similarly, miR-24 was also shown to target topoisomerase I and promote etoposide-induced apoptosis [615,616]. Nevertheless, of most relevance is the report describing a polymorphism in DHFR gene, which impairs its regulation by miR-24 and promotes resistance to the treatment with MTX [617]. Authors describe a naturally occurring change in the 3'UTR region of DHFR gene that renders it insensitive to the miR-24. However, the effect of miR upregulation or inhibition on the levels of DHFR were carried out in the HT1090 cells, and the frequency of SNP or its impact on the MTX in primary human cancer was never tested.

1.6 Objectives

We hypothesise that peripheral blood monocytes from patients with drug-resistant RA have distinct miR signatures, which could be informative of underlying pathogenic processes. Therefore the aims of this study were:

1. To identify miR species, which are differentially regulated in patients with poor response to treatment with conventional DMARDs agents, or biologics therapies compared to those who have good disease control with one or two DMARD agents

2. Once identified, to determine factors that regulate these novel miRs in PB monocytes

3. To identify and utilise an experimental model, which allows manipulation of the miR expression, aiding the discovery of molecular targets and function of these miRs

4. To explore the role of these miRs in the inflammation and drug resistance of RA

2 Materials and Methods

2.1 General Buffers and Reagents

Complete RPMI- RPMI 1640 media supplemented with 10% foetal calf serum (FCS), 2mM L-Glutamine, 100 U/ml penicillin, 100 µg/ml streptomycin (all Invitrogen).

Complete DMEM- DMEM media supplemented with 10% FCS 2 mM L-Glutamine, 100 U/ml penicillin, 100 µg/ml streptomycin (all Invitrogen).

Wash media- RPMI 1640 medium supplemented with 100 U/ml penicillin, 100 µg/ml streptomycin.

MACs/FACs Buffer- Dulbeccos Phosphate Buffered Saline (dPBS) supplemented with 2 % FCS and 100 U/ml penicillin, 100 µg/ml streptomycin.

ELISA Wash buffer- 1x dPBS was supplemented with Tween 20 to a final concentration of 0.05 % (v/v).

ELISA Assay Buffer- 1x dPBS was supplemented with bovine serum albumin (BSA) (Sigma) to a final concentration of 0.5 % (w/v).

Tris-acetate EDTA (TAE) buffer- concentrated 50x stock solution of TAE includes dissolved 242 g Tris base in 750 ml deionized water. To this, add 57.1 ml glacial acetic acid and 100 ml of 0.5 M EDTA (pH 8.0). Adjust the solution to a final volume of 1 litre.

SOC medium- 2 g of Tryptone, 0.5 g yeast extract, 2 ml of 5 M NaCl, 2.5 ml of 1 M KCl, 10 ml of 1 M $MgCl_2$, 10 ml of 1 M $MgSO_4$ and 20 ml of glucose made up to 100 ml with distilled water and autoclaved.

5X STOP Dye- 4 gram of sucrose, 1.5 ml of 0.5 M EDTA (pH 8.0), 1 ml of 1 M KCl and 0.2 ml of Tris-HCl (pH 8.0), 20 mg of bromophenol blue made up to 10 ml with distilled water.

Luria Bertani (LB) media- 10 g tryptone, 5 g yeast extract, 10 g NaCl made up to 1 litre with deionised water, pH adjusted to 7.5 with NaOH and autoclaved.

Luria Bertani (LB) Agar media- 10 g tryptone, 5 g yeast extract, 10 g NaCl made up to 1 litre with distilled water and autoclaved.

TE buffer- 1ml of Tris-HCl (pH 8.0) and 0.2 ml of 0.5M EDTA made up to 100 ml with distilled water.

2.2 Cell Culture

Cell culture experiments were performed in the laminar flow hood. Cells were cultured in the appropriate medium (see below), in an incubator with 5% CO_2 /95% O_2 at 37°C, unless otherwise stated.

2.2.1 Culture of Primary Human Cells

2.2.1.1 Patient blood samples

Recruitment of patients took place between March 2010 and September 2011 under the ethical approval from Local research Ethics Committee (West of Scotland) REC ref Number 10/S0703/4 (R&D Ref: GN09RH699). All participants gave their written informed consent to participation. Study patients were recruited across three different sites: at Glasgow Royal Infirmary, Stobhill General Hospital and Gartnavel General Hospital as a part of rheumatology outpatient clinic or day unit. Dr Derek Baxter primarily conducted recruitment with the help from Professor Iain McInnes, Dr Duncan Porter and fellow Dr Eva Ruzicka. All participating patients had a clinical diagnosis of RA meeting 1987 ACR criteria. Other inclusion and exclusion criteria are listed in Table 2.1. Clinical assessment and blood samples for epigenetic analysis were taken on the same day to minimise variation in the clinical status between the patients. Patients were categorised as Responders or Non-responders to the treatment according to the disease activity score based on the 28 joints count (DAS28 score) at the time of the recruitment.

The treatment category of disease modifying anti-rheumatic drugs (DMARDs) involved patients who were on active treatment with Methotrexate,

Sulphasalazine, Hydroxycholoquine or combination of 2 or 3 of these medications. The other category included patients on biological agents, such as anti-TNFα therapy (Infliximab, Etanercept and Adalimumab) or patients receiving either anti-CD20 agent Rituximab or anti-IL-6R agent Tocilizumab.

Group	Inclusion Criteria	Exclusion Criteria
1. Healthy Controls	• Lack of current inflammatory, degenerative or otherwise symptomatic disease at the time of recruitment	• Current or recent joint injury • Family history of established inflammatory or autoimmune disease
2. DMARDs Responder Patients	• Rheumatoid Arthritis (meeting ACR 1987 criteria) • DAS28-ESR (or CRP) less then 3.2 • Disease duration greater then ten years • Prior therapy with two or fewer DMARDs lasting greater then three months	• DAS28-ESR or CRP above 3.2 at the time of recruitment • Previous use of third DMARD or biologic agent • Active disease within recent 3 months
3. DMARDs Resistant Patients	Eligibility of biologic therapy according to BSR 2010 criteria: • DAS28-ESR or CRP >5.1 on 2 occasions a month apart • Failing at least 2 previous DMARDs, including Methotrexate and • Positive RF or anti-CCP antibodies	• Active infection, septic arthritis of native or prosthetic joint within last year • NYHA grade 3 or 4 heart failure • Demyelinating disease • Malignancy
4. Biologics Resistant Patients	• Rheumatoid Arthritis (meeting ACR 1987 criteria) • DAS28-ESR or CRP > 3.2 • Previous treatment with two or more biologic agents	• Active infection • Recent surgery • Malignancy

Table 2.1 Inclusion and exclusion criteria for healthy controls and patient cohort study.

2.2.1.2 Separation of peripheral blood mononuclear cells

Blood samples from RA patients and healthy volunteers were processed by senior technician Lynn Stewart. Buffy coats obtained from Scottish National Blood Transfusion Service (SNBTS) were processed by myself. For the separation of PBMCs samples or buffy coats: each was diluted with equal amounts of wash media and layered over Histopaque®-1077 (Sigma) and centrifuged at 21,00 rpm for 20 minutes at room temperature. Next, the layer of mononuclear cells was collected in a new sterile 50 ml tube and washed with equal amount of wash media. After this step, cells were resuspended in 25 ml of cold MACS buffer and

kept on ice for further processing. Live cell number was counted with trypan blue exclusion (Sigma).

2.2.1.3 Isolation of $CD14^+$ monocytes from PBMCs

Isolation of $CD14^+$ monocytes in RA patient's cohort and healthy volunteers was performed by senior technician Lynn Stewart. Isolations of $CD14^+$ monocytes from buffy coats and subsequent RA patient samples were performed by myself. AutoMacs (Miltenyi Biotec) separator was used for this procedure and original protocol was followed. According to it, cells were resuspended in 80 µl MACs buffer per $1x10^7$ cells and appropriate volume (usually 500 µl), depending on the required number of cells, was transferred to a new sterile 15 ml tube and filtered using 70 µm filters (BD Falcon). Samples and anti-CD14 conjugated magnetic beads (Miltenyi Biotec) were then placed in the appropriate AutoMacs racks, the PosselD programme, which ensures highest resulting cell purity, was used for automatic separation. Purity of cells was assessed by flow cytometry and was typically >95%.

2.2.1.4 Culture of primary human monocytes

For the experiments with primary human monocytes, cells were cultured at a density of $0.25x10^6$ cells per well of 48-well plate in 250 µl of complete RPMI medium, supplemented with 50 ng/ml of M-CSF or GM-CSF medium (both Peprotech). Cells were kept in these conditions for 24 hours before any stimuli were added..

2.2.1.5 Culture of primary human macrophages

For differentiation of human macrophages, isolated $CD14^+$ cells were cultured at a density of $0.25x10^6$ cells per well in a 24-well plate in 500 µl of complete RPMI medium, supplemented with 50 ng/ml of M-CSF or GM-CSF medium for 7 days (both Peprotech). The medium was replaced on day 3.

2.2.2 Culture of Human Cell Lines

2.2.2.1 THP-1 Cells

THP-1 cell line cells were cultured in 25 ml of complete RPMI medium in T75 tissue culture flasks (Corning). Cells were passaged three times a week. Before passage, cells were washed in complete RPMI, centrifuged at 1,500 rpm for 5 minutes and then counted. Cells were seeded at a density of $2x10^6$ in 25 ml of complete RPMI and cultured under normal culture conditions.

2.2.2.2 miR-23a~24-2~27a sponge THP-1 cells

THP-1 cells were stably transfected with of miR-sponge constructs or empty vector control and were cultured in 25 ml of complete RPMI medium in T75 tissue culture flask or in 10 ml of complete RPMI medium in T25 tissue culture flask (Corning; details of sponge constructs are described in Chapter 5). For selection, these cells were cultured along with 800 µg/ml of the antibiotic Geneticin (G418, Invitrogen). Cells were seeded at a density of $1x10^5$/ml in complete RPMI.

2.2.2.3 PMA differentiation of THP-1 cells and THP-1 miR sponges

Before plating, THP-1 cells were counted and washed with wash medium. Cells were seeded at $0.25x10^6$ cells per well of a 24-well plate in 500 µl of complete RPMI medium, supplemented with 25 ng/ml of PMA medium and cultured for 7 days. Optimisation of culture conditions indicated that best results were achieved if complete RPMI medium was replaced on day 3 only.

2.2.2.4 HEK293 Cells

HEK293 cells were cultured in complete DMEM medium in T75 tissue culture flasks (Corning) and passaged twice a week. To dissociate cells from the flask: media was removed, cells gently washed with sterile Dulbeccos PBS (Gibco; dPBS) and then incubated for 3 minutes at 37°C with 5 ml 0.05% Trypsin EDTA (Invitrogen). Following this, 7 ml of complete DMEM was added to the flask to inactivate trypsin and cells centrifuged at 1,500 rpm for 5 minutes at room temperature. Cells were then seeded at a density of $5x10^4$/ml in a fresh T75 Flask in 15 ml complete DMEM and cultured under normal culture conditions.

2.2.2.5 Cryopreservation of the cell lines

For future use, cell lines were stored in liquid nitrogen. Cells were frozen in cryovials at a concentration of $1x10^6$ in 10% DMSO and complete RPMI medium. Cells were stored at -80°C overnight and then transferred to liquid nitrogen.

2.2.3 Cell Stimulation

Primary human $CD14^+$ monocytes, differentiated human macrophages and THP-1 cells were stimulated with cytokines and TLR ligands to determine their effects on the expression of miR-23a~24~27a cluster and cytokine production. Stimuli were added to individual wells in the pre-concentrated form in 50 µl of medium. Stimulatory conditions varied for each experiment and details are stated in the figure legend for each graph.

2.2.4 Cell Transfection

Transfection of primary cells and cell lines were performed using transfection protocols and reagents that were deemed most effective from published literature and previous experience within the laboratory.

2.2.4.1 Transfection of primary human monocytes

Primary human monocytes isolated from buffy coats or from freshly donated samples were transfected with miR mimics and miR inhibitors using N-TER™ reagent (Sigma). N-TER™ is a peptide-based transfection reagent optimised specifically for the delivery of siRNA and miR.

Enriched peripheral blood (PB) or buffy coat $CD14^+$ monocytes were seeded in 24-well plates at a concentration of $3.5x10^5$ cells in complete RPMI 1640 media. Cells were transfected with either mimics for miR-23a, miR-24, miR-27a or scrambled control at a concentration of 20 nM. N-TER™ peptide and 5 µM stock of mimic were thawed at room temperature for ~10 minutes. Samples were prepared as shown in Table 2.2. Contents of Tube A were added to Tube B, vortexed briefly and allowed to sit at room temperature for 15-20 minutes. Transfection complex was then added directly onto the cells. Cells were placed in incubator for 24-48 hours prior to analysis.

Reagent	Tube A		Reagent	Tube B
miRNA (5 µM)	3.25 µl		N-TER™	2 µl
siRNA Dilution Buffer	9.25 µl		Water	10.5 µl
Final Volume	12.5 µl		Final Volume	12.5 µl

Table 2.2 Preparation of N-TER™ transfections for single well of 24-well plate.

2.2.4.2 Transfection of HEK293 cells

HEK293 cells were seeded shortly before transfection at a density of $1x10^5$ per well of 24-well plate in 500 µl of complete DMEM. Next, 400 ng of plasmid DNA was diluted in 60 µl of OPTIMEM (Invitrogen). To this 2.8 µl of 2 µM miR mimic was added to the diluted DNA giving a final concentration when added to the cells of 10 µM. To the DNA-miR mix, 1.5 µl of Attractene (Qiagen) transfection reagent was added then mixed by vortexing. Sample was then incubated for 10-15 minutes at room temperature before being added drop-wise to the cells. Cells were incubated for 24-48 hours prior to analysis.

Transfections with plasmid alone were performed as described above omitting miR.

2.2.4.3 Generation of stably transfected THP-1 cells

Prior to transfection, 10 µg of plasmid DNA was linearized using 20 units of *Ase*I (NEB) in a 50 µl reaction in CutSmart™ Buffer. Once digested DNA was sterilized by ethanol precipitation. The DNA pellet was resuspended in 100 µl of dPBS. Next, $1x10^7$ THP-1 cells were spun down at 300 g for 5 minutes, supernatant removed and cell pellet resuspended in 700 µl of dPBS before being added to the linearized plasmid DNA. The cell/DNA mixture was then added into a 4 mm electroporation cuvette (Invitrogen) and placed into Gene Pulser II (Bio-Rad). The electroporation cuvette was pulsed using parameters set to 310 V, 950 µF and resistance infinite. Cells were then removed into 20 ml of complete RPMI

media in a T75 tissue culture flask and incubated overnight. The following day G418 (Invitrogen) was added to a concentration of 800 µg/ml. After 1 week cells were split 1 in 5 in fresh media containing G418 and allowed to grow undisturbed for 2-3 weeks until stably transfected clones appeared.

2.3 Flow Cytometry

2.3.1 Extracellular staining protocol

Before staining, $1x10^6$ cells were resuspended in 1 ml of FACS staining buffer and, from this, 100 µl of cells were added per FACS tube (BD). Each experiment had tubes for unstained cells, viability staining, individual fluorochrome tubes for the compensation setting, isotypes, fluorescence minus one (FMO) tubes that had all other antibodies apart from the antibody of interested (instead, isotype was added) and final tube with all staining antibodies. For the purity check CD14-PE conjugated and associated IgG-PE isotype controls were used (Miltenyi Biotech). For the surface IL-6R staining Il-6R-PE conjugated and IgG-PE isotype were used (Biolegend).

After each step cells were washed with 500 µl of FACS buffer followed by centrifugation at 300 g for 5 minutes. First, cells were incubated with 10 µl of Human Fc block (Miltenyi Biotech) for 20 minutes at room temperature to prevent non-specific binding. After second wash, appropriate antibodies and isotypes were added in the quantities indicated by the manufacturer's and cells were incubated for 25 minutes at 4°C. Following this, cells were washed with 500 µl of FACS buffer and resuspended in 300 µl of FACS buffer, if there were to be analysed immediately.

If analysis was to be done the next day, cells were resuspended in 300 µl of 4% v/v paraformaldehyde solution (PFA; diluted in dPBS from 16% w/v formaldehyde solution, methanol free, Pierce) vortexed and stored in the dark at 4°C until required . FACSCalibur™ (BD) or MACS Quant (Miltenyi Biotech) were used for the analysis.

2.3.2 Intracellular staining of phosphorylated STAT3

Intracellular phosphorylated STAT3 staining was performed using mouse anti-human STAT3 (pY705) antibody from (BD Biosciences). THP-1 cells were stained as follows. Prior to staining, BD Cytofix™ buffer was pre-warmed at 37°C for 5-10 before use. $1x10^6$ of THP-1 cells in a volume of 1 ml were placed in FACS tubes (BD Biosciences) and stimulated with IL-6 (Biolegend) at a final concentration 100 ng/ml for 13 minutes at 37°C before being fixed with 1 ml of BD Cytofix™ followed by incubation at 37°C for 10 minutes. Cells were then centrifuged at 300 g for 5 minutes and supernatant removed. Pellet was then disrupted by vortex and cells permeablised by adding BD™Phosphflow Perm Buffer II followed by incubation on ice for 30 minutes. Cells were spun at 300 g for 5 minutes, supernatant removed and cells washed with BD Pharmingen™ Stain Buffer, this step was repeated twice. After the second wash, cell pellet was resuspended in 100 µl BD Pharmingen™ Stain Buffer. To this 10 µl of mouse anti-STAT3 (pY705) was added directly to the cells. Cells were mixed gently and incubated at room temperature for 30 minutes. Cells were then pelleted by centrifugation at 300 g for 5 minutes, supernatant discarded and finally the pellet was resuspended in 2 ml of BD Pharmingen™ Stain Buffer. FACS analysis was performed using either FACSCalibur™ (BD) or MACS Quant (Miltenyi Biotech). Mouse IgG2a κ-PE was used as an isotype control (BD Bioscience).

2.3.3 Assessment of transfection efficiency

For the assessment of transfection efficiency fluorescent Dy547-labeled control mimic of scrambled miRs derived from C. elegans (cel-miR-67) was used (Thermo Scientific). This compound has absorbance/emission of 557/570 nanometres allowing detection on the FACS analyser. In experiments where cells were transfected with cells transfected with Dy547-labeled control were also included to allow estimation of transfection efficiencies. Cells were collected into a FACS tube and washed with FACS buffer, before centrifugation at 400 g for 5 minutes. Cells were then resuspended in 300 µl of FACS buffer and analysed by FACS.

2.3.4 Assessment of cellular viability

If cells were to be analysed live then 5 µl of 7AAD viability staining solution (Biolegend) was added direct to cells 10 minutes before analysis on the flow cytometer.

If cells were to be fixed and stored overnight in 4% PFA solution, Fixable Viability Dye eFluor®506 (eBioscience) was used. The viability staining was performed in a separate step, after completing surface staining. For this cells were resuspended in 1 ml of FACS buffer and 1 µl of viability dye added per test tube during vortexing. Cell where than incubated for 30 minutes at 4°C in the dark, before a final wash with FACS buffer and re-suspension in 300 µl of 4% PFA fixing solution.

2.4 Quantitative Polymerase Chain Reaction (qPCR)

2.4.1 RNA Isolation from Cells

Total RNA was purified using Qiagen's miRNeasy kit, which is specifically formulated to retrieve the maximal amount of miRs from cells. Mature miRs in particular are purified with lower efficiencies from standard RNA isolation kits due to their tight association with the RISC complex. In all cases the protocol was used as described in the manufacturer's instructions. I will therefore discuss it only briefly here.

Cells, either purified $CD14^+$ cells isolated from PB or buffy coats, or THP-1 cells were initially spun at 300 g for 3 minutes to remove media. Cells were then washed with dPBS, spun again at 300 g for 3 minutes and dPBS removed. The cells were lysed by the addition of 700 µl of Qiazol reagent. As a rule of thumb, 700 µl was used for any cell number up to 3 million cells. Cell lysates were vortexed for 30 seconds and allowed to stand at room temp for 5 minutes. At this stage 140 µl of chloroform was added to each sample and shaken vigorously by hand. Samples were then spun at 12,000 g for 15 minutes at 4°C. After centrifugation the upper (clear) aqueous phase was carefully removed and transferred in to a new 1.5 ml tube followed by 525 µl of 100 % ethanol. The samples were mixed by inversion before being pipetted into individual RNeasy spin columns. Columns were spun at 8,000 g for 15 seconds at room temperature and the flow through discarded. The RNA at this stage is bound to the column.

Columns were then washed with 700 µl of RWT buffer and spun at 8,000 g for 15 seconds. Flow-through from columns were discarded as before. The next stage of the protocol involves the columns being washed with 500 µl of RPE buffer, spun at 8,000 g for 1 minute and the flow-through discarded, this step was repeated twice. The samples were then spun for 1 minute at 8,000 g to dry the columns. In the final elution step, the columns were transferred into fresh RNAse-free 1.5 ml micro-centrifuge tubes and 30-50 µl of nuclease free water added carefully to the bottom of each column. Columns were allowed to stand at room temperature for 1 minute before being centrifuged at 8,000 g for 1 minute. Finally, the column was discarded and the RNA samples placed on ice for immediate use or stored at -20°C or -80°C for short or long-term storage respectively.

Note DNAse digests were not generally performed on samples as all qPCR assays were designed to span or overlap exon-intron junctions meaning that they were specific for cDNA.

2.4.2 Measuring Nucleic Acid Concentration

The quantity and quality of RNA or DNA samples were determined using a Nanodrop ND-1000 spectrophotometer (ThermoScientific). Depending on the type of nucleic acid being quantified the Nanodrop was set to measure DNA or RNA. The sample was blanked against nuclease free water prior to measurements. Two microliters of sample was typically measured. The Nanodrop returns readings of nucleic acid concentration (ng/ml) along with 260/280 and 230/260 ratios. A 260/280 reading of ~1.8 and ~2.0 are expected from pure DNA and RNA samples respectively. The 230/260 measurement gives a secondary indication of sample purity, ideal readings should be ~2.0, values significantly lower than this generally indicate contamination with carbohydrates or phenols.

2.4.3 SYBR Green Protocol

SYBR green qPCR was used to detect both mRNA and miR expression levels.

2.4.3.1 cDNA Synthesis from mRNA

Depending on the nature of the target RNA to be quantified different cDNA kits were used.

Where only target mRNA levels were to be quantified I used the High Capacity cDNA kit (Applied BioSystems). cDNA reactions were performed according to manufacturer's instructions and will be described only in brief here.

Initially nanodrop quantified RNA samples were normalised to a concentration of 10 ng/µl. A 2x cDNA reaction master-mix was prepared in thin-walled 200 µl PCR tubes (Starlab) as shown in Table 2.3. To this 10 µl (100 ng) of RNA was added and samples incubated in a thermocycler using the cycling conditions shown in Table 2.4. Prior to use samples were diluted 1 in 10 in nuclease-free water. For short-term storage, 1 or 2 days, samples were stored at 4°C or at -20°C for longer-term storage.

Component	Volume per reaction (µl)
10xRT Buffer	2.0
dNTP (100mM)	0.8
10XRT Random Primers	2.0
MultiScribe™ Reverse Transcriptase	1.0
RNase Inhibitor	1.0
Nuclease-free water	3.2
Total per reaction	10.0

Table 2.3 High Capacity 2x master mix.

Settings	Step 1	Step 2	Step 3	Step 4
Temp	25°C	37°C	85°C	4°C
Time	10 minutes	120 minutes	5 minutes	∞

Table 2.4 Cycling parameters High Capacity cDNA synthesis

2.4.3.2 cDNA synthesis miRNA & mRNA

In instances where miRNA or miRNA and mRNA levels were required to be quantified Qiagen's miScript II Reverse Transcription kit was used. This kit offered two options depending on whether miR only or both miRNA and mRNA were to be measured. The miRNA-only protocol used the HiSpec buffer, while the HiFlex buffer was used for miRNA and mRNA quantification. In either instance the manufacturer's instructions were followed. Briefly, RNA samples were normalised to concentrations of 10 ng/ml. A 2x cDNA reaction master-mix was prepared in thin-walled 200 µl PCR tubes (Starlab), as shown in Table 2.5 below. To this 10 µl (100 ng) of RNA was added and samples incubated in a thermocycler using the cycling conditions shown in Table 2.6. Prior to use samples were diluted 1 in 10 in nuclease-free water. For short-term storage, 1 or 2 days, samples were stored at 4°C, for longer term at -20°C.

Component	Volume per reaction (µl)
5xHiFlex or HiSpec Buffer	4.0
10x Nucleics mix	2.0
Nuclease free water	2.0
Reverse Transcriptase	2.0
RNA	10.0
Total per reaction	20.0

Table 2.5 miScript II RT reaction.

Settings	Step 1	Step 2	Step 3
Temp	37°C	95°C	4°C
Time	60 minutes	5 minutes	∞

Table 2.6 Cycling parameters miScript II cDNA synthesis

2.4.3.3 SYBR green PCR mRNA detection

SYBR green PCR were performed using SYBR® Select master-mix (Applied Biosystems). Reactions were set up according to manufacturer's instructions, outlined in Table 2.7.

Component	Volume per reaction (µl)
SYBR® Select master-mix	5.0
Forward and Reverse Primers (5nM each primer)	1.0
cDNA template	1.0
Nuclease free water	3.0
Total per reaction	10.0

Table 2.7 Components per well SYBR® Select reaction.

Reactions were plated in triplicate into either 96 or 384-well plate formats depending on the size of the experiment. Plates were sealed with a MicroAmp optical adhesive cover (Applied Biosystems). A no template control was included for each primer set used. Plates were centrifuged for 300 g for 1 minute before being placed in a StepOnePlus™ Real-Time PCR System, for 96-well plate or a QuantStudio™ 12K Flex Real-Time PCR System for a 384-well plate format. Cycling parameters used are shown in Table 2.8. A melt curve was performed after each run to confirm the presence of a single amplified product. QPCR primers used in this thesis are listed in Table 2.11.

Step	Temperature	Duration	Cycles
UDG* Activation	50°C	2 minutes	1X
AmpliTaq Fast DNA polymerase, UP activation	95°C	2 minutes	1X
Denature	95°C	1 seconds	40X
Anneal/Extend	60°C	30 seconds	

Table 2.8 Fast cycling parameters for SYBR® select qPCR
* Uracil DNA Glycosylase

2.4.3.4 SYBR green PCR for microRNA quantification

SYBR green PCR for miRs were performed using miScript SYBR Green PCR kit (Qiagen). Reactions were set up according to manufacturer's instructions, outlined in Table 2.9.

Component	Volume per reaction (µl)
QuantiTect SYBR Green master mix	5.0
10x miScript Universal Primer	1.0
10x miScript miR-specific primer	1.0
Template*	1.0
Nuclease free water	2.0
Total per reaction	10.0

Table 2.9 Components per well QuantiTect SYBR® reaction
* cDNA prepared using miScript II Reverse Transcription kit (Qiagen).

Reactions were plated in triplicate into either 96 or 384-well plate format depending on the size of the experiment. Plates were sealed with a MicroAmp optical adhesive cover (Applied Biosystems). No template controls were included for each primer set used. Plates were centrifuged for 300 g for 1 minute before being placed in a StepOnePlus™ Real-Time PCR System, for 96-well plate or a QuantStudio™ 12K Flex Real-Time PCR System for a 384-well plate format. Cycling parameters used are shown in Table 2.10. Primer assays for hsa-miR-23a, hsa-miR-24, hsa-miR-27a, hsa-miR-23b, hsa-miR-27b and RNU6 were purchased from Qiagen.

Step	Temperature	Duration	Cycles
Taq Polymerase activation	95°C	2 minutes	1X
Denature	95°C	15 seconds	40X
Annealing	55°C	30 seconds	
Extension	70°C	30 seconds	

Table 2.10 Cycling conditions for miScript SYBR green PCR.

2.4.4 Analysis of PCR Results

For each target gene a relevant and unchanging housekeeping gene was included, GAPDH or 18S for mRNA or RNU6 for miRs. The Cycle Threshold (Ct) values of each well were exported in to an EXCEL spreadsheet (Microsoft) for analysis as described in the next two sections.

2.4.4.1 $2^{-\Delta Ct}$ quantification

The expression of target genes was expressed as $2^{-\Delta CT}$. This involved the subtraction of the Ct value of the housekeeping gene from the Ct value of the target gene producing a ΔCt value for each sample. The final value was then expressed as $2^{-\Delta CT}$.

2.4.4.2 $2^{-\Delta\Delta CT}$ Quantification- Fold change Relative Quantification

Relative Quantification (RQ) represents gene expression values as fold change relative to control samples. Initially the Ct value of housekeeping gene was subtracted from target gene generating ΔCt value for each sample. The ΔCt value of the control sample was then subtracted from the experimental sample giving the samples ΔΔCt value. The final value was then expressed as $2^{-\Delta\Delta Ct}$, the resulting value indicating the fold change of experimental sample relative to control.

2.4.4.3 Absolute quantification

Standard curves of known target template copy numbers were generated by dilution of plasmid DNA containing the amplicon of the qPCR primers. A top standard of 10^7 copies was diluted 1 in 10 to 100 copies. Standards were generated for both target and housekeeping genes. Standards were run on qPCR machine to generate Ct values. The standard curve was created by plotting $\log_{10}$(copy number) versus Ct value. Copy numbers of experimental samples were interpolated from the standard curve. Values then presented as copies of target per 10,000 copies of GAPDH or per 10^6 copies of 18S.

2.4.4.4 QPCR primers

Primer name	Sequence
sIL-6R Fw	TCTCCACAAGCGCCTTCG
sIL-6R Rev	CTCAGGGCTGAGATGCCG
mIL-6R Fw	TGCAATAACCACCCCTGACC
mIL-6R Rev	GTGCCCATGCTACATTTGCC
Total IL-6R Fw	AGGGAGACAGCTCTTTCTACATA
Total IL-6R Rev	AGGCTGCAAGATTCCACAA
GAPDH Fw	GAAGGACTCATGACCACAGT
GAPDH Fw	GTAGAGGCAGGGATGATGTT
Pri-miR-23a Fw	CGTGTTCACAGTGGCTAAGT
Pri-miR-23a Rev	AACTGTGTTTCAGCTCAGTAGG
MTHFR Fw	CTTCATGTTCTGGAAGGACGAG
MTHFR Rev	GTCGTGGATGTACTGGATGATG
DHFR Fw	AATCACCCAGGCCATCTTAAAC
DHFR Rev	ACACCTGGGTATTCTGGCA

Table 2.11 List of QPCR primers

2.5 Molecular Cloning

2.5.1 Creation of Luciferase reporter plasmids

To validate the interaction between miR and its target mRNAs, I created a luciferase reporter plasmid in which regions containing putative miR-binding site were cloned downstream of luciferase open reading frame (ORF) in the pGLOMS2BD vector (gift of Dr Derek Gilchrist) Figure 2.1. Regions of interest were amplified by PCR using proof reading polymerase *Pfu* (Stratagene). A typical reaction is shown in Table 2.12. Genomic DNA isolated from HEK293 cells was used as template. Primers for the amplification of putative miR-23a cluster binding sites were designed using Integrated DNA Technologies (IDT) online PrimerQuest program (https://eu.idtdna.com/site). Primer melting temperature design parameter were set at 60°C.

Regions to be amplified were screened for presence of *Pme*I and *Xho*I sites; if none were present these restriction enzymes (RE) were used for sub-cloning into pGLOMS2BD vector (Figure 2.1 A). If not, alternative compatible restriction enzymes were selected. Once their presence had been excluded, *Pme*I site (GTTTAAAC) would be added onto the 5'end of the Fw primer and *Xho*I site (CTCGAG) onto the 5' end of Rev primers. Primers were manufactured by IDT. A list of the primers used in this work can be found in Table 2.17. Once amplified, PCR reactions were run on a 0.8 % (w/v) agarose TAE gel. Bands of the correct size were excised from the gel and DNA fragments purified using Qiagen's QIAquick gel extraction kit (See section 2.5.6.4).

Component	Volume per Reaction (µl)
10X PfuUltra II buffer	5.0
dNTP mix (25 mM)	0.5
Genomic DNA template	1.0
Fw Primer (10 µM)	1.0
Rev Primer (10 µM)	1.0
PfuUltra II fusion HS DNA polymerase	1.0
Nuclease free water	40.5
Total Reaction Volume	50.0

Table 2.12 Components of *Pfu*Ultra PCR reaction.

Step	Temperature	Duration	Cycles
Denaturation of genomic DNA template	95°C	2 minutes	1X
Denature	95°C	20 seconds	30X
Annealing	55°C	20 seconds	
Extension	72°C	15 seconds per kilobase	
Final extension	72°C	3 minutes	1X

Table 2.13 PCR cycling parameters for the amplification of putative MBS from genomic DNA.

As target regions had been amplified using the proof-reading polymerase *Pfu*, they did not contain terminal 3' adenosine overhangs that are required for the subsequent TOPO cloning into pCR2.1 TOPO (Invitrogen). To overcome this, purified PCR products were incubated with *Taq* DNA polymerase that adds 3' A overhang onto the template DNA. A typical 'A-tailing' reaction is shown in Table 2.14. Reactions were prepared in 200 µl thin walled PCR tubes (Starlab) and incubated in a thermocycler for 30 minutes at 72°C. After treatment with *Taq* polymerase, samples were directly cloned using the TOPO TA Cloning® kit into pCR2.1 TOPO, described in section 2.5.6.4.

Component	Volume per Reaction (µl)
10x *Taq* DNA polymerase buffer	2.5
dATP (25 mM)	0.5
Purified PCR product	20.0
Taq DNA polymerase (5 units/ µl)	1.0
Nuclease free water	1.0
Total Reaction Volume	25.0

Table 2.14 Components of A tailing reaction.

Samples incubated at 72°C for 30 minutes.

Plasmids containing the correct insert were identified by RE digest. The cloning site of pCR2.1 TOPO vector is flanked by *Eco*RI sites, which was used to identify the presence of inserts of the correct size. A typical restriction digest is shown in Table 2.15. Once confirmed, plasmid DNAs were digested with *Pme*I and *Xho*I along with pGLOMS2BD which was digested with *Pme*I and *Sal*I (*Sal*I and *Xho*I generate compatible ends). After RE digestion, 5 µl of STOP dye was added to each sample before being run on a 0.8 % TAE agarose gel alongside a 1 Kb(+) DNA ladder (Invitrogen). Bands corresponding to the insert and cut pGLOMS2BD DNAs were excised from the gel and subsequently purified using QIAquick gel purification kit (Qiagen) described in section 2.5.6.4.

Component	Volume per reaction (µl)
10X CutSmart™ Buffer	2.0
Plasmid DNA (500ng)	Variable
Nuclease free water	Variable
Restriction Enzyme (New England BioLabs) (10 units/µl)	0.5
Total per reaction	20.0

Table 2.15 Standard restriction enzyme digest reaction.

HF enzymes from New England BioLabs were used in these experiments. Reactions were incubated at 37°C for 1 hour.

Purified insert and pGLOMS2BD DNAs were then ligated together using T4 DNA ligase (NEB). A typical ligation reaction is shown in Table 2.16. Ligations were incubated at room temperature for 10 minutes before being transformed into competent DH5α as described in section 2.5.5. Plasmid DNA was isolated from the resulting clones as described in section 2.5.6.1. The correct identity of the plasmids was confirmed by RE digest with *Bam*HI (NEB). Example DNA fragment patterns of pGLOMS2BD and pGLOMS2BD-IL10 are shown in Figure 2.1. Plasmids were then sequenced using the sequencing service provided by Source Bioscience. A forward sequencing primer located at the 3' end of the luciferase ORF, called GLOseq was used (see Table 2.23 for primer sequence). Cultures containing the correct plasmids were next used to inoculate 100 ml of LP broth containing 50 µg/ml ampicillin and grown overnight at 37°C with shaking (200 rpm). Plasmid DNA was then purified from the resulting cultures using the method described in section 2.5.6.2.

Component	Volume per reaction (µl)
10X T4 DNA ligase Buffer	2.0
Vector (100ng)	Variable
Insert (3x molar excess of vector)	Variable
T4 DNA ligase (NEB) (20 units/µl)	1.0
Nuclease free water	Variable
Total per reaction	20.0

Table 2.16 Standard T4 DNA ligase reaction.
Reactions were incubated at room temp for 10 minutes before being transformed in *E. coli*.

Primer name	Sequence
IL-6R 3'UTR (1) Fw	AGATATCAAGCATGCATCCGCCGTACTCTTT
IL-6R 3'UTR (1) Rev	AGTCGACACAGGGTCTCACTTGCTCTGTCA
IL-6R 3'UTR (2) FW	AGTTTAAACTAATCCTAGCACTTTGGGAGGCCA
IL-6R 3'UTR (2) Rev	AGTCGACCAGCCTTTGGTATTTGCTTTCAGG
IL-6ST 3'UTR Fw	AGTTTAAACGCTACATGCCTCAGTGAAGGACTA
IL-6ST 3'UTR Rev	AGTCGACACTGTCCCTAAGCCACTCTGATGA
ERAP1 3'UTR Fw	AGTTTAAACCTTGCCAGGTTCCTGTTATCT
ERAP1 3'UTR Rev	AGTCGACCCAACACTTGGGTTTACGTTG

Table 2.17 List of luciferase assay primers

A

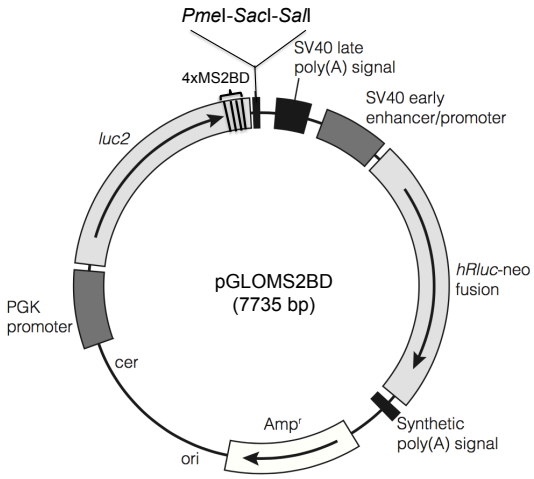

B

```
<Serial Cloner V2.5> -- <20 Nov 2016   14:07>

Restriction analysis of pGLOMSBD2 .xdna [Circular]
Incubated with BamHI

2 fragments generated.

   1:    4,521 bp  -  From BamHI[2792]   To  BamHI[7313]

   2:    3,214 bp  -  From BamHI[7313]   To  BamHI[2792]
```

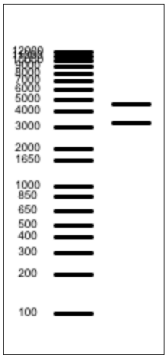


```
<Serial Cloner V2.5> -- <20 Nov 2016   14:11>

Restriction analysis of pGLOMS2BD-IL10.xdna [Circular]
Incubated with BamHI

2 fragments generated.

   1:    4,521 bp  -  From BamHI[2792]   To  BamHI[7313]

   2:    3,708 bp  -  From BamHI[7313]   To  BamHI[2792]
```

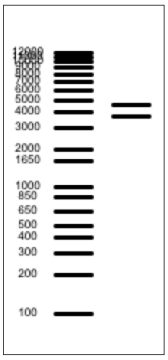

Figure 2.1 Plasmid map of pGLOMS2BD and representative screening RE digests of pGLOMS2BD-3'UTR clones.

(A) *Luc*2 the luciferase gene driven by the Phospho-glycerate kinase (PGK) promoter, a multiple cloning site containing unique *Pme*I, *Sac*I and *Sal*I sites is positioned immediately downstream of the luc2 ORF and terminated by SV40 late poly(A) signal. Plasmid contains a humanised Renilla-neo fusion (hRluc-neo) gene driven by the SV40 early enhancer/promoter terminated by synthetic poly(A) signal. Bacterial resistance gene conferring Amp^r encodes Beta lactamase. (B) Virtual digest produced using the SerialCloner program. Original pGLOMS2BD is shown for comparison.

2.5.2 Generation of miR-23a~miR-24~miR-27a sponge expression constructs.

In this section I will describe the methods used to design and create miR-sponge expression constructs. miR-sponges specific for each member of the miR-23a cluster individually and in all combinations were created, see Figure 5.7. miR-sponges are essentially concatomers of near perfect MBS for the miRs they are designed against. To decrease Slicer activity associated with highly complementary miR/MBS interactions that results in the rapid degradation of target mRNAs, a 3 bp mismatch was introduced into the MBS corresponding to position 8 in the miR. This was intended to cause the sponge transcript and with it its Ago2 complexed miRs to be sequestered rather than degraded [618]. Here I developed a novel strategy to create miR-sponges taking advantage of recent availability of bespoke gene synthesis. One of the main limitations of this type of gene synthesis is that it cannot include significant regions of repetitive sequence. This obstacle was over come by introducing different sequences in the bulge regions of the sponge MBS and in the sequences linking the MBS. Using this approach I was able to design a single sequence that contained 5 MBS for each member of the miR-23a cluster that was capable of being synthesised by IDT. Sponge sequence is shown Table 2.18.

miR23-24-27 sponge sequence
AGTTTAAACCTCGAGCCCGGGTAATCCGACCAATGTGATAATGGTAATCCGCTCAATGTGA TGCAGGTAATCCTCACAAT GTGATTATGGTAATCCAACCAATGTGATTTGGGTAATCCAGTCAATGTGATAGTACTGTTC CTGCCTGACTGAGCCAAAT CTGTTCCTGCAACACTGAGCCAGCACTGTTCCTGCGACACTGAGCCATATCTGTTCCTGCG CTACTGAGCCATTGCTGTT CCTGCAACACTGAGCCAGCTGCGGAACTCGACACTGTGAAATTGCGGAACTGCTCACTGTG AAGGCGCGGAACTACGCAC TGTGAAGGCGCGGAACTGTCCACTGTGAATATGCGGAACTGGTCACTGTGAAGATATCGtc

Table 2.18 Multiple sponge sequence.

The resulting plasmid called pIDT23~24~27 sponge is shown in Figure 2.2. Each of the different sponge units is separated with sites for different blunt cutting enzymes- *Sma*I, *Sca*I, *Pvu*II and *Eco*RV, this allowed for all combinations of the sponge to be generated from a single construct by restriction digest followed by re-ligation. For example, miR-23 sponge was made by digesting pIDT23~24~27 sponge with *Sca*I/*Eco*RV. Digested vector was run an 0.8% agarose TAE gel and the band corresponding to the vector excised, gel purified and re-ligated in a T4 DNA ligation reaction. The same approach was used to generate the other 6 sponge combinations. The combinations of RE used to generate sponge combinations is shown in Table 2.19.

Next, the number of MBS per sponge was doubled by digesting the sponge constructs produced in the previous step (e.g. pIDT23) with *Xho*I and *Xho*I+*Sal*I. The *Xho*I linearized vector and the *Xho*I/*Sal*I released insert containing the sponge sequence were excised and gel purified. The *Xho*I cut vector was treated with Calf Intestinal Phosphatase (NEB) to remove phosphate from the 5' end. This prevented the re-ligation of the vector. The sponge fragment released in the *Xho*I+*Sal*I digest was then ligated into the *Xho*I site, doubling the size of sponge (10x MBS). As inserts were not cloned directionally, plasmids were sequenced to confirm orientation.

Finally, the sponge sequences were cloned into the mammalian expression construct pGLOMS2BD (shown in Figure 2.1). This was achieved by digesting the doubled sponge constructs with *Pme*I and *Not*I, the released insert was then cloned into the same sites in pGLOMS2BD creating final constructs.

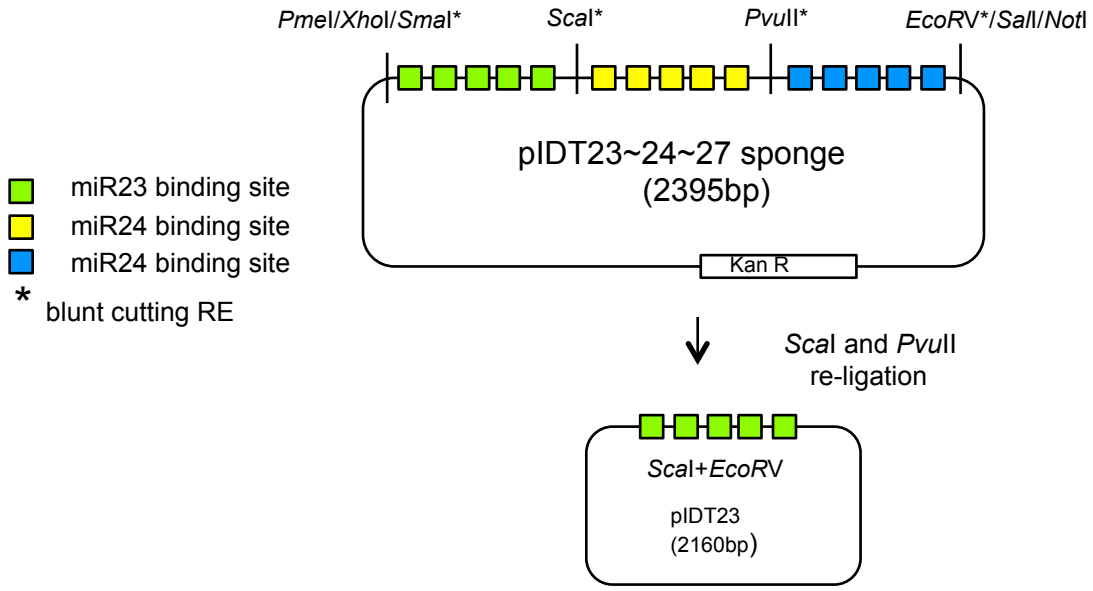

Figure 2.2 Schematic showing sponge cloning strategy

Sponge plasmid	Parental Plasmid	Enzyme Combination
pIDT23	pIDT23~24~27 sponge	*Sca*I+*Eco*RV
pIDT24	pIDT24+27	*Pvu*II+*Eco*RV
pIDT27	pIDT23~24~27 sponge	*Pvu*II+*Sma*I
pIDT23+24	pIDT23~24~27 sponge	*Pvu*II+*Eco*RV
pIDT23+27	pIDT23~24~27 sponge	*Sca*I+*Pvu*II
pIDT24+27	pIDT23~24~27 sponge	*Sma*I+*Sca*I
pIDT23+24+27	pIDT23~24~27 sponge	NA

Table 2.19 Restriction digest used in the generation of sponge combinations

2.5.2.1 Creation of pEF6-sponge constructs.

The human Phospho Glycerate Kinase promoter in the pGLOMS2BD sponge vectors was replaced by the Elongation factor 1 alpha promoter (EF1α). This was achieved by synthesising a G-block encoding the EF1α promoter containing 20 bp homology arms at the 5' and 3' ends corresponding to the sequences 5' to the *Mlu*I site and 3' to the *Sma*I site of pGLOMS2BD. The G-block was then inserted into pGLOMS2BD digested with *Mlu*I and *Sma*I using Gibson assembly (see section 2.5.4) creating pEF6-Luc. The various sponge inserts were then cloned into the *Pme*I and *Not*I sites of this vector producing the final pEF6-Sponge vectors.

2.5.3 TOPO cloning of PCR products.

Taq DNA polymerase amplified or treated PCR products were cloned directly in pCR2.1 TOPO using the TOPO TA Cloning® kit (Invitrogen). Four microlitres of PCR reactions were added directly into a TOPO cloning reaction, along with 1 µl of salt solution and 1 µl of pCR2.1 TOPO. The reaction was incubated for 10 minutes at room temperature then 2 µl removed and transformed into chemically competent One Shot® TOP10 *E. coli* that were provided with the kit. A detailed transformation protocol can be found in Section 2.5.5.

2.5.4 Gibson Assembly® Method

During the course of my PhD the availability of G-blocks and the development of the Gibson Assembly cloning meant that the generation of luciferase reporter constructs could be streamlined. Instead of using the PCR and conventional sub-cloning methods described in section 2.5.1 to produce these constructs, I could using G-blocks and Gibson Assembly to generate luciferase reporter constructs along with constructs in which MBS were mutated in a single cloning step.

Regions containing putative miR-23a cluster binding sites within genes of interest were identified using one of the miR target prediction programs described in section 2.9. Sequences containing these regions were copied from ENSEMBL genome browser (http://www.ensembl.org/index.html) and pasted into SerialCloner where the 20 bp homology arms specific for the insertion into the *Pme*I/*Sal*I sites of pGLOMS2BD were added (see Table 2.20).

Generally sequences of approximately 450 bp were used with the target MBS positioned close to the middle. This could be extended to 700 bp if the inclusion of nearby MBS was required. Once designed the G-blocks were ordered from Intergrated DNA technologies. pGLOMS2BD was digested with *Pme*I/*Sal*I, separated by gel electrophoresis and purified using QIAquick gel purification kit (Qiagen). The resulting gel fragment was used in a Gibson Assembly reaction along with the previously designed G-block, see Table 2.21. Samples were prepared in 200 µl thin walled PCR tubes (Starlab) and incubated at 50°C for 60 minutes. The reactions where then transformed into MAX Efficiency® DH5α™ (Invitrogen) as described in section 2.5.5. Table 2.22 shows the sequences of G-block used in this thesis.

5' Homology arm	3'UTR Sequence	3' Homology arm
GTCTGCAGAGATCTGTTT	<Target sequence>	GTCTAGAGTCGACCTGCAG

Table 2.20 Luciferase reporter G-block template.

Component	Volume per reaction (µl)
2X Gibson Assembly master mix (NEB)	10.0
Vector (100ng)	Variable
G-block (3x molar excess of vector)	Variable
Nuclease free water	Variable
Total per reaction	20.0

Table 2.21 Standard Gibson Assembly reaction

Name - MTHFR wt gBlocks® Gene Fragments 437 base pairs

```
5'- GTC TGC AGA GAT CTG TTT CCA GCA TCC AGC CTG TGT GTT CTG TAA TGG AAC TGA CCC CCT CCC CTG AAA
ACG AAG GGG CCC CGG GGC TGG CAA GCA GGG AAA GCT CCA CGG TGC GTG GCT GTG GCA CAG ACT TCT GGA AGG
CTG GCT GAG TGG AAT GCA GGG AAG AGG GCA GTA CCT GGG AAA GGA CCC ACC CAT CTT CCT GCT GCT GTA ACT
GCT GAG CCA CTC GCA GTC GCA GGA TCC GCT GCC ACC ACG TCT GCC AGG CCC ATC TCA GGT GCC ACT CCC TGA
GCT TTG GGG ACA GTT GGC AGA GAA GGC CTC TTG TGC TCA CGC TCC CCC GCA GTC CCC AGC CCT TCT GCC TTT
CTC CCC CGA CAC TGC TGC ACC AGA GTG AAA GGG CTA TGG CAA GGG GGT GTC ATC TGA GGA GGT CTA GAG TCG
ACC TGC AG -3'
```

Name - MTHFR Mt gBlocks® Gene Fragments 429 base pairs

```
5'- GTC TGC AGA GAT CTG TTT CCA GCA TCC AGC CTG TGT GTT CTG TAA TGG AAC TGA CCC CCT CCC CTG AAA
ACG AAG GGG CCC CGG GGC TGG CAA GCA GGG AAA GCT CCA CGG TGC GTG GCT GTG GCA CAG ACT TCT GGA AGG
CTG GCT GAG TGG AAT GCA GGG AAG AGG GCA GTA CCT GGG AAA GGA CCC ACC CAT CTT CCT GCT GCT GTA ACT
GCT CGC AGT CGC AGG ATC CGC TGC CAC CAC GTC TGC CAG GCC CAT CTC AGG TGC CAC TCC CTG AGC TTT GGG
GAC AGT TGG CAG AGA AGG CCT CTT GTG CTC ACG CTC CCC CGC AGT CCC CAG CCC TTC TGC CTT TCT CCC CCG
ACA CTG CTG CAC CAG AGT GAA AGG GCT ATG GCA AGG GGG TGT CAT CTG AGG AGG TCT AGA GTC GAC CTG CAG
-3'
```

Name - DHFR wt gBlocks® Gene Fragments 437 base pairs

```
5'- GTC TGC AGA GAT CTG TTT TAT GAA GGT GTT TTC TAG TTT AAG TTG TTC CCC CTC CCT CTG AAA AAA GTA
TGT ATT TTT ACA TTA GAA AAG GTT TTT TGT TGA CTT TAG ATC TAT AAT TAT TTC TAA GCA ACT AGT TTT TAT
TCC CCA CTA CTC TTG TCT CTA TCA GAT ACC ATT TAT GAG ACA TTC TTG CTA TAA CTA AGT GCT TCT CCA AGA
CCC CAA CTG AGT CCC CAG CAC CTG CTA CAG TGA GCT GCC ATT CCA CAC CCA TCA CAT GTG GCA CTC TTG CCA
GTC CTT GAC ATT GTC GGG CTT TTC ACA TGT TGG TAA TAT TTA TTA AAG ATG AAG ATC CAC ATA CCC TTC AAC
TGA GCA GTT TCA CTA GTG GAA ATA CCA AAA GCT TCC TAC GTG TAT ATC CAG AGG TTT GTA GGT CTA GAG TCG
ACC TGC AG -3'
```

Name - DHFR mt2 gBlocks® Gene Fragments 430 base pairs

```
5'- GTC TGC AGA GAT CTG TTT AGC GAT TCT CCT GCC TCA GGC TCC CAA GTA GCT AGG ACC AGG TGC GCG CCA
CCA CGC CCG GCT AAT TTT TGT ATT TTG TAT TTT TAG TAG AGA TGG GGT TTC ACC ATG TTG GTC AGG CTA GTC
TCG AAC TCG TGA CCG CAA GCG ATT CAC CCA CCT CAG CCT CCC AAA GTG CTG GGA TTA CCG GCT CCA CAC CCG
GCA CAT CTT CAT TCT TTT TAT GTA GTA AAA AGT ATA AGG CCA CAC ATG GTT TAT TTG AAG TAT TTT ATA ATT
TAA AAA AAT ACA GAA GCA GGA AAA CCA ATT ATA AGT TCA AGT GAG GGA TGA TGG TTG CTT GAA CCA AAG GGT
TGC ATG TAG TAA GAA ATT GTG ATT TAA GAT ATA TTT TAA AGT TAT AAG TAG CAG GTC TAG AGT CGA CCT GCA G
-3'
```

Name - DHFR wt2 gBlocks® Gene Fragments 437 base pairs

```
5'- GTC TGC AGA GAT CTG TTT AGC GAT TCT CCT GCC TCA GGC TCC CAA GTA GCT AGG ACC AGG TGC GCG CCA
CCA CGC CCG GCT AAT TTT TGT ATT TTG TAT TTT TAG TAG AGA TGG GGT TTC ACC ATG TTG GTC AGG CTA GTC
TCG AAC TCG TGA CCG CAA GCG ATT CAC CCA CCT CAG CCT CCC AAA GTG CTG GGA TTA CCG GCT TGA GCC ACC
ACA CCC GGC ACA TCT TCA TTC TTT TTA TGT AGT AAA AAG TAT AAG GCC ACA CAT GGT TTA TTT GAA GTA TTT
TAT AAT TTA AAA AAA TAC AGA AGC AGG AAA ACC AAT TAT AAG TTC AAG TGA GGG ATG ATG GTT GCT TGA ACC
AAA GGG TTG CAT GTA GTA AGA AAT TGT GAT TTA AGA TAT ATT TTA AAG TTA TAA GTA GCA GGT CTA GAG TCG
ACC TGC AG -3'
```

Name - DHFR mt gBlocks® Gene Fragments 427 base pairs

```
5'- GTC TGC AGA GAT CTG TTT TAT GAA GGT GTT TTC TAG TTT AAG TTG TTC CCC CTC CCT CTG AAA AAA GTA
TGT ATT TTT ACA TTA GAA AAG GTT TTT TGT TGA CTT TAG ATC TAT AAT TAT TTC TAA GCA ACT AGT TTT TAT
TCC CCA CTA CTC TTG TCT CTA TCA GAT ACC ATT TAT GAG ACA TTC TTG CTA TAA CTA AGT GCT TCT CCA AGA
CCC CCC AGC ACC TGC TAC AGT GAG CTG CCA TTC CAC ACC CAT CAC ATG TGG CAC TCT TGC CAG TCC TTG ACA
TTG TCG GGC TTT TCA CAT GTT GGT AAT ATT TAT TAA AGA TGA AGA TCC ACA TAC CCT TCA ACT GAG CAG TTT
CAC TAG TGG AAA TAC CAA AAG CTT CCT ACG TGT ATA TCC AGA GGT TTG TAG GTC TAG AGT CGA CCT GCA G -3'
```

Table 2.22 List of G-blocks sequences

2.5.5 Transformation

Transformation of bacterial cells, in this case *E. coli*, refers to the introduction of DNA, most often in the form of a plasmid containing a bacterial origin of replication and a gene conferring antibiotic resistance to the bacteria that have taken up the foreign DNA. This is most commonly achieved using either chemically competent or electro-competent *E. coli*. In my studies I used only chemically competent *E. coli*. Chemically competent *E. coli* are made by incubating bacteria until the mid log phase of their growth in culture. At this

point cells are pelleted then incubated on ice in the presence of various salts, classically calcium chloride. This process renders the cells permeable to DNA.

The type of *E. coli* used in transformation depended on the source of the plasmid DNA being used. Plasmids generated from TOPO cloning were transformed into highly competent One Shot® TOP10 *E. coli* provided with the kit (Invitrogen). Plasmids generated using Gibson Assembly or site-directed mutagenesis were transformed into MAX Efficiency® DH5α™ (Invitrogen). Finally, plasmids generated by conventional sub-cloning methods, using T4 DNA ligase were transformed into Sub-cloning Efficiency™ DH5α™ (Invitrogen). The transformation method used in each case was the same and outlined below.

1. Competent *E. coli* were thawed on ice.

2. Two microlitres of plasmid DNA was added to 50 µl of competent cells in a sterile 1.5 micro-centrifuge tube, gently mixed by flicking and incubated on ice for 30 minutes.

3. Cells were then 'heat shocked' at 42°C in a water bath for 30 seconds before being returned to ice for 2-3 minutes.

4. Competent cells were then transferred to 15 ml falcon tube along with 300 µl of SOC media and incubated at 37°C with shaking (200 rpm) for 45 minutes. This gives the transformed bacteria time to express the plasmid's antibiotic resistance gene.

6. Finally, 100 µl of bacterial culture was spread onto LB agar plates containing 50 µg/ml ampicillin and incubated overnight at 37°C.

The following day, 2 or 3 colonies were picked and used to inoculate 5 ml of LB broth containing 50 µg/ml ampicillin and grown overnight at 37°C with shaking (200 rpm). The next morning bacterial cultures where *E. coli* had grown were visibly turbid. These cultures were selected for plasmid purification, described in detail in section 2.5.8.

2.5.6 DNA Extraction

2.5.6.1 Small scale plasmid purification from bacterial cultures

Plasmid DNA was isolated from small (5 ml) bacterial cultures using QIAprep Spin Miniprep Kit (Qiagen) kit according to manufacturer's instructions. Briefly, 1.5 ml of overnight culture was transferred in to 1.5 ml micro-centrifuge tube and spun at 17,900 g for 3 minutes. The supernatant was discarded and the pellet resuspended in 250 µl of Buffer P1, supplemented with RNAse A (100 µg/ml final concentration). Next, 250 µl of P2 was added followed by mixing by inversion. At this stage the bacterial solution becomes clear and viscous as the bacteria are lysed. This is followed by the addition of 350 µl of buffer N3 followed by mixing by inversion. This serves to neutralise buffer P2, causing the precipitation of the proteins and genomic DNA that are bound by the SDS in buffer P2. The samples are then clarified by centrifugation at 17,900 g for 10 minutes. The supernatant was then added to the Qiaprep spin column and spun for 15 seconds at 17,900 g. The flow through was discarded and 500 µl of PB buffer added to the column. The columns were spun at 17,900 g for 15 seconds and the flow through discarded. The columns were washed with 750 µl PE buffer and spun at 17,900 g for 15 seconds. The columns were then spun for 2 minutes at 17,900 g to remove any residual wash buffer. Finally, the columns were transferred to a fresh 1.5ml micro-centrifuge tube and 50 µl of nuclease free water added. Columns were allowed to stand for 1 minute before being centrifuged at 17,900 g for 1 minute. The plasmid DNA eluted from the column was collected in the tube. Plasmid DNA was stored at 4°C until required.

2.5.6.2 Large-scale plasmid purification from bacterial cultures

For purification of plasmid DNA from larger bacterial cultures Qiagen's Plasmid Maxi kit was used. For plasmid DNAs that were intended for transfection into mammalian cells Qiagen's Endofree Plasmid Maxi kit was used. Both kits involved essentially the same steps apart from an endotoxin removal step that will be discussed below. In both cases, the purifications were performed according to the manufacturer's instructions.

Briefly, 100 ml overnight cultures were spun in two 50 ml falcon tubes at 3,000 rpm for 30 minutes. The supernatants were discarded and the pellets

resuspended in a single volume of 10 ml. Next, 10 ml of buffer P2 was added to the resuspended sample and mixed thoroughly by inversion. Samples were allowed to stand at room temperature for 5 minutes. Samples were then neutralised by the addition of cold buffer P3, mixed by inversion and allowed to sit on ice for 5 minutes. Samples were then centrifuged at 5,000 rpm for 30 minutes at 4°C.

For endotoxin free preparations, supernatants were carefully removed into a fresh 50 ml falcon tube and 2.5 ml of ER (endotoxin removal) buffer added. Samples were mixed by inversion and placed on ice for 30 minutes. During this time maxi-prep columns were equilibrated by the addition of 10 ml of QBT buffer. This was allowed to pass through the column under gravity.

At this stage both non-endofree and endofree samples were poured into equilibrated columns and allowed to drain by gravity. After the sample has passed through the column, 30 ml of QC buffer was added and allowed to flow through, this was repeated twice. The plasmid DNA was eluted from the column into a fresh 50 ml falcon tube, by the addition of 15 ml of QF buffer. The eluted plasmid DNA was then precipitated by the addition of 10 ml of 100% isopropanol. The samples were carefully mixed before being centrifuged at 5,000 rpm for 30 minutes at 4°C. The supernatants were carefully poured off and pellet washed with 5 ml of 70% ethanol followed by centrifugation at 5,000 rpm for 10 minutes at room temperature. The supernatant was carefully poured off and the visible DNA pellet allowed to air dry for 5 minutes. Finally the DNA was dissolved in 500 µl of TE buffer. Plasmid DNAs were stored at 4°C until required.

2.5.6.3 Genomic DNA isolation

Genomic DNA was isolated from mammalian cells using the Cell Lysis solution from the GeneArt Genomic cleavage detection kit (Invitrogen) according to manufacturer's instructions. Typically, genomic DNA was prepared from $5x10^5$ cells. Cells were spun at 300 g for 3 minutes and culture media discarded. The cell pellet was resuspended in 50 µl of Cell Lysis buffer supplemented with 2 µl of Protein Degrader and sample transferred to 200 µl thin walled PCR tube. Samples were incubated at 68°C for 15 minutes, followed by 95°C for 10 min. At this stage samples could be used directly in PCR reactions or stored at -20°C.

2.5.6.4 DNA isolation from Agarose Gels

DNA was purified from gel slices excised from agarose TAE gels using the QIAquick Gel purification kit (Qiagen) according to manufacturer's instructions. Briefly, DNA containing gel slices were incubated with 450 µl of QG buffer, at 55°C for 10 minutes with mixing every 2 minutes. This served to dissolve the agarose gel, liberating the DNA. To this, 150 µl of isopropanol was added and mixed by vortex. The sample was then pipetted into the QIAquick spin column and spun at 17,900 g for 15 seconds. The flow through was discarded and 750 µl of PE wash buffer added to the column followed by centrifugation at 17,900 g for 15 seconds. The flow through was discarded and the column spun again at 17,900 g for 2 minutes to dry the column's filter. The column was then placed into a fresh tube and 50 µl of nuclease free water added. Samples were allowed to stand at room temperature for 1 minute before being centrifuged at 17,900 g for 1 minute. The purified DNA sample was collected in the flow through in the tube and the column discarded.

2.5.7 Agarose Gel Electrophoresis

DNA samples were separated according to their size by agarose gel electrophoresis. The concentration of agarose used varied according to the size of the fragments that were run. Typically for fragments from 500 bp to 8,000 bp a 0.8% (w/v) agarose gel was used. Gels were made by weighing the required amount of agarose into a Pyrex conical flask. To this 100 ml of 1xTAE buffer was added and the sample heated in the microwave until the agarose had completely dissolved. The agarose-TAE mixture was allowed to cool for 1-2 minutes. Next, 10 µl of ethidium bromide (10 mg/ml, Sigma) was added and the agarose poured into the casting tray of the Sub-Cell GT electrophoresis gel apparatus (Bio-Rad). The gel was allowed to set at room temperature for 15-30 minutes. In the meantime samples were prepared for loading by the addition of 5X STOP dye solution. Once set the agarose gel was placed into the gel tank and submerged in 1xTAE running buffer. Samples were then pipetted into wells alongside 1 Kb(+) DNA ladder (Invitrogen) and run at 100V for approximately 30 minutes. The DNA bands in the gel were then visualized in UV trans-illuminator (Gel Logic 200).

2.5.8 Sequencing of Plasmids

Plasmids were sequenced by SourceBioscience using primers listed in Table 2.23.

Primer Name	Sequence
GLOseq	GAGAAGGAGATCGTGGACTATG
M13 Fw	GTAAAACGACGGCCAG
M13 Rev	CAGGAAACAGCTATGAC

Table 2.23 List of Sequencing Primers

2.5.9 Site directed mutagenesis

Site-directed mutagenesis was used to mutate the seed regions of putative miR target sequences cloned into luciferase reporter constructs using the QuikChange Lightning Site-Directed Mutagenesis kit (Agilent Technologies) according to manufacturer's instructions. In brief, the sequence to be mutated was pasted into the online QuikChange Primer design program (www.agilent.com/genomics/qcpd). This program allows the user to make desired changes in the sequences. The program then generates two complimentary sequences corresponding to the desired mutations. These are generally between 25 and 45 bases in length and have melting temperature of ≥78°C. Oligonucleotides were synthesised and HPLC purified by IDT. These primers were then used to amplify the template plasmid. A standard reaction is shown in Table 2.24. Reactions were prepared in 200 µl thin walled PCR tubes (Starlab) then incubated in thermocycler using the cycling parameters outlined in Table 2.25. Once finished, 2 µl of *Dpn*I enzyme was added to the reaction, mixed gently and incubated at 37°C for 5 minutes. Two microlitres of reaction was transformed into MAX Efficiency® DH5α™ (Invitrogen) as described in section 2.5.5. In all cases, mutations were confirmed by sequencing. Site-directed mutagenesis primers used in this thesis are shown in Table 2.26.

Component	Volume per Reaction (µl)
10x *QuikChange* buffer	5.0
dNTP (25 mM)	1.0
Plasmid Template (25 ng/µl)	1.0
Fw Primer (100 ng/µl)	1.25
Rev Primer (100 ng/µl)	1.25
QuikSolution Reagent	1.5
QuikChange Lightning Enzyme	1.0
Nuclease free water	34.0
Total Reaction Volume	50.0

Table 2.24 Standard QuikChange Lightning Site-directed mutagenesis reaction.

Step	Temperature	Duration	Cycles
Denaturation of genomic DNA template	95°C	2 minutes	1X
Denature	95°C	20 seconds	18X
Annealing	60°C	10 seconds	
Extension	68°C	30 seconds/kb of plasmid length	
Final extension	68°C	5 minutes	1x

Table 2.25 Cycling parameters for QuikChange Lightning Site-directed Mutagenesis.

Primer name	Sequence
IL6R1-23SDM+	GCCTCTGTATTCAGCAAATGCCTAGGATCATCATTGGATCCTAGCAAAATGCTAATGAGGAACTAATTATAATTCT
IL6R1-23SDM-	AGAATTATAATTAGTTCCTCATTAGCATTTTGCTAGGATCCAATGATGATCCTAGGCATTTGCTGAATACAGAGGC
IL6R1-27SDM-	TCCAAAGAGTCTTGATATGGTTCTCTTGGATCCGGCCCAAGTTCACTCTAGCCCCTTTAA
IL6R1-27SDM+	TTAAAGGGGCTAGAGTGAACTTGGGCCGGATCCAAGAGAACCATATCAAGACTCTTTGGA

Table 2.26 Site-directed mutagenesis primers

2.6 Characterisation of 5' and 3' of mRNA ends

2.6.1 5' Rapid Extension of cDNA ends (5'RACE)

5'RACE was used to amplify the 5' ends of primary-miR-23a cluster transcript (pri-miR-23a). In the initial step the 5' end of the pri-miR-23a was converted into cDNA using a gene-specific primer (Pri23a 5'RACE GSP1). 200 ng of total RNA in a volume of 9 µl was added to 200 µl thin walled PCR tube and denatured by heating at 75°C for minutes in a thermocycler then rapidly chilled on ice. The denatured RNA was then used as template in the reverse transcription reaction shown in Table 2.27. Reaction was incubated at 37°C for 60 minutes. Next the excess primers were removed by diluting the reaction to a final volume of 2 ml in water which was then applied to a Centricon-100 micro-concentrator and centrifuged at 1,000 g at 4°C for 20 minutes. This step was then repeated. The flow-through containing pri-miR-23a cDNA was then transferred to a fresh 0.5 ml micro-centrifuge tube and the volume reduced to ~10 µl in a rotary vacuum evaporator. The resulting 9 µl of cDNA was then added into terminal transferase reaction (Shown in Table 2.28) that adds a polyadenosine tail onto the 3' end of the cDNA corresponding to the 5' end of the pri-miR-23a. Reaction was incubated at 37°C for 15 minutes followed by 80°C for 3 minutes to inactivate the terminal transferase. The sample was then diluted in TE buffer to a final volume of 1 ml. Finally the following PCR reaction was performed using a Gene-specific primer (Pri23a 5'RACE GSP2) nested within the first gene-specific primer and QT-adaptor primer 5' shown in Table 2.29. PCR reaction was performed using AmpiTaq Gold® 360 master mix set up as shown Table 2.30. The cycling parameters used are shown in Table 2.31. Finally PCR products were analysed using gel electrophoresis (see section 2.5.7) 5'RACE bands were excised and cloned into pCR2.1 TOPO before being sent off for sequencing. Sequences were aligned against the human genome using BLAST (https://blast.ncbi.nlm.nih.gov/Blast.cgi). Primer sequences used in 5'RACE of the pri-miR-23a cluster are shown in Table 2.32.

Component	Volume per Reaction (µl)
5x Reverse Transcriptase buffer	4.0
dNTP (20 mM)	1.0
Denatured RNA (200 ng)	9.0
Gene-specific primer (10 µM)	4.0
Placental RNase inhibitor (20 units/µl)	1.0
Reverse Transcriptase (100 units/µl) (Applied Biosystems)	1.0
Total Reaction Volume	20.0

Table 2.27 5'RACE Reverse transcription reaction

Component	Volume per reaction (µl)
5X TdT Buffer (NEB)	5.0
$CoCl_2$ (2.5 mM)	5.0
dATP (10 mM)	1.0
cDNA	10.0
Terminal Transferase (20 units/µl) NEB	1.0
Total per reaction	20.0

Table 2.28 5'RACE terminal transferase reaction.

Primer Name	Primer Sequence
Q_T	CCAGTGAGCAGAGTGACGAGGACTCGAGCTCAAGC TTTTTTTTTTTTTTTT
Q_0	CCAGTGAGCAGAGTGACG
Q_I	GAGGACTCGAGCTCAAGC

Table 2.29 Primers used in 5' and 3' RACE

Component	Volume per Reaction (µl)
2x Amplitaq Gold 360 master mix (Invitrogen)	25.0
QT primer (10 µM)	1.6
Q0 primer (10 µM)	3.2
GSP2 primer (10 µM)	3.2
Diluted cDNA from previous step	5.0
Nuclease free water	10.5
Total Reaction Volume	50.0

Table 2.30 Final stage PCR 5'RACE reaction.

Cycle Number	Denature	Annealing	Extension
1	5 min at 94˚C	5 min at 55˚C	40 min at 72˚C
2-31	40 sec at 94˚C	1 min at 55˚C	3 min at 72˚C

Table 2.31 Cycling parameters used in 5'RACE PCR.

Primer Name	Sequence
Pri23a 5'RACE GSP1	GCCAGTGTACACAAACCAAC
Pri23a 5'RACE GSP2	CGGAACTTAGCCACTGTGAA

Table 2.32 Primers used in 5'RACE of pri-miR-23a transcript.

2.6.2 3' Rapid Extension of cDNA ends (3'RACE)

The protocol described here has been adapted from the excellent Nature Protocols method described by Scotto-Lavino et al. [619]. A schematic of the technique is shown in Figure 2.3.

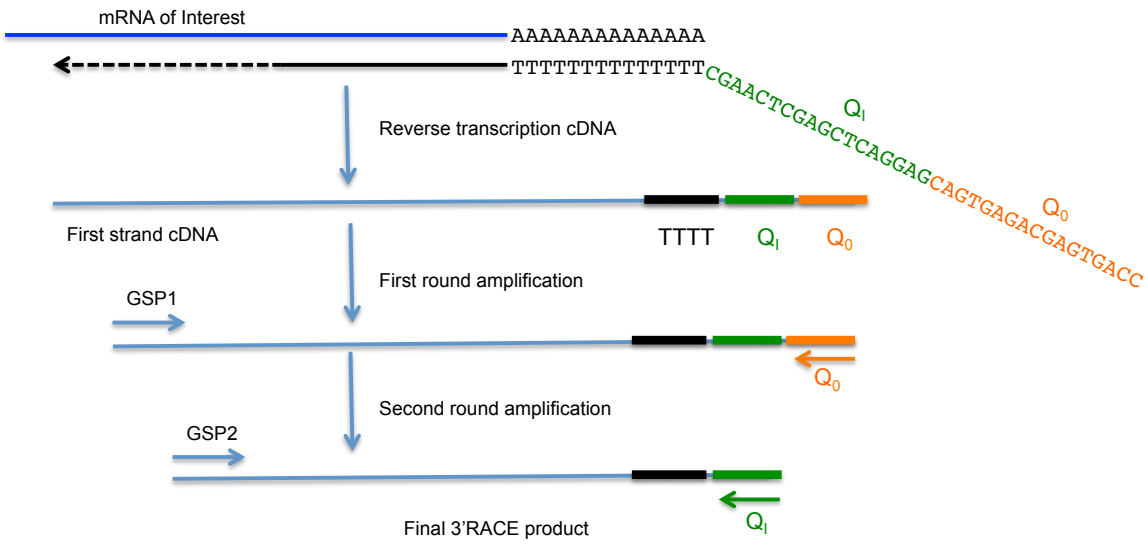

Figure 2.3 Overview of 3'RACE protocol

Figure adapted from Scott-Livino et al., Nature Protocols, 2007.

In the first step of this protocol 500 ng of total RNA in a volume of 10 µl, isolated from THP-1 cells, was placed into a 200 µl thin-walled PCR tube and heated to 80°C for 3 minutes. The sample was then rapidly cooled on ice. The denatured RNA was then used as template in the reverse transcription reaction shown in Table 2.33. Reaction was incubated at room temperature for 5 minutes then placed into a thermocycler were the sample was incubated at 42°C for 60 minutes followed by 10 minutes at 55°C. The reverse transcriptase was inactivated at 70°C for 5 minutes. Next 1.5 units of RNase H (Invitrogen) was added to the sample and incubated at 37°C for 20 minutes to destroy RNA template. Sample was then diluted to 1 ml in TE.

Component	Volume per Reaction (µl)
5x Reverse Transcriptase buffer	4.0
dNTP (20 mM)	1.0
Denatured RNA (500 ng)	10.0
Q_T primer (10 µM)*	0.5
Placental RNase inhibitor (20 units/µl)	1.0
Reverse Transcriptase (100 units/µl) (Applied Biosystems)	1.0
Nuclease free water	2.5
Total Reaction Volume	20.0

Table 2.33 3' RACE Reverse transcription reaction
* Sequence of Q_T primer shown in Table 2.29.

The cDNA generated from the first step was then used as template in PCR containing the nested primer (Q_I) incorporated into the cDNA by the Q_T primer and a forward primer specific for my gene of interest (GSP1). The reaction was set up according Table 2.34. Sample was the incubated in a thermocycler using the cycling parameters shown in Table 2.35.

Component	Volume per Reaction (µl)
2x Amplitaq Gold 360 master mix (Invitrogen)	25.0
Q_0 primer (10 µM)	1.25
GSP1primer (10 µM)	1.25
Diluted cDNA from previous step	1.0
Nuclease free water	21.5
Total Reaction Volume	50.0

Table 2.34 First round PCR 3'RACE reaction

Cycle Number	Denature	Annealing	Extension
1	5 min at 98°C	2 min at 55°C	40 min at 72°C
2-30	10 sec at 94°C	10 min at 55°C	3 min at 72°C
31	10 sec at 94°C	10 min at 55°C	15 min at 72°C

Table 2.35 Cycling parameters used in first and second round 3'RACE PCRs

Reaction from the first round PCR was then diluted 1 in 20 in TE before being used as template in the second round PCR. The reaction is as shown in Table 2.34, except Q0 and GSP1 primers were replaced with QI and GSP2. The PCR was performed using the parameters shown in Table 2.35. Finally PCR products were analysed using gel electrophoresis (see 2.5.7) 3'RACE bands were excised and cloned into pCR2.1 TOPO before being sent off for sequencing. Sequences were screened for presence of non-genomic stretches of polyA sequences and presence of consensus polyA signal located 5' of polyA tail. Gene specific primers used in this thesis are shown in Table 2.36.

Primer Name	Sequence
IL6R GSP1	GAGGGTGAGTGGGTGAATAAT
IL6R GSP2	CCTGGGTAACTAGGGAAGATAA
sIL6R GSP2	CCTCCCAGGTTCAAGAAGAC
CSFR1 GSP1	TGCAGCCCAACAACTATCA
CSFR1 GSP2	CTCCCACAAACTTCAACTCCT
pri23a 3'Race GSP1	CATTGCCAGGGATTTCCAAC
pri23a-3'Race GSP2	GATTTCCAACCGACCCTGA

Table 2.36 Gene specific 3'RACE primers

2.7 Luciferase reporter assay

Luciferase reporter assays have become the *de facto* method for validating miR target interactions. In these experiments sequences containing putative miR binding sites were cloned down stream of a luciferase reporter conferring sensitivity to the miR thought to bind it. Co-transfection of luciferase reporter plasmid into a cell line (commonly HEK293 cells) along with miR mimic should reduce luciferase activity compared to scrambled miR control if the MBS is

targeted by the test miR. If the ability of the miR to reduce luciferase activity is lost upon the mutation of the MBS's seed region, the miR is deemed to directly regulate target mRNA expression via this MBS. The method used to create Luciferase reporter constructs is described in section 2.5.1. Here I shall briefly describe the Dual Luciferase® reporter assay system (Promega). Cells were co-transfected with luciferase reporter constructs containing the putative MBS along with the miR mimic that targets it or scrambled control using the method described in 2.2.4.2. Cells were grown for 24 hours after which they were washed once in dPBS. The dPBS was then removed and replaced with 250 µl of 1x Passive Lysis Buffer, included in kit, and incubated with shaking for 15 minutes at room temperature. 50 µl of each sample was plated in duplicate into white 96-well plate (Greiner) followed by 50 µl of LAR II solution. Samples were incubated for 10 minutes at room temperature with shaking. The luminescence produced by each sample was measured using luminometer counter (MicroBeta Trilex, Perkin Elmer). Next, 50 µl of STOP & GLO® solution was added to each well and the plate incubated for a further 10 minutes at room temperature. This solution quenches luciferase activity while providing a substrate for renilla internal control. The plate was then read again in the luminometer counter.

Values were normalised by dividing luciferase activity by renilla activity. Values of miR-treated samples were then expressed as a percentage of those treated with scrambled control.

2.8 Cytokine quantification

2.8.1 Enzyme-Linked-Immunosorbent assay (ELISA)

Human ELISA Cytoset kits (Invitrogen) for detection of IL-6, sIL-6R, TNFα and IL-10 were used to determine cytokine concentrations in cell supernatants according manufacturer's instructions. A generalized protocol will be briefly described here. A 96-well microtitre plate was coated with capture antibody in dPBS, covered and incubated overnight at 4°C. The following day the plate was washed once with ELISA Wash buffer (dPBS, 0.05% Tween 20) and blocked by the addition of 200 µl of Assay buffer (dPBS, 0.5% BSA) for 1 hour at room temperature. Next, a standard curve was generated using recombinant human cytokine standards dissolved in Assay buffer. A top standard of 2,000 pg/ml was

serially diluted 1:2 across 7 samples. 100 µl of each standard was added in duplicate to the plate along with two wells containing only assay buffer. Samples were tested neat or diluted with assay buffer, depending on cytokine and experimental set up, with 100 µl being added to each well in duplicate. The detection antibody was then added in to each well. The plate was then covered and incubated for 2 hours at room temperature with shaking. Next, the plate was washed 5 times with ELISA wash buffer and 100 µl of streptavidin-HRP added to each well. Plates were then incubated for 30 minutes at room temperature, washed as before and 100 µl of TMB chromagen (Biosource) added to each well. The reaction was then stopped by addition of 50 µl of Stop solution to each well (Biosource). Finally, plates were read at 450 nm on a MTX TC II microplate reader (Dynex Technologies).

2.8.2 Luminex Assay

A human cytokine 25-plex assay (Invitrogen) was used to determine the concentration of 25 cytokines and chemokines simultaneously within RA patient cohort and health control serum samples. The assay was carried out by senior technician Lynn Stewart following manufacturer's instructions. Briefly, the plate was pre-wetted using the wash buffer provided. Antibody beads were vortexed for 30 seconds then sonicated for 30 seconds immediately before being added into each well. Wells were then washed twice with 200 µl of 1x Wash buffer. Next 50 µl of Incubation buffer was added into each well followed by the diluted standards. Samples were diluted 1:1 with Assay buffer and 100 µl added per well. Plate was then covered with an opaque lid and incubated on an orbital shaker at 500-600 rpm for 2 hours at room temperature. Next wells were washed twice in Wash buffer followed by the addition of 1x biotinylated antibody solution. Plate was then incubated at room temperature on an orbital shaker for 1 hour. Wells were then washed twice in Wash buffer and 100 µl of 1x streptavidin-RPE added to each well followed by shaking for 30 minutes. Liquid was then removed and each well washed 3X in Wash buffer. Finally, 150 µl of Wash buffer was plated into each well, plate then shaken for 3 minutes in orbital shaker before being read on the Luminex® 100/200™ system.

2.9 Target prediction

There are a number of well established online miR-target prediction tools that can be used to identify potential miR-mRNA interactions (Reviewed in Chapter 1). They have their own strengths and weaknesses and generally rely on identifying sequences complementary to miR seed region as the basis for their predictions. A list of the programs used in this work is shown in Table 2.37. As a starting point I used human Targetscan to identify miR-23a cluster binding sites in RA and monocyte relevant genes. Targetscan has the advantage of being simple to use and has one of the better false positive rates with respect to the other prediction programs available. Once identified I then screened the other databases listed in Table 2.37. MBS that are predicted by more than one program in most cases have an increased predictive value [620]. A list of the programs used together with their web addresses is shown in Table 2.38. I used Diana tools-TarBase website which is a curated database of miR-target interactions supported by experimental evidence to search for previously identified interactions or interactions that were supported by HITS-CLIP, PAR-CLIP or CLASH methodologies.

Target Prediction Algorithm	Features		Accuracy
	Parameters used in binding site prediction	Cross-species conservation	
Targetscan	Seed match, 3' complementarity local AU content and position contribution	Given scoring for each result	21-48%*
miRanda	Complimentary and free energy binding	Uses conservation filter	49%
PicTar	Seed match	Requires pairing at conserved positions	48%
PITA	Target site accessibility energy	User-defined	NA
Rna22	Pattern recognition and folding energy	Not used	NA

Table 2.37 List of Target prediction programs.

Target prediction program	Web address
Targetscan-Human	http://www.targetscan.org/vert_71/
miRanda	http://www.microrna.org/microrna/home.do
PITA	https://omictools.com/pita-tool
PicTar	https://omictools.com/pita-tool
Rna22	https://cm.jefferson.edu/rna22/Interactive/
miRwalk	http://zmf.umm.uni-heidelberg.de/apps/zmf/mirwalk2/index.html
Diana Tools	http://diana.imis.athena-innovation.gr/DianaTools/index.php?r=tarbase/index

Table 2.38 Web addresses of online miR target prediction algorithms

2.10 Statistical Analysis

Statistical analysis was done using PRISM6 platform. Results from measurements conducted in the RA patient cohort were analysed by non-parametric Kruskal-Wallis test with Dunn's correction for multiple comparisons. Experiments with primary human cells were analysed by non-parametric methods, such as Kruskal-Wallis test with Dunn's correction for multiple comparisons, Mann-Whitney test for the comparison of unpaired samples and Wilcoxon test for the paired samples accordingly. Data from THP-1 cells lines were analysed with parametric methods, such as Ordinary One-Way ANOVA with Dunnett's correction for multiple comparisons and paired or unpaired t test. In all analysis $p<0.05$ was considered significant. Details of all statistical methods used and number of experimental replicates for each experiment are stated in the figure legend.

3 Profiling of miR species in drug resistant RA

3.1 Introduction

Rheumatoid arthritis is a chronic autoimmune condition and as such has a diverse spectrum of intensity and presentation in patients. This is rarely reflected in the therapeutic approach such that standard treatment protocols are offered to new patients during the first six months post diagnosis. Although it is likely that a variety of clinical presentations exhibit subtle differences in pathological processes from the start, they are not readily exploitable in the clinical setting due to the lack of biomarkers or other measurable parameters to inform clinical decision making from the onset. In essence we lack a suitable clinically relevant endotype. Moreover, it has been previously shown that patients failing multiple modes of treatment are likely to respond less well to newer biologic medications such as anti-TNFα, regardless of the mode of action, especially if they are female with high disease activity and multiple co-morbidities [621]. Based on this we hypothesise that aligning the right patients with the right drug, particularly in early RA, could deliver improved treatment outcome.

Inability to stratify patients and to accurately predict clinical response is a significant stumbling block in the era of readily available new therapeutics. The importance of this task goes hand-in-hand with a well-excepted general strategy to treat aggressively from the onset in an attempt to establish early disease control and limit “chronicity” of the active disease [64]. Understanding how available treatments intersect with disease pathogenesis is both informative of undergoing pathological processes and will highlight pitfalls in current clinical practice. Further understanding and stratification of patients according to their response to therapy will undoubtedly lead to more tailored evidence-based treatment of RA.

This chapter will introduce a cohort of patients with rheumatoid arthritis (RA) selected on the basis of clinical response to or failing of different modes of treatment. Furthermore, emerging evidence of the importance of epigenetics and, particularly, miRs in the pathogenesis of RA prompted us to study miR

signatures in peripheral blood monocytes from these patients to identify pathways that correlate with pathology and drug response in RA [511].

3.2 Patient cohort

We gathered a cohort of patients with established diagnosis of RA and matched healthy controls. Patients were recruited by Dr Derek Baxter at the Glasgow Royal Infirmary and by Dr Duncan Porter at the Gartnavel General Hospital. Patients were selected and stratified by their clinical response to different modes of treatment, resulting in three distinct patient groups plus an additional group of healthy sex-matched controls.

The first group consisted of 21 healthy controls recruited predominantly from patient's family members and amongst the staff in the Institute of Infection, Immunity and Inflammation of the University of Glasgow. The second group was formed from 16 patients with disease duration more than ten years with good clinical response to treatment with a maximum of two DMARD agents (ever), designated 'DMARDs responders'. The third group, 'DMARDs resistant' comprised of 22 patients with high disease activity (measured by DAS28-ESR or CRP). These patients had recently qualified for biological treatment after failing several DMARDs but did not start the treatment yet. Finally, the fourth group involved 41 patients with active disease despite treatment with two or more biologic agents; this group was termed - 'Biologics Resistant'.

3.2.1 Patient demographics

Patient information regarding disease duration, severity and clinical findings are summarised in Table 3.1, together with information on 21 Healthy controls recruited in the study. Due to the nature of RA, the majority of recruited patients were females, percentages ranging from 56% in DMARDs responders group to 77% in DMARDs resistant group and 85% in Biologics resistant group. This was reflected in healthy control group, as 86% of volunteers were female (Table 3.1). Average age between patient groups was 61 years. However, healthy control were recruited from the volunteers in the institute and were younger at an average of 48 years of age. All patients had established longstanding disease at the time of recruitment, with the average duration of 18, 12 and 21 years for

the DMARDs responsive, DMARDs resistant and Biologics resistant groups respectively (Table 3.1). Patients in the DMARD resistant group had significantly shorter disease duration than patients from the DMARD responders group, indicating more aggressive disease despite multiple DMARD therapies.

RF and anti-CCP antibodies were measured in all groups as 'gold standard' biomarkers of RA [622]. The vast majority of patients (81%, 90% and 78% in DMARD responders, DMARD resistant and Biologic resistant patient groups respectively) were RF positive, while only one person in healthy controls group (5%) had a weakly positive result. Similarly, the majority of patients had a high titre of anti-CCP antibodies (81%, 84% and 68% in DMARD responders, DMARD resistant and Biologic resistant patient groups respectively) while the same person in the controls group had a very weakly positive test for anti-CCP and comprised 5% of the healthy controls, Table 3.1. This indicates that in a majority of cases our patients suffered from seropositive RA, associated with increased risk of erosive joint damage and functional impairment [623-625].

CRP and ESR levels were measured as indicators of overall inflammation. In the healthy controls group both measurements were within normal limits, that is within the upper limit of 1.0mg/dl (10mg/L) CRP and 10 mmHg ESR as per laboratory guidelines. Median CRP levels in all three patient groups were on average within normal limits (Median (25%, 75%) of 0.98 (0.34, 1.5), 1.0 (0.6, 3.4) and 1.0 (0.5, 3.3), respectively) and were significantly higher than in the healthy controls group. The second parameter, ESR, was on average above the accepted normal range limit in patient groups, and was particularly raised in patients failing DMARDs treatment when compared to healthy controls, indicating higher level of inflammation (Median (25%, 75%) of 27 (11, 57) vs. 8.0 (4.0, 15) mm/h, respectively, Table 3.1). Moreover, clinical evaluation of patients revealed a significant difference in tender joint count (TJC) between DMARDs responders group and both groups failing treatment (Mean±SD of 1.4±2.5 vs. 14±7.1 and 9.5±5.4, respectively). Additionally, average swollen joint counts (SJC) were also higher in DMARDs resistant and biologics resistant groups when compared to DMARDs responders (11.0±5.1 and 9.4±3.0 vs. 2.1±1.5, respectively), Table 3.1.

	Healthy controls	DMARDs Responders	DMARDs Resistant	Biologics Resistant	Notes
Age in years, mean (SD)	48 (7.9)**	64 (11)	59 (10)	58.8 (10.1)	** Healthy controls were significantly younger than patients in all other groups
Sex – Female/Male	18/3	9/7	17/5	35/6	
Mean (SD) disease duration, months	N/A	249 (134)	148 (101)*	220.1 (101.1)	* DMARD responsive patients had longer disease duration than patients resistant to DMARDs
% RF+	5***	81	90	78	*** Healthy controls had significantly lower RF+ titer than any of the patient groups, although there was no difference between patient groups themselves
RF titer, IU/ml, median (25,75%)	11 (10, 11)	64 (19, 238)	359 (117, 754)	72 (13,192)	
% anti-CCP+	5***	81	84	68	*** Healthy controls had significantly lower anti-CCP titer than patient groups, no difference between patient groups themselves
Anti-CCP titer, IU/ml, median (25,75%)	1.9 (1.3, 3.2)	201 (15, 340)	316 (165, 340)	213 (13,340)	Note - values over 340 are above detectable level
Mean (SD) tender joint count (TJC)	N/A	1.4 (2.5)****	14 (7.1)	9.5 (5.4)	**** Significantly lower TJC in DMARDs responders compared to both patients groups failing treatment
Mean (SD) swollen joint count (SJC)	N/A	2.1 (1.5)****	11 (5.1)	9.4 (3.0)	**** Significantly lower SJC in DMARDs responders compared to both patients groups failing treatment
Median (25,75%) CRP, mg/dl	0.15 (0.05, 0.4)	0.98** (0.34, 1.5)	1.0*** (0.6, 3.4)	1.0*** (0.5,3.3)	**-*** Significant difference between CRP levels in healthy controls and all patient groups
Median (25,75%) ESR, mm/h	8.0*** (4.0, 15)	13 (11, 25)	27 (11, 57)	23.5 (11,39)	*** Significant difference between ESR levels in healthy controls and DMARDs resistant patients only

Table 3.1 Rheumatoid arthritis patient cohort and healthy controls, demographics.

Table shows demographic data from patient groups and matched healthy controls. Statistical analysis between groups was done by one-way ANOVA. Parameters that exhibited normal Gaussian distribution are represented by mean with 95% standard deviation (Mean (SD)). Non-parametric data are represented by median with 25% and 75% percentiles (Median (25,75%)). Statistical significance is represented by * - $p<0.05$, ** - $p<0.01$, *** - $p<0.001$, **** - $p<0.0001$.

3.2.2 Disease activity scores

To assess disease severity, progression and effect of treatment, several validated clinical scores were used, amongst which was the primary clinical measurement tool – disease activity score 28 (DAS28) [69,70,626]. The score is based on separate counts of swollen and painful joints amongst preselected 28 joints assessed by the clinician, visual analogue scale (VAS) for the average pain estimate by the patient and inflammatory marker CRP or ESR, making DAS28-CRP or DAS28-ESR scores, as described in Chapter 1. DAS28 score is a continuous scale, in which a DAS of >5.1 represents high disease activity, DAS28 score between >3.2 and <5.1 results in moderate activity, while the DAS28 score in the range of 2.6-3.2 is a mark of low disease activity at the time of assessment. Clinical remission is classified with the DAS28 score of <2.6. A change of 1.2 in the score of the individual patient is considered a clinically significant change.

In our patient cohort, mean values (±SD) of the DAS28-CRP were 3.0±0.7 for the DMARDs responders, 5.7±1.2 for the DMARDs resistant and 5.1±0.9 for biologics resistant patients as stated in Table 3.2. Similarly, DAS28-ESR was 3.2±0.6, 6.0±1.3 and 5.3±1.2 in DMARD responders, DMARD resistant and Biologic resistant groups respectively (Table 3.2). Overall, there was a significant difference between DAS28-CRP and DAS28-ESR scores between DMARDs responders and both groups of patients failing current treatment, $p<0.0001$. DMARDs responders group included patients with low disease activity (DAS28 ≤3.2) established and maintained on the current DMARD treatment despite longer overall disease duration compared to other patient groups. This group also had the highest number of male subjects (7/16, 44%). Since male sex has been associated with higher chance of achieving drug related low disease activity [621] we have confirmed that there was no difference in disease activity scores between males and females across DMARDs responders group (Mean±SD, 2.9±0.4 vs 3.0±0.9 in DAS28-CRP, respectively; 3.1±0.15 and 3.2±0.8 in DAS28-ESR, respectively). Maintained DAS28 response is also a good prognostic factor and predicts a better long-term outcome for all patients [70,71]. In contrast to this, the two later disease groups included patients with high disease activity on current DMARDs and/or biologics treatment as evident from DAS28 scores ≥5.1 indicating poor prognostic outcome despite shorter disease duration in the case of DMARDs resistant patients (Table 3.2). Patients in the later two groups have also

experienced a variety of DMARDS or biologic agents and as such can be classified as patients with true treatment resistant disease.

Regarding individual components of DAS28 score, the significant disparity was found in counts of tender and swollen joints in both treatment failure groups compared to good responders (Table 3.1). Additionally, we observed an increase in the patient's global score in DMARDs resistant group when compared to DMARDs responders (61±25 vs. 38±23, respectively, Table 3.2), indicating a significant overall impact of high disease activity. As stated previously, all patient groups had normal CRP levels and raised ESR marker. However, no significant difference was measured between the groups (Table 3.1).

The Clinical Disease Activity Index (CDAI) and the Simplified Disease Activity Index (SDAI) are two other continuous measures used in this study as the most recent tools for the clinical trials outcomes [77,627]. Similarly to DAS28, the SDAI score involves 28 joint counts for tender and swollen joints, acute reactant CRP (mg/dl) and patient's global assessment, with addition of the physician's global assessment also measured on 0-10 Likert scale. Although more details on clinical scoring using SDAI can be found in Chapter 1, most importantly high disease activity is measured by scoring >26, moderate range is 12-26, mild <3.4-11, and remission is suggested with SDAI of <3.3. 22 points represent a major change, while an improvement in 10 to 21 points is considered a minor change.

Given that CRP results are not always available at the time of the patient's appointment, CDAI score was developed to be interpretable at the clinic and includes the sum of 28 TJC and SJC, patient's global assessment and patient's overall pain score. No acute phase reactant is necessary for the CDAI score. High disease activity is represented by score >22, moderate range lies between 11-22, low disease activity is within the score of 2.9-10, and remission is <2.8. Latest ACR guidelines on evaluation of disease activity in RA suggest that use of DAS28, CDAI and SDAI scores incorporating CRP are all valid discriminative measures and prediction of clinical outcomes correlate with each other [80,627].

	Healthy controls	DMARDs Responders	DMARDs Resistant	Biologics Resistant	Notes
Mean (SD) DAS28 (CRP)	N/A	3.0 (0.7)****	5.7 (1.2)	5.1 (0.9)	**** Significant difference in DAS CRP score between DMARD responders and both patient groups failing treatment
Mean (SD) DAS28 (ESR)	N/A	3.2 (0.6)****	6.0 (1.3)	5.3 (1.2)	**** Significant difference in DAS ESR between DMARD responders and both patient groups failing treatment
SDAI, median (25, 75%)	N/A	8.7**** (6.2, 10)	40 (28, 47)	31 (24, 38)	**** Significant difference in SDAI between DMARD responders and both patient groups failing treatment
CDAI, median (25,75%)	N/A	7.6 **** (4.9, 9.5)	37 (27, 44)	29 (20, 34)	**** Significant difference in CDAI score between DMARD responders and both patient groups failing treatment
Mean (SD) patients pain score	N/A	38 (23)	61 (25)*	48 (22)	* DMARD resistant patients report significantly higher pain score than DMARD responsive patients
Mean (SD) patient's global assessment	N/A	30 (20)	66 (24)***	50 (25)*	***-* Significant difference in patients global assessment between DMARD responders and both patients groups failing treatment, respectfully
Mean (SD) physicians global assessment	N/A	1.6 (0.6)****	6.4 (2.4)	4.5 (1.9)	**** Significant difference in Physicians global assessment between DMARD responders and both patients groups failing treatment

Table 3.2 Rheumatoid arthritis patient cohort - clinical scores.

Table shows clinical data from patient groups. These score are not applicable to healthy controls group. Statistical analysis between groups was done by one-way ANOVA. Parameters that exhibited normal Gaussian distribution are represented by mean with 95% standard deviation (Mean (SD)). Non-parametric data are represented by median with 25% and 75% percentiles (Median (25,75%)). Statistical significance is represented by * - $p<0.05$, *** - $p<0.001$, **** - $p<0.0001$.

In this patient cohort, SDAI and CDAI scores did not exhibit normal Gaussian distribution and are represented as median values with 25th and 75th percentile. The SDAI score in the group of patients responding to DMARDs treatment was below the active disease threshold and was significantly lower compared to both treatment failure groups (Median (25, 75%) of 8.7 (6.2,10) in DMARD responders group vs. 40 (28,47) in DMARD resistant group and 31 (24,38) in Biologic resistant group, $p<0.0001$, Table 3.2). Similarly, median CDAI score in DMARDs responders group confirmed low disease activity (7.6 (4.9, 9.5)), while the median score in DMARDs resistant and biologics resistant groups was significantly higher at 37 (27, 44) and 29 (20,34), $p<0.0001$, respectively (Table 3.2).

With regards to individual components of the scores, significantly higher TJC and SJC in therapy failing groups were major indicators of high disease activity, as shown previously in Table 3.1. Besides those, high patient global assessment (30±20 vs. 66±24, $p<0.0001$ and vs. 50±25, $p<0.01$ in DMARD responders vs. DMARD resistant and Biologic resistant groups respectively) and higher physician's global assessment (1.6±0.6 vs. 6.4±2.4 and vs. 4.5±1.9, $p<0.0001$ in DMARD responders vs. DMARD resistant and Biologic resistant groups respectively) were significantly higher in the latter two groups failing treatment and were other main contributors to the overall raised clinical scores.

In summary, the DMARDs responders group comprised patients with long-established but well-managed disease with low disease activity recorded by all clinical tools used. The DMARDs resistant group included patients with shorter disease duration compared to the previous group, with high disease activity as evident from the clinical tools used and additionally with increased inflammatory response, significantly higher patients pain and global scores and higher physician's global assessment indicating poorly controlled disease despite current treatment. Finally, biologic resistant patients also exhibited high disease activity on all clinical scores, raised ESR inflammatory marker and significantly higher patient's and physician's global scores confirming the presence of disease refractory to the use of more than one biologic agent.

3.2.3 Treatment protocols in patient groups

All patients in the DMARDs responsive group received a single treatment agent at the time of the recruitment. The majority of these were on monotherapy with Sulfasalazine (10 patients, 62.5%), and then Methotrexate (5 patients, 31.25%), with one remaining patient (6.25%) on historically established gold therapy (Table 3.3). DMARDs resistant patients have previously experienced a median of 3 DMARDs ranging from 2 to 6 different agents, including double or triple therapy with Sulfasalazine, Methotrexate and/or Hydroxychloroquine or historically used single agents like Leflunomide, Azithromycin, Gold or Penicillamine. At the time of recruitment 13 patients (59.5%) were on Methotrexate, 2 patients (9%) on Sulfasalazine, four patients (18%) on Leflunomide, and one patient (4.5%) receiving Hydroxychloroquine, Gold or Penicillamine each. Patients in the biologics resistant group were also highly experienced with DMARDs agents with a median of 6 drugs, ranging from 2 to 8. Alike previous group, majority of patients (29 patients (71.2%)) were on therapy with Methotrexate, with 3 patients (7.2%) on Sulfasalazine or Hydroxycholoquine, 2 patients (4.8%) on Leflunomide and 1 subject (2.4%) with no DMARD treatment or rarely used single agents like Azithromycin, Gold or even Prednisolone respectively, Table 3.3.

Similar to the DMARDs treatment group, patients in the biologic resistant group had also experienced a wide range of biologic agents before recruitment for this study, listed in Table 3.4. Overwhelmingly, first choice biologic was a TNFα inhibitor, mainly Adalimumab (19 patients, 46.3%), Etanercept (17 patients, 41.5%) or Infliximab in 4 patients (9.75%). One patient (2.45%) was started on treatment with Abatacept, an anti-T cell agent, as a part of a clinical trial. The mean number of biologic agents per patient was 3, ranging from 2 to 5. Most popular second choice, for 73.2% of patients, was a second TNFα inhibitor or, alternatively, 26.8% were switched to a B-cell inhibition with Rituximab. Later choices have seen an addition of anti-IL-6 agent Tocilizumab and, again, anti-T cell agent Abatacept, while the last choice was based entirely on options alternative to an anti-TNFα agent.

	DMARDs Responders	DMARDs Resistant	Biologics Resistant
Current DMARDs	16 total	22 total	41 total
None	-	-	1 (2.4%)
Methotrexate	5 (31.25%)	13 (59.5%)	29 (71.2%)
Sulfasalazine	10 (62.5%)	2 (9%)	3 (7.2%)
Hydroxychloroquine	-	1 (4.5%)	3 (7.2%)
Leflunomide	-	4 (18%)	2 (4.8%)
Azithromycin	-	-	1 (2.4%)
Gold	1 (6.25%)	1 (4.5%)	1 (2.4%)
Prednisolone	-	-	1 (2.4%)
Penicillamine	-	1 (4.5 %)	-

Table 3.3 The list of current DMARDs in each of patient groups.

Table shows numbers of patients and the percentage of all patients in the group being treated with particular disease modifying anti-rheumatic drugs (DMARDs) at the time of the study recruitment.

	Current biologic	1st	2nd	3rd	4th	5th
Adalimumab	-	19	15	4	-	-
Etanercept	4 (9.6%)	17	13	4	1	-
Infliximab	-	4	2	7	1	-
Rituximab	20 (49%)	-	11	14	1	1
Abatacept	1 (2.4%)	1 (Trial)	-	-	1	2
Tocilizumab	5 (12%)	-	-	4	3	1
None	11 (27%)	-	-	-	-	-

Table 3.4 The list of current biologic therapy and history of different agents used in the treatment of biologics resistant patient group.

The column of current biologics shows the total number and the percentage of patients treated with specific biologic agent at the time of recruitment for the study. Additionally, the table shows the most popular choices for the alternative therapy switch in this patient group.

There are many causes of treatment failure in patients. In this case, discontinuation of the first biologic agent could be explained by either primary or secondary loss of efficacy or the presence of side effects. Amongst them, 11 patients (27%) have not achieved a meaningful clinical improvement (measured by DAS28 ESR or CRP change of >1.2) within 6 months of treatment initiation and were classified as a primary failure. A secondary failure occurred in 14 patients (34%) that had meaningful improvement within first 6 months but progressed to develop active disease with an increase in the DAS28 score to the level observed prior to the start of the treatment at a later point. However, the majority of patients (16, 39%) had to stop with first therapeutic due to the side effects, most common ones being the injection/infusion site reaction and infection. Study entry criteria for the Biologic resistant group were, therefore, based on a failure of 2 or more biologic agents to reflect a true inefficacy rather than the presence of side effects.

Along with the above treatment, all patients with high disease activity were given ’rescue’ steroids in the intramuscular or intra-articular form to rapidly reduce the inflammation and provide symptomatic relief until the onset of action of DMARD or biologic therapy. Daily oral steroids were used in one patient from DMARD responders group, while intravenous methylprednisolone was routinely administered before Rituximab infusion in an effort to prevent an adverse reaction to the drug.

3.3 MiR array in RA patients and healthy controls

Here I set out to investigate the miR expression profile of purified CD14+ monocytes derived from the peripheral blood of rheumatoid arthritis patients and comparable healthy controls. Our hypothesis was that global analysis of miR expression profiles would highlight miR-regulated disease pathways. To this end, the Affymetrix 3.0 miR Array platform was used for these experiments. Principal component analysis of all patient and healthy control groups is shown in Figure 3.1. It uses statistical test with orthogonal transformation to identify a possible correlation between parameters within one group that are linearly uncorrelated at first glance. Here we see that principal component 1 (PC1) is clearly distinguishing the group of DMARDs responsive patients, likely due to the meticulous clinical categorisation. However, neither PC1 nor PC2 is capable of distinguishing between all other groups as they show increased variability. Inability to clearly separate clinically distinctive groups of patients from each other or healthy controls even in the single cell study points to difficult and, likely, multifactorial pathogenesis of this disease. Even so, monocytes and macrophages continue to be the cell type of interest for this study as we sought to analyse the effects of treatment or the lack thereof in RA.

Further miR array analysis identified 493 differentially expressed miRs between biologics resistant and DMARDs responder patients, while the smallest difference (63 miRs) was found between good responders and healthy controls groups, pointing towards different epigenetic changes in high disease activity state (Venn diagram, Figure 3.2). Therefore, we decided to focus on differences in miRNA expression between DMARDs responders and both patient groups failing multiple modes of treatment to highlight pathways in progressive disease and treatment resistance.

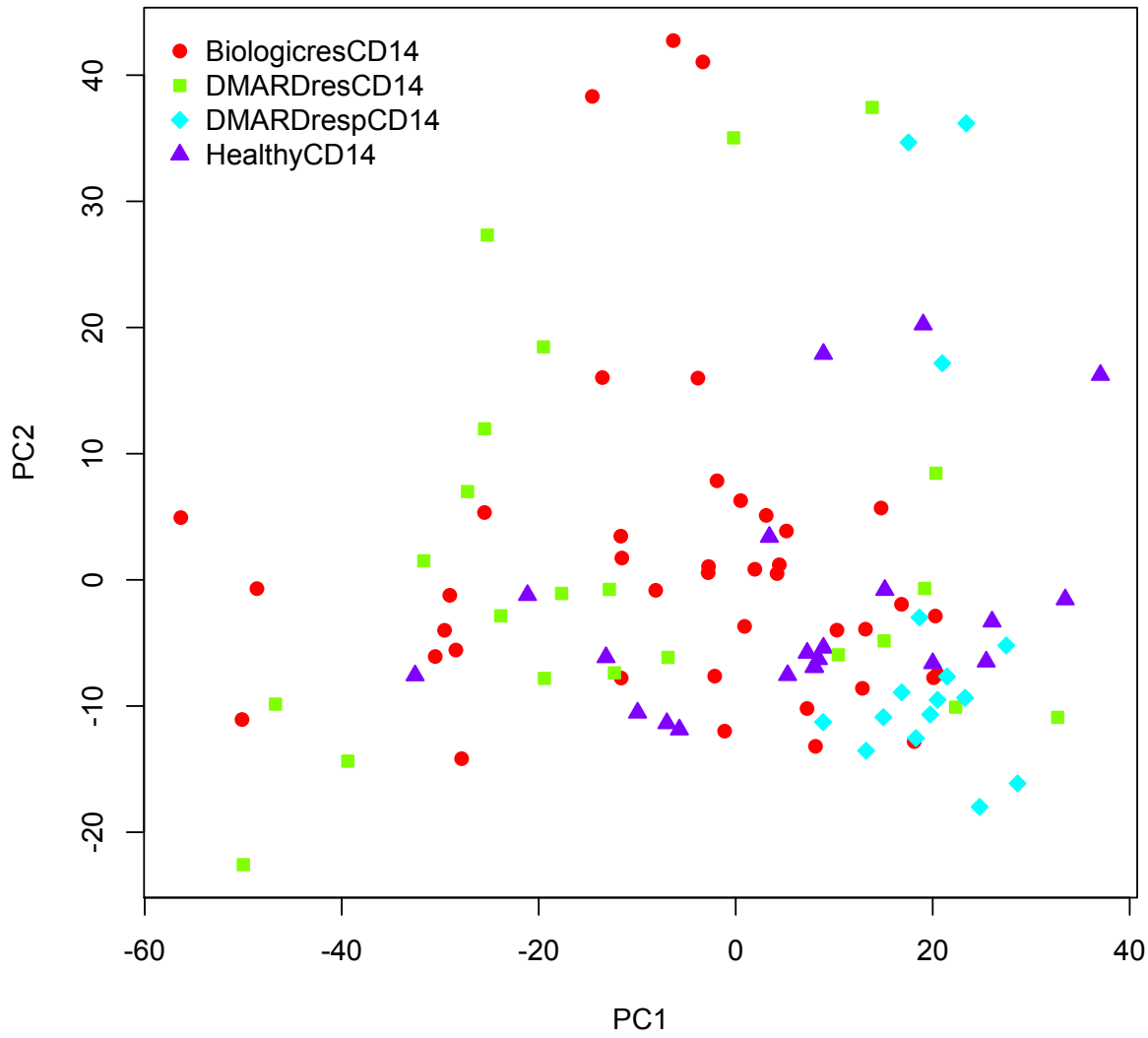

Figure 3.1 Principal component analysis of miR Array in all patient groups and healthy controls.

Principal component analysis identified two principle components – PC1 and PC2 shown above, to allow categorisation of each group. MiR Array was performed on CD14+ monocytes isolated from peripheral blood of participants. DMARDs responder patients (DMARDresCD14) have formed a tight expression cluster and are clearly distinguished by PC1. DMARDs resistant (DMARDresCD14), Biologics resistant (BiologicresCD14) patients and healthy controls (HealthyCD14) have disseminated expression patterns and could not be easily distinguished by PC1 or PC2.

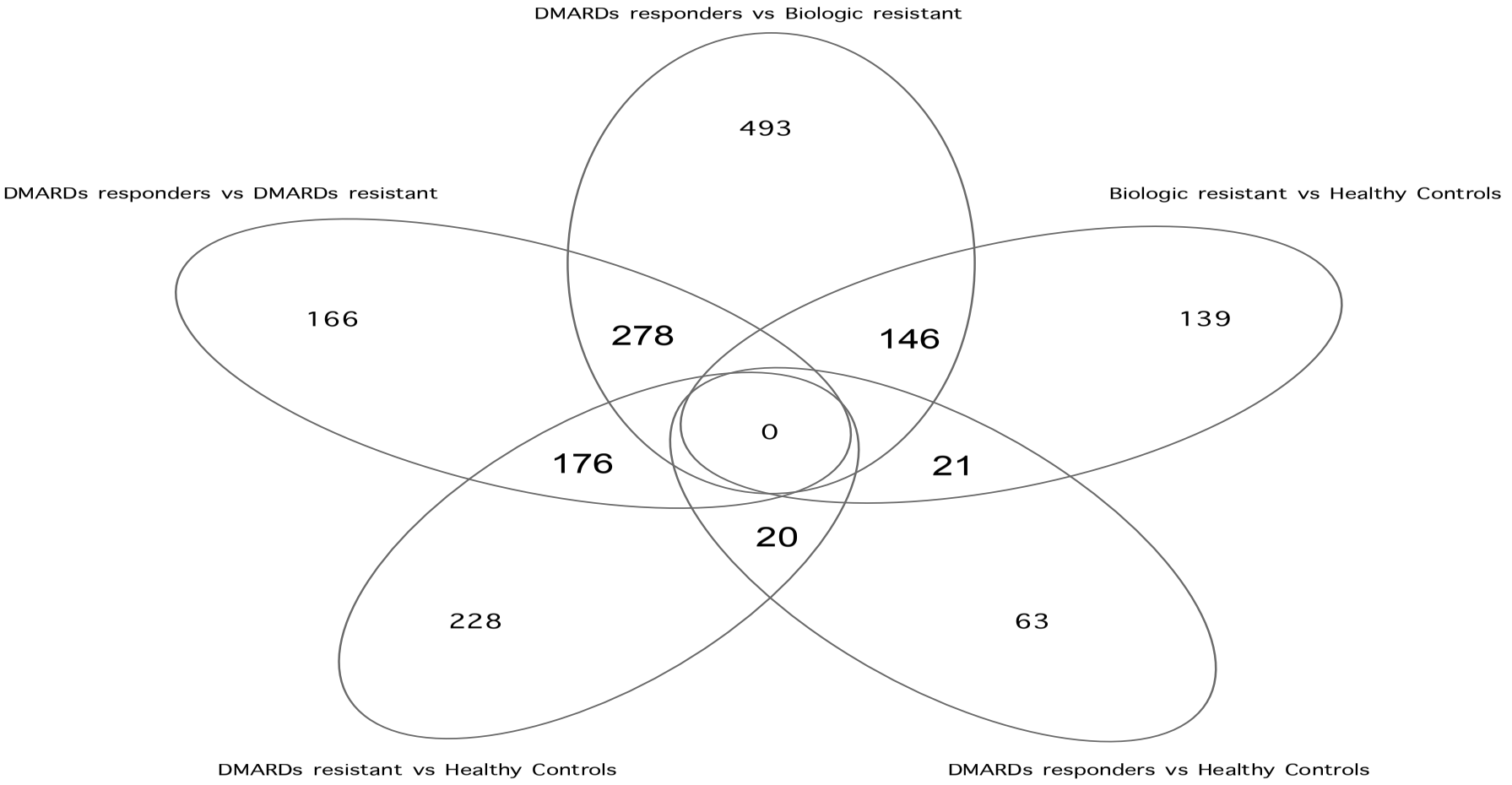

Figure 3.2 Venn diagram shows individually compared differentially expressed miRs across all patient and healthy control groups.

Figure shows sum of differentially expressed miRs from $CD14^{+}$ monocytes. Comparison is made between all patient and control groups. Analysis included miRs with statistically significant differential expression between the each comparison ($p<0.05$).

3.3.1 MiR-27 and miR-23 are differentially expressed between treatment responders and non-responders.

Comparing miR signatures in treatment-responsive and resistant RA: here we list the top 50 miRs differentially expressed between DMARDs responders and DMARDs resistant groups (Figure 3.3). We identified miR-27a and miR-27b as being expressed significantly lower in DMARDs resistant patients when compared to good responders. Similarly, analysis of top 50 differentially expressed miRs between DMARDs responders and biologic resistant groups (Figure 3.4) identified hairpin miR-27a probe, miR-23a and miR-23b to be downregulated in difficult to treat patients.

Interestingly, these miRs derive from two almost identical miR clusters - miR-23a~24-2~27a and miR-23b~24-1~27b each of them expressed as a single primary transcript. Multiple studies have gathered data to support a strong synergistic effect of miRs derived from a single cluster, as they have the capacity to target multiple molecules of the same pathway and, therefore, exhibit increased overall impact. For example, miR-19, miR-212 and miR-132 are a part of the cluster collectively targeting transcription factor FOXO3 in haematopoietic stem cells regulating cell survival [628]. Moreover, the previous investigation of this particular miR-23a~24~27a cluster has shown the cooperative function of cluster members in several human diseases and cancer [567]. Given that multiple members of miR-23a and miR-23b clusters were differentially expressed in patients failing multiple modes of treatment when compared to good responders, here we chose to further investigate the expression of miR-23-24-27 clusters in peripheral blood monocytes in treatment-resistant RA.

Expression of mature miRs from both miR 23~24~27 clusters across all treatment and control groups is shown in Figure 3.5. MiR-27a is downregulated in both groups failing treatment when compared to healthy controls (Median (25, 75%), 10.38 (9.7, 10.8) and 10.52 (10.2, 10.8) vs. 10.8 (10.7, 10.9) in DMARD resistant, Biologic resistant vs. healthy control groups, $p<0.01$ in both comparisons respectively) and when compared to DMARDs responders (Median (25, 75%) 10.7 (10.6, 10.8) in DMARD responders vs. 10.4 (9.7, 10.8) in DMARD resistant groups, $p<0.05$; hp-hsa-miR-27a_st probe, 1.96 (1.84, 2.18) in DMARD responders vs. 1.5 (1.3, 1.7) in Biologic resistant groups, $p<0.01$ respectively).

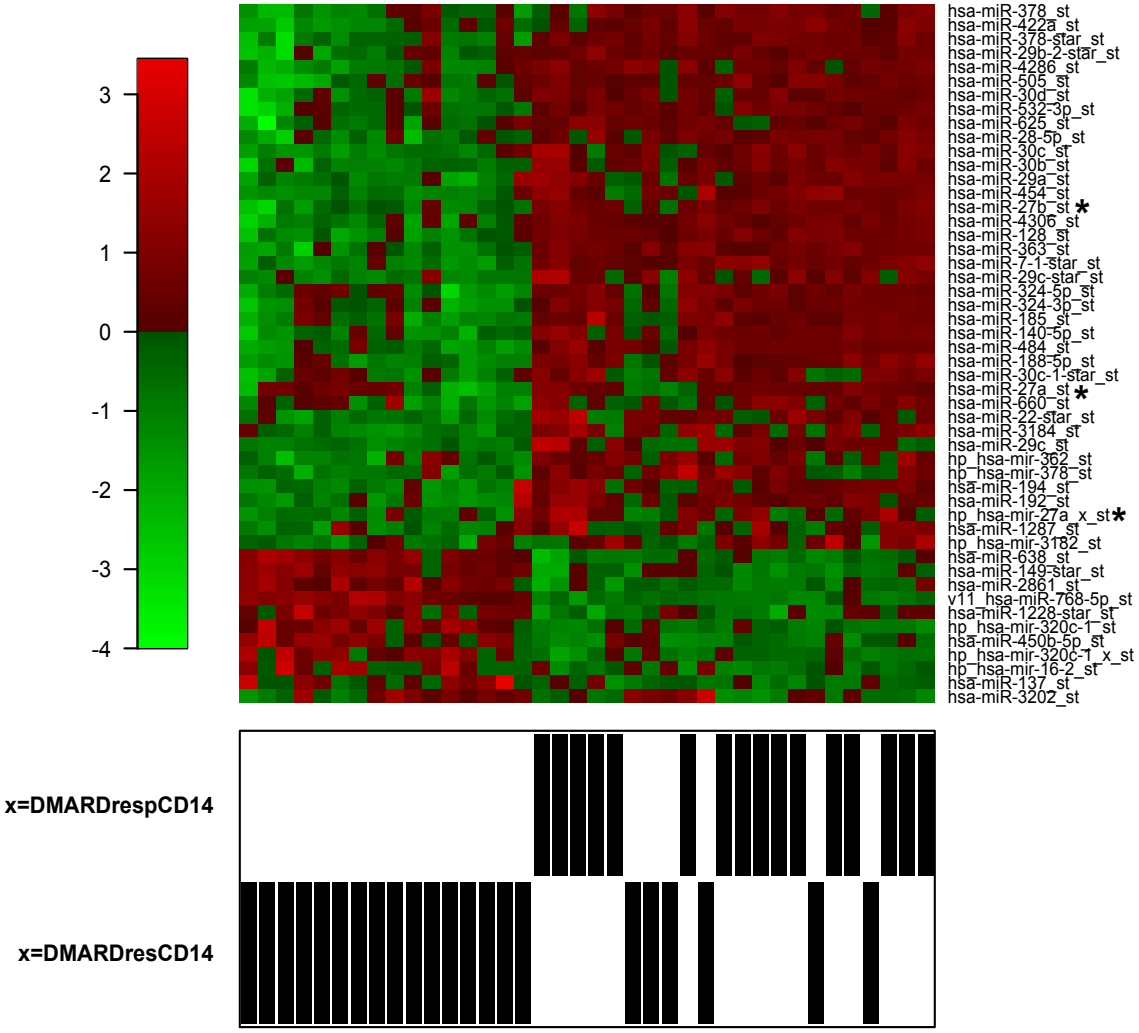

Figure 3.3 Heat-map of top 50 differentially expressed miRs in DMARDs responders and DMARDs resistant groups.

This figure shows the heat-map of differentially expressed miRs between DMARDs responders (x=DMARDrespCD14) and DMARDs failures (x=DMARDresCD14). The left side of the plot shows **Log2** expression intensity scale where red stipulates overexpressed (max +3.4) and green symbolises underexpressed genes (min -4). The right side of the heat-map lists miR probes. Star symbol is marking probes identifying mature miR-27a and miR-27b and hairpin miR-27a probe.

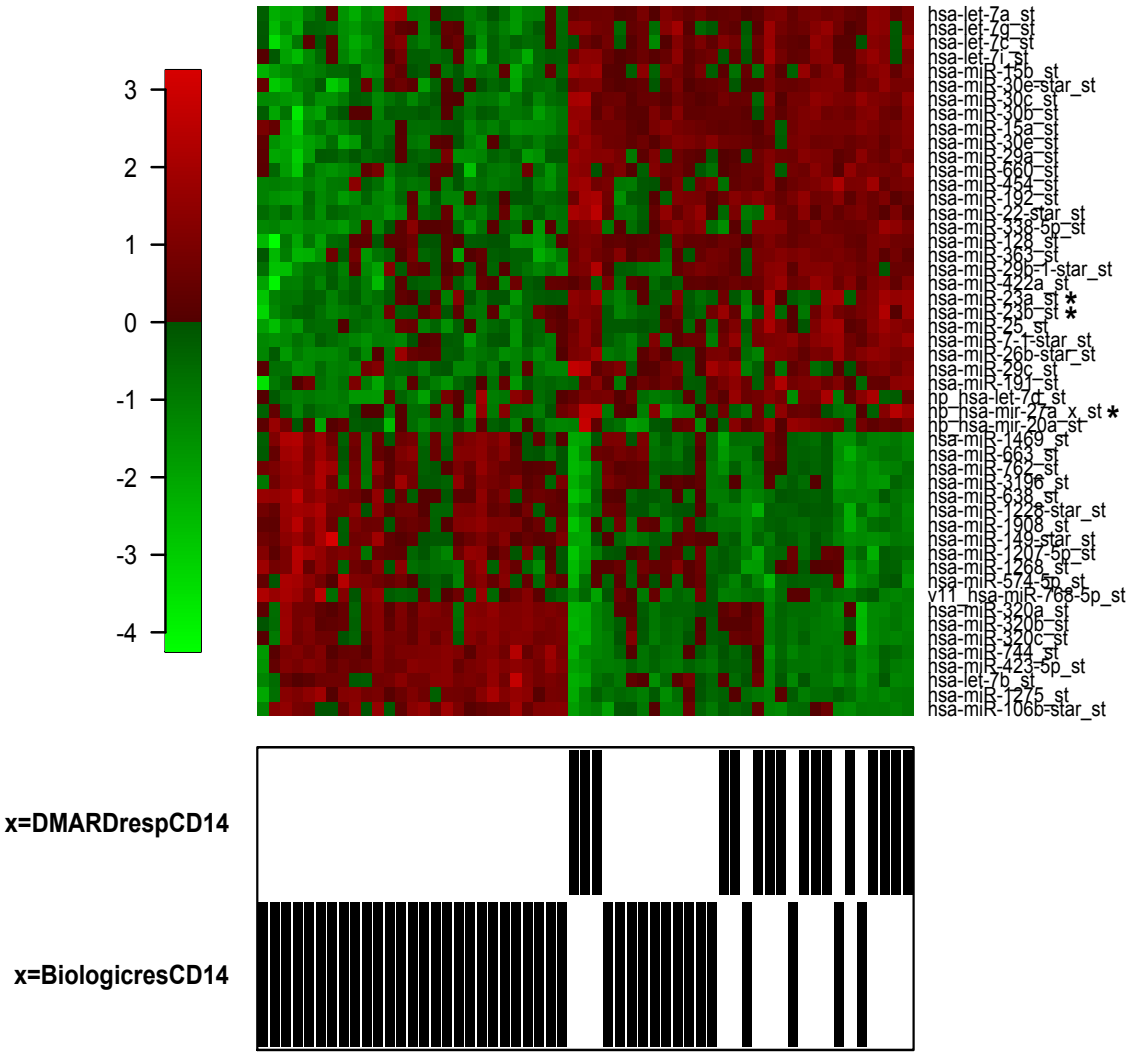

Figure 3.4 Heat-map of top 50 differentially expressed miRs between DMARDs responders and Biologics resistant groups.

This figure shows the heat-map of differentially expressed miRs between DMARDs responders (x=DMARDrespCD14) and Biologics treatment failures (x=BiolodicresCD14). The left side of the plot shows **Log2** expression intensity scale where red stipulates overexpressed (max +3.2) and green symbolises underexpressed genes (min -4.2). The right side of the heat-map lists miR probes. Star symbol is marking probes identifying mature miR-23a and miR-23b and hairpin miR-27a probe.

Similarly, miR-27b is downregulated in DMARDs resistant patients when compared to healthy controls (Median (25,75%) 6.56(6.1,6.93) in DMARD resistant vs. 7.2(7.1,7.4) in healthy controls, $p<0.01$) and in both treatment failure groups when compared to good responders (6.56(6.1,6.93) and 6.9(6.6,7.2) vs. 7.35(7.2,7.5) in DMARD resistant, Biologic resistant and DMARD responders groups, respectively, $p<0.0001$). There was no statistical difference in miR-27a or miR-27b expression between healthy controls and good responder groups.

Next, we investigated the expression of miR-24. The sequence of mature miR-24 is identical in both miR-23~24~27 clusters and could not be distinguished in detection in this assay. Therefore a single probe can identify its total expression. The log2 intensity of miR-24 probe is decreased in DMARDs responders group compared to all other groups (Mean±SD 12.75±0.19 in DMARD resistant vs. 12.87±0.07 in healthy controls, 12.88±0.07 in DMARD responders and 12.93±0.11 in Biologic resistant groups, $p<0.05$, $p<0.05$ and $p<0.0001$ respectively), Figure 3.5 plot D.

Lastly, Figure 3.5 plots **E** shows expression of miR-23a to be significantly increased in DMARDs responders group compared to healthy controls (Median (25, 75%) 13.3 (13.2, 13.4) in DMARD responders vs. 13.13 (13.1, 13.2) in control groups, $p<0.01$), but also in comparison with biologics resistant patients (13.3 (13.2, 13.4) in DMARD responders vs. 13.15 (13.1, 13.2) in Biologic resistant groups, $p<0.001$). Moreover, this pattern is consistent with expression of miR-23b, Figure 3.5 plot **F,** which is found to be higher in DMARDs responders compared to all other groups (Median (25, 75%) 11.3 (11.2, 11.4) in DMARD responders vs. 11.1 (11, 11.2) in healthy controls, 11.2 (11, 11.3) in DMARD resistant and 11.1 (11, 11.2) in Biologic resistant groups, $p<0.05$, $p<0.05$ and $p<0.001$ respectively).

DMARDs and biologics treatment resistant groups have varied only in expression of mature miR-23a, which is found to be decreased in the Biologic resistant group (Median (25, 75%) 13.2 (13.1, 13.4) in DMARD resistant and 13.15 (13.1, 13.2) in Biologic resistant groups, $p<0.05$) and in miR-24 expression, which was decreased in DMARDs treatment failures (Mean±SD 12.75±0.19 in DMARD resistant vs. 12.93±0.11 in Biologic resistant groups, $p<0.0001$), Figure 3.5.

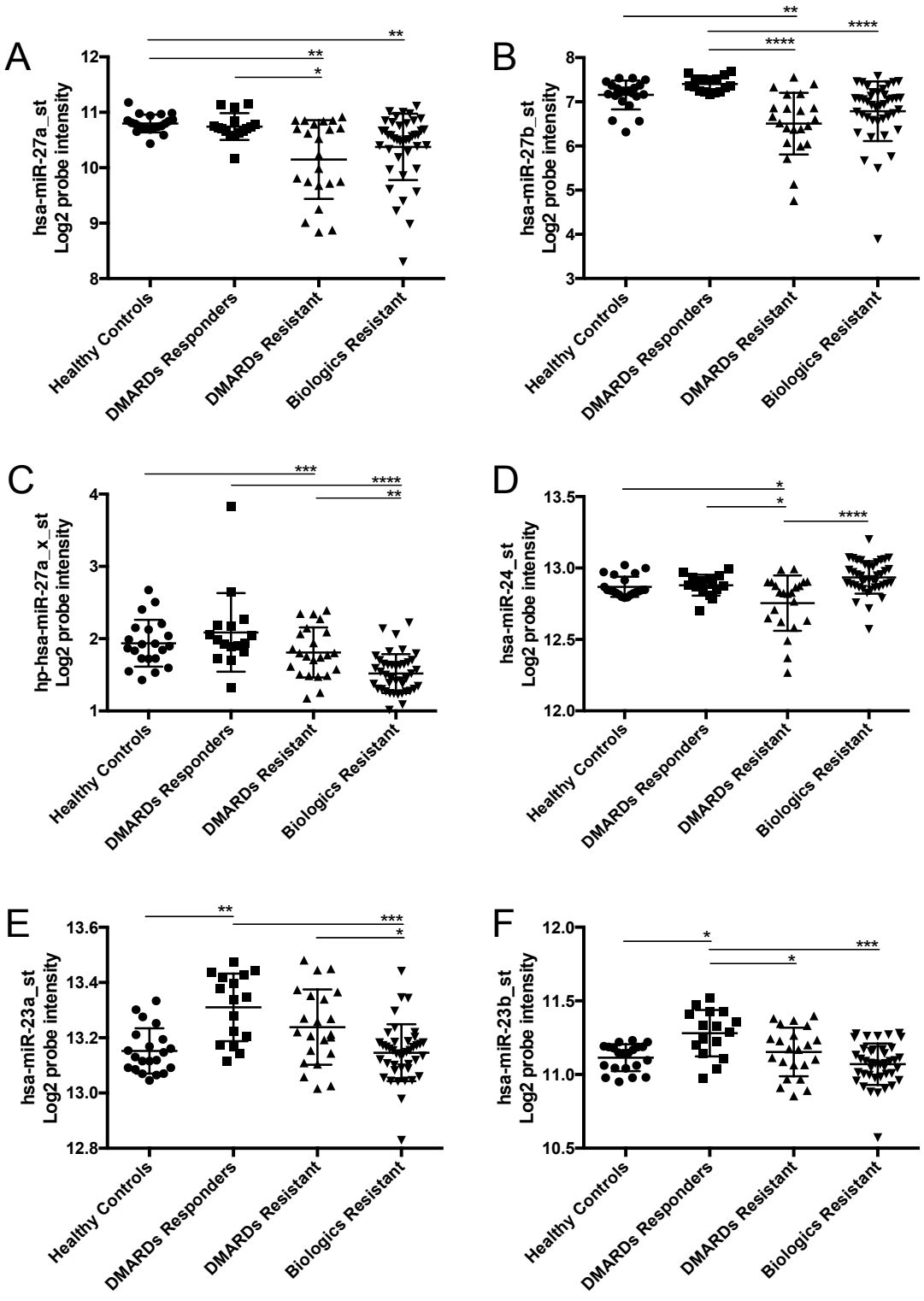

Figure 3.5 Expression of mature miRs from miR-23a~24-2~27a and miR-23b~24-1~27b clusters in miR Array from CD14+ monocytes of RA patients and healthy controls.

This figure shows Log2 intensity of the miR Array probes identifying mature miR-27a **(A)**, mature miR-27b **(B)**, hairpin loop probe of miR-27a **(C)**, mature miR-24 **(D)**, mature miR-23a **(E)** and mature miR-23b **(F)**. Statistical analysis for all probes apart from miR-24 was done using non-parametric multiple comparisons Kruskal-Wallis test with Dunn's correction. Expression of miR-24 across all groups passed D'Agostino and Pearson's normality test and was analysed using one-way ANOVA test with Tukey's test for multiple comparisons. Statistical significance is shown by * - $p<0.05$, ** - $p<0.01$, *** - $p<0.001$, **** - $p<0.0001$.

3.3.2 Mature miRs derived from the single cluster do not correlate in their expression.

Figure 3.6 shows the relative log2 intensity of expression of mature miRs derived from both miR-23~24~27 clusters. All probes are expressed at different intensities and are within the assay's detection limit as evident from standard array platform controls, here exemplified by positive AFFX-CreX-3_at and negative AFFX-ThrX-3_st controls (Mean±SD 14.90±0.06 and 1.13±0.13, respectively).

Unexpectedly, no significant correlation was found between expression of miR-23a and miR-27a. This was true for expression in all patient and healthy controls groups, as well as in all samples analysed together (Table 3.5). MiR-24 also did not correlate with expression with other two members of miR-23a~24-2~27a cluster. This finding could be explained by the nature of the miR-24 sequence and our inability to distinguish its origins between 'a' or 'b' clusters.

In the second cluster, miR-27b has correlated with miR-23b levels ($r=0.37$, $p=0.0001$) and with miR-24 ($r=0.25$, $p=0.012$) across all samples. However, individual group analysis has shown that significant moderate correlation occurred only in DMARDs resistant group (Table 3.5).

These data point towards likely posttranscriptional regulation of mature miR expression from the primary transcript, which has been described previously for miR-23~24~27 clusters [629].

	miR-23a~24-2~27a cluster (r, p values)			miR-23b~24-1~27b cluster (r, p values)		
	miR-23a vs miR-24	miR-23a vs miR-27a	miR-24 vs miR27a	miR-23b vs miR-24	miR-23b vs miR-27b	miR-24 vs miR27b
All groups	-0.03, 0.77	-0.1, 0.32	-0.002, 0.98	-0.045, 0.65	**0.37, 0.0001**	**0.25, 0.0122**
Healthy Controls	0.27, 0.23	0.06, 0.79	-0.37, 0.1	0.03, 0.9	0.29, 0.21	-0.15, 0.51
DMARDs Responder Patients	-0.23, 0.39	0.13, 0.63	-0.08, 0.77	-0.45, 0.08	0.43, 0.09	-0.35, 0.19
DMARDs Resistant Patients	0.22, 0.32	-0.37, 0.09	-0.06, 0.8	0.04, 0.87	**0.43, 0.0459**	**0.52, 0.013**
Biologics Resistant Patients	0.097, 0.55	-0.046, 0.78	-0.13, 0.42	0.23, 0.16	0.29, 0.07	0.03, 0.84

Table 3.5 Expression correlation of mature members of miR-23a~24-2~27a and miR-23b~24-1~27b clusters across all samples or individual groups.

Table shows correlation intensity (r) and significance (p) between all mature miR members of the same miR cluster believed to be expressed from a single primary transcript. Numbers in bold mark statistically significant correlations according to Pearson's correlation coefficients.

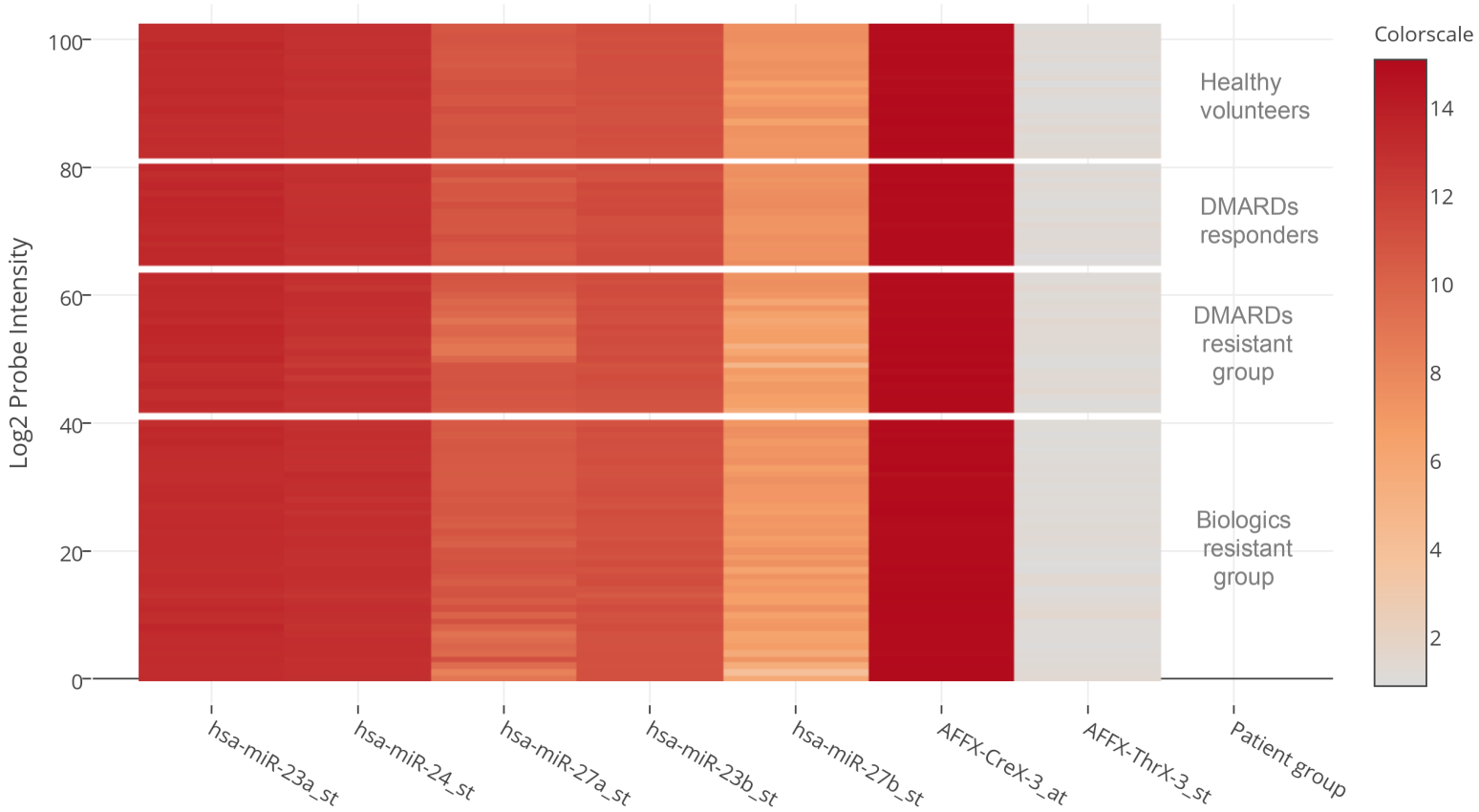

Figure 3.6 Intensity of mature miR Array probes from 'a' and 'b' miR-23-24-27 clusters across all patient groups.

This figure shows the heat map of log2 intensity of all individual probes identifying mature miRs derived from both miR-23~24~27 clusters. Probe identities are listed below. AFFX-CreX-3_at is a positive control probe. AFFX-ThrX-3_st is a negative control probe. Reference colour scale is represented on the right side (min – 1; max - 15).

3.3.3 Primary miR-23a~24-2~27a but not pri-miR-23b~24-1~27b transcript is expressed in CD14+ monocytes.

The miR-23a~24-2~27a cluster is expressed as a single transcript whereas miR-23b~24-1~27b is thought to be co-expressed with its host C9ORF3. Differential expression of mature miRs prompted us to investigate the expression of primary miR transcript levels in the patient cohort.

In the Affymetrix 3.0 miR Array, there are two hairpin loop probes for each member of the miR-23a~24-2~27a cluster and a single probe for each member of the primary miR-23b~24-1~27b sequence. Intensities of hairpin loop probes designed to identify primary miR sequences from both clusters are depicted in Figure 3.7.

Surprisingly, the only strong hybridization signal was detected from extended primary miR-23a probe (hp_hsa-miR-23a_x_st probe, Mean±SD 6.94±0.23), with significantly lower expression detected by both miR-27a probes (hp_hsa-mir-27a_st and hp_hsa-mir-27a_x_st, 1.85±0.39 and 1.62±0.35, $p<0.0001$, respectively). The mean intensity of all probes designed to detect primary transcript of miR-23b~24-1~27b was below the arbitrary cut-off of 1.3 (the log2 intensity of control negative probes on the array, including AFFx-ThrX-3_st probe) and was significantly lower than pri-miR-23a probe above (Figure 3.7).

The presence of mature miRs from miR-23b~24-1~27b cluster with absence of primary transcript could be explained by extended longer half-life of mature miRs compared to rapidly processed primary transcripts, but also there is a possibility that the methods used are not sensitive enough to fully distinguish one nucleotide difference between mature miRs of ‘a’ and ‘b’ cluster, therefore recognising miR-23a for miR-23b, for example.

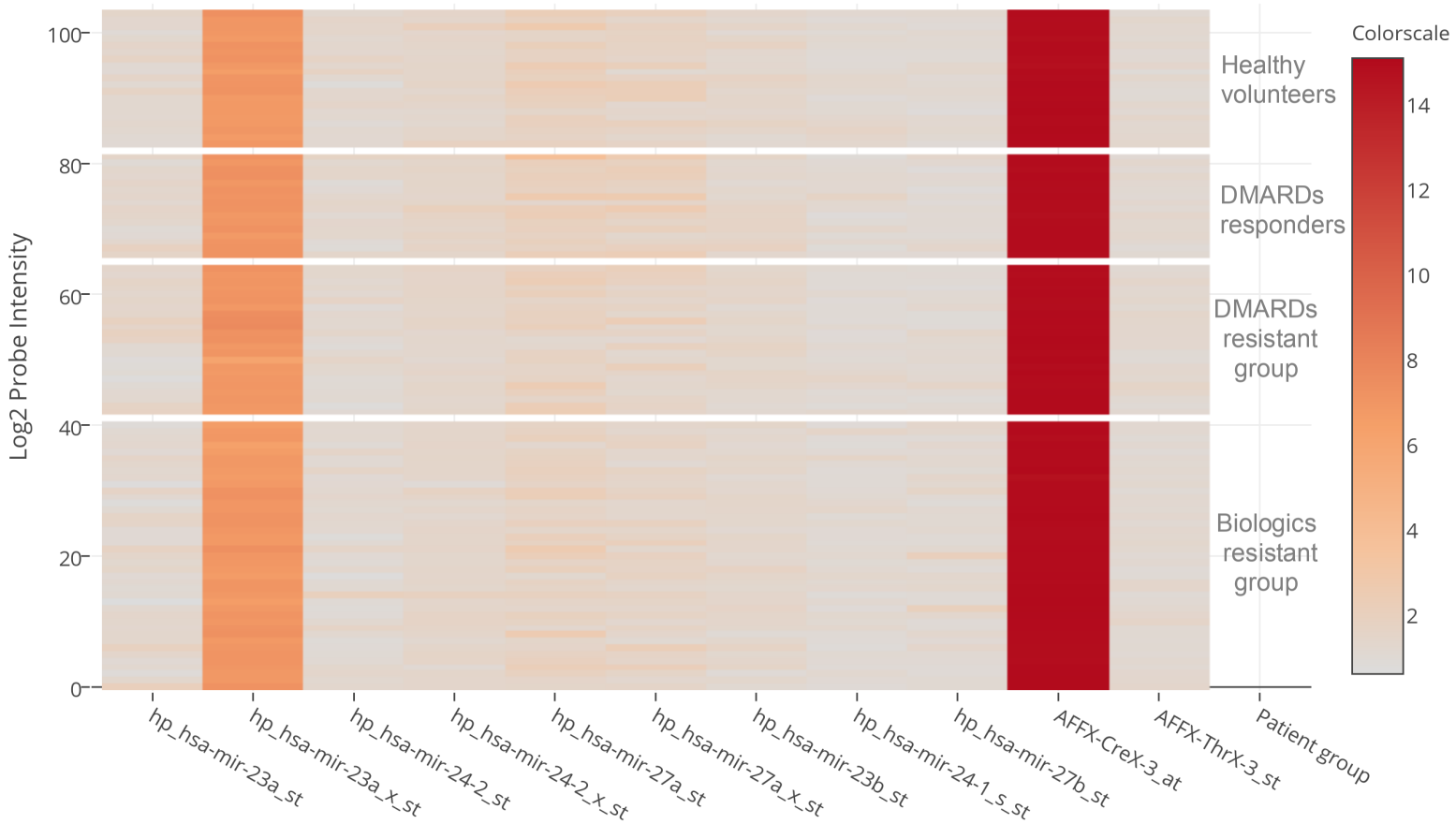

Figure 3.7 Intensity of the primary transcript probes for 'a' and 'b' miR-23-24-27 clusters across all patient groups.

This figure shows the heat map of log2 intensity of all probes identifying primary miRs transcripts of both miR-23~24~27 clusters. Probe identities are listed below. AFFX-CreX-3_at is a positive control probe. AFFX-ThrX-3_st is a negative control probe. Reference colour scale is represented on the right side (min – 1; max - 15).

3.3.4 Array probes lack specificity to distinguish between miRs with single nucleotide difference.

To investigate the potential cross-reactivity of the miR probes we correlated probes with single nucleotide differences. Certainly, strong correlation between expression of mature miR-23a and miR-23b ($r=0.75$, $p<0.0001$) and miR-27a and miR-27b ($r=0.66$, $p<0.0001$) would support the hypothesis of probe cross-reactivity. Furthermore, linear regression showed that overall 56.4% of detected miR-23b could be explained by the expression of miR-23a ($r^2=0.5637$, $p<0.0001$) and 44% of the miR-27b level by miR-27a transcript ($r^2=0.4379$, $p<0.0001$), Table 3.6. This association, however, was not statistically significant in the healthy control group and DMARDs resistant patients with regards to miR-27a and miR-27b expression (Table 3.6).

To further explore the option of cross-reactivity between other mature miRs with similar sequences, we have identified miR-155 and miR-505 to have single nucleotide difference between the human and mouse forms, both of which are present on the Affymetrix 3.0 miR Array platform including probes for other 151 organisms. As expected, mouse miR-155 and miR-505 probes were able to detect a human sample but with lesser intensity than original human probes (Mean±SD of log2 probe intensity, 2.61±0.64 vs. 9.91±0.29 for miR-155 and 1.32±0.36 vs. 4.02±1.08 for miR-505, mouse and human probes respectively, Figure 3.8). Also, the significant correlation between human and mouse miR-155 ($r^2=0.3994$, $p<0.0001$) was observed. Mouse and human miR-505 expressions exhibited weak correlation with only tendency for significance ($r^2=0.1823$, $p=0.0695$) pointing towards lower limits of accuracy in lowly expressed probes (<1.5 log2 intensity). Overall, this example confirms that cross-hybridisation of sequences with single nucleotide difference occurs in the array platform used for the analysis of this cohort and, as such, significant degree of detection of mature members of miR-23b~24-1~27b cluster depended on the intensity of the expression of miR-23a~24-2~27a cluster, where highly expressed transcripts like miR-23a had higher chance of cross-hybridization.

	miR-23a vs. miR-23b		miR-27a vs. miR-27b	
	Correlation (r, p)	Linear regression (R^2)	Correlation (r, p)	Linear regression (R^2)
All groups	**0.75, <0.0001**	**0.5637**	**0.66, <0.0001**	**0.4379**
Healthy Controls	0.33, 0.14	0.1095	0.01, 0.96	0.0001
DMARDs Responder Patients	**0.73, <0.0012**	**0.5382**	**0.51, 0.0423**	**0.2629**
DMARDs Resistant Patients	**0.70, <0.0002**	**0.4971**	0.33, 0.1280	0.1120
Biologics Resistant Patients	**0.75, <0.0001**	**0.5621**	**0.80, <0.0001**	**0.6414**

Table 3.6 Correlation and linear regression between the expression of 'a' and 'b' forms of miR-23 and miR-27 across all samples or individual groups.

This table shows correlation intensity (r), significance (p) and linear regression (R^2) between miR-23a and miR-23b in the left column and miR-27a and miR-27b in the right column. Numbers in bold mark statistically significant correlations (Pearson's correlation coefficients) and linear regression.

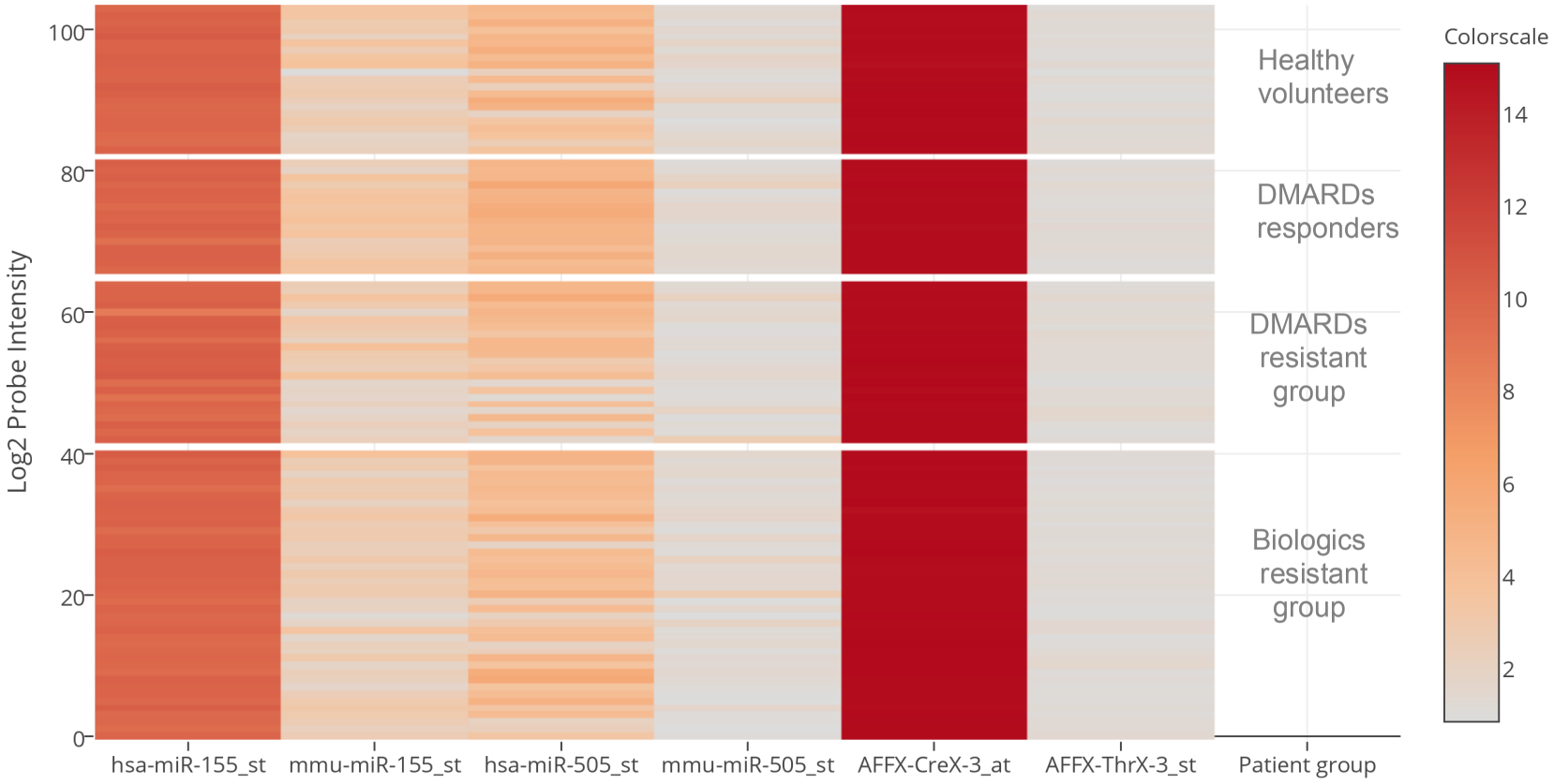

Figure 3.8 Two examples of cross-hybridization of human and mouse probes in miR species with single nucleotide difference on Affymetrix 3.0 miRNA Array.

This figure shows the heat map of log2 intensity of all probes identifying human (hsa-) and mouse (mmu-) probes of miR-155 and miR-505 (probe identities are listed on the x axis). AFFX-CreX-3_at is a positive control probe. AFFX-ThrX-3_st is a negative control probe. Reference colour scale is represented on the right side (min – 1; max - 15)..

3.4 Increased expression of miR-27a and miR-27b in DMARDs responders is validated by qPCR.

Quantitative PCR is a more sensitive method of detecting transcript expression and is therefore widely accepted for validating results of the miR array. Before testing valuable clinical samples we explored the sensitivity of miR qPCR primers and their ability to distinguish sequences with a single nucleotide difference. I selected the option of testing this with Qiagen miR SYBR Green qPCR primers.

For this purpose, we created miR standards from commercially available miR-27a and miR-27b mimics diluted with sterile RNase free water to the concentration of 10^9 – 10^7 – 10^5 - 10^3 molecules per 2µl of the solution. These miR standards were then detected with both miR-27a and miR-27b primers in qPCR reaction. Here we established that miR-27a primers can detect miR-27b mimic with a significantly lower efficacy resulting in 7 to 9 PCR cycles delay (Figure 3.9, A). As expected in this case, detected levels of miR-27b linearly correlated with miR-27a and could be fully explained by the affinity of the miR-27a primer for the miR-27b sequence ($r=0.9978$, $R^2=0.9956$, $p=0.0022$). Likewise, miR-27b primers were able to detect miR-27a sequence with equal 7 to 9 PCR cycles delay, again creating a 10^2-10^3 gap and significantly depending on the affinity of miR-27b primers ($r=0.9977$, $R^2=0.9954$, $p=0.0023$), Figure 3.9, A. Although there is obvious cross-reactivity between these assays, our biological samples do not express more than 10^3-10^5 copies of miR per test, allowing us to account for the contamination which is in this case negligibly small. Meaning that qPCR method would be acceptable quantifying the expression of miRs with a single nucleotide difference like miR-23a/b and miR-27a/b.

Quantitative PCR analysis of the RA patient samples confirmed significantly increased expression of miR-27a in DMARDs responders when compared to healthy controls (Median (25,75%) 0.96 (0.8, 1.3) vs. 0.54 (0.36, 0.69) respectively, $p=0.01$) and both groups failing treatments (0.23 (0.11,0.38) in DMARDs failures and 0.37(0.16,0.58) in Biologics failures, $p<0.0001$ in both comparisons, Figure 3.9, B left). Equally, miR-27b was found to be significantly higher in DMARDs responders when compared to healthy controls (Median (25,75%) 0.07 (0.06, 0.08) and 0.04 (0.03, 0.05) respectively, $p=0.05$) and both non-responder groups (0.04 (0.01, 0.05) in DMARD resistant and 0.04 (0.02, 0.09)

in Biologic resistant groups, p=0.01 in both comparisons, Figure 3.9 B, right). The miR-27b expression is on average 10-fold lower than of miR-27a and could not be explained solely by the cross reactivity of qPCR primers, indicating a minor presence of mature miR-27b in the samples. For this analysis, three samples from healthy controls and ten samples from Biologics resistant group were excluded from the testing due to the very low content and poor purity of RNA in the samples, confirmed by NanoDrop measurement.

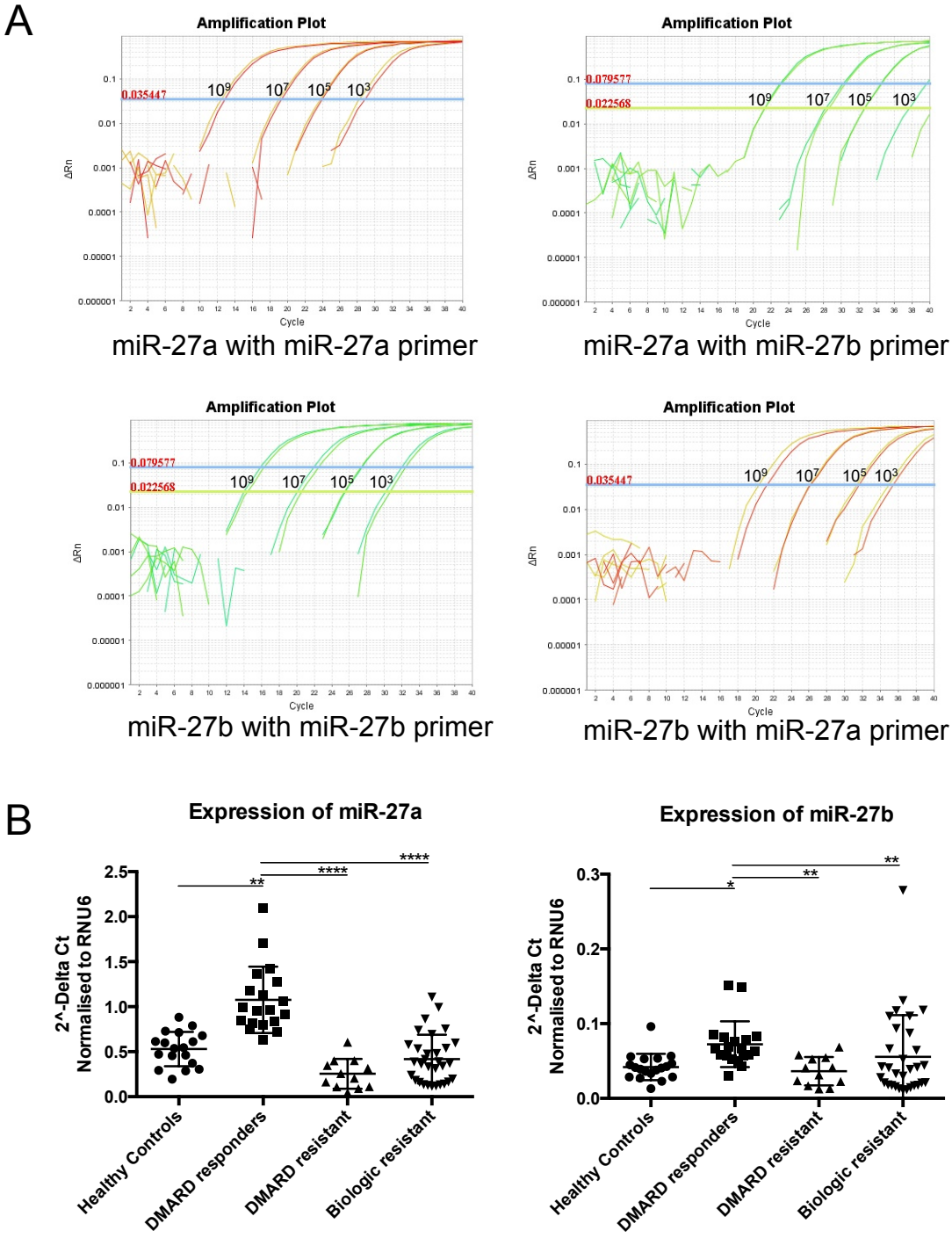

Figure 3.9 Validating the expression of miR-27a and miR-27b by qPCR.

Qiagen SYBR-green mature miR Assays were used for the qPCR of miR-27a and miR-27b in CD14+ cells from RA patients and healthy controls. (**A**) Representative amplification plots for the specificity of Qiagen miR primers detecting miR standards derived from mature miR mimic cDNA reconstituted with water to the concentration of 10^9, 10^7, 10^5 and 10^3 molecules/µl. Numbers in red represent assay detection threshold. MiR-27a standards detected with miR-27a primers (top left), miR-27a standards detected with miR-27b primers (top right), miR-27b standards detected with miR-27b primers (bottom left) and miR-27b standards detected with miR-27a primers (bottom right). (**B**). Expression of mature miR-27a and miR-27b in primary CD14+ monocytes from all RA patients and healthy controls. QPCR method, data displayed as Mean±SD of 2^-dCT normalized to RNU6 control gene. Data analyzed by Kruskal-Wallis test for multiple comparisons with Dunn's correction, * - p<0.05, ** - p<0.01, **** - p<0.0001.

3.5 Expression of miR-27a but not miR-27b correlates with multiple clinical outcomes.

One of the goals of this study was to identify single or multiple miRs that can, in future work, be evaluated for their biomarker potential and further inform clinical and therapeutic choices. Addressing this, we analysed the correlation of miR-27a and miR-27b qPCR expression with clinical measures captured during categorisation of the patient cohort.

MiR-27a but not miR-27b showed significant negative correlation with multiple clinical outcomes and scores. Tender joint count (TJC) and swollen joint count (SJC) both correlated negatively with miR-27a expression ($r=-0.3751$ and $r=-0.4125$, $p<0.01$ respectively), Figure 3.10 A. Although no correlation was found with inflammatory markers like ESR and CRP or subjective parameters like patients VAS pain score, miR-27a has significantly negatively correlated with both DAS28-ESR and DAS28-CRP scores ($r=-0.3974$ and $r=-0.3974$, $p<0.002$ respectively), Figure 3.10 B.

Likewise, miR-27a had significant negative correlation with SDAI and CDAI scores ($r=-0.4531$ and $r=-0.4389$, $p<0.001$ respectively), Figure 3.10 C. This is likely based on the correlation with TJC and SJC since there was no significant association of miR-27a expression with other individual components of SDAI or CDAI scores including patients or physician's global scores.

Reassuringly, there was no obvious correlation between miR-27a or miR-27b expression and patients/volunteers age indicating that expression of these miRs is not driven purely by senescence. Interestingly, no association was found with disease duration amongst patients, inflammatory markers (CRP and ESR) or autoimmune antibodies (RF or anti-CCP). This taken together with significant correlation with SJC and TJC points towards the specific association of miR-27a with synovial inflammation rather than general inflammation, serology or age. The negative correlation of miR-27a with these parameters further supports our hypothesis of the protective role of this miR in the monocyte-mediated synovial inflammation in the context of RA.

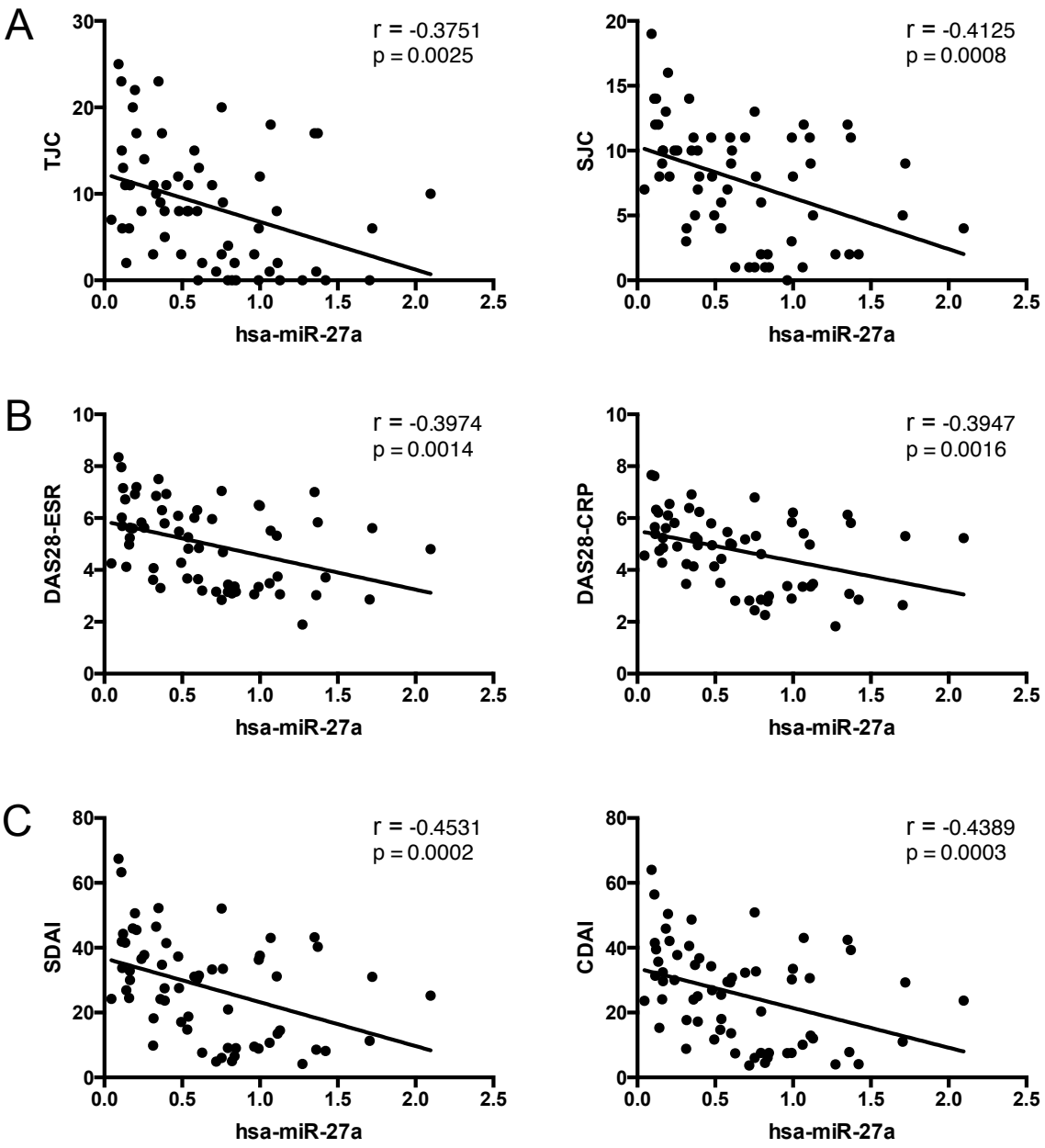

Figure 3.10 Expression of miR-27a correlates with clinical data from all RA patients.

Plots show all RA patients recruited for the study. (A) Here, tender joint count (TJC) on the left and swollen joint count (SJC) on the right show moderate negative correlation with qPCR miR-27a expression (Pearson's parametric correlation coefficient, r=-0.3751, p=0.0025 and r=-0.04125, p=0.0008, respectively). (B) Both clinical scores DAS28-ESR (left) and DAS28-CRP (right) negatively correlate with qPCR miR-27a expression (Pearson's parametric correlation coefficient r=-0.3974, p=0.0014 and r=-0.3947, p=0.0016, respectively). (C) SDAI (left) and CDAI (right) clinical score also negatively correlate with qPCR miR-27a expression (r=-0.4531, p=0.0002 and r=-0.4389, p0.0003, respectively). For this analysis Spearman's non-parametric correlation coefficient was used since SDAI and CDAI scores exhibit non-parametric distribution.

3.6 Discussion

RA is an autoimmune, chronic and likely pathogenically diverse disease. Treatment options are based on immune suppression. Whether it is DMARDs or biologic treatments, drug-free remission is too rare [630] [621]. More importantly, trials have shown that it is early recognition, clinical judgment and an aggressive treat to target approaches that are key factors in achieving remission in patients. For example, TICORA (Tight Control of RA) study showed that improving clinical practice and implementing tight control protocols can increase the clinical remission rate with DAS score <1.6 to 65% after 18 months, compared to only 16% success rate in the routine group [64]. The success of the routine group, in this case, is also comparable with the overall efficacy of 12 months of TNFα treatment after DMARDs failure, with 26%, 21%, and 17% DAS28 remission rates with adalimumab, etanercept and infliximab respectively [631]. The negative outcome of the Triple Therapy in Early RA (TEAR) study posing a valuable question whether remission rates could be further improved by starting the treatment with triple DMARD therapy in every patient, has taught us that "one drug for all" no matter how intense is not appropriate for the treatment of RA [65]. Moreover, it is still recommended that Methotrexate as a single agent should be the first line treatment for the majority of RA patients with expected efficacy in more than one-third of cases [632]. The clinical data above support the hypothesis of this study that "right patient and right treatment/treatments" should be identified early for the improved efficacy. To study this we have turned to the detailed clinical categorisation of patients with different treatment response to a variety of therapeutics.

For this, we selected three patient groups and matched healthy controls. All patients met the ACR 1987 diagnostic RA criteria and had established disease. They were further subdivided into groups. The first clinical group involved good responders with low disease activity on DMARDs, mostly a single agent, with disease duration over ten years. These were patients with low disease activity (DAS28<3.2) rather than patients in remission (DAS28<2.6) which made recruiting in the given timescale possible. This group was then compared to the patients with high disease activity (DAS28>5.1) despite treatment with several DMARDs and shorter overall disease duration. Lastly, we have compared the good responders to a group involving patients with high disease activity (DAS>5.1) on 2

or more biologic treatments. Unfortunately we failed to recruit a group of patients with good response to biologic treatment, and this is a shortcoming of this study. However, the principle separation of patients into responders and non-responders is still valid. Although the separation of medical treatments to DMARDs and biologics therapies is a crude approach to segregating treatments, it is the most historically established one. DMARDs agents vary greatly in the mechanism of action, efficacy and side effects as described in Chapter 1. Similarly, a variety of biologic treatments could be easily separated further according to the cell type they affect. Moreover, new therapies like small molecule inhibitors have a distinct mechanism of action but do not strictly adhere to any of these categories and would pose a further dilemma on the classification of the treatments used. The major contribution of biologic agents was, therefore, a variety of treatment options for patients whose disease does not respond to a number of DMARD agents. Having further treatment options in such an evasive disease is critical for the clinical success which is why understanding the pathogenesis behind the clinical response to single treatment agent and direct comparison to the multiple treatment failures is a valuable characteristic of this study.

Moreover, we selected CD14+ monocytes as blood derived precursors that are not only central to the pathogenesis of RA but also serve as a primary therapeutic target for the majority of treatments used from DMARDs to biologic agents. It has been shown that Methotrexate increases CD95 marker expression in blood mononuclear cells sensitising them to apoptosis [633]. Similar antiproliferative and apoptotic effect of Methotrexate was shown in the THP-1 human monocytic cell line [43]. These findings could explain why the number of circulating $CD14^{+high}$ cells was predictive of clinical response to Methotrexate [634].

Amongst biologic agents, most commonly used anti-TNFα treatment has a direct influence on monocytes recruitment and activity in the RA synovium. Earlier studies have clearly shown reduced number of CD68+ve macrophages in the lining and the sublining of the synovial joint as early as two weeks post first therapeutic infusion [365]. Further studies have confirmed that anti-TNFα treatment significantly reduces the influx of monocytes to the affected joints and likely increases the efflux, overall contributing to the reduction of

inflammation [635]. Responders to treatment with Tocilizumab, an anti-IL6R monoclonal antibody, were also shown to have less circulating monocytes and myeloid DCs [636]. Even Abatacept, a CTLA4 antagonist known for its effect on T cells has been shown to reduce the expression of adhesion molecules in monocytes and macrophages after few weeks of treatments and therefore reduce the endothelial adhesion and migration [637].

From this, I conclude that the majority of current RA treatments primarily target peripheral blood monocytes and macrophages when exuding their therapeutic effect. Therefore this study is unique in the sense that it describes miR profiling of primary pathogenic $CD14^+$ cells in clinically well-defined groups of difficult to treat patients with RA. Such studies including this number of patients are very laborious and represent a classic example of extensive bench to bedside collaboration. Often miR array results have a large number of confounding factors, yet, by narrowing the clinical criteria and isolating a specific cell population we were hoping to better address the question of miR-dysregulation in RA monocytes. Similar approaches have been taken in more recent studies investigated miR profiles of monocytes from patients with systemic juvenile idiopathic arthritis (sJIA), monocyte activation syndrome (MAS) and Sjögren's syndrome [638] [639]. Another study, done on a significantly smaller scale, has compared the miR profile of $CD14^+$ cells derived from synovial tissue obtained during joint replacement in RA and OA patients [640]. Here, authors identified miR-223 as critical regulator of aryl hydrocarbon receptor (AHR) in synovial macrophages from RA patients. The most recent study, published only as an abstract from 2015 ACR meeting has described a miR profile in $CD14^+CD16^+$ populations of peripheral blood monocytes from RA patients and healthy volunteers. However, they have predominantly focused on the atherogenic risk and cardiovascular disease in RA [641]. The most relevant study to date analysed circulating serum derived miRs in 95 RA patients undergoing combined TNFα and DMARDs treatment. Although no speculation was made to the cell types accounting for the differences found, this group has shown that non-responders to combination treatment failed to upregulate miR-23 and miR-223 in the serum, in concordance with our results and additionally underscoring prominent role of miRs in drug-disease interplay [642].

Our patient and healthy volunteer cohort includes predominantly women (56-85%). This is consistent with previous reports of higher incidence of RA in the female sex. It is also well established that joint destruction as a result of inflammation is more pronounced in women (50%) than in men (27%) and requires more often surgical interventions [643]. Seropositivity for RF in our cohort (78-90%) was also comparable to that from the general population of RA patients (80%) and is highly predictive of more aggressive disease [644]. Between 68-84% of recruited RA patients were positive for anti-CCP Ab, other hallmark antibodies in RA associated with joint destruction [645] [646] [647]. Healthy controls were predominantly younger women with mean age of 48 years, and all apart from one were seronegative. One seropositive healthy control had a low RF and anti-CCP titres and denied any clinical signs of the disease, therefore did not meet the exclusion criteria, Table 3.1. These data show no significant differences in age, sex or serological findings between patient groups indicating that these were not likely contributors to the disease resistance seen here. As mentioned before, patients in DMARDs responders group had longer disease than the two groups failing treatment also indicating that treatment resistance is an attribute of the disease pathogenesis rather than duration.

Interestingly, inflammatory markers ESR and CRP were within normal limits in all patient groups. Nonetheless, CRP was significantly higher than in healthy controls group, likely indicating chronic low-grade inflammation. Large studies conducted in subjects with cardiovascular disease have clearly shown an association between the marginal rise in CRP and increased risk of a fatal cardiovascular outcome, despite overall 'normal' levels of the marker [648]. This points towards an overall cumulative effect of the low-grade chronic inflammation exemplified by the small increase in CRP we observed in patient groups. Other clinical parameters were measured only in patient groups where differences between treatment responders and non-responders were obvious. Namely, all clinical scores – DAS28 ESR and CRP, SDAI and CDAI scores as well as independent clinical parameters such as TJC and SJC, patients and physician's global scales were indicating low disease activity in DMARDs responders and were significantly increased in both groups failing treatment confirming the severe on-going inflammatory process, Table 3.2. A separate analysis of DMARDs responder groups demonstrated the equal contribution of both sexes with

regards to low disease activity scores. Overall, we found no clinical idiosyncrasies that would render these data atypical and outcomes are suitable for generalizability to RA.

Array technology on purified $CD14^{+}$ve cells allows for broad, extensive profiling of the miR expression signatures. Group analysis showed a higher proportion of differentially expressed miRs in patients failing DMARDs and biologic treatment compared to DMARDs responders or healthy controls, Figure 3.2. The coherent nature of DMARDs responders was also evident from the principal component analysis when patients in these groups could be easily identified by the first principle component. Treatment-resistant groups and healthy controls group, were significantly more diverse, Figure 3.1. As Leo Tolstoy remarked, “Happy families are all alike; every unhappy family is unhappy in its own way”. Lack of other similar studies and no principle component analysis of those published limit the possibility of comparison and speculation on the coherence of miR expression patterns in drug resistant RA. True to the aim of this project, we investigated and compared drug-resistant and responder groups rather than how they relate to healthy controls.

Comparing miR expression profiles from DMARDs responders and both groups failing treatment, we identified several miRs that have known association with autoimmune or inflammatory conditions. Amongst the top 50 differentially expressed miRs were miR-505, miR-128, miR-422, miR-378, miR-30, miR-29, miR-27 and miR-23, Figure 3.3 and Figure 3.4. For example, miR-505 was recently recognised in a small group of patients as a potential serum biomarker for primary biliary cirrhosis [649]. The immunological role of miR-128 was described in overexpression transgenic mice model with reduced generation of precursors and mature B cells while seeing an increase in common lymphoid progenitor cells [650]. Existing data on miR-422a is limited to 23 reports overwhelmingly in the context of cancer cells. However, a recent publication has demonstrated direct targeting of kallikrein-related peptidase 4 and the role of miR in SLE nephritis [651]. MiR-378 is best known for its effect in muscle strain and certain cancers. However, its immunological role was recognised in the ability to negatively regulate NK cells cytotoxicity, the ability that it shares with miR-30e [652]. Additionally, overexpression of miR-30b has been shown to attenuate antigen presentation capacity of primary human macrophages and dendritic cells [595].

MiR-29 has multiple roles in the immune and inflammatory processes. Our group has shown a decisive role of miR-29 in tendon inflammation and how it regulates the onset and perpetuation of tendinopathy [653]. MiR-29 is also well known for regulating wound healing and for its ability to influence fibrosis, including intestinal fibrosis in inflammatory bowel disease [654]. Lastly, miR-23 and miR-27 are one of the first miRs to be discovered and as such have been studied in a variety of cancers [517] [655] [656]. There is a growing body of work highlighting their important role in autoimmune disease, described in detail in Chapter 1.

Interestingly, there are a number of other miRs known for their importance in RA that have not featured in our analysis. Amongst them are miR-155, miR-146a, miR-223 and miR-34a. Mir-155 is a proinflammatory miR and overexpressed in RA patients. Our group has shown that miR-155 is expressed at a particularly high level in synovial tissue cells compared to PBMCs from RA patients [550]. Furthermore, we have shown that miR-155 expression has a profound effect on migration of monocytes through the regulation of chemokines and chemokine receptors [552]. Next, miR-146a and b are both known for their anti-inflammatory properties in RA myeloid cells. MiR-146a expression is induced by proinflammatory cytokines like TNFα or through LPS stimulation, and in return, they inhibit NFκB signalling by directly binding to IRAK1 and TRAF6 [657]. A further report by Pauley et al. confirmed upregulated miR-146a expression in PBMCs from RA patients and the significant impact it exhibits on TNFα production [554]. Furthermore, miR-223 is known for its stimulating role in osteoclastogenesis by repressing the M-CSF inhibitor NF1A [562]. Both of these miRs were also detected RA and OA synovium [658]. Lastly, we have shown that miR-34a is expressed at high levels in RA SF macrophages and in PB monocytes in difficult to treat patients (Tange, C. E, unpublished data) [659]. The profound role of these miRs in maturation, activation and migration of macrophages may not be as readily reflected in circulating precursor monocytes, therefore explaining why they are not prominently featured in our dataset. Secondly, there is no significant body of data linking these miRs to the effect of medications in RA. Therefore, they might not play a role in treatment response for which this study was designed. As a result, we have focused our further effort on understanding the role of miR-23~24~27 in the treatment-resistant RA

as it contains two members prominently dysregulated in our miR array analysis that may exhibit a synergistic effect in $CD14^+$ RA monocytes.

Briefly, I will touch on the subject of the sensitivity of the miR array detection in the context of the miR-23~24~27 cluster which is of particular interest when accounting for significant similarities between the 'a' and 'b' miR forms. Three principle methods are used for detecting miRs: RT-qPCR, miR array hybridization and next generation sequencing methods. Amongst them, miR array is the least equipped method to distinguish between single nucleotide differences in mature miRs, predominantly because the entire sequence of the miR is used as a probe resulting in the great variability of melting temperatures [660]. Recent technological advancements include higher overall hybridization temperature to decrease the cross-hybridisation or, alternatively, the use of locked nucleic acid bases to increase specificity. However, single nucleotide difference could be distinctively evaluated only by the costly Next-Generation sequencing method [660]. Our data would certainly suggest that Affymetrix miR Array 3.0 platform is not sensitive enough to adequately distinguish between miR-23a and miR-23b or between miR-27a and miR-27b as a high degree of correlation was established in those pairs, Table 3.6. This finding was further exemplified by the clear hybridization signal from relevant murine miR probes in the absence of murine sequences, Figure 3.8. Despite limited sensitivity, it appears that all mature miRs from both 'a' and 'b' miR-23~24~27 clusters were present, even taking into account the higher expression levels of miR-23a and miR-27a compared to their counterparts from the miR-23b~24-1~27b cluster. Even so, we struggled to identify primary transcript identifying miR-23b~24-1~27b cluster. This phenomenon was previously explained in the literature by likely rapid processing of the primary transcript [517]. This is hardly surprising in the context of the overall lower expression of the miR-23b~24-1~27b cluster, which was shown to be expressed at low levels in myeloid cells [593].

The expression of pri-miR-23a~24~27a did not correlate with the expression of mature miRs, Table 3.5. There are several possible explanations for this finding. Firstly, miR-24 is indistinguishable between both clusters and should not correlate with either pri-miR transcript. Secondly, mature miRs have greater stability and longer half-life than primary transcripts. Thirdly, mature miRs from

these clusters are known to have differential processing of the mature forms dependent on the context [567].

Validating this data with qPCR has confirmed that miR-27a and miR-27b are differentially expressed in different treatment groups. Taking into account the healthy controls group it appears that both miRs are upregulated in good responders to DMARDs treatment, Figure 3.9. Failure to upregulate the expression miR-27a in DMARDs and biologics treatment groups showed a negative correlation with all clinical scores – DAS28 ESR and CRP, SDAI and CDAI scores, Figure 3.10. MiR-27a but not miR-27b levels were also found to correlate with the essential clinical parameters – TJC and SJC. Blood-derived parameters that have the ability to correlate with clinical synovial inflammation are quite rare, and biomarker potential of miR-27a could be further explored in the plasma levels and tested in the independent RA cohort, although this would be beyond the spectrum of this investigation. The above-mentioned clinical correlations suggest that miR-23~24~27 cluster may play a role in treatment responses in RA patients.

Summarising my data so far, we have found miR-23a~24-2~27a cluster to be highly expressed in $CD14^{+}$ monocytes from healthy controls or good responders to DMARD treatment with low disease activity. On the contrary, miR-23a and miR-27a expression was significantly reduced in patients failing all modes of treatment that have perpetually increased inflammatory burden, as evident from raised disease activity scores. This inverse correlation is summarised below in Figure 3.11. The next chapter will explore what regulates the miR-23a~24-2~27a cluster in blood-derived monocytes and mature macrophages.

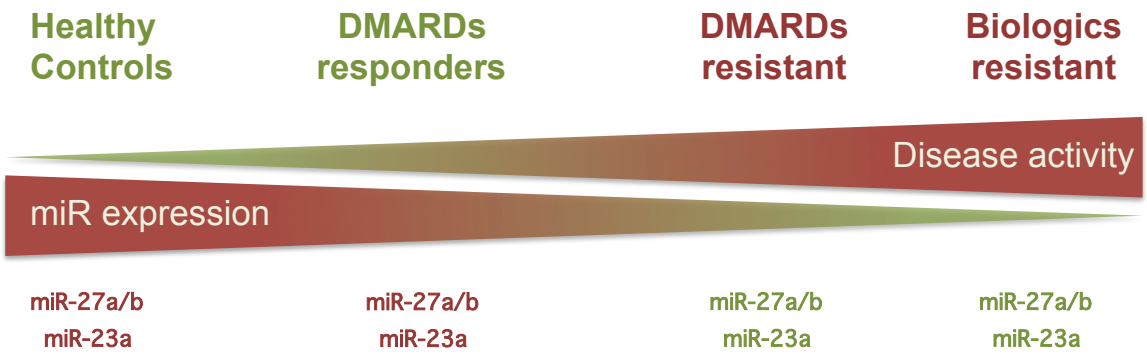

Figure 3.11 Depiction of inverse correlation of miR-23 and miR-27 in CD14^{+} monocytes from RA patients and healthy controls with disease activity.

Study included 21 Healthy controls, 16 DMARDs responders patients, 22 DMARDs resistant patients and 41 Biologics resistant patients. Red colour represents 'higher' values; green colour represents 'lower' values. Arrows represent transformation from no or low disease activity in healthy controls and DMARDs responders (left two groups) to higher disease activity states in DMARDs and Biologics non-responders (right two groups), as measured by DAS28, SDAI and CDAI scores. In contrast, the expression of miR-23 and miR-27 exhibit the opposite distribution.

4 Factors regulating miR-23a~24-2~27a cluster in monocytes and macrophages

4.1 Introduction

MiR-23~24~27 clusters have been implicated in a variety of physiologic and pathologic processes including oncogenesis, tumour metastasis, apoptosis and myelopoiesis (Chapter 1)[567]. This versatility of functions and context-dependent expression of miR-23~24~27 clusters is enabled by a range of regulatory transcription factors (TF). In myeloid cells, miR-23~24~27 was shown to play different roles depending on several TFs crucial to development, maturation and activation of the cells. Amongst them, PU.1 which is necessary for the myeloid lineage commitment [253]. It is the regulation of miR-23~24~27 cluster by PU.1 that plays a decisive role in the promotion of myelopoiesis over B cell lymphopoiesis from progenitor cells in mice [568]. Additionally, miR-23a~24-2~27a can also influence erythropoiesis when regulated by NFκB p65 in bone marrow-derived cells [661,662]. In maturation, terminating expression of miR-24 was necessary to allow M-CSF-driven differentiation of human monocytes into macrophages [663]. Considering that M-CSF is a driving and survival force for the majority, if not all of recruited inflammatory monocytes, this suggests a prime role for miR-23~24~27 clusters in the regulation of innate immune response. This role was further confirmed by reports of direct binding of NFκB p65 to miR-23b promoter upon IL-17A and other cytokine stimulations [593]. Indeed, this data indicates that other pro-inflammatory cytokines acting through NFκB activation like TNFα or TLR ligands could have an effect on miR-23~24~27 clusters [664]. In fact, stimulating mature macrophages with TLR3, TLR4 and TLR9 ligands decreased the expression of miR-23a and relieved the repression on its direct target TNFAIP3 (A20), a negative regulator of NFκB [665]. Regulation of NFκB/A20 pathway is vital not only for autophagy and antifungal properties of macrophages but also for continuation of chronic inflammation [666,667]. Genome-wide association studies (GWAS) have linked polymorphisms in the A20 loci with susceptibility to RA and other auto-immune diseases [668,669]. Further investigation of the regulation of miR-23~24~27 clusters in human myeloid cells will be informative of miR biology as well as of the regulation of monocyte activation under inflammatory conditions like RA.

Reassuringly, human myeloid cells were found to have all the necessary components to process miRs in the usual way, therefore limiting the mechanistic difficulties with interpretation of results [663]. MiR-23a~24-2~27a is expressed as single transcript under the control of its promoter [670]. Its paralogue, the miR-23b~24-1~27b cluster has an intronic location within its host gene C9ORF3 with which it is thought to be exclusively co-expressed [567]. Despite being present in a variety of contexts, it seems that miR-23a-24-2~27a is primarily expressed in blood derived cells while its paralogue is predominantly present in tissues [567]. Investigating the transcriptional regulation of miR expression requires quantification of primary miR transcripts rather than mature forms. It is here we can measure rapid changes in the rate of expression that would otherwise be difficult to detect in what are often significant pools of relatively stable mature miRs [517,670]. This underscores the importance of focusing on early time points when investigating the stimuli and pathways responsible for regulating the expression of pri-miR-23a~24-2~27a [517,670]. In this chapter, I will elucidate the influence of pro-inflammatory cytokines on the expression of the primary miR-23~24~27 transcript in human monocytes and macrophages.

4.2 Results

4.2.1 Expression of miR-23~24~27 clusters in CD14$^+$ monocytes.

Circulating monocytes are abundant and versatile blood cells typically distinguished by CD14$^+$ cell surface marker [671]. Purified CD14$^+$ cells from four buffy coats were tested for the expression of miR-23~24~27 clusters (Figure 4.1). Primary miR-23a~24-2~27a cluster transcript was expressed at significantly higher levels than pri-miR-23b~24-1~27b (Figure 4.1, A). Pri-miR-23a~24-2~27a was also found to be highly expressed in CD14$^+$CD16$^-$ monocytes when compared to total CD14$^+$ cells (Figure 4.1, B). These "classical" monocytes are thought to have less contribution to overall inflammation in such autoimmune diseases as RA and SLE than pro-inflammatory CD14^{low}CD16$^+$ cells, in keeping with our hypothesis that miR-23a cluster may have an anti-inflammatory role in RA [672,673].

While, mature miR-23a, miR-24 and miR-27a are readily detectable in CD14$^+$ cells they do not appear to accumulate at equal numbers, with miR-24 levels being significantly higher than miR-23a or miR 27a (Figure 4.1, C). I also observed no significant difference between levels of miR-23a and miR-27a, this is in contrast to a previous report in mouse CD14$^+$ monocytes which showed reduced expression of miR-23a compared to others [568]. Although found at similar levels, miR-23a and miR-27a did not correlate with their expression in these samples ($r=0.495$, $p=0.505$). As expected, mature members of the paralogue cluster, miR-23b and miR-27b, were expressed 100-fold less than the ‘a’ cluster (Figure 4.1, D). Within this data, miR-23b is present at significantly higher levels than miR-27b (Figure 4.1, D). There is an almost linear correlation between the expression ‘a' and ‘b' miR family members, which strongly suggests there is significant primer cross-reactivity in the mature ‘a' and ‘b' qPCR assays in keeping with observations recorded in Chapter 3 (Figure 4.1, E).

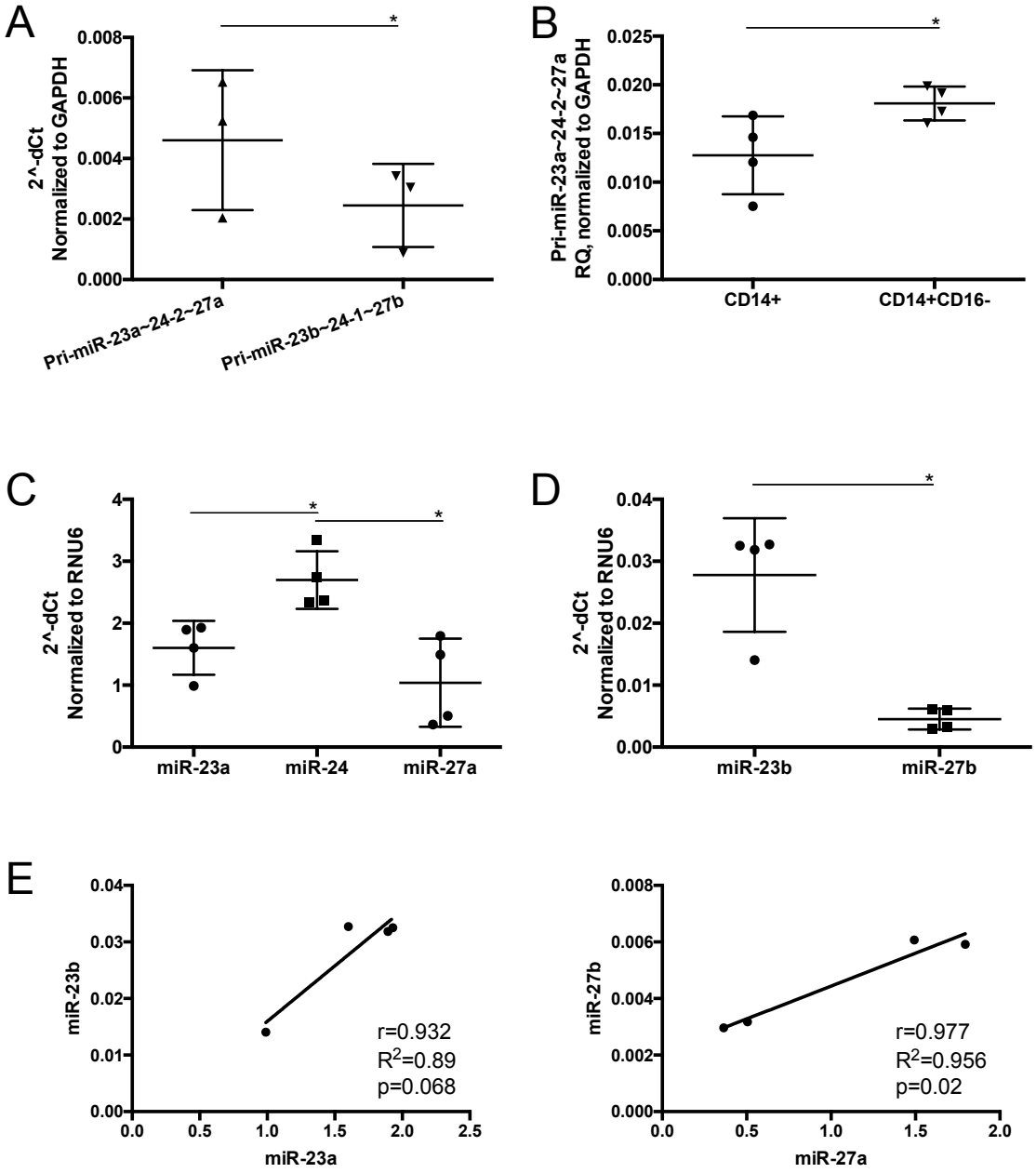

Figure 4.1 Expression of the miR-23~24~27 cluster in buffy coat derived monocytes.

Primary human $CD14^+$ monocytes were used for each experiment. Results are obtained by the qPCR method and displayed as 2^-dCT relative to GAPDH (control for mRNA) or RNU6 (control for miR) genes. (**A**) $CD14^+$ cells were purified from 3 buffy coat donors and tested for expression of primary miR-23a~24-2~27a and miR-23b~24-1~27b transcripts. Data was analysed by Mann-Whitney's test. (**B**) $CD14^+$ and $CD14^+CD16^-$ cells from 4 buffy coat donors were tested for expression of pri-miR-23a~24-2~27a. Data was analysed by Mann-Whitney's test. (**C**) $CD14^+$ cells from 4 buffy coat donors were tested for the expression of mature members of miR-23a~24-2~27a cluster. Data was analysed by Kruskal-Wallis test with Dunn's correction for multiple comparisons. (**D**) $CD14^+$ cells from 4 buffy coat donors were tested for the expression of mature miR-23b and miR-27b. Data was analysed by Mann-Whitney's test. (**E**) Correlation plots between mature members of 'a' and 'b' cluster: miR-23a and miR-23b, r=0.9, p=0.068 (E); miR-27a and miR-27b, r=0.977, p=0.02. Data was analysed by Pearson's correlation coefficient. * - p≤0.05, ** - p≤0.01.

4.2.2 Influence of cytokines on the expression of miR-23a~24-2~27a cluster in monocytes.

Inflammatory cytokines influence activation, expression of adhesion molecules, maturation and T cell priming abilities of monocytes [674]. For example, TNFα stimulation of $CD14^+$ cells aides differentiation of monocyte and T cell priming through increased expression of IL-17A [675]. Both cytokines have been shown to activate NFκB and promote inflammation [676]. Antibody blockade of both is currently successfully used in the clinical practice of multiple inflammatory conditions (Chapter 1). In these experiments, neither TNFα nor IL-17A had any influence on the expression of pri-miR-23a~24-2~27a transcript in $CD14^+$ cells form 4 buffy coat donors (Figure 4.2, A, B).

4.2.2.1 Gamma and beta interferon stimulation of human $CD14^+$ monocytes reduce miR-23a~24-2~27a cluster expression.

I next sought to examine the effect that type I (IFNα and IFNß) and type II (IFNγ) interferons had on miR-23a~24-2~27a cluster expression. $CD14^+$ monocytes from 4 buffy coat donors were treated separately with IFNα, IFNß and IFNγ. IFNα showed no significant effect on pri-miR-23a expression, although did trend towards an increase (Figure 4.2, C). Treatment with IFNγ produced a significant reduction in pri-miR-23a expression after 4 and 24 hours of stimulation (Figure 4.2, D). A similar reduction was also observed in IFNß treated cells (Figure 4.2, E).

JAK1-STAT1 are shared between IFNß and IFNγ signalling pathways, suggesting that these maybe involved in the direct regulation of pri-miR-23a expression [677,678]. Even so, this is an unexpected observation given the apparent different functional effects elicited by type I and II interferons on monocyte function [678].

4.2.2.2 Interleukin 6 and CCL2 stimulation of human CD14$^+$ monocytes reduces miR-23a~24-2~27a cluster expression

Next, CD14$^+$ monocytes were stimulated with IL-6, to assess its influence on pri-miR-23a expression. IL-6 has a well-characterised role in the chronicity of RA, which is reflected in clinical practice where the biologic agent tocilizumab targeting IL-6R shows significant efficacy [679]. In CD14$^+$ monocytes, IL-6 reduced the expression of pri-miR-23a~24-2~27a after 24 hours of exposure (Figure 4.2, F). The lack of effect of IL-6 after 4 hours suggests that IL-6 may act indirectly.

In contrast to this, treatment of CD14$^+$ monocytes with the migratory inflammatory chemokine CCL2 led to the significant decrease in the expression of pri-miR-23a~24-2~27a transcript after 4 but not at 24 hours indicating the direct ability of the chemotactic molecule to regulate the expression of miR-23a in primary human monocytes (Figure 4.2, G).

Interestingly, none of the inflammatory stimuli tested above led to the increased expression of this miR cluster, which may simply reflect the already high levels of miR expression within CD14$^+$ cells. The reduction in pri-miR-23a transcript following stimulation with pro-inflammatory cytokines is in keeping with the low levels of miR-23a~24-2~27a found in the CD14$^+$ cells derived from RA patients failing DMARD or biologic treatment. Analysis of the potential transcription factors mediating this is to follow.

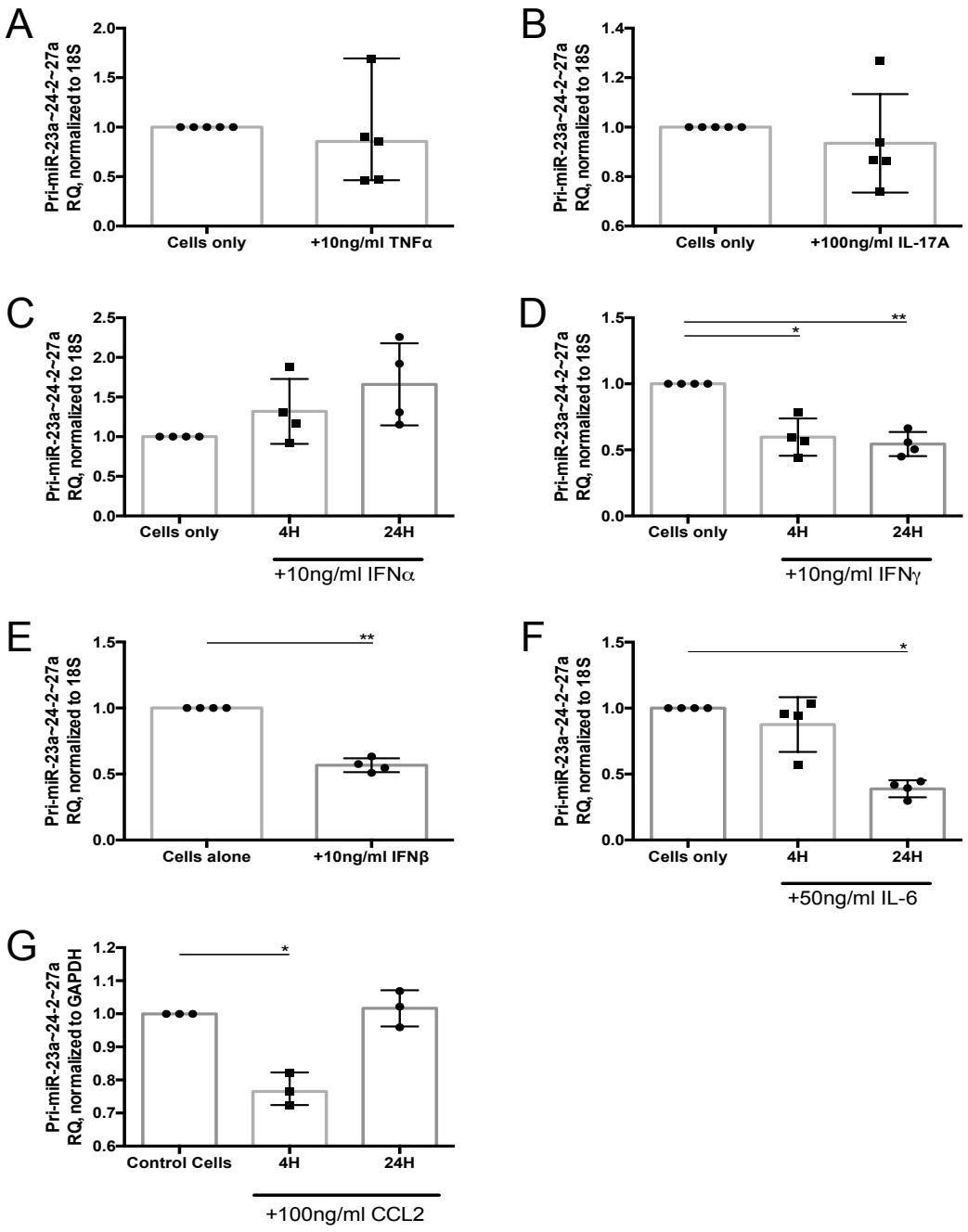

Figure 4.2 Influence of proinflammatory cytokines and CCL2 chemokine on the expression of miR-23a~24-2~27a cluster in CD14$^+$ monocytes.

Primary human CD14$^+$ monocytes from 4 buffy coat donors were used for **A-F** experiments, and 3 buffy coat donors samples were used for the experiment **G**. Results are obtained by the qPCR method measuring pri-miR-23a~24-2~27a and displayed as Mean±SD of RQ (2^-ddCT) relative to 18S or GAPDH genes and control cells. (**A**) Cells were incubated with 50 ng/ml of M-CSF and 10 ng/ml of TNFα for 24H. (**B**) Cells were incubated with 50 ng/ml of M-CSF and 100ng/ml of IL-17A for 24H. (**C,D**) Cells were incubated with 50 ng/ml of M-CSF and 10ng/ml of IFNα (**C**) and 10 ng/ml of IFNγ (**D**) for 4 and 24 hours and (**E**) Cells were incubated with 50 ng/ml of M-CSF and 10 ng/ml of IFNβ for 4 hours. (**F**) Cells were incubated with 50 ng/ml of M-CSF and 50 ng/ml of IL-6 for 4 and 24 hours. (**G**) Cells were incubated with 50 ng/ml of M-CSF and 100 ng/ml of CCL2 for 4 and 24 hours. Data for **A**, **B** and **E** were analysed by Wilcoxon's test; data for **C**-**G** were analysed by Kruskal-Wallis test with Dunn's correction for multiple comparisons. * - p≤0.05, ** - p≤0.01.

4.2.3 Influence of TLR stimulants on the expression of miR-23a~24-2~27a cluster in monocytes.

Activation of monocyte/macrophages by microbial components and also by endogenously arising DAMPS, signaling via Toll-like receptors (TLRs 1-9) results in the production of a variety of proinflammatory responses many of which are hallmarks of RA [680,681]. A recent study reported that TLR3/4 induced NFκB/p65 directly regulated the miR-23a cluster expression in leukaemic cells and erythroid precursors [661]. With this in mind, I decided to explore the effect of TLR stimulation on miR-23a~24-2~27a expression.

4.2.3.1 TLR activation does not regulate miR-23a~24-2~27a expression in human CD14$^+$cells

To examine the potential role of TLR signalling in the regulation of miR-23a~24-2~27a cluster expression I stimulated CD14$^+$ cells from 4 buffy coat donors and measured pri-miR-23a by qPCR.

Pam3CSK4 (Pam3) a ligand for the TLR1/2 pathway had no effect on the expression of pri-miR-23a (Figure 4.3, A). TLR4 activation via LPS stimulation showed a non-significant increase in pri-miR-23a levels after 4 hours of exposure, but no effect after 24 hours (Figure 4.3, B). Upon closer scrutiny of this data revealed an upregulation of pri-miR-23a~24-2~27a by LPS in 3 out of 4 samples (p=0.06). It is possible that the addition of more donors this study could have reached significance. Exposure of monocytes derived from peripheral blood of 3 healthy controls and 3 RA patients with active disease confirmed that TLR4 activation has an inconsistent effect on miR-23~24~27 cluster expression with no statistically significant change in expression (Figure 4.3, C). Again, this could be due to the limited number of participants.

TLR3 ligand, Poly(I:C) that mimics viral double-stranded RNA, was used to stimulate CD14$^+$ cells. I found no change in miR-23a cluster expression (Figure 4.3, D). Similarly, CLO97, which is structurally comparable to single-stranded RNA that activates TLR7/8 signaling, had no effect on the expression of pri-miR-23a (Figure 4.3, E). TLR9 ligands were not included in this study as this receptor is largely absent from human monocytes, which are as a consequence unresponsive to them [682]. TNFα production was measured in each sample as a

positive control for TLR stimulation (Figure 4.3, F). In all cases, an increase in TNFα was observed in cells treated with TLR ligands, indicating that signaling had taken place in samples assessed for pri-miR-23a levels. As expected, TNFα production in cells stimulated by Pam3 resulted in a very modest escalation of the cytokine release, in keeping with previous reports [683].

The results above show that pri-miR-23a expression is largely unaffected by TLR activation which is at odds with a report demonstrating that miR-23a cluster expression is up-regulated in response to NFκB/p65 activation [661]. Our failure to reproduce the author's findings likely stems from the use of different cell types, monocytes rather than leukemic cell lines. I did note a trend towards increased expression upon LPS stimulation, which may have reached significance with the inclusion of more donors. Another potential reason that no increase in pri-miR-23a expression was observed may have been due to their already high expression, meaning that any induction could be difficult to detect.

Lastly, I have investigated the effect of hypoxia on the levels of miR-23a cluster. Hypoxic conditions are present in the inflamed arthritic joints and are thought to be a powerful driver of angiogenesis, immune cell migration and perpetuation of inflammation [684,685]. With the lack of modular incubator, hypoxia in mammalian cells can be induced with cobalt (II) chloride hexahydrate solution ($CoCl_2$) resulting in activation of hypoxia-induced factor 1α (HIF1α) [686]. Exposure of $CD14^+$ monocytes from 7 buffy coat donors to $CoCl_2$ solution for 24 hours did not alter the expression of pri-miR-23a~24-2~27a transcript, negating the effect of chemically induced hypoxia (Figure 4.3, G). This experimental model of hypoxia also failed to induce TNFα expression during 24-hour stimulation by $CoCl_2$ (Figure 4.3, H)

Above investigations conclude that cytokine cross-talk rather than bacterial and viral danger signals modulate the expression of miR-23~24-2~27a cluster in peripheral blood monocytes. Other environmental stimuli such as hypoxia, are characteristic for arthritic joints and have no direct influence on the expression of miR-23a~24-2~27a.

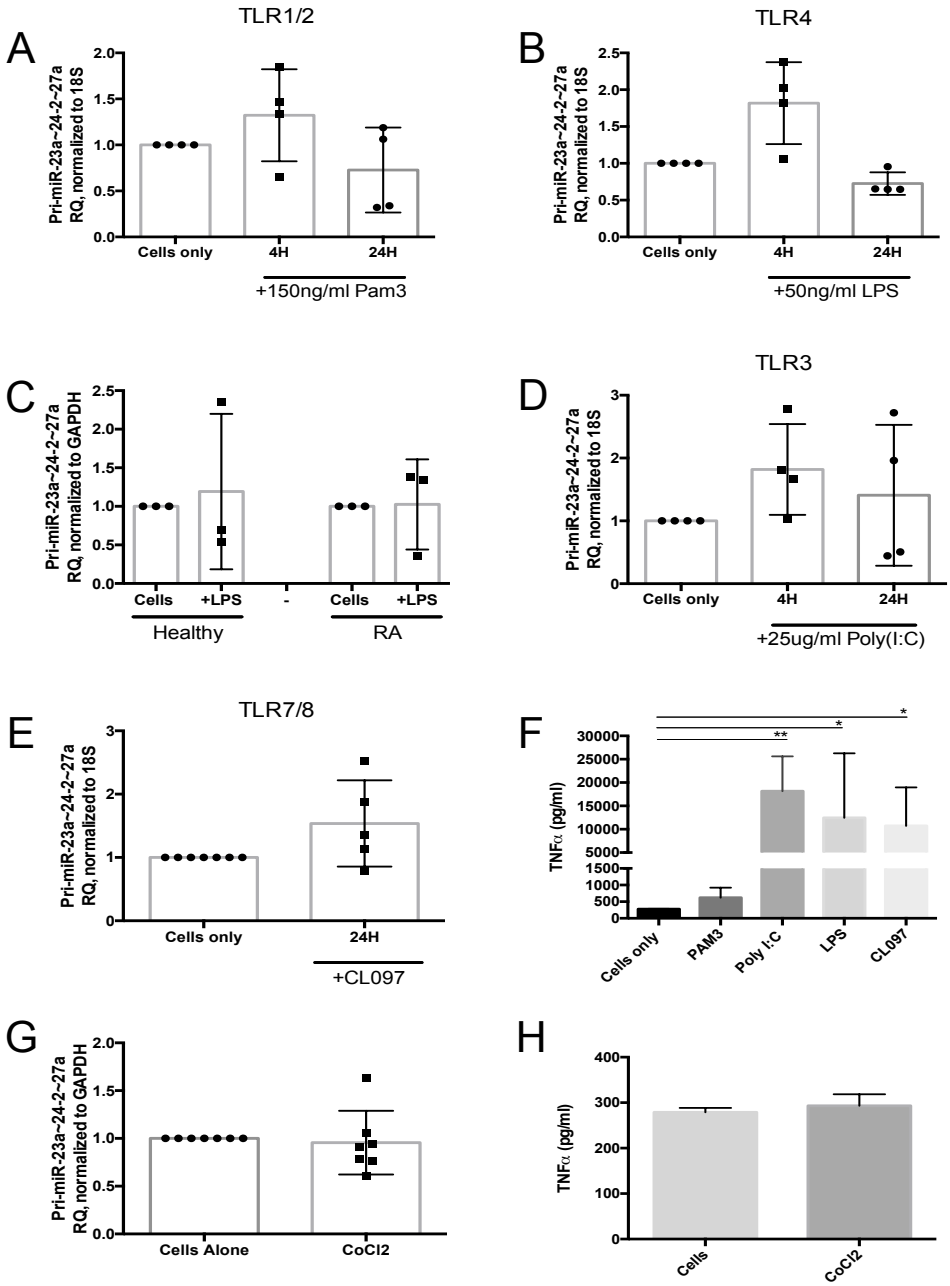

Figure 4.3 Influence of TLR ligands on miR-23a~24-2~27a cluster expression in CD14$^+$ monocytes.

Primary CD14$^+$ monocytes were used for each experiment. Results for A-E, G are obtained by the qPCR method measuring pri-miR-23~24~27 and displayed as RQ (2^-ddCT) relative to 18S or GAPDH genes and control cells, represented by Mean±SD. Results for F and H are obtained by ELISA method and are displayed as the concentration of TNFα cytokine (pg/ml) (**A**, **B**, **D**) CD14$^+$ cells from 4 buffy coat donors were incubated for 4 and 24 hours with 50 ng/ml of M-CSF and 150 ng/ml Pam3CSK4 (Pam3), 50 ng/ml LPS and 25 µg/ml Poly(I:C), respectively. (**C**) CD14$^+$ cells from 3 HC and 3 RA patients were incubated for 24 hours with 50ng/ml of M-CSF and 50 ng/ml of LPS. (**E**) CD14$^+$ cells from 4 buffy coat donors were incubated with 50 ng/ml of M-CSF and 1 µg/ml of CL097. (**F**) Showing TNFα levels in the supernatant of cells after TLR stimulations from A, B, D and E. (**G**) CD14$^+$ cells from 7 buffy coat donors were incubated with 50 ng/ml of M-CSF and 100 µM $CoCl_2$ for 24 hours. (**H**) Showing TNFα levels in the supernatant of cells from experiment G. Data for A, B, D and F were analysed by Kruskal-Wallis test with Dunn's correction for multiple comparisons. Data for C were analysed by Wilcoxon test for each pair. Data for E, G and H, were analysed by Mann-Whitney test. Non-significant p≥0.05 for A-E, G-H, * - p≤0.05, ** - p≤0.01.

4.2.4 Expression of miR-23a~24-2~27a cluster in macrophages.

Macrophage-colony stimulating factor (M-CSF) is the accepted primary lineage regulator of almost all mononuclear phagocytes and resident macrophages [687]. M-CSF 1 receptor (CSF1R) is expressed on the majority if not all macrophages and some types of dendritic cells [245]. As such, M-CSF/CSF1R pathway is the main driver of maturation of monocytes into macrophages in response to inflammation [251]. Thus, I sought to determine if M-CSF-driven maturation of monocytes into macrophages had any effect on the expression levels of the miR-23a~24-2~27a cluster.

4.2.4.1 miR-23a~24-2~27a cluster is down regulated in M-CSF matured macrophages.

To determine the effect of M-CSF-driven maturation of monocytes on the expression of pri-miR-23a cluster expression, $CD14^{+}$ blood-derived monocytes were treated with M-CSF. Pri-miR-23a and pri-miR-23b cluster expressions were measured on 0, 3 and 7 days post stimulation with M-CSF. Exposure of monocytes with M-CSF resulted in significant downregulation of pri-miR-23a~24-2~27a by day 3 with expression levels dropping close to undetectable levels by day 7 of maturation (Figure 4.4, A). At the same time, primary transcript of the paralogue miR-23b~24-2~27b cluster shows a significant increase by day 3 and day 7 of M-CSF exposure in keeping with published data suggesting that miR-23b is relevant in joint derived tissue cells (Figure 4.4) [593].

4.2.4.2 miR-23a~24-2~27a cluster is down regulated in GM-CSF matured macrophages.

GM-CSF is an alternative macrophage maturation factor and plays many roles in promoting innate and adaptive immune responses far beyond its traditional role in myelopoiesis [277]. So much so, that a substantial case has been made for a clinical targeting of GM-CSF in RA and initial clinical trial results remain hopeful [277,688]. GM-CSF polarised monocytes behaved in a similar way to M-CSF polarisation when assessed for the expression of primary transcripts of both miR clusters (Figure 4.4, B). GM-CSF significantly reduced the levels of pri-miR-23a transcript after 3 days of maturation and levels of miR expression remained low after 7 days (Figure 4.4, left). Pri-miR-23b cluster, on the other hand, was significantly increased after 3- and 7-day exposure to GM-CSF (Figure 4.4, right).

As expected, monocyte to macrophage maturation upon exposure to M-CSF or GM-CSF also resulted in the reduction of expression of all mature members of the miR-23a~24~27a cluster, although all miRs were still detectible on day 7 (Figure 4.5, A-C). The longer half-life of mature miR species is likely ensuring continued functionality during the transition period from miR-23a~24-2~27a to miR-23b~4-1~27b cluster in mature macrophages.

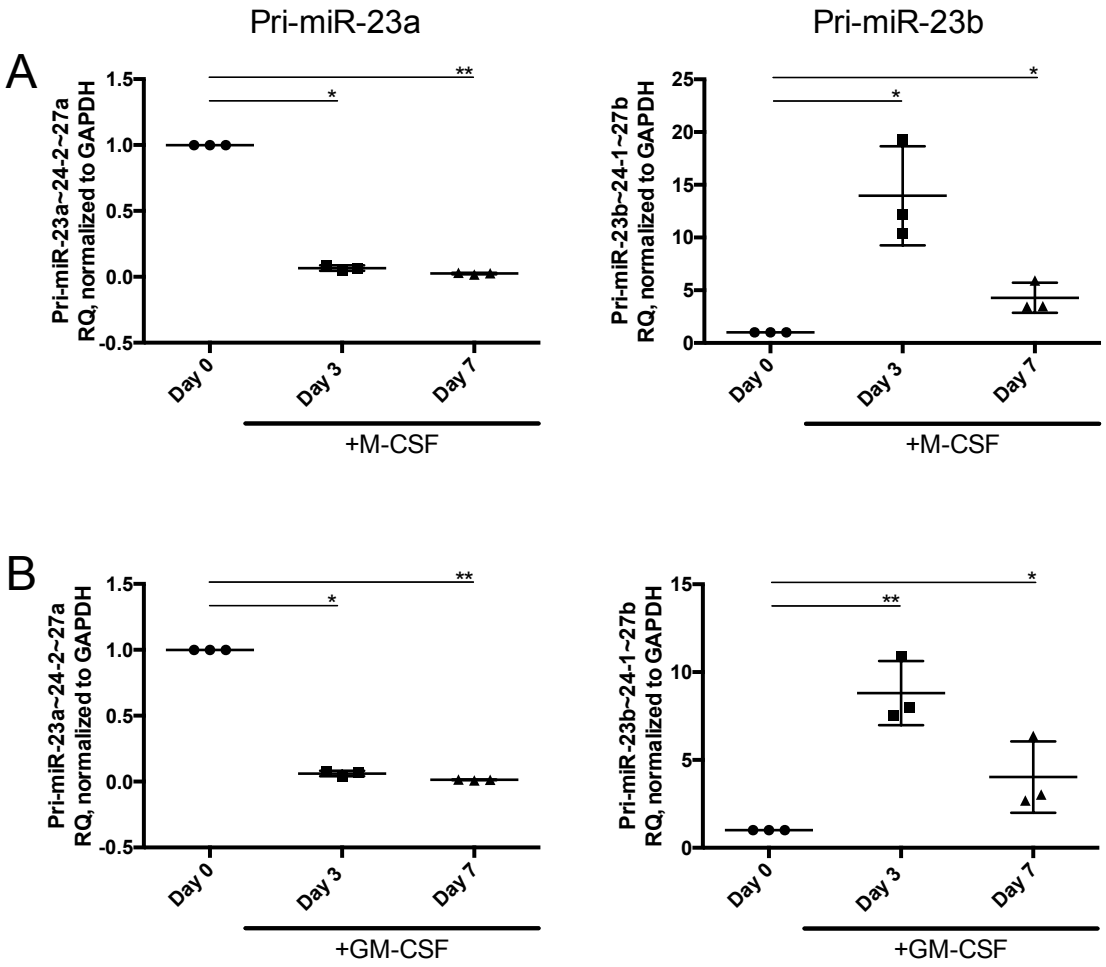

Figure 4.4 Expression of both miR-23~24~27 clusters in maturation of macrophages

Primary $CD14^+$ monocytes from 3 buffy coat donors were used for each experiment. Expression of pri-miR-23a~24-2~27a (left) and pri-miR-23b~24-1~27b (right) transcripts was done on day 0, 3 and 7. Results are obtained by the qPCR method and displayed as RQ (2^-ddCT) relative to GAPDH gene and control cells. (**A**) $CD14^+$ cells were incubated for 7 days with 50ng/ml of M-CSF. (**B**) $CD14^+$ cells were incubated for 7 days with 50ng/ml of GM-CSF. Data were analysed by Kruskal-Wallis test with Dunn's correction for multiple comparisons. * - p≤0.05, ** - p≤0.01.

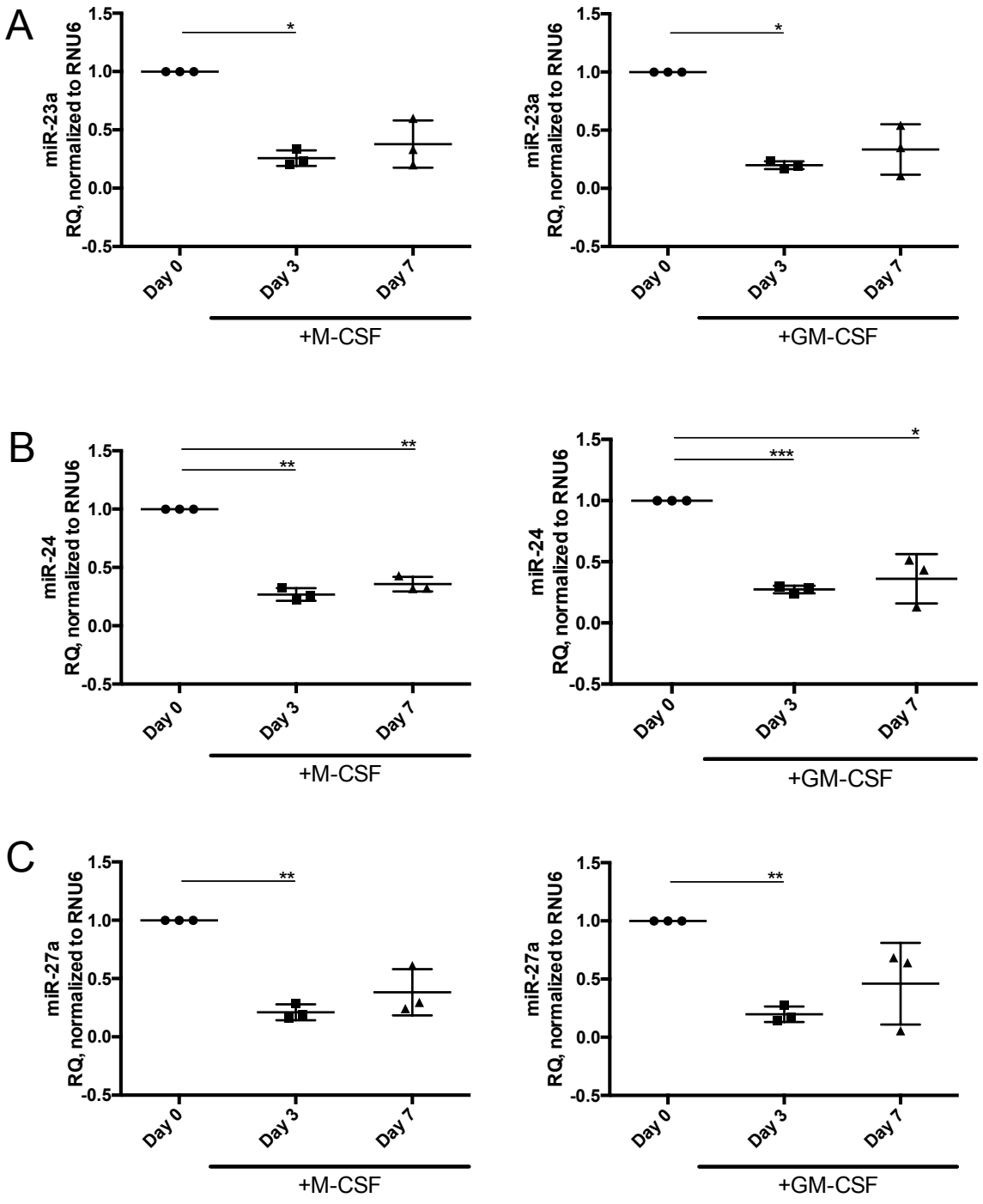

Figure 4.5 Expression of mature miRs from miR-23a~24-2~27a cluster in maturation of macrophages.

Primary $CD14^+$ monocytes from 3 buffy coat donors were used for each experiment. Cells were incubated for 7 days with 50ng/ml of M-CSF (left) or 50ng/ml of GM-CSF (right). Expression of mature miRs was done on day 0, 3 and 7. Results are obtained by the qPCR method and displayed as Mean±SD of RQ (2^-ddCT) relative to RNU6 gene and control cells. (**A**) Shows expression of miR-23a. (**B**) Shows expression of miR-24. (**C**) Shows expression of miR-27a. Data were analysed by Kruskal-Wallis test with Dunn's correction for multiple comparisons. * - p≤0.05, ** - p≤0.01, *** - p≤0.001.

4.2.4.3 Expression of miR-23a~24-2~27a cluster in polarisation and activation of macrophages.

Although part of the innate immune response, monocyte-derived macrophages have the ability to adapt to the environment guided by locally produced cytokines. Many reports have advocated a broad classification of activated macrophages into two main groups – classically activated with IFNγ or LPS (M1) and alternatively activated with IL-4 (M2) [257-259]. Recently, a revised nomenclature demanded a more detailed description of experimentally generated macrophages to understand the generated phenotype clearly as well as to encourage reproducibility of the results [260]. Here I sought to investigate the effect of further polarisation of M-CSF and GM-MSF macrophages into M1 and M2 phenotypes on miR-23a~24-2~27a expression.

4.2.4.4 The polarisation of M-CSF and GM-CSF macrophages into M1 and M2 phenotypes has no effect on miR-23a~24-2~27a cluster expression.

$CD14^+$ monocytes from 3 buffy coat donors were isolated and polarised for 6 days with either 50 ng/ml of M-CSF or GM-CSF. Upon differentiation into macrophages different polarising stimuli were added: IFNγ, LPS or the combination of the two for the classical activation and IL-4 for alternative activation. Polarising conditions were applied for 24 hours before cells were analysed for miR-23a~24-2~27a cluster expression (Figure 4.6, A). The previous monocyte to macrophage differentiation showed a reduction in primary miR-23a~24-2~27a cluster transcript. This experiment indicates that further classical or alternative polarisation of macrophages does not influence the expression of pri-miR-23a cluster (Figure 4.6, A, B). Polarised macrophages were then assessed for the expression of pro-inflammatory TNFα and regulatory IL-10 cytokines (Figure 4.6, C-F). As expected, both M-CSF and GM-CSF differentiated cells stimulated with LPS and the combination with IFNγ expressed large levels of TNFα in keeping with M1 phenotype (Figure 4.6, C and D, respectively). Moreover, M-CSF driven macrophages also expressed IL-10 upon LPS and combination stimuli (Figure 4.6, E). This effect was not seen in GM-CSF polarised macrophages (Figure 4.6, F). Moreover, here observed minimal expression of IL-10 from M2 M-CSF and IL-4 driven cells was likely due to the short exposure to IL-4 necessary for the measurement of primary miR-23a transcript. Further regulatory phenotype could

be obtained by longer exposure to IL-4 and IL-13 that has not been further pursued.

Apart from the well-accepted polarising stimuli, monocytes and macrophages recruited into the chronic inflammatory environment can become activated by the variety of other cytokines. For example, IL-17A, TNFα and IL-6 are all highly expressed in the joint synovial inflammation and perpetuate inflammation [689]. 24-hour stimulation of M-CSF matured macrophages with either TNFα (Figure 4.7, A), IL-17A (Figure 4.7, B) or IL-6 (Figure 4.7, C) had little to no effect on the expression of pri-miR-23a~24-2~27a. Exposure of M-CSF polarised macrophages to LPS has again shown variable results with upregulation of pri-miR-23a~24-2~27a in 2 out of 4 donors and no overall significant effect (Figure 4.7, D). These inconclusive results could be explained by the small concentration of the stimulant and by small power of the study, both of which could be clarified on further investigation. The effects of repetitive exposure to LPS, such as in tolerance induction, have not been explored here [690].

Overall these results show that polarising stimuli or exposure to cytokines fails to recover the expression of miR-23a~24-2~27a cluster seen in blood derived monocytes, as it is unequivocally terminated by M-CSF and GM-CSF exposure during maturation process.

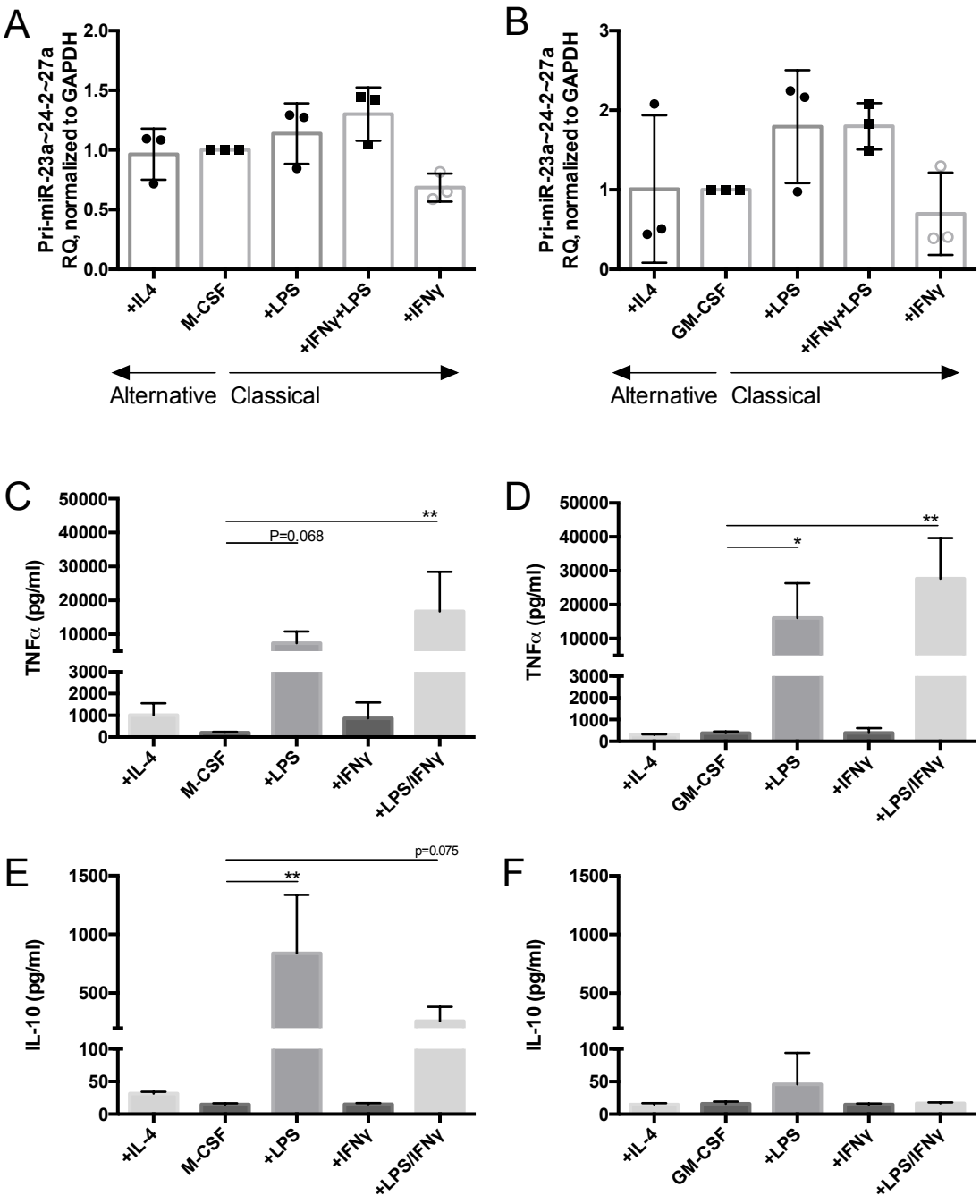

Figure 4.6 Influence of cytokine polarization on miR-23a~24-2~27a cluster expression in mature macrophages.

Results for A and B are obtained by the qPCR method and displayed as of RQ (2^-ddCT) relative to GAPDH gene and control cells, Mean±SD. Results for C-F are obtained by ELISA method and display concentration of the measured cytokine (pg/ml), Mean±SD. (**A, B**) Purified $CD14^+$ cells from 3 buffy coat donors were incubated for 6 days with 50 ng/ml of M-CSF (**A**) or 50 ng/ml GM-CSF (**B**) than stimulated for 24 hours with 100ng/ml IL-4, 15 ng/ml LPS, 20ng/ml IFNγ and the combination of LPS with IFNγ. (**C, D**) Shows TNFα (pg/ml) levels in the supernatant solution of the cells after 24 hours of stimulation as stated in A and B, respectively. (**E, F**) Shows IL-10 (pg/ml) levels in the supernatant solution of the cells after 24 hours of stimulation as stated in A and B, respectively. Data were analysed by Kruskal-Wallis test with Dunn's correction for multiple comparisons. * - p≤0.05, ** - p≤0.01,

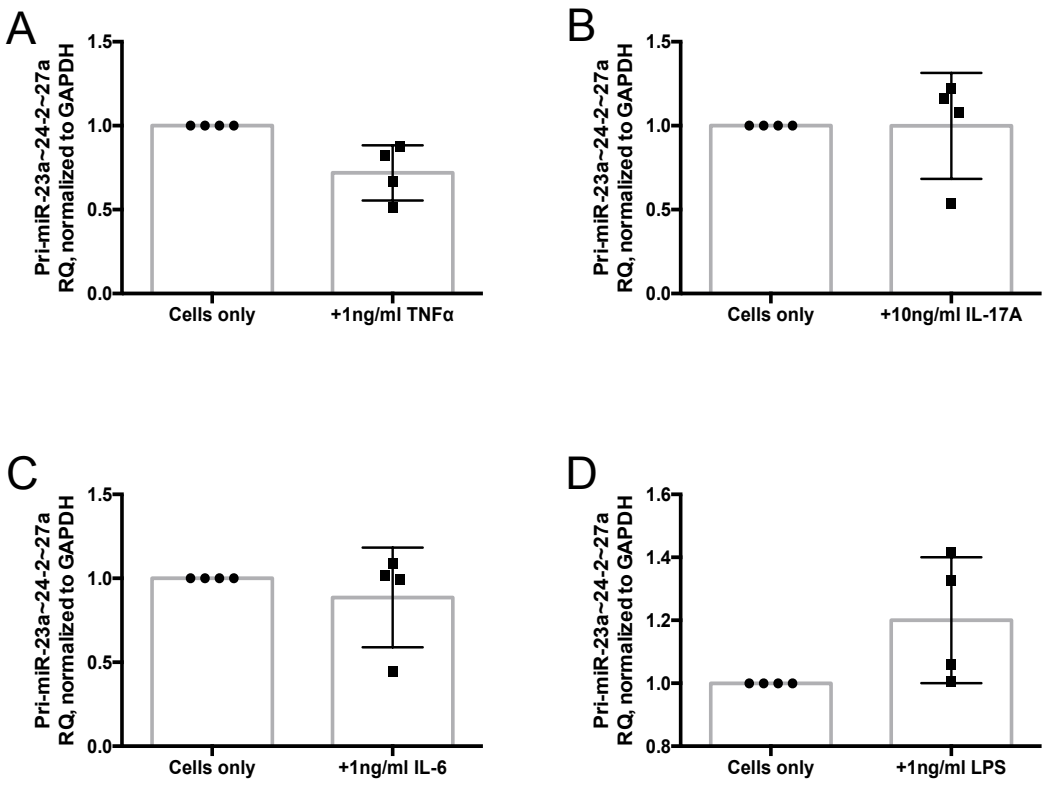

Figure 4.7 Influence of proinflammatory cytokines on miR-23a~24-2~27a cluster expression in mature macrophages.

Results are obtained by the qPCR method and displayed as RQ (2^-ddCT) relative to GAPDH gene and control cells (Mean±SD). Purified $CD14^+$ cells from 4 buffy coat donors were incubated for 7 days with 50ng/ml of M-CSF than stimulated with 1ng/ml TNFα (**A**), 10ng/ml IL-17A (**B**), 1ng/ml IL-6 (**C**) and 1ng/ml LPS (**D**). Data were analysed by Mann-Whitney test. Non-significant $p \geq 0.05$ for all comparisons

4.2.5 Cytokines influencing miR-23a~24-2~27a expression in serum of patients with RA

Reproducing the cytokine milieu that is present in vivo in the chronic inflammatory conditions is not without difficulty, therefore understanding what impacted the expression of miR-23a~24-2~27a cluster in the patients with the drug-resistant RA is challenging. Previous data from this chapter has identified IL-6, CCL2, IFNβ, and IFNγ as regulating the expression of miR-23a~24~27a cluster in blood-derived monocytes. Here, these and other potent proinflammatory cytokines were assessed in the serum samples from patients with drug responsive or resistant RA and healthy controls described in detail in Chapter 3.

4.2.5.1 IL-6 is increased in serum of DMARDs and biologic resistant patients.

The levels of pro-inflammatory cytokines present in cohort samples were measured by Luminex. IL-6 was significantly increased in the serum of DMARDs and biologics resistant patients when compared to levels found in healthy controls (Figure 4.8, A). Intermediate IL-6 levels detected in DMARDs responder patients were not significantly different from other groups. I next analysed TNFα, which was elevated in DMARDs resistant patients when compared to healthy controls, reflecting increased level of inflammation in these patients (Figure 4.8, B). As expected, TNFα levels in biologics resistant group were reduced due to the current treatment with anti-TNFα agents in some patients (Figure 4.8, B).

Following this, members of the interferon family were analysed. IFNα, a type I interferon, was found at higher levels in DMARDs failures when compared to both control groups (Figure 4.8, C). Similarly, IFNα was raised in biologics resistant patients compared to healthy controls (Figure 4.8, C). Association of type I interferon's with RA is well established, although their therapeutic and biomarker potentials remain somewhat controversial [691]. Type II member, IFNγ, was detected in only 3 patients from DMARDs resistant group and in 1 patient amongst DMARDs responders (Figure 4.8, D). The absence of IFNγ from majority of the cohort serum samples indicates that it was not a key driver influencing the expression of pri-miR-23a~24-2~27a in this cohort of RA patients.

Unfortunately, IFNβ was not included on the Luminex panel. Therefore this and limited sample availability meant that I could not assess its levels in these patient groups.

The high presence of inflammatory cytokines results in activation of peripheral blood monocytes, however, it is the growth factors and chemokines that ensure migration into affected tissues and differentiation into macrophages. Data shown in this chapter confirms previously published finding that maturation of monocytes with either M-CSF or as seen above with GM-CSF results in a decrease in the expression of pri-miR-23a~24-2~27a cluster as cells progress to become macrophages (Figure 4.5). Unfortunately, assessment of M-CSF growth factor in the serum samples from RA patients was not available on the platform used, however, levels of GM-CSF and a chemotactic chemokine CCL2 were measured. Serum GM-CSF was not detected in any healthy control subjects, while all three patient groups had insignificant elevation of the cytokine (Figure 4.8, E). Interestingly, chemokine CCL2, otherwise named monocyte chemoattractant protein (MCP1), was raised in both groups failing multiple modes of treatment compared to good responders and healthy controls, overall mirroring the expression pattern of miR-23~24~27 clusters (Figure 4.8, F).

To explore the link between expression of miR-27a in $CD14^+$ monocytes and levels of pro-inflammatory cytokines and chemokines in patient's serum, correlation coefficients were calculated. Unfortunately, miR-27a expression in monocytes failed to reach significance when correlated with IL-6 expression ($r=-0.25$, $p=0.06$ in biologics resistant patients). Furthermore, both miR-27a and miR-27b failed to correlate with IL-6 or CCL2 and representative plots in biologic resistant patients are shown below (Figure 4.9, A and B). This is possibly caused by the longer half-life of miRs, which can be sequestered in the cell for prolonged periods of time, therefore, creating cumulative picture of the expression, unlike secretable cytokines. As a control, IL-6 had significant correlation with acute inflammatory response marker CRP ($r=0.5908$, $p=0.0003$), but not with the disease activity score DAS28-CRP, since it involves additional components, not dependant on IL-6 expression (Figure 4.9, E and F).

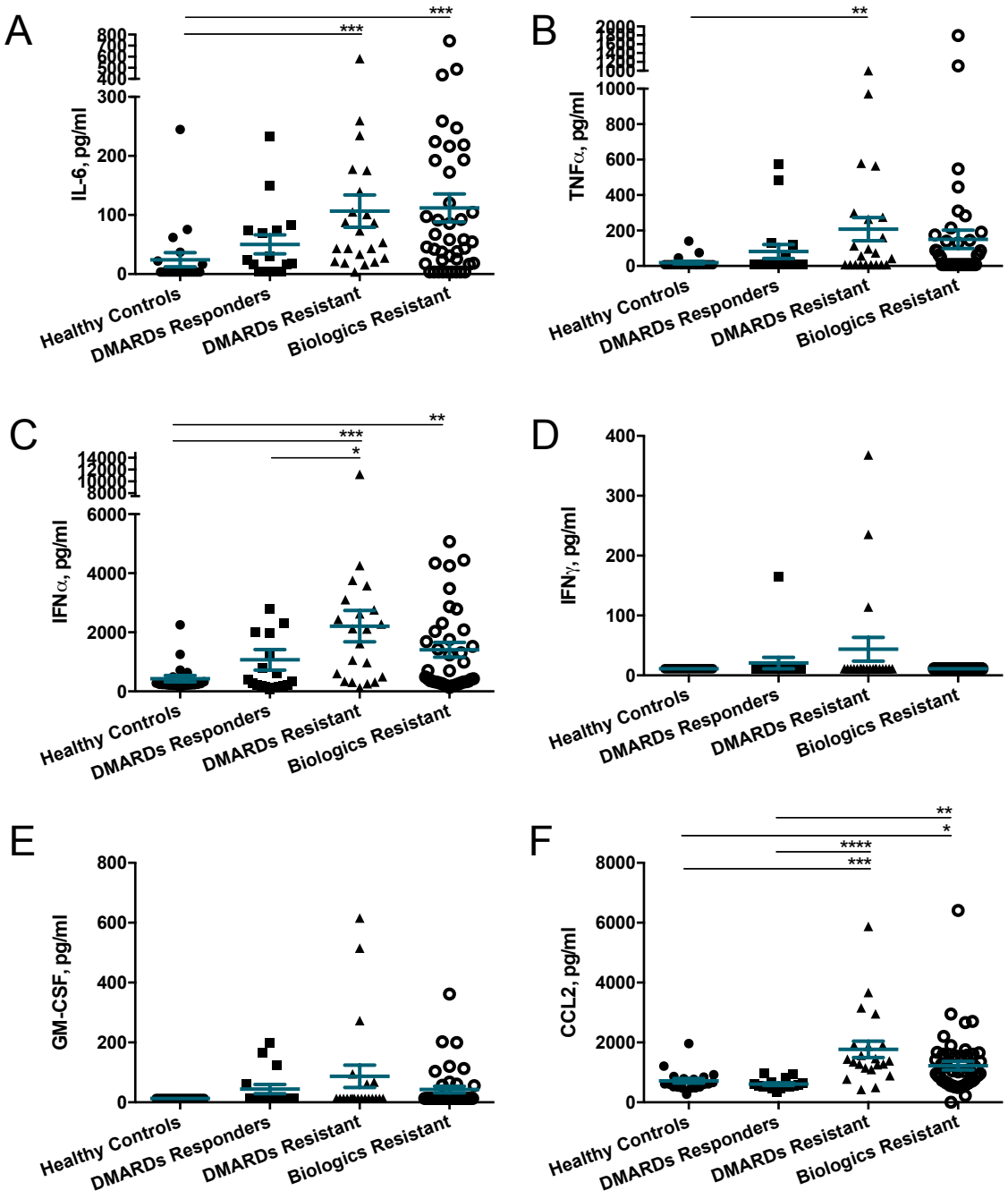

Figure 4.8 Expression of proinflammatory cytokines in serum samples from RA patient cohort.

RA patient and healthy controls cohort involve 4 groups: 21 healthy controls, 16 DMARDs responders, 22 DMARDs resistant and 41 biologics resistant patients. Results are obtained by the Luminex method and displayed as concentration of the cytokine in the 1ml of the serum (pg/ml). Measured cytokines involve IL-6 pg/ml (**A**), TNFα pg/ml (**B**), IFNα pg/ml (**C**), IFNγ pg/ml (**D**), GM-CSF pg/ml (**E**) and chemokine CCL2 pg/ml (**F**). Data were analysed by Kruskal-Wallis test with Dunn's correction for multiple comparisons. * - p≤0.05, ** - p≤0.01, *** - p≤0.001.

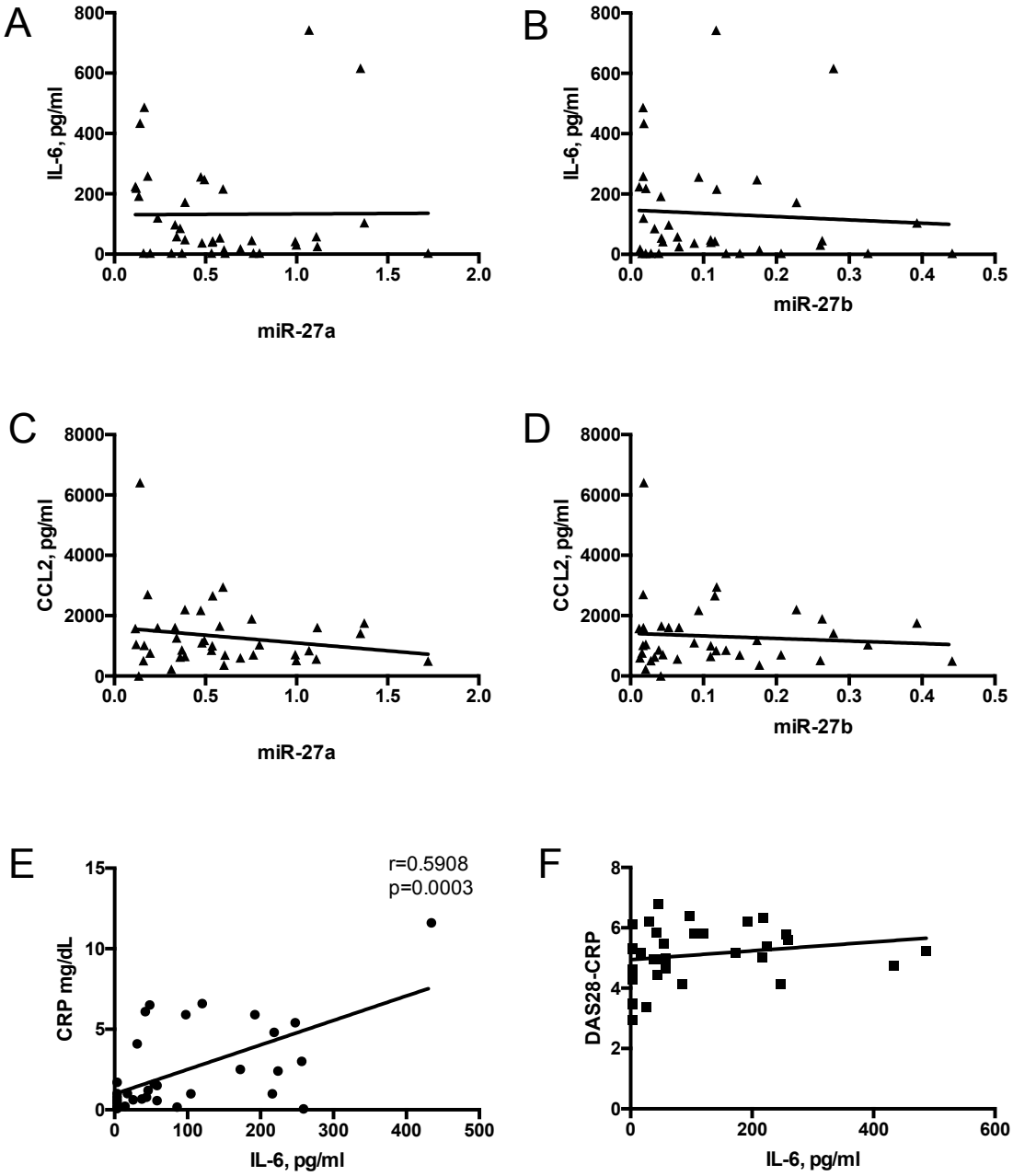

Figure 4.9 Correlation of IL-6 and CCL2 from RA biologics resistant patient's serum with expression of miR-27a and miR-27b in CD14^{+} monocytes.

Correlation plots between mature miR expression in CD14+ monocytes (qPCR, 2^-ddCT) and serum samples from 38 RA patient resistant to biologics treatment. (**A**) Correlation between IL-6 (pg/ml) and miR-27a (r=-0.25, p=0.06) (**B**) Correlation between IL-6 (pg/ml) and miR-27b (r=-0.16, p=0.17). (**C**) Correlation between CCL2 (pg/ml) and miR-27a (r=-0.1, p=0.27). (**D**) Correlation between CCL2 (pg/ml) and miR-27b (r=0.02, p=0.44). (**E**) Correlation between CRP (mg/dl) and IL-6 (pg/ml) (r=0.5908, p=0.0003). (**F**) Correlation between DAS28-CRP clinical score and IL-6 (pg/ml) (r=0.1955, p=0.2677). Data were analyzed by Spearman's correlation coefficient, p≥0.05 is non-significant.

4.2.6 MiR-23a~24-2~27a cluster promoter analysis

4.2.6.1 *In silico* characterisation of the miR-23a~24-2~27a promoter.

Here I sought to identify the regulatory elements in the promoter of miR-23a~miR-27a~miR-24-2 that could be responsible for regulation of the cluster described in the previous sections. Typically this requires the identification of the promoter followed by the bioinformatic prediction of putative transcription factor binding sites. The miR-23a~24-2~27a clusters promoter and transcriptional start site (TSS) has been previously described in Hela cells [570]. Current methodologies such as Cap Analysis of Gene Expression (CAGE), which can precisely capture the sequences associated with 5' cap, are inadequate for the detection of primary miR transcripts as they are below detectable level in their capped form. The authors used 5' RACE to capture the TSS in this cell line showing it to be located 7bp upstream from the miR-23a's coding sequence. As TSS often vary between cell types, bringing the expression of the associated genes under the control of different promoter elements it is important to define the miR-23a~24-2~27a cluster promoter within the context of myeloid linage cells.

As miR primary transcripts exist only transiently before being rapidly processed into their trimmed precursor forms, capturing their 5' ends and inferred transcriptional start sites represents a significant challenge. To overcome this, Drosha, a protein that is essential for the processing of pri-miR to pre-miR forms was knocked-down by siRNA in THP-1 cells resulting in an increase in the levels of the primary miR-23a~24-2~27a cluster transcript (Figure 4.10, A-B). 5'RACE performed on the total RNA purified from these cells yielded a single band which when sequenced revealed a TSS that was identical to the one previously described in Hela cells (Figure 4.10, C) [570].

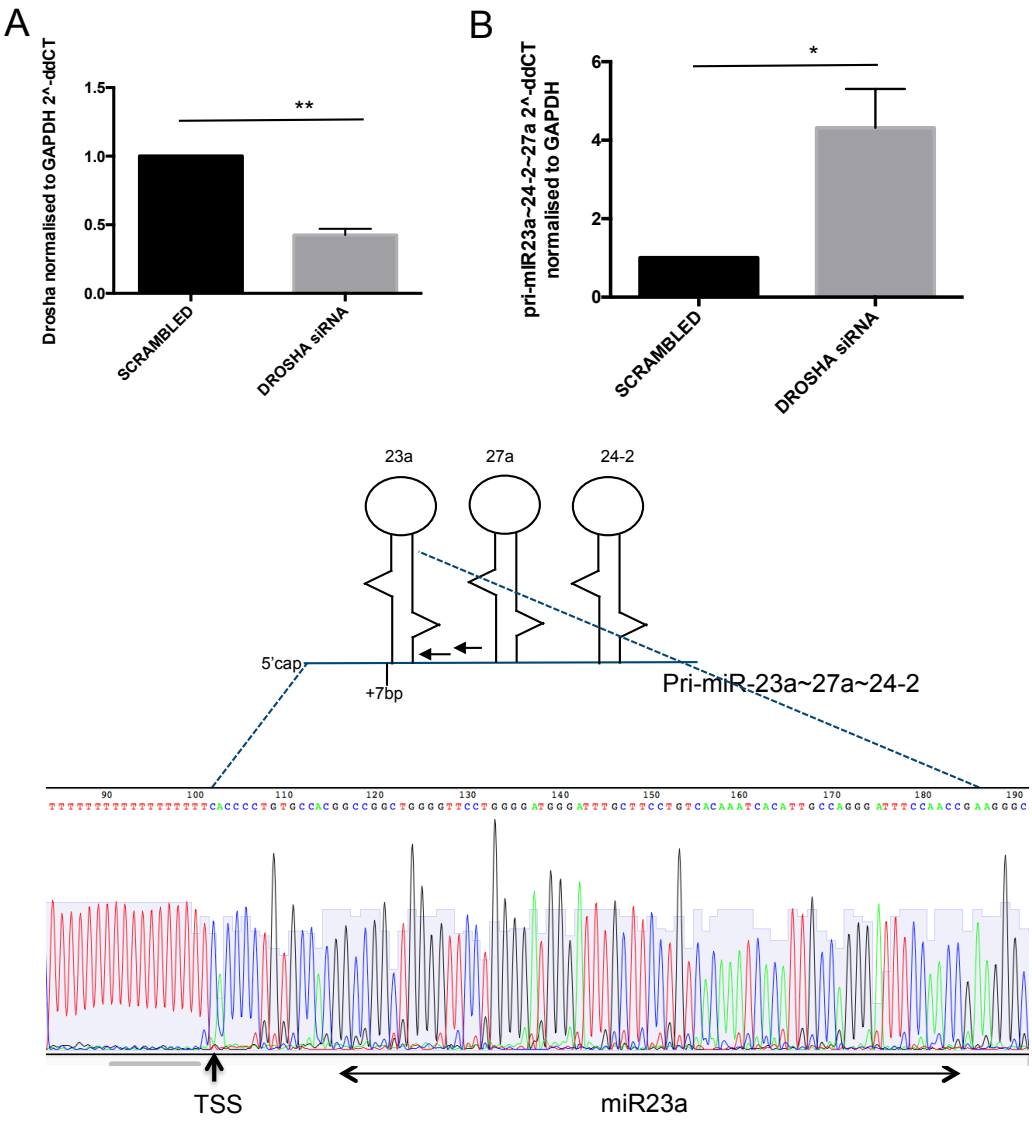

Figure 4.7: Charaterisation of 5' transcriptional start site by 5'Rapid Extension of cDNA Ends.

Figure 4.10 Characterization of 5' transcriptional start site by 5'Rapid Extension of cDNA Ends.

Experiments done in THP-1 cells in 3 technical replicates. (**A**) THP-1 cells transfected with DROSHA siRNA. Results obtained by qPCR method showing Mean±SD of 2^-ΔΔCT of DROSHA expression normalised to GAPDH and control cells. (**B**) THP-1 cells transfected with DROSHA siRNA. Results obtained by qPCR method showing Mean±SD of 2^-ΔΔCT of pri-miR-23a~24-2~27a expression normalised to GAPDH and control cells. (**C**) Schematic of 5'Cap, TSS and pri-mir-23a~24-2~27a cluster sequence with underlying data from 5'RACE sequencing showing intensity of the signal starting from 124 bp preceding pre-miR-23a sequence.

Next, bioinformatic analysis using MatInspector was performed on the 2kb sequence directly upstream of the TSS. The aim of this was to identify putative regulatory elements that had potential relevance to monocyte/macrophage biology (Table 4.1). MatInspector identified potential IRF and STAT binding sites both of which are known to regulate target gene expression within Interferon gamma and IL-6 signalling pathways [387,692]. A number of putative SMAD binding sites were also highlighted suggesting that the cluster could be regulated by TGFß [693]. This observation is supported by the finding that the miR-23a cluster is up-regulated in monocyte-derived DCs and CD8 T cells stimulated with TGFß [577,609].

Intriguingly, there are 13 predicted retinoic X receptor (RXR) binding sites within 2kb upstream from miR-23a's TSS. There is a large body of literature relating to RXR's role in monocyte/macrophage biology [694]. RXR acts as a homodimer or as a heterodimer with a number of binding partners (LXRα, PPARγ, VDR and others). It also plays a vital role in the regulation of cholesterol, fatty acid and glucose metabolism [695]. Recent studies have shown that vitamin D inhibits the production of pro-inflammatory cytokines by monocytes and macrophages through the action of heterodimers of RXRα and VDR [696,697]. A heterodimer of RXRα/liver X receptor alpha (LXRα) pathway has been shown to be upregulated in the synovial macrophages of patients with RA, and this pathway increased the production of pro-inflammatory cytokines [698]. Interestingly, the alpha subunit of RXRα is predicted to have binding sites for both miR-27a and miR-24. A common feature of miR biology is auto-regulatory feedback loops in which the expression of a miR is regulated by a transcription factor which is in turn targeted by the same miR [699].

There are two predicted Activator protein-1 (AP1) sites in miR-23a's promoter. AP1 activity is induced by a variety of stimuli affecting a wide range of cellular processes. However, one important role is the regulation of cell proliferation and survival [700]. Pertinently, methotrexate has been shown to induce the activity of AP1 in RA patients and could potentially effect the expression of miR-23a cluster in treated cells [701].

Transcription factor	Family Information	Matrix SIM	SEQ
V$RXRF	RXR heterodimer binding sites	0.91	gcggatcacctgaggtcaggaggtc
V$RORA	v-ERB and RAR-related orphan receptor alpha	0.92	atcacctgaggtcaggaggtcgaga
V$RXRF	RXR heterodimer binding sites	0.82	tcacctgaggtcaggaggtcgagac
V$EREF	Estrogen response elements	0.917	tgaggtcaggaggtcgaga
V$SMAD	Vertebrate SMAD family of transcription factors	0.967	ctggtctcgac
V$RXRF	RXR heterodimer binding sites	0.742	gtagctgggattacaggtgcccgcc
V$RXRF	RXR heterodimer binding sites	0.838	ttgcttgaactctggaggtggaggt
V$SMAD	Vertebrate SMAD family of transcription factors	0.974	agagtctcgcc
V$IRFF	Interferon regulatory factors	0.941	aaaaaaaaaaaaaagaaaagaaaaa
V$IRFF	Interferon regulatory factors	0.932	aaagaaaagaaaaagaaaaaattag
V$RXRF	RXR heterodimer binding sites	0.886	gcaggggtgcaatcacagctcactg
V$RXRF	RXR heterodimer binding sites	0.877	gagagtcacctgaggccaggagttc
V$AP1F	AP1, Activating protein 1	0.861	aggagagtcacct
V$P53F	p53 tumor suppressor	0.862	acaggcgtgagccgccatgcttggc
V$GREF	Glucocorticoid responsive and related elements	0.893	aatgaacacgtggtcctct
V$GREF	Glucocorticoid responsive and related elements	0.921	agaggaccacgtgttcatt
V$HIFF	Hypoxia inducible factor, bHLH/PAS protein family	0.96	gaggaccacgtgttcat
V$FAST	FAST-1 SMAD interacting proteins	0.848	ccacgtgttcattttgc
V$RXRF	RXR heterodimer binding sites	0.794	tatcttgccctggtgctgggcactt
V$RXRF	RXR heterodimer binding sites	0.784	gtaagtgcccagcaccagggcaaga
V$AP1F	AP1, Activating protein 1	0.87	tactgagtgacat
V$HIFF	Hypoxia inducible factor, bHLH/PAS protein family	0.934	tccccccccgtggcccg
V$MZF1	Myeloid zinc finger 1 factors	0.996	gggggggaggcc
V$NFKB	Nuclear factor kappa B/c-rel	0.932	gggggggaggccctgg
V$STAT	Signal transducer and activator of transcription	0.964	ccacttcctagaagcctgg
V$STAT	Signal transducer and activator of transcription	0.951	aggcttctaggaagtggcg
V$SMAD	Vertebrate SMAD family of transcription factors	0.963	agtggcgccag
V$RXRF	RXR heterodimer binding sites	0.783	ccccatggccccatttggcctgccc
V$RXRF	RXR heterodimer binding sites	0.76	tgggcaggccaaatggggccatggg
V$RXRF	RXR heterodimer binding sites	0.774	ccatttggcctgcccagggctcaat
V$RXRF	RXR heterodimer binding sites	0.756	cattgagccctgggcaggccaaatg
V$MZF1	Myeloid zinc finger 1 factors	0.996	gggggggagctt
V$P53F	p53 tumor suppressor	0.826	gggagcttggccatgcaagttgctg
V$SMAD	Vertebrate SMAD family of transcription factors	0.953	ggtggctcctg
V$MZF1	Myeloid zinc finger 1 factors	0.992	gaggggaggtg
V$MZF1	Myeloid zinc finger 1 factors	0.992	gaggggagaaa
V$GLIF	GLI zinc finger family	0.903	ggtgccccccctcacccc
V$RXRF	RXR heterodimer binding sites	0.763	gccggccgtggcacaggggtgaggg

Table 4.1 The list of potential binding sites upstream of the miR-23a~24-2~27a cluster.

A 2kb sequence upstream from the TSS was subjected to bioinformatics analysis using the MatInspector algorithm from Genomatix -https://www.genomatix.de/online_help/help_matinspector. This searches for known transcription factor binding site sequences. Matrix Sim is a measure of similarity to the consensus sequences, with perfect matches scoring 1. Transcription factor gene symbols used by the program are listed on the left, with the description in the centre, predictive binding score (Sim) to the centre right and binding sequence in context to the right.

There are two predicted response elements for hypoxia-inducible factor 1 (HIF1). My data suggests that, at least in monocytes, hypoxia does not influence the expression of miR-23a cluster (Figure 4.3, F). However, this may not be the case in other cell types.

A single NFκB site lies within the 400 bp upstream from the TSS. NFκB is the down stream regulators of IL-1β, TLR1-9 and TNFα signalling pathways [664,702]. My data does not support a role for this, neither TLR ligands nor TNFα induced changes in the expression levels of miR-23a~27a~24-2. Despite this, NFκB has been shown to directly regulate miR-23a cluster expression in Jurkat cells [662]. A more recent study showed that NFκB regulated miR-23a expression in murine macrophages [665,703].

The archetypal tumour suppressor p53 has a single predicted binding site in the miR-23a promoter. It has been reported that p53 increased the expression of miR-23a in human hepatocellular carcinoma cells treated with the cytotoxic agent etoposide [614]. In turn, miR-23a directly targets p53 transcripts completing an auto-regulatory feed back loop.

The prediction of a STAT binding site in the miR-23a cluster promoter is particularly interesting. STAT1, 3 and 5 lie downstream of the IFNγ signalling pathway in monocytes and macrophages [461,704]. It is an obvious candidate for the transcription factor responsible for the down regulation of miR-23a cluster expression seen in IFNγ treated cells (Figure 4.2, B and C). As different STAT family members bind to similar sequences, it is possible that other STATs can also bind to the promoter of miR-23a cluster. Thus the decrease in miR-23a expression seen in IFNβ stimulated monocytes may be influenced by STAT1 or STAT2 [678]. A schematic of miR-23a promoter and associated binding sites is illustrated in the Figure 4.11, A.

A comparison of miR-23a promoter sequences shows significant conservation between species (Figure 4.11, B). A well-conserved 200 bp region upstream from the TSS contains the predicted NFκB, RXR, SMAD and STAT binding sites hinting at their functional importance [681].

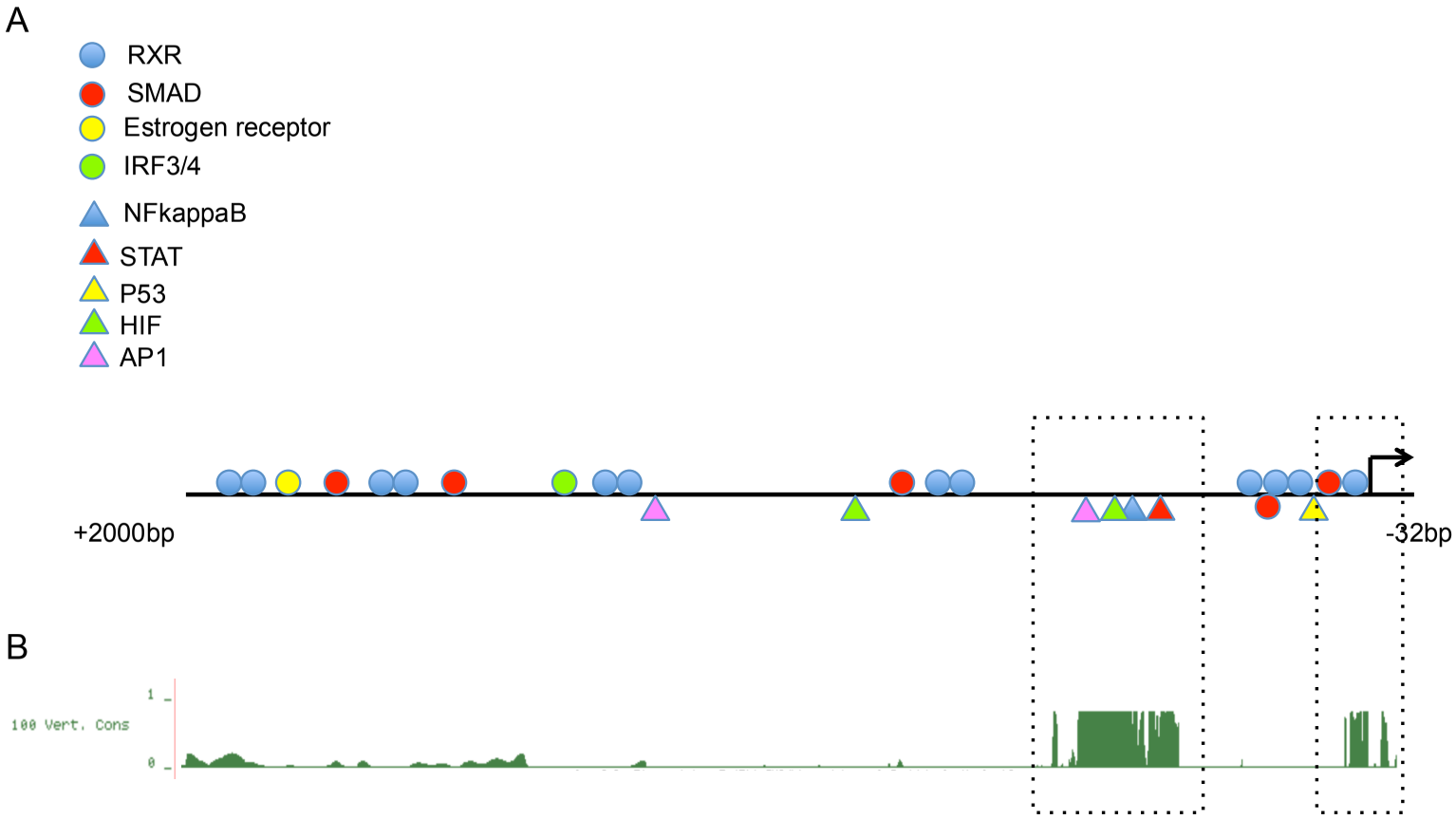

Figure 4.11 Schematic of miR-23a~24-2~27a promoter region showing positions and level of conservation of potential transcription factor binding sites.

(**A**) Relevant myeloid transcription factors predicted by Matinspector in the 2kb sequence directly upstream of the TSS. (**B**) Sequence conservation between 100 vertebrates species (100 Vert. Cons, left axis, in green) generated using Basewise Conservation by PhyloP on the UCGS Genome Browser.

4.2.6.2 Characterization of the 3' end of pri-miR-23a~miR-24-2~miR-27a transcripts.

Inspection of the miR-23a cluster in the UCSC Genome Browser poly(A) track identifies the presence of polyadenylation sites within each member of the cluster (Figure 4.12, A). These corresponded to data from polyASeq (Figure 4.12, B). PolyASeq is a targeted RNA sequencing technique of the 3' ends of polyadenylated transcripts first described by Derti et al [546]. As alternative polyadenylation could, in theory, uncouple the expression of poly-cistronic miR clusters, resulting in a post-transcriptional mechanism for modulating mature miR levels produced from a single primary transcript. As noted in Chapter 3, levels of the mature forms of the miR-23a cluster did not correlate with each other as one might expect given that they are derived from a single primary transcript. To see if the forms identified in polyASeq data are bona fide, 3'Rapid Extension of cDNA Ends (3'RACE) was performed to characterise the 3'ends of the pri-miR-23a transcript. The same RNA samples from the Drosha-depleted THP-1 cells used previously for 5'RACE were used (Figure 4.10, A). Two different sets of forward primers were designed for the amplification of the 3' end, giving rise to individual bands (Figure 4.12, C). Each band was cloned and sequenced. Both amplicons had identical polyA tails that were not present in the genomic sequence, indicating that they were added post-transcriptionally (Figure 4.12, B). The beginning of the polyA tail was located 14 bp downstream from the predicted Drosha cleavage site. Surprisingly, there was no canonical polyA signal sequence upstream of the polyA tail, which is essential for polyadenylation [705]. As far as I am aware there are no reports of polyadenylation of Drosha generated pre-miRNAs. I could not detect any of the transcripts that corresponded to the species highlighted in UCSC Genome Browser poly(A) track. It may be that these forms are not present in THP-1 cells or that they are present at levels that even in Drosha-depleted samples are too low for detection using 3'RACE. Similarly, the previously reported polyadenylated species, which had a polyA signal at position +1752-1757 were also not detected [570]. The length of this species with respect to the forward primers used here may have been too long to be efficiently amplified. Repeating the 3'RACE with primers designed closer to the predicted end of this transcript may have increased the likelihood of detecting this transcript.

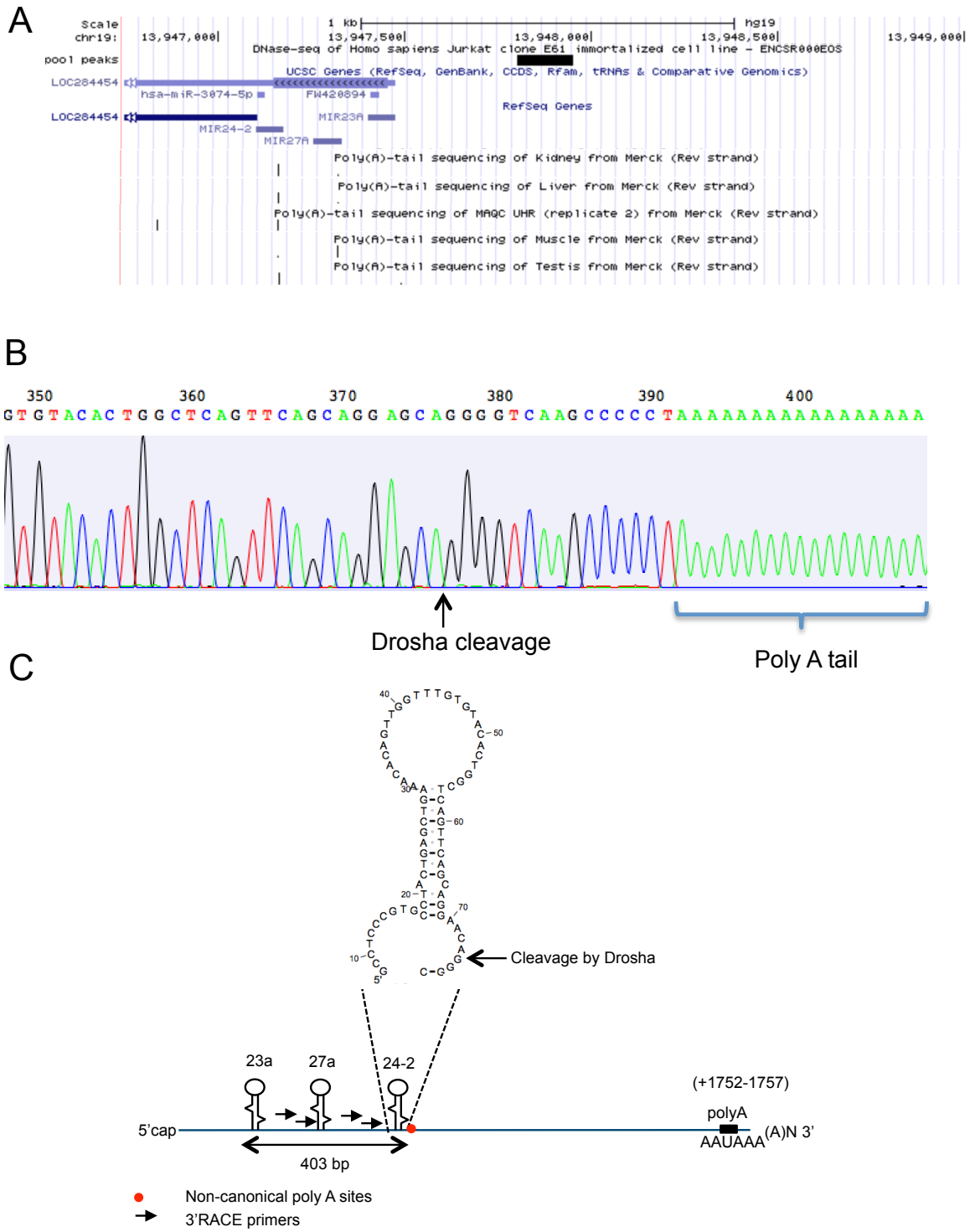

Figure 4.12 Characterization of 3' transcriptional polyadenylation sites by 3'RACE method.

Experiments done in THP-1 cells in 3 technical replicates. (**A**) Shows polyAseq tract of the miR-23a cluster loci from ENCODE genome browser. (**B**) 3'RACE performed in THP-1 cells transfected with DROSHA siRNA; the resulting amplicon was then sequenced. Figure shows the sequence at the 390 bp position in the pri-miR-23a transcript. (**C**) Schematic of the newly identified polyadenylation site proximal to Drosha cleavage site of pri-mir-23a~24-2~27a transcript. Schematic also shows the placement of 3'RACE primers for amplification.

4.3 Discussion

Myeloid cells are the mainstay of the innate immune response. Although heavily studied in the context of provoked immunity, we still lack a full understanding of what drives monocytes and macrophages in the chronic inflammatory conditions and disables the termination of the process. This is of particular interest in inflammatory monocytes that not only change upon activation by certain stimuli but also have the ability to mature, migrate and differentiate into macrophages, further transferring the problem into tissues. The biology behind these processes involves a tight interplay between homeostatic maintenance and an acute response to an insult, most commonly involving change of TF and miR species to help regulate this process. Similar features have been clearly demonstrated in the priming of T cells when the turnover of the entire population of miR species in the cell is required to achieve a new phenotype [706]. Considering implications of miR-23~24~27 clusters in chronic inflammatory processes, understanding what regulates these clusters in monocytes is paramount to capturing the triggers of chronicity.

Blood-derived myeloid cells are collectively labelled as $CD14^+$ cells. This cell marker is a part of TLR4 pattern recognition receptor and is present on the majority of myeloid cells. Recently, expression of CD14 and CD16 (FcγRIII) markers on the surface of monocytes were utilised to describe three distinct cell populations. The most prevalent classical $CD14^+CD16^-$ cells expressing CCR2 and resembling $Ly6C^{hi}$ murine monocytes; proinflammatory 'intermediate' $CD14^+CD16^+$ cells and non-classical $CD14^-CD16^+$ cells known for their ability to patrol vascular wall endothelial cells [212,221,707-710]. Both $CD16^+$ populations account for less than 10% of all monocytes [710]. Nonetheless, $CD14^+CD16^+$ population has been implicated in autoimmune diseases such as RA [641]. Data above confirms that miR-23a~24-2~27a cluster is not only highly expressed in $CD14^+$ blood-derived monocytes, but that it is present at particularly high levels in classical $CD14^+CD16^-$ cells (Figure 4.1, B). Unfortunately, investigating the expression of miR-23a cluster in purified $CD16^+$ cells was not performed at the time, yet, these data raise the possibility that the remaining highly inflammatory $CD14^+CD16^+$ population could have a very low expression of miR cluster which could be contributing to their aggressive phenotype and certainly requires further investigation. It is therefore also possible that treatment-

resistant patients reviewed in Chapter 3 had a higher proportion of $CD14^+CD16^+$ cells resulting in lower overall expression of miR-23a and miR-27a than treatment responders or healthy controls. Unfortunately at the time of this study only $CD14^+$ cells were analysed and the frequency of $CD16^+$ cells in these samples was unknown. However, RA patients with active disease, such as patients in DMARDs and biologics resistant groups, were previously found to have an increased proportion of $CD14^+CD16^+$ population in peripheral blood [641].

The importance of miR-23~24~27 clusters in myeloid cells was previously established with links to the promotion of myelopoiesis during lineage commitment, phagocytosis and antigen presentation during inflammation [568,595,711]. Even so, there are no studies to date that explore the role and regulation of miR-23~24~27 cluster in inflammatory monocytes, while several reports focus on the role in mature macrophages and dendritic cells [594,712]. Reports in cancer research and other studies have suggested regulators of miR-23 clusters include NFκB and M-CSF. Here we set out to investigate if inflammatory cytokines and TLR stimuli have an effect on pri-miR-23a~24~27a expression in human monocytes. Unfortunately, variety of inflammatory stimuli including IL-17A, TNFα and LPS utilising NFκB signalling failed to exhibit any effect on the expression of primary miR-23a~24-2~27a transcript in monocytes (Figure 4.2, A; Figure 4.3, B). From these, it is the effect of LPS stimulation through TLR4 that is the most puzzling one. LPS stimulation in buffy coat derived $CD14^+$ cells, healthy controls and RA patients resulted in the upregulation of primary miR-23a~24-2~27a transcript in a number of subjects, while others demonstrated no effect (Figure 4.3, B and C). This variability could be more prominent due to the small number of participants in each group. However, the possibility of other unknown factors, such as the availability of the CD14 receptor following cell purification, for example, could be influencing the expression of miR-23a cluster in these circumstances and cannot be wholly excluded. Other TLR ligands to TLR1/2, TLR3 and TLR7/8, did not regulate the miR-23a cluster expression (Figure 4.3, A, D, E).

Instead, the ability of IL-6 to downregulate the expression of miR-23a cluster was discovered (Figure 4.2, D). IL-6 is a genuinely pleiotropic cytokine expressed by almost all stromal and immune cells that exhibit hormone-like as well as proinflammatory functions [373]. Its effects are mediated through IL-6Rα/GP130

signalling involving JAK1/Tyk2 and STAT3 kinases [387]. This signalling cascade is negatively controlled by suppressors of cytokine signalling (SOCS) with the absence of SOCS3 leading to inhibitory effects of IL-6, resembling that of IL-10 [391,410]. Nonetheless, lack of SOCS3 in the chronic inflammatory setting allows sustained STAT1 and STAT3 signalling causing exacerbated inflammation [713]. Activation of IL-6 pathway through STAT1 and STAT3 are good indicators of therapy response [714,715]. It is, therefore, understandable that patients failing DMARDs and biologics treatment had increased concentration of serum IL-6 cytokine (Figure 4.8, A). High levels of IL-6 trended towards a negative correlation with low expression of miR-27a in biologics resistant patients. However, this has not reached statistical significance ($r=-0.25$, $p=0.06$) (Figure 4.9, A). Cofounding factors of this analysis include some patients on treatment with tocilizumab targeting IL-6R and modifying IL-6 pathway and limited sample size to reflect the magnitude of this relationship. Nonetheless, *in vitro* experiments would support IL-6 as a candidate, capable of regulating the expression of miR-23a~24-2~27a cluster in this RA patient cohort.

Involvement of the JAK1 signalling pathway is further supported by the discovery of the inhibitory effect of IFNγ, which strongly and continuously reduced the expression of primary miR-23a~24-2~27a transcript (Figure 4.2, C). This provides a new mechanism by which T cells, and in particular Th1 cells, mediate activation of monocytes and induce maturation similarly to M-CSF or GM-CSF growth factors. IFNγ and M-CSF both reduced the expression of miR-23a cluster; it would be interesting to explore if these stimuli lead to same functional outcome through miR pathway targeting that will be discussed later. Even though IFNγ significantly influenced miR-23a~24-2~27a cluster expression in *in vitro* experiments, it is not likely that it had a significant impact in monocytes from RA patients, given low serum concentrations of the cytokine in the majority of participants (Figure 4.8, D). Contrary to this, type I interferon - IFNα was highly present in patient serum samples, however, had insignificant effect on miR-23a~24-2~27a expression when tested in *in vitro* (Figure 4.8, C and Figure 4.2, B). The previous report would suggest that type I interferon can downregulate miR-27a expression in murine M-CSF exposed macrophages [596]. My data on human M-CSF-derived macrophages showed that differentiation significantly reduces miR-23a cluster expression in its own right, so much so that

further reduction obtained by IFNα exposure might not be relevant. The lack of reports on the impact of type I interferons on miR expression in monocytes does not allow comparison and requires further investigations. Especially when considering the puzzling effect of IFNß which downregulated miR-23a cluster similarly to IFNγ rather than to its family member IFNα. This similarity might be explained by the involvement of JAK1 signalling cascade, shared by all cytokines exerting influence on miR-23a~24-2~27a expression and could be further tested by exposure of cytokine-stimulated monocytes to tofacitinib, a JAK1/JAK3 inhibitor and a clinically used small molecule.

Upon encountering pathogens, cytokines and other activators, blood-derived monocytes migrate to affected tissues guided by homing chemokines like CCL2. Exposure to tissue inflammation triggers the maturation of monocytes into phagocytic macrophages, and this process is primarily governed by M-CSF growth factor [245,716]. Previously published and this data have clearly demonstrated that miR-23a~24-2~27a is actively abolished during M-CSF guided maturation process and is at the limit of detection after 3 days of exposure (Figure 4.4, A) [594]. Instead, its functions are replaced by the newly triggered expression of pri-miR-23b~24-1~27b paralogue cluster (Figure 4.4, A). This switch is reflected in the expression of mature miRs (Figure 4.5). Both growth factors M-CSF and GM-CSF signal through reciprocal receptors and are responsible for the maintenance of myeloid cells [717]. Other potential ligands of CSF1R include VEGFA and IL-3. However, they are not considered a major influence in RA arthritis and were not tested here. GM-CSF guided maturation of monocytes also obliterated expression of pri-miR-23a cluster after 3 days of exposure (Figure 4.4, B). Similarly, GM-CSF exposure led to a significant increase in the expression of the paralogue pri-miR-23b cluster (Figure 4.4, B). The intronic placement of miR-23b~24-1~27b cluster and likely co-expression with the host gene C9ORF3 poses the question on the function of the host gene and its importance in macrophage growth. Nonetheless, the fact that miR-23a~24-2~27a expression was reduced by both M-CSF and GM-CSF exposure points towards critical role of this cluster in all myeloid maturation, including monocyte-derived DCs and alveolar macrophages that are in mice thought to be primarily governed by GM-CSF [249,718]. Indeed, persistent expression of miR-24 in human M-CSF and GM-CSF differentiated macrophages and DCs did not only influence the phenotype of

cells but also severely affected their ability to produce cytokines upon stimulation with LPS, ultimately impairing their function [594]. It is still unclear if instead expressed miR-23b~24-1~27b cluster differs in functions or serves as an equivalent to miR-23a~24-2~27a myeloid regulator in the tissues. *In silico* analysis of the potential miR functions will be analysed in the following chapter however one nucleotide difference in mature sequences between 'a' and 'b' miRs and identical 'seed' region would certainly suggest that they have a capacity to bind to the same mRNA targets.

Maturation and migration into tissues allow monocyte-derived macrophages to encounter a variety of cytokines that help to decide future fate of the cells. Described in this manner classically activated with IFNγ and LPS macrophages exhibit proinflammatory phenotype and are designated M1 cells, while others activated by IL-4 and IL-13 are termed M2 macrophages, known for their regulatory abilities. In recent years a variety of laboratory protocols and the many ways in which one can grow and activate macrophages has led to some confusion between different phenotypes and difficulty in reproducing certain results. At best, this proposed scale should be viewed as shades of grey rather than monochrome absolute phenotypes. This has prompted Murray et al. to systematically review the nomenclature in attempt to limit confusion [260]. My data showed that neither LPS, IFNγ or LPS with IFNγ nor IL-4 exposure of M-CSF or GM-CSF grown macrophages led to recovery of primary miR-23a~24-2~27a transcript expression (Figure 4.6, A). Arguably, longer exposure to these stimuli could have had a different effect. However, a short 24 hour stimulation allows measurement of primary transcript and shows the initiation of transcription or lack there off in this case. M-CSF differentiated macrophages stimulated with other inflammatory cytokines including TNFα, IL-17A and IL-6 also failed to resume pri-miR-23a expression (Figure 4.6, B-D). These data collectively indicate that miR-23a~24-2~27a cluster is switched off during monocyte to macrophage differentiation. Therefore, it is possible that M-CSF exposure of peripheral blood monocytes from difficult to treat RA patients was the driving force behind the start of the migration process and caused decreased expression of miR-23a and miR-27a. Unfortunately, M-CSF measurement was not available to me at the time of the assay. However, high presence of migratory chemokine CCL2 in patients with high disease activity indicates increased recruitment of monocytes

to the inflamed tissues and could further explain the low expression of miR-23a and miR-27a in difficult to treat patients (Figure 4.8, F). Additionally, stimulation of monocytes with CCL2 chemokine also caused decrease of the pri-miR-23a expression, as a part of cell maturation priming (Figure 4.2, G).

Here we confirmed the TSS of miR-23a cluster in THP-1 monocytic cell line. Using the TSS site to define the likely location of the miR-23a cluster's promoter allowed us to take advantage of the up to date in silico analysis software (MatInspector) that could predict the presence of binding sites in the 2kB sequence immediately upstream of the TSS. This analysis revealed the presence of binding sites for a number of monocyte/macrophage transcription factors. The presence of NFκB and STAT binding sites was of particular interest. A recent study also identified the presence of NFκB and STAT binding sites in the murine miR-23a promoter [703]. The presence of regulatory elements for these transcription factors would provide a possible mechanism for the reduction in pri-miR-23a cluster expression seen in response to IL-6, IFNβ and IFNγ, all 3 of which are thought to induce JAK/STAT signalling [678] [719]. While in silico analysis, although suggestive, does not in itself prove the observed transcriptional changes are a direct result JAK/STAT, it does provide the framework for additional experiments that could. Cloning the miR-23a cluster promoter upstream of a luciferase promoter would allow the functional role of STAT signalling to be further interrogated. If for example, the transfection of a miR-23a promoter luciferase plasmid into a relevant cell type (e.g. THP-1) followed by treatment with IL-6/IFNγ re-capitulated the reduction in expression levels observed in primary $CD14^+$ cells this would confirm that the necessary regulatory elements were present in the selected region. Mutation of the predicted STAT binding sites would further localise the elements essential for IL-6/IFNγ regulation of miR-23a cluster expression. However, the ultimate de facto proof of STAT regulation of the cluster requires specific STAT Chromatin Immuno Precipitation (ChIP) of the miR-23a promoter or indeed an Electro Mobility Shift Assay. Unfortunately, due to time constraints, I was unable to perform these studies. However, this will be pursued in my future work.

Analysis of the polyAseq data on the UCSC Genome Browser revealed the presence of a number of polyA peaks between each member of the cluster

raising the possibility that the cluster could be controlled post-transcriptionally via alternative polyadenylation. While there are as far as I am aware no reports describing such a mechanism the possibility was too intriguing to ignore. To study this, I performed 3' RACE to capture the polyadenylated form of the pri-miR-23a~24-2~27a transcript. I was able to identify a polyadenylated transcript from the miR-23a loci; it was not one that had previously been reported. The 3' end of this transcript corresponded to a site 14 bp down steam from the predicted Drosha cleavage site of miR-24-2. While this transcript did contain a non-genomic encoded polyA tail, it did not, however, include an associated polyA sequence (typically AAUAAA) [705].

In this chapter, I have identified a number of key stimuli that influence the expression of the miR-23a cluster in primary human myeloid cells along with their potential regulatory elements within the miR-23a clusters promoter.

5 Validating THP-1 myeloid cell line as a model system to study miR-23~24~27 cluster interactions

5.1 Introduction

The human THP-1 myeloid cell line was established in 1980 from a patient with an acute monocytic leukaemia [720]. Ever since THP-1 cells have been extensively used for the modelling of human myeloid biology. Phenotypic studies confirmed that although cancerous, THP-1 cells did not loose their myeloid properties and morphologically resemble monocytes with distinctive surface markers [720]. Upon stimulation with phorbol-12-myristate-13-acetate (PMA) or vitamin D_3 THP-1 cells mature into adherent phagocytizing cells resembling primary macrophages [721]. The PMA method is preferred as it leads to increased phagocytosis and higher expression of CD14 and CD11b surface markers resembling mature primary macrophages [722]. Also, similarly to macrophages, THP-1 cells secrete M-CSF and support maturation in an autocrine manner, yet in vitro stimulation with M-CSF leads to incomplete maturation of the cells, unlike those with PMA [723,724]. Other immortalised human myeloid cell lines include U937, ML-2 and Mono Mac 6 cells that exhibit more immature phenotypes and have not been used in this work.

Technical advantages gained by studying THP-1 cells are many. Primarily, stable genetic background reduces phenotype variability often found in primary human specimens [725]. Secondly, THP-1 cells are significantly more suitable for transfections with DNA plasmids and miRs, while the efficacy of these procedures in primary human monocytes can be low and cause cell apoptosis [726]. Among transfection methods available, electroporation is a suitable way of delivering plasmid DNA into THP-1 cells without consequences to cell viability or function [727,728]. Thirdly, THP-1 cells are indefinitely stored in liquid nitrogen and can be recovered without damage to morphology or myeloid phenotype of the cells. Additionally, primary human monocytes account for up to 10% of peripheral blood leukocytes and can be difficult to recover in numbers suitable for an extensive mechanistic experiment In contrast THP-1 cells are easily maintained and readily available.

In inflammation, several functions of primary monocytes have been compared to that of THP-1 cells. TNFα stimulated THP-1s have been shown to adhere to endothelial cells in the same way as blood-derived monocytes [729]. The transcriptome of THP-1 cells after LPS activation is largely similar to that observed in primary human monocytes. Similarly, PMA differentiated THP-1s resembled M-CSF, and to a lesser extent, GM-CSF matured macrophages, although some subtle differences have been noted [730,731]. Some studies have reported that THP-1 cells retain the ability to differentiate into phenotypes that mimic M1 or M2 macrophages, depending on the cytokine exposure [732,733].

Taking this into consideration I sought to explore the possibility of using THP-1 cells to dissect the complex roles of the mIR-23a~24-2~27a cluster in monocyte/macrophage biology that would have otherwise been difficult to examine on primary monocytes. To this end, I tested the suitability of THP-1 cells as a model system by reproducing the data obtained from primary human $CD14^{+}$ cells in Chapter 4 along with a characterization of some of the most general features of monocyte biology. Having reassured myself as to the suitability of THP-1 cells to study the functional significance of the miR-23a~24-2~27a cluster in monocyte/macrophage biology. I set about to create THP-1 cell lines that were deficient in miR-23, miR-24 and miR-27 activities by engineering THP-1 cells to express miR-sponge transcripts designed to bind and sequester endogenous miR-23, miR-24 and miR-27. This ambitious strategy allowed the functional depletion of each miR within the miR-23a cluster along with all possible combination of each from the relevant THP-1 cell line.

5.2 Results

5.2.1 Demonstrating the suitability of THP-1 cells as a model system to study miR-23a~24-2~27a cluster's role in monocyte function

The aim of this study was to systematically explore the role that the miR-23a cluster plays in monocyte/macrophage biology. To accomplish this, I had to identify a human monocytic cell line that retained essential features of a primary monocyte, namely the abilities to respond to inflammatory stimuli, to produce pro-inflammatory and anti-inflammatory cytokines, to mature into a 'macrophage' like cell and express the miR-23a~24-2~27a cluster. The available literature would suggest that THP-1 cells meet most of these requirements. However, little is know about miR-23a cluster in these cells. To this end, I aimed to evaluate miR-23a cluster expression and regulation within THP-1 cells.

5.2.1.1 THP-1 cells express miR-23a and miR-23b clusters THP-1 cells.

Both miR-23~24~27 clusters were detected in undifferentiated THP-1 cells. As previously seen in blood-derived monocytes, they express higher levels of the primary miR-23a cluster than its paralogue, pri-miR-23b (Figure 5.1, A). The similarities with primary monocytes are also reflected in the expression of mature members, as miR-24 was found at significantly higher levels than miR-23a or miR-27a (Figure 5.1, A).

5.2.1.2 PMA maturation supresses pri-miR-23a~24~27a expression

Next, I have explored the expression of both miR clusters during PMA driven maturation of THP-1 cells, which is thought to mimic M-CSF-driven maturation of primary human monocytes into macrophages. For this, THP-1 cells were cultured with 25 ng/ml of PMA for three days followed by the replacement of the medium, not containing any PMA for the next four days. This protocol was designed to allow full differentiation and adherence of THP-1 cells while minimising toxicity of the PMA that can occur if exposure exceeds 72 hours. Here, expression of primary miR-23a~24~27a transcript was significantly reduced after 4 and 24 hours, as well as after seven days of maturation (Figure 5.1, B). However, there was no significant difference in the pri-miR-23a expression after three days of maturation, possibly due to the developing toxicity of PMA before

the change of medium. On the contrary, the pri-miR-23b cluster expression was immediately reduced after 4 hours of exposure, followed by the steady increase in levels until day 7 (Figure 5.1, B). As a result, primary miR-23b cluster transcript was present at higher levels than pri-miR-23a after seven days of maturation, similarly to that observed in primary human M-CSF-derived macrophages. In contrast to this, I detected a significant steady increase in the expression of mature members of miR-23a cluster during the PMA exposure of THP-1 cells, with the highest change observed in the levels of miR-23a (Figure 5.1, D-F).

Together, these data confirm that THP-1 cells continuously express both miR clusters in a steady state or during cell differentiation. The pattern of expression in monocytic THP-1 cells largely mimics that of primary monocytes, while PMA matured THP-1 cells appear different from M-CSF or GM-CSF matured primary macrophages. Given that this work primarily focuses on the role of blood-derived monocytes, undifferentiated monocytic THP-1 cells will be the focus of this and next chapter.

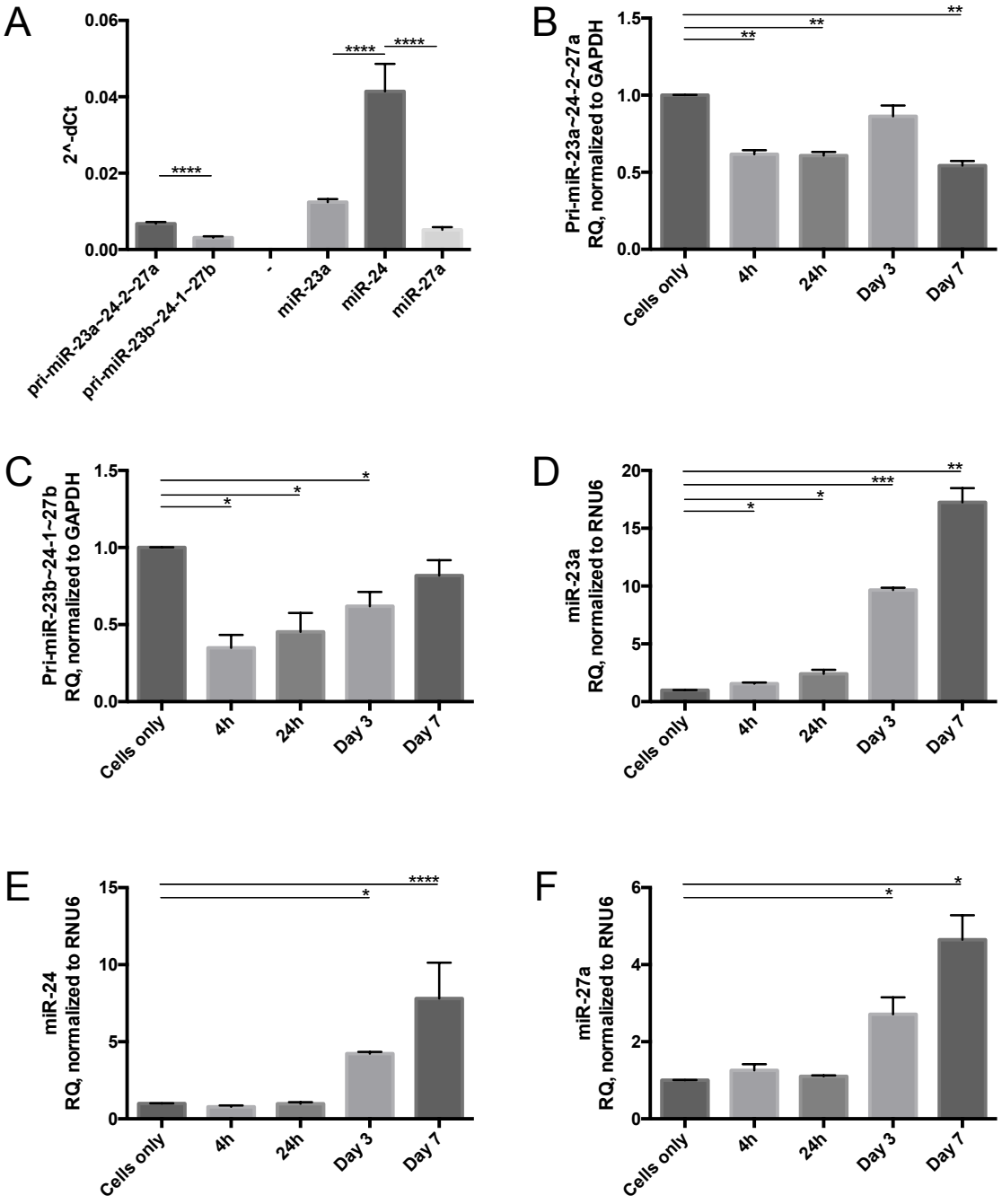

Figure 5.1 The expression of miR-23a~24-2~27a cluster in THP-1 monocytic cell line

THP-1 cells were used in each experiment. Data represented by Mean±SD, n=3. Results are obtained by the qPCR method and displayed as RQ (2^-ddCT) relative to GAPDH or RNU6 genes and control cells. (**A**) Expression of the primary transcript of miR-23a~24-2~27a and miR-23b~24-1~27b clusters and mature miR-23a, miR-24, miR-27a in undifferentiated THP-1 cells (2^-dCT). Expression normalised to GAPDH and analysed by ordinary one-way ANOVA with Sidak's correction for multiple comparisons. (**B**) Expression of pri-miR-23a~24-2~27a transcript in THP-1 cells during 7-day maturation with 25 ng/ml PMA normalised to GAPDH control. (**C**) Expression of the pri-miR-23b~24-1~27b transcript in THP-1 cells during 7-day maturation with 25 ng/ml PMA, normalised to GAPDH control. (**D-F**) Expression of mature miR-23a, miR-24 and miR-27a in THP-1 cells during 7-day maturation with 25 ng/ml PMA, respectively; expression normalised to RNU6 control. Data from experiments **B-F** analyzed by ordinary one-way ANOVA with Dunnett's correction for multiple comparisons, * - p≤0.05, ** - p≤0.01, *** - p≤0.001, **** - p≤0.0001.

5.2.1.3 Expression of pri-miR-23a~24-2~27a in THP-1 cells under inflammatory stimuli.

Like primary $CD14^+$ cells, THP-1 cells have previously been shown to express TNFR1 and IL17RA and respond to TNFα and IL-17A cytokines, respectively [734,735]. THP-1 cells have also been shown to express both Interferon gamma (IFNGR1) and IL-6R receptors [736,737]. Thus, I went on to investigate whether miR-23a cluster expression within THP-1 cells respond in the same way as that observed in $CD14^+$ cells upon pro-inflammatory cytokine stimulation.

5.2.1.3.1 TNFα and IL-17A do not effect pri-miR-23a~24-2~27a expression in THP-1 cells.

Dose-dependant stimulation of THP-1 cells with TNFα and IL-17A was used to explore their effect on NFκB signalling cytokines on miR-23a expression, a dose-dependent stimulation of THP-1 cells was performed. Despite a considerable range of doses, neither TNFα nor IL-17A had any significant effect on the expression of the primary transcript of miR-23a~24-2~27a cluster (Figure 5.2, A and B). This finding is in keeping with that previously observed in human blood-derived monocytes (Chapter 4). Published work conducted in murine models would suggest that NFκB activation reduces the expression of miR-23a in murine macrophages and that IL-17A directly downregulates the expression of mature miR-23b in the embryonic kidney cell line [593,703]. However, neither of these was observed in human monocytes or THP-1 cells, which might reflect differences between the two species or simply reflect the different cell types studied. It is interesting to note that proposed NFκB binding site reported is conserved between species and that NFκB/p65 has been shown to bind to this site in an erythroblast cell line [661].

5.2.1.3.2 IFNγ represses the expression of pri-miR-23a~24-2~27a cluster in THP-1 cells.

Previous investigation of what impacts miR-23a cluster expression in primary human monocytes has identified IFNγ as having a significant repressive effect on the expression of the cluster at a concentration of 10 ng/ml. This finding was reproduced here in THP-1 cells where IFNγ stimulation resulted in downregulation of pri-miR-23a~24-2~27a expression in a dose-dependent manner (Figure 5.2, C). The dose of 50 ng/ml of IFNγ had a potentially toxic effect on

the THP-1 cells and failed to further downregulate the expression of the pri-miR-23a cluster (Figure 5.2, C). Indeed, high levels of IFNγ have been reported to induce apoptosis in THP-1 cells [738]. In line with this, physiologic levels of IFNγ, detected in human serum samples, are significantly below 25 ng/ml and predominantly vary from 10 pg/ml to 150 pg/ml in patients with severe infection, such as leprosy [739].

5.2.1.3.3 THP-1 cells express functional IL-6R.

Next, I explored the effect of IL-6 on the expression of miR-23a cluster since it had the ability to suppress its expression in fresh human monocytes after 24 hours of exposure. Unfortunately, exposure of THP-1 cells to various doses of IL-6 failed to exhibit any effect on the levels of primary miR-23a transcript (Figure 5.2, D). However, this lack of effect was not due to a non-functional IL-6R pathway as THP-1 cells as the surface expression of IL-6 receptor matched the levels found in PBMC derived CD14+ monocytes (Figure 5.3, A). Further assessment revealed that IL-6 receptor is fully functional in THP-1 cells and induces phosphorylation of STAT3 signalling upon encounter with a cocktail of cytokines or IL-6 cytokine alone (Figure 5.3, B). Interestingly, the strongest signal of STAT3 phosphorylation occurred after 13 minutes stimulation of THP-1 cells with IL-6. However, the combination of IL-6 and soluble IL-6R prolonged the window of STAT3 phosphorylation up to 30 minutes, most likely due to the trans-signaling through membrane-bound subunit GP130 (Figure 5.3, B) [740,741]. Thus providing evidence of a highly expressed and fully functional IL-6R pathway in THP-1 cells. Although lacking the ability to regulate the miR-23a cluster expression in THP-1 cells, the presence of functional IL-6R pathway allows us to investigate further the effect that mature members of the miR-23a cluster have on targets within the IL-6R pathway in the inflammatory context.

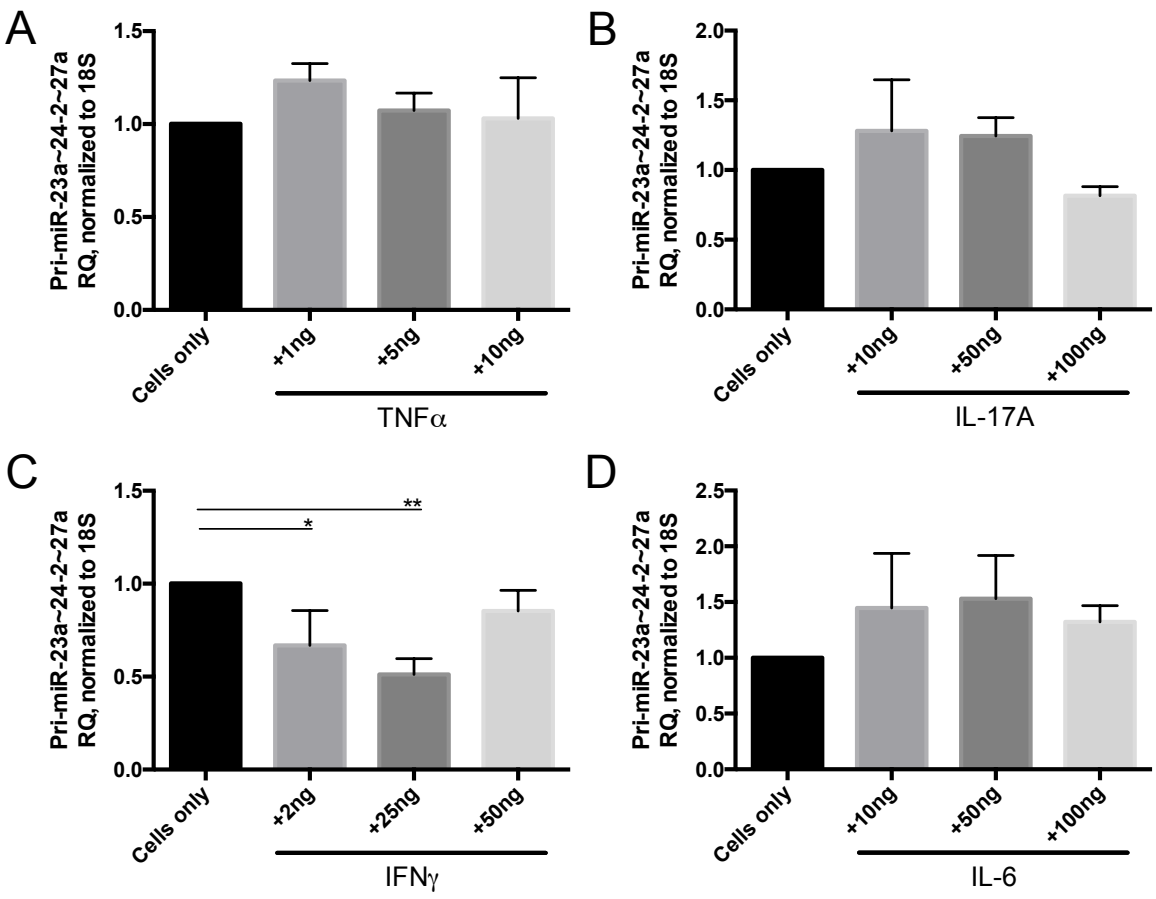

Figure 5.2 Influence of proinflammatory cytokines on the expression of miR-23a~24-2~27a cluster in The THP-1 monocytic cell line.

THP-1 cells were used for each experiment. Data represented by Mean±SD, experiments were conducted on 3 separate occasions. Results were obtained by the qPCR method measuring pri-miR-23~24~27 and displayed as RQ (2^-ddCT) relative to 18S gene and control cells. (**A**) THP-1 cells were incubated with 1, 5 or 10 ng/ml of TNFα for 24 hours. (**B**) THP-1 cells were incubated with 10, 50 or 100 ng/ml of IL-17A for 24 hours. (**C**) THP-1 cells were incubated with 2, 25 or 50 ng/ml of IFNγ for 24 hours. (**D**) THP-1 cells were incubated with 10, 50 or 100 ng/ml of IL-6 for 24 hours. On all occasions, data were analysed with One-Way ANOVA test with Dunnett's correction for multiple comparisons. * - p≤0.05, ** - p≤0.01.

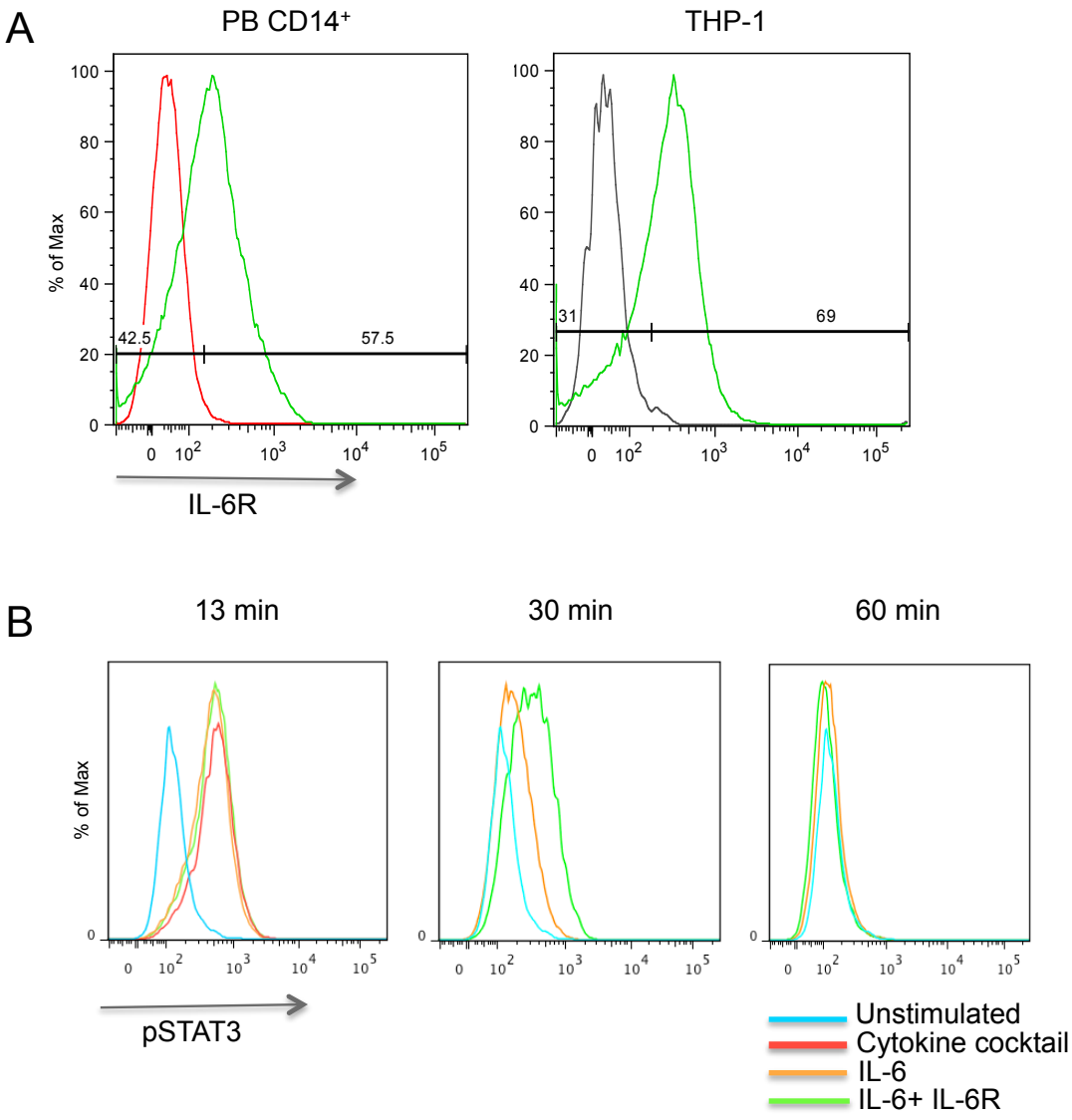

Figure 5.3 Functional assessment of IL-6/IL-6R pathway in THP-1 monocytic cell line.

THP-1 cella were used for each experiment. Results were obtained by the FACS. (**A**) Representative histogram of surface IL-6R expression in PB CD14^{+} cells (left) and in THP-1 cells (right). Matching isotype is shown in red (left) and grey (right), IL-6R staining shown in green. (**B**) Representative plot of phosphorylated STAT3 staining in THP-1 cells: unstimulated cells (blue), upon stimulation with cytokine cocktail (25 ng/ml IFNγ, 50 ng/ml IL-6 and 20 ng/ml IL-4) (red), 50 ng/ml IL-6 (orange) or 50 ng/ml IL-6 with 25 ng/ml soluble IL-6R (green) after 13' (left), 30' (middle) and 60' (right).

5.2.1.4 Expression of pri-miR-23a~24-2~27a in THP-1 cells under TLR stimuli.

The ability to respond to pathogen-associated molecular pattern (PAMP) signals is a mainstay of monocytic function, which is preserved in THP-1 cells as they continue to express TLR receptors [742,743] [744,745]. Here I sought to examine the effect of TLR stimulation on miR-23a cluster expression.

5.2.1.4.1 THP-1 cells up-regulate miR-23a~24-2~27a expression in response to stimulation with LPS or Pam3.

Stimulation of THP-1 cells with Poly(I:C) and CL097 activators of the intracellular TLR3 and TLR7/8 pathways did not have any measurable impact on the expression of pri-miR-23a cluster, repeating the finding previously observed in primary human monocytes (Figure 5.4, B and C).

However, stimulation of THP-1 cells with Pam3CSK4 surface TLR1/2 ligand led to increased expression of miR-23a cluster (Figure 5.4, A). Similarly, stimulation of THP-1 cells with LPS ligand to TLR4 has shown a dose-dependent increase in the expression of primary miR-23a cluster transcript (Figure 5.4, C).

THP-1 cells produced proinflammatory cytokines TNFα, IL-6 and soluble IL-6R upon LPS stimulation in a dose-dependent manner (Figure 5.5, A-C). Similar response is observed from primary human monocytes, which were shown to produce TNFα, IL-6 and IL-6R upon stimulation with LPS [746,747].

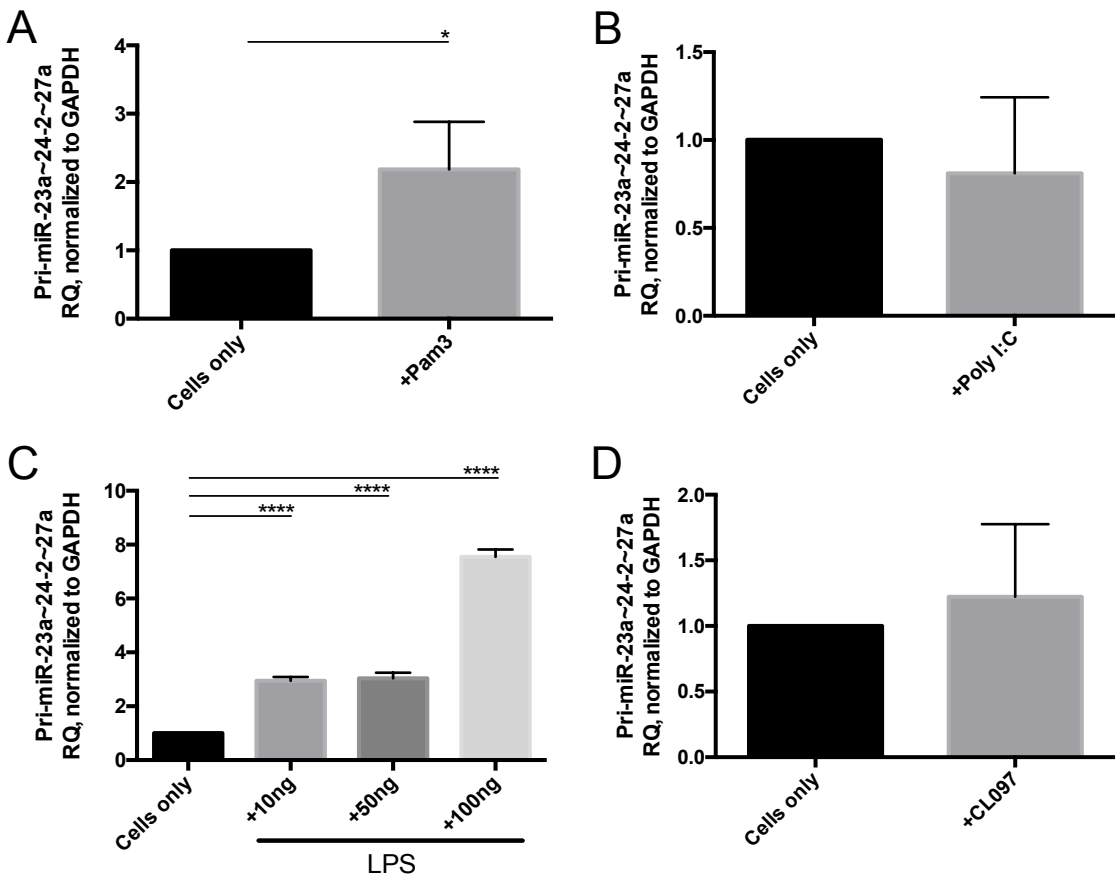

Figure 5.4 Influence of TLR ligands on the expression of miR-23a~24-2~27a cluster in the THP-1 monocytic cell line.

THP-1 cells were for each experiment. Data represented by Mean±SD, experiments were conducted on 3 separate occasions. Results are obtained by the qPCR method measuring pri-miR-23a~24~27a and displayed as RQ (2^-ddCT) relative to GAPDH gene and control cells. (**A**) THP-1 cells were incubated with 150 ng/ml of Pam3 for 24 hours. (**B**) THP-1 cells were incubated with 50 µg/ml Poly(I:C) for 24 hours. (**C**) THP-1 cells were incubated with 10, 50 or 100 ng/ml of LPS for 24 hours. (**D**) THP-1 cells were incubated with 1 µg/ml of CL097 for 24 hours. On all occasions, data were analysed with One-Way ANOVA test with Dunnett's correction for multiple comparisons. * - $p \leq 0.05$, **** - $p \leq 0.0001$.

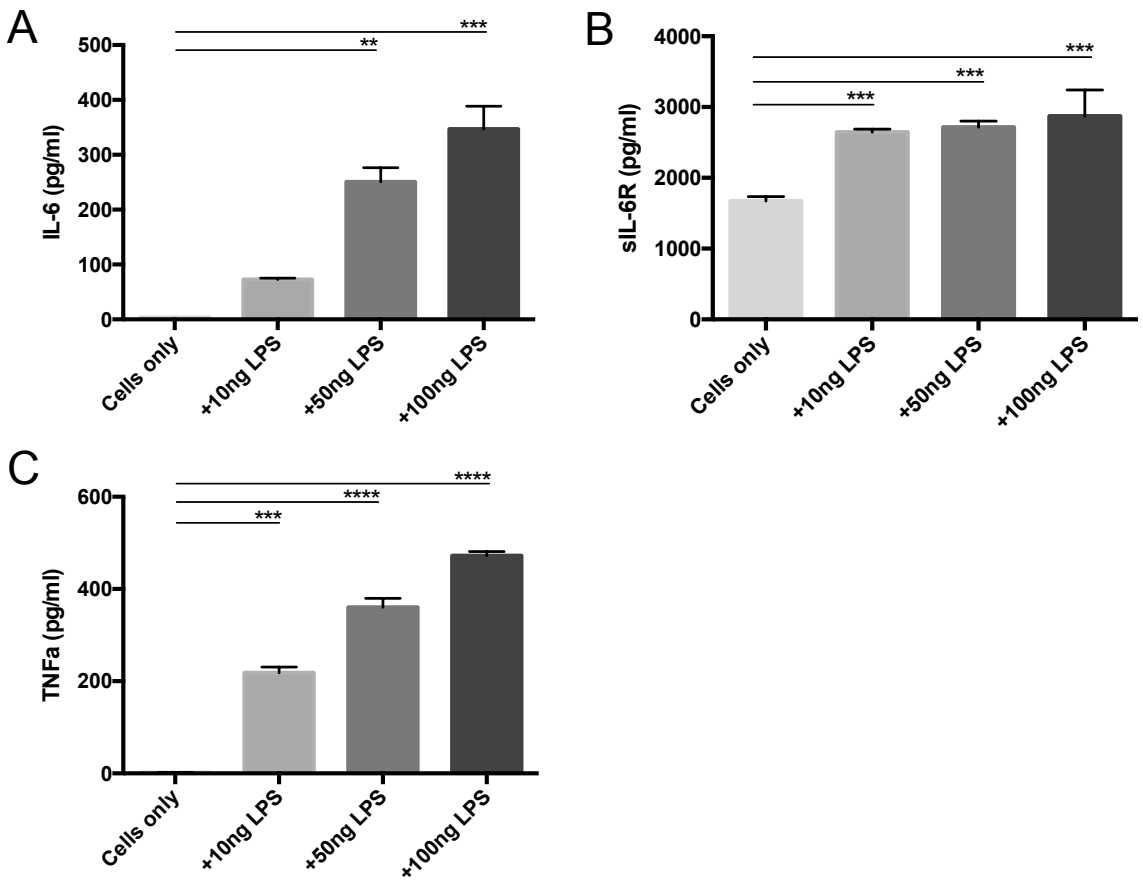

Figure 5.5 Expression of proinflammatory cytokines by THP-1 cells upon stimulation with TLR4 ligand LPS.

THP-1 cells were used for each experiment. Data represented by Mean±SD, experiments were conducted on 3 separate occasions. Results are obtained by the ELISA method and displayed as concentration (pg/ml) of cytokines in the supernatant of the THP-1 cells stimulated with 10, 50 or 100 ng/ml of LPS for 24 hours. (**A**) IL-6 levels (pg/ml). (**B**) Soluble IL-6R levels (pg/ml). (**C**) TNFα levels (pg/ml). On all occasions, data were analysed with One-Way ANOVA test with Dunnett's correction for multiple comparisons. * - p≤0.05, ** - p≤0.01.

5.2.2 Creating miR-23~24~27 knock-out THP-1 cell lines

5.2.2.1 Principal of miR sponge for technical knock-out of miRs

Ebert and colleagues first introduced the concept of miR sponges for the creation of loss of function of endogenously expressed miRs [618]. MicroRNA sponges inhibit miR function by swamping the cell with transcripts containing multiple (typically >5) high-affinity miR binding sites. These sponge transcripts compete with the endogenous miR targets, obscuring them from inhibition (Figure 5.6). In addition to this simple decoy role, sponges are typically designed to have a mismatch or a 3 base pair 'bulge' sequence at the 5' end of the seed region (Figure 5.6, B). The aim of this imperfect match is to induce the sequestering of the target rather than its degradation removing bound miRs from the active pool of the RISC-associated miRs, leaving their endogenous targets unregulated (Figure 5.6, A). One of the main advantages of miR sponges is that they have broad specificity for miR families i.e. a sponge against miR-23a will in most cases also target miR-23b and c species.

Recently there have been some reports where the authors used miR-sponges against multiple miR targets to investigate the collective roles of these miRs in the cell function and diseases [748,749].

To study the miR-23a cluster miRs we designed sponges that would target each miR within the cluster along with all possible combinations (Figure 5.7). The resulting miR sponge constructs and stably transfected miR sponge cell lines were extensively validated for their ability to be targeted by both exogenous and endogenous miRs.

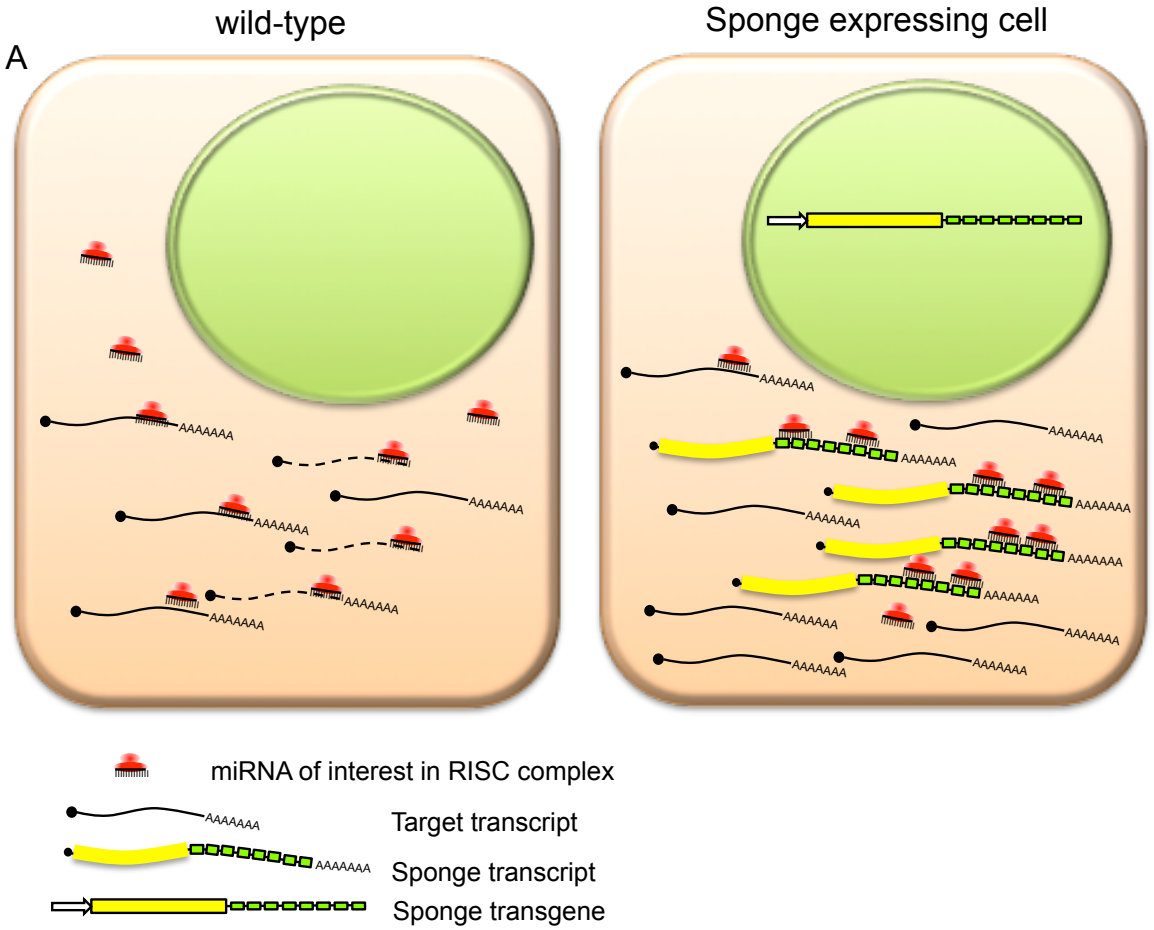

B

```
5'ctgttcctgc n n n actgagcca 3'   miR24 sponge
3'gacaaggacg a c u ugacucggu 5'   miR-24

5'ggtaatcc n n n caatgtgat 3'     miR23 sponge
  ccauuagg     guuacacua 5'     miR-23a
         g ac c

5'gcggaact n n n cactgtgaa 3' miR27 sponge
3'cgccuuga     a tc g gugacacuu 5' miR-27a
```

Figure 5.6 Schematic diagram of the principle of miR sponges.

(**A**) Schematic showing of the mechanism by which miR sponges relieve the inhibition of endogenous target genes. (**B**) Sponge miR binding site units with imperfect pairing between a miR and a sponge 'bulge' sequences introduced to promote sequestration over endonucleolytic cleavage by Argonaute 2 complex.

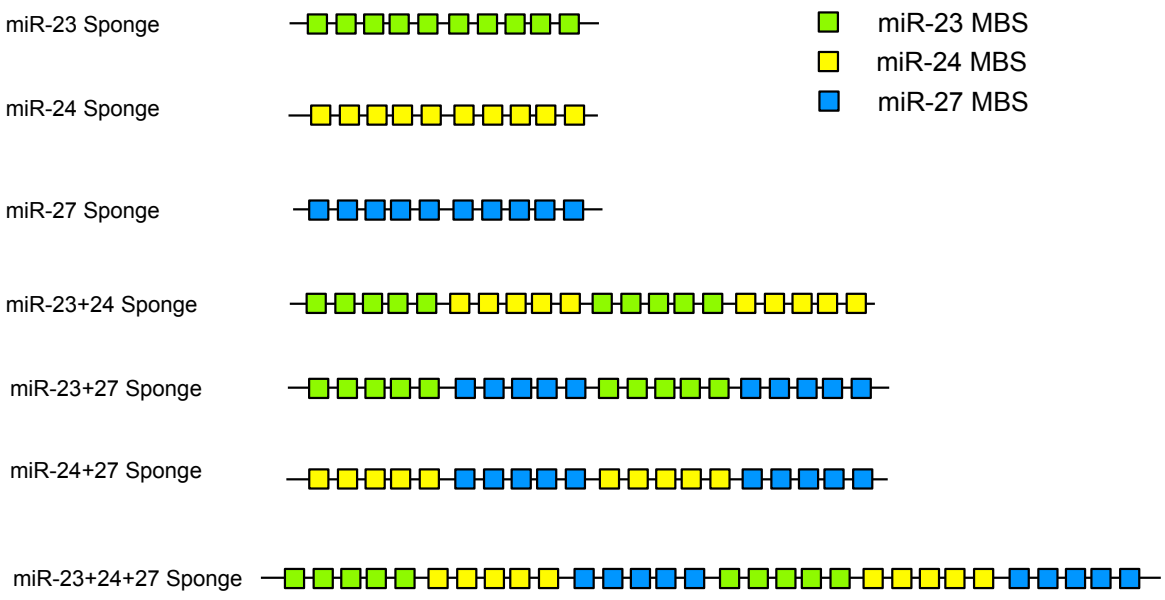

Figure 5.7 Schematic representation of multiple combinations miR-23~24~27 sponges.

Each green, yellow and blue square represents the individual miR binding site (MBS) for miR-23, miR-24 and miR-27, respectively. Each miR sponge construct contains 10 MBSs for each individual miR. See materials and methods for more details (Section 2.5.2).

5.2.2.2 Construction of miR sponge expression constructs

The method used to generate the miR-23~24~27 sponge transgenes is described in detail in the material and methods (Chapter 2) and will be discussed only briefly here. Previously described methods for generating sponge transcripts involved the concatemerization of double-stranded oligonucleotides encoding optimised miR binding sites (MBS) [750]. MBS are designed to contain a 3 nucleotide ‘bulge' or mismatch with positions 9-12 of the miR sequence which is thought to better mimic physiological miR:mRNA interaction (Figure 5.6, B). It is believed that these types of interactions promote sequestration rather than degradation, resulting in a more efficient loss of function of target miRs [618,751,752]. While this approach is adequate for the generation of sponges against single miR targets, it would have been laborious for the production of the various sponges required for this work. Taking advantage of recent developments in gene synthesis, I developed a novel design strategy in which sponge MBS arrays were synthesised using commercial gene synthesis technologies. (Figure 5.8, A). One of the main limitations of gene synthesis is that they cannot contain significant repeat regions. At first glance, this should have precluded their use for the generation of miR sponges, which are effectively repeats of MBS. However, as mentioned above, as sponge MBS are designed to contain a 3 base bulge it was possible to alter this sequence along with a 5 bp ‘spacer' sequence between each MBS. Decreasing the level of repetitiveness in each sponge to the extent that it permitted the synthesis of a single sequence containing 5 MBS each of miR-23, miR-27 and miR-24. The spacers between each miRs sponge were designed to contain restriction sites for different blunt-cutting restriction enzymes that permitted the rapid generation of all possible sponge combinations simply by restriction enzyme digest followed by religation of the plasmid (Figure 5.8, A). Similarly, the number of MBS in each sponge was doubled to contain 10 MBS per miR by cloning the sponge sequence into the parental vector. The final step was to clone each of the seven sponge combinations downstream of the luciferase of pGLOMS2BD vector, transcriptionally fusing the sponge with a luciferase reporter gene under the control of the Phospho-Glycerate-Kinase (PGK) promoter (Figure 5.8, B). Linking each sponge to a luciferase reporter allowed sponge activity to be monitored and validated. The following sections will describe the functional validation of the miR sponge constructs.

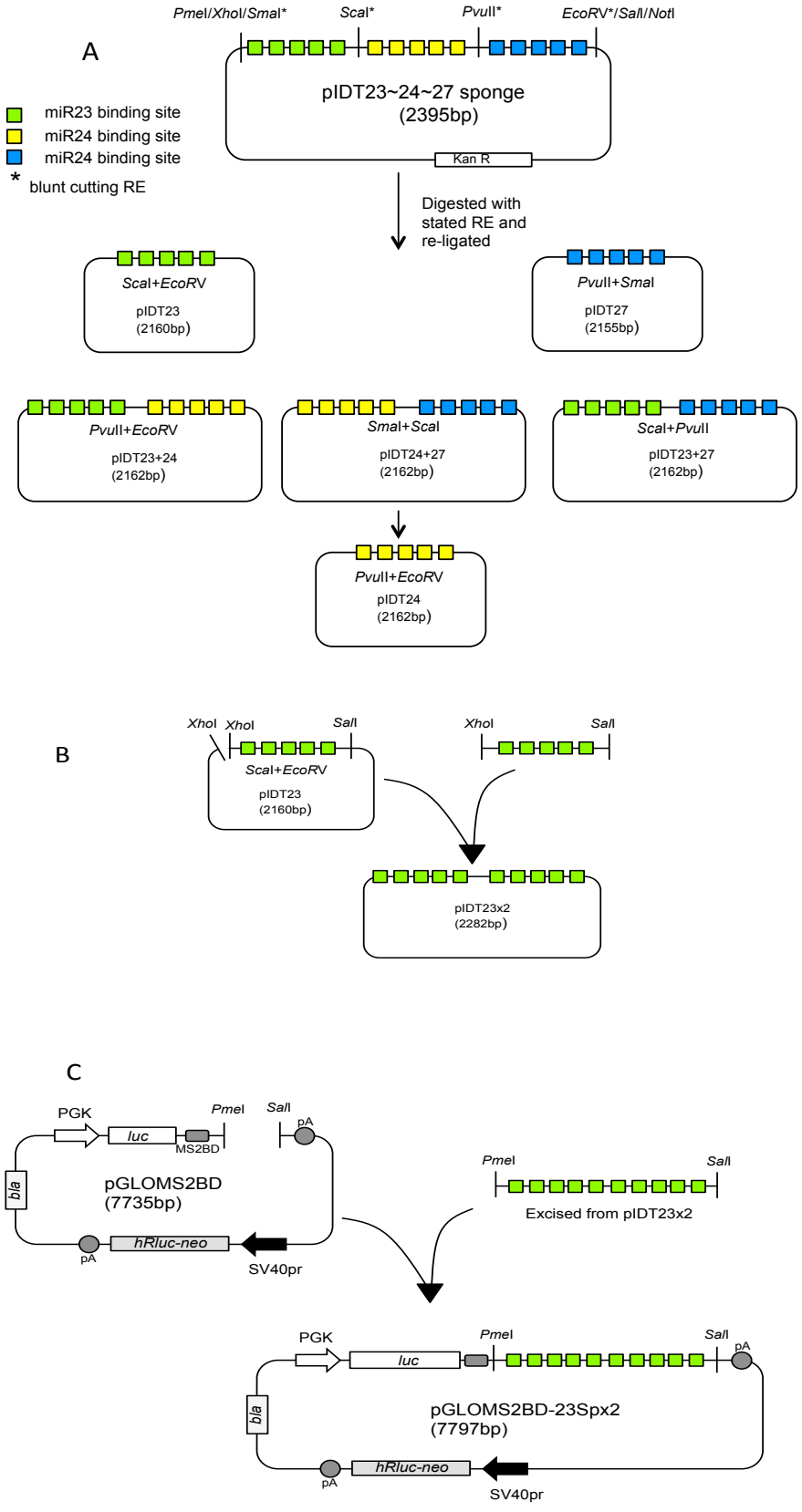

Figure 5.8 Schematic showing the cloning strategy of miR-23, miR-24 and miR-27 sponge transgenes. (**A**) miR-23~24~27 sponge gene was created using Gene Synthesis method. Individual miR sponges were created using the combination of restriction enzymes (RE). (**B**) miR sponge gene was double using specially designed restriction sites. (**C**) miR Sponge gene was cloned into Luciferase expressing plasmid - pGLOMS2BD. See materials and methods for more details (Section 2.5.2).

5.2.2.3 Overview of functional validation of constructs and generation of stable THP-1 cells lines containing miR sponges.

5.2.2.3.1 Testing sponge constructs in HEK293 cells

As an initial step, I sought to confirm that each of the seven miR sponge constructs was targetable by the miRs to for which they were designed. To achieve this sponge constructs were co-transfected along with miR mimics and scrambled negative control mimic into HEK293 cells. One day later luciferase activity was measured. In all cases, the level of luciferase activity was significantly reduced compared to scrambled control (**Figure 5.9**, A-H). It is worth noting that while the luciferase activity of miR-23 sponge decreased with the addition of miR-23a mimic it was reduced less than in miR-24 and miR-27 sponges with their corresponding miR-mimics, indicating that miR-23 sponge may be less efficient at reducing the miR-23a activity in high expressing cells.

5.2.2.3.2 Creation of stable THP-1 miR sponge cell lines

As previously described, THP-1 cells are a useful model system to study myeloid function. These cells are relatively easy to grow and, importantly for this study, to genetically modify. The seven sponge constructs along with empty vector control were electroporated into THP-1 cells. Stably transfected cells were selected for by their resistance to G418, which is conferred by the neomycin resistance gene contained with the sponge-expression constructs. G418-resistant cells emerged 3-4 weeks after electroporation and were grown continuously in the presence of G418 thereafter. Genotyping of sponge cells showed that they all contained the correct sponge transgenes (Figure 5.10, A). A luciferase assays performed on sponge cells revealed that they all expressed both luciferase and renilla (Figure 5.10, B). However, the normalised luciferase activity measured in miR-27 and miR-23+24+27 sponge cells was less than 10% that of the empty vector, suggesting that these sponge transcripts were saturated by endogenous miRs raising the possibility that target miRs were not entirely depleted in these cells (Figure 5.10, C). To overcome this potentially confounding problem I decided to make new constructs that would express sponge transcripts at higher levels.

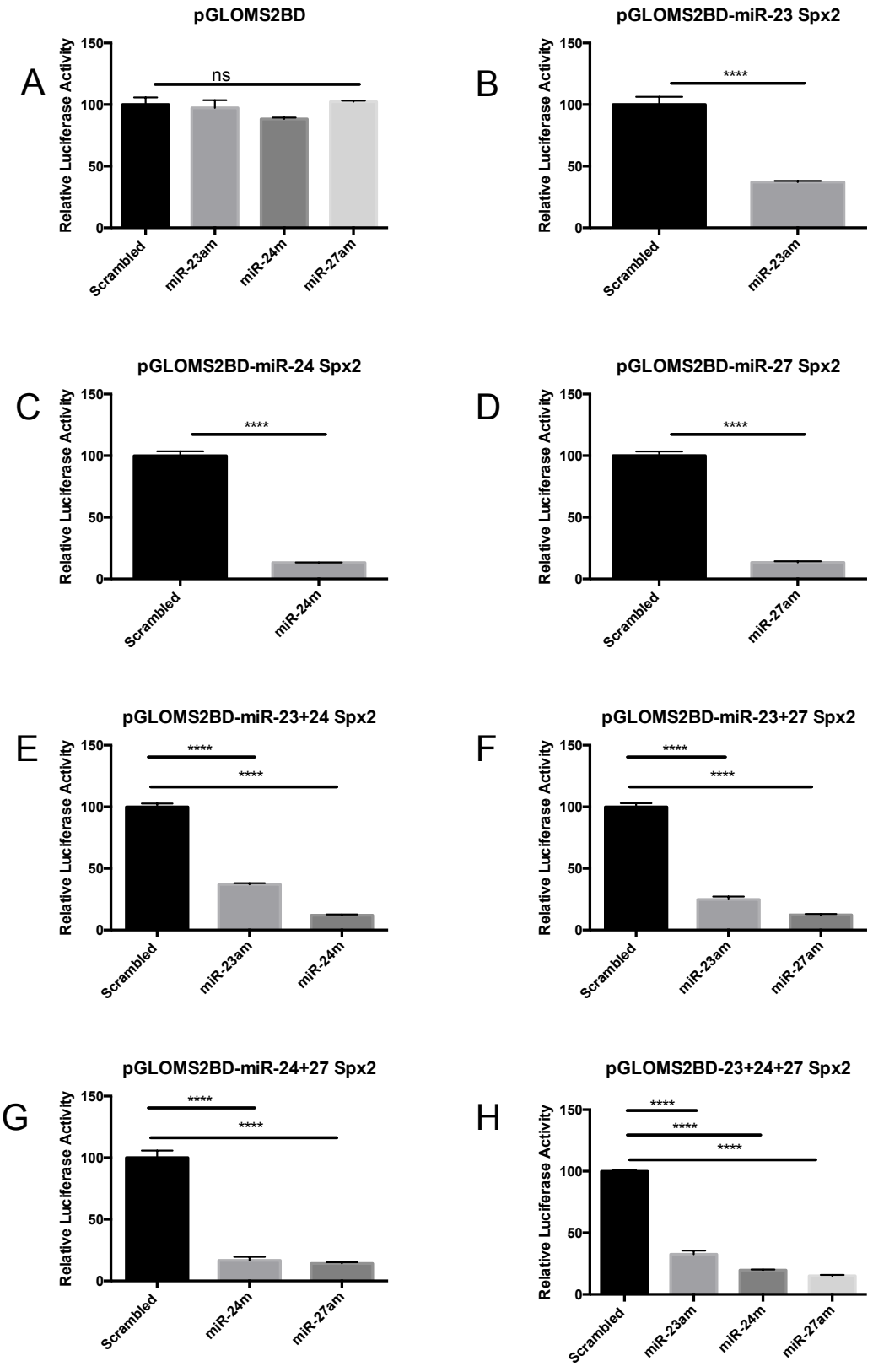

Figure 5.9 MiR-23a~24-2~27a sponge constructs are efficiently targeted by miR-23a, miR-24 and miR-27a mimics.

HEK293 cells were co-transfected with sponge plasmids in pGLOMS5BD vector and with either scrambled control or miR mimics (miR-23am, miR-24m, miR-27am). Luciferase activities were measured after 24 hours. Data analysed by ordinary One way ANOVA and represented by Mean±SD of 3 separate experiments. **** - p≤0.0001 versus scrambled control, ns – p>0.05.

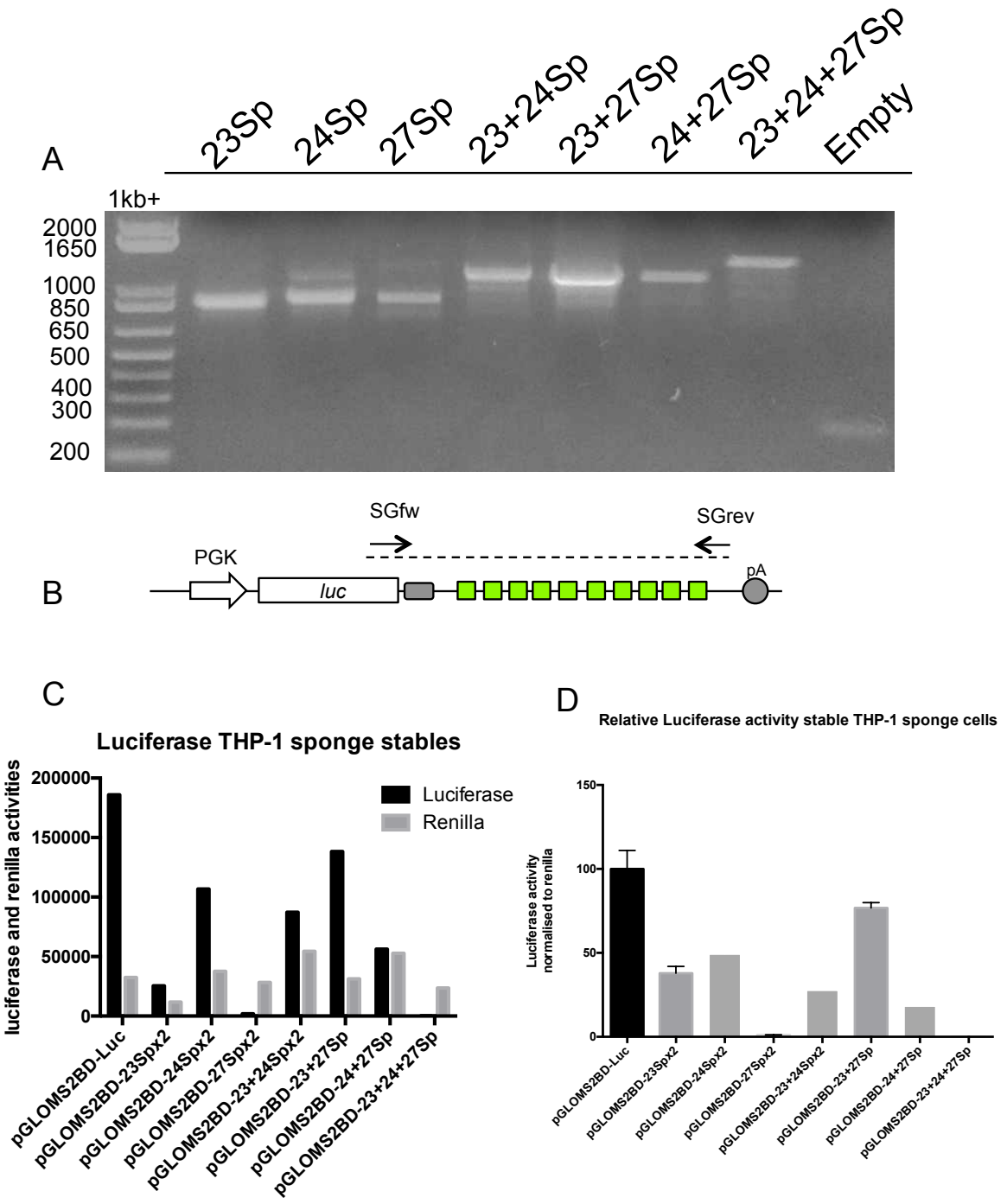

Figure 5.10 Characterization of stable THP-1 sponge cell lines.

(**A**) PCR genotyping of THP-1 stables confirmed presence of sponge transgenes. (**B**) Schematic showing of genotyping strategy, arrows indicate the location of primers. (**C**) Luciferase and renilla activity measure (arbitrary units) on 100,000 sponge cells. (**D**) Luciferase activities of THP-1 sponge cells normalised to renilla and expressed as a percentage of the pGLOMS2BD-LUC control vector.

5.2.2.3.3 Creation of miR sponge constructs with increased expression

To increase sponge transcript expression levels the relatively weak PGK promoter was replaced with the stronger elongation factor 1 alpha (EF1a) promoter [753]. This was accomplished by replacing the PGK promoter of pGLOMS2BD with the human EF1α promoter. The EF1α promoter was synthesised as a G-block and cloned by Gibson Assembly using the strategy shown in Figure 5.11, A. The resulting construct (pEF6-Luc) produced >10 fold increase in normalised luciferase activity compared to the original pGLOMS2BD plasmid when transfected into HEK293 cells (Figure 5.11, BC). The decision was therefore taken to convert the sponge plasmids to the new pEF6-Luc construct.

5.2.2.3.4 pEF6-Sponge constructs are targeted by their corresponding miRs

Once made, the pEF6-Sponge constructs were transfected into HEK293 to test their luciferase activity (Figure 5.12, A). All constructs showed increased luciferase compared to the equivalent pGLOMS2BD sponge constructs. To confirm that the pEF6 sponge targets were targeted by their corresponding miRs, sponge constructs along with miR mimics were co-transfected into HEK293 cells and luciferase activity measured (Figure 5.12, B). In all instances, miRs significantly reduced luciferase activity compared to scrambled control. Notably, luciferase activity in most cases did not drop below 50% of the control, suggesting that there was still ample sponge capacity remaining within the cell despite supra-physiological levels of target miRs introduced by transfection.

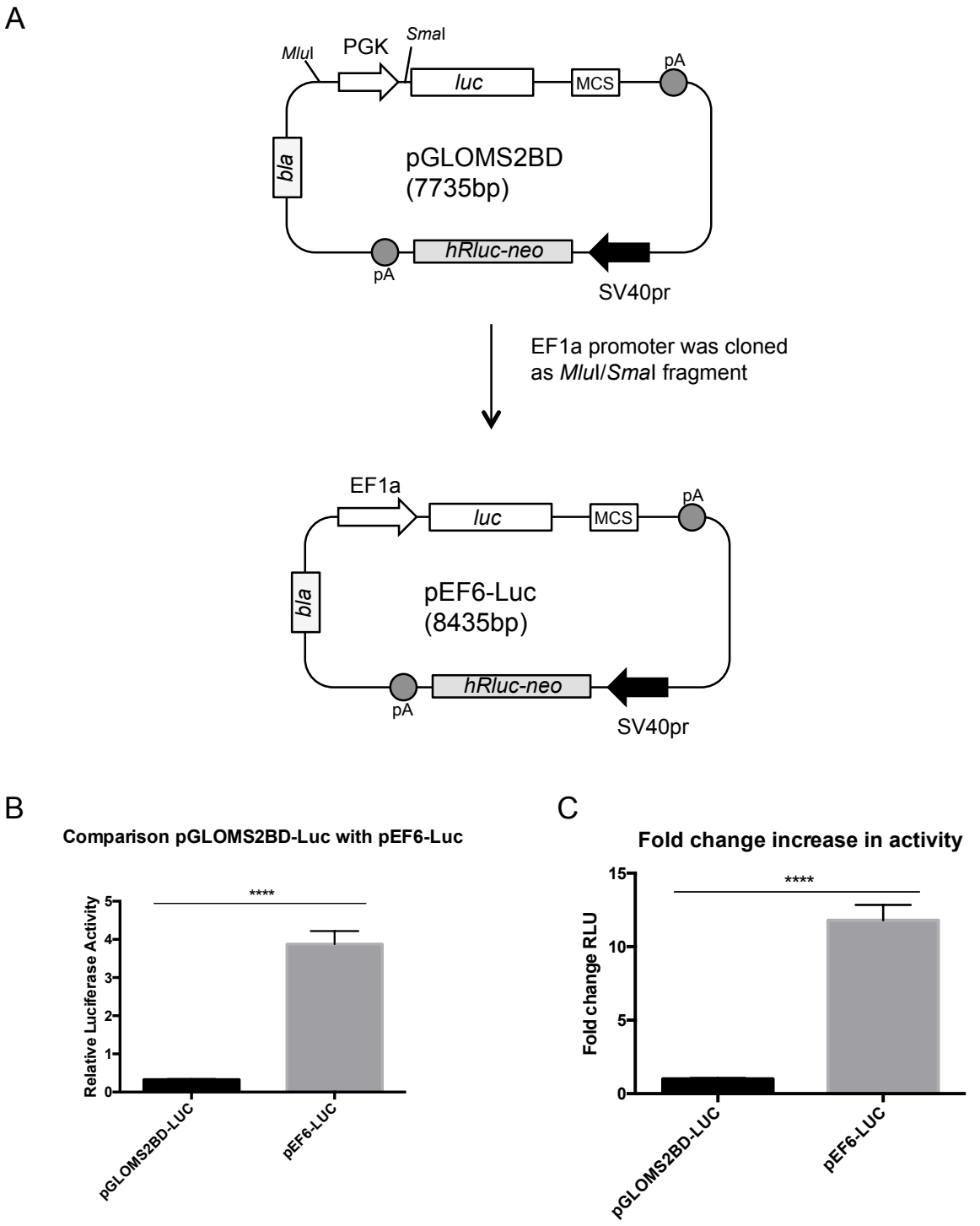

Figure 5.11 Creation of high-expressing sponge constructs.

(**A**) Schematic showing the conversion of pGLOMS2BD to pEF6-Luc. (**B**) Comparison of relative luciferase activity produced by pGLOMS2BD and pEF6-Luc Vectors transfected into HEK293 cells. Luciferase activity measured using Dual-Glo luciferase assay, values normalised to Renilla. (**C**) Relative increased in normalised luciferase activity of pEF6-Luc Vector compared to pGLOMS2BD Vector. Data were analysed by ordinary Student's t, **** - p≤0.0001.

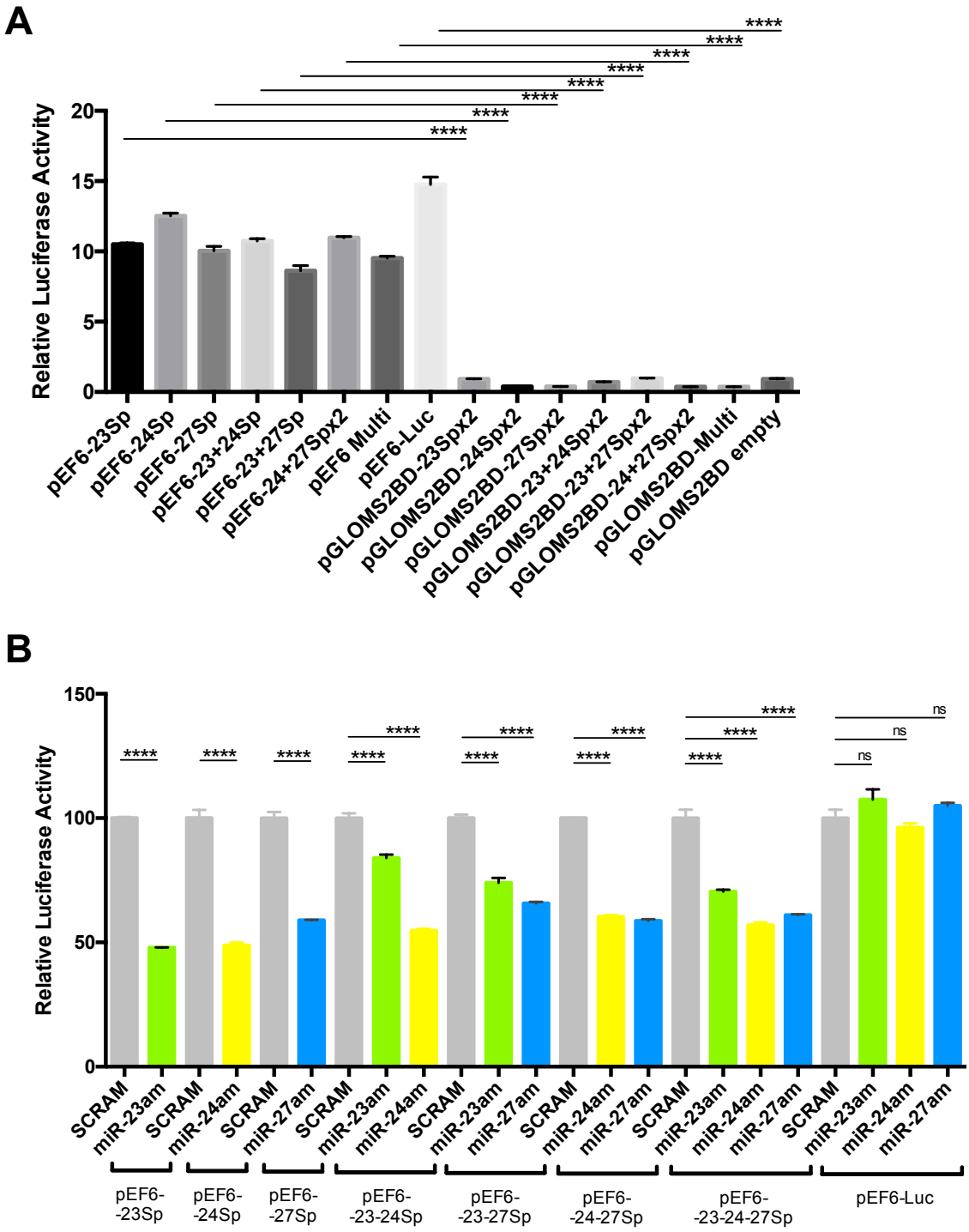

Figure 5.12 EF6-Sponge constructs are targeted by their cognate miRs.

HEK293 cell line was used for transfection experiments; luciferase activity was measured after 24 hours using Dual-Glo Luciferase assay. Luciferase activities were normalised to renilla (A, B) and to scrambled control (B) and displayed as Mean±SD of Relative Luciferase Activity, n=3 for each experiment. (**A**) All pEF6-Luc sponge and pGLOMS2BD-sponge constructs were transfected into HEK293 cells. (**B**) HEK293 cells were co-transfected with sponge pEF6-Luc plasmids and with either miR mimics (miR-23am, miR-24m, miR-27am) or scrambled control mimic (SCRAM). Data were analysed by ordinary One way ANOVA test with Sidak's correction for multiple comparisons, **** - p≤0.0001, ns – p>0.05.

5.2.2.4 Creation and validation of THP-1 pEF6-Sponge cell lines

Stable THP-1 cells lines were made as described in Section 5.2.2.3.2. After electroporation with the 7 EF6-sponge constructs plus empty vector, each clone was genotyped by PCR and shown to contain the correct sponge transgene (Figure 5.13, A and B). Dual luciferase assays were performed on the resulting G418 resistant clones (Figure 5.13, C). All EF6-sponge cell lines showed robust luciferase activity, indicating that they all contained functional EF6-sponge transgenes.

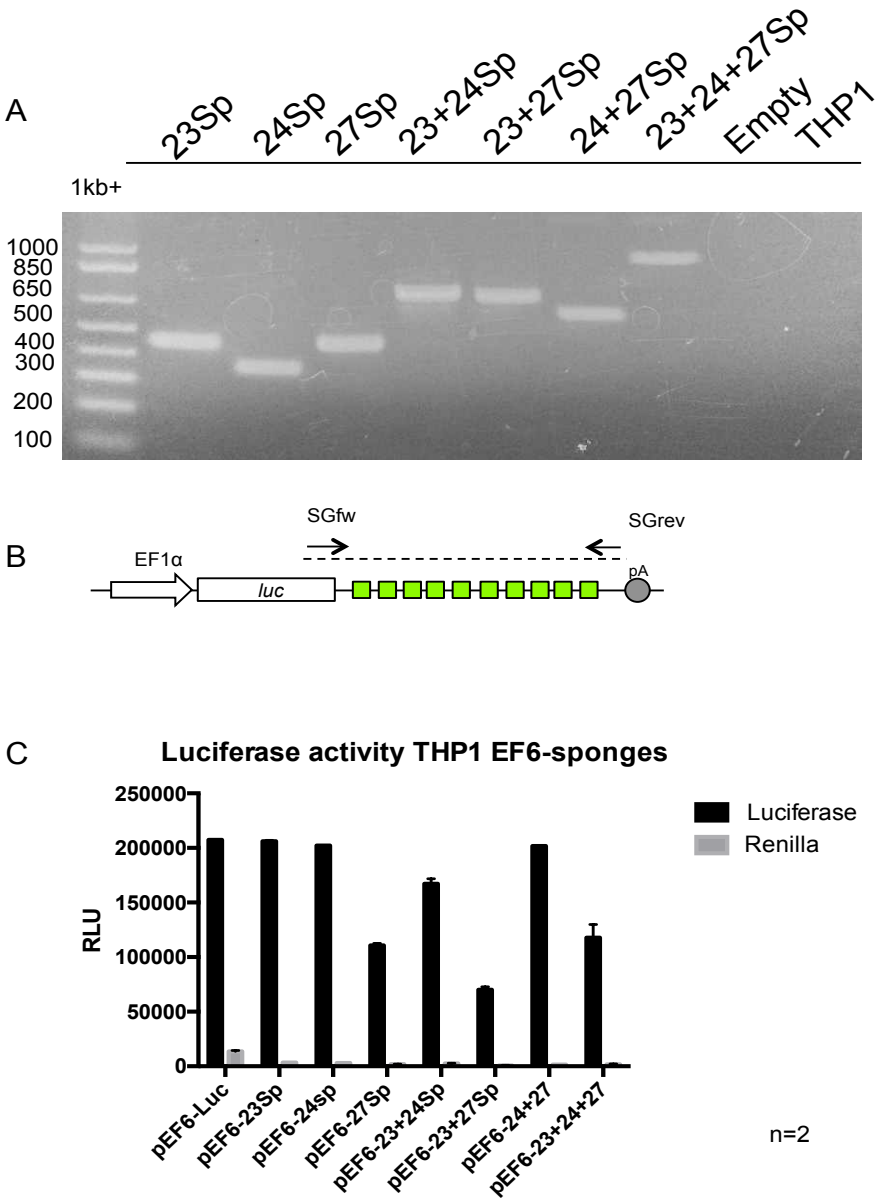

Figure 5.13 Characterization of stable THP-1 EF6-sponge cell lines.

(**A**) PCR genotyping of THP-1 stably transfected cell lines (stables) confirmed presence of sponge transgenes. (**B**) Schematic showing of genotyping strategy, arrows indicate the location of primers. (**C**) Luciferase and renilla activity was measured on two separate occasions, displayed as Mean±SD of Relative Luciferase activity (RLU, arbitrary units) on 100,000 sponge cells.

5.2.2.4.1 THP-1 EF6-sponge cells are actively targeted by miR-23-miR-24-miR-27 family miRs

To further validate the THP-1 EF6-sponge cell lines, I transfected them with both miR mimics and miR-inhibitors. The ability of miR mimics to target or inhibitors to relieve the expression of sponge transcripts was inferred from measured luciferase activity compared to scrambled control (Figure 5.14, A-H). In all cases, mimics were able to reduce luciferase expression compared to scrambled control. Conversely, miR-inhibition resulted in a significant increase in luciferase expression as they alleviated the repression of endogenous miRs. Demonstrating sponge transcripts were being actively targeted by endogenous miRs. The only exception to this was EF6-miR-23-24-27 sponge cells which while showing a significant decrease in luciferase activity upon the overexpression of miR-23a, miR-24 and miR-27a were unaffected by the inhibition of individual miRs this was likely due to the targeting of the miR-23-24-27 sponge by all three endogenous miRs (Figure 6.8 H). Alleviation of the repressive activity of one miR was insufficient to de-repress the translation of luciferase ORF by the other two. However, the fact that it was able to bind further miRs when artificially introduced suggests that it has not reached its maximal ‘sponge' capacity and therefore may still be of use experimentally.

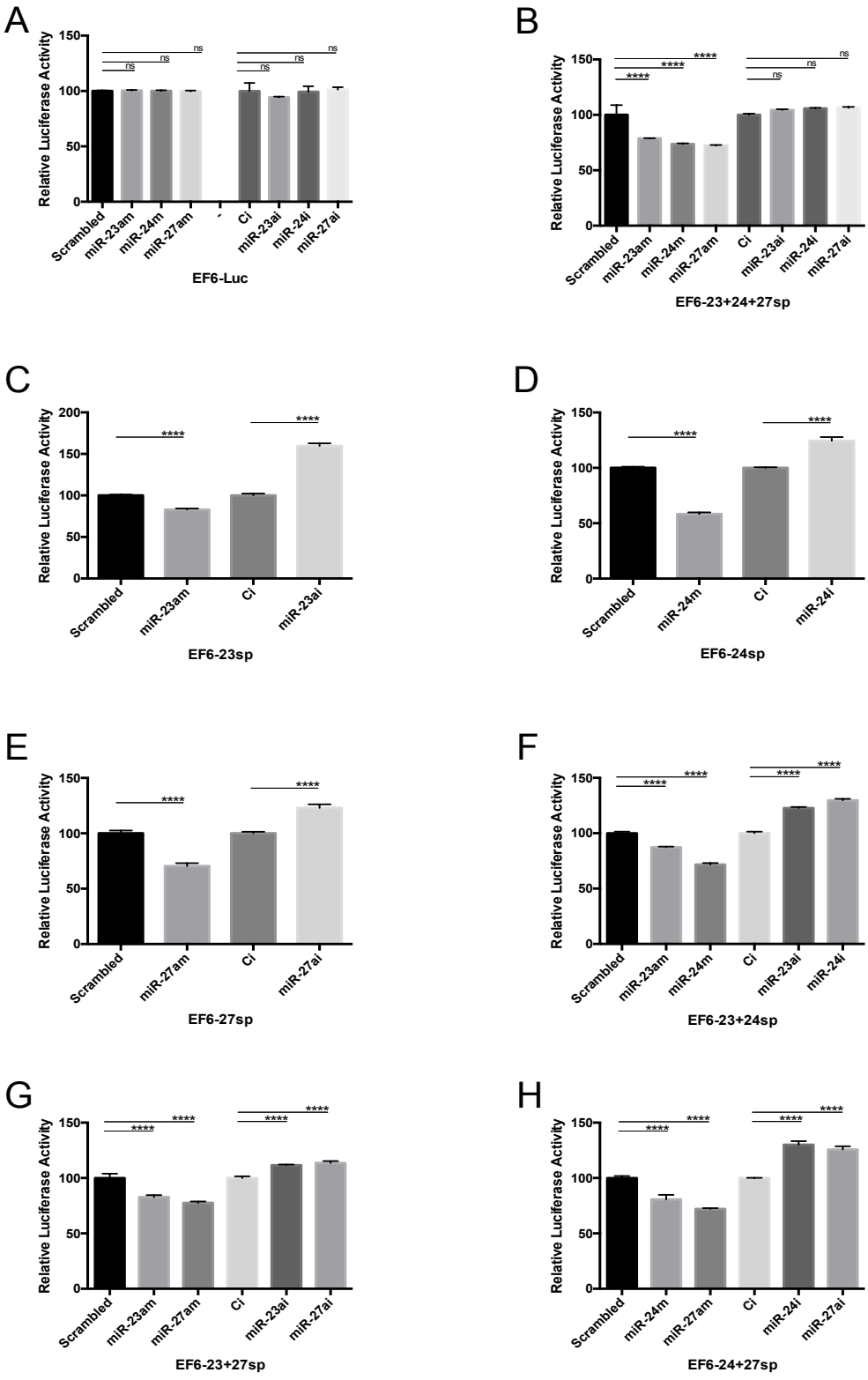

Figure 5.14 Stable THP-1 EF6-sponge cells are targeted by their corresponding miRs.

Stable THP-1 sponge cell lines were transfected with scrambled control mimic (Scrambled), miR mimics (miR-23am, miR-24m, miR-27am), Control inhibitors (Ci) and miR inhibitors (miR-23ai, miR-24i, miR-27ai). Luciferase activity was measured after 24hours. Luciferase activities are normalised to renilla and corresponding control (Scrambled for miR mimics and Control inhibitor for miR inhibitors). Data is displayed as Mean±SD of Relative Luciferase activity of 3 separate experiments and analysed by ordinary One way ANOVA test, **** - $p \leq 0.00001$, ns – $p > 0.05$.

5.2.2.5 THP-1 EF6-sponge transcripts are targeted by miRs from both ‘a' and ‘b' clusters.

As previously discussed, miR-23a and b and miR-27a and b paralogues are closely related and vary from each other by a single base at position 19. The sponge, while designed against the ‘a' cluster, should share sufficient complementarity with the ‘b' cluster miRs to target it with similar efficiency. To test this, miR mimics corresponding to miR-23 and miR-27 from both clusters were transfected into EF6-23+24+27 THP-1 cells, and their effect on luciferase activity measured (Figure 5.15). In all cases, mimics significantly reduced luciferase activity compared to scrambled control. However, there was no significant difference between ‘a' and ‘b' miRs, suggesting that the sponge transcripts bind both species with comparable efficiency.

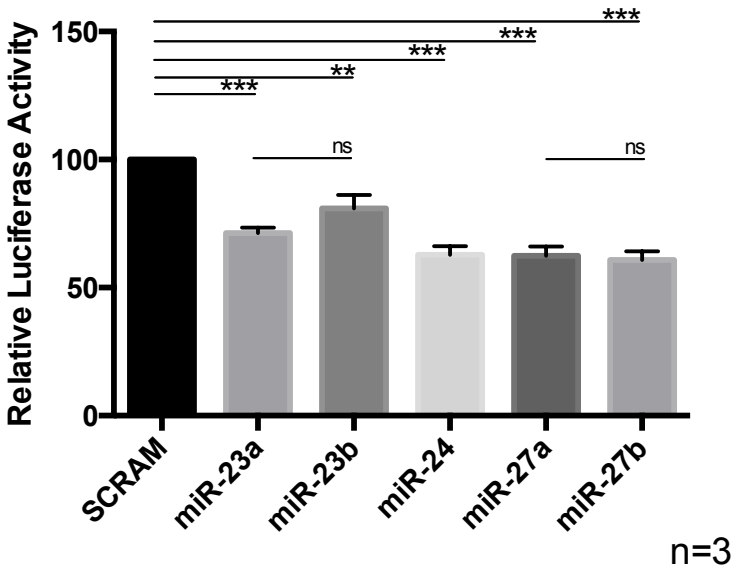

Figure 5.15 pEF6-23-24-27 sponge is targeted with equal efficiency by family members of both miR-23a and miR-23b clusters.

THP-1 cells expressing the miR-23-24-27 sponge were transfected with the scrambled control mimic (SCRAM) and with miR mimics of miR-23a, miR-23b, miR-24, miR-27a, miR-27b. Luciferase activity was measured after 24 hours. Luciferase activities are normalised to renilla and displayed as Mean±SD of the percentage of scrambled control vector from 3 separate experiments. Data were analysed by ordinary One way ANOVA test, ** - $p \leq 0.01$, *** - $p \leq 0.001$, ns – $p \geq 0.05$.

5.2.2.6 Mature miR-23a, miR-24 and miR-27a levels are increased in THP-1 cells, containing their cognate sponge transcripts.

There are a number of papers that have reported significant drops in mature miR levels in sponge expressing cells [749,754]. These reports are somewhat puzzling as miR sponges, unlike antagomir inhibition, are not thought to directly induce degradation of target miRs or by binding them change their chemical properties such that they are inefficiently purified using standard protocols [755]. There is no cellular process yet described that would provide a reasonable mechanistic explanation for the decreased levels of miRs reported in these publications. Taking an open-minded approach, I decided to see if the presence of sponge activity had any effect on the amount of mature miRs produced by the miR-23a cluster. Therefore the levels of the mature forms were quantified by qPCR on RNA prepared from THP-1 EF6-sponge cells (Figure 5.16, A).

To my surprise, the levels of miR-24 and miR-27a were dramatically increased in cells containing compatible sponge transcripts up to 100 fold in the case of miR-27a in the EF6-23-27 sponge cell line (Figure 5.16, A). MiR-23a sponge capacity did not have any significant effect on mature miR-23a levels. There have been other reports describing the imbalanced production of mature miRs from pri-miR-23a cluster. Chhabra and colleagues reported that miR-23a was not generated from the over-expression of pri-miR-23a cluster while miR-27a and miR-24-2 were [574]. Similarly, another study described that miR-23a maturation was blocked when over-expressed in HEK293 cells but not in HeLa cells [756]. Neither authors postulated a mechanism for these observations.

My findings could not be explained by an increase in the expression of the pri-23a~24-2~27a transcript in THP-1 sponge cells (Figure 5.16, B). In fact, conversely pri-23a~24-2~27a levels were decreased rather than increased in sponge cells (Figure 5.16, B). MiR expression is often controlled by feedback loops, whereby transcription factors controlling the expression of the miR are themselves directly targeted by the same miRs [699]. In this instance a transcriptional repressor may be directly targeted by miR-23a/24-2/27a, de-repression by sponge transcripts would result in increased levels of the transcriptional repressor and consequently a decrease in primary transcript levels. It is worth noting that earlier in this and previous chapters I described how IFNγ and IFNβ reduced pri-miR-23a cluster expression in THP-1 cells and

primary CD14 monocytes. It is tempting to speculate that TFs at the end of those signalling pathways may be direct targets of the miR-23a/miR-24/miR-27a. Indeed target analysis in chapter 6 predicted that the miRs in this cluster directly target various TFs including STATs and AP-1.

This of course does not provide a mechanistic explanation for the observed increase in mature miRs seen in sponge cells. These changes must be due to some process operating post-transcriptionally, possibly by prolonging the stability of sponge-targeted miRs. Indeed, it has been reported that sequestered miRs containing ‘bulges’, as is the case with miR-23a/24/27a sponges, exhibit increased half-lives compared to those without [757]. This would provide an obvious mechanistic explanation for the increased levels miRs seen here.

The observed increase in levels of mature miR-27a and miR-24 seen in sponge cells does raise concern as to the utility of these sponges to achieve an effective reduction in miR activity. Data produced from over-expression and inhibition studies in Section 5.2.2.4.1 would suggest that there is still sufficient ‘sponge' capacity to lower target miR activity within the THP-1 EF6-Sponge cells effectively. However, to directly address this concern I decided to measure absolute copy numbers of sponge transcripts in each of the sponge cell lines.

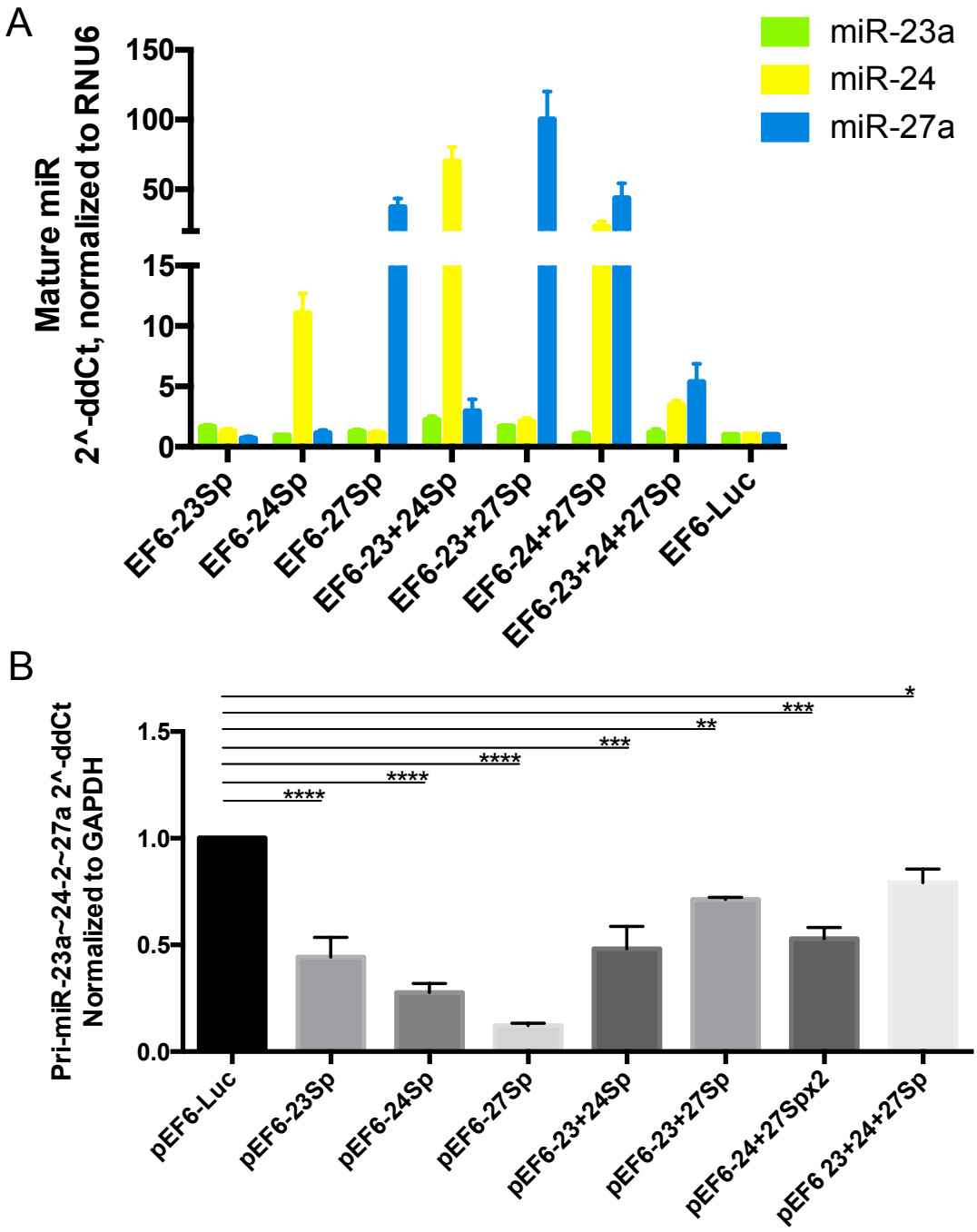

Figure 5.16 Expression levels of pri-miR-23a~24-2~27a cluster and mature miRs in THP-1 sponge cells.

pEF6 THP-1 Sponge cells were used for both experiments. (**A**) Mature miR-23a, miR-24 and miR-27a levels were measured by SYBR green qPCR. Data shown as Mean±SD of RQ (2^-ddCT) normalised to house keeping gene RNU6 and relative to pEF6-Luc (Empty Vector control**).** (**B**) Levels of pri-miR-23a~24-~27a transcript were measured by SYBR green qPCR. Data shown as Mean±SD of RQ (2^-ddCT) normalised to house keeping gene GAPDH and relative to pEF6-Luc (Empty Vector control). Data were analyzed by ordinary One way ANOVA test, * - p≤0.05, ** - p≤0.01, *** - p≤0.001, **** - p≤0.0001.

5.2.2.7 Copies of sponge transcripts are present in excess of endogenous miR-23a, miR-24 and miR-27a in THP-1 EF6-sponge cells.

Absolute quantification of sponge transcripts expressed within the THP-1 EF6-sponge cells was performed along with the measurement of mature miR-23a, miR-24 and miR-27a levels. The pEF6-luc plasmid along with miR mimics of miR-23a, miR-24 and miR-27a were used to generate a qPCR copy number standard curve. This allowed me to determine the copy numbers of sponge transcripts and mature miR-23a, miR-24 and miR-27a in sponge cells (Figure 5.17, A and B). It has been estimated that a single cell contains 10-30 pg of RNA; here I assumed 20 pg [758]. The results clearly show that in each of the EF6-Sponge cell lines, except EF6-23+24+27sp, sponge transcripts are present at higher levels than the miRs to which they are designed. Given that each sponge contains 10 miR-binding sites, the level of sponge capacity within these cells is far in excess of target miRs. However, some caution should be taken in the interpretation of data generated from EF6-23+24+27 cells, which may be inefficient at depleting the activity of miR-23a, miR-24 and mIR-27a.

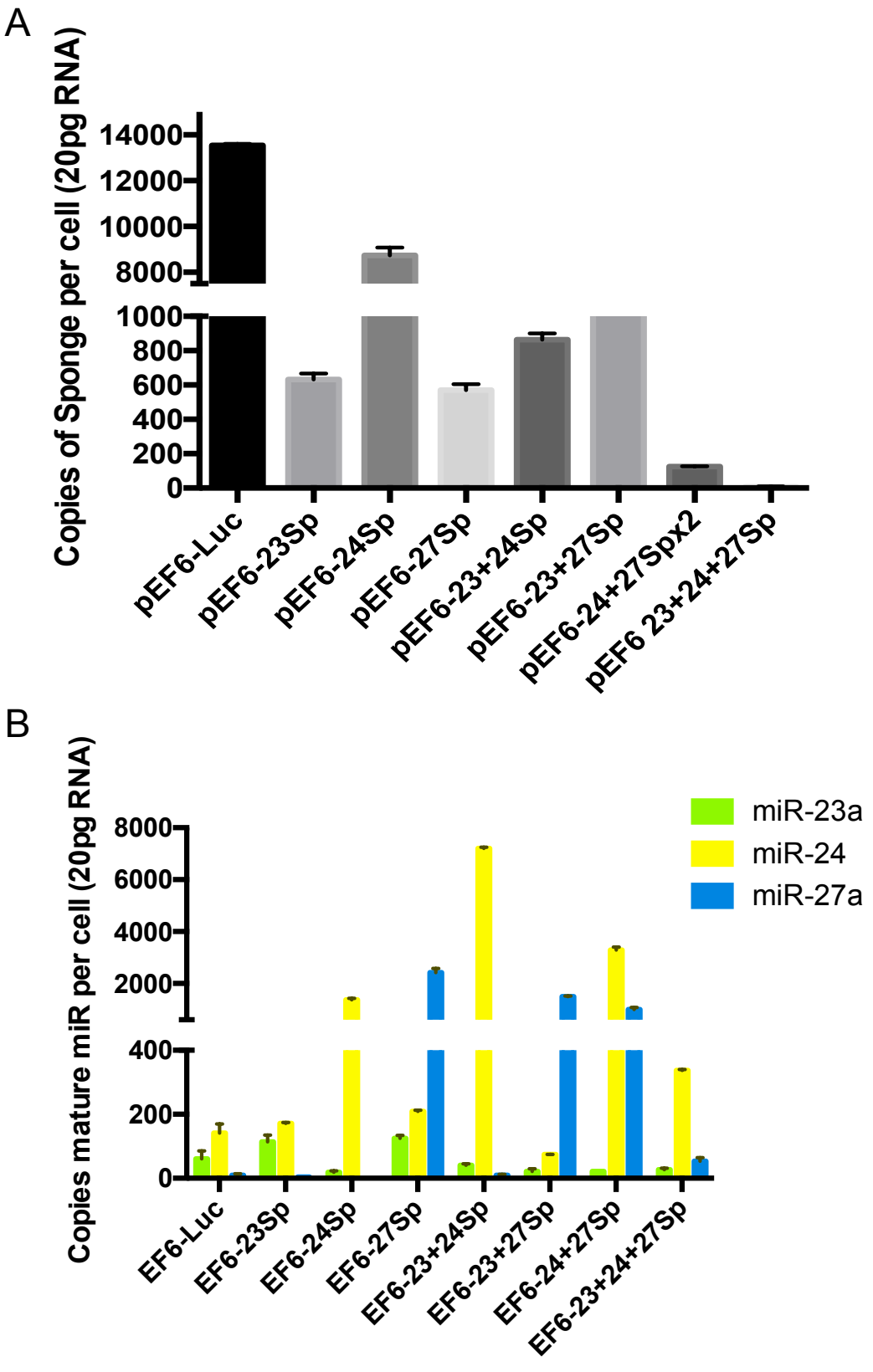

Figure 5.17 Copy numbers of miR and Sponge transcripts per cell (20pg RNA).

(**A**) Absolute Copies of each Sponge transcript was measured from cDNA prepared from THP-1 sponge cell lines, by qPCR against a standard curve of know copies generated from the pEF6Luc plasmid. (**B**) Absolute copies of mature miR-23a, miR-24 and miR-27a were measured from THP-1 sponge cell lines by qPCR against a standard curve of known copies of cDNA prepared from denatured miR mimics. In both A and B, values were normalised to 20 pg of input RNA and expressed as copies per cell where the assumed RNA per cell is 20 pg.

5.3 Discussion

The aim of the work described in this chapter was to generate miR-23-24-27 cluster deficient monocytic cell line for further functional and mechanistic studies.

First I tested the suitability of THP-1 cells as a functional surrogate for human $CD14^+$ monocytes. THP-1 cells have been exploited experimentally for over three decades in the study of monocyte biology [759]. I confirmed that THP-1s show many of the features synonymous with monocyte function: ability to respond to and produce pro-inflammatory stimuli and capacity to mature into macrophage like cells, being amongst the most carefully studied aspects.

Here, I found that the THP-1 cells expressed pri-miR-23a transcript and resulting mature miR-23a, miR-24-2 and miR-27a forms; and that the ratio of the expression of each of the mature forms was similar to that of primary human $CD14^+$ cells. Likewise, the miR-23a cluster was the predominant form expressed in THP-1 cells. THP-1s upon treatment with PMA, an activator of Protein Kinase C, quickly adopt a macrophage-like phenotype [722,760]. This process sees a sharp decrease in primary miR-23a cluster expression, which was also observed in M-CSF and GM-CSF matured primary macrophage cultures. In keeping with my previous data in primary monocytes, I found no change in pri-miR-23a cluster upon stimulation with either TNFα or IL-17A. NFκB is the primary transcriptional regulator downstream from both TNFα and IL-17a signalling pathways. The miR-23a cluster has previously been shown to be directly upregulated by NFκB/P65 via a binding site in the promoter [661]. In fact, stimulation of THP-1 cells with TLR2 and TLR4 ligands (Pam3 and LPS, respectively) also utilising NFκB/P65 signalling did increase cluster expression levels, in concordance with previously published data. Curiously, treatment with IL-6 while having a significant negative effect on the expression of pri-miR-23a expression in $CD14^+$ cells had no effect on THP-1 cells, despite the presence of an active IL-6R rapidly inducing phosphorylation of STAT3. A number of other studies have demonstrated the presence of robust IL-6 signalling in THP-1 cells [761]. The reason for the discrepancy between THP-1 and primary cells is not apparent.

Next, I described the generation of miR-sponge constructs designed to specifically deplete endogenous miR-23/miR-24/miR-27 in THP-1 cells. This decision has been made in attempt to stay true to investigating human biology, without resorting to mouse knock out models whilst deciphering the full scope of the miR-23a~24~27a functions. This approach involved the creation of a novel cloning strategy that for the first time describes a quick and reliable method for the production of sponge transcripts using commercially available gene synthesis [762]. This a significant improvement in terms of speed and ease of manufacture compared to previously described methods [762]. I went on to create and functionally validate constructs that would express miR-sponge transcripts targeting all 7 combinations of miRs produced from miR-23a cluster (Figure 5.7). In all cases the resulting miR-sponges were targeted with high efficiency by their corresponding miRs. THP-1 cells that stably expressed the 7 sponge transcripts along with the empty vector controls were created. Subsequently upon the characterization of these cell lines, I observed that in some instances (miR-27 and miR-23+24+27) sponge transcript levels as measured by the expression of transcriptionally coupled luciferase gene were almost undetectable, suggesting that they had been completely saturated by endogenous miRs. Concerned that endogenous miRs might be expressed at levels higher than their corresponding sponge transcripts, I took the decision to remake the sponge constructs replacing the initial PGK promoter with the stronger EF1α promoter [753]. This resulted in a 10 fold increase in expression. THP-1 cells stably expressing the new pEF6-sponge transgenes were created and subjected to an extensive set of experiments designed to confirm the identity and efficacy of the sponge expressing cells. In all cases over-expression or inhibition of miR-23a, miR-24 and miR-27a THP-1s expressing the corresponding sponge exhibited the expected change in the luciferase activity. Interestingly, mature levels of miR-24 and miR-27a were significantly increased in THP-1s expressing sponges designed against them, while miR-23a levels were unaffected. This increase was not due to an increase in primary transcript expression. Indeed, primary transcript levels were decreased in the sponge expressing constructs. It is possible that this was due to a stabilisation of miR-24 and miR-27 that has been reported upon miR binding to transcripts that contain ‘bulge’ sequences [757]. The significant increase seen is potentially the result of long-term sponge expression in these cells that over time results in an accumulation of these miRs.

The sponge cell lines could provide an excellent platform to study the complex interaction of the miR-23a cluster. By measuring the differences that depletion of each of the miRs within the cluster in turn and in combination, make to the transcriptome, proteome and metabolome of THP-1 offers the opportunity to study their role in unparalleled detail. Taking a ‘Systems Biology' approach, using the latest bioinformatics analytic techniques to integrate these data sets would provide an incredible insight into the complex interplay of roles these miRs play in monocyte/macrophage biology [763].

In summary, THP-1 largely recapitulate the findings I observed in primary human $CD14^{+}$ cells, suggesting that they are a rational model to study the role of miR-23a~24-2~27a in monocyte function. To functionally study them in this context I created 7 THP-1 cell lines in which every combination of the miR-23a cluster was functionally depleted providing an excellent experimental platform for their study in a monocytic cell line. Investigation of the functional role of miR-23a~24~27a cluster in THP-1 cells and primary human monocytes is to follow.

6 Identification and verification of miR-23a~24-2~27a molecular targets.

6.1 Introduction

My previous data have shown that treatment-resistant RA patients lack the expression of the miR-23a cluster in $CD14^+$ monocytes as a consequence of raised pro-inflammatory stimuli, such as IL-6, but also when stimulated by IFNγ and IFNß in the *in vitro* setting. Moreover, a decrease in the expression of this miR cluster was observed during M-CSF and GM-CSF differentiation into macrophages, suggesting some possible role in monocyte maturation. Therefore, this chapter will look into the role of miR-23a~24~27a in peripheral blood monocytes and elucidate how this relates to the pathogenesis of RA in general, and, more specifically, to the drug resistance observed in the patient cohort.

The key to understanding miR functions is the identification of their molecular targets. To identify potential interactions of this miR cluster, several in silico prediction algorithms were used including: Targetscan, MiRanda, miR22, Pictar2, PITA and miRwalk, all of which are described in detail the Chapter 1. Once potential targets were identified, they were integrated with pathways active in monocytes and macrophages using the Ingenuity pathway analysis platform. Ingenuity pathway analysis was initially based on published interactions, however recently this platform expanded to incorporate published and predicted miR:mRNA transcript interactions based on the validated interactions from TarBase and miRecords databases, as well as the in-silico analysis from TargetScan algorithm.

From all identified interactions, relevant potential targets were experimentally validated for the ability to bind and be regulated by specific miRs. These interactions were then further tested in THP-1 cells as well as in generated miR-23 cluster sponge THP-1 cells and primary inflammatory monocytes to elucidate the roles of miR-23a, miR-24 and miR-27a in immunity.

6.2 MiR-23a and miR-27a are predicted to target the IL-6R pathway

In-silico prediction algorithms and Ingenuity pathway analysis highlighted the IL-6 pathway as being heavily targeted by the miR-23a cluster (Figure 6.1). Zhu et al. demonstrated miR-23a's interaction with IL-6R in gastric adenocarcinoma cells [764]. However, here I identified both miR-23a and miR-27a to have potential binding sites in the 3'UTR region of IL-6R. Further comprehensive analysis of the IL-6R pathway also identified IL-6R co-receptor GP130 as another possible target of both miR-23a and miR-27a. Additionally, ERAP1 aminopeptidase, implicated in the cleavage of IL-6R into a soluble form, is a predicted target of miR-27a [397]. With regards to the intracellular compartment of this pathway, miR-23a is predicted to regulate key signalling molecules: JAK1/2 and STAT1/3, while miR-24 has two potential binding sites in the 3'UTR of STAT3. The coordinated suppression of JAK/STAT signalling by all members of this miR cluster was demonstrated this year in human acute erythroid leukaemia cells. Nevertheless implications for IL-6 signalling in the inflammatory context has not been explored [765].

While suggestive, all algorithms used to predict miRNA target interactions suffer from significant false discovery rates; therefore experimental validation is required and will follow next.

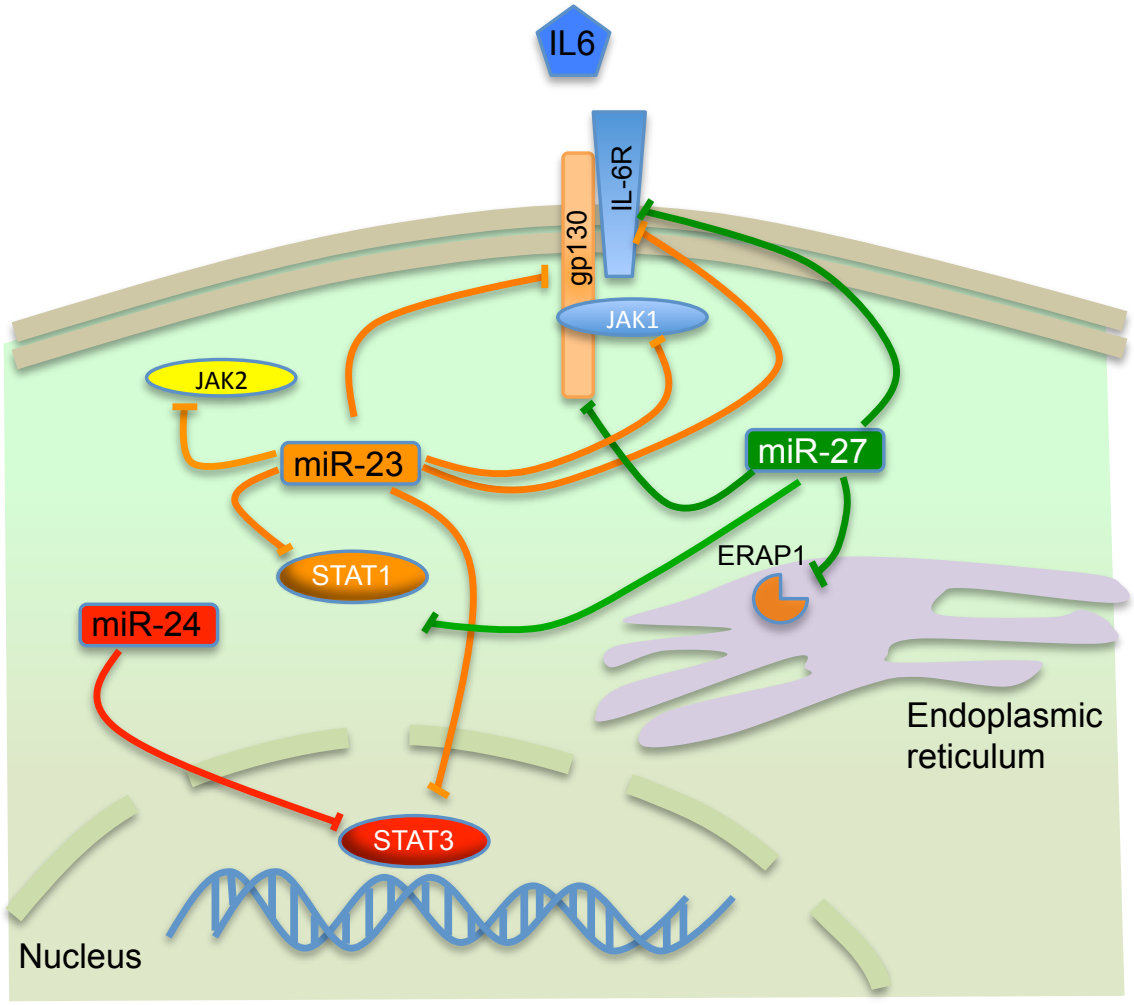

Figure 6.1 Schematic showing the predicted miR23a~24-2~27a regulatory network of the IL-6 signalling pathway.

In silico predicted targets of miR-23a include IL-6R, GP130, JAK1, JAK2 and STAT1 molecules (depicted in orange). MiR-24 is predicted to target STAT3 signaling molecule (depicted in red), while miR-27a has predicted binding sites in the 3'UTR of IL-6R, GP130, STAT1 and ERAP1 (depicted in green). In silico analysis was performed using available algorythms, such as Targetscan, miRanda, RNA22, miRWalk, PicTar2 and PITA.

6.2.1 Membrane and Soluble IL-6R transcripts share polyadenylation signals that contain miR-23 and miR-27 binding sites

Alternative splicing of IL-6R transcripts results in membrane-spanning IL-6R (mIL-6R) and soluble-IL-6R (sIL-6R). Both of these forms form active receptor complexes with co-receptor IL-6ST (GP130). Secretion of the soluble form of IL-6R can confer IL-6 responsiveness to cells that do not express IL-6R by utilising the ubiquitously expressed GP130 co-receptor trans-signalling. Trans-signalling was shown to have significant implications in RA pathogenesis and was reviewed in detail in Chapter 1 and in [373]. The analysis IL-6R transcripts using the ENSEMBL genome browser appeared to show that mIL-6R and sIL-6R transcripts vary not only in the inclusion or exclusion of exon 9 respectively but also in the length of their 3'UTR sequence by potentially utilising alternative polyadenylation signals (Figure 6.2, A). This raises the possibility that sIL-6R may be regulated by only a subset of miRs that target mIL-6R.

To see if this was indeed the case I characterised the 3' ends of both sIL-6R and mIL-6R using 3'RACE. I designed primers that were specific for either variant. The resulting bands were cloned and sequenced. Inspection of the sequences in both cases corresponded to the shorter annotated sequences in the 3'UTR of IL-6R (Figure 6.2, B). This strongly suggests that both soluble and membrane IL-6R variants use the same proximal polyadenylation signal, previously described only in the soluble form. Furthermore, both sequences contained stretches of non-genomically encoded tracts of adenosines, which is a hallmark of polyadenylation. Finally, identification of a variant polyA signal (AAGAAA) upstream of the polyA tail provided the final evidence that the amplified sequences did indeed represent the 3' ends of both IL-6R transcripts (Figure 6.2, B).

I did not, however, identify 3' species corresponding to the longer 4070 bp 3'UTR which is attributed to the mIL-6R in ENSEMBL (ENST00000368485.7). However, this may have been due to the length of amplification necessary to detect it. The 3'RACE strategy used here was designed to see if both IL-6R variants utilised the same polyadenylation signal and designing primers closer to the distal most polyA signal may have allowed the identification of longer 3'UTR forms.

Notably, the proximal 3'UTR identified in both forms lies adjacent to the polyA site reported for sIL-6R (ENST00000344086.8) (Figure 6.2, C). The previously annotated ENSEMBL transcript appears to be an artefact result from mispriming of oligodT to a genomically encoded stretch of adenosine residues rather than a true polyA tail added posttranscriptionally. Such events are well-described confounders of the 3'RACE method [619]. Significantly, this form and the 3' end of the annotated sIL-6R transcript in ENSEMBL lack obvious canonical or non-canonical polyA signals, further supporting the conclusion that the transcript annotated in the ENSEMBL's database is an artefact of oligodT primed reverse transcription.

Superimposing identified miR-23a and miR-27a binding sites onto the longer and shorter 3'UTR sequences demonstrates that both mIL-6R and sIL-6R retain MBS to these miRs (Figure 6.2, C). Here I showed that both mIL-6R and sIL-6R share polyA signals, have similar 3'UTR and are therefore likely to be co-regulated by the same cadre of miRs.

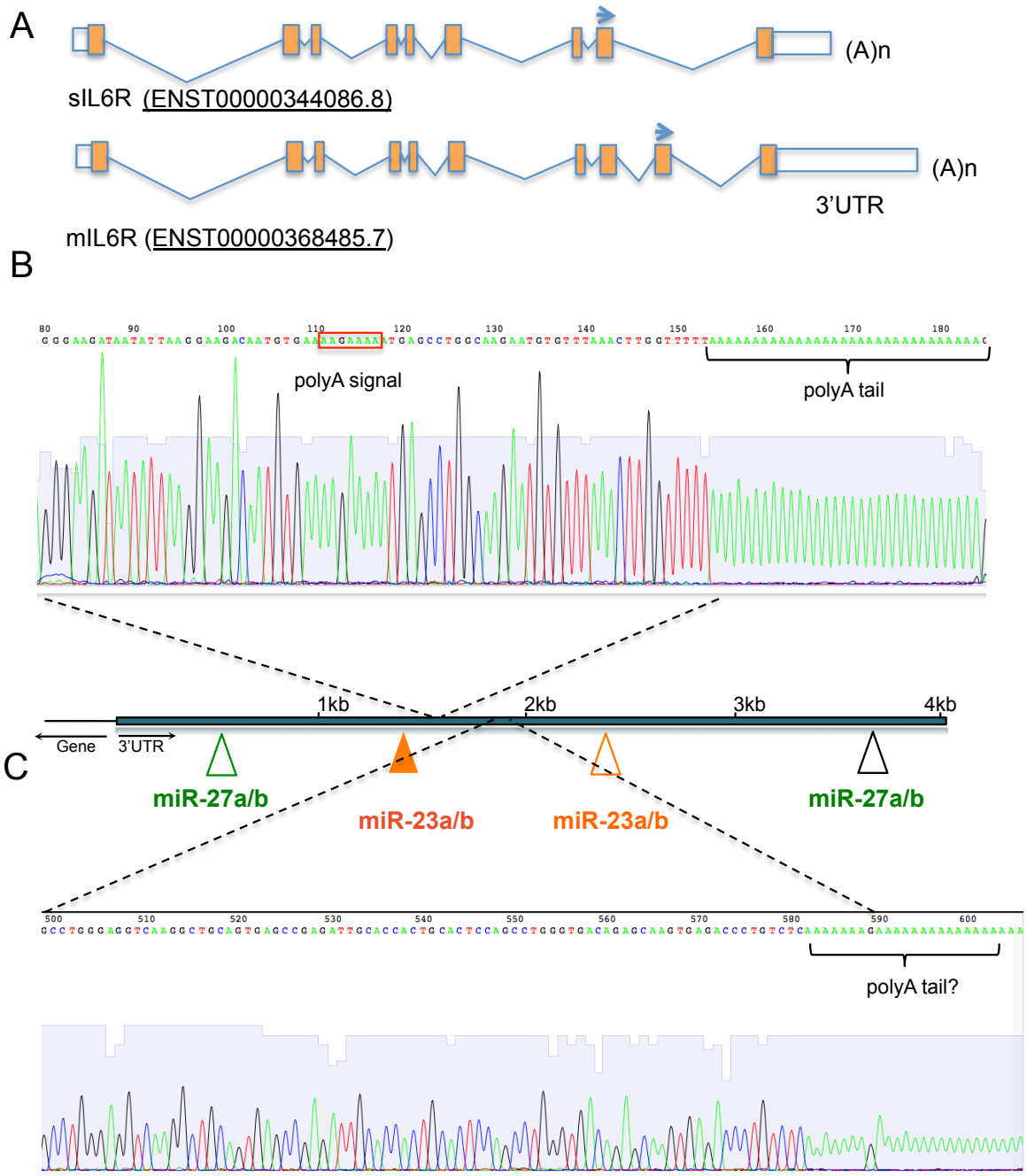

Figure 6.2 Membrane and soluble IL6R utilise the same polyA signals.

(**A**) A schematic showing of the exon structure of human soluble and membrane IL-6R transcripts annotated in ENSEMBL database. Blue arrows show the variant-specific primers used in 3'RACE. 3'RACE was performed on total RNA purified from THP-1 cells, using variant-specific primers (blue arrows). Amplified 3'ends were cloned into pCR2.1 TOPO and sequenced. (**B**) The chromatogram shown is representative of the cloned sequences. The red box shows the position of predicted polyA signal. The position of the 3' end is mapped onto a schematic of the IL-6R 3'UTR showing the positions of predicted miR-23a and mIR-27a binding sites. Open triangles represent poorly conserved sites as determined by Targetscan. (**C**) 3'RACE product corresponding to the 3' end of the sIL-6R (ENST00000344086.8) is an artefact amplified from genomically encoded stretch of adenosine residues and is not a genuine polyadenylated species.

6.2.2 MiR-23a and miR-27a directly target membrane and soluble forms of IL-6R

Here I set out to experimentally validate molecular targeting of IL-6R's 3'UTR by miR-23a and miR-27a. Firstly, bioinformatic analysis using a number of miR target prediction algorithms (MiRWalk, miRanda, PicTar2, PITA, RNA22 and Targetscan) was done to identify miR-23a cluster binding sites within IL-6R 3'UTR (Table 6.1).

Table 6.1 Summary of miR-23a and miR-27a predicted binding sites by selected algorithms
Green and red indicate presence or absence of miR binding site respectively.

Using these algorithms, I was able to identify two potential binding sites for both miR-23a and miR-27a in the IL-6R 3'UTR and each case these sites were predicted by at least 3 out of the 6 programs used (Figure 6.3, A). To experimentally validate these sites, I amplified a 2.1 kb region encompassing 3 out of the 4 predicted sites (Figure 6.3, B). This region was cloned downstream from the luciferase reporter gene. The resulting plasmid was co-transfected into HEK293 cells along with miR mimics corresponding to miR-23a, miR-27a or scrambled control. After 24 hours the luciferase activity was measured using a dual-luciferase assay.

These experiments showed that both miR-23a and miR-27a significantly reduced luciferase expression compared to scrambled control, suggesting that they directly target IL-6R (Figure 6.3, C). Subsequent mutation of the predicted binding site ameliorated the effect of miR mimics, demonstrating conclusively that this effect was due to the direct interaction of miR-23a and miR-27a with IL-6R 3'UTR (Figure 6.3, C).

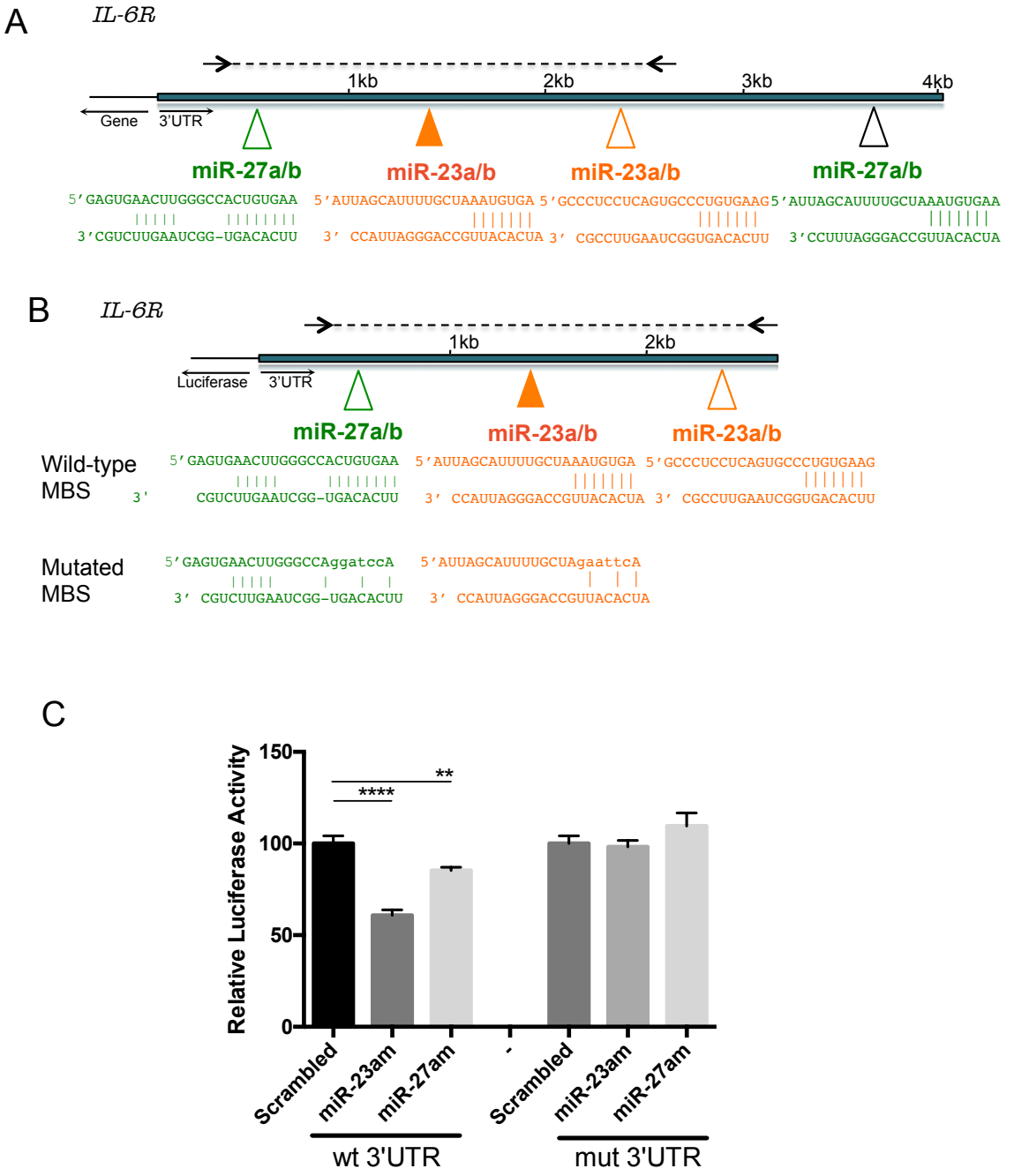

Figure 6.3 MiR-23a and miR-27a directly target IL-6R.

(**A**) A schematic showing of the position and sequences of predicted miR-23a and miR-27a sites in the IL-6R 3'UTR. MiR-23a/b and miR-27a/b sites are indicated by orange and green triangles respectively. Open triangles represent poorly conserved sites as determined by Targetscan. (**B**) Shows region cloned into pmiRGLO luciferase reporter construct. Alignments of miRs with predicted binding sites are shown along with the changes made in the seed regions of mutated controls. (**C**) Luciferase activity in HEK293 cells co-transfected with wild-type or mutated IL6R 3'UTR luciferase reporter and miR-23a, miR-27a or scrambled control mimics. Activities were normalised to renilla internal control and values expressed as % of scrambled controls, (n =3). Data analyzed by Student's t-test, **p<0.01, ****p<0.0001 versus scrambled control.

6.2.3 Overexpression of miR-23a or miR-27a reduces IL-6R transcript levels in THP-1 cells

Having demonstrated that miR-23a and miR-27a can functionally interact with sequences within the IL-6R 3'UTR I then set out to see if they could reduce transcript levels when over-expressed in THP-1 cells. THP-1 cells were transfected with miR-23a, miR-24, mIR-27a mimics and scrambled control and membrane, soluble and total IL-6R mRNA levels measured by q-PCR (Figure 6.4). In these experiments, miR-23a and miR-27a significantly reduced the levels of the membrane and total IL-6R transcript levels (Figure 6.4 A). However, only miR-27a significantly lowered soluble IL-6R levels (Figure 6.4 B). In keeping with target predictions, miR-24 did not alter IL-6R transcript levels (Figure 6.4, C). While artificial overexpression of miRs can demonstrate the potential of a miR to regulate its target mRNAs, it tells us nothing about whether it does so under normal physiological conditions. Generally, the pool of miRs is small in comparison to the number of potential target mRNAs meaning that most are not actively targeted [541]. Gaining insight into whether a specific miR is actively regulating a defined target requires the inhibition of miR. This can be accomplished using specific miR inhibitors or by over-expressing 'sponge' transcripts containing multiple high-affinity miR binding sites. In the previous chapter, I described the creation and validation of sponge constructs against miR-23/24/27. In this next section, I will use these cells to discover if miR-23a and miR-27a are actively regulating IL-6R expression in THP1 cells. To this end mIL-6R, sIL-6R and total IL-6R mRNAs were quantified by qPCR in THP-1 sponge expressing cells (Figure 6.5).

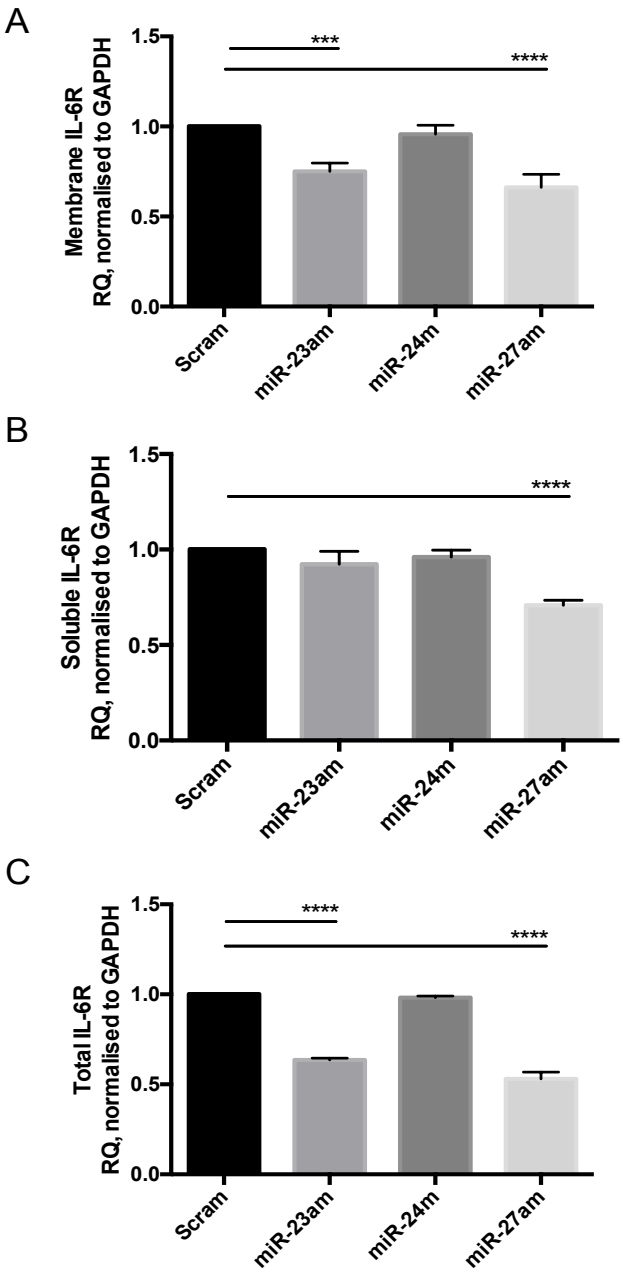

Figure 6.4 Overexpression of mIR-23a and miR-27a reduces IL-6R expression in THP-1 cells.

Results obtained by qPCR method performed on RNA prepared from THP-1 cells, measuring (**A**) membrane IL-6R; (**B**) soluble IL-6R; (**C**) total IL-6R. Data represented by Mean±SD of a relative quantification (RQ, 2-^ddCT) relative to GAPDH control gene and scrambled control mimic, n=3. Data analysed by ordinary one-way ANOVA with Dunnett's correction for multiple comparisons, *** - $p \leq 0.001$, **** - $p \leq 0.0001$.

6.2.4 MiR-23a and miR-27a are actively regulating IL-6R transcript levels in THP-1 sponge cells

I have previously demonstrated that miR-23a and miR-27a have the potential to directly decrease IL-6R expression when over–expressed in THP-1 cells. Here I investigated whether they are actively doing so under normal homeostatic conditions. To test this, I measured IL-6R mRNA levels in THP-1 cells that stably express sponge transgenes targeting each of the miRs within the miR-23a cluster individually and in combination.

QPCR measurements of the membrane, soluble and total IL-6R mRNAs in each of the sponge cell lines showed that both mIL-6R and sIL-6R levels were increased in cells with miR-23 sponge activity compared to empty vector control (Figure 6.5). Cells expressing miR-27 sponges showed a significant increase in mIL-6R levels and trend towards increase in sIL-6R and total IL-6R levels. In keeping with the fact that miR-24 is not predicted to target IL-6R, miR-24-Sponge expressing cells had no effect on IL-6R mRNA levels. Interestingly, a sponge combination targeting both miR-23 and miR-27 yielded the most significant increase in IL-6R expression suggesting that IL-6R expression is being concurrently regulated by both miRs (Figure 6.5).

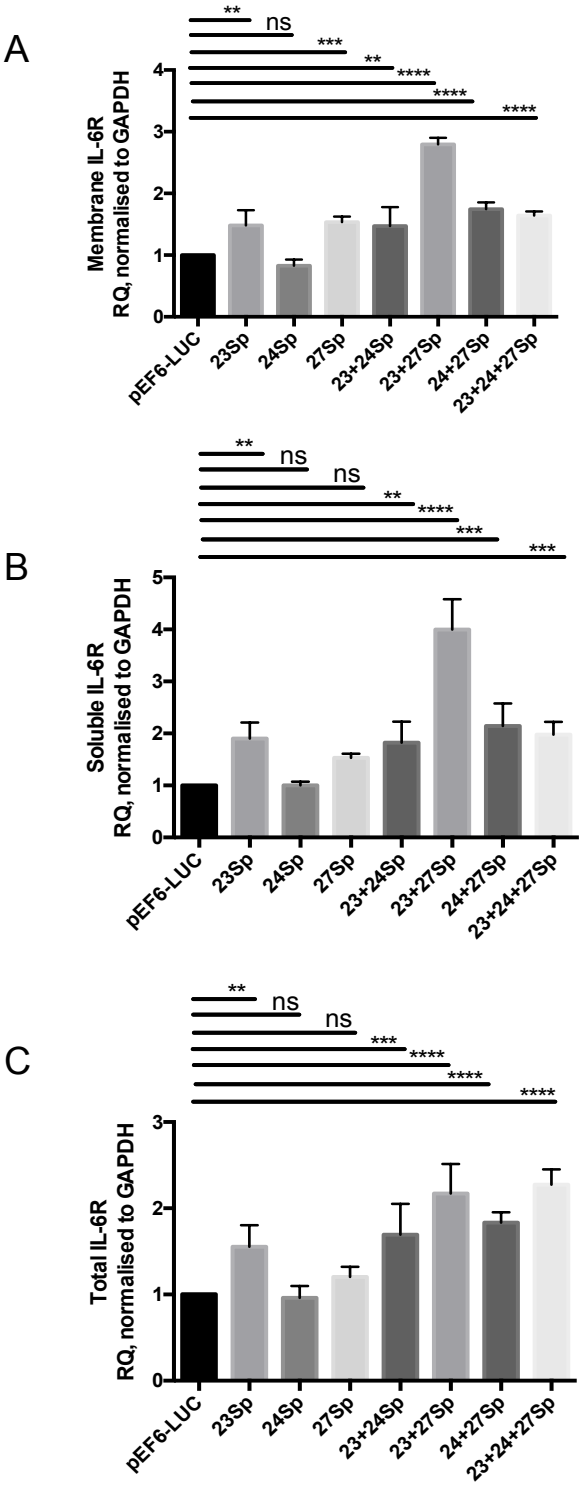

Figure 6.5 IL-6R mRNA expression is increased in miR-23 and miR-27 sponge expressing THP-1 cells.

Results obtained by qPCR method performed on RNA prepared from THP-1 sponge cells measuring (**A**) membrane IL-6R; (**B**) soluble IL-6R; (**C**) total IL-6R. Data represented by Mean±SD of a RQ (2^ddCT) relative to GAPDH control gene and scrambled control mimic, n=3. Data analyzed by ordinary one-way ANOVA with Dunnett's correction for multiple comparisons, **p≤0.01, *** - p≤0.001, **** - p≤0.0001, ns - p≥0.05.

6.2.5 Overexpression of miR-23a or miR-27a reduces IL-6R transcript levels in primary human CD14$^+$ monocytes.

Previously I have shown that overexpression of miR-23a and miR-27a in THP-1 decreases IL-6R mRNA levels. Here I tested this observation in primary human CD14$^+$ monocytes. To this end, CD14$^+$ cells were isolated from the blood of healthy donors and transfected with miR-23a, miR-27a and scrambled negative control and the levels of the membrane, soluble and total IL-6R mRNAs levels measured by qPCR.

Overexpression of miR-27a resulted in a significant decrease in both IL-6R variants suggesting that IL-6R transcripts are regulatable by miR-27a in primary CD14$^+$ monocytes as well as in THP-1 cells (Figure 6.6). However, overexpression of miR-23a failed to exhibit the same effect. This finding appears at odds with the analogous experiment in THP-1 cells where miR-23a expression did reduce the expression of membrane and total IL-6R. From previous work, we know that miR-23a is expressed at a higher level in primary CD14$^+$ monocytes than miR-27a creating a possibility that endogenous miR-23a is already saturating IL-6R MBSs. Thus overexpression of the miR did not have an additive effect (see Figure 4.1, C). This is also supported by data from THP-1 sponge cells which showed that IL-6R levels are highest in miR-23-sponge expressing cells, suggesting that miR-23a is regulating IL-6R expression to a greater degree than miR-27a. That said, de-repression of IL-6R expression is greatest in miR23+miR27 sponge expressing cells demonstrating that synergistic effect of both miRs takes place (Figure 6.5, A and B). Arguably, inhibition of endogenous miR-23a and miR-27a with the corresponding antagomir would have been more informative with regards to the effect of endogenous miRs.

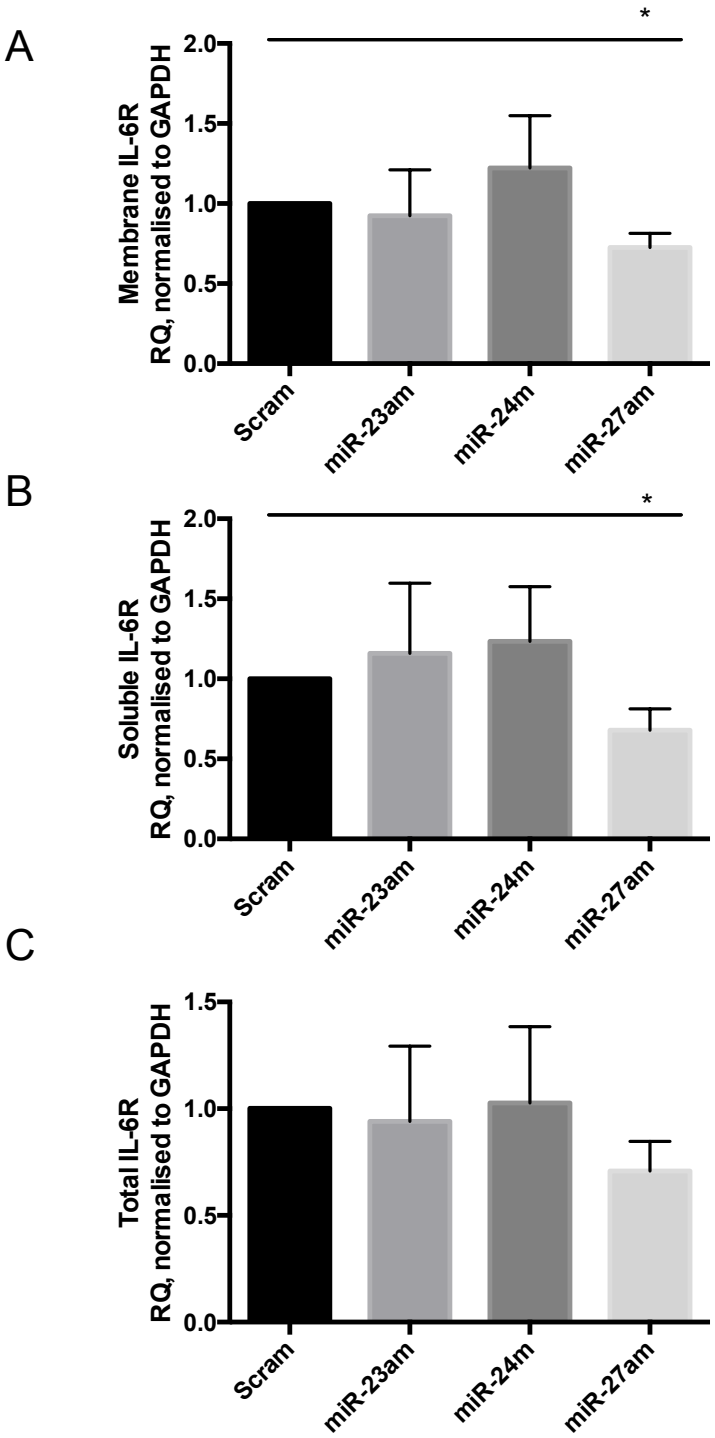

Figure 6.6 Overexpression of miR-27a decreases IL-6R mRNA expression in human CD14$^+$ monocytes.

Results obtained by qPCR method performed on RNA prepared from isolated CD14$^+$ cells measuring (**A**) membrane IL-6R; (**B**) soluble IL-6R; (**C**) total IL-6R. Data represented by Mean±SD of a fold change (2^ddCT) relative to GAPDH control gene and scrambled control mimic, n=3. Data analysed by ordinary one-way ANOVA with Dunnett's correction for multiple comparisons, * - $p \leq 0.05$.

6.2.6 Inhibition of miR-23a and miR-27a increases IL-6R surface expression in THP-1 cells and promotes pro-inflammatory phenotype

With the effects of miR-23a and miR-27a on the IL-6R transcript levels evaluated previously, I next investigated the effect of miR-23a and miR-27a on the IL-6R protein level in miR sponge expressing cells as well as in THP-1 transfected with miR inhibitors.

Surface IL-6R levels on THP-1 cells expressing various combinations of sponge transcripts were measured by FACS (Figure 6.7, A). Cells expressing miR-23 and miR-27 sponges showed significantly higher surface IL-6R staining compared to cells expressing the empty vector control demonstrating that loss of either miR-23 or miR-27 activities from the cells resulted in a corresponding increase in IL-6R protein expression. Again, in keeping with the fact that miR-24 is not predicted to target IL-6R and in concordance with previously seen lack of effect on the transcript level, miR-24 sponge THP-1 cells had levels of surface IL-6R identical to those of control reporter cells. THP-1 cells containing miR-23 and miR-27 double sponge also had raised levels of surface protein, similar to those of miR-23 sponge alone. Interestingly, the highest expression of surface IL-6R protein was found in the multiple sponge cells containing binding elements to all three miRs of the cluster.

As miR-sponges seem to be agnostic whether they bind 'a' or 'b' miR species it is possible that the results presented here could represent the effect of the paralogue miR-23b-cluster activity. To test this, I transfected THP-1 cells with specific miR-27a and miR-27b inhibitors, which exhibit more sequence specificity than miR-sponges. Cells transfected with miR-27a inhibitors had increased surface IL-6R levels (Figure 6.7, B). In contrast, inhibition of miR-27b only had a tendency to affect surface IL-6R expression confirming miR-27a, and not miR-27b, as the dominant species regulating IL-6R expression in THP-1 cells. These data demonstrate that modulation of endogenous miR-23a and miR-27a affect the IL-6R levels at the protein level as well as at the transcript level.

Furthermore, to investigate if inhibition of miR-23 and miR-27 has an effect on the way cells respond to inflammatory stimuli they were exposed to a range of

concentrations of LPS. Firstly, THP-1 sponge cells were matured for 6 days with PMA, with the change of medium after day 3, as stated in the protocols. On day 6, the medium was once again changed, and cells were stimulated with 1 ng/ml, 10 ng/ml or 100 ng/ml of LPS for 24 hours. The next day, supernatants were collected, and levels of IL-6 and TNFα were measured (Figure 6.7, C and D, respectively). Indeed, matured miR-23 sponge cells produced significantly higher levels of IL-6 and TNFα, especially when stimulated with 100 ng/ml of LPS. However, stimulation of miR-27 sponge cells resulted in raised levels of IL-6, but not of TNFα. Nevertheless, double miR-23 and miR-27 sponge cells expressed significantly higher levels of both IL-6 and TNFα when exposed to as little as 1 ng/ml of LPS. Suggesting that myeloid cells lacking miR-23 and miR-27 not only exhibit pro-inflammatory phenotype but also act synergistically to amplify this response if both miRs are inhibited, as is the case in biologic non-responder RA patients, described in Chapter 3.

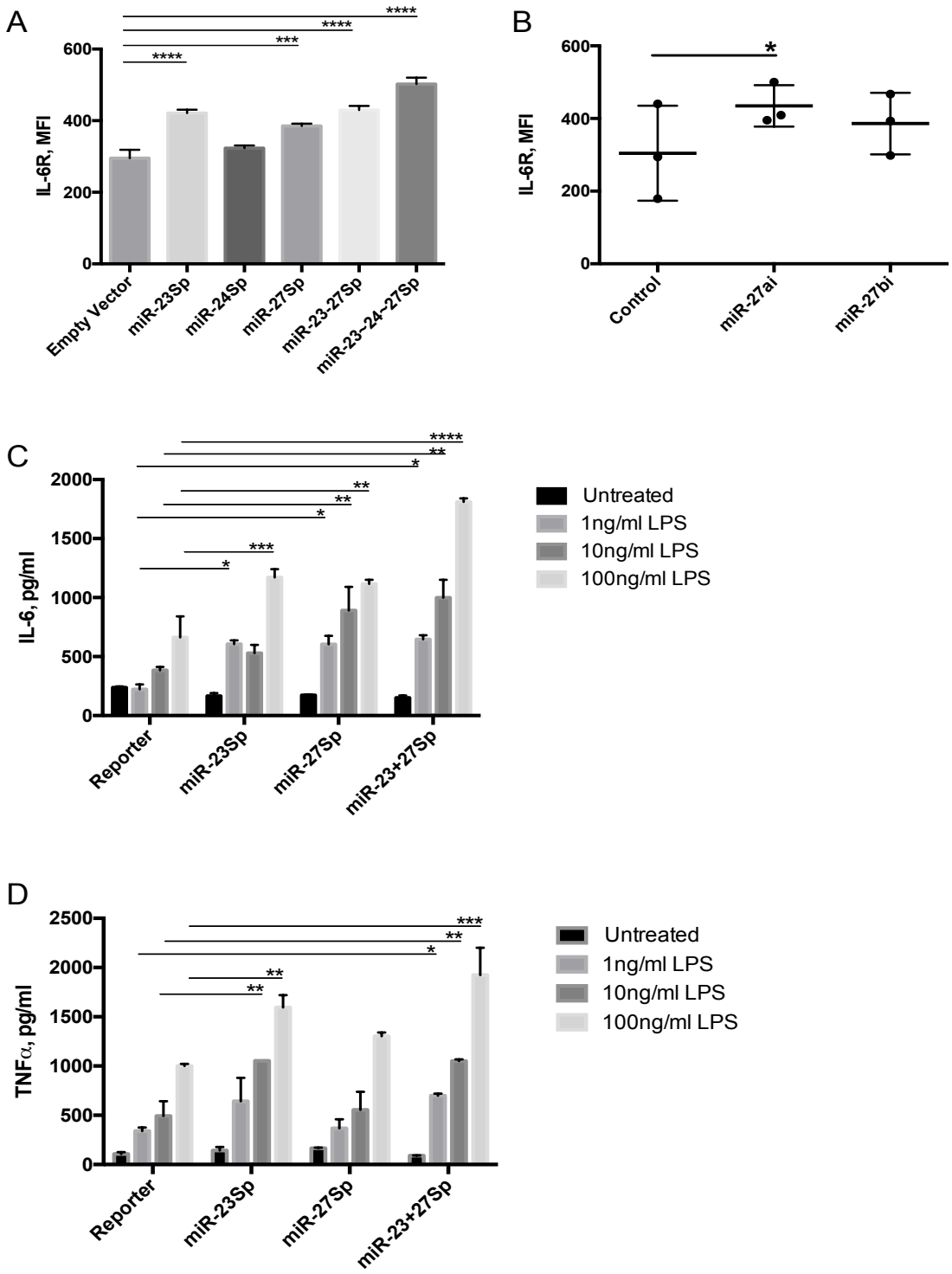

Figure 6.7 Inhibition of miR-27a increases surface IL-6R expression in THP-1 cells.

Results for (**A**) and (**B**) are obtained by FACS method and show surface IL-6R staining in (**A**) miR-23a, miR-24 and miR-27a THP-1 sponge cells; (**B**) THP-1 cells transfected with control, miR-27a or miR-27b inhibitors (Control, miR-27ai or miR-27bi, respectively). Data displayed as Mean±SD of mean fluorescence intensity (MFI) of surface IL-6R staining (n=3). (**C**) Reporter and miR-23, miR-27 and miR-23+27 sponge THP-1 cells were matured with PMA for 6 days (protocol described in Chapter 2) and then stimulated with 1 ng/ml, 10 ng/ml or 100ng/ml of LPS for 24 hours. After stimulation, supernatants were collected, and ELISA measurement of TNFα and IL-6 were done. Data displayed as Mean±SD of pg/ml concentration of IL-6 (**C**) and TNFα (**D**), (n=3). Data are analysed by Ordinary One-way ANOVA test with Dunnett's correction for multiple comparisons, * - p≤0.05, **** - p≤).0001.

6.2.7 Biologic resistant patients have increased levels of membrane and soluble IL-6R compared to DMARDs responders

Next, I investigated if the RA patients, described in Chapter 3, have altered levels of soluble or membrane IL-6R, as would the *in-vitro* data suggest. For this, the qPCR method was used to measure the transcript levels of mIL-6R, sIL-6R and miR-27a on the remaining RNA samples from the cohort (Figure 6.8). The results showed that mIL-6R levels were significantly increased in biologic resistant patients compared to all other groups, while soluble IL-6R transcript levels were significantly increased in both biologic and DMARD resistant patients compared to healthy controls (Figure 6.8, A and B, respectively). Measuring serum sIL-6R from the various patient groups showed that levels were increased in biologic resistant patients reflecting the observed increases in transcript levels (Figure 6.8, C). It is important to note that a part of the detected soluble IL-6R protein was also likely generated by the shedding from the membrane receptor by ADAM10 or 17 sheddases [373].

In Chapter 3 (Figure 6.9, A) I showed that miR-27a levels were decreased in the biologic resistant patients compared to DMARD responders. Microarray data also suggest that miR-23a levels were low in these patients (Figure 3.4). To investigate this relation, expression of the membrane and soluble IL-6R were correlated with the levels of miR-27a measured by qPCR in the same samples (Figure 6.8, D and E, respectively). Unfortunately, only 10 samples from the biologic resistant group of 41 patients had data available for this analysis, and although this is a very limited sample size, there was no indication that miR levels correlated with those of its target. This is not a surprising result, especially when one considers the differences in the turn over rate of these two very different RNA species.

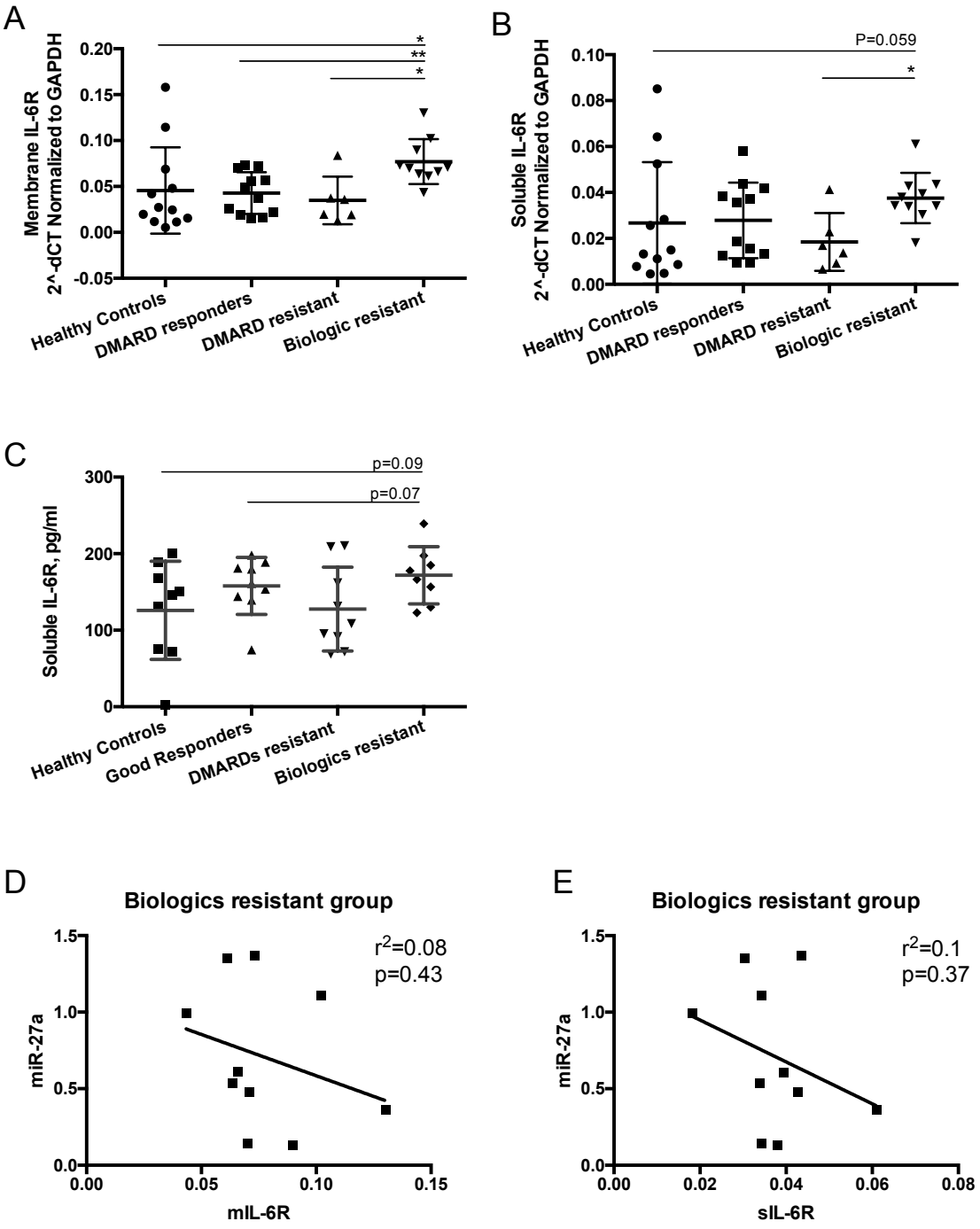

Figure 6.8 IL-6R expression is increased in RA patients resistant to Biologic therapies.

Expression of mIL-6R (**A**) and sIL-6R (**B**) was measured by qPCR method in samples from RA patient cohort and healthy controls, described in Chapter 3. Note lower numbers of samples in each group are due to the limited amount of available RNA following miRarray and other testes, performed previously. (**C**) Levels of soluble IL-6R were measured in serum samples from RA cohort patients and healthy controls. Results obtained by ELISA method and displayed in pg/ml. Expression of miR-27a, measured by qPCR was correlated with the levels of mIL-6R (**D**) and sIL-6R (**E**) in 10 samples from Biologics resistant patients, which had both measurements available.

6.2.8 Expression of IL-6R splice variants is more coordinated in patients failing DMARD and Biologic therapies.

Membrane and soluble IL-6R isoforms are expressed primarily from the same gene via alternative splicing where the inclusion or exclusion of exon 9 produces transcripts that express mIL-6R or sIL-6R forms, respectively. Here I looked at the correlation of sIl-6R and mIL-6R mRNA levels in healthy controls, DMARD-responsive, DMARD-resistant and biologics resistant patients.

Strikingly I found that correlation coefficient increased in value and significance in every subsequent group compared to the previous one until there was an almost perfect correlation between mIL-6R vs. sIL-6R forms in patients resistant to DMARDs and Biologic therapies, r=0.9387 and r=0.9961 respectively (Figure 6.9). Why IL-6R splice variant selection should become more coordinated in these patient groups is unclear. Moreover, this phenomenon could only be investigated by designing specific primers for each of the splicing forms separately and not by screening methods, such as mRNA array or even transcription sequencing as they lack required specificity. Whether this observation is related to a decrease in repression by miR-23a and miR-27a remains to be determined. This could be tested experimentally by examining the effect that inhibition of miR-23a and miR-27a has on the correlation between mIL-6R vs. sIL-6R in $CD14^{+}$ monocytes. Whatever the cause of this phenomenon it evidentially involves some disease related mechanism that is worthy of further investigation.

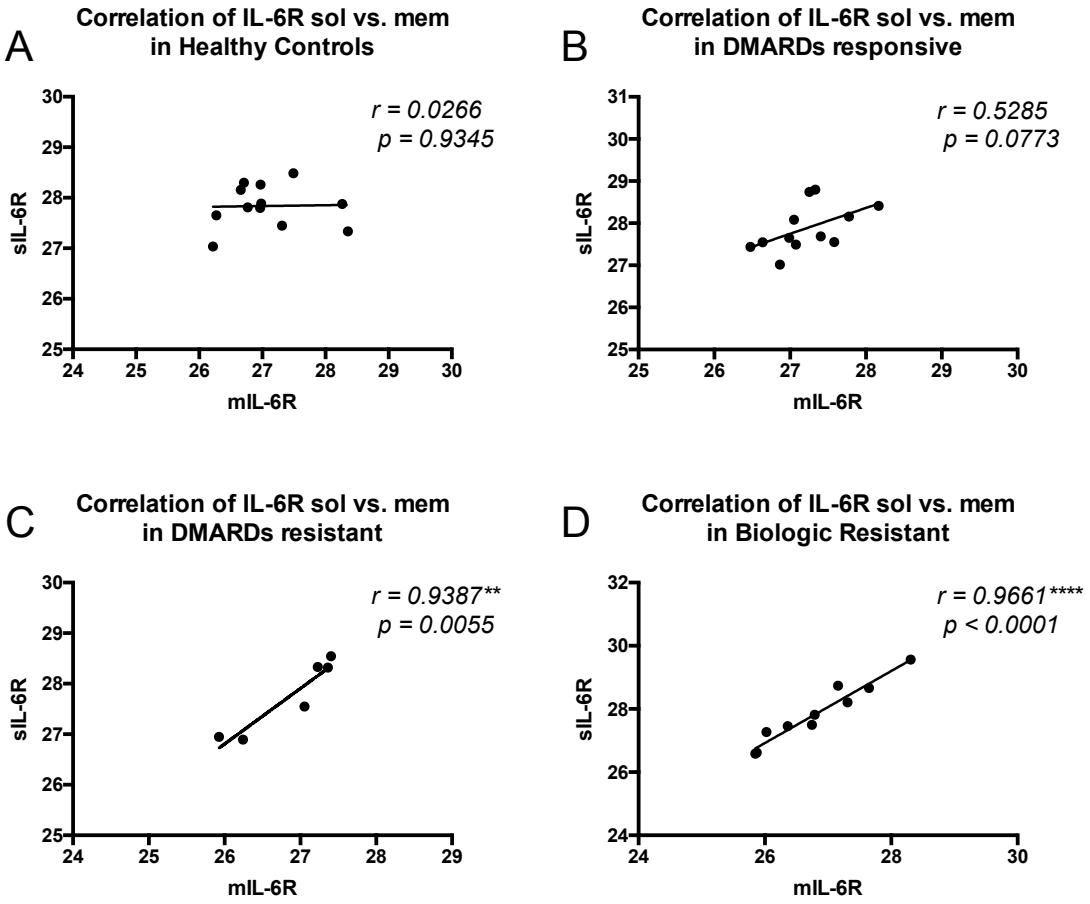

Figure 6.9 mIL-6R vs. sIL-6R correlation increases in DMARD and Biologic resistant patients.

qPCR CT values of soluble (sIL-6R) and membrane (mIL-6R) mRNA levels of IL-6R were correlated in (**A**) healthy controls, (**B**) DMARD-responders, (**C**) DMARD-resistant and (**D**) biologic resistant patients. Data were analysed by Pearson's correlation coefficient. ** - p≤0.01, ****- p≤0.0001.

6.3 IL-6RST (GP130) is not targeted by miR-23a or miR-27a

Having previously shown that IL-6R is targeted by both miR-23a and miR-27a I next sought to explore the possibility that members of the miR-23a cluster may also target its co-receptor IL-6R Signal Transducer (IL-6ST), otherwise known as GP130. IL-6ST is a ubiquitously expressed receptor and acts as co-receptor in receptor complexes for numerous cytokines including IL-27, IL-11, LIF, OSM and CNTF, cardiotrophin1, cardiotrophin-like cytokine and IL-6 (Reviewed in Chapter 1). However, my interest stems from its fundamental role in the IL-6R signalling complex. Searching IL-6ST 3'UTR for potential miR-23a cluster MBSs revealed potential binding sites for both miR-23a and miR-27a (Table 6.2).

Gene	miRNA	miRWalk	miRanda	Pictar2	PITA	RNA22	Targetscan
GP130	miR-23a-3p						
GP130	miR-27a-3p						
GP130	miR-27a-3p						

Table 6.2 Summary of target predictions for IL-6ST.
Green and red indicate presence or absence of miR binding site respectively.

To functionally validate miR-23a and miR-27a targeting of IL-6ST I constructed two luciferase reporter assays. The first contained approximately 2kb region with both miR-27a binding sites (IL-6ST-1), while the other included a 400bp region containing the predicted miR-23a site (IL-6ST-2). Both regions were amplified by PCR before being cloned downstream of luciferase ORF in pGLOMS2BD vector (Figure 6.10 A). The resulting constructs were co-transfected along with either miR-23a, miR-27a mimic or scrambled control and luciferase activity was measured after 24 hours. Plasmids pGLOMS2BD-23sp and pGLOMS2BD-27sp sponge constructs were included as positive controls. Neither miR-23a nor miR-27a reduced luciferase activity when introduced along with the IL-6ST luciferase reporter constructs (Figure 6.10, B). These results would appear to conclusively show that IL-6ST is not directly regulated by miR-23a or miR-27a. However, a recent report by Su and colleagues present evidence in the form of luciferase assay that shows miR-27a does indeed directly target IL-6ST

[765]. Furthermore, the authors show that miR-27a regulates IL-6ST via the poorly conserved site and not highly conserved one. The reason for the discrepancies in our data is unclear. The region used by Su et al. in their luciferase reporter assay was smaller than the one used here (629 bp, versus 1978bp) this could have influenced our results in a number of ways. The region that I amplified may have contained multiple polyA signals, which could have been active in the luciferase-IL-6ST(1) transcript effectively excising the active miR-27a MBS, rendering the reporter transcript insensitive to miR-27a regulation. Alternatively, Including a larger 3'UTR fragment might have inadvertently included another highly active miR MBS for a highly expressed miR that preferential targets the reporter transcript meaning that exogenous miR-23a has little impact.

Searches of HITS-CLIP and CLASH databases identified HITS-CLIP peaks corresponding to interactions between IL-6ST and miR-27a [766]. Interestingly the same study identified an interaction between miR-24 and IL-6ST. None of the target prediction algorithms I used here identified a miR-24 binding site in IL-6ST. It is becoming increasingly clear that the dogma that miR-target interactions rely primarily on complementarity between target and seed region needs to be re-considered in light of the massive unbiased data sets generated from studies using HITS-CLIP, PAR-CLIP and CLASH technologies suggest that as many as 40% of miRNA/target interactions are non-canonical [767]. Therefore, it may be that a yet to be identified miR-24 binding site is waiting to be discovered that interacts with sequences other than the 3'UTR or via complimentary outside the seed region.

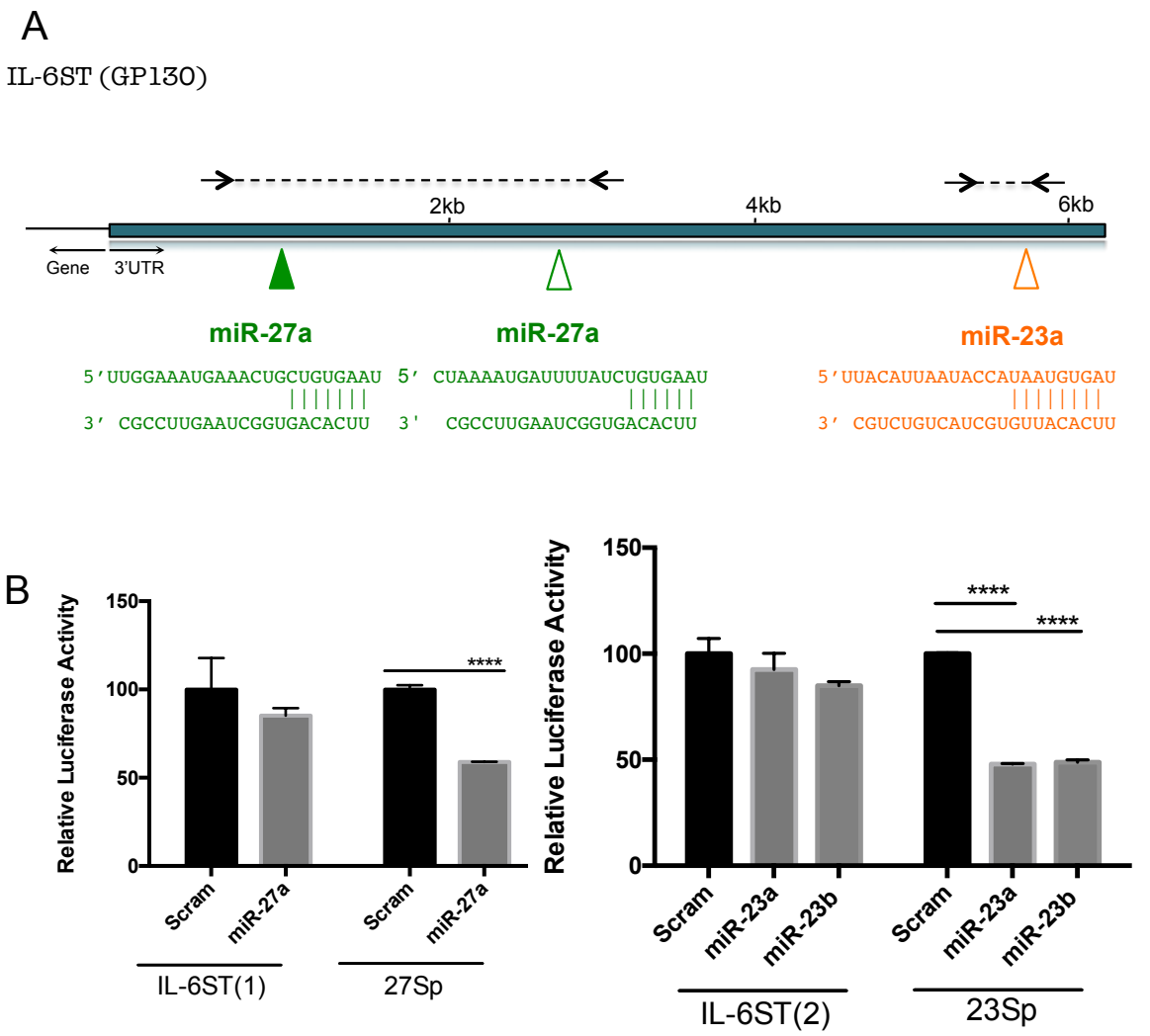

Figure 6.10 Neither miR-23a/b or miR-27a target IL-6ST

(**A**) Schematic representation of IL-6ST's 3'UTR showing the location of predicted miR-23a/b and miR-27a binding sites. MiR-23a/b and miR-27a/b sites are indicated by orange and green triangles respectively. Open triangles represent poorly conserved sites; filled triangles well-conserved sites as determined by Targetscan. The arrows and dotted line show the regions amplified by PCR that were cloned into pmiRGLO. The alignment of miRs with their MBS is shown below in green. (**B**) Luciferase activity in HEK293 cells co-transfected with IL-6ST (1) and (2) luciferase reporter plasmids and miR-27a, miR-27b or scrambled control mimics. pGLOMS2BD-23Sp and pGLOMS2BD-27Sp were used as positive controls. Activities were normalised to Renilla internal control and values expressed as % of scrambled controls. (n =3). Data were analysed by Student's t-test, **** - p<0.0001 versus scrambled control.

6.4 ERAP-1 (ARTS1) is not targeted by miR-27a

The bioinformatic analysis highlighted ERAP-1 as a predicted target of miR-27a. ERAP-1 is an aminopeptidase localised in the endoplasmic reticulum where it plays a role in the processing of antigen peptides for presentation by MHC class 1 molecules [768]. Amongst its other activities are the cleavage of TNFRI, IL-1 receptor II and mIL-6R where it acts by ‘shedding' them from the membrane [397]. Significantly, after HLA-B27, ERAP-1 has the second strongest association (26%) with ankylosing spondylitis. However, no implications for RA were found to date [769].

Here I set out to determine if ERAP-1 was a direct target of miR-27a. As a first step, I searched for miR-27a binding sites in ERAP-1 3'UTR using 6 different target prediction algorithms. Two out of the 6 programs (Targetscan and PITA) identified a single poorly conserved miR-27a binding site (Table 6.3).

Gene	miRNA	miRWalk	miRanda	Pictar2	PITA	RNA22	Targetscan
ERAP1	miR-27a-3p						

Table 6.3 Summary of target predictions for ERAP-1.
Green and red indicate presence or absence of miR binding site respectively.

Given ERAP-1's association with IL-6 signalling, I have tested this interaction by constructing a luciferase reporter assay, in which a 450 bp region containing the predicted miR-27a binding site was cloned downstream of luciferase ORF. The resulting construct was co-transfected along with either miR-27a mimic or scrambled control and luciferase activity measured after 24 hours. The pGLOMS2BD-27 sponge was fused to miR-27 sponge were used as a positive control. Neither, miR-27a nor miR-27b reduced luciferase activity when introduced along with the ERAP-1 luciferase reporter (Figure 6.11). However, both significantly reduced luciferase activity of the positive control. This result strongly suggests that ERAP-1 is not a target of miR-27. Further bio-informatic analysis of HITS-CLIP and CLASH databases failed to pick up any interactions between ERAP-1 and miR-27a/b further supporting my conclusion that miR-27 does not target ERAP-1.

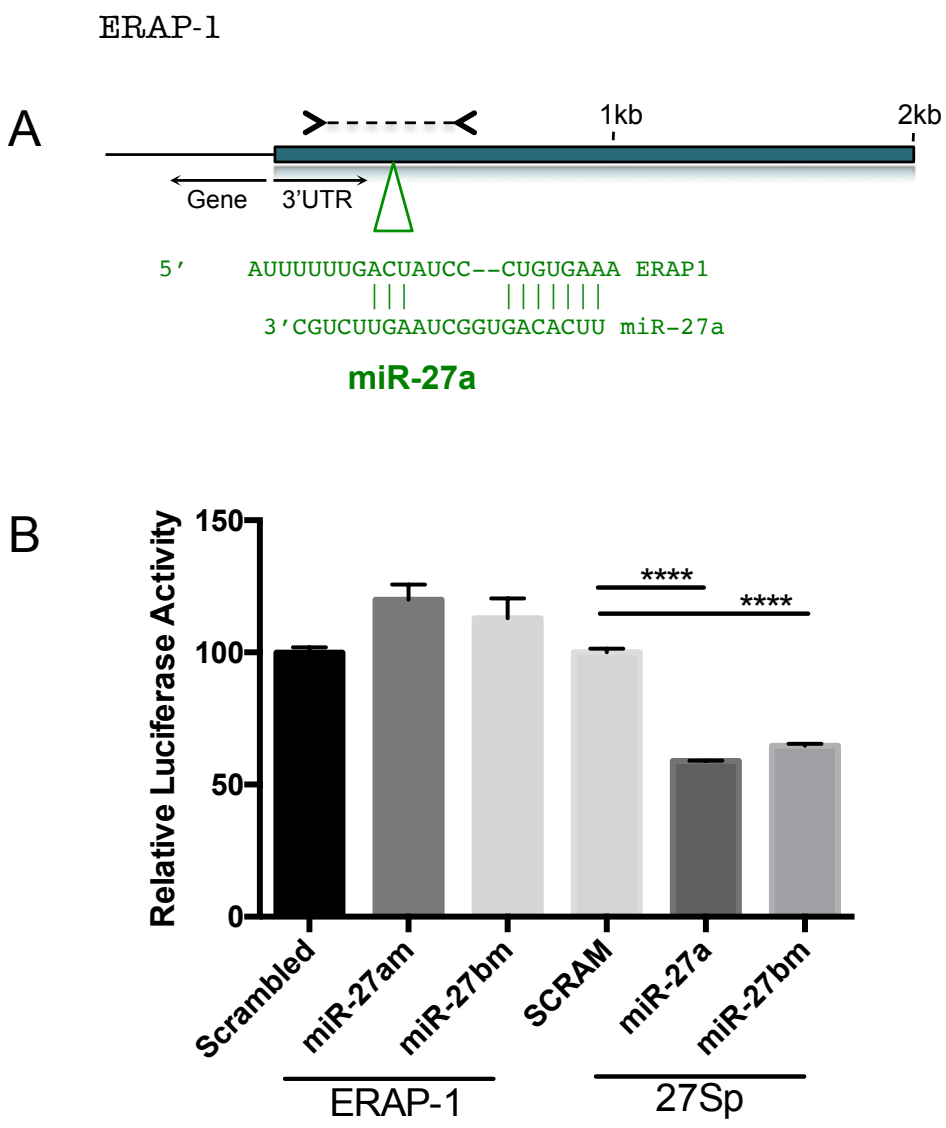

Figure 6.11 ERAP-1 is not a direct target of miR-27a or miR-27b

(**A**) Schematic representation of ERAP-1 3'UTR showing the location of predicted poorly conserved miR-27a binding site. The arrows and dotted line show the region amplified by PCR and cloned into pGLOMS2BD vector. The alignment of miR-27a with its MBS is shown in green. (**B**) Luciferase activity in HEK293 cells co-transfected with ERAP-1 luciferase reporter plasmid and miR-27a, miR-27b or scrambled control mimics. pGLOMS2BD-27sp was used as positive control. Activities were normalised to Renilla and values expressed as % of scrambled controls. (n =3). Data were analysed by Student's t-test, **** - $p<0.0001$ versus scrambled control.

6.5 MiR-24 targets MTHFR, but not DHFR

I have previously shown that the miR-23a cluster expression is lower in DMARD-resistant and biologic-resistant patients compared to DMARD-responders and healthy controls. While it is unlikely that lower miR-23a cluster expression causes treatment failure in these patients, I decided to use Ingenuity Pathway analysis to see if there were any obvious targets/pathways that could contribute towards a resistant phenotype. This highlighted dihydrofolate reductase (DHFR) and methylene tetrahydrofolate reductase MTHFR genes, which are of particular relevance to my study since they are actively implicated in the methotrexate pathway.

6.5.1 DHFR is not regulated by miR-24.

DHFR is a predicted target of miR-24 as identified by various target prediction algorithms (Table 6.4). Initial screening of DHFR for miR-23a cluster binding sites identified a single predicted miR-24 site at position +2192 in the 3'UTR (annotated here as DHFR#2). However, Mishra and colleagues reported that DHFR was indeed targeted by miR-24 but at another site (+1258, annotated here as DHFR#1). Notably, the miR-24 site described in this work was not identified by any of the target predictions used here likely due to imperfect base-pairing in the seed region (Figure 6.12, A). As the authors did not use reporter assay to validate this target, I choose to investigate it along with the other predicted miR-24 site. Regions containing both MBS were synthesised as G-blocks and cloned directly into pGLOMS2BD using Gibson Assembly (Figure 6.12, A).

Table 6.4 Summary of predicted miR-24 binding sites in DHFR.

Green and red indicate presence or absence of miR binding site respectively.

The resulting plasmids were co-transfected into HEK293 cells along with miR-24 or scrambled control. The pGLOMS2BD-24 sponge construct was used as a positive control. After 24 hours the luciferase activity was measured using a dual-luciferase assay. In these experiments miR-24 did not reduce luciferase activity in either DHFR#1 or DHFR#2 reporter assays compared to scrambled control (Figure 6.12, B). In contrast luciferase activity in positive controls was significantly reduced. This data suggests that miR-24 does not target DHFR via either site.

The reason for the disparity between my results and those described by Mishra et al. is unclear. Notably, the authors did not validate a miR-24 interaction with a DHFR by reporter assay. Instead, the authors showed that overexpression of miR-24 reduced DHFR protein levels by western blot. A limitation of this approach is that it does not differentiate between direct and indirect effects of miR-24 overexpression. They presented data showed that miR-24's interaction with DHFR was dependent on the sequence immediately downstream from the miR-24 binding site. Furthermore, authors state that C829T polymorphism abolishes this regulation by increasing local secondary structure (Figure 6.12, A). Significantly, the sequence used in my reporter assay corresponded to the ‘active’ 829C variant meaning that it should be sensitive to miR-24.

To further interrogate my finding I measured the effect that miR-24 modulation had on DHFR transcript levels in THP-1 and $CD14^+$ cells (Figure 6.13). Overexpression of miR-24 in THP-1 cells and $CD14^+$ monocytes did not significantly change the expression of DHFR compared to the scrambled control. Similarly, DHFR expression levels were unchanged in THP-1 expressing miR-24 sponge cells compared to empty vector control. These experiments confirm that miR-24 modulation does not impact DHFR levels as measured by qPCR.

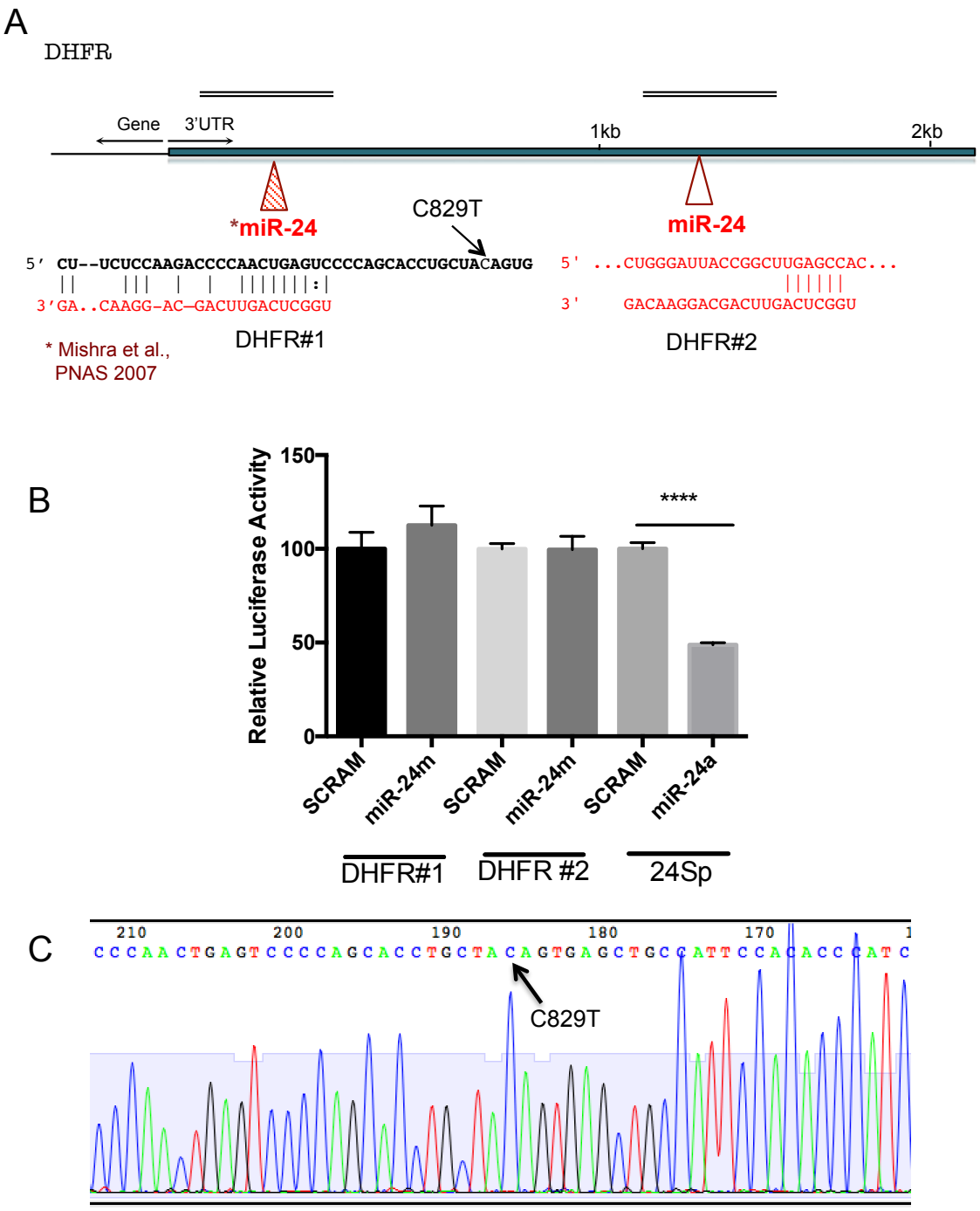

Figure 6.12 DHFR is not targeted by miR-24.

(**A**) Schematic representation of the DHFR 3'UTR showing the location of predicted miR-24 binding sites, below alignments of miR-24 with MBS and location of the C829T polymorphism are shown. Double lines correspond to G-block sequences used to generate DHFR luciferase reporter assay. (**B**) Luciferase activity in HEK293 cells co-transfected with DHFR luciferase reporter plasmid and miR-24 or scrambled control mimics. PGLOMS2BD-24sp was used as positive control. Activities were normalised to Renilla and values expressed as % of scrambled controls. (n =3). Data were analysed by Student's t-test, **** - p<0.0001 versus scrambled control. (**C**) Chromatogram showing the sequence of DHFR#1 region from THP-1.

It is possible that miR-24 regulates DHFR strictly by translational repression leaving transcript levels unchanged. However, Mirsha and colleagues reported that transcripts carrying the 829T variant had a longer half-life than the 829C miR-24-senstive variant, suggesting that miR-24 regulates DHFR by transcript destabilisation. To rule out the possibility that DHFR in THP-1 cells carried the 829T miR-24-insenstitive variant the corresponding genomic region was amplified by PCR and sequenced, showing that THP-1 cells encoded the 829C supposedly miR-24 sensitive variant (Figure 6.12 C). Furthermore, secondary structure analysis of the region surrounding C829T polymorphism showed that 829T, contrary to the findings of Mirsha et al., did not increase local secondary structure but rather reduced it compared to the 829C variant (Figure 6.14).

Finally, searches of HITS-CLIP and CLASH databases failed to pick up any interactions between DHFR and miR-24 further supporting my conclusion that miR-24 does not target DHFR.

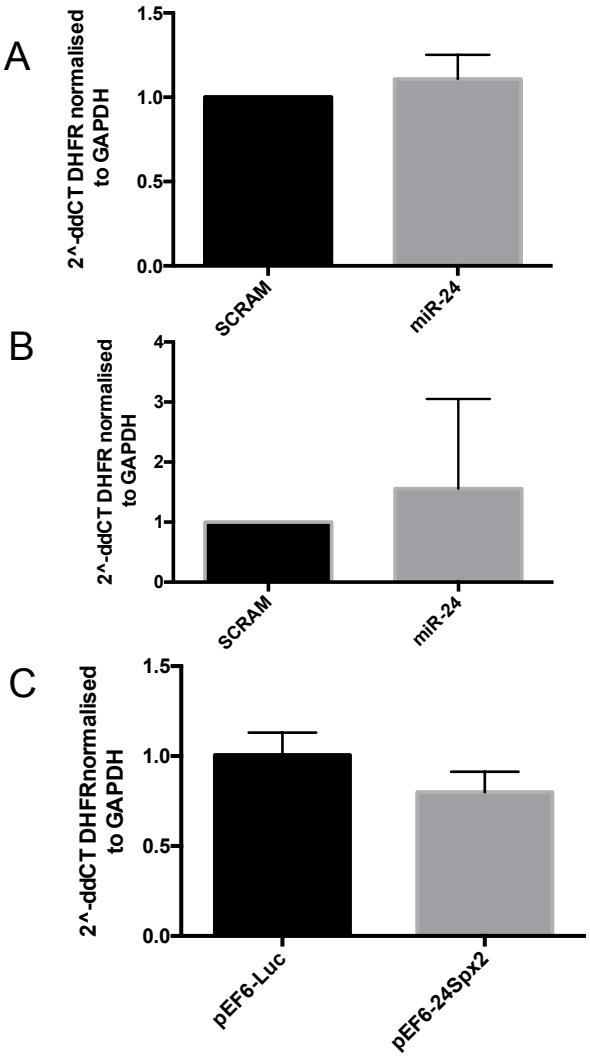

Figure 6.13 Modulation of miR-24 expression does not alter DHFR in THP-1 cells or CD14$^+$ monocytes

(**A**) THP-1 cells and (**B**) CD14$^+$ monocytes were transfected with miR-24 mimic along with scrambled negative control and DHFR mRNA were measured by qPCR. (**C**) DHFR mRNA was measured in THP-1 cells expressing miR-24 sponge transcript. Measurements were conducted on 3 separate occasions (**A** and **C**) or with cells derived from 3 buffy coat donors (**B**) and analysed by Paired student's t test (**A**), Wilcoxon paired test (**B**) and Unpaired student's t test (**C**). Transfection efficiencies were measured by FACS method, detecting fluorescent control mimic; only samples with >80% efficiency were processed further.

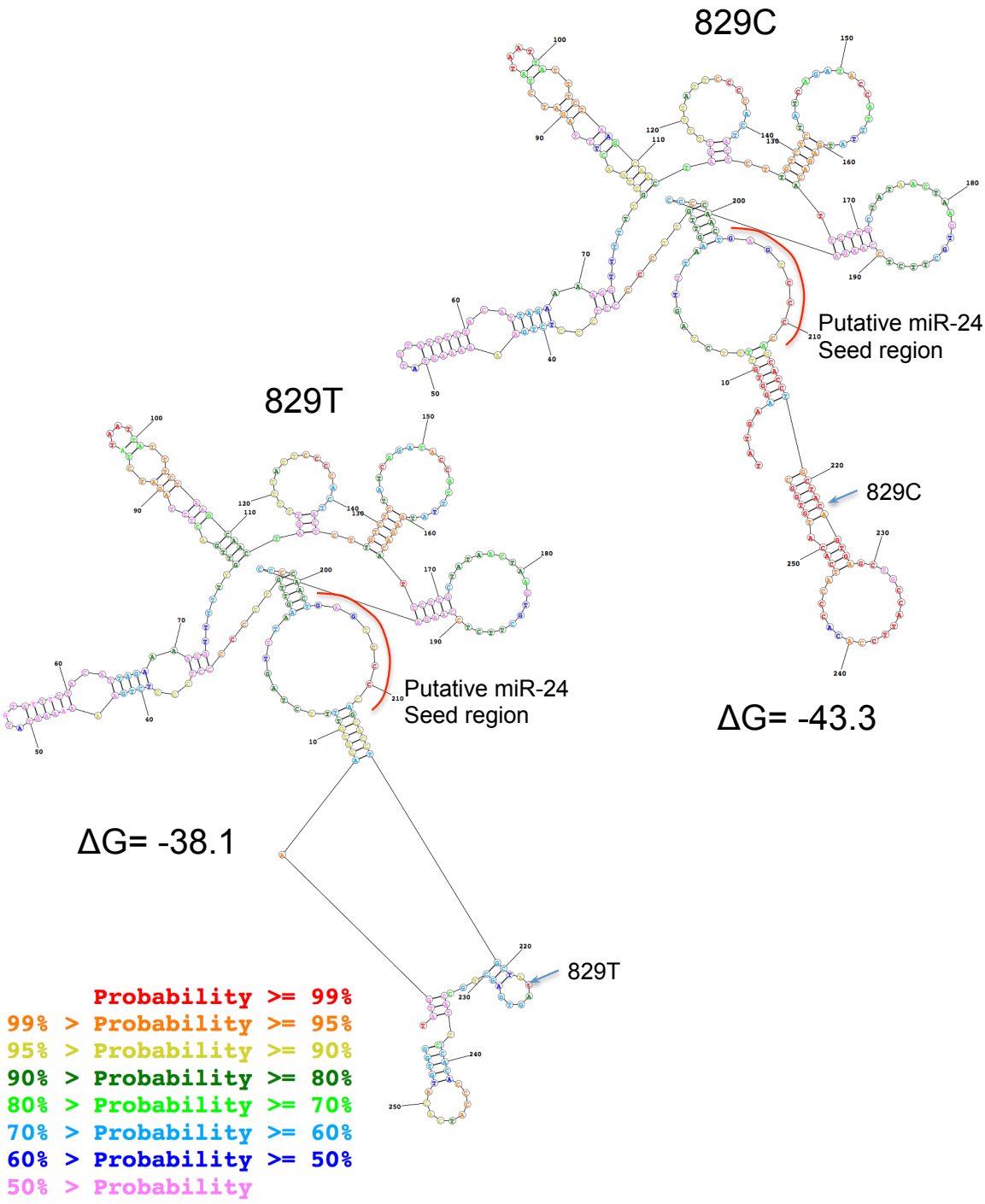

Figure 6.14 DHFR 829T reduces RNA secondary structure around potential miR-24 site

Secondary structure prediction shows that 829T variant has lower free energy (ΔG=-38.1) than the 829C variant (ΔG=-43.3), indicating that this isoform has less stable tertiary structure. Putative miR-24 is indicated by a red curved line. Secondary structures generated using RegRNA2 program.

6.5.2 MiR-24 targets MTHFR

As discussed briefly in the previous sections, patients fail DMARD treatments for two main reasons lack of efficacy and or lack of tolerance to the drugs. Studies have shown that around 40% of RA patients treated with MTX will experience adverse effects from the result of the treatment. Half of these patients will have severe adverse effects including worsening of nodulosis, pneumonitis, neurologic toxicity, gastrointestinal complications including nausea, vomiting and diarrhea, transaminitis, hematologic abnormalities, rash, stomatitis, and alopecia [770].

Methotrexate related toxicity in RA patients has been associated with two common polymorphisms (C667T and A1298C) that reduce the activity of MTHFR [771]. Along with DHFR, MTHFR is a critical enzyme in the folate pathway, converting 5,10-methylenetetrahydrofolate to 5-methyltetrahydrofolate, which acts as the methyl donor for re-methylation of homocysteine to methionine. MTX inhibition of DHFR prevents the conversion of dihydrofolate to tetrahydrofolate (THF). The resulting depletion of THF consequently prevents MTHFR production of 5-methyltetrahydrofolate causing an accumulation of homocysteine (Figure 6.15). It is ultimately increased serum homocysteine levels that are responsible for much of MTX toxicity [772].

Here I have identified MTHFR as a target of miR-24 and speculate that increased miR-24 levels may play a role in MTX-associated toxicity.

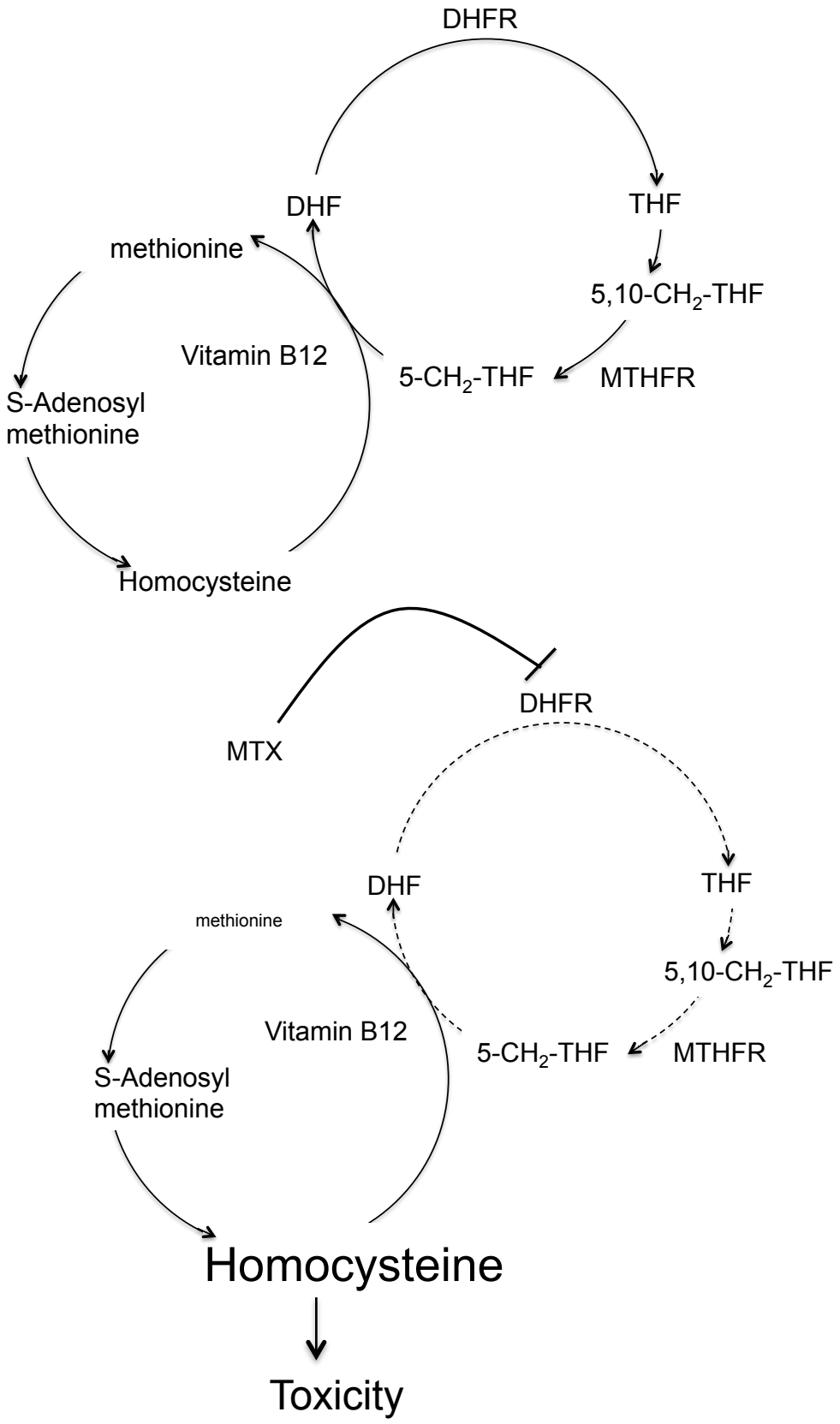

Figure 6.15 Diagram showing methotrexate's effect on methionine biosynthesis pathways leading to increased homocysteine production and toxicity.

Dihydrofolate reductase (DHFR), Dihydrofolate (DHF), Tetrahydrofolate (THF), 5,10-methylenetetrahydrofolate (5,10-CH2-THF) and to 5-methyltetrahydrofolate (5-CH2-THF)

MTHFR has 2 predicted miR-24 binding sites in its 3'UTR, with the distal site (MTHFR#2) being highly conserved amongst vertebrates (Table 6.5). Analysis of these sites using the available target prediction programs showed that 5 out of 6 algorithms predicted the MTHFR#2 site, while MTHFR#1 was only identified by 3 of the 6. For this reason, I decided to focus my attention on validating the MTHFR#2 site as a miR-24 target.

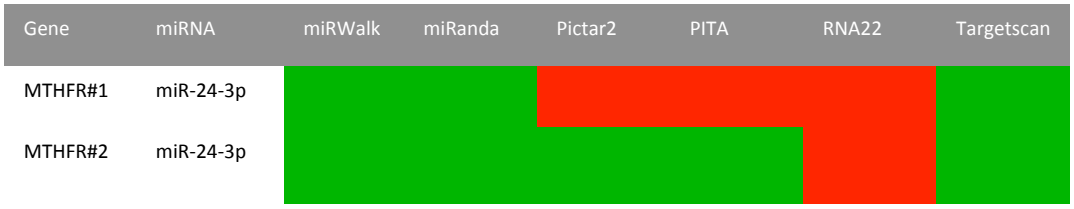

Table 6.5 Summary of predicted miR-24 binding sites in MTHFR.
Green and red indicate presence or absence of miR binding site respectively.

To that end, I made a luciferase reporter assay containing MTHFR#2 binding site using G-Blocks and Gibson assembly. In parallel, I created reporter assay in which the seed region of the putative miR-24 binding site was mutated (Figure 6.16, A). The resulting plasmids were co-transfected into HEK293 cell along with miR-24 mimic or scrambled negative control. The following day, luciferase activity was measured by dual-luciferase assay. The results showed that miR-24 significantly reduced luciferase activity of the wild-type MTHFR#2 reporter assay; this reduction was ameliorated by mutation of the seed region (Figure 6.16, B).

These results conclusively show that MTHFR is a direct target of miR-24 and that this interaction is mediated via a conserved site in its 3'UTR. Interestingly, analysis of microarray data from an experiment where miR-24 was over-expressed in human keratinocytes showed a significant corresponding decrease in MTHFR expression [773].

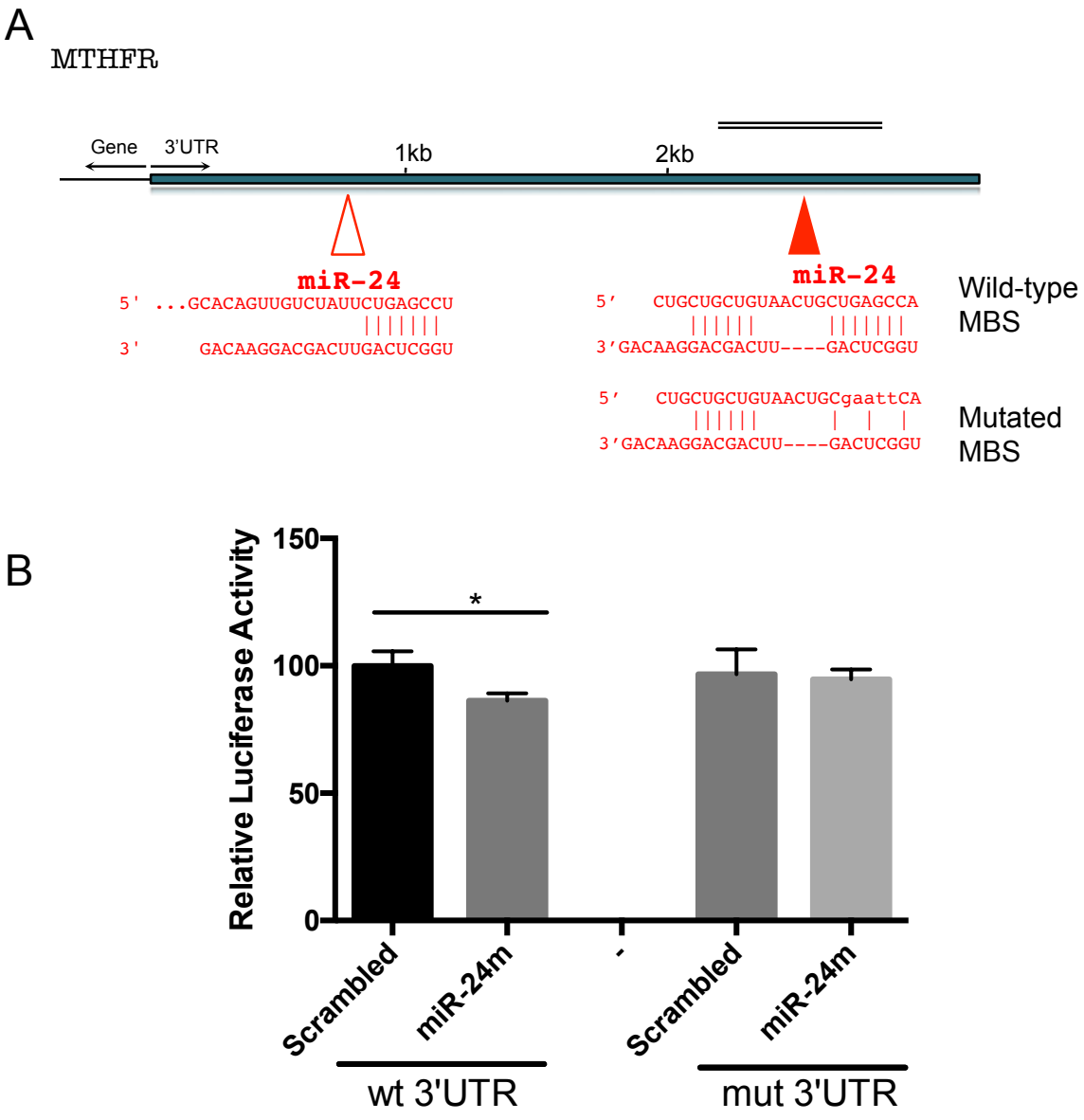

Figure 6.16 miR-24 targets MTHFR via a conserved site in 3'UTR

(**A**) Schematic of the MTHFR 3'UTR showing location of predicted miR-24 binding sites, below are alignments of miR-24 with wild-type and mutated MBSs. Double lines correspond to G-block sequences used to generate MTHFR#2 luciferase reporter assay. (**B**) Luciferase activity in HEK293 cells co-transfected with wild-type or mutated MTHFR luciferase reporter plasmids along with miR-24 or scrambled control mimics. Activates were normalised to Renilla and values expressed as % of scrambled controls. (n =3). Data were analysed by Student's t-test, * - $p<0.01$ versus scrambled control.

6.5.3 Modulation of miR-24 alters MTHFR expression in THP-1 cells

To further characterise miR-24's regulation of MTHFR, I next looked to see what effect overexpression of miR-24 had on the levels of endogenous MTHFR. For this, THP-1 cells were transfected with miR-24 mimic along with scrambled control mimic and grown for 24 hours. MTHFR transcript levels were measured by qPCR. Results showed a significant decrease in MTHFR expression compared to scrambled control (Figure 6.17, A). I then performed the analogous experiment in human $CD14^+$ monocytes purified from fresh blood of 3 separate donors. Cells were allowed to rest overnight before being transfected with miR-24 or scrambled control (transfection efficiencies were >80%). After transfection, cells were incubated for 24 hours before MTHFR transcript levels were measured by qPCR (Figure 6.17, B). Although the differences between scrambled and miR-24 treated samples were not significant, there was a trend towards lower MTHFR expression in miR-24 treated samples. Repeating this experiment with more donors may drive these data towards significance.

Having over-expressed miR-24, I next looked at MTHFR expression in THP-1 miR-24 sponge expressing cells in which miR-24 activity is functionally depleted (Figure 6.17, C). MTHFR levels were increased in miR-24 sponge cells compared to the control cell line (pEF6-luc). This further supports a role for miR-24 in the regulation of MTHFR. Moreover, it suggests that miR-24 is actively regulating it in THP-1 cells.

Although the data presented here demonstrates a clear, direct effect of miR-24 on MTHFR expression, its significance to toleration of MTX in RA patients has not yet been established. However, a number of studies have linked polymorphisms (C667T and A1298C) in MTHFR that affect or lower the activity of the enzyme with increased intolerance to methotrexate amongst RA patients [774]. Therefore it is tempting to speculate that patients with higher miR-24 expression would have lower MTHFR and consequently be less tolerant to MTX treatment. Patients in this category will more often than not be moved onto other DMARD treatments such as sulfasalazine (SSZ). While this clinical scenario will not apply to all patients on SSZ, it will do for many of them. While acknowledging these limitations I sought to test my hypothesis that higher miR-24 levels reduce

MTHFR expression driving MTX intolerance in RA patients by comparing miR-24 expression in SSZ patients compared to those on MTX. Figure 6.17 shows the results of the analysis. While the difference between the two groups is not statistically significant, there is a clear trend towards lower levels or miR-24 in patients who are tolerating MTX treatment. While not by any means conclusive it does generally support my hypothesis.

As discussed previously, this comparison is not ideal one to test miR-24's role in MTX intolerance. Moreover, due to the lack of sufficient patient RNA miR-24 probe intensities were used as a measure of miR-24 expression levels. This study requires further validation by qPCR. A better comparison would be qPCR quantification of miR-24 levels in patients who tolerate MTX with those suffering side effects.

Given more time, I would carry out further studies on MTHFR. Specifically, I would like to see if miR-24 regulation affects MTHFR protein levels and ultimately its activity in THP-1 cells and $CD14^+$ cells. Going further I would see if miR-24 repression of MTHFR activity within monocytes had any effect on the folate pathway. Specifically, MTHFR catalysed conversion of 5,10-methylenetetrahydrofolate to 5-methyltetrahydrofolate production and accumulation of homocysteine in treated cells. These studies could ultimately be extended to a comparison of miR-24 levels in patients tolerating MTX with those showing adverse effects. Further stratification of these patients for the presence of the common C667T and A1298C polymorphisms and high miR-24 could also provide a valuable insight into RA patient MTX-insensitivity.

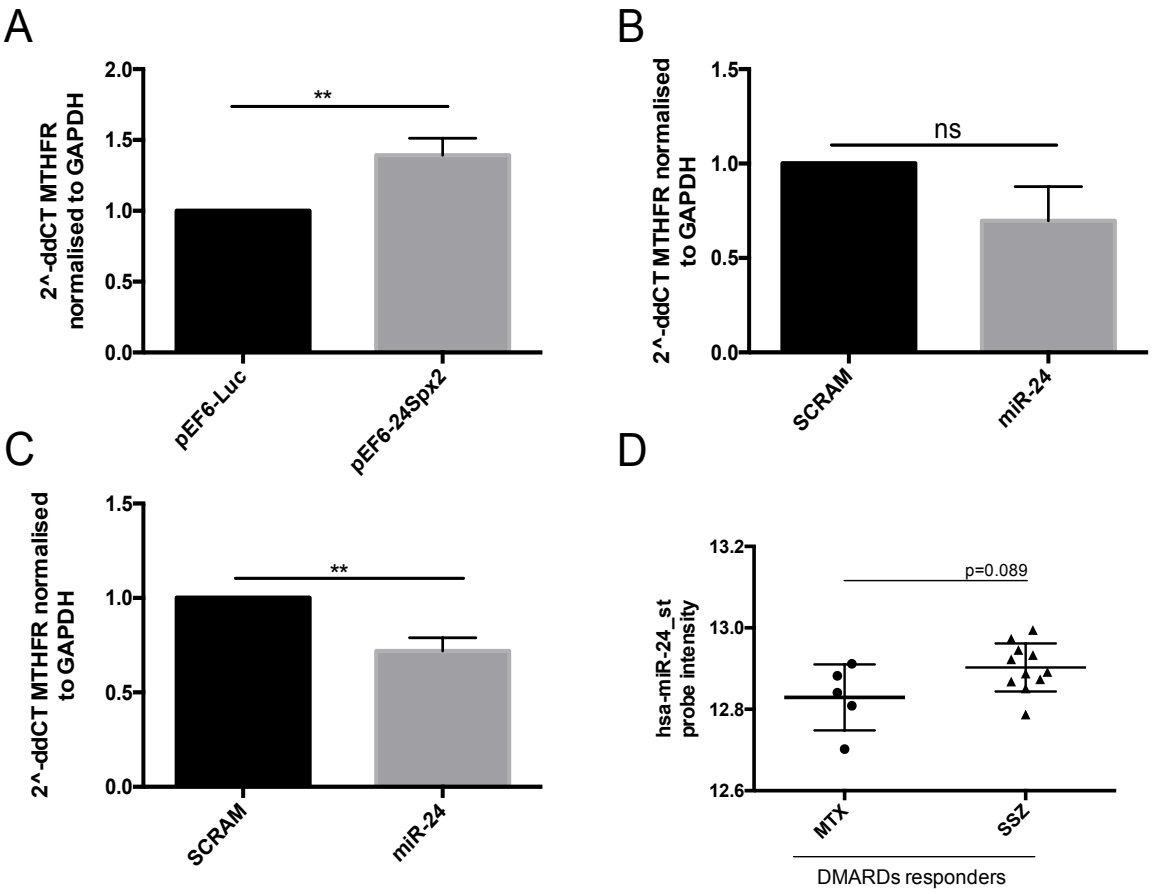

Figure 6.17 Modulation of miR-24 alters MTHFR expression in THP-1 cells

(**A**) MTHFR mRNA was measured in THP-1 cells containing miR-24 sponge (pEF6-24SpX2) or control vector (pEF6-Luc). MTHFR mRNA was also measured by qPCR in Buffy coat CD14+ monocytes (**B**) and THP-1 cells (**C**) transfected with miR-24 mimic (miR-24) along with scrambled negative control (SCRAM) for 24 hours. Experiments were done on 3 separate occasions and analysed by Student's t test for (**A**) and (**C**) and by Mann-Whitney's test for (**B**). (**D**) MiR-24 probe intensities from samples taken from DMARD responder patients being treated with MTX or SSZ. Data analysed using Mann Whitney's test.

6.6 Macrophage colony stimulating factor receptor 1 is a direct target of miR-24

There are ample data supporting the hypothesis that IL-6 stimulation of monocytes triggers M-CSF dependant maturation into macrophages [401,402]. With now abundant evidence that the miR-23a~24~27a cluster is implicated in the IL-6 pathway and also with a rapid decrease in the clusters expression following exposure to M-CSF, observed in chapter 4, I have analysed the M-CSF pathway for potential direct targets these miRs, which would explain the observed interactions.

Indeed, CSF1R has two conserved predicted miR-24 binding sites in its 3'UTR. Sites were identified by 2/6 and 3/6 target prediction algorithms used (Table 6.6). While this did not look overly promising, given that greater consensus between target prediction programs correlates with lower false positive rates, the extended base-pairing outside the seed region encouraged me to experimentally validate miR-24 and CSF1R interaction (Figure 6.18, A).

Table 6.6 Summary of predicted miR-24 binding sites in CSF1R.
Green and red indicate presence or absence of miR binding site respectively.

To functionally validate CSF1R as a miR-24 target I created a luciferase reporter assay in which the 3'UTR of CSF1R containing both putative miR-24 sites was amplified by PCR and cloned downstream of the luciferase ORF in pGLOMS2DB. A reporter assay in which the two miR-24 seed regions were mutated was also created (Figure 6.18 A). The resulting plasmids were co-transfected into HEK293 cells along with miR-24 mimic or scrambled negative control. Luciferase activity was measured 24 hours later. The results showed that miR-24 significantly reduced the luciferase activity of the wild-type CSF1R reporter assay; this reduction was ameliorated by seed-region mutation (Figure 6.18, B).

These results conclusively show that CSF1R is a direct target of miR-24. As both binding sites were mutated in the G-block used to create the mutated pGLOMS2BD-CSF1R assay it is not possible to say whether miR-24 targets via one or both of the predicted sites. Unfortunately, I did not have time during my PhD studies to further characterise miR-24 interactions with CSF1R. However, given that it is so fundamentally important to monocyte/macrophage biology it is an intriguing target worthy of further investigation.

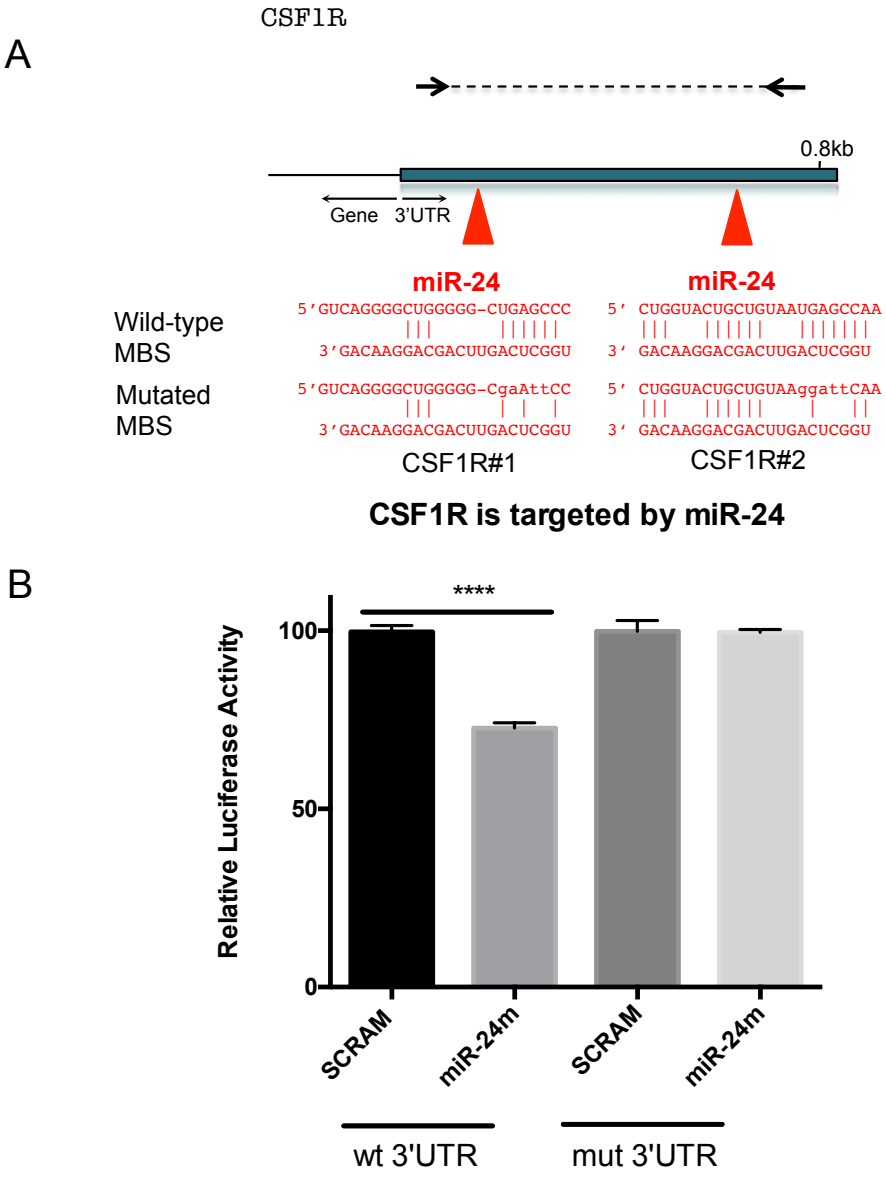

Figure 6.18 CSF1R is a direct target of miR-24

(**A**). Schematic representation of the CSF1R 3'UTR showing location of predicted miR-24 binding sites. Below are alignments of miR-24 with wild-type and mutated MBSs. Dotted lines show the PCR amplified region used to generate pGLOMS2BD-CSF1R luciferase reporter assay. (**B**) Luciferase activity in HEK293 cells co-transfected with wild-type or mutated CSF1R luciferase reporter plasmids along with miR-24 or scrambled control mimics. Activity was normalised to Renilla and values expressed as % of scrambled controls. (n =3). Data were analysed by Student's t test, * - $p<0.01$, versus scrambled control.

6.7 Discussion

Interleukin 6 is a potent activator of myeloid cells and contributes to overall inflammatory phenotype. Targeting of the IL-6 pathway has been particularly successful in the clinical setting [679]. Difficulties with cytokine inhibition as well as the complexity of the cis and trans IL-6 signalling meant that IL-6R receptor, and not the cytokine was a preferred clinical target [373]. Therefore, miR targeting of the receptor, as well as GP130, could have a profound impact on the IL-6 pathway in monocytes activation and its implications for IL-6R targeted treatment.

Here I have identified IL-6R as a direct target of two members of this cluster – miR-23a and miR-27a. Further investigation has confirmed that these interactions have functional consequences for the IL-6 pathway in myeloid cells. Namely, overexpression of both miRs led to the reduction of IL-6R transcript levels. Moreover, THP-1 sponge cells lacking each of the miRs or both of them in combination had increased levels of IL-6R transcript and protein. Investigation of miR-23 and miR-27-sponge cells demonstrated synchronicity in the function of cluster miRs, by which combined repression of both miR-23a and miR-27a has an additive effect on levels of IL-6R protein. This finding is of particular importance since miRs from this cluster are co-expressed, and their function should be viewed in its entirety.

Further investigation of single or combinatorial inhibition of miRs in THP-1 sponge cells allowed assessment of overall phenotype of cells lacking the miR-23a cluster. Thus, stimulation with LPS triggered significantly higher expression of IL-6 and TNFα cytokines in sponge cells lacking miR-23a, miR-27a or both. Roles of increased IL-6 and TNFα in RA are well recognised, not least as they are successfully targeted in the clinical setting (discussed in detail in Chapter 1). Therefore, lack of miR-23a and miR-27a that was previously demonstrated in $CD14^{+}$ cells from biologics resistant patients are likely to perpetuate chronicity of the disease by increasing both soluble and membrane-bound forms of IL-6R and cells responsiveness to its cytokine. This was confirmed by both increased levels of circulating IL-6 and IL-6R found in biologics resistant patients and by raised expression of the membrane and soluble IL-6R transcripts. Unfortunately, I found that miR-27a levels did not correlate with those of IL-6R transcripts.

However, this could be due to the small number of patients receiving anti-IL-6 treatment before the start of this study, which could have a potential impact on the levels of IL-6R found. Moreover, the relationship between miR-23a and miR-27a expression and effects of Tocilizumab need to be explored in detail. Further experiments on miR-23a cluster in the regulation of JAK/STAT signalling pathways would also be of vital importance since recent work from Su et al. describing the role of miR-23a and miR-27a regulation of JAK1 and STAT3 [765]. If proven applicable to primary human monocytes, and particularly $CD14^{+}$ cells derived from patients with the disease, these finding can have significant implications for the clinical use of new synthetic DMARDs, such as Jakinibs [452].

The THP-1 sponge cells created and used in my work are a valuable tool in the investigation of other aspects of inflammatory response, such as chemokine secretion, migration, antigen presentation and maturation into macrophages [775,776]. Unfortunately, due to the time constraints, I did not explore these here. However, they would provide valuable insight into the role of miR-23a cluster in other traits of myeloid cells and would pose a challenge for future work.

Interestingly, other predicted interactions of miR-23a cluster with members of IL-6R pathway, such as GP130 and ERAP-1 yielded negative results. In my analysis, miR-27a had a tendency to repress GP130 expression in the context of luciferase reporter assay. However, this finding was not statistically significant. This finding is in disagreement with recently published data that shows direct targeting of GP130 by miR-27a in an analogous luciferase reporter assay [765]. It is possible that the larger segment of GP130 3'UTR used in my experiments included other MBSs and as a result was targeted by highly expressed endogenous miRs in HEK293 cells. Therefore repeat of the evaluation of these particular binding site would be required for conclusive results. Lack of efficacy of miR-27a in the context of larger 3'UTR segment raises the question of its biological efficacy. For this, assessment of GP130 transcript and protein in THP-1 sponge cells would be informative and will be assessed in the future.

Detailed exploration of IL-6R transcripts revealed that presence of exon 9 coding for a membrane-spanning unit of the receptor distinguishes two distinct isoforms – soluble and membrane with their corresponding 3'UTRs. Our group and others

have demonstrated that transcripts can become insensitive to miR regulatory elements by shortening transcript's 3'UTR using alternative polyadenylation sites [653]. Given that miR-23a cluster binding sites where spread out along entire 3'UTR of IL-6R, it was important to identify if the transcripts present in THP-1 cells are sensitive to miR regulation. For this purpose 3'RACE method was utilised and contrary to the previously described long 3'UTR in membrane transcript and short 3'UTR in the soluble transcript, both IL-6R isoforms detected here utilised identical proximal polyadenylation site. Significantly, this shorter 3'UTR retained the active miR-23 and miR-27 sites identified here. Nevertheless, this discrepancy instigated a series of experiments in which I measured both soluble and membrane bound IL-6R transcripts. Although both mRNAs were constitutively expressed in THP-1 cells and isolated $CD14^+$ monocytes, it is the results obtained in the RA patient cohort that is of particular interest. Membrane and soluble IL-6R transcripts exhibited no correlation in healthy control individuals and only mildly so in patients who are good responders to DMARD treatment. However, in both treatment failure groups and particularly in biologic resistant patients, mIL-6R and sIL-6R transcripts displayed an almost linear correlation. The mechanism behind this observation is unclear, and this phenomenon has, to my knowledge, not been described before. Further evaluation would be required to understand if this is associated with disease activity or drug resistance.

Published data in cancer research has highlighted the role of miR-23a cluster in the regulation of apoptosis, but also in inhibition of topoisomerases and resistance to concomitant cancer treatments, such as etoposide. Work from Mishra et al. directly implicated miR-24 in the regulation of DHFR and sensitivity to MTX. Thus this pathway was assessed in the context of this RA cohort of drug-resistant patients. As discussed in Chapter 3, patients fail DMARD and Biologic treatments for two broad clinical reasons, lack of efficacy and lack of tolerance to the drugs. MTX is in most cases the first line treatment for RA. While MTX's mode of action in RA is unclear a number of putative mechanisms have been proposed (reviewed in the introduction). One of these is its well-defined role as a folate antagonist via the inhibition of Dihydrofolate reductase (DHFR) and Thymidylate synthetase (TYMS) [777]. Loss of activity of these two enzymes results in a reduction of thymidine synthesis, causing reduced DNA synthesis and

ultimately cytostasis [778,779]. *In vitro* studies have shown that primary T lymphocytes treated with low doses of MTX have reduced levels of ATP and GTP compared to untreated controls. Consequently, MTX-treated T cells proliferate less and are more apoptotic, the same observations have been demonstrated in T cells isolated from RA patients [780].

Despite this, clinical studies in patients receiving MTX and concomitant folate showed no loss of clinical benefit suggesting that folate pathway inhibition was not central to the anti-inflammatory activity of MTX [781]. Furthermore, MTX resistance in oncological conditions arises from compensatory gene amplification and increases in DHFR expression. This indicates that significant alterations in DHFR levels could bind MTX and limit its effectiveness by reducing its intracellular availability. Therefore, lower levels of miR-24 could lead to a rise in intracellular DHFR and titrating out intracellular MTX limiting its activity. Unfortunately, despite the extensive analysis of DHFR pathway and miR-24 associated SNPs, DHFR does not appear to be a direct target of miR-24. The lack of direct validation miR assay in previously published work makes it difficult to understand if our failure to find evidence of miR-24 regulation of DHFR were due to technical differences. The fact that I did not observe changes in DHFR transcript levels, when miR-24 was overexpressed or inhibited also suggest that this interaction does not occur. Genotyping of THP-1 showed that they carry the C829 polymorphism which should according to Mishra et al. be targetable by miR-24. Furthermore, the authors finding that the 829T variant increased local secondary structure making the miR-24 binding site inaccessible to miR-24-RISC complex was not the case, in fact, the opposite was true. Finally, none of the publically available HITS-CLIP, PAR-CLIP and CLASH databases identifies miR-24:DHFR interactions. Taking this into account I can only conclude that DHFR is not targeted by miR-24.

Nevertheless, further exploration of this pathway identified the closely related MTHFR gene as a direct target of miR-24. This interaction has potential implications for tolerability of MTX in RA patients rather than the efficacy of the drug. Several polymorphisms in MTHFR gene were previously described to have an effect on its activity, as well as on serum homocysteine levels, which mediates MTX-related toxicity. C677T polymorphism of MTFR is associated with decreased activity of the enzyme and raised homocysteine levels in the general

population [782]. In RA, an association of C677T effect on serum homocysteine levels remains controversial [783]. Second identified MTHFR polymorphism, A1298C, is shown to have a protective role in RA. Higher frequency of 1298CC was found in RA patients when compared to the general population (24,7% vs. 12,8%) and was associated with lower rate of MTX side effects [771]. My data showed that miR-24 overexpression reduces levels of MTHFR transcript, while the level was increased in THP-1 sponge cells lacking this miR. Although this is by no means a conclusive analysis, it indicates that reduced expression of miR-24 could improve MTX tolerability. For this, I have investigated the expression of miR-24 miRarray probe in patients from DMARDs responders group who have been tolerating long-term treatment with MTX for years. Indeed, this group of patients had a tendency towards reduced expression of miR-24 in PB $CD14^+$ cells, compared to SSZ treated patients. Patients from DMARDs responders group had a long-standing disease with duration of ten years and had tried 2 or fewer DMARDs, therefore constitute true responders to a particular medication. Significantly, subjects included in this analysis were receiving a single DMARD at the time of recruitment, limiting the effect of polypharmacy. However, future work would require assessment of the miR-24 expression, serum homocysteine levels, MTHFR polymorphisms and MTX tolerability in a prospective study to evaluate biomarker potential of this miR. This is particularly relevant when real world data is considered since drug prescription analysis would suggest that many of our patients do not take MTX on a regular basis and lose valuable time to control the disease activity or maintain the benefits.

Lastly, in silico analysis, but not Ingenuity pathway analysis has identified CSF1R as a direct target of miR-24. This was subsequently confirmed by the luciferase validation assay. Unfortunately, the lack of time has prevented me from exploring this interaction further. However, this finding could have considerable implications for the maturation and activation of blood-derived monocytes in the arthritic joint. As discussed in Chapter 1, CSF1R mediates maturation and survival of blood derived monocyte and synovial macrophages, which was clearly demonstrated in $csf1r^{op/op}$ mice [784]. M-CSF signalling through CSF1R is also required for expression of RANKL and differentiation of osteoclasts, implicating it in the development of bone erosions is RA [199]. Thus miR-24 regulation of the CSF pathway, or the lack of thereof could have important implications for

disease pathogenesis. Concordantly, new therapeutic strategies are being developed to target this pathway in RA [785].

The observed interaction between miR-24 and M-CSF pathway in this work allows the postulation of a hypothesis, by which M-CSF and GM-CSF stimulation of blood-derived $CD14^{+}$ monocytes reduce the expression of miR-24 and promotes differentiation of the cells, by de-repressing its receptor CSF1R. The fact that miR-24 plays an important role in these processes was recently demonstrated by Fordham et al. who showed that overexpression of miR-24 led to a significant reduction in levels of TNFα and IL-6 cytokines in M-CSF matured primary human macrophages [594]. Although the authors did not speculate on the mechanism behind this observation, miR-24's targeting of CSF1R could offer a mechanistic explanation.

7 General Discussion

The aim of my PhD project was to investigate miR signatures in peripheral blood monocytes of patients with therapy-resistant RA. We hypothesised that epigenetic changes, and in particular miR dysregulation, contributes to the pathogenic phenotype of difficult to treat disease. We believed that investigating peripheral blood monocytes would be of particular importance, since these cells serve as central orchestrators of the many other pathogenic cells in RA, including inflammatory macrophages, dendritic cells and osteoclasts.

To study specific molecular signatures that may be associated with therapeutic resistance requires a meticulous approach using highly phenotyped patients. This phenotyping and the decision to opt for purification of a specific cell population were underlying factors designed to increase the likelihood of success for this project.

Firstly we identified clinically distinct groups of patients with established RA who either had well-controlled disease on two or less first line medications or who had progressed to require multiple DMARDs and then biologic agents, and exhibited serial therapeutic resistance. It is now well established that approximately 30% of patients gain clinical benefit from treatment with a single DMARD agent such as MTX, and thereafter progress little and have limited need of other therapeutics. Others are progressors of variable rapidity, thus representing functionally distinct subsets of RA patients [63]. It has been thought that longstanding disease has a stable underlying pathogenic signature; failure of response to initial treatment is a poor prognostic factor for future therapies [355]. However, it should be noted that the underlying phenotype of immunity in RA need not necessarily be a constant over time and as such a reappraisal of the immune status in patients with discrete phenotypes seems reasonable. Therefore, patients with specific therapeutic responses were selected for this study in order to investigate whether underlying pathogenic signatures represent a possible route to identifying functionally relevant endotypes.

For the purpose of this study profiling of the total $CD14^{+}$ population was conducted. Recently, distinct monocyte subsets, such as CD14+CD16+ cells, were

implicated in RA pathogenesis [227]. Profiling of the miR signature of these subsets would be an interesting subject to explore in my future work. Nevertheless, the purified $CD14^+$ peripheral blood monocytes isolated from the various patient groups were subjected to miR array analysis, and yielded dysregulated miR species. From these, I decided to further investigate the miR-23a~24-27a cluster, which was downregulated in both groups of difficult to treat patients when compared to good responders.

First and foremost, my analyses identified IL-6R pathway as a potential candidate target of this cluster. High IL-6 serum levels, mirroring cluster dysregulation were found in all treatment failure patients, supporting this hypothesis. Investigation of the function of miR-23a~24-2~27a cluster implicated miR-23a and miR-27a in an IL-6 regulatory pathway feedback loop. Specifically, IL-6 signalling of $CD14^+$ monocytes reduces the expression of the miR-23a cluster, which in turn de-represses its direct targets namely IL-6R and JAK/STAT signalling molecules (demonstrated by [765]), thus rendering cells more responsive to IL-6. Compatible with this, I have demonstrated that functional knockdown of miR-23a and miR-27a in THP-1 sponge cells results in increased expression of soluble IL-6R, which serves as an (accessory) alarmin and empowers cells not otherwise expressing IL-6R to become sensitive to the effects of IL-6 cytokine by virtue of trans signalling. Commensurate with this, I found raised expression of IL-6R transcripts and serum levels of soluble IL-6R in the biologics resistant patient group, consistent with an important role for these pathways. During RA inflammation, activated macrophages, as well as activated FLSs and B cells, are the major source of IL-6; it is possible that this regulatory feedback loop could operate in other lineages and this should be investigated in future [90,160,786].

Additionally, I have discovered that the miR-23a cluster expression is regulated by cytokines with dominant antiviral properties, namely IFNγ and IFNß. Some years ago, raised levels of IFNγ were found in synovial fluid from patients with RA and were associated with a notional pathogenic T_H1 response [90,93]. More recently, activated T cells producing both IFNγ and IL-17 were identified in RA providing another mechanism by which antiviral responses within a chronic inflammatory setting such as RA can potentially trigger suppression of miR-23a cluster in an IL-6 independent way [98]. This hypothesis needs further

exploration in primary blood-derived monocytes. Nevertheless, this is the first study to my knowledge to provide a mechanism by which antiviral cytokines such as the interferons can ultimately influence IL-6 pathway activation by regulating IL-6R levels via miR-23a and miR-27a.

Interestingly, the ability to regulate the miR-23a cluster was demonstrated with IFNß but not IFNα. This is somewhat contrary to what one would expect, not least of all as these cytokines share intracellular JAK/STAT signalling pathways [468]. Moreover, a distinct IFNα signature was reported in a subgroup of RA patients, which was associated with increased activity of the innate immune system, consistent with my hypothesis [457]. pDCs are a major source of INFα, while IFNß expression is attributed to activated FLSs cells in RA [283,458]. This provides an interesting scenario whereby FLSs secrete mediators capable of suppressing miR-23a cluster expression in blood-derived monocytes and thus promoting IL-6 sensitivity (Figure 7.1). Exploring these pathways in primary cells, as well as understanding how this influences monocyte-T cell or -FLS cross talk in arthritic joints would be an interesting and enticing task for me, going forward.

Next, I have identified that monocyte maturation processes governed by M-CSF or GM-CSF growth factors induce rapid suppression of miR-23a~24-2~27a cluster. Both of these cytokines are indispensable for maturation of inflammatory monocytes into macrophages, osteoclasts and DCs in the RA synovium. In turn, miR-24 directly targets and regulates expression of CSF1R. This suggests that stimulation with M-CSF could promote expression of its receptor by suppressing miR-24 (Figure 7.1). Additionally, blood-derived monocytes exposed to IL-6 or antiviral mediators like IFNß and IFNγ could elevate CSF1R expression by inhibiting miR-23a cluster expression and promoting maturation of cells (Figure 7.1). In fact, the ability of IL-6 to promote M-CSF-driven maturation has been recognised previously, however, a mechanism for this phenomenon was never described [373].

Finally, my data implicate miR-24 in the regulation of MTHFR and potential implications for MTX tolerability. This again would require further assessment in an independent cohort of RA patients, receiving MTX as a first DMARD. This investigation would allow assessment of potential biomarker properties of the miR-23a~miR-24-2~27a cluster.

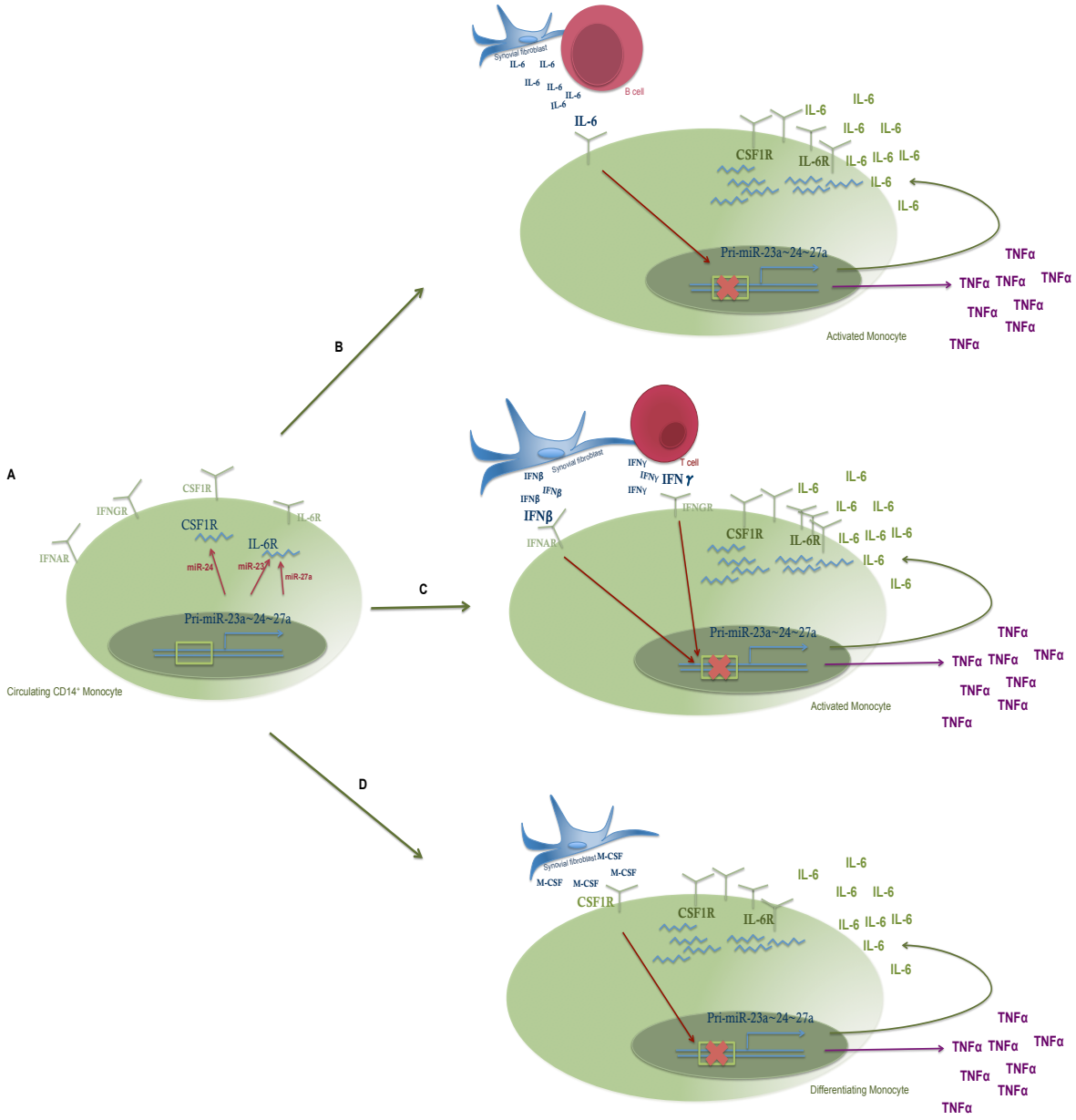

Figure 7.1 Summary of the proposed miR-23a~miR-27a~IL-6R in RA.

(**A**) A steady state of circulating monocyte with high expression of miR-23a~24~27a cluster. (**B**) Shows proposed IL-6/IL-6R/miR-23a/miR-27a regulatory pathway in activated monocytes. (**C**) Depicts proposed effect of IFNβ and IFNγ on miR-23a~24~27a cluster expression in monocyte activation. (**D**) Summary of the effect of M-CSF driven monocyte maturation on miR-23a~24~27a cluster and expression of pro-inflammatory cytokines.

The stability of serum miRs and easy measurement renders them good potential biomarkers that could be of clinical use. In fact, upregulation of miR-23a alongside miR-223 was suggested as biomarkers of clinical response to TNFα/DMARDs combination treatment in patients with early RA [642]. Going forward I would like to explore the biomarker potential of miR-23a and miR-27a for prediction of IL-6 and JAK inhibitor treatments, while it would be interesting to evaluate miR-24 in the context of MTX tolerability. Having a clear idea of the mechanism behind the function of this miR cluster helps to understand how they interplay with disease pathogenesis and effect of drugs, thus improving their biomarker potential.

In summary, data contained herein confirm a postulated anti-inflammatory role for the miR-23a~24-2~27a cluster in the context of RA monocytes and suggests that dysregulation of this miR cluster could impose significant consequences upon implicated cells, resulting in production of pro-inflammatory cytokines, such as TNFα and IL-6, via a pathogenic feedback loop thus promoting chronicity. My studies in the longer term have greater consequence beyond this specific pathway. They lay out a framework upon which to develop novel biomarker profiles that have functional coherence and plausibility. I am now about to embark on more detailed analyses using highly phenotyped clinical cohorts contained in the Scottish Early RA Cohort. Moreover they give reason to believe that there are endotypes contained within the wider RA population that will have functional, prognostic and therapeutic consequence. That discrete immunologic setpoints exist in RA manifest in discrete miR expression in monocytes in the blood compartment strongly alludes that the existence of such endotpyes has at least some epigenetic underpinning. This in turn can offer future therapeutic options – either by directly targeting miRs or by using them as bait to elucidate novel pathways by virtue of their identified target pathways. As such they speak to an exciting future in the area of integrated biomarker and pathogenesis studies.

Bibliography

1. Scott DL, Coulton BL, Symmons DPM, Popert AJ. LONG-TERM OUTCOME OF TREATING RHEUMATOID ARTHRITIS: RESULTS AFTER 20 YEARS. The Lancet. Elsevier; 1987;329:1108–11.

2. Robertson J, Peters MJ, McInnes IB, Sattar N. Changes in lipid levels with inflammation and therapy in RA: a maturing paradigm. Nat Rev Rheumatol. 2013;9:513–23.

3. Dale J, Paterson C, Tierney A, Ralston SH, Reid DM, Basu N, et al. The Scottish Early Rheumatoid Arthritis (SERA) Study: an inception cohort and biobank. BMC Musculoskeletal Disorders. BioMed Central; 2016;17:461.

4. Sparks JA, Chang S-C, Liao KP, Lu B, Fine AR, Solomon DH, et al. Rheumatoid Arthritis and Mortality Among Women During 36 Years of Prospective Follow-Up: Results From the Nurses' Health Study. Arthritis Care Res (Hoboken). 2016;68:753–62.

5. Solomon DH. Cardiovascular Morbidity and Mortality in Women Diagnosed With Rheumatoid Arthritis. Circulation. 2003;107:1303–7.

6. BENNETT GA, COBB S, JACOX R, JESSAR RA, ROPES MW. Proposed diagnostic criteria for rheumatoid arthritis. Bull Rheum Dis. 1956;7:121–4.

7. Arnett FC, Edworthy SM, Bloch DA, McShane DJ, Fries JF, Cooper NS, et al. The American Rheumatism Association 1987 revised criteria for the classification of rheumatoid arthritis. Arthritis Rheum. 1988;31:315–24.

8. Council TJCOTMR, Nuffield Foundation on Clinical Trials of Cortisone, A.C.T.H., Diseases OTMICR. A COMPARISON of cortisone and aspirin in the treatment of early cases of rheumatoid arthritis; a report by the Joint Committee of the Medical Research Council and Nuffield Foundation on Clinical Trials of Cortisone, A.C.T.H., and Other Therapeutic Measures in Chronic Rheumatic Diseases. Br Med J. BMJ Group; 1954;1:1223–7.

9. Smyth CJ. Indomethacin in rheumatoid arthritis. A comparative objective evaluation with adrenocorticosteroids. Arthritis Rheum. 1965;8:921–42.

10. Chandler GN. INTRA-ARTICULAR THERAPY IN RHEUMATOID ARTHRITIS. The Lancet. 1958;272:1336.

11. Weiser HI. INTRA-ARTICULAR THERAPY IN RHEUMATOID ARTHRITIS. The Lancet. 1958;272:1182.

12. Rylance HJ, Chalmers TM, Elton RA. Clinical trials of intra-articular aspirin in rheumatoid arthritis. Lancet. 1980;2:1099–102.

13. Gross D, Enderlin M, Fehr K. [Immunosuppresive therapy of progredient chronic polyarthritis using antimetabolites and cytostatics]. Schweiz Med Wochenschr. 1967;97:1301–10.

14. Urowitz MB, Gordon DA, Smythe HA, Pruzanski W, Ogryzio MA. Azathioprine in rheumatoid arthritis. A double-blind, cross over study. Arthritis Rheum. 1973;16:411–8.

15. Mason M, Currey HL, Barnes CG, Dunne JF, Hazleman BL, Strickland ID. Azathioprine in rheumatoid arthritis. Br Med J. 1969;1:420–2.

16. Currey HL, Harris J, Mason RM, Woodland J, Beveridge T, Roberts CJ, et al. Comparison of azathioprine, cyclophosphamide, and gold in treatment of rheumatoid arthritis. Br Med J. 1974;3:763–6.

17. Sigler JW, Bluhm GB, Duncan H, Sharp JT, Ensign DC, McCrum WR. Gold salts in the treatment of rheumatoid arthritis. A double-blind study. Ann. Intern. Med. 1974;80:21–6.

18. O'BRIEN WM. A controlled trial of gold salt therapy in rheumatoid arthritis. Arthritis Rheum. 1973;16:353–8.

19. Sharp JT, Lidsky MD, Duffy J. Clinical responses during gold therapy for rheumatoid arthritis. Changes in synovitis, radiologically detectable erosive lesions, serum proteins, and serologic abnormalities. Arthritis Rheum. 1982;25:540–9.

20. Menkes CJ. Is there a place for chemical and radiation synovectomy in rheumatic diseases? Rheumatol Rehabil. 1979;18:65–77.

21. Strober S, Tanay A, Field E, Hoppe RT, Calin A, Engleman EG, et al. Efficacy of total lymphoid irradiation in intractable rheumatoid arthritis. A double-blind, randomized trial. Ann. Intern. Med. 1985;102:441–9.

22. Trentham DE, Weinblatt ME, Austen KF. Total lymphoid irradiation in tertiary care for rheumatoid arthritis. Ann. Intern. Med. 1985;102:544–5.

23. Paulus HE. The use of combinations of disease-modifying antirheumatic agents in rheumatoid arthritis. Arthritis Rheum. 1990;33:113–20.

24. McCarty DJ, Carrera GF. Intractable rheumatoid arthritis. Treatment with combined cyclophosphamide, azathioprine, and hydroxychloroquine. JAMA. 1982;248:1718–23.

25. Ward JR. Role of disease-modifying antirheumatic drugs versus cytotoxic agents in the therapy of rheumatoid arthritis. Am. J. Med. 1988;85:39–44.

26. Iannuzzi L, Dawson N, Zein N, Kushner I. Does drug therapy slow radiographic deterioration in rheumatoid arthritis? N. Engl. J. Med. 1983;309:1023–8.

27. Weinblatt ME, Coblyn JS, Fox DA, Fraser PA, Holdsworth DE, Glass DN, et al. Efficacy of low-dose methotrexate in rheumatoid arthritis. N. Engl. J. Med. Massachusetts Medical Society; 1985;312:818–22.

28. Pullar T, Hunter JA, Capell HA. Sulphasalazine in rheumatoid arthritis: a double blind comparison of sulphasalazine with placebo and sodium aurothiomalate. Br Med J (Clin Res Ed). BMJ Group; 1983;287:1102–4.

29. Wenger ME, Alexander S, Bland JH, Blechman WJ. Auranofin versus placebo

in the treatment of rheumatoid arthritis. Am. J. Med. 1983;75:123–7.

30. Bunch TW, O'Duffy JD, Tompkins RB, O'Fallon WM. Controlled trial of hydroxychloroquine and D-penicillamine singly and in combination in the treatment of rheumatoid arthritis. Arthritis Rheum. 1984;27:267–76.

31. Dougados M, Amor B. Cyclosporin A in rheumatoid arthritis: preliminary clinical results of an open trial. Arthritis Rheum. 1987;30:83–7.

32. Sinclair RJ, Duthie JJ. Salazopyrin in the Treatment of Rheumatoid Arthritis. Ann. Rheum. Dis. 1949;8:226–31.

33. Van der Heijde DM, van Riel PL, Nuver-Zwart IH, Gribnau FW, vad de Putte LB. Effects of hydroxychloroquine and sulphasalazine on progression of joint damage in rheumatoid arthritis. Lancet. 1989;1:1036–8.

34. Van der Heijde DM, van Riel PL, Nuver-Zwart IH, van de Putte LB. Sulphasalazine versus hydroxychloroquine in rheumatoid arthritis: 3-year follow-up. Lancet. 1990;335:539.

35. Hannonen P, Möttönen T, Hakola M, Oka M. Sulfasalazine in early rheumatoid arthritis. A 48-week double-blind, prospective, placebo-controlled study. Arthritis Rheum. 1993;36:1501–9.

36. Weber CK, Liptay S, Wirth T, Adler G, Schmid RM. Suppression of NF-kappaB activity by sulfasalazine is mediated by direct inhibition of IkappaB kinases alpha and beta. Gastroenterology. 2000;119:1209–18.

37. Okada Y, Wu D, Trynka G, Raj T, Terao C, Ikari K, et al. Genetics of rheumatoid arthritis contributes to biology and drug discovery. Nature. 2014;506:376–81.

38. Lawrence T, Natoli G. Transcriptional regulation of macrophage polarization: enabling diversity with identity. Nat. Rev. Immunol. Nature Publishing Group; 2011;11:750–61.

39. Li P, Schwarz EM, O'Keefe RJ, Ma L, Boyce BF, Xing L. RANK signaling is not required for TNFalpha-mediated increase in CD11(hi) osteoclast precursors but is essential for mature osteoclast formation in TNFalpha-mediated inflammatory arthritis. J. Bone Miner. Res. John Wiley and Sons and The American Society for Bone and Mineral Research (ASBMR); 2004;19:207–13.

40. Moreno JL, Kaczmarek M, Keegan AD, Tondravi M. IL-4 suppresses osteoclast development and mature osteoclast function by a STAT6-dependent mechanism: irreversible inhibition of the differentiation program activated by RANKL. Blood. American Society of Hematology; 2003;102:1078–86.

41. Jones JR, Barrick C, Kim K-A, Lindner J, Blondeau B, Fujimoto Y, et al. Deletion of PPARgamma in adipose tissues of mice protects against high fat diet-induced obesity and insulin resistance. Proceedings of the National Academy of Sciences. National Acad Sciences; 2005;102:6207–12.

42. MacMullan PA, Madigan AM, Paul N, Peace AJ, Alagha A, Nolan KB, et al. Sulfasalazine and its metabolites inhibit platelet function in patients with

inflammatory arthritis. Clin. Rheumatol. Springer London; 2016;35:447–55.

43. Cutolo M, Bisso A, Sulli A, Felli L, Briata M, Pizzorni C, et al. Antiproliferative and antiinflammatory effects of methotrexate on cultured differentiating myeloid monocytic cells (THP-1) but not on synovial macrophages from patients with rheumatoid arthritis. J. Rheumatol. 2000;27:2551–7.

44. Cohen HB, Briggs KT, Marino JP, Ravid K, Robson SC, Mosser DM. TLR stimulation initiates a CD39-based autoregulatory mechanism that limits macrophage inflammatory responses. Blood. 2013;122:1935–45.

45. Fishman P, Cohen S. The A3 adenosine receptor (A3AR): therapeutic target and predictive biological marker in rheumatoid arthritis. Clin. Rheumatol. 2016;35:2359–62.

46. Hall GH, Jones BJ, Head AC, Jones VE. Intra-articular methotrexate. Clinical and laboratory study in rheumatoid and psoriatic arthritis. Ann. Rheum. Dis. 1978;37:351–6.

47. Weinblatt ME, Trentham DE, Fraser PA, Holdsworth DE, Falchuk KR, Weissman BN, et al. Long-term prospective trial of low-dose methotrexate in rheumatoid arthritis. Arthritis Rheum. 1988;31:167–75.

48. Andersen PA, West SG, O'Dell JR, Via CS, Claypool RG, Kotzin BL. Weekly pulse methotrexate in rheumatoid arthritis. Clinical and immunologic effects in a randomized, double-blind study. Ann. Intern. Med. 1985;103:489–96.

49. Morgan SL, Baggott JE, Vaughn WH, Young PK, Austin JV, Krumdieck CL, et al. The effect of folic acid supplementation on the toxicity of low-dose methotrexate in patients with rheumatoid arthritis. Arthritis Rheum. 1990;33:9–18.

50. Alarcóan GS, Billingsley LM, Clegg DO, Hardin JG, Klippel J, Luggen ME, et al. Lack of association between hla–dr2 and clinical response to methotrexate in patients with rheumatoid arthritis. Arthritis Rheum. John Wiley & Sons, Inc; 1987;30:218–20.

51. Kremer JM, Rynes RI, Bartholomew LE. Severe flare of rheumatoid arthritis after discontinuation of long-term methotrexate therapy. Double-blind study. Am. J. Med. 1987;82:781–6.

52. Mackenzie AH. Antimalarial drugs for rheumatoid arthritis. Am. J. Med. 1983;75:48–58.

53. A randomized trial of hydroxychloroquine in early rheumatoid arthritis: the HERA Study. Am. J. Med. 1995;98:156–68.

54. Fox RI. Mechanism of action of hydroxychloroquine as an antirheumatic drug. Semin. Arthritis Rheum. 1993;23:82–91.

55. Paulus HE, Egger MJ, Ward JR, James Williams H. Analysis of improvement in individual rheumatoid arthritis patients treated with disease-modifying antirheumatic drugs, based on the findings in patients treated with placebo. Arthritis Rheum. John Wiley & Sons, Inc; 1990;33:477–84.

56. Williams HJ. Combination second-line therapy for rheumatoid arthritis. Br. J. Rheumatol. 1994;33:603–4.

57. Wilske KR, Healey LA. Remodeling the pyramid--a concept whose time has come. J. Rheumatol. 1989;16:565–7.

58. Nisar M, Carlisle L, Amos RS. Methotrexate and sulphasalazine as combination therapy in rheumatoid arthritis. Br. J. Rheumatol. 1994;33:651–4.

59. O'Dell JR, Leff R, Paulsen G, Haire C, Mallek J, Eckhoff PJ, et al. Treatment of rheumatoid arthritis with methotrexate and hydroxychloroquine, methotrexate and sulfasalazine, or a combination of the three medications: results of a two-year, randomized, double-blind, placebo-controlled trial. Arthritis Rheum. Wiley Subscription Services, Inc., A Wiley Company; 2002;46:1164–70.

60. O'Dell JR, Haire CE, Erikson N, Drymalski W, Palmer W, Eckhoff PJ, et al. Treatment of rheumatoid arthritis with methotrexate alone, sulfasalazine and hydroxychloroquine, or a combination of all three medications. N. Engl. J. Med. Massachusetts Medical Society; 1996;334:1287–91.

61. Calgüneri M, Pay S, Calişkaner Z, Apraş S, Kiraz S, Ertenli I, et al. Combination therapy versus monotherapy for the treatment of patients with rheumatoid arthritis. Clin. Exp. Rheumatol. 1999;17:699–704.

62. Möttönen T, Hannonen P, Leirisalo-Repo M, Nissilä M, Kautiainen H, Korpela M, et al. Comparison of combination therapy with single-drug therapy in early rheumatoid arthritis: a randomised trial. FIN-RACo trial group. Lancet. 1999;353:1568–73.

63. O'Dell JR, Haire C, Erikson N, Drymalski W, Palmer W, Maloley P, et al. Efficacy of triple DMARD therapy in patients with RA with suboptimal response to methotrexate. J Rheumatol Suppl. 1996;44:72–4.

64. Grigor C, Capell H, Stirling A, McMahon AD, Lock P, Vallance R, et al. Effect of a treatment strategy of tight control for rheumatoid arthritis (the TICORA study): a single-blind randomised controlled trial. The Lancet. 2004;364:263–9.

65. Saunders SA, Capell HA, Stirling A, Vallance R, Kincaid W, McMahon AD, et al. Triple therapy in early active rheumatoid arthritis: A randomized, single-blind, controlled trial comparing step-up and parallel treatment strategies. Arthritis Rheum. Wiley Subscription Services, Inc., A Wiley Company; 2008;58:1310–7.

66. O'Dell JR, Curtis JR, Mikuls TR, Cofield SS, Bridges SL, Ranganath VK, et al. Validation of the methotrexate-first strategy in patients with early, poor-prognosis rheumatoid arthritis: results from a two-year randomized, double-blind trial. Arthritis Rheum. 2013;65:1985–94.

67. Porter D. Intensive management of early rheumatoid arthritis: the TICORA and TEAR studies. Clin. Exp. Rheumatol. 2012;30:S32–4.

68. Van der Heijde DM, van 't Hof MA, van Riel PL, Theunisse LA, Lubberts EW, van Leeuwen MA, et al. Judging disease activity in clinical practice in

rheumatoid arthritis: first step in the development of a disease activity score. Ann. Rheum. Dis. 1990;49:916–20.

69. Van der Heijde DM, van 't Hof M, van Riel PL, van de Putte LB. Validity of single variables and indices to measure disease activity in rheumatoid arthritis. J. Rheumatol. 1993;20:538–41.

70. Goekoop-Ruiterman YPM, de Vries-Bouwstra JK, Kerstens PJSM, Nielen MMJ, Vos K, van Schaardenburg D, et al. DAS-driven therapy versus routine care in patients with recent-onset active rheumatoid arthritis. Ann. Rheum. Dis. 2010;69:65–9.

71. Wells G, Becker J-C, Teng J, Dougados M, Schiff M, Smolen J, et al. Validation of the 28-joint Disease Activity Score (DAS28) and European League Against Rheumatism response criteria based on C-reactive protein against disease progression in patients with rheumatoid arthritis, and comparison with the DAS28 based on erythrocyte sedimentation rate. Ann. Rheum. Dis. 2009;68:954–60.

72. van Riel PLCM. The development of the disease activity score (DAS) and the disease activity score using 28 joint counts (DAS28). Clin. Exp. Rheumatol. 2014;32:S–65–74.

73. Marhadour T, JOUSSE-JOULIN S, CHALES G, GRANGE L, HACQUARD C, LOEUILLE D, et al. Reproducibility of Joint Swelling Assessments in Long-lasting Rheumatoid Arthritis: Influence on Disease Activity Score-28 Values (SEA-Repro Study Part I). J. Rheumatol. [Internet]. 2010;37:932–7. Available from: http://www.jrheum.org/cgi/doi/10.3899/jrheum.090879

74. Dale J, Stirling A, Zhang R, Purves D, Foley J, Sambrook M, et al. Targeting ultrasound remission in early rheumatoid arthritis: the results of the TaSER study, a randomised clinical trial. Ann. Rheum. Dis. 2016;75:1043–50.

75. Haavardsholm EA, Aga A-B, Olsen IC, Lillegraven S, Hammer HB, Uhlig T, et al. Ultrasound in management of rheumatoid arthritis: ARCTIC randomised controlled strategy trial. BMJ. 2016;354:i4205.

76. Deighton C, Deighton C, Hyrich K, Hyrich K, Ding T, Ding T, et al. BSR and BHPR rheumatoid arthritis guidelines on eligibility criteria for the first biological therapy. Rheumatology [Internet]. 2010;49:1197–9. Available from: http://rheumatology.oxfordjournals.org/content/49/6/1197.long

77. Smolen JS. A simplified disease activity index for rheumatoid arthritis for use in clinical practice. Rheumatology. 2003;42:244–57.

78. Aletaha D, Funovits J, Keystone EC, Smolen JS. Disease activity early in the course of treatment predicts response to therapy after one year in rheumatoid arthritis patients. Arthritis Rheum. Wiley Subscription Services, Inc., A Wiley Company; 2007;56:3226–35.

79. Aletaha D, Nell VPK, Stamm T, Uffmann M, Pflugbeil S, Machold K, et al. Acute phase reactants add little to composite disease activity indices for rheumatoid arthritis: validation of a clinical activity score. Arthritis Res. Ther. 2005;7:R796–806.

80. Anderson J, Caplan L, Yazdany J, Robbins ML, Neogi T, Michaud K, et al. Rheumatoid arthritis disease activity measures: American College of Rheumatology recommendations for use in clinical practice. Arthritis Care Res (Hoboken) [Internet]. 2012;64:640–7. Available from: http://doi.wiley.com/10.1002/acr.21649

81. Felson DT, Anderson JJ, Boers M, Bombardier C, Chernoff M, Fried B, et al. The American college of rheumatology preliminary core set of disease activity measures for rheumatoid arthritis clinical trials. Arthritis Rheum. John Wiley & Sons, Inc; 1993;36:729–40.

82. Felson DT, Anderson JJ, Boers M, Bombardier C, Furst D, Goldsmith C, et al. American College of Rheumatology. Preliminary definition of improvement in rheumatoid arthritis. Arthritis Rheum. 1995;38:727–35.

83. Pincus T, Stein CM. ACR 20: clinical or statistical significance? Arthritis Rheum. 1999;42:1572–6.

84. Felson DT, Anderson JJ, Lange MLM, Wells G, LaValley MP. Should imporvement in rheumatoid arthritis clinical trials be defined as fifty percent or seventy percent improvement in core set measures, rather than twenty percent? Arthritis Rheum. John Wiley & Sons, Inc; 1998;41:1564–70.

85. van Gestel AM, Anderson JJ, van Riel PL, Boers M, Haagsma CJ, Rich B, et al. ACR and EULAR improvement criteria have comparable validity in rheumatoid arthritis trials. American College of Rheumatology European League of Associations for Rheumatology. J. Rheumatol. 1999;26:705–11.

86. Felson DT, Smolen JS, Wells G, Zhang B, van Tuyl LHD, Funovits J, et al. American College of Rheumatology/European League Against Rheumatism Provisional Definition of Remission in Rheumatoid Arthritis for Clinical Trials. Ann. Rheum. Dis. BMJ Publishing Group Ltd and European League Against Rheumatism; 2011;70:404–13.

87. O'Dell JR, Mikuls TR. To improve outcomes we must define and measure them: toward defining remission in rheumatoid arthritis. Arthritis Rheum. Wiley Subscription Services, Inc., A Wiley Company; 2011;63:587–9.

88. Holoshitz J. The rheumatoid arthritis HLA–DRB1 shared epitope. Curr Opin Rheumatol. 2010;22:293–8.

89. Silman AJ, MACGREGOR AJ, Thomson W, HOLLIGAN S, CARTHY D, FARHAN A, et al. TWIN CONCORDANCE RATES FOR RHEUMATOID ARTHRITIS: RESULTS FROM A NATIONWIDE STUDY. Rheumatology. 1993;32:903–7.

90. McInnes IB, Schett G. Cytokines in the pathogenesis of rheumatoid arthritis. Nat. Rev. Immunol. 2007;7:429–42.

91. Toh M-L, Miossec P. The role of T cells in rheumatoid arthritis: new subsets and new targets. Curr Opin Rheumatol. 2007;19:284–8.

92. Lundy SK, Sarkar S, Tesmer LA, Fox DA. Arthritis Res. Ther. 2007;9:202.

93. Wilson CB, Rowell E, Sekimata M. Epigenetic control of T-helper-cell

differentiation. Nat. Rev. Immunol. 2009;9:91–105.

94. Ho I-C, Tai T-S, Pai S-Y. GATA3 and the T-cell lineage: essential functions before and after T-helper-2-cell differentiation. Nat. Rev. Immunol. 2009;9:125–35.

95. Leavy O. T-cell development: CD40–CD40L crosstalk in TH17-cell differentiation. Nat. Rev. Immunol. 2009;9:76–6.

96. Niedbala W, Besnard A-G, Nascimento DC, Donate PB, Sonego F, Yip E, et al. Nitric oxide enhances Th9 cell differentiation and airway inflammation. Nat Commun. 2014;5:4575.

97. van den Berg WB, Miossec P. IL-17 as a future therapeutic target for rheumatoid arthritis. Nat Rev Rheumatol. 2009;5:549–53.

98. Cosmi L, Cimaz R, Maggi L, Santarlasci V, Capone M, Borriello F, et al. Evidence of the transient nature of the Th17 phenotype of CD4+CD161+ T cells in the synovial fluid of patients with juvenile idiopathic arthritis. Arthritis Rheum. 2011;63:2504–15.

99. Nistala K, Adams S, Cambrook H, Ursu S, Olivito B, de Jager W, et al. Th17 plasticity in human autoimmune arthritis is driven by the inflammatory environment. Proceedings of the National Academy of Sciences. 2010;107:14751–6.

100. Nistala K, Moncrieffe H, Newton KR, Varsani H, Hunter P, Wedderburn LR. Interleukin-17–producing T cells are enriched in the joints of children with arthritis, but have a reciprocal relationship to regulatory T cell numbers. Arthritis Rheum. 2008;58:875–87.

101. Alonso MN, Wong MT, Zhang AL, Winer D, Suhoski MM, Tolentino LL, et al. TH1, TH2, and TH17 cells instruct monocytes to differentiate into specialized dendritic cell subsets. Blood. 2011;118:3311–20.

102. Campbell IK, van Nieuwenhuijze A, Segura E, O'Donnell K, Coghill E, Hommel M, et al. Differentiation of Inflammatory Dendritic Cells Is Mediated by NF- B1-Dependent GM-CSF Production in CD4 T Cells. The Journal of Immunology. 2011;186:5468–77.

103. Sakaguchi S, Ono M, Setoguchi R, Yagi H, Hori S, Fehervari Z, et al. Foxp3+CD25+CD4+ natural regulatory T cells in dominant self-tolerance and autoimmune disease. Immunological Reviews. 2006;212:8–27.

104. Herrath J, Müller M, Amoudruz P, Janson P, Michaëlsson J, Larsson PT, et al. The inflammatory milieu in the rheumatic joint reduces regulatory T-cell function. European Journal of Immunology. 2011;41:2279–90.

105. Wehrens EJ, Mijnheer G, Duurland CL, Klein M, Meerding J, van Loosdregt J, et al. Functional human regulatory T cells fail to control autoimmune inflammation due to PKB/c-akt hyperactivation in effector cells. Blood. 2011;118:3538–48.

106. Korn T, Reddy J, Gao W, Bettelli E, Awasthi A, Petersen TR, et al. Myelin-

specific regulatory T cells accumulate in the CNS but fail to control autoimmune inflammation. Nat. Med. 2007;13:423–31.

107. O'Connor RA, Malpass KH, Anderton SM. The Inflamed Central Nervous System Drives the Activation and Rapid Proliferation of Foxp3+ Regulatory T Cells. The Journal of Immunology. 2007;179:958–66.

108. Chauhan SK, Annan El J, Ecoiffier T, Goyal S, Zhang Q, Saban DR, et al. Autoimmunity in Dry Eye Is Due to Resistance of Th17 to Treg Suppression. The Journal of Immunology. 2009;182:1247–52.

109. Stummvoll GH, DiPaolo RJ, Huter EN, Davidson TS, Glass D, Ward JM, et al. Th1, Th2, and Th17 Effector T Cell-Induced Autoimmune Gastritis Differs in Pathological Pattern and in Susceptibility to Suppression by Regulatory T Cells. The Journal of Immunology. 2008;181:1908–16.

110. van Amelsfort JMR, van Roon JAG, Noordegraaf M, Jacobs KMG, Bijlsma JWJ, Lafeber FPJG, et al. Proinflammatory mediator–induced reversal of CD4+,CD25+ regulatory T cell–mediated suppression in rheumatoid arthritis. Arthritis Rheum. 2007;56:732–42.

111. Baecher-Allan C, Viglietta V, Hafler DA. Inhibition of Human CD4+CD25+high Regulatory T Cell Function. The Journal of Immunology. 2002;169:6210–7.

112. Ashley CW, Baecher-Allan C. Cutting Edge: Responder T Cells Regulate Human DR+ Effector Regulatory T Cell Activity via Granzyme B. The Journal of Immunology. 2009;183:4843–7.

113. Chen X, Subleski JJ, Kopf H, Howard OMZ, Mannel DN, Oppenheim JJ. Cutting Edge: Expression of TNFR2 Defines a Maximally Suppressive Subset of Mouse CD4+CD25+FoxP3+ T Regulatory Cells: Applicability to Tumor-Infiltrating T Regulatory Cells. The Journal of Immunology. 2008;180:6467–71.

114. Valencia X. TNF downmodulates the function of human CD4+CD25hi T-regulatory cells. Blood. 2006;108:253–61.

115. BAYRY J, SIBERIL S, TRIEBEL F, TOUGH D, KAVERI S. Rescuing CD4+CD25+ regulatory T-cell functions in rheumatoid arthritis by cytokine-targeted monoclonal antibody therapy. Drug Discovery Today. 2007;12:548–52.

116. Nadkarni S, Mauri C, Ehrenstein MR. Anti–TNF-α therapy induces a distinct regulatory T cell population in patients with rheumatoid arthritis via TGF-β. Journal of Experimental Medicine. 2007;204:33–9.

117. McGovern JL, Nguyen DX, Notley CA, Mauri C, Isenberg DA, Ehrenstein MR. Th17 cells are restrained by Treg cells via the inhibition of interleukin-6 in patients with rheumatoid arthritis responding to anti-tumor necrosis factor antibody therapy. Arthritis Rheum. 2012;64:3129–38.

118. Coulthard LR, Geiler J, Mathews RJ, Church LD, Dickie LJ, Cooper DL, et al. Differential effects of infliximab on absolute circulating blood leucocyte counts of innate immune cells in early and late rheumatoid arthritis patients. Clin. Exp. Immunol. 2012;170:36–46.

119. Carvalheiro H, Duarte C, Silva-Cardoso S, da Silva JAP, Souto-Carneiro MM. CD8+ T Cell Profiles in Patients With Rheumatoid Arthritis and Their Relationship to Disease Activity. Arthritis & Rheumatology. 2015;67:363–71.

120. Cho B-A, Sim JH, Park JA, Kim HW, Yoo W-H, Lee S-H, et al. Characterization of Effector Memory CD8+ T Cells in the Synovial Fluid of Rheumatoid Arthritis. Journal of Clinical Immunology. 2012;32:709–20.

121. Romio M, Reinbeck B, Bongardt S, Huls S, Burghoff S, Schrader J. Extracellular purine metabolism and signaling of CD73-derived adenosine in murine Treg and Teff cells. AJP: Cell Physiology. 2011;301:C530–9.

122. Weinblatt ME, Maddison PJ, Bulpitt KJ, Hazleman BL, Urowitz MB, Sturrock RD, et al. CAMPATH-1H, a humanized monoclonal antibody, in refractory rheumatoid arthritis. An intravenous dose-escalation study. Arthritis Rheum. 1995;38:1589–94.

123. Olsen NJ, Brooks RH, Cush JJ, Lipsky PE, St Clair EW, Matteson EL, et al. A double-blind, placebo-controlled study of anti-CD5 immunoconjugate in patients with rheumatoid arthritis. The Xoma RA Investigator Group. Arthritis Rheum. 1996;39:1102–8.

124. van der Lubbe PA, Dijkmans BA, Markusse HM, Nässander U, Breedveld FC. A randomized, double-blind, placebo-controlled study of CD4 monoclonal antibody therapy in early rheumatoid arthritis. Arthritis Rheum. 1995;38:1097–106.

125. Genovese MC, Becker J-C, Schiff M, Luggen M, Sherrer Y, Kremer J, et al. Abatacept for rheumatoid arthritis refractory to tumor necrosis factor alpha inhibition. N Engl J Med. Massachusetts Medical Society; 2005;353:1114–23.

126. Weinblatt M, Combe B, Covucci A, Aranda R, Becker J-C, Keystone E. Safety of the selective costimulation modulator abatacept in rheumatoid arthritis patients receiving background biologic and nonbiologic disease-modifying antirheumatic drugs: A one-year randomized, placebo-controlled study. Arthritis Rheum. Wiley Subscription Services, Inc., A Wiley Company; 2006;54:2807–16.

127. Kremer JM, Genant HK, Moreland LW, Russell AS, Emery P, Abud-Mendoza C, et al. Results of a two-year followup study of patients with rheumatoid arthritis who received a combination of abatacept and methotrexate. Arthritis Rheum. Wiley Subscription Services, Inc., A Wiley Company; 2008;58:953–63.

128. Zaiss MM, Axmann R, Zwerina J, Polzer K, Gückel E, Skapenko A, et al. Treg cells suppress osteoclast formation: A new link between the immune system and bone. Arthritis Rheum. Wiley Subscription Services, Inc., A Wiley Company; 2007;56:4104–12.

129. Schett G, Gravallese E. Bone erosion in rheumatoid arthritis: mechanisms, diagnosis and treatment. Nat Rev Rheumatol. 2012;8:656–64.

130. Weinblatt ME, Schiff M, Valente R, van der Heijde D, Citera G, Zhao C, et al. Head-to-head comparison of subcutaneous abatacept versus adalimumab for rheumatoid arthritis: findings of a phase IIIb, multinational, prospective, randomized study. Arthritis Rheum. Wiley Subscription Services, Inc., A Wiley

Company; 2013;65:28–38.

131. Alzabin S, Abraham SM, Taher TE, Palfreeman A, Hull D, McNamee K, et al. Incomplete response of inflammatory arthritis to TNFα blockade is associated with the Th17 pathway. Ann. Rheum. Dis. BMJ Publishing Group Ltd and European League Against Rheumatism; 2012;71:1741–8.

132. Genovese MC, Durez P, Richards HB, Supronik J, Dokoupilová E, Mazurov V, et al. Efficacy and safety of secukinumab in patients with rheumatoid arthritis: a phase II, dose-finding, double-blind, randomised, placebo controlled study. Ann. Rheum. Dis. BMJ Publishing Group Ltd and European League Against Rheumatism; 2013;72:863–9.

133. Genovese MC, Durez P, Richards HB, Supronik J, Dokoupilová E, Aelion JA, et al. One-year efficacy and safety results of secukinumab in patients with rheumatoid arthritis: phase II, dose-finding, double-blind, randomized, placebo-controlled study. J. Rheumatol. The Journal of Rheumatology; 2014;41:414–21.

134. Genovese MC, Greenwald M, Cho C-S, Berman A, Jin L, Cameron GS, et al. A phase II randomized study of subcutaneous ixekizumab, an anti-interleukin-17 monoclonal antibody, in rheumatoid arthritis patients who were naive to biologic agents or had an inadequate response to tumor necrosis factor inhibitors. Arthritis Rheumatol. 2014;66:1693–704.

135. Pavelka K, Chon Y, Newmark R, Lin S-L, Baumgartner S, Erondu N. A study to evaluate the safety, tolerability, and efficacy of brodalumab in subjects with rheumatoid arthritis and an inadequate response to methotrexate. J. Rheumatol. 2015;42:912–9.

136. Mease PJ, McInnes IB, Kirkham B, Kavanaugh A, Rahman P, van der Heijde D, et al. Secukinumab Inhibition of Interleukin-17A in Patients with Psoriatic Arthritis. N Engl J Med. 2015;373:1329–39.

137. Janssen R. **A Study of the Effectiveness and Safety of Ustekinumab (STELARA) and CNTO 1959 Administered Under the Skin of Patients With Active Rheumatoid Arthritis, Despite Existing Methotrexate Therapy**

[Internet]. Available from: https://clinicaltrials.gov/ct2/show/results/NCT01645280?sect=X70156&term=ustekinumab+rheumatoid+arthritis&rank=1#outcome1

138. Kunkel HG, Williams RC. Rheumatoid Arthritis. Annual Review of Medicine. Annual Reviews 4139 El Camino Way, P.O. Box 10139, Palo Alto, CA 94303-0139, USA; 1964;15:37–52.

139. Feldmann M, Brennan FM, Maini RN. Rheumatoid Arthritis. Cell. 1996;85:307–10.

140. Edwards JC, Cambridge G. Sustained improvement in rheumatoid arthritis following a protocol designed to deplete B lymphocytes. Rheumatology. 2001;40:205–11.

141. Bugatti S, Vitolo B, Caporali R, Montecucco C, Manzo A. B cells in rheumatoid arthritis: from pathogenic players to disease biomarkers. Biomed Res

Int. Hindawi Publishing Corporation; 2014;2014:681678–14.

142. Tobón GJ, Izquierdo JH, Cañas CA. B lymphocytes: development, tolerance, and their role in autoimmunity-focus on systemic lupus erythematosus. Autoimmune Diseases. Hindawi Publishing Corporation; 2013;2013:827254–17.

143. LeBien TW, Tedder TF. B lymphocytes: how they develop and function. Blood. American Society of Hematology; 2008;112:1570–80.

144. Meffre E. The establishment of early B cell tolerance in humans: lessons from primary immunodeficiency diseases. Annals of the New York Academy of Sciences. Blackwell Publishing Inc; 2012;1246:1–10.

145. Samuels J, Ng Y-S, Coupillaud C, Paget D, Meffre E. Impaired early B cell tolerance in patients with rheumatoid arthritis. Journal of Experimental Medicine. Rockefeller University Press; 2005;201:1659–67.

146. Menard L, Samuels J, Ng Y-S, Meffre E. Inflammation-independent defective early B cell tolerance checkpoints in rheumatoid arthritis. Arthritis Rheum. Wiley Subscription Services, Inc., A Wiley Company; 2011;63:1237–45.

147. Rapetti L, Chavele K-M, Evans CM, Ehrenstein MR. B cell resistance to Fas-mediated apoptosis contributes to their ineffective control by regulatory T cells in rheumatoid arthritis. Ann. Rheum. Dis. BMJ Publishing Group Ltd and European League Against Rheumatism; 2015;74:294–302.

148. Bosello S, Youinou P, Daridon C, Tolusso B, Bendaoud B, Pietrapertosa D, et al. Concentrations of BAFF correlate with autoantibody levels, clinical disease activity, and response to treatment in early rheumatoid arthritis. J. Rheumatol. 2008;35:1256–64.

149. Bombardieri M, Kam N-W, Brentano F, Choi K, Filer A, Kyburz D, et al. A BAFF/APRIL-dependent TLR3-stimulated pathway enhances the capacity of rheumatoid synovial fibroblasts to induce AID expression and Ig class-switching in B cells. Ann. Rheum. Dis. BMJ Publishing Group Ltd and European League Against Rheumatism; 2011;70:1857–65.

150. Alsaleh G, François A, Knapp A-M, Schickel J-N, Sibilia J, Pasquali J-L, et al. Synovial fibroblasts promote immunoglobulin class switching by a mechanism involving BAFF. European Journal of Immunology. WILEY-VCH Verlag; 2011;41:2113–22.

151. Avalos AM, Busconi L, Marshak-Rothstein A. Regulation of autoreactive B cell responses to endogenous TLR ligands. Autoimmunity. 2010;43:76–83.

152. Herlands RA, Christensen SR, Sweet RA, Hershberg U, Shlomchik MJ. T Cell-Independent and Toll-like Receptor-Dependent Antigen-Driven Activation of Autoreactive B Cells. Immunity. 2008;29:249–60.

153. Sweet RA, Ols ML, Cullen JL, Milam AV, Yagita H, Shlomchik MJ. Facultative role for T cells in extrafollicular Toll-like receptor-dependent autoreactive B-cell responses in vivo. Proc. Natl. Acad. Sci. U.S.A. National Acad Sciences; 2011;108:7932–7.

154. Lundberg K, Bengtsson C, Kharlamova N, Reed E, Jiang X, Kallberg H, et al. Genetic and environmental determinants for disease risk in subsets of rheumatoid arthritis defined by the anticitrullinated protein/peptide antibody fine specificity profile. Ann. Rheum. Dis. 2013;72:652–8.

155. Amara K, Steen J, Murray F, Morbach H, Fernandez-Rodriguez BM, Joshua V, et al. Monoclonal IgG antibodies generated from joint-derived B cells of RA patients have a strong bias toward citrullinated autoantigen recognition. Journal of Experimental Medicine. 2013;210:445–55.

156. Bobbio-Pallavicini F, Alpini C, Caporali R, Avalle S, Bugatti S, Montecucco C. Autoantibody profile in rheumatoid arthritis during long-term infliximab treatment. Arthritis Res. Ther. 2004;6:R264.

157. Leadbetter EA, Rifkin IR, Hohlbaum AM, Beaudette BC, Shlomchik MJ, Marshak-Rothstein A. Chromatin–IgG complexes activate B cells by dual engagement of IgM and Toll-like receptors. Nature. Nature Publishing Group; 2002;416:603–7.

158. Lanzavecchia A. Antigen Uptake and Accumulation in Antigen-Specific B Cells. Immunological Reviews. Blackwell Publishing Ltd; 1987;99:39–51.

159. Takemura S, Klimiuk PA, Braun A, Goronzy JJ, Weyand CM. T cell activation in rheumatoid synovium is B cell dependent. The Journal of Immunology. American Association of Immunologists; 2001;167:4710–8.

160. Barr TA, Shen P, Brown S, Lampropoulou V, Roch T, Lawrie S, et al. B cell depletion therapy ameliorates autoimmune disease through ablation of IL-6-producing B cells. J. Exp. Med. Rockefeller University Press; 2012;209:1001–10.

161. Yeo L, Toellner K-M, Salmon M, Filer A, Buckley CD, Raza K, et al. Cytokine mRNA profiling identifies B cells as a major source of RANKL in rheumatoid arthritis. Ann. Rheum. Dis. BMJ Publishing Group Ltd and European League Against Rheumatism; 2011;70:2022–8.

162. Schlegel PM, Steiert I, Kötter I, Müller CA. B cells contribute to heterogeneity of IL-17 producing cells in rheumatoid arthritis and healthy controls. Rosenberger P, editor. PLoS ONE. 2013;8:e82580.

163. Einfeld DA, Brown JP, Valentine MA, Clark EA, Ledbetter JA. Molecular cloning of the human B cell CD20 receptor predicts a hydrophobic protein with multiple transmembrane domains. EMBO J. European Molecular Biology Organization; 1988;7:711–7.

164. Valentine MA, Meier KE, Rossie S, Clark EA. Phosphorylation of the CD20 phosphoprotein in resting B lymphocytes. Regulation by protein kinase C. J. Biol. Chem. 1989;264:11282–7.

165. Stashenko P, Nadler LM, Hardy R, Schlossman SF. Expression of cell surface markers after human B lymphocyte activation. Proceedings of the National Academy of Sciences. National Acad Sciences; 1981;78:3848–52.

166. Press OW, Appelbaum F, Ledbetter JA, Martin PJ, Zarling J, Kidd P, et al. Monoclonal antibody 1F5 (anti-CD20) serotherapy of human B cell lymphomas.

Blood. 1987;69:584–91.

167. Czuczman MS. Rituximab in Combination With Fludarabine Chemotherapy in Low-Grade or Follicular Lymphoma. Journal of Clinical Oncology. 2005;23:694–704.

168. Leget GA, Czuczman MS. Use of rituximab, the new FDA-approved antibody. Current Opinion in Oncology. 1998;10:548–51.

169. Emery P, Fleischmann R, Filipowicz-Sosnowska A, Schechtman J, Szczepanski L, Kavanaugh A, et al. The efficacy and safety of rituximab in patients with active rheumatoid arthritis despite methotrexate treatment: results of a phase IIB randomized, double-blind, placebo-controlled, dose-ranging trial. Arthritis Rheum. Wiley Subscription Services, Inc., A Wiley Company; 2006;54:1390–400.

170. Cohen SB, Emery P, Greenwald MW, Dougados M, Furie RA, Genovese MC, et al. Rituximab for rheumatoid arthritis refractory to anti-tumor necrosis factor therapy: Results of a multicenter, randomized, double-blind, placebo-controlled, phase III trial evaluating primary efficacy and safety at twenty-four weeks. Arthritis Rheum. Wiley Subscription Services, Inc., A Wiley Company; 2006;54:2793–806.

171. Keystone E, Burmester GR, Furie R, Loveless JE, Emery P, Kremer J, et al. Improvement in patient-reported outcomes in a rituximab trial in patients with severe rheumatoid arthritis refractory to anti-tumor necrosis factor therapy. Arthritis Rheum. Wiley Subscription Services, Inc., A Wiley Company; 2008;59:785–93.

172. Keystone E, Emery P, Peterfy CG, Tak PP, Cohen S, Genovese MC, et al. Rituximab inhibits structural joint damage in patients with rheumatoid arthritis with an inadequate response to tumour necrosis factor inhibitor therapies. Ann. Rheum. Dis. 2009;68:216–21.

173. Cohen SB, Keystone E, Genovese MC, Emery P, Peterfy C, Tak P-P, et al. Continued inhibition of structural damage over 2 years in patients with rheumatoid arthritis treated with rituximab in combination with methotrexate. Ann. Rheum. Dis. 2010;69:1158–61.

174. Keystone EC, Cohen SB, Emery P, Kremer JM, Dougados M, Loveless JE, et al. Multiple courses of rituximab produce sustained clinical and radiographic efficacy and safety in patients with rheumatoid arthritis and an inadequate response to 1 or more tumor necrosis factor inhibitors: 5-year data from the REFLEX study. J. Rheumatol. 2012;39:2238–46.

175. Vos K, Thurlings RM, Wijbrandts CA, van Schaardenburg D, Gerlag DM, Tak PP. Early effects of rituximab on the synovial cell infiltrate in patients with rheumatoid arthritis. Arthritis Rheum. Wiley Subscription Services, Inc., A Wiley Company; 2007;56:772–8.

176. Kavanaugh A, Rosengren S, Lee SJ, Hammaker D, Firestein GS, Kalunian K, et al. Assessment of rituximab's immunomodulatory synovial effects (ARISE trial). 1: clinical and synovial biomarker results. Ann. Rheum. Dis. 2008;67:402–8.

177. Thurlings RM, Vos K, Gerlag DM, Tak PP. Disease activity-guided rituximab therapy in rheumatoid arthritis: the effects of re-treatment in initial nonresponders versus initial responders. Arthritis Rheum. Wiley Subscription Services, Inc., A Wiley Company; 2008;58:3657–64.

178. Vital EM, Dass S, Rawstron AC, Buch MH, Goëb V, Henshaw K, et al. Management of nonresponse to rituximab in rheumatoid arthritis: predictors and outcome of re-treatment. Arthritis Rheum. Wiley Subscription Services, Inc., A Wiley Company; 2010;62:1273–9.

179. Greenwald MW, Shergy WJ, Kaine JL, Sweetser MT, Gilder K, Linnik MD. Evaluation of the safety of rituximab in combination with a tumor necrosis factor inhibitor and methotrexate in patients with active rheumatoid arthritis: results from a randomized controlled trial. Arthritis Rheum. Wiley Subscription Services, Inc., A Wiley Company; 2011;63:622–32.

180. Emery P, Deodhar A, Rigby WF, Isaacs JD, Combe B, Racewicz AJ, et al. Efficacy and safety of different doses and retreatment of rituximab: a randomised, placebo-controlled trial in patients who are biological naive with active rheumatoid arthritis and an inadequate response to methotrexate (Study Evaluating Rituximab's Efficacy in MTX iNadequate rEsponders (SERENE)). Ann. Rheum. Dis. 2010;69:1629–35.

181. McGonagle D, Tan AL, Madden J, Taylor L, Emery P. Rituximab use in everyday clinical practice as a first-line biologic therapy for the treatment of DMARD-resistant rheumatoid arthritis. Rheumatology (Oxford). Oxford University Press; 2008;47:865–7.

182. Porter D, van Melckebeke J, Dale J, Messow CM, McConnachie A, Walker A, et al. Tumour necrosis factor inhibition versus rituximab for patients with rheumatoid arthritis who require biological treatment (ORBIT): an open-label, randomised controlled, non-inferiority, trial. Lancet. 2016;388:239–47.

183. van Vollenhoven RF, Wax S, Li Y, Tak PP. Safety and efficacy of atacicept in combination with rituximab for reducing the signs and symptoms of rheumatoid arthritis: a phase II, randomized, double-blind, placebo-controlled pilot trial. Arthritis Rheumatol. 2015;67:2828–36.

184. Genovese MC, Bojin S, Biagini IM, Mociran E, Cristei D, Mirea G, et al. Tabalumab in rheumatoid arthritis patients with an inadequate response to methotrexate and naive to biologic therapy: a phase II, randomized, placebo-controlled trial. Arthritis Rheum. Wiley Subscription Services, Inc., A Wiley Company; 2013;65:880–9.

185. Firestein GS. Invasive fibroblast-like synoviocytes in rheumatoid arthritis. Passive responders or transformed aggressors? Arthritis Rheum. John Wiley & Sons, Inc; 1996;39:1781–90.

186. Meinecke I, Cinski A, Baier A, Peters MA, Dankbar B, Wille A, et al. Modification of nuclear PML protein by SUMO-1 regulates Fas-induced apoptosis in rheumatoid arthritis synovial fibroblasts. Proceedings of the National Academy of Sciences. National Acad Sciences; 2007;104:5073–8.

187. Müller-Ladner U, Kriegsmann J, Franklin BN, Matsumoto S, Geiler T, Gay RE,

et al. Synovial fibroblasts of patients with rheumatoid arthritis attach to and invade normal human cartilage when engrafted into SCID mice. Am. J. Pathol. American Society for Investigative Pathology; 1996;149:1607–15.

188. Lefèvre S, Knedla A, Tennie C, Kampmann A, Wunrau C, Dinser R, et al. Synovial fibroblasts spread rheumatoid arthritis to unaffected joints. Nat. Med. Nature Publishing Group; 2009;15:1414–20.

189. Bartok B, Firestein GS. Fibroblast-like synoviocytes: key effector cells in rheumatoid arthritis. Immunological Reviews. Blackwell Publishing Ltd; 2010;233:233–55.

190. Edwards JCW, LEIGH RD, Cambridge G. Expression of molecules involved in B lymphocyte survival and differentiation by synovial fibroblasts. Clin. Exp. Immunol. Blackwell Science Ltd; 1997;108:407–14.

191. Valencia X, Higgins JMG, Kiener HP, Lee DM, Podrebarac TA, Dascher CC, et al. Cadherin-11 provides specific cellular adhesion between fibroblast-like synoviocytes. Journal of Experimental Medicine. Rockefeller University Press; 2004;200:1673–9.

192. Chang SK, Noss EH, Chen M, Gu Z, Townsend K, Grenha R, et al. Cadherin-11 regulates fibroblast inflammation. Proc. Natl. Acad. Sci. U.S.A. National Acad Sciences; 2011;108:8402–7.

193. McInnes IB, Buckley CD, Isaacs JD. Cytokines in rheumatoid arthritis - shaping the immunological landscape. Nat Rev Rheumatol. 2016;12:63–8.

194. Firestein GS, Yeo M, Zvaifler NJ. Apoptosis in rheumatoid arthritis synovium. Journal of Clinical Investigation. American Society for Clinical Investigation; 1995;96:1631–8.

195. Matsumoto S, Müller-Ladner U, Gay RE, Nishioka K, Gay S. Ultrastructural demonstration of apoptosis, Fas and Bcl-2 expression of rheumatoid synovial fibroblasts. J. Rheumatol. 1996;23:1345–52.

196. Kumkumian GK, Lafyatis R, Remmers EF, Case JP, Kim SJ, Wilder RL. Platelet-derived growth factor and IL-1 interactions in rheumatoid arthritis. Regulation of synoviocyte proliferation, prostaglandin production, and collagenase transcription. The Journal of Immunology. 1989;143:833–7.

197. Lotz M, Guerne PA. Interleukin-6 induces the synthesis of tissue inhibitor of metalloproteinases-1/erythroid potentiating activity (TIMP-1/EPA). J. Biol. Chem. 1991;266:2017–20.

198. Shigeyama Y, Pap T, Kunzler P, Simmen BR, Gay RE, Gay S. Expression of osteoclast differentiation factor in rheumatoid arthritis. Arthritis Rheum. John Wiley & Sons, Inc; 2000;43:2523–30.

199. Schett G, Teitelbaum SL. Osteoclasts and Arthritis. J. Bone Miner. Res. John Wiley and Sons and The American Society for Bone and Mineral Research (ASBMR); 2009;24:1142–6.

200. Guerne PA, Zuraw BL, Vaughan JH, Carson DA, Lotz M. Synovium as a source

of interleukin 6 in vitro. Contribution to local and systemic manifestations of arthritis. Journal of Clinical Investigation. American Society for Clinical Investigation; 1989;83:585–92.

201. Palmer CD, Mutch BE, Page TH, Horwood NJ, Foxwell BMJ. Bmx regulates LPS-induced IL-6 and VEGF production via mRNA stability in rheumatoid synovial fibroblasts. Biochem. Biophys. Res. Commun. 2008;370:599–602.

202. Kim K-W, Cho M-L, Kim H-R, Ju J-H, Park M-K, Oh H-J, et al. Up-regulation of stromal cell–derived factor 1 (CXCL12) production in rheumatoid synovial fibroblasts through interactions with T lymphocytes: Role of interleukin-17 and CD40L–CD40 interaction. Arthritis Rheum. Wiley Subscription Services, Inc., A Wiley Company; 2007;56:1076–86.

203. Firestein GS, Nguyen K, Aupperle KR, Yeo M, Boyle DL, Zvaifler NJ. Apoptosis in rheumatoid arthritis: p53 overexpression in rheumatoid arthritis synovium. Am. J. Pathol. American Society for Investigative Pathology; 1996;149:2143–51.

204. Yamanishi Y, Boyle DL, Green DR, Keystone EC, Connor A, Zollman S, et al. p53 tumor suppressor gene mutations in fibroblast-like synoviocytes from erosion synovium and non-erosion synovium in rheumatoid arthritis. Arthritis Res. Ther. BioMed Central; 2005;7:R12–8.

205. Harty LC, Biniecka M, O'Sullivan J, Fox E, Mulhall K, Veale DJ, et al. Mitochondrial mutagenesis correlates with the local inflammatory environment in arthritis. Ann. Rheum. Dis. 2012;71:582–8.

206. Karouzakis E, Gay RE, Gay S, Neidhart M. Epigenetic deregulation in rheumatoid arthritis. Adv. Exp. Med. Biol. 2011;711:137–49.

207. Nakamachi Y, Kawano S, Takenokuchi M, Nishimura K, Sakai Y, Chin T, et al. MicroRNA-124a is a key regulator of proliferation and monocyte chemoattractant protein 1 secretion in fibroblast-like synoviocytes from patients with rheumatoid arthritis. Arthritis Rheum. Wiley Subscription Services, Inc., A Wiley Company; 2009;60:1294–304.

208. Stanczyk J, Ospelt C, Karouzakis E, Filer A, Raza K, Kolling C, et al. Altered expression of microRNA-203 in rheumatoid arthritis synovial fibroblasts and its role in fibroblast activation. Arthritis Rheum. 2011;63:373–81.

209. Genovese MC, Jarosova K, Cieślak D, Alper J, Kivitz A, Hough DR, et al. Apremilast in Patients With Active Rheumatoid Arthritis: A Phase II, Multicenter, Randomized, Double-Blind, Placebo-Controlled, Parallel-Group Study. Arthritis Rheumatol. 2015;67:1703–10.

210. Rosengren S, Corr M, Firestein GS, Boyle DL. The JAK inhibitor CP-690,550 (tofacitinib) inhibits TNF-induced chemokine expression in fibroblast-like synoviocytes: autocrine role of type I interferon. Ann. Rheum. Dis. 2012;71:440–7.

211. Hoeffel G, Chen J, Lavin Y, Low D, Almeida FF, See P, et al. C-Myb+ Erythro-Myeloid Progenitor-Derived Fetal Monocytes Give Rise to Adult Tissue-Resident Macrophages. Immunity. 2015;42:665–78.

212. Geissmann F, Jung S, Littman DR. Blood monocytes consist of two principal subsets with distinct migratory properties. Immunity. 2003;19:71–82.

213. Misharin AV, Cuda CM, Saber R, Turner JD, Gierut AK, Haines GK III, et al. Nonclassical Ly6C− Monocytes Drive the Development of Inflammatory Arthritis in Mice. Cell Rep. 2014;9:591–604.

214. Boring L, Gosling J, Chensue SW, Kunkel SL, Farese RV Jr, Broxmeyer HE, et al. Impaired monocyte migration and reduced type 1 (Th1) cytokine responses in C-C chemokine receptor 2 knockout mice. Journal of Clinical Investigation. 1997;100:2552–61.

215. Serbina NV, Pamer EG. Monocyte emigration from bone marrow during bacterial infection requires signals mediated by chemokine receptor CCR2. Nat. Immunol. 2006;7:311–7.

216. Hamilton JA, Achuthan A. Colony stimulating factors and myeloid cell biology in health and disease. Trends Immunol. 2013;34:81–9.

217. Croxford AL, Lanzinger M, Hartmann FJ, Schreiner B, Mair F, Pelczar P, et al. The Cytokine GM-CSF Drives the Inflammatory Signature of CCR2+ Monocytes and Licenses Autoimmunity. Immunity. 2015;43:502–14.

218. Udalova IA, Mantovani A, Feldmann M. Macrophage heterogeneity in the context of rheumatoid arthritis. Nat Rev Rheumatol. 2016;12:472–85.

219. Auffray C, Fogg D, Garfa M, Elain G, Join-Lambert O, Kayal S, et al. Monitoring of Blood Vessels and Tissues by a Population of Monocytes with Patrolling Behavior. Science. 2007;317:666–70.

220. MA I, R S, C L, et al. Comparison of gene expression profiles between human and mouse monocyte subsets. Blood. 2010;115(3):e10-e19. Blood. 2010;116:857–7.

221. Ingersoll MA, Spanbroek R, Lottaz C, Gautier EL, Frankenberger M, Hoffmann R, et al. Comparison of gene expression profiles between human and mouse monocyte subsets. Blood. 2010;115:e10–9.

222. Ziegler-Heitbrock L, Ancuta P, Crowe S, Dalod M, Grau V, Hart DN, et al. Nomenclature of monocytes and dendritic cells in blood. Blood. 2010;116:e74–e80.

223. Baeten D, Boots AMH, Steenbakkers PGA, Elewaut D, Bos E, Verheijden GFM, et al. Human cartilage gp-39+,CD16+ monocytes in peripheral blood and synovium: Correlation with joint destruction in rheumatoid arthritis. Arthritis Rheum. 2000;43:1233–43.

224. Chara L, Sánchez-Atrio A, Pérez A, Cuende E, Albarrán F, Turrión A, et al. Monocyte populations as markers of response to adalimumab plus MTX in rheumatoid arthritis. Arthritis Res. Ther. 2012;14:R175.

225. Wijngaarden S, van Roon JAG, Bijlsma JWJ, van de Winkel JGJ, Lafeber FPJG. Fcgamma receptor expression levels on monocytes are elevated in rheumatoid arthritis patients with high erythrocyte sedimentation rate who do

not use anti-rheumatic drugs. Rheumatology. 2003;42:681–8.

226. Kawanaka N, Yamamura M, Aita T, Morita Y, Okamoto A, Kawashima M, et al. CD14+,CD16+ blood monocytes and joint inflammation in rheumatoid arthritis. Arthritis Rheum. 2002;46:2578–86.

227. Rossol M, Kraus S, Pierer M, Baerwald C, Wagner U. The CD14brightCD16+ monocyte subset is expanded in rheumatoid arthritis and promotes expansion of the Th17 cell population. Arthritis Rheum. 2012;64:671–7.

228. Iwahashi M, Yamamura M, Aita T, Okamoto A, Ueno A, Ogawa N, et al. Expression of toll-like receptor 2 on CD16+ blood monocytes and synovial tissue macrophages in rheumatoid arthritis. Arthritis Rheum. 2004;50:1457–67.

229. Cooper DL, Martin SG, Robinson JI, Mackie SL, Charles CJ, Nam J, et al. FcγRIIIa Expression on Monocytes in Rheumatoid Arthritis: Role in Immune-Complex Stimulated TNF Production and Non-Response to Methotrexate Therapy. Proost P, editor. PLoS ONE. 2012;7:e28918.

230. Abrahams VM, Cambridge G, Lydyard PM, Edwards JCW. Induction of tumor necrosis factor α production by adhered human monocytes: A key role for Fcγ receptor type IIIA in rheumatoid arthritis. Arthritis Rheum. 2000;43:608.

231. Yoon BR, Yoo S-J, Choi YH, Chung Y-H, Kim J, Yoo IS, et al. Functional Phenotype of Synovial Monocytes Modulating Inflammatory T-Cell Responses in Rheumatoid Arthritis (RA). Shin E-C, editor. PLoS ONE. 2014;9:e109775.

232. Tsou C-L, Peters W, Si Y, Slaymaker S, Aslanian AM, Weisberg SP, et al. Critical roles for CCR2 and MCP-3 in monocyte mobilization from bone marrow and recruitment to inflammatory sites. Journal of Clinical Investigation. 2007;117:902–9.

233. Kruger T, Brown E, Malik R, Majid A, Baier J. Interleukin-4 (IL-4) and Interleukin-13 (IL-13) inhibit IL-1β induction of Interleukin-8 (IL-8) and Epithelial neutrophil activating protein (ENA-78) in alveolar type II cells. 1958. Pediatric Research. 1998;43:334–4.

234. Tsuboi N, Yoshikai Y, Matsuo S, Kikuchi T, Iwami KI, Nagai Y, et al. Roles of Toll-Like Receptors in C-C Chemokine Production by Renal Tubular Epithelial Cells. The Journal of Immunology. 2002;169:2026–33.

235. Brown Z, Gerritsen ME, Carley WW, Strieter RM, Kunkel SL, Westwick J. Chemokine gene expression and secretion by cytokine-activated human microvascular endothelial cells. Differential regulation of monocyte chemoattractant protein-1 and interleukin-8 in response to interferon-gamma. Am. J. Pathol. 1994;145:913–21.

236. Proudfoot AEI, Handel TM, Johnson Z, Lau EK, LiWang P, Clark-Lewis I, et al. Glycosaminoglycan binding and oligomerization are essential for the in vivo activity of certain chemokines. Proceedings of the National Academy of Sciences. 2003;100:1885–90.

237. Allen SJ, Crown SE, Handel TM. Chemokine: receptor structure, interactions, and antagonism. Annual Review of Immunology. 2007;25:787–820.

238. Jia T, Serbina NV, Brandl K, Zhong MX, Leiner IM, Charo IF, et al. Additive Roles for MCP-1 and MCP-3 in CCR2-Mediated Recruitment of Inflammatory Monocytes during Listeria monocytogenes Infection. The Journal of Immunology. 2008;180:6846–53.

239. Charo IF, Ransohoff RM. The Many Roles of Chemokines and Chemokine Receptors in Inflammation. N. Engl. J. Med. 2006;354:610–21.

240. Weber C. Specialized roles of the chemokine receptors CCR1 and CCR5 in the recruitment of monocytes and TH1-like/CD45RO+ T cells. Blood. 2001;97:1144–6.

241. Zernecke A. Deficiency in CCR5 but not CCR1 protects against neointima formation in atherosclerosis-prone mice: involvement of IL-10. Blood. 2006;107:4240–3.

242. Jakubzick C, Gautier EL, Gibbings SL, Sojka DK, Schlitzer A, Johnson TE, et al. Minimal Differentiation of Classical Monocytes as They Survey Steady-State Tissues and Transport Antigen to Lymph Nodes. Immunity. 2013;39:599–610.

243. Merad M, Manz MG, Karsunky H, Wagers A, Peters W, Charo I, et al. Langerhans cells renew in the skin throughout life under steady-state conditions. Nat. Immunol. 2002;3:1135–41.

244. Martinez FO, Gordon S, Locati M, Mantovani A. Transcriptional Profiling of the Human Monocyte-to-Macrophage Differentiation and Polarization: New Molecules and Patterns of Gene Expression. The Journal of Immunology. 2006;177:7303–11.

245. Hume DA. Macrophages as APC and the dendritic cell myth. J Immunol. American Association of Immunologists; 2008;181:5829–35.

246. Ginhoux F, Greter M, Leboeuf M, Nandi S, See P, Gokhan S, et al. Fate mapping analysis reveals that adult microglia derive from primitive macrophages. Science. American Association for the Advancement of Science; 2010;330:841–5.

247. Wang Y, Szretter KJ, Vermi W, Gilfillan S, Rossini C, Cella M, et al. IL-34 is a tissue-restricted ligand of CSF1R required for the development of Langerhans cells and microglia. Nat. Immunol. Nature Research; 2012;13:753–60.

248. Stanley E, Lieschke GJ, Grail D, Metcalf D, Hodgson G, Gall JA, et al. Granulocyte/macrophage colony-stimulating factor-deficient mice show no major perturbation of hematopoiesis but develop a characteristic pulmonary pathology. Proceedings of the National Academy of Sciences. 1994;91:5592–6.

249. Dranoff G, Crawford A, Sadelain M, Ream B, Rashid A, Bronson R, et al. Involvement of granulocyte-macrophage colony-stimulating factor in pulmonary homeostasis. Science. 1994;264:713–6.

250. Niida S, Kaku M, Amano H, Yoshida H, Kataoka H, Nishikawa S, et al. Vascular endothelial growth factor can substitute for macrophage colony-stimulating factor in the support of osteoclastic bone resorption. J. Exp. Med. Rockefeller University Press; 1999;190:293–8.

251. Chitu V, Stanley ER. Colony-stimulating factor-1 in immunity and inflammation. Current Opinion in Immunology. 2006;18:39–48.

252. Genovese MC, Hsia E, Belkowski SM, Chien C, Masterson T, Thurmond RL, et al. Results from a Phase IIA Parallel Group Study of JNJ-40346527, an Oral CSF-1R Inhibitor, in Patients with Active Rheumatoid Arthritis despite Disease-modifying Antirheumatic Drug Therapy. J. Rheumatol. 2015;42:1752–60.

253. Schulz C, Perdiguero EG, Chorro L, Szabo-Rogers H, Cagnard N, Kierdorf K, et al. A Lineage of Myeloid Cells Independent of Myb and Hematopoietic Stem Cells. Science. American Association for the Advancement of Science; 2012;336:86–90.

254. Mass E, Ballesteros I, Farlik M, Halbritter F, Günther P, Crozet L, et al. Specification of tissue-resident macrophages during organogenesis. Science. 2016;353:aaf4238–8.

255. Leddin M, Perrod C, Hoogenkamp M, Ghani S, Assi S, Heinz S, et al. Two distinct auto-regulatory loops operate at the PU.1 locus in B cells and myeloid cells. Blood. 2011;117:2827–38.

256. FOWLES LF, STACEY KJ, MARKS D, Hamilton JA, Hume DA. Regulation of urokinase plasminogen activator gene transcription in the RAW264 murine macrophage cell line by macrophage colony-stimulating factor (CSF-1) is dependent upon the level of cell-surface receptor. Biochemical Journal. 2000;347:313–20.

257. Gordon S, Taylor PR. Monocyte and macrophage heterogeneity. Nat. Rev. Immunol. Nature Publishing Group; 2005;5:953–64.

258. Gordon S, Martinez FO. Alternative Activation of Macrophages: Mechanism and Functions. Immunity. 2010;32:593–604.

259. Stein M. Interleukin 4 potently enhances murine macrophage mannose receptor activity: a marker of alternative immunologic macrophage activation. Journal of Experimental Medicine. Rockefeller University Press; 1992;176:287–92.

260. Murray PJ, Allen JE, Biswas SK, Fisher EA, Gilroy DW, Goerdt S, et al. Macrophage activation and polarization: nomenclature and experimental guidelines. Immunity. 2014;41:14–20.

261. Ravasi T, Wells C, Forest A, Underhill DM, Wainwright BJ, Aderem A, et al. Generation of Diversity in the Innate Immune System: Macrophage Heterogeneity Arises from Gene-Autonomous Transcriptional Probability of Individual Inducible Genes. The Journal of Immunology. American Association of Immunologists; 2002;168:44–50.

262. Schroder K, Irvine KM, Taylor MS, Bokil NJ, Le Cao K-A, Masterman K-A, et al. Conservation and divergence in Toll-like receptor 4-regulated gene expression in primary human versus mouse macrophages. Proc. Natl. Acad. Sci. U.S.A. National Acad Sciences; 2012;109:E944–53.

263. O'Neill LAJ, Pearce EJ. Immunometabolism governs dendritic cell and

macrophage function. The Journal of Cell Biology. 2016;212:2121OIA306.

264. Wang N, Liang H, Zen K. Molecular Mechanisms That Influence the Macrophage M1â€“M2 Polarization Balance. Front Immunol. 2014;5:889.

265. Kennedy A, Fearon U, Veale DJ, Godson C. Macrophages in Synovial Inflammation. Front Immunol. 2011;2.

266. Ginhoux F, Jung S. Monocytes and macrophages: developmental pathways and tissue homeostasis. Nat. Rev. Immunol. Nature Research; 2014;14:392–404.

267. Burmester GR, Locher P, Koch B, Winchester RJ, Dimitriu-Bona A, Kalden JR, et al. The tissue architecture of synovial membranes in inflammatory and non-inflammatory joint diseases. Rheumatol. Int. 1983;3:173–81.

268. Kinne RW, Stuhlmüller B, Burmester GR. Cells of the synovium in rheumatoid arthritis. Macrophages. Arthritis Res. Ther. 2007;9:224.

269. Sebbag M, Parry SL, Brennan FM, Feldmann M. Cytokine stimulation of T lymphocytes regulates their capacity to induce monocyte production of tumor necrosis factor-α, but not interleukin-10: Possible relevance to pathophysiology of rheumatoid arthritis. European Journal of Immunology. 1997;27:624–32.

270. Cassetta L, Cassol E, Poli G. Macrophage Polarization in Health and Disease. The Scientific World JOURNAL. 2011;11:2391–402.

271. Martinez FO. Macrophage activation and polarization. Frontiers in Bioscience. 2008;13:453.

272. Brühl H, Cihak J, Plachý J, Kunz-Schughart L, Niedermeier M, Denzel A, et al. Targeting of Gr-1+,CCR2+ monocytes in collagen-induced arthritis. Arthritis Rheum. 2007;56:2975–85.

273. Thurlings RM, Wijbrandts CA, Bennink RJ, Dohmen SE, Voermans C, Wouters D, et al. Monocyte Scintigraphy in Rheumatoid Arthritis: The Dynamics of Monocyte Migration in Immune-Mediated Inflammatory Disease. Boswell A, editor. PLoS ONE. 2009;4:e7865.

274. Evans HG, Gullick NJ, Kelly S, Pitzalis C, Lord GM, Kirkham BW, et al. In vivo activated monocytes from the site of inflammation in humans specifically promote Th17 responses. Proc. Natl. Acad. Sci. U.S.A. National Acad Sciences; 2009;106:6232–7.

275. Burger D, Dayer J-M. The role of human T-lymphocyte-monocyte contact in inflammation and tissue destruction. Arthritis Research. 2002;4:S169.

276. Zhang S-Y, Boisson-Dupuis S, Chapgier A, Yang K, Bustamante J, Puel A, et al. Inborn errors of interferon (IFN)-mediated immunity in humans: insights into the respective roles of IFN-α/β, IFN-γ, and IFN-λ in host defense. Immunological Reviews. Blackwell Publishing Ltd; 2008;226:29–40.

277. Wicks IP, Roberts AW. Targeting GM-CSF in inflammatory diseases. Nat Rev Rheumatol. 2015;12:37–48.

278. Lebre MC, Vergunst CE, Choi IYK, Aarrass S, Oliveira ASF, Wyant T, et al.

Why CCR2 and CCR5 Blockade Failed and Why CCR1 Blockade Might Still Be Effective in the Treatment of Rheumatoid Arthritis. Khoury JE, editor. PLoS ONE. Public Library of Science; 2011;6:e21772.

279. van Vuuren AJ, van Roon JAG, Walraven V, Stuij I, Harmsen MC, McLaughlin PMJ, et al. CD64-Directed Immunotoxin Inhibits Arthritis in a Novel CD64 Transgenic Rat Model. The Journal of Immunology. American Association of Immunologists; 2006;176:5833–8.

280. van Roon JAG, Van Vuuren AJ, Wijngaarden S, Jacobs KMG, Bijlsma JWJ, Lafeber FPJG, et al. Selective elimination of synovial inflammatory macrophages in rheumatoid arthritis by an Fc? receptor I-directed immunotoxin. Arthritis Rheum. Wiley Subscription Services, Inc., A Wiley Company; 2003;48:1229–38.

281. Germano G, Frapolli R, Belgiovine C, Anselmo A, Pesce S, Liguori M, et al. Role of Macrophage Targeting in the Antitumor Activity of Trabectedin. Cancer Cell. 2013;23:249–62.

282. Siegal FP. The Nature of the Principal Type 1 Interferon-Producing Cells in Human Blood. Science. 1999;284:1835–7.

283. Haniffa M, Collin M, Ginhoux F. Ontogeny and Functional Specialization of Dendritic Cells in Human and Mouse. Development and Function of Myeloid Subsets. Elsevier; 2013. pp. 1–49.

284. Yu CI, Becker C, Metang P, Marches F, Wang Y, Toshiyuki H, et al. Human CD141 +Dendritic Cells Induce CD4 +T Cells To Produce Type 2 Cytokines. The Journal of Immunology. 2014;193:4335–43.

285. Jongbloed SL, Kassianos AJ, McDonald KJ, Clark GJ, Ju X, Angel CE, et al. Human CD141 +(BDCA-3) +dendritic cells (DCs) represent a unique myeloid DC subset that cross-presents necrotic cell antigens. Journal of Experimental Medicine. 2010;207:1247–60.

286. Nizzoli G, Krietsch J, Weick A, Steinfelder S, Facciotti F, Gruarin P, et al. Human CD1c+ dendritic cells secrete high levels of IL-12 and potently prime cytotoxic T-cell responses. Blood. 2013;122:932–42.

287. Hemont C, Neel A, Heslan M, Braudeau C, Josien R. Human blood mDC subsets exhibit distinct TLR repertoire and responsiveness. Journal of Leukocyte Biology. 2013;93:599–609.

288. Segura E, Touzot M, Bohineust A, Cappuccio A, Chiocchia G, Hosmalin A, et al. Human Inflammatory Dendritic Cells Induce Th17 Cell Differentiation. Immunity. 2013;38:336–48.

289. León B, López-Bravo M, Ardavín C. Monocyte-Derived Dendritic Cells Formed at the Infection Site Control the Induction of Protective T Helper 1 Responses against Leishmania. Immunity. 2007;26:519–31.

290. Hammad H, Plantinga M, Deswarte K, Pouliot P, Willart MAM, Kool M, et al. Inflammatory dendritic cells—not basophils—are necessary and sufficient for induction of Th2 immunity to inhaled house dust mite allergen. Journal of Experimental Medicine. 2010;207:2097–111.

291. Coutant F, Miossec P. Altered dendritic cell functions in autoimmune diseases: distinct and overlapping profiles. Nat Rev Rheumatol. 2016.

292. Kaneko K, Miyabe Y, Takayasu A, Fukuda S, Miyabe C, Ebisawa M, et al. Chemerin activates fibroblast-like synoviocytes in patients with rheumatoid arthritis. Arthritis Res. Ther. 2011;13:R158.

293. Eisinger K, Bauer S, Schäffler A, Walter R, Neumann E, Buechler C, et al. Chemerin induces CCL2 and TLR4 in synovial fibroblasts of patients with rheumatoid arthritis and osteoarthritis. Experimental and Molecular Pathology. 2012;92:90–6.

294. Bondue B, Wittamer V, Parmentier M. Chemerin and its receptors in leukocyte trafficking, inflammation and metabolism. Cytokine Growth Factor Rev. 2011;22:331–8.

295. Janeway CA Jr., Medzhitov R. I NNATEI MMUNER ECOGNITION. Annual Review of Immunology. 2002;20:197–216.

296. Gallo PM, Gallucci S. The Dendritic Cell Response to Classic, Emerging, and Homeostatic Danger Signals. Implications for Autoimmunity. Front Immunol. 2013;4.

297. Page G, Miossec P. Paired synovium and lymph nodes from rheumatoid arthritis patients differ in dendritic cell and chemokine expression. The Journal of Pathology. John Wiley & Sons, Ltd; 2004;204:28–38.

298. Page G, Lebecque S, Miossec P. Anatomic Localization of Immature and Mature Dendritic Cells in an Ectopic Lymphoid Organ: Correlation with Selective Chemokine Expression in Rheumatoid Synovium. The Journal of Immunology. 2002;168:5333–41.

299. Manzo A, Bombardieri M, Humby F, Pitzalis C. Secondary and ectopic lymphoid tissue responses in rheumatoid arthritis: from inflammation to autoimmunity and tissue damage/remodeling. Immunological Reviews. 2010;233:267–85.

300. Pitzalis C, Kelly S, Humby F. New learnings on the pathophysiology of RA from synovial biopsies. Curr Opin Rheumatol. 2013;25:334–44.

301. Tucci M, Ciavarella S, Strippoli S, Dammacco F, Silvestris F. Oversecretion of Cytokines and Chemokines in Lupus Nephritis Is Regulated by Intraparenchymal Dendritic Cells. Annals of the New York Academy of Sciences. 2009;1173:449–57.

302. Segura E, Valladeau-Guilemond J, Donnadieu M-H, Sastre-Garau X, Soumelis V, Amigorena S. Characterization of resident and migratory dendritic cells in human lymph nodes. J. Exp. Med. Rockefeller University Press; 2012;209:653–60.

303. Schlitzer A, McGovern N, Teo P, Zelante T, Atarashi K, Low D, et al. IRF4 Transcription Factor-Dependent CD11b+ Dendritic Cells in Human and Mouse Control Mucosal IL-17 Cytokine Responses. Immunity. 2013;38:970–83.

304. Swiecki M, Colonna M. The multifaceted biology of plasmacytoid dendritic

cells. Nat. Rev. Immunol. 2015;15:471–85.

305. Jongbloed SL, Lebre MC, Fraser AR, Gracie JA, Sturrock RD, Tak PP, et al. Enumeration and phenotypical analysis of distinct dendritic cell subsets in psoriatic arthritis and rheumatoid arthritis. Arthritis Res. Ther. 2006;8:R15.

306. Walsh KP, Mills KHG. Dendritic cells and other innate determinants of T helper cell polarisation. Trends Immunol. 2013;34:521–30.

307. Lebre MC, Jongbloed SL, Tas SW, Smeets TJM, McInnes IB, Tak PP. Rheumatoid Arthritis Synovium Contains Two Subsets of CD83−DC-LAMP− Dendritic Cells with Distinct Cytokine Profiles. Am. J. Pathol. 2008;172:940–50.

308. Tournadre A, Lenief V, Eljaafari A, Miossec P. Immature muscle precursors are a source of interferon-β in myositis: Role of Toll-like receptor 3 activation and contribution to HLA class I up-regulation. Arthritis Rheum. 2012;64:533–41.

309. Miossec P, Kolls JK. Targeting IL-17 and TH17 cells in chronic inflammation. Nat Rev Drug Discov. 2012;11:763–76.

310. Reynolds G, Gibbon JR, Pratt AG, Wood MJ, Coady D, Raftery G, et al. Synovial CD4+ T-cell-derived GM-CSF supports the differentiation of an inflammatory dendritic cell population in rheumatoid arthritis. Ann. Rheum. Dis. 2016;75:899–907.

311. Benedetti G, Miossec P. Interleukin 17 contributes to the chronicity of inflammatory diseases such as rheumatoid arthritis. European Journal of Immunology. 2014;44:339–47.

312. Litinskiy MB, Nardelli B, Hilbert DM, He B, Schaffer A, Casali P, et al. DCs induce CD40-independent immunoglobulin class switching through BLyS and APRIL. Nat. Immunol. 2002;3:822–9.

313. Le Bon A, Thompson C, Kamphuis E, Durand V, Rossmann C, Kalinke U, et al. Cutting Edge: Enhancement of Antibody Responses Through Direct Stimulation of B and T Cells by Type I IFN. The Journal of Immunology. 2006;176:2074–8.

314. Thomas R. Dendritic cells and the promise of antigen-specific therapy in rheumatoid arthritis. Arthritis Res. Ther. 2013;15:204.

315. Idoyaga J, Fiorese C, Zbytnuik L, Lubkin A, Miller J, Malissen B, et al. Specialized role of migratory dendritic cells in peripheral tolerance induction. Journal of Clinical Investigation. 2013.

316. Benham H, Nel HJ, Law SC, Mehdi AM, Street S, Ramnoruth N, et al. Citrullinated peptide dendritic cell immunotherapy in HLA risk genotype-positive rheumatoid arthritis patients. Science Translational Medicine. 2015;7:290ra87–7.

317. Hilkens CMU, Isaacs JD. Tolerogenic dendritic cell therapy for rheumatoid arthritis: where are we now? Clin. Exp. Immunol. 2013;172:148–57.

318. Van der Heijde DM. Joint erosions and patients with early rheumatoid arthritis. Br. J. Rheumatol. 1995;34 Suppl 2:74–8.

319. Boyle WJ, Simonet WS, Lacey DL. Osteoclast differentiation and activation. Nature. 2003;423:337–42.

320. Teitelbaum SL, Ross FP. Genetic regulation of osteoclast development and function. Nat. Rev. Genet. 2003;4:638–49.

321. Yoshida H, Hayashi S, Kunisada T, Ogawa M, Nishikawa S, Okamura H, et al. The murine mutation osteopetrosis is in the coding region of the macrophage colony stimulating factor gene. Nature. 1990;345:442–4.

322. Yasuda H, Shima N, Nakagawa N, Yamaguchi K, Kinosaki M, Mochizuki S, et al. Osteoclast differentiation factor is a ligand for osteoprotegerin/osteoclastogenesis-inhibitory factor and is identical to TRANCE/RANKL. Proceedings of the National Academy of Sciences. 1998;95:3597–602.

323. Gravallese EM, Manning C, Tsay A, Naito A, Pan C, Amento E, et al. Synovial tissue in rheumatoid arthritis is a source of osteoclast differentiation factor. Arthritis Rheum. 2000;43:250–8.

324. Herman S, Müller RB, Krönke G, Zwerina J, Redlich K, Hueber AJ, et al. Induction of osteoclast-associated receptor, a key osteoclast costimulation molecule, in rheumatoid arthritis. Arthritis Rheum. Wiley Subscription Services, Inc., A Wiley Company; 2008;58:3041–50.

325. Ji JD, Park-Min KH, Shen Z, Fajardo RJ, Goldring SR, McHugh KP, et al. Inhibition of RANK Expression and Osteoclastogenesis by TLRs and IFN- in Human Osteoclast Precursors. The Journal of Immunology. American Association of Immunologists; 2009;183:7223–33.

326. Lam J, Takeshita S, Barker JE, Kanagawa O, Ross FP, Teitelbaum SL. TNF-α induces osteoclastogenesis by direct stimulation of macrophages exposed to permissive levels of RANK ligand. Journal of Clinical Investigation. 2000;106:1481–8.

327. Takayanagi H. Osteoimmunology and the effects of the immune system on bone. Nat Rev Rheumatol. 2009;5:667–76.

328. Meyer O. Anticitrullinated protein/peptide antibody assays in early rheumatoid arthritis for predicting five year radiographic damage. Ann. Rheum. Dis. 2003;62:120–6.

329. Harre U, Georgess D, Bang H, Bozec A, Axmann R, Ossipova E, et al. Induction of osteoclastogenesis and bone loss by human autoantibodies against citrullinated vimentin. Journal of Clinical Investigation. 2012;122:1791–802.

330. Pettit AR, Ji H, Stechow von D, Müller R, Goldring SR, Choi Y, et al. TRANCE/RANKL Knockout Mice Are Protected from Bone Erosion in a Serum Transfer Model of Arthritis. Am. J. Pathol. 2001;159:1689–99.

331. Redlich K, Hayer S, Maier A, Dunstan CR, Tohidast-Akrad M, Lang S, et al. Tumor necrosis factor α-mediated joint destruction is inhibited by targeting osteoclasts with osteoprotegerin. Arthritis Rheum. John Wiley & Sons, Inc; 2002;46:785–92.

332. Ohno H, Uemura Y, Murooka H, Takanashi H, Tokieda T, Ohzeki Y, et al. The orally-active and selective c-Fms tyrosine kinase inhibitor Ki20227 inhibits disease progression in a collagen-induced arthritis mouse model. European Journal of Immunology. WILEY-VCH Verlag; 2008;38:283–91.

333. Cohen SB, Dore RK, Lane NE, Ory PA, Peterfy CG, Sharp JT, et al. Denosumab treatment effects on structural damage, bone mineral density, and bone turnover in rheumatoid arthritis: A twelve-month, multicenter, randomized, double-blind, placebo-controlled, phase II clinical trial. Arthritis Rheum. 2008;58:1299–309.

334. Schett G, Stach C, Zwerina J, Voll R, Manger B. How antirheumatic drugs protect joints from damage in rheumatoid arthritis. Arthritis Rheum. Wiley Subscription Services, Inc., A Wiley Company; 2008;58:2936–48.

335. Matzelle MM, Gallant MA, Condon KW, Walsh NC, Manning CA, Stein GS, et al. Resolution of inflammation induces osteoblast function and regulates the Wnt signaling pathway. Arthritis Rheum. Wiley Subscription Services, Inc., A Wiley Company; 2012;64:1540–50.

336. Diarra D, Stolina M, Polzer K, Zwerina J, Ominsky MS, Dwyer D, et al. Dickkopf-1 is a master regulator of joint remodeling. Nat. Med. Nature Publishing Group; 2007;13:156–63.

337. Poole KES, van Bezooijen RL, Loveridge N, Hamersma H, Papapoulos SE, Löwik CW, et al. Sclerostin is a delayed secreted product of osteocytes that inhibits bone formation. FASEB J. Federation of American Societies for Experimental Biology; 2005;19:1842–4.

338. Wittkowski H, Foell D, af Klint E, De Rycke L, De Keyser F, Frosch M, et al. Effects of intra-articular corticosteroids and anti-TNF therapy on neutrophil activation in rheumatoid arthritis. Ann. Rheum. Dis. BMJ Publishing Group Ltd and European League Against Rheumatism; 2007;66:1020–5.

339. Sarraj B, Ludányi K, Glant TT, Finnegan A, Mikecz K. Expression of CD44 and L-selectin in the innate immune system is required for severe joint inflammation in the proteoglycan-induced murine model of rheumatoid arthritis. The Journal of Immunology. American Association of Immunologists; 2006;177:1932–40.

340. Eyles JL, Hickey MJ, Norman MU, Croker BA, Roberts AW, Drake SF, et al. A key role for G-CSF-induced neutrophil production and trafficking during inflammatory arthritis. Blood. American Society of Hematology; 2008;112:5193–201.

341. Kelchtermans H, Schurgers E, Geboes L, Mitera T, Van Damme J, Van Snick J, et al. Effector mechanisms of interleukin-17 in collagen-induced arthritis in the absence of interferon-γ and counteraction by interferon-γ. Arthritis Res. Ther. BioMed Central; 2009;11:R122.

342. Chakravarti A, Raquil MA, Tessier P, Poubelle PE. Surface RANKL of Toll-like receptor 4-stimulated human neutrophils activates osteoclastic bone resorption. Blood. American Society of Hematology; 2009;114:1633–44.

343. Assi LK, Wong SH, Ludwig A, Raza K, Gordon C, Salmon M, et al. Tumor

necrosis factor α activates release of B lymphocyte stimulator by neutrophils infiltrating the rheumatoid joint. Arthritis Rheum. Wiley Subscription Services, Inc., A Wiley Company; 2007;56:1776–86.

344. Wright HL, Moots RJ, Edwards SW. The multifactorial role of neutrophils in rheumatoid arthritis. Nat Rev Rheumatol. 2014;10:593–601.

345. Cross A, Bucknall RC, Cassatella MA, Edwards SW, Moots RJ. Synovial fluid neutrophils transcribe and express class II major histocompatibility complex molecules in rheumatoid arthritis. Arthritis Rheum. Wiley Subscription Services, Inc., A Wiley Company; 2003;48:2796–806.

346. Romero V, Fert-Bober J, Nigrovic PA, Darrah E, Haque UJ, Lee DM, et al. Immune-mediated pore-forming pathways induce cellular hypercitrullination and generate citrullinated autoantigens in rheumatoid arthritis. Science Translational Medicine. American Association for the Advancement of Science; 2013;5:209ra150–0.

347. Derouet M, Thomas L, Cross A, Moots RJ, Edwards SW. Granulocyte macrophage colony-stimulating factor signaling and proteasome inhibition delay neutrophil apoptosis by increasing the stability of Mcl-1. J. Biol. Chem. American Society for Biochemistry and Molecular Biology; 2004;279:26915–21.

348. Robinson J, Watson F, Bucknall RC, Edwards SW. Activation of neutrophil reactive-oxidant production by synovial fluid from patients with inflammatory joint disease. Soluble and insoluble immunoglobulin aggregates activate different pathways in primed and unprimed cells. Biochemical Journal. Portland Press Limited; 1992;286 (Pt 2):345–51.

349. Weinmann P, Moura RA, Caetano-Lopes JR, Pereira PA, Canhao H, Queiroz MV, et al. Delayed neutrophil apoptosis in very early rheumatoid arthritis patients is abrogated by methotrexate therapy. Clin. Exp. Rheumatol. 2007;25:885–7.

350. Brinkmann V, Reichard U, Goosmann C, Fauler B, Uhlemann Y, Weiss DS, et al. Neutrophil extracellular traps kill bacteria. Science. American Association for the Advancement of Science; 2004;303:1532–5.

351. Lande R, Ganguly D, Facchinetti V, Frasca L, Conrad C, Gregorio J, et al. Neutrophils activate plasmacytoid dendritic cells by releasing self-DNA-peptide complexes in systemic lupus erythematosus. Science Translational Medicine. American Association for the Advancement of Science; 2011;3:73ra19–9.

352. Khandpur R, Carmona-Rivera C, Vivekanandan-Giri A, Gizinski A, Yalavarthi S, Knight JS, et al. NETs are a source of citrullinated autoantigens and stimulate inflammatory responses in rheumatoid arthritis. Science Translational Medicine. American Association for the Advancement of Science; 2013;5:178ra40–0.

353. Chen X, Oppenheim JJ. Therapy: Paradoxical effects of targeting TNF signalling in the treatment of autoimmunity. Nat Rev Rheumatol. 2016;12:625–6.

354. Williams RO, Feldmann M, Maini RN. Anti-tumor necrosis factor ameliorates joint disease in murine collagen-induced arthritis. Proceedings of the National Academy of Sciences. National Acad Sciences; 1992;89:9784–8.

355. Feldmann M, Maini RN. Anti-TNF Therapy, from Rationale to Standard of Care: What Lessons Has It Taught Us? The Journal of Immunology. 2010;185:791–4.

356. Moreland LW, O'Dell JR, Paulus HE, Curtis JR, Bathon JM, St Clair EW, et al. A randomized comparative effectiveness study of oral triple therapy versus etanercept plus methotrexate in early aggressive rheumatoid arthritis: the treatment of Early Aggressive Rheumatoid Arthritis Trial. Arthritis Rheum. Wiley Subscription Services, Inc., A Wiley Company; 2012;64:2824–35.

357. Weinblatt ME, Kremer JM, Bankhurst AD, Bulpitt KJ, Fleischmann RM, Fox RI, et al. A trial of etanercept, a recombinant tumor necrosis factor receptor:Fc fusion protein, in patients with rheumatoid arthritis receiving methotrexate. N. Engl. J. Med. Massachusetts Medical Society; 1999;340:253–9.

358. Maini R, St Clair EW, Breedveld F, Furst D, Kalden J, Weisman M, et al. Infliximab (chimeric anti-tumour necrosis factor alpha monoclonal antibody) versus placebo in rheumatoid arthritis patients receiving concomitant methotrexate: a randomised phase III trial. ATTRACT Study Group. Lancet. 1999;354:1932–9.

359. Choy EHS, Hazleman B, Smith M, Moss K, Lisi L, Scott DGI, et al. Efficacy of a novel PEGylated humanized anti-TNF fragment (CDP870) in patients with rheumatoid arthritis: a phase II double-blinded, randomized, dose-escalating trial. Rheumatology. 2002;41:1133–7.

360. Smolen JS, Kay J, Doyle MK, Landewé R, Matteson EL, Wollenhaupt J, et al. Golimumab in patients with active rheumatoid arthritis after treatment with tumour necrosis factor alpha inhibitors (GO-AFTER study): a multicentre, randomised, double-blind, placebo-controlled, phase III trial. Lancet. 2009;374:210–21.

361. Kremer J, Ritchlin C, Mendelsohn A, Baker D, Kim L, Xu Z, et al. Golimumab, a new human anti-tumor necrosis factor alpha antibody, administered intravenously in patients with active rheumatoid arthritis: Forty-eight-week efficacy and safety results of a phase III randomized, double-blind, placebo-controlled study. Arthritis Rheum. Wiley Subscription Services, Inc., A Wiley Company; 2010;62:917–28.

362. Lipsky PE, Van der Heijde DM, St Clair EW, Furst DE, Breedveld FC, Kalden JR, et al. Infliximab and methotrexate in the treatment of rheumatoid arthritis. Anti-Tumor Necrosis Factor Trial in Rheumatoid Arthritis with Concomitant Therapy Study Group. N. Engl. J. Med. Massachusetts Medical Society; 2000;343:1594–602.

363. Keystone E, Heijde DVD, Mason D, Landewé R, Vollenhoven RV, Combe B, et al. Certolizumab pegol plus methotrexate is significantly more effective than placebo plus methotrexate in active rheumatoid arthritis: findings of a fifty-two-week, phase III, multicenter, randomized, double-blind, placebo-controlled, parallel-group study. Arthritis Rheum. Wiley Subscription Services, Inc., A Wiley Company; 2008;58:3319–29.

364. Charles P, Elliott MJ, Davis D, Potter A, Kalden JR, Antoni C, et al. Regulation of cytokines, cytokine inhibitors, and acute-phase proteins following

anti-TNF-alpha therapy in rheumatoid arthritis. The Journal of Immunology. 1999;163:1521–8.

365. Taylor PC, Peters AM, Paleolog E, Chapman PT, Elliott MJ, McCloskey R, et al. Reduction of chemokine levels and leukocyte traffic to joints by tumor necrosis factor α blockade in patients with rheumatoid arthritis. Arthritis Rheum. John Wiley & Sons, Inc; 2000;43:38–47.

366. Paleolog EM, Hunt M, Elliott MJ, Feldmann M, Maini RN, Woody JN. Deactivation of vascular endothelium by monoclonal anti-tumor necrosis factor alpha antibody in rheumatoid arthritis. Arthritis Rheum. 1996;39:1082–91.

367. Armuzzi A, Lionetti P, Blandizzi C, Caporali R, Chimenti S, Cimino L, et al. anti-TNF agents as therapeutic choice in immune-mediated inflammatory diseases: focus on adalimumab. Int J Immunopathol Pharmacol. 2014;27:11–32.

368. Cavalli G, Dinarello CA. Treating rheumatological diseases and co-morbidities with interleukin-1 blocking therapies. Rheumatology (Oxford). Oxford University Press; 2015;54:2134–44.

369. Jiang Y, Genant HK, Watt I, Cobby M, Bresnihan B, Aitchison R, et al. A multicenter, double-blind, dose-ranging, randomized, placebo-controlled study of recombinant human interleukin-1 receptor antagonist in patients with rheumatoid arthritis: radiologic progression and correlation of Genant and Larsen scores. Arthritis Rheum. John Wiley & Sons, Inc; 2000;43:1001–9.

370. Hoffman HM, Throne ML, Amar NJ, Sebai M, Kivitz AJ, Kavanaugh A, et al. Efficacy and safety of rilonacept (interleukin-1 trap) in patients with cryopyrin-associated periodic syndromes: Results from two sequential placebo-controlled studies. Arthritis Rheum. Wiley Subscription Services, Inc., A Wiley Company; 2008;58:2443–52.

371. Lachmann HJ, Kone-Paut I, Kuemmerle-Deschner JB, Leslie KS, Hachulla E, Quartier P, et al. Use of Canakinumab in the Cryopyrin-Associated Periodic Syndrome. N. Engl. J. Med. Massachusetts Medical Society; 2009;360:2416–25.

372. Cavalli G, Franchini S, Aiello P, Guglielmi B, Berti A, Campochiaro C, et al. Efficacy and safety of biological agents in adult-onset Still's disease. Scand. J. Rheumatol. Informa Healthcare; 2015;44:309–14.

373. Hunter CA, Jones SA. IL-6 as a keystone cytokine in health and disease. Nat. Immunol. Nature Research; 2015;16:448–57.

374. Yasukawa K, Hirano T, Watanabe Y, Muratani K, Matsuda T, Nakai S, et al. Structure and expression of human B cell stimulatory factor-2 (BSF-2/IL-6) gene. EMBO J. European Molecular Biology Organization; 1987;6:2939–45.

375. Woloski BM, Fuller GM. Identification and partial characterization of hepatocyte-stimulating factor from leukemia cell lines: comparison with interleukin 1. Proceedings of the National Academy of Sciences. National Acad Sciences; 1985;82:1443–7.

376. Rohleder N, Aringer M, Boentert M. Role of interleukin-6 in stress, sleep, and fatigue. Annals of the New York Academy of Sciences. Blackwell Publishing

Inc; 2012;1261:88–96.

377. Bethin KE, Vogt SK, Muglia LJ. Interleukin-6 is an essential, corticotropin-releasing hormone-independent stimulator of the adrenal axis during immune system activation. Proceedings of the National Academy of Sciences. National Acad Sciences; 2000;97:9317–22.

378. Kraakman MJ, Kammoun HL, Allen TL, Deswaerte V, Henstridge DC, Estevez E, et al. Blocking IL-6 trans-Signaling Prevents High-Fat Diet-Induced Adipose Tissue Macrophage Recruitment but Does Not Improve Insulin Resistance. Cell Metabolism. 2015;21:403–16.

379. Hodes GE, Pfau ML, Leboeuf M, Golden SA, Christoffel DJ, Bregman D, et al. Individual differences in the peripheral immune system promote resilience versus susceptibility to social stress. Proceedings of the National Academy of Sciences. 2014;111:16136–41.

380. Kopf M, Baumann H, Freer G, Freudenberg M, Lamers M, Kishimoto T, et al. Impaired immune and acute-phase responses in interleukin-6-deficient mice. Nature. Nature Publishing Group; 1994;368:339–42.

381. Fraunberger P, Wang Y, Holler E, Parhofer KG, Nagel D, Walli AK, et al. PROGNOSTIC VALUE OF INTERLEUKIN 6, PROCALCITONIN, AND C-REACTIVE PROTEIN LEVELS IN INTENSIVE CARE UNIT PATIENTS DURING FIRST INCREASE OF FEVER. Shock. 2006;26:10–2.

382. Mroczko B, Groblewska M, Gryko M, Kędra B, Szmitkowski M. Diagnostic usefulness of serum interleukin 6 (IL-6) and C-reactive protein (CRP) in the differentiation between pancreatic cancer and chronic pancreatitis. Journal of Clinical Laboratory Analysis. Wiley Subscription Services, Inc., A Wiley Company; 2010;24:256–61.

383. Hibi M, Murakami M, Saito M, Hirano T, Taga T, Kishimoto T. Molecular cloning and expression of an IL-6 signal transducer, gp130. Cell. Cell Press; 1990;63:1149–57.

384. Taga T, Hibi M, Hirata Y, Yamasaki K, Yasukawa K, Matsuda T, et al. Interleukin-6 triggers the association of its receptor with a possible signal transducer, gp130. Cell. Cell Press; 1989;58:573–81.

385. Jones GW, McLoughlin RM, Hammond VJ, Parker CR, Williams JD, Malhotra R, et al. Loss of CD4+ T cell IL-6R expression during inflammation underlines a role for IL-6 trans signaling in the local maintenance of Th17 cells. J Immunol. American Association of Immunologists; 2010;184:2130–9.

386. Yoshida K, Taga T, Saito M, Suematsu S, Kumanogoh A, Tanaka T, et al. Targeted disruption of gp130, a common signal transducer for the interleukin 6 family of cytokines, leads to myocardial and hematological disorders. Proceedings of the National Academy of Sciences. National Acad Sciences; 1996;93:407–11.

387. HEINRICH PC, BEHRMANN I, HAAN S, Hermanns HM, Müller-Newen G, Schaper F. Principles of interleukin (IL)-6-type cytokine signalling and its regulation. Biochemical Journal. 2003;374:1–20.

388. McFarland-Mancini MM, Funk HM, Paluch AM, Zhou M, Giridhar PV, Mercer CA, et al. Differences in wound healing in mice with deficiency of IL-6 versus IL-6 receptor. J Immunol. American Association of Immunologists; 2010;184:7219–28.

389. Mauer J, Chaurasia B, Goldau J, Vogt MC, Ruud J, Nguyen KD, et al. Signaling by IL-6 promotes alternative activation of macrophages to limit endotoxemia and obesity-associated resistance to insulin. Nat. Immunol. Nature Research; 2014;15:423–30.

390. Skiniotis G, Boulanger MJ, Garcia KC, Walz T. Signaling conformations of the tall cytokine receptor gp130 when in complex with IL-6 and IL-6 receptor. Nature Structural & Molecular Biology. Nature Publishing Group; 2005;12:545–51.

391. Croker BA, Krebs DL, Zhang J-G, Wormald S, Willson TA, Stanley EG, et al. SOCS3 negatively regulates IL-6 signaling in vivo. Nat. Immunol. 2003;4:540–5.

392. Schöbitz B, Pezeshki G, Pohl T, Hemmann U, Heinrich PC, Holsboer F, et al. Soluble interleukin-6 (IL-6) receptor augments central effects of IL-6 in vivo. The FASEB Journal. 1995;9:659–64.

393. Atreya R, Finotto S, Mudter J, Mullberg J, Jostock T, Holtmann M, et al. Blockade of IL-6 transsignaling abrogates established experimental colitis in mice by suppression of T cell resistance against apoptosis. Gastroenterology. W.B. Saunders; 2000;118:A863.

394. Briso EM, Dienz O, Rincon M. Cutting edge: soluble IL-6R is produced by IL-6R ectodomain shedding in activated CD4 T cells. The Journal of Immunology. American Association of Immunologists; 2008;180:7102–6.

395. Jones SA, Novick D, Horiuchi S, Yamamoto N, Szalai AJ, Fuller GM. C-reactive protein: a physiological activator of interleukin 6 receptor shedding. Journal of Experimental Medicine. Rockefeller University Press; 1999;189:599–604.

396. Marin V, Montero-Julian F, Grès S, Bongrand P, Farnarier C, Kaplanski G. Chemotactic agents induce IL-6Rα shedding from polymorphonuclear cells: involvement of a metalloproteinase of the TNF-α-converting enzyme (TACE) type. European Journal of Immunology. WILEY-VCH Verlag; 2002;32:2965–70.

397. Cui X, Rouhani FN, Hawari F, Levine SJ. An aminopeptidase, ARTS-1, is required for interleukin-6 receptor shedding. J. Biol. Chem. American Society for Biochemistry and Molecular Biology; 2003;278:28677–85.

398. Garbers C, Jänner N, Chalaris A, Moss ML, Floss DM, Meyer D, et al. Species specificity of ADAM10 and ADAM17 proteins in interleukin-6 (IL-6) trans-signaling and novel role of ADAM10 in inducible IL-6 receptor shedding. Journal of Biological Chemistry. American Society for Biochemistry and Molecular Biology; 2011;286:14804–11.

399. McLoughlin RM, Hurst SM, Nowell MA, Harris DA, Horiuchi S, Morgan LW, et al. Differential Regulation of Neutrophil-Activating Chemokines by IL-6 and Its Soluble Receptor Isoforms. The Journal of Immunology. American Association of Immunologists; 2004;172:5676–83.

400. Romano M, Sironi M, Toniatti C, Polentarutti N, Fruscella P, Ghezzi P, et al. Role of IL-6 and Its Soluble Receptor in Induction of Chemokines and Leukocyte Recruitment. Immunity. 1997;6:315–25.

401. Chomarat P, Banchereau J, Davoust J, Palucka AK. IL-6 switches the differentiation of monocytes from dendritic cells to macrophages. Nat. Immunol. 2000;1:510–4.

402. Jenkins BJ, Grail D, Inglese M, Quilici C, Bozinovski S, Wong P, et al. Imbalanced gp130-dependent signaling in macrophages alters macrophage colony-stimulating factor responsiveness via regulation of c-fms expression. Molecular and Cellular Biology. American Society for Microbiology; 2004;24:1453–63.

403. Suzuki M, Hashizume M, Yoshida H, Shiina M, Mihara M. IL-6 and IL-1 synergistically enhanced the production of MMPs from synovial cells by up-regulating IL-6 production and IL-1 receptor I expression. Cytokine. 2010;51:178–83.

404. Ma CS, Deenick EK, Batten M, Tangye SG. The origins, function, and regulation of T follicular helper cells. J. Exp. Med. Rockefeller University Press; 2012;209:1241–53.

405. Korn T, Mitsdoerffer M, Croxford AL, Awasthi A, Dardalhon VA, Galileos G, et al. IL-6 controls Th17 immunity in vivo by inhibiting the conversion of conventional T cells into Foxp3+ regulatory T cells. Proc. Natl. Acad. Sci. U.S.A. National Acad Sciences; 2008;105:18460–5.

406. Jones SA, Scheller J, Rose-John S. Therapeutic strategies for the clinical blockade of IL-6/gp130 signaling. J. Clin. Invest. American Society for Clinical Investigation; 2011;121:3375–83.

407. Sharma MD, Huang L, Choi J-H, Lee E-J, Wilson JM, Lemos H, et al. An Inherently Bifunctional Subset of Foxp3+ T Helper Cells Is Controlled by the Transcription Factor Eos. Immunity. 2013;38:998–1012.

408. Stumhofer JS, Silver JS, Laurence A, Porrett PM, Harris TH, Turka LA, et al. Interleukins 27 and 6 induce STAT3-mediated T cell production of interleukin 10. Nat. Immunol. Nature Publishing Group; 2007;8:1363–71.

409. McGeachy MJ, Bak-Jensen KS, Chen Y, Tato CM, Blumenschein W, McClanahan T, et al. TGF-β and IL-6 drive the production of IL-17 and IL-10 by T cells and restrain TH-17 cell–mediated pathology. Nat. Immunol. Nature Publishing Group; 2007;8:1390–7.

410. Yasukawa H, Ohishi M, Mori H, Murakami M, Chinen T, Aki D, et al. IL-6 induces an anti-inflammatory response in the absence of SOCS3 in macrophages. Nat. Immunol. 2003;4:551–6.

411. IL6R Genetics Consortium Emerging Risk Factors Collaboration, Sarwar N, Butterworth AS, Freitag DF, Gregson J, Willeit P, et al. Interleukin-6 receptor pathways in coronary heart disease: a collaborative meta-analysis of 82 studies. Lancet. 2012;379:1205–13.

412. Mehta NN. Large-Scale Association Analysis Identifies 13 New Susceptibility Loci for Coronary Artery Disease. Circulation: Cardiovascular Genetics. 2011;4:327–9.

413. Fishman D, Faulds G, Jeffery R, Mohamed-Ali V, Yudkin JS, Humphries S, et al. The effect of novel polymorphisms in the interleukin-6 (IL-6) gene on IL-6 transcription and plasma IL-6 levels, and an association with systemic-onset juvenile chronic arthritis. Journal of Clinical Investigation. 1998;102:1369–76.

414. Lu ZY, Brochier J, Wijdenes J, Brailly H, Bataille R, Klein B. High amounts of circulating interleukin (IL)-6 in the form of monomeric immune complexes during anti-IL-6 therapy. Towards a new methodology for measuring overall cytokine production in human in vivo. European Journal of Immunology. WILEY-VCH Verlag GmbH; 1992;22:2819–24.

415. Sato K, Tsuchiya M, Saldanha J, Koishihara Y, Ohsugi Y, Kishimoto T, et al. Reshaping a human antibody to inhibit the interleukin 6-dependent tumor cell growth. Cancer Research. 1993;53:851–6.

416. Maini RN, Taylor PC, Szechinski J, Pavelka K, Bröll J, Balint G, et al. Double-blind randomized controlled clinical trial of the interleukin-6 receptor antagonist, tocilizumab, in European patients with rheumatoid arthritis who had an incomplete response to methotrexate. Arthritis Rheum. Wiley Subscription Services, Inc., A Wiley Company; 2006;54:2817–29.

417. Genovese MC, McKay JD, Nasonov EL, Mysler EF, da Silva NA, Alecock E, et al. Interleukin-6 receptor inhibition with tocilizumab reduces disease activity in rheumatoid arthritis with inadequate response to disease-modifying antirheumatic drugs: the tocilizumab in combination with traditional disease-modifying antirheumatic drug therapy study. Arthritis Rheum. Wiley Subscription Services, Inc., A Wiley Company; 2008;58:2968–80.

418. Kremer JM, Blanco R, Brzosko M, Burgos-Vargas R, Halland A-M, Vernon E, et al. Tocilizumab inhibits structural joint damage in rheumatoid arthritis patients with inadequate responses to methotrexate: results from the double-blind treatment phase of a randomized placebo-controlled trial of tocilizumab safety and prevention of structural joint damage at one year. Arthritis Rheum. Wiley Subscription Services, Inc., A Wiley Company; 2011;63:609–21.

419. Garnero P, Thompson E, Woodworth T, Smolen JS. Rapid and sustained improvement in bone and cartilage turnover markers with the anti-interleukin-6 receptor inhibitor tocilizumab plus methotrexate in rheumatoid arthritis patients with an inadequate response to methotrexate: results from a substudy of the multicenter double-blind, placebo-controlled trial of tocilizumab in inadequate responders to methotrexate alone. Arthritis Rheum. Wiley Subscription Services, Inc., A Wiley Company; 2010;62:33–43.

420. Gabay C, Emery P, van Vollenhoven R, Dikranian A, Alten R, Pavelka K, et al. Tocilizumab monotherapy versus adalimumab monotherapy for treatment of rheumatoid arthritis (ADACTA): a randomised, double-blind, controlled phase 4 trial. Lancet. 2013;381:1541–50.

421. Dennis G, Holweg CT, Kummerfeld SK, Choy DF, Setiadi A, Hackney JA, et al. Synovial phenotypes in rheumatoid arthritis correlate with response to

biologic therapeutics. Arthritis Res. Ther. BioMed Central; 2014;16:R90.

422. Buckley F, Finckh A, Huizinga TWJ, Dejonckheere F, Jansen JP. Comparative Efficacy of Novel DMARDs as Monotherapy and in Combination with Methotrexate in Rheumatoid Arthritis Patients with Inadequate Response to Conventional DMARDs: A Network Meta-Analysis. Journal of Managed Care & Specialty Pharmacy. Academy of Managed Care Pharmacy; 2015;21:409–23.

423. Bijlsma JWJ, Welsing PMJ, Woodworth TG, Middelink LM, Pethö-Schramm A, Bernasconi C, et al. Early rheumatoid arthritis treated with tocilizumab, methotrexate, or their combination (U-Act-Early): a multicentre, randomised, double-blind, double-dummy, strategy trial. Lancet. 2016;388:343–55.

424. van Nies JAB, Tsonaka R, Gaujoux-Viala C, Fautrel B, van der Helm-van Mil AHM. Evaluating relationships between symptom duration and persistence of rheumatoid arthritis: does a window of opportunity exist? Results on the Leiden early arthritis clinic and ESPOIR cohorts. Ann. Rheum. Dis. BMJ Publishing Group Ltd and European League Against Rheumatism; 2015;74:806–12.

425. Schwartz DM, Bonelli M, Gadina M, O'Shea JJ. Type I/II cytokines, JAKs, and new strategies for treating autoimmune diseases. Nat Rev Rheumatol. 2016;12:25–36.

426. Giovannoni G, Gold R, Selmaj K, Havrdova E, Montalban X, Radue E-W, et al. Daclizumab high-yield process in relapsing-remitting multiple sclerosis (SELECTION): a multicentre, randomised, double-blind extension trial. Lancet Neurol. 2014;13:472–81.

427. Schmidt-Weber CB. Anti-IL-4 as a new strategy in allergy. Chem Immunol Allergy. Basel: KARGER; 2012;96:120–5.

428. Kim H-R, Hwang K-A, Park S-H, Kang I. IL-7 and IL-15: Biology and Roles in T-Cell Immunity in Health and Disease. Critical Reviews™ in Immunology. Begel House Inc; 2008;28:325–39.

429. Ogata Y, Kukita A, Kukita T, Komine M, Miyahara A, Miyazaki S, et al. A novel role of IL-15 in the development of osteoclasts: inability to replace its activity with IL-2. The Journal of Immunology. 1999;162:2754–60.

430. McInnes IB, Leung BP, Sturrock RD, Field M, Liew FY. Interleukin-15 mediates T cell-dependent regulation of tumor necrosis factor-alpha production in rheumatoid arthritis. Nat. Med. 1997;3:189–95.

431. Deshpande P, Cavanagh MM, Le Saux S, Singh K, Weyand CM, Goronzy JJ. IL-7- and IL-15-mediated TCR sensitization enables T cell responses to self-antigens. J Immunol. American Association of Immunologists; 2013;190:1416–23.

432. Baslund B, Tvede N, Danneskiold-Samsoe B, Larsson P, Panayi G, Petersen J, et al. Targeting interleukin-15 in patients with rheumatoid arthritis: a proof-of-concept study. Arthritis Rheum. Wiley Subscription Services, Inc., A Wiley Company; 2005;52:2686–92.

433. Knevel R, Krabben A, Brouwer E, Posthumus, Wilson AG, Saxne T, et al. Genetic variants in IL-15 associate with progression of joint destruction in

rheumatoid arthritis, a multi cohort study. Ann. Rheum. Dis. BMJ Publishing Group Ltd and European League Against Rheumatism; 2012;71:A56.3–A57.

434. Cornish AL, Campbell IK, McKenzie BS, Chatfield S, Wicks IP. G-CSF and GM-CSF as therapeutic targets in rheumatoid arthritis. Nat Rev Rheumatol. 2009;5:554–9.

435. Caux C, Vanbervliet B, Massacrier C, Dezutter-Dambuyant C, de Saint-Vis B, Jacquet C, et al. CD34+ hematopoietic progenitors from human cord blood differentiate along two independent dendritic cell pathways in response to GM-CSF+TNF alpha. Journal of Experimental Medicine. Rockefeller University Press; 1996;184:695–706.

436. Zhan Y, Xu Y, Lew AM. The regulation of the development and function of dendritic cell subsets by GM-CSF: More than a hematopoietic growth factor. Molecular Immunology. 2012;52:30–7.

437. Codarri L, Gyülvészi G, Tosevski V, Hesske L, Fontana A, Magnenat L, et al. RORγt drives production of the cytokine GM-CSF in helper T cells, which is essential for the effector phase of autoimmune neuroinflammation. Nat. Immunol. Nature Research; 2011;12:560–7.

438. Bär E, Whitney PG, Moor K, Reis e Sousa C, LeibundGut-Landmann S. IL-17 Regulates Systemic Fungal Immunity by Controlling the Functional Competence of NK Cells. Immunity. 2014;40:117–27.

439. Weber GF, Chousterman BG, Hilgendorf I, Robbins CS, Theurl I, Gerhardt LMS, et al. Pleural innate response activator B cells protect against pneumonia via a GM-CSF-IgM axis. J. Exp. Med. Rockefeller University Press; 2014;211:1243–56.

440. la Rubia de J, Martínez C, Solano C, Brunet S, Cascón P, Arrieta R, et al. Administration of recombinant human granulocyte colony-stimulating factor to normal donors: results of the Spanish National Donor Registry. Bone Marrow Transplantation. Nature Publishing Group; 1999;24:723–8.

441. Stösser S, Schweizerhof M, Kuner R. Hematopoietic colony-stimulating factors: new players in tumor-nerve interactions. J. Mol. Med. Springer-Verlag; 2011;89:321–9.

442. Schweizerhof M, Stösser S, Kurejova M, Njoo C, Gangadharan V, Agarwal N, et al. Hematopoietic colony–stimulating factors mediate tumor-nerve interactions and bone cancer pain. Nat. Med. Nature Publishing Group; 2009;15:802–7.

443. Cook AD, Pobjoy J, Sarros S, Steidl S, Dürr M, Lacey DC, et al. Granulocyte-macrophage colony-stimulating factor is a key mediator in inflammatory and arthritic pain. Ann. Rheum. Dis. BMJ Publishing Group Ltd and European League Against Rheumatism; 2013;72:265–70.

444. Ryan PC, Sleeman MA, Rebelatto M, Wang B, Lu H, Chen X, et al. Nonclinical safety of mavrilimumab, an anti-GMCSF receptor alpha monoclonal antibody, in cynomolgus monkeys: Relevance for human safety. Toxicology and Applied Pharmacology. 2014;279:230–9.

445. Burmester GR, Weinblatt ME, McInnes IB, Porter D, Barbarash O, Vatutin M, et al. Efficacy and safety of mavrilimumab in subjects with rheumatoid arthritis. Ann. Rheum. Dis. BMJ Publishing Group Ltd and European League Against Rheumatism; 2013;72:1445–52.

446. McInnes IB, Burmester GR, Kremer JM, Miranda P, Korkosz M, Vencovsky J, et al. SAT0189 Rapid Onset of Clinical Benefit in Patients with RA Treated with Mavrilimumab, A Fully Human Monoclonal Antibody Targeting GM–CSFR-ALPHA: Subanalysis of the Phase IIB Earth Explorer 1 Study. Ann. Rheum. Dis. BMJ Publishing Group Ltd and European League Against Rheumatism; 2015;74:723.3–724.

447. Burmester GR, McInnes IB, Kremer JM, Miranda P, Korkosz M, Vencovsky J, et al. OP0034 Efficacy and Safety of Mavrilimumab, A Fully Human Gm–CSFR-Alpha Monoclonal Antibody in Patients with Rheumatoid Arthritis: Primary Results from the Earth Explorer 1 Study. Ann. Rheum. Dis. BMJ Publishing Group Ltd and European League Against Rheumatism; 2015;74:78.1–78.

448. Weinblatt M, McInnes I, Kremer J, Miranda P, Vencovsky J, Godwood A, et al. SAT0146 Earth Explorer 2, A Phase IIB Exploratory Study Evaluating Efficacy and Safety of Mavrilimumab, A Fully Human Granulocyte-Macrophage Colony-Stimulating Factor Receptor-Alpha Monoclonal Antibody, and The Tumor Necrosis Factor Antagonist Golimumab in Rheumatoid Arthritis. Ann. Rheum. Dis. BMJ Publishing Group Ltd and European League Against Rheumatism; 2016;75:717.2–718.

449. Borden EC, Sen GC, Uze G, Silverman RH, Ransohoff RM, Foster GR, et al. Interferons at age 50: past, current and future impact on biomedicine. Nat Rev Drug Discov. 2007;6:975–90.

450. Krause I, Shoenfeld Y. Intravenous Immunoglobulin Treatment for Fibrosis, Atherosclerosis, and Malignant Conditions. Adoptive Immunotherapy. New Jersey: Humana Press; 2004. pp. 403–8.

451. Parlato S, Bruni R, Fragapane P, Salerno D, Marcantonio C, Borghi P, et al. IFN-α regulates Blimp-1 expression via miR-23a and miR-125b in both monocytes-derived DC and pDC. Zissel G, editor. PLoS ONE. Public Library of Science; 2013;8:e72833.

452. O'Shea JJ, Plenge R. JAK and STAT Signaling Molecules in Immunoregulation and Immune-Mediated Disease. Immunity. 2012;36:542–50.

453. Hertzog P, Forster S, Samarajiwa S. Systems Biology of Interferon Responses. Journal of Interferon & Cytokine Research. Mary Ann Liebert, Inc. 140 Huguenot Street, 3rdDMARD resistant Floor New Rochelle, NY 10801 USA; 2011;31:5–11.

454. Forster S. Interferon signatures in immune disorders and disease. Immunol. Cell Biol. 2012;90:520–7.

455. Higgs BW, Liu Z, White B, Zhu W, White WI, Morehouse C, et al. Patients with systemic lupus erythematosus, myositis, rheumatoid arthritis and scleroderma share activation of a common type I interferon pathway. Ann. Rheum. Dis. BMJ Publishing Group Ltd and European League Against

Rheumatism; 2011;70:2029–36.

456. Ruiz-Riol M, Armengol Barnils MDP, Colobran Oriol R, Sánchez Pla A, Borràs Serres F-E, Lucas-Martin A, et al. Analysis of the cumulative changes in Graves' disease thyroid glands points to IFN signature, plasmacytoid DCs and alternatively activated macrophages as chronicity determining factors. J. Autoimmun. 2011;36:189–200.

457. van der Pouw Kraan TCTM, Wijbrandts CA, van Baarsen LGM, Voskuyl AE, Rustenburg F, Baggen JM, et al. Rheumatoid arthritis subtypes identified by genomic profiling of peripheral blood cells: assignment of a type I interferon signature in a subpopulation of patients. Ann. Rheum. Dis. BMJ Publishing Group Ltd and European League Against Rheumatism; 2007;66:1008–14.

458. van Holten J. Expression of interferon in synovial tissue from patients with rheumatoid arthritis: comparison with patients with osteoarthritis and reactive arthritis. Ann. Rheum. Dis. 2005;64:1780–2.

459. Rönnblom L, Eloranta M-L. The interferon signature in autoimmune diseases. Curr Opin Rheumatol. 2013;25:248–53.

460. Gordon RA, Grigoriev G, Lee A, Kalliolias GD, Ivashkiv LB. The interferon signature and STAT1expression in rheumatoid arthritis synovial fluid macrophages are induced by tumor necrosis factor α and counter-regulated by the synovial fluid microenvironment. Arthritis Rheum. Wiley Subscription Services, Inc., A Wiley Company; 2012;64:3119–28.

461. Hervas-Stubbs S, Perez-Gracia JL, Rouzaut A, Sanmamed MF, Le Bon A, Melero I. Direct effects of type I interferons on cells of the immune system. Clin. Cancer Res. American Association for Cancer Research; 2011;17:2619–27.

462. Li J, Fu Q, Cui H, Qu B, Pan W, Shen N, et al. Interferon-α priming promotes lipid uptake and macrophage-derived foam cell formation: a novel link between interferon-α and atherosclerosis in lupus. Arthritis Rheum. Wiley Subscription Services, Inc., A Wiley Company; 2011;63:492–502.

463. Merrill JT, Wallace DJ, Petri M, Kirou KA, Yao Y, White WI, et al. Safety profile and clinical activity of sifalimumab, a fully human anti-interferon monoclonal antibody, in systemic lupus erythematosus: a phase I, multicentre, double-blind randomised study. Ann. Rheum. Dis. BMJ Publishing Group Ltd and European League Against Rheumatism; 2011;70:1905–13.

464. McBride JM, Jiang J, Abbas AR, Morimoto A, Li J, Maciuca R, et al. Safety and pharmacodynamics of rontalizumab in patients with systemic lupus erythematosus: Results of a phase I, placebo-controlled, double-blind, dose-escalation study. Arthritis Rheum. Wiley Subscription Services, Inc., A Wiley Company; 2012;64:3666–76.

465. van Baarsen LG, Wijbrandts CA, Rustenburg F, Cantaert T, van der Pouw Kraan TC, Baeten DL, et al. Regulation of IFN response gene activity during infliximab treatment in rheumatoid arthritis is associated with clinical response to treatment. Arthritis Res. Ther. BioMed Central; 2010;12:R11.

466. Thurlings RM, Boumans M, Tekstra J, van Roon JA, Vos K, van Westing DM,

et al. Relationship between the type I interferon signature and the response to rituximab in rheumatoid arthritis patients. Arthritis Rheum. Wiley Subscription Services, Inc., A Wiley Company; 2010;62:3607–14.

467. Park JK. Rheumatoid arthritis subgroup with type I interferon signature: Comment on the article by Thurlings et al. Arthritis Rheum. Wiley Subscription Services, Inc., A Wiley Company; 2011;63:4033–3.

468. O'Shea JJ, Holland SM, Staudt LM. JAKs and STATs in immunity, immunodeficiency, and cancer. N Engl J Med. 2013;368:161–70.

469. Macchi P, Villa A, Giliani S, Sacco MG, Frattini A, Porta F, et al. Mutations of Jak-3 gene in patients with autosomal severe combined immune deficiency (SCID). Nature. Nature Publishing Group; 1995;377:65–8.

470. Russell SM, Tayebi N, Nakajima H, Riedy MC, Roberts JL, Aman MJ, et al. Mutation of Jak3 in a patient with SCID: essential role of Jak3 in lymphoid development. Science. 1995;270:797–800.

471. Ouyang W, Rutz S, Crellin NK, Valdez PA, Hymowitz SG. Regulation and functions of the IL-10 family of cytokines in inflammation and disease. Annual Review of Immunology. Annual Reviews; 2011;29:71–109.

472. Changelian PS, Flanagan ME, Ball DJ, Kent CR, Magnuson KS, Martin WH, et al. Prevention of organ allograft rejection by a specific Janus kinase 3 inhibitor. Science. American Association for the Advancement of Science; 2003;302:875–8.

473. O'Shea JJ, Schwartz DM, Villarino AV, Gadina M, McInnes IB, Laurence A. The JAK-STAT pathway: impact on human disease and therapeutic intervention. Annual Review of Medicine. Annual Reviews; 2015;66:311–28.

474. Fleischmann R, Kremer J, Cush J, Schulze-Koops H, Connell CA, Bradley JD, et al. Placebo-controlled trial of tofacitinib monotherapy in rheumatoid arthritis. N Engl J Med. Massachusetts Medical Society; 2012;367:495–507.

475. Strand V, Lee EB, Fleischmann R, Alten RE, Koncz T, Zwillich SH, et al. Tofacitinib versus methotrexate in rheumatoid arthritis: patient-reported outcomes from the randomised phase III ORAL Start trial. RMD Open. EULAR; 2016;2:e000308.

476. Burmester GR, Blanco R, Charles-Schoeman C, Wollenhaupt J, Zerbini C, Benda B, et al. Tofacitinib (CP-690,550) in combination with methotrexate in patients with active rheumatoid arthritis with an inadequate response to tumour necrosis factor inhibitors: a randomised phase 3 trial. Lancet. 2013;381:451–60.

477. van der Heijde D, Tanaka Y, Fleischmann R, Keystone E, Kremer J, Zerbini C, et al. Tofacitinib (CP-690,550) in patients with rheumatoid arthritis receiving methotrexate: twelve-month data from a twenty-four-month phase III randomized radiographic study. Arthritis Rheum. Wiley Subscription Services, Inc., A Wiley Company; 2013;65:559–70.

478. van Vollenhoven RF, Fleischmann R, Cohen S, Lee EB, García Meijide JA, Wagner S, et al. Tofacitinib or adalimumab versus placebo in rheumatoid arthritis. N Engl J Med. Massachusetts Medical Society; 2012;367:508–19.

479. Lee EB, Fleischmann R, Hall S, Wilkinson B, Bradley JD, Gruben D, et al. Tofacitinib versus methotrexate in rheumatoid arthritis. N Engl J Med. Massachusetts Medical Society; 2014;370:2377–86.

480. Mascarenhas J, Hoffman R. Ruxolitinib: the first FDA approved therapy for the treatment of myelofibrosis. Clin. Cancer Res. American Association for Cancer Research; 2012;18:3008–14.

481. Genovese MC, Kremer J, Zamani O, Ludivico C, Krogulec M, Xie L, et al. Baricitinib in Patients with Refractory Rheumatoid Arthritis. N Engl J Med. Massachusetts Medical Society; 2016;374:1243–52.

482. Dougados M, van der Heijde D, Chen YC, Greenwald M, Drescher E, Liu J, et al. LB0001 Baricitinib, an Oral Janus Kinase (JAK)1/JAK2 Inhibitor, in Patients with Active Rheumatoid Arthritis (RA) and An Inadequate Response to CDMARD Therapy: Results of the Phase 3 RA-Build Study:. Ann. Rheum. Dis. BMJ Publishing Group Ltd and European League Against Rheumatism; 2015;74:79.2–79.

483. He Y, Wong AYS, Chan EW, Lau WCY, Man KKC, Chui CSL, et al. Efficacy and safety of tofacitinib in the treatment of rheumatoid arthritis: a systematic review and meta-analysis. BMC Musculoskeletal Disorders. 2013;14:298.

484. Wollenhaupt J, Silverfield J, Lee EB, Curtis JR, Wood SP, Soma K, et al. Safety and efficacy of tofacitinib, an oral janus kinase inhibitor, for the treatment of rheumatoid arthritis in open-label, longterm extension studies. J. Rheumatol. 2014;41:837–52.

485. Winthrop KL, Yamanaka H, Valdez H, Mortensen E, Chew R, Krishnaswami S, et al. Herpes zoster and tofacitinib therapy in patients with rheumatoid arthritis. Arthritis Rheumatol. 2014;66:2675–84.

486. van Vollenhoven RF, Tanaka Y, Lamba M, Collinge M, Hendrikx T, Hirose T, et al. THU0178 Relationship Between NK Cell Count and Important Safety Events in Rheumatoid Arthritis Patients Treated with Tofacitinib. Ann. Rheum. Dis. 2015;74:258.3–259.

487. Winthrop KL, Silverfield J, Racewicz A, Neal J, Lee EB, Hrycaj P, et al. The effect of tofacitinib on pneumococcal and influenza vaccine responses in rheumatoid arthritis. Ann. Rheum. Dis. 2016;75:687–95.

488. Kume K. Tocilizumab Improves Arterial Stiffness As Well As Other Biologics with Methotrexate-Resistant Active Rheumatoid Arthritis-An Open Label, Randomized Cohort Multi Center Study. OMICS Journal of Radiology. 2015;04.

489. Scheller J, Garbers C, Rose-John S. Interleukin-6: from basic biology to selective blockade of pro-inflammatory activities. Seminars in Immunology. 2014;26:2–12.

490. Charles-Schoeman C, Fleischmann R, Davignon J, Schwartz H, Turner SM, Beysen C, et al. Potential mechanisms leading to the abnormal lipid profile in patients with rheumatoid arthritis versus healthy volunteers and reversal by tofacitinib. Arthritis Rheumatol. 2015;67:616–25.

491. Moisan A, Lee Y-K, Zhang JD, Hudak CS, Meyer CA, Prummer M, et al. White-to-brown metabolic conversion of human adipocytes by JAK inhibition. Nature Cell Biology. 2015;17:57–67.

492. Vanhoutte FP, Mazur M, Namour F, van der Aa A, Wigerinck P, van t Klooster GAE. OP0263 Efficacy and safety of GLPG0634, a selective JAK1 inhibitor, after short-term treatment of rheumatoid arthritis; results of a phase IIA trial. Ann. Rheum. Dis. 2014;71:145.1–145.

493. MacGregor AJ, Snieder H, Rigby AS, Koskenvuo M, Kaprio J, Aho K, et al. Characterizing the quantitative genetic contribution to rheumatoid arthritis using data from twins. Arthritis Rheum. 2000;43:30–7.

494. van der Woude D, Houwing-Duistermaat JJ, Toes REM, Huizinga TWJ, Thomson W, Worthington J, et al. Quantitative heritability of anti-citrullinated protein antibody-positive and anti-citrullinated protein antibody-negative rheumatoid arthritis. Arthritis Rheum. 2009;60:916–23.

495. Lenz TL, Deutsch AJ, Han B, Hu X, Okada Y, Eyre S, et al. Widespread non-additive and interaction effects within HLA loci modulate the risk of autoimmune diseases. Nat. Genet. 2015;47:1085–90.

496. Stahl EA, Wegmann D, Trynka G, Gutierrez-Achury J, Do R, Voight BF, et al. Bayesian inference analyses of the polygenic architecture of rheumatoid arthritis. Nat. Genet. 2012;44:483–9.

497. Horton R, Wilming L, Rand V, Lovering RC, Bruford EA, Khodiyar VK, et al. Gene map of the extended human MHC. Nat. Rev. Genet. 2004;5:889–99.

498. Gregersen PK, Silver J, Winchester RJ. The shared epitope hypothesis. an approach to understanding the molecular genetics of susceptibility to rheumatoid arthritis. Arthritis Rheum. 1987;30:1205–13.

499. Anderson KM, Roark CL, Portas M, Aubrey MT, Rosloniec EF, Freed BM. A Molecular Analysis of the Shared Epitope Hypothesis: Binding of Arthritogenic Peptides to DRB1*04 Alleles. Arthritis & Rheumatology. 2016;68:1627–36.

500. Bossini-Castillo L, de Kovel C, Kallberg H, van 't Slot R, Italiaander A, Coenen M, et al. A genome-wide association study of rheumatoid arthritis without antibodies against citrullinated peptides. Ann. Rheum. Dis. 2015;74:e15–5.

501. Wagner CA, Sokolove J, Lahey LJ, Bengtsson C, Saevarsdottir S, Alfredsson L, et al. Identification of anticitrullinated protein antibody reactivities in a subset of anti-CCP-negative rheumatoid arthritis: association with cigarette smoking and HLA-DRB1 “shared epitope” alleles. Ann. Rheum. Dis. 2015;74:579–86.

502. Han B, Diogo D, Eyre S, Kallberg H, Zhernakova A, Bowes J, et al. Fine Mapping Seronegative and Seropositive Rheumatoid Arthritis to Shared and Distinct HLA Alleles by Adjusting for the Effects of Heterogeneity. The American Journal of Human Genetics. 2014;94:522–32.

503. Fortune MD, Guo H, Burren O, Schofield E, Walker NM, Ban M, et al.

Statistical colocalization of genetic risk variants for related autoimmune diseases in the context of common controls. Nat. Genet. 2015;47:839–46.

504. Vahedi G, Kanno Y, Furumoto Y, Jiang K, Parker SCJ, Erdos MR, et al. Super-enhancers delineate disease-associated regulatory nodes in T cells. Nature. 2015;520:558–62.

505. Hrdlickova B, Kumar V, Kanduri K, Zhernakova DV, Tripathi S, Karjalainen J, et al. Expression profiles of long non-coding RNAs located in autoimmune disease-associated regions reveal immune cell-type specificity. Genome Medicine. 2014;6:88.

506. Li G, Diogo D, Wu D, Spoonamore J, Dancik V, Franke L, et al. Human Genetics in Rheumatoid Arthritis Guides a High-Throughput Drug Screen of the CD40 Signaling Pathway. McCarthy MI, editor. PLoS Genetics. 2013;9:e1003487.

507. Evans CH, Ghivizzani SC, Robbins PD. Arthritis gene therapy and its tortuous path into the clinic. Transl Res. 2013;161:205–16.

508. Hohmann EL. Gene therapy--still a work in clinical and regulatory progress. N Engl J Med. 2009;361:193–5.

509. Hampton T. Arthritis gene therapy trial resumes. JAMA. American Medical Association; 2008 Jan 2;:28–8.

510. Viatte S, Plant D, Han B, Fu B, Yarwood A, Thomson W, et al. Association of HLA-DRB1 Haplotypes With Rheumatoid Arthritis Severity, Mortality, and Treatment Response. JAMA. 2015;313:1645.

511. Bottini N, Firestein GS. Epigenetics in rheumatoid arthritis: a primer for rheumatologists. Curr Rheumatol Rep. Springer US; 2013;15:372.

512. Ghildiyal M, Zamore PD. Small silencing RNAs: an expanding universe. Nat. Rev. Genet. 2009;10:94–108.

513. Ha M, Kim VN. Regulation of microRNA biogenesis. Nature Reviews Molecular Cell Biology. 2014;15:509–24.

514. Graves P, Zeng Y. Biogenesis of Mammalian MicroRNAs: A Global View. Genomics, Proteomics & Bioinformatics. 2012;10:239–45.

515. Im H-I, Kenny PJ. MicroRNAs in neuronal function and dysfunction. Trends in Neurosciences. 2012;35:325–34.

516. Qu Z, Li W, Fu B. MicroRNAs in autoimmune diseases. Biomed Res Int. Hindawi Publishing Corporation; 2014;2014:527895–8.

517. Lee Y, Jeon K, Lee J-T, Kim S, Kim VN. MicroRNA maturation: stepwise processing and subcellular localization. EMBO J. European Molecular Biology Organization; 2002;21:4663–70.

518. Roush S, Slack FJ. The let-7 family of microRNAs. Trends in Cell Biology. 2008;18:505–16.

519. Ozsolak F, Poling LL, Wang Z, Liu H, Liu XS, Roeder RG, et al. Chromatin

structure analyses identify miRNA promoters. Genes Dev. 2008;22:3172–83.

520. Davis BN, Hata A. Mechanisms of control of microRNA biogenesis. Journal of Biochemistry. 2010.

521. Han J, Pedersen JS, Kwon SC, Belair CD, Kim Y-K, Yeom K-H, et al. Posttranscriptional Crossregulation between Drosha and DGCR8. Cell. 2009;136:75–84.

522. Kadener S, Rodriguez J, Abruzzi KC, Khodor YL, Sugino K, Marr MT, et al. Genome-wide identification of targets of the drosha-pasha/DGCR8 complex. RNA. Cold Spring Harbor Lab; 2009;15:537–45.

523. BOHNSACK MT. Exportin 5 is a RanGTP-dependent dsRNA-binding protein that mediates nuclear export of pre-miRNAs. RNA. 2004;10:185–91.

524. Ketting RF. Dicer functions in RNA interference and in synthesis of small RNA involved in developmental timing in C. elegans. Genes Dev. 2001;15:2654–9.

525. Hammond SM. Argonaute2, a Link Between Genetic and Biochemical Analyses of RNAi. Science. 2001;293:1146–50.

526. Huntzinger E, Izaurralde E. Gene silencing by microRNAs: contributions of translational repression and mRNA decay. Nat. Rev. Genet. 2011;12:99–110.

527. Vlachos IS, Paraskevopoulou MD, Karagkouni D, Georgakilas G, Vergoulis T, Kanellos I, et al. DIANA-TarBase v7.0: indexing more than half a million experimentally supported miRNA:mRNA interactions. Nucleic Acids Res. Oxford University Press; 2015;43:D153–9.

528. Peterson SM, Thompson JA, Ufkin ML, Sathyanarayana P, Liaw L, Congdon CB. Common features of microRNA target prediction tools. Frontiers in Genetics. Frontiers; 2014;5.

529. Cloonan N. Re-thinking miRNA-mRNA interactions: Intertwining issues confound target discovery. BioEssays. 2015;37:379–88.

530. M Witkos T, Koscianska E, J Krzyzosiak W. Practical Aspects of microRNA Target Prediction. Current Molecular Medicine. 2011;11:93–109.

531. Krek A, Grün D, Poy MN, Wolf R, Rosenberg L, Epstein EJ, et al. Combinatorial microRNA target predictions. Nat. Genet. Nature Publishing Group; 2005;37:495–500.

532. Lewis BP, Burge CB, Bartel DP. Conserved Seed Pairing, Often Flanked by Adenosines, Indicates that Thousands of Human Genes are MicroRNA Targets. Cell. 2005;120:15–20.

533. Friedman RC, Farh KK-H, Burge CB, Bartel DP. Most mammalian mRNAs are conserved targets of microRNAs. Genome Res. 2009;19:92–105.

534. Nielsen CB, Shomron N, Sandberg R, Hornstein E, Kitzman J, Burge CB. Determinants of targeting by endogenous and exogenous microRNAs and siRNAs. RNA. Cold Spring Harbor Lab; 2007;13:1894–910.

535. Alexiou P, Maragkakis M, Papadopoulos GL, Reczko M, Hatzigeorgiou AG. Lost in translation: an assessment and perspective for computational microRNA target identification. Bioinformatics. Oxford University Press; 2009;25:3049–55.

536. Kertesz M, Iovino N, Unnerstall U, Gaul U, Segal E. The role of site accessibility in microRNA target recognition. Nat. Genet. Nature Publishing Group; 2007;39:1278–84.

537. Yue D, Liu H, Huang Y. Survey of Computational Algorithms for MicroRNA Target Prediction. Curr. Genomics. 2009;10:478–92.

538. Miranda KC, Huynh T, Tay Y, Ang Y-S, Tam W-L, Thomson AM, et al. A Pattern-Based Method for the Identification of MicroRNA Binding Sites and Their Corresponding Heteroduplexes. Cell. 2006;126:1203–17.

539. Hafner M, Landthaler M, Burger L, Khorshid M, Hausser J, Berninger P, et al. Transcriptome-wide Identification of RNA-Binding Protein and MicroRNA Target Sites by PAR-CLIP. Cell. 2010;141:129–41.

540. Takagi S, Nakajima M, Kida K, Yamaura Y, Fukami T, Yokoi T. MicroRNAs regulate human hepatocyte nuclear factor 4alpha, modulating the expression of metabolic enzymes and cell cycle. Journal of Biological Chemistry. American Society for Biochemistry and Molecular Biology; 2010;285:4415–22.

541. Jens M, Rajewsky N. Competition between target sites of regulators shapes post-transcriptional gene regulation. Nat. Rev. Genet. 2014;16:113–26.

542. Selbach M, Schwanhäusser B, Thierfelder N, Fang Z, Khanin R, Rajewsky N. Widespread changes in protein synthesis induced by microRNAs. Nature. 2008;455:58–63.

543. Licatalosi DD, Mele A, Fak JJ, Ule J, Kayikci M, Chi SW, et al. HITS-CLIP yields genome-wide insights into brain alternative RNA processing. Nature. 2008;456:464–9.

544. Helwak A, Kudla G, Dudnakova T, Tollervey D. Mapping the Human miRNA Interactome by CLASH Reveals Frequent Noncanonical Binding. Cell. 2013;153:654–65.

545. Ørom UA, Lund AH. Isolation of microRNA targets using biotinylated synthetic microRNAs. Methods. 2007;43:162–5.

546. Derti A, Garrett-Engele P, MacIsaac KD, Stevens RC, Sriram S, Chen R, et al. A quantitative atlas of polyadenylation in five mammals. Genome Res. 2012;22:1173–83.

547. Kuhn DE, Martin MM, Feldman DS, Terry AV, Nuovo GJ, Elton TS. Experimental validation of miRNA targets. Methods. 2008;44:47–54.

548. Vicente R, Noël D, Pers Y-M, Apparailly F, Jorgensen C. Deregulation and therapeutic potential of microRNAs in arthritic diseases. Nat Rev Rheumatol. 2016;12:211–20.

549. Tili E, Michaille JJ, Cimino A, Costinean S, Dumitru CD, Adair B, et al. Modulation of miR-155 and miR-125b Levels following Lipopolysaccharide/TNF-

Stimulation and Their Possible Roles in Regulating the Response to Endotoxin Shock. The Journal of Immunology. 2007;179:5082–9.

550. Kurowska-Stolarska M, Alivernini S, Ballantine LE, Asquith DL, Millar NL, Gilchrist DS, et al. MicroRNA-155 as a proinflammatory regulator in clinical and experimental arthritis. Proc. Natl. Acad. Sci. U.S.A. 2011;108:11193–8.

551. Wang P, Hou J, Lin L, Wang C, Liu X, Li D, et al. Inducible microRNA-155 Feedback Promotes Type I IFN Signaling in Antiviral Innate Immunity by Targeting Suppressor of Cytokine Signaling 1. The Journal of Immunology. 2010;185:6226–33.

552. Elmesmari A, Fraser AR, Wood C, Gilchrist D, Vaughan D, Stewart L, et al. MicroRNA-155 regulates monocyte chemokine and chemokine receptor expression in Rheumatoid Arthritis. Rheumatology (Oxford). Oxford University Press; 2016;:kew272.

553. Alivernini S, Kurowska-Stolarska M, Tolusso B, Benvenuto R, Elmesmari A, Canestri S, et al. MicroRNA-155 influences B-cell function through PU.1 in rheumatoid arthritis. Nat Commun. 2016;7:12970.

554. Pauley KM, Satoh M, Chan AL, Bubb MR, Reeves WH, Chan EK. Upregulated miR-146a expression in peripheral blood mononuclear cells from rheumatoid arthritis patients. Arthritis Res. Ther. BioMed Central; 2008;10:R101.

555. Li J, Wan Y, Guo Q, Zou L, Zhang J, Fang Y, et al. Altered microRNA expression profile with miR-146a upregulation in CD4+ T cells from patients with rheumatoid arthritis. Arthritis Res. Ther. 2010;12:R81.

556. Stanczyk J, Pedrioli DML, Brentano F, Sanchez-Pernaute O, Kolling C, Gay RE, et al. Altered expression of MicroRNA in synovial fibroblasts and synovial tissue in rheumatoid arthritis. Arthritis Rheum. 2008;58:1001–9.

557. Murata K, Yoshitomi H, Tanida S, Ishikawa M, Nishitani K, Ito H, et al. Plasma and synovial fluid microRNAs as potential biomarkers of rheumatoid arthritis and osteoarthritis. Arthritis Res. Ther. 2010;12:R86.

558. Zhou Q, Haupt S, Kreuzer JT, Hammitzsch A, Proft F, Neumann C, et al. Decreased expression of miR-146a and miR-155 contributes to an abnormal Treg phenotype in patients with rheumatoid arthritis. Ann. Rheum. Dis. 2015;74:1265–74.

559. Nakasa T, Shibuya H, Nagata Y, Niimoto T, Ochi M. The inhibitory effect of microRNA-146a expression on bone destruction in collagen-induced arthritis. Arthritis Rheum. 2011;63:1582–90.

560. Dai R, Phillips RA, Zhang Y, Khan D, Crasta O, Ahmed SA. Suppression of LPS-induced Interferon- and nitric oxide in splenic lymphocytes by select estrogen-regulated microRNAs: a novel mechanism of immune modulation. Blood. 2008;112:4591–7.

561. Fulci V, Scappucci G, Sebastiani GD, Giannitti C, Franceschini D, Meloni F, et al. miR-223 is overexpressed in T-lymphocytes of patients affected by rheumatoid arthritis. Human Immunology. 2010;71:206–11.

562. Li Y-T, Chen S-Y, Wang C-R, Liu M-F, Lin C-C, Jou I-M, et al. Brief Report: Amelioration of collagen-induced arthritis in mice by lentivirus-mediated silencing of microRNA-223. Arthritis Rheum. Wiley Subscription Services, Inc., A Wiley Company; 2012;64:3240–5.

563. Pandis I, Ospelt C, Karagianni N, Denis MC, Reczko M, Camps C, et al. Identification of microRNA-221/222 and microRNA-323-3p association with rheumatoid arthritis via predictions using the human tumour necrosis factor transgenic mouse model. Ann. Rheum. Dis. 2012;71:1716–23.

564. Zhang Q, Wu J, Cao Q, Xiao L, Wang L, He D, et al. A critical role of Cyr61 in interleukin-17â "dependent proliferation of fibroblast-like synoviocytes in rheumatoid arthritis. Arthritis Rheum. 2009;60:3602–12.

565. Niederer F, Trenkmann M, Ospelt C, Karouzakis E, Neidhart M, Stanczyk J, et al. Down-regulation of microRNA-34a* in rheumatoid arthritis synovial fibroblasts promotes apoptosis resistance. Arthritis Rheum. 2012;64:1771–9.

566. Miao C-G, Yang Y-Y, He X, Huang C, Huang Y, Qin D, et al. MicroRNA-152 modulates the canonical Wnt pathway activation by targeting DNA methyltransferase 1 in arthritic rat model. Biochimie. 2014;106:149–56.

567. Chhabra R, Dubey R, Saini N. Cooperative and individualistic functions of the microRNAs in the miR-23a~27a~24-2 cluster and its implication in human diseases. Molecular Cancer. 2010;9:232.

568. Kong KY, Owens KS, Rogers JH, Mullenix J, Velu CS, Grimes HL, et al. MIR-23A microRNA cluster inhibits B-cell development. Exp. Hematol. 2010;38:629–640.e1.

569. Saini HK, Griffiths-Jones S, Enright AJ. Genomic analysis of human microRNA transcripts. Proceedings of the National Academy of Sciences. 2007;104:17719–24.

570. Lee Y, Kim M, Han J, Yeom K-H, Lee S, Baek SH, et al. MicroRNA genes are transcribed by RNA polymerase II. EMBO J. EMBO Press; 2004;23:4051–60.

571. Tanzer A, Stadler PF. Molecular Evolution of a MicroRNA Cluster. Journal of Molecular Biology. 2004;339:327–35.

572. Tanzer A, Riester M, Hertel J, Bermudez-Santana CI, Gorodkin J, Hofacker IL, et al. Evolutionary Genomics of microRNAs and Their Relatives. Evolutionary Genomics and Systems Biology. Hoboken, NJ, USA: John Wiley & Sons, Inc; 2010. pp. 295–327.

573. Yuan X, Liu C, Yang P, He S, Liao Q, Kang S, et al. Clustered microRNAs' coordination in regulating protein-protein interaction network. BMC Syst Biol. 2009;3:65.

574. Chhabra R, Adlakha YK, Hariharan M, Scaria V, Saini N. Upregulation of miR-23a~27a~24-2 Cluster Induces Caspase-Dependent and -Independent Apoptosis in Human Embryonic Kidney Cells. Blagosklonny MV, editor. PLoS ONE. 2009;4:e5848.

575. Huang S, He X, Ding J, Liang L, Zhao Y, Zhang Z, et al. Upregulation of miR-23a~27a~24 decreases transforming growth factor-beta-induced tumor-suppressive activities in human hepatocellular carcinoma cells. Int. J. Cancer. 2008;123:972–8.

576. Wang Q, Huang Z, Xue H, Jin C, Ju XL, Han JDJ, et al. MicroRNA miR-24 inhibits erythropoiesis by targeting activin type I receptor ALK4. Blood. 2008;111:588–95.

577. Min S, Li L, Zhang M, Liang X, Xie Y, He Q, et al. TGF-ß-associated miR-27a inhibits dendritic cell-mediated differentiation of Th1 and Th17 cells by TAB3, p38 MAPK, MAP2K4 and MAP2K7. Genes Immun. 2012;13:621–31.

578. Chan MC, Hilyard AC, Wu C, Davis BN, Hill NS, Lal A, et al. Molecular basis for antagonism between PDGF and the TGFß family of signalling pathways by control of miR-24 expression. EMBO J. 2009;29:559–73.

579. Mertens-Talcott SU, Noratto GD, Li X, Angel-Morales G, Bertoldi MC, Safe S. Betulinic acid decreases ER-negative breast cancer cell growth in vitro and in vivo: role of Sp transcription factors and microRNA-27a:ZBTB10. Mol. Carcinog. Wiley Subscription Services, Inc., A Wiley Company; 2013;52:591–602.

580. Urbich C, Kaluza D, Fromel T, Knau A, Bennewitz K, Boon RA, et al. MicroRNA-27a/b controls endothelial cell repulsion and angiogenesis by targeting semaphorin 6A. Blood. 2012;119:1607–16.

581. Ma Y, Yu S, Zhao W, Lu Z, Chen J. miR-27a regulates the growth, colony formation and migration of pancreatic cancer cells by targeting Sprouty2. Cancer Lett. 2010;298:150–8.

582. Veliceasa D, Biyashev D, Qin G, Misener S, Mackie AR, Kishore R, et al. Therapeutic manipulation of angiogenesis with miR-27b. Vasc Cell. 2015;7:6.

583. Poliseno L, Tuccoli A, Mariani L, Evangelista M, Citti L, Woods K, et al. MicroRNAs modulate the angiogenic properties of HUVECs. Blood. American Society of Hematology; 2006;108:3068–71.

584. Guttilla IK, White BA. Coordinate regulation of FOXO1 by miR-27a, miR-96, and miR-182 in breast cancer cells. J. Biol. Chem. American Society for Biochemistry and Molecular Biology; 2009;284:23204–16.

585. Mertens-Talcott SU, Chintharlapalli S, Li X, Safe S. The oncogenic microRNA-27a targets genes that regulate specificity protein transcription factors and the G2-M checkpoint in MDA-MB-231 breast cancer cells. Cancer Research. American Association for Cancer Research; 2007;67:11001–11.

586. Lin S-C, Liu C-J, Lin J-A, Chiang W-F, Hung P-S, Chang K-W. miR-24 up-regulation in oral carcinoma: Positive association from clinical and in vitro analysis. Oral Oncology. 2010;46:204–8.

587. Qin W, Shi YZBYCJLMJJY. miR-24 Regulates Apoptosis by Targeting the Open Reading Frame (ORF) Region of FAF1 in Cancer Cells [electronic resource]. Public Library of Science.

588. Lal A, Navarro F, Maher CA, Maliszewski LE, Yan N, O'Day E, et al. miR-24 Inhibits Cell Proliferation by Targeting E2F2, MYC, and Other Cell-Cycle Genes via Binding to “Seedless” 3′UTR MicroRNA Recognition Elements. Molecular Cell. 2009;35:610–25.

589. Saumet A, Vetter G, Bouttier M, Portales-Casamar E, Wasserman WW, Maurin T, et al. Transcriptional repression of microRNA genes by PML-RARA increases expression of key cancer proteins in acute promyelocytic leukemia. Blood. American Society of Hematology; 2009;113:412–21.

590. Schultz J, Lorenz P, Gross G, Ibrahim S, Kunz M. MicroRNA let-7b targets important cell cycle molecules in malignant melanoma cells and interferes with anchorage-independent growth. Cell Research. Nature Publishing Group; 2008;18:549–57.

591. Abu-Elneel K, Liu T, Gazzaniga FS, Nishimura Y, Wall DP, Geschwind DH, et al. Heterogeneous dysregulation of microRNAs across the autism spectrum. neurogenetics. Springer Berlin Heidelberg; 2008;9:153–61.

592. Perkins DO, Jeffries CD, Jarskog LF, Thomson JM, Woods K, Newman MA, et al. microRNA expression in the prefrontal cortex of individuals with schizophrenia and schizoaffective disorder. Genome Biology. BioMed Central; 2007;8:R27.

593. Zhu S, Pan W, Song X, Liu Y, Shao X, Tang Y, et al. The microRNA miR-23b suppresses IL-17-associated autoimmune inflammation by targeting TAB2, TAB3 and IKK-α. Nat. Med. Nature Research; 2012;18:1077–86.

594. Fordham JB, Naqvi AR, Nares S. Regulation of miR-24, miR-30b, and miR-142-3p during macrophage and dendritic cell differentiation potentiates innate immunity. Journal of Leukocyte Biology. 2015;98:195–207.

595. Naqvi AR, Fordham JB, Ganesh B, Nares S. miR-24, miR-30b and miR-142-3p interfere with antigen processing and presentation by primary macrophages and dendritic cells. Sci Rep. 2016;6:32925.

596. Zheng Q, Hou J, Zhou Y, Yang Y, Cao X. Type I IFN-Inducible Downregulation of MicroRNA-27a Feedback Inhibits Antiviral Innate Response by Upregulating Siglec1/TRIM27. J Immunol. 2016;196:1317–26.

597. Saha B, Bruneau JC, Kodys K, Szabo G. Alcohol-induced miR-27a regulates differentiation and M2 macrophage polarization of normal human monocytes. J Immunol. American Association of Immunologists; 2015;194:3079–87.

598. Hassan MQ, Gordon JAR, Beloti MM, Croce CM, Wijnen AJV, Stein JL, et al. A network connecting Runx2, SATB2, and the miR-23a 27a 24-2 cluster regulates the osteoblast differentiation program. Proceedings of the National Academy of Sciences. 2010;107:19879–84.

599. Shi D-L, Shi G-R, Xie J, Du X-Z, Yang H. MicroRNA-27a Inhibits Cell Migration and Invasion of Fibroblast-Like Synoviocytes by Targeting Follistatin-Like Protein 1 in Rheumatoid Arthritis. Mol. Cells. Korean Society for Molecular and Cellular Biology; 2016;39:611–8.

600. Chen S-Z, Xu X, Ning L-F, Jiang W-Y, Xing C, Tang Q-Q, et al. miR-27 impairs the adipogenic lineage commitment via targeting lysyl oxidase. Obesity (Silver Spring). 2015;23:2445–53.

601. Zhu Y, Zhang X, Ding X, Wang H, Chen X, Zhao H, et al. miR-27 inhibits adipocyte differentiation via suppressing CREB expression. Acta Biochim. Biophys. Sin. (Shanghai). 2014;46:590–6.

602. Sun L, Trajkovski M. MiR-27 orchestrates the transcriptional regulation of brown adipogenesis. Metabolism. 2014.

603. Xie W, Li L, Zhang M, Cheng H-P, Gong D, Lv Y-C, et al. MicroRNA-27 Prevents Atherosclerosis by Suppressing Lipoprotein Lipase-Induced Lipid Accumulation and Inflammatory Response in Apolipoprotein E Knockout Mice. Zhang Y, editor. PLoS ONE. 2016;11:e0157085.

604. Lozano-Velasco E, Galiano-Torres J, Jodar-Garcia A, Aranega AE, Franco D. miR-27 and miR-125 Distinctly Regulate Muscle-Enriched Transcription Factors in Cardiac and Skeletal Myocytes. Biomed Res Int. 2015;2015:391306.

605. Di Y, Zhang D, Hu T, Li D. miR-23 regulate the pathogenesis of patients with coronary artery disease. Int J Clin Exp Med. 2015;8:11759–69.

606. Zhang B, Liu S-Q, Li C, Lykken E, Jiang S, Wong E, et al. MicroRNA-23a Curbs Necrosis during Early T Cell Activation by Enforcing Intracellular Reactive Oxygen Species Equilibrium. Immunity. 2016;44:568–81.

607. Cho S, Wu C-J, Yasuda T, Cruz LO, Khan AA, Lin L-L, et al. miR-23~27~24 clusters control effector T cell differentiation and function. The Journal of Cell Biology. 2016;212:212422.

608. Pua HH, Steiner DF, Patel S, Gonzalez JR, Ortiz-Carpena JF, Kageyama R, et al. MicroRNAs 24 and 27 Suppress Allergic Inflammation and Target a Network of Regulators of T Helper 2 Cell-Associated Cytokine Production. Immunity. 2016.

609. Chandran PA, Keller A, Weinmann L, Seida AA, Braun M, Andreev K, et al. The TGF-ß-inducible miR-23a cluster attenuates IFN-γ levels and antigen-specific cytotoxicity in human $CD8^+$ T cells. Journal of Leukocyte Biology. 2014;96:633–45.

610. Sanchez-Martínez D, Krzywinska E, Rathore MG, Saumet A, Cornillon A, Lopez-Royuela N, et al. All-trans retinoic acid (ATRA) induces miR-23a expression, decreases CTSC expression and granzyme B activity leading to impaired NK cell cytotoxicity. The International Journal of Biochemistry & Cell Biology. 2014;49:42–52.

611. Ahmadian-Elmi M, Bidmeshki Pour A, Naghavian R, Ghaedi K, Tanhaei S, Izadi T, et al. miR-27a and miR-214 exert opposite regulatory roles in Th17 differentiation via mediating different signaling pathways in peripheral blood CD4+ T lymphocytes of patients with relapsing-remitting multiple sclerosis. Immunogenetics. 2016;68:43–54.

612. Zhu H, Wu H, Liu X, Evans BR, Medina DJ, Liu C-G, et al. Role of MicroRNA miR-27a and miR-451 in the regulation of MDR1/P-glycoprotein expression in

human cancer cells. Biochemical Pharmacology. 2008;76:582–8.

613. Zhang H, Li M, Han Y, Hong L, Gong T, Sun L, et al. Down-Regulation of miR-27a Might Reverse Multidrug Resistance of Esophageal Squamous Cell Carcinoma. Digestive Diseases and Sciences. Springer US; 2009;55:2545–51.

614. Wang N, Zhu M, Tsao S-W, Man K, Zhang Z, Feng Y. MiR-23a-mediated inhibition of topoisomerase 1 expression potentiates cell response to etoposide in human hepatocellular carcinoma. Molecular Cancer. BioMed Central; 2013;12:119.

615. Brunner S, Herndler-Brandstetter D, Arnold CR, Wiegers GJ, Villunger A, Hackl M, et al. Upregulation of miR-24 is associated with a decreased DNA damage response upon etoposide treatment in highly differentiated CD8(+) T cells sensitizing them to apoptotic cell death. Aging Cell. 2012;11:579–87.

616. Bu H, Baraldo G, Lepperdinger G, Jansen-Dürr P. mir-24 activity propagates stress-induced senescence by down regulating DNA topoisomerase 1. Exp Gerontol. 2016;75:48–52.

617. Mishra PJ, Humeniuk R, Mishra PJ, Longo-Sorbello GSA, Banerjee D, Bertino JR. A miR-24 microRNA binding-site polymorphism in dihydrofolate reductase gene leads to methotrexate resistance. PNAS. 2007;104:13513–8.

618. Ebert MS, Neilson JR, Sharp PA. MicroRNA sponges: competitive inhibitors of small RNAs in mammalian cells. Nat. Methods. 2007;4:721–6.

619. Scotto Lavino E, Du G, Frohman MA. 3′ End cDNA amplification using classic RACE. Nature Protocols. 2007;1:2742–5.

620. Ritchie W, Flamant S, Rasko JEJ. Predicting microRNA targets and functions: traps for the unwary. Nat. Methods. 2009;6:397–8.

621. Vastesaeger N, Kutzbach AG, Amital H, Pavelka K, Lazaro MA, Moots RJ, et al. Prediction of remission and low disease activity in disease-modifying anti-rheumatic drug-refractory patients with rheumatoid arthritis treated with golimumab. Rheumatology (Oxford). Oxford University Press; 2016;55:1466–76.

622. Shmerling RH, Delbanco TL. How useful is the rheumatoid factor? An analysis of sensitivity, specificity, and predictive value. Arch. Intern. Med. 1992;152:2417–20.

623. McInnes IB, Schett G. The Pathogenesis of Rheumatoid Arthritis. N Engl J Med. 2011;365:2205–19.

624. Vallbracht I, Rieber J, Oppermann M, Förger F, Siebert U, Helmke K. Diagnostic and clinical value of anti-cyclic citrullinated peptide antibodies compared with rheumatoid factor isotypes in rheumatoid arthritis. Ann. Rheum. Dis. 2004;63:1079–84.

625. Bukhari M, Thomson W, Naseem H, Bunn D, Silman A, Symmons D, et al. The performance of anti-cyclic citrullinated peptide antibodies in predicting the severity of radiologic damage in inflammatory polyarthritis: results from the Norfolk Arthritis Register. Arthritis Rheum. 2007;56:2929–35.

626. Mäkinen H. Is DAS28 an appropriate tool to assess remission in rheumatoid arthritis? Ann. Rheum. Dis. 2005;64:1410–3.

627. Aletaha D, Smolen JS. The Simplified Disease Activity Index (SDAI) and Clinical Disease Activity Index (CDAI) to monitor patients in standard clinical care. Best Practice & Research Clinical Rheumatology [Internet]. 2007;21:663–75. Available from: http://eutils.ncbi.nlm.nih.gov/entrez/eutils/elink.fcgi?dbfrom=pubmed&id=17678828&retmode=ref&cmd=prlinks

628. Mehta A, Zhao JL, Sinha N, Marinov GK, Mann M, Kowalczyk MS, et al. The MicroRNA-132 and MicroRNA-212 Cluster Regulates Hematopoietic Stem Cell Maintenance and Survival with Age by Buffering FOXO3 Expression. Immunity. 2015;42:1021–32.

629. Buck AH, Perot JCMAKDSTLCVMLDLLPS. Post-transcriptional regulation of miR-27 in murine cytomegalovirus infection [electronic resource]. Cold Spring Harbor Laboratory Press.

630. Tiippana-Kinnunen T, Paimela L, Kautiainen H, Laasonen L, Leirisalo-Repo M. Can disease-modifying anti-rheumatic drugs be discontinued in long-standing rheumatoid arthritis? A 15-year follow-up. Scand. J. Rheumatol. 2010;39:12–8.

631. Hetland ML, Christensen IJ, Tarp U, Dreyer L, Hansen A, Hansen ITN, et al. Direct comparison of treatment responses, remission rates, and drug adherence in patients with rheumatoid arthritis treated with adalimumab, etanercept, or infliximab: Results from eight years of surveillance of clinical practice in the nationwide Danish DANBIO registry. Arthritis Rheum. Wiley Subscription Services, Inc., A Wiley Company; 2010;62:22–32.

632. Sethi MK, O'Dell JR. Combination conventional DMARDs compared to biologicals: what is the evidence? Curr Opin Rheumatol. 2015;27:183–8.

633. Seitz M, Zwicker M, Loetscher P. Effects of methotrexate on differentiation of monocytes and production of cytokine inhibitors by monocytes. Arthritis Rheum. 1998;41:2032–8.

634. Chara L, Sánchez-Atrio A, Pérez A, Cuende E, Albarrán F, Turrión A, et al. The number of circulating monocytes as biomarkers of the clinical response to methotrexate in untreated patients with rheumatoid arthritis. J Transl Med. BioMed Central; 2015;13:2.

635. Herenius MMJ, Thurlings RM, Wijbrandts CA, Bennink RJ, Dohmen SE, Voermans C, et al. Monocyte migration to the synovium in rheumatoid arthritis patients treated with adalimumab. Ann. Rheum. Dis. BMJ Publishing Group Ltd and European League Against Rheumatism; 2011;70:1160–2.

636. Richez C, Barnetche T, Khoryati L, Duffau P, Kostine M, Contin-Bordes C, et al. Tocilizumab treatment decreases circulating myeloid dendritic cells and monocytes, 2 components of the myeloid lineage. J. Rheumatol. 2012;39:1192–7.

637. Bonelli M, Ferner E, Göschl L, Blüml S, Hladik A, Karonitsch T, et al. Abatacept (CTLA-4IG) treatment reduces the migratory capacity of monocytes in patients with rheumatoid arthritis. Arthritis Rheum. Wiley Subscription Services,

Inc., A Wiley Company; 2013;65:599–607.

638. Schulert G, Fall N, Shen N, Grom A. Differential monocyte microrna expression profiles in children with active systemic juvenile idiopathic arthritis. Pediatric Rheumatology. 2014;12:P59.

639. Williams AEG, Choi K, Chan AL, Lee YJ, Reeves WH, Bubb MR, et al. Sjögren's syndrome-associated microRNAs in CD14+ monocytes unveils targeted TGFß signaling. Arthritis Res. Ther. BioMed Central; 2016;18:554.

640. Ogando J, Tardáguila M, Díaz-Alderete A, Usategui A, Miranda-Ramos V, Martínez-Herrera DJ, et al. Notch-regulated miR-223 targets the aryl hydrocarbon receptor pathway and increases cytokine production in macrophages from rheumatoid arthritis patients. Sci Rep. Nature Publishing Group; 2016;6:20223.

641. Barbarroja N, Ruiz-Limon P. … Profiling of CD14+ and CD16+ Monocyte Subtypes in Rheumatoid Arthritis. Alterations Related to Cardiovascular Disease and Endothelial Dysfunction. ARTHRITIS & …; 2015.

642. Castro-Villegas C, Perez-Sanchez C, Escudero A, Filipescu I, Verdu M, Ruiz-Limon P, et al. Circulating miRNAs as potential biomarkers of therapy effectiveness in rheumatoid arthritis patients treated with anti-TNFα. Arthritis Res. Ther. 2015;17:131.

643. Weyand CM, Schmidt D, Wagner U, Goronzy JJ. The influence of sex on the phenotype of rheumatoid arthritis. Arthritis Rheum. 1998;41:817–22.

644. Firestein GS. Evolving concepts of rheumatoid arthritis. Nature. Nature Publishing Group; 2003;423:356–61.

645. Huizinga TWJ, Amos CI, van der Helm-van Mil AHM, Chen W, van Gaalen FA, Jawaheer D, et al. Refining the complex rheumatoid arthritis phenotype based on specificity of the HLA-DRB1 shared epitope for antibodies to citrullinated proteins. Arthritis Rheum. 2005;52:3433–8.

646. van Gaalen FA, van Aken J, Huizinga TWJ, Schreuder GMT, Breedveld FC, Zanelli E, et al. Association between HLA class II genes and autoantibodies to cyclic citrullinated peptides (CCPs) influences the severity of rheumatoid arthritis. Arthritis Rheum. 2004;50:2113–21.

647. Kroot EJ, de Jong BA, van Leeuwen MA, Swinkels H, van den Hoogen FH, van't Hof M, et al. The prognostic value of anti-cyclic citrullinated peptide antibody in patients with recent-onset rheumatoid arthritis. Arthritis Rheum. John Wiley & Sons, Inc; 2000;43:1831–5.

648. Sattar N, Murray HM, Welsh P, Blauw GJ, Buckley BM, Cobbe S, et al. Are Markers of Inflammation More Strongly Associated with Risk for Fatal Than for Nonfatal Vascular Events? Turnbull FM, editor. PLoS Medicine. 2009;6:e1000099.

649. Ninomiya M, Kondo Y, Funayama R, Nagashima T, Kogure T, Kakazu E, et al. Distinct microRNAs expression profile in primary biliary cirrhosis and evaluation of miR 505-3p and miR197-3p as novel biomarkers. Ansari AA, editor. PLoS ONE. 2013;8:e66086.

650. Yang Y, Xu J, Chen H, Fei X, Tang Y, Yan Y, et al. MiR-128-2 inhibits common lymphoid progenitors from developing into progenitor B cells. Oncotarget. 2016;7:17520–31.

651. Krasoudaki E, Banos A, Stagakis E, Loupasakis K, Drakos E, Sinatkas V, et al. Micro-RNA analysis of renal biopsies in human lupus nephritis demonstrates up-regulated miR-422a driving reduction of kallikrein-related peptidase 4. Nephrol. Dial. Transplant. Oxford University Press; 2015;:gfv374.

652. Wang P, Gu Y, Zhang Q, Han Y, Hou J, Lin L, et al. Identification of resting and type I IFN-activated human NK cell miRNomes reveals microRNA-378 and microRNA-30e as negative regulators of NK cell cytotoxicity. J Immunol. American Association of Immunologists; 2012;189:211–21.

653. Millar NL, Gilchrist DS, Akbar M, Reilly JH, Kerr SC, Campbell AL, et al. MicroRNA29a regulates IL-33-mediated tissue remodelling in tendon disease. Nat Commun. 2015;6:6774.

654. Giuffrida P, Pinzani M, Corazza GR, Di Sabatino A. Biomarkers of intestinal fibrosis - one step towards clinical trials for stricturing inflammatory bowel disease. United European Gastroenterol J. SAGE Publications; 2016;4:523–30.

655. Scheibner KA, Teaboldt B, Hauer MC, Civin CI. The Mir-23a~Mir-27a~Mir-24 Cluster Acts as a Tumor Suppressor In Leukemias by Post-Transcriptional Regulation of 14-3-3 Proteins. Blood. 2010;116:3145.

656. Li X, Liu X, Xu W, Zhou P, Gao P, Jiang S, et al. c-MYC-regulated miR-23a/24-2/27a Cluster Promotes Mammary Carcinoma Cell Invasion and Hepatic Metastasis by Targeting Sprouty2. Journal of Biological Chemistry. 2013;288:18121–33.

657. Nakasa T, Miyaki S, Okubo A, Hashimoto M, Nishida K, Ochi M, et al. Expression of microRNA-146 in rheumatoid arthritis synovial tissue. Arthritis Rheum. Wiley Subscription Services, Inc., A Wiley Company; 2008;58:1284–92.

658. Kriegsmann M, Randau TM, Gravius S, Lisenko K, Altmann C, Arens N, et al. Expression of miR-146a, miR-155, and miR-223 in formalin-fixed paraffin-embedded synovial tissues of patients with rheumatoid arthritis and osteoarthritis. Virchows Archiv. Springer Berlin Heidelberg; 2016;469:93–100.

659. Kurowska-Stolarska M, Ballantine L, Stolarski B, Hunter J, Hueber A, Gracie JA, et al. miR-155 and miR-34a regulate proinflammatory cytokine production by human monocytes. Ann. Rheum. Dis. BMJ Publishing Group Ltd and European League Against Rheumatism; 2010;69:A30–0.

660. Git A, Dvinge H, Salmon-Divon M, Osborne M, Kutter C, Hadfield J, et al. Systematic comparison of microarray profiling, real-time PCR, and next-generation sequencing technologies for measuring differential microRNA expression. RNA. 2010;16:991–1006.

661. Zhang Y-C, Ye H, Zeng Z, Chin YE, Huang Y-N, Fu G-H. The NF-κB p65/miR-23a-27a-24 cluster is a target for leukemia treatment. Oncotarget. Impact Journals; 2015;6:33554–67.

662. Rathore MG, Saumet A, Rossi J-F, de Bettignies C, Tempé D, Lecellier C-H, et al. The NF-κB member p65 controls glutamine metabolism through miR-23a. The International Journal of Biochemistry & Cell Biology. 2012;44:1448–56.

663. Luers AJ, Loudig OD, Berman JW. MicroRNAs are expressed and processed by human primary macrophages. Cell. Immunol. 2010;263:1–8.

664. Schütze S, Wiegmann K, Machleidt T, Krönke M. TNF-induced activation of NF-kappa B. Immunobiology. 1995;193:193–203.

665. Peng P, Li Z, Liu X. Reduced Expression of miR-23a Suppresses A20 in TLR-stimulated Macrophages. Inflammation. Springer US; 2015;38:1787–93.

666. Matmati M, Jacques P, Maelfait J, Verheugen E, Kool M, Sze M, et al. A20 (TNFAIP3) deficiency in myeloid cells triggers erosive polyarthritis resembling rheumatoid arthritis. Nat. Genet. 2011;43:908–12.

667. Kanayama M, Inoue M, Danzaki K, Hammer G, He Y-W, Shinohara ML. Autophagy enhances NFκB activity in specific tissue macrophages by sequestering A20 to boost antifungal immunity. Nat Commun. 2015;6:5779.

668. Tavares RM, Turer EE, Liu CL, Advincula R, Scapini P, Rhee L, et al. The ubiquitin modifying enzyme A20 restricts B cell survival and prevents autoimmunity. Immunity. 2010;33:181–91.

669. Bowes J, Lawrence R, Eyre S, Panoutsopoulou K, Orozco G, Elliott KS, et al. Rare variation at the TNFAIP3 locus and susceptibility to rheumatoid arthritis. Hum. Genet. 2010;128:627–33.

670. CAI X. Human microRNAs are processed from capped, polyadenylated transcripts that can also function as mRNAs. RNA. Cold Spring Harbor Lab; 2004;10:1957–66.

671. Ferrero E, Goyert SM. Nucleotide sequence of the gene encoding the monocyte differentiation antigen, CD14. Nucleic Acids Res. 1988;16:4173.

672. Hepburn AL. Expression of Fc and complement receptors on peripheral blood monocytes in systemic lupus erythematosus and rheumatoid arthritis. Rheumatology. Oxford University Press; 2004;43:547–54.

673. Mukherjee R, Kanti Barman P, Kumar Thatoi P, Tripathy R, Kumar Das B, Ravindran B. Non-Classical monocytes display inflammatory features: Validation in Sepsis and Systemic Lupus Erythematous. Sci Rep. Nature Publishing Group; 2015;5:13886.

674. van Furth R. Human monocytes and cytokines. Res. Immunol. 1998;149:719–20.

675. Iwamoto S, Iwai S-I, Tsujiyama K, Kurahashi C, Takeshita K, Naoe M, et al. TNF-alpha drives human CD14+ monocytes to differentiate into CD70+ dendritic cells evoking Th1 and Th17 responses. The Journal of Immunology. 2007;179:1449–57.

676. Griffin GK, Newton G, Tarrio ML, Bu DX, Maganto-Garcia E, Azcutia V, et al. IL-17 and TNF- Sustain Neutrophil Recruitment during Inflammation through

Synergistic Effects on Endothelial Activation. The Journal of Immunology. 2012;188:6287–99.

677. Zhao L-J, Hua X, He S-F, Ren H, Qi Z-T. Interferon alpha regulates MAPK and STAT1 pathways in human hepatoma cells. Virology Journal. BioMed Central; 2011;8:157.

678. Platanias LC. Mechanisms of type-I- and type-II-interferon-mediated signalling. Nat. Rev. Immunol. Nature Publishing Group; 2005;5:375–86.

679. Smolen JS, Beaulieu A, Rubbert-Roth A, Ramos-Remus C, Rovensky J, Alecock E, et al. Effect of interleukin-6 receptor inhibition with tocilizumab in patients with rheumatoid arthritis (OPTION study): a double-blind, placebo-controlled, randomised trial. Lancet. 2008;371:987–97.

680. Huang Q-Q, Pope RM. The role of toll-like receptors in rheumatoid arthritis. Curr Rheumatol Rep. 2009;11:357–64.

681. Brentano F, Kyburz D, Gay S. Toll-like receptors and rheumatoid arthritis. Methods Mol. Biol. Totowa, NJ: Humana Press; 2009;517:329–43.

682. Hornung V, Rothenfusser S, Britsch S, Krug A, Jahrsdörfer B, Giese T, et al. Quantitative expression of toll-like receptor 1-10 mRNA in cellular subsets of human peripheral blood mononuclear cells and sensitivity to CpG oligodeoxynucleotides. The Journal of Immunology. American Association of Immunologists; 2002;168:4531–7.

683. KREUTZ M, ACKERMANN U, HAUSCHILDT S, KRAUSE SW, RIEDEL D, BESSLER W, et al. A comparative analysis of cytokine production and tolerance induction by bacterial lipopeptides, lipopolysaccharides and Staphyloccocus aureus in human monocytes. Immunology. 1997;92:396–401.

684. Doust JWL. Differential Tissue and Organ Anoxia in Disease: The Measurement of Peri-Articular Oxygen Saturation Levels in Patients with Arthritis. Ann. Rheum. Dis. 1951;10:269–76.

685. Quiñonez-Flores CM, González-Chávez SA, Pacheco-Tena C. Hypoxia and its implications in rheumatoid arthritis. J. Biomed. Sci. 2016;23:62.

686. Wu D, Yotnda P. Induction and Testing of Hypoxia in Cell Culture. Journal of Visualized Experiments. 2011;:e2899–9.

687. Stanley ER, Berg KL, Einstein DB, Lee PS, Pixley FJ, Wang Y, et al. Biology and action of colony--stimulating factor-1. Mol. Reprod. Dev. Wiley Subscription Services, Inc., A Wiley Company; 1997;46:4–10.

688. Behrens F, Tak PP, Østergaard M, Stoilov R, Wiland P, Huizinga TW, et al. MOR103, a human monoclonal antibody to granulocyte-macrophage colony-stimulating factor, in the treatment of patients with moderate rheumatoid arthritis: results of a phase Ib/IIa randomised, double-blind, placebo-controlled, dose-escalation trial. Ann. Rheum. Dis. BMJ Publishing Group Ltd and European League Against Rheumatism; 2015;74:1058–64.

689. Moura RA, Cascao R, Perpetuo I, Canhao H, Sousa E, Mourao AF, et al.

Cytokine profile in serum and synovial fluid of patients with established rheumatoid arthritis. Ann. Rheum. Dis. 2010;69:A51–1.

690. O'Carroll C, Fagan A, Shanahan F, Carmody RJ. Identification of a unique hybrid macrophage-polarization state following recovery from lipopolysaccharide tolerance. J Immunol. 2014;192:427–36.

691. Conigliaro P, Perricone C, Benson RA, Garside P, Brewer JM, Perricone R, et al. The type I IFN system in rheumatoid arthritis. Autoimmunity. 2010;43:220–5.

692. Honda K, Taniguchi T. IRFs: master regulators of signalling by Toll-like receptors and cytosolic pattern-recognition receptors. Nat. Rev. Immunol. 2006;6:644–58.

693. Werner F, Jain MK, Feinberg MW, Sibinga NE, Pellacani A, Wiesel P, et al. Transforming growth factor-beta 1 inhibition of macrophage activation is mediated via Smad3. J. Biol. Chem. American Society for Biochemistry and Molecular Biology; 2000;275:36653–8.

694. Glass CK, Ogawa S. Combinatorial roles of nuclear receptors in inflammation and immunity. Nat. Rev. Immunol. 2006;6:44–55.

695. Tall AR, Yvan-Charvet L. Cholesterol, inflammation and innate immunity. Nat. Rev. Immunol. 2015;15:104–16.

696. Mora JR, Iwata M, Andrian von UH. Vitamin effects on the immune system: vitamins A and D take centre stage. Nat. Rev. Immunol. 2008;8:685–98.

697. Bettoun DJ, Burris TP, Houck KA, Buck DW, Stayrook KR, Khalifa B, et al. Retinoid X receptor is a nonsilent major contributor to vitamin D receptor-mediated transcriptional activation. Mol. Endocrinol. 2003;17:2320–8.

698. Asquith DL, Ballantine LE, Nijjar JS, Makdasy MK, Patel S, Wright PB, et al. The liver X receptor pathway is highly upregulated in rheumatoid arthritis synovial macrophages and potentiates TLR-driven cytokine release. Ann. Rheum. Dis. 2013;72:2024–31.

699. Tsang J, Zhu J, van Oudenaarden A. MicroRNA-mediated feedback and feedforward loops are recurrent network motifs in mammals. Molecular Cell. 2007;26:753–67.

700. Shaulian E, Karin M. AP-1 as a regulator of cell life and death. Nature Cell Biology. Nature Publishing Group; 2002;4:E131–6.

701. Spurlock CF, Tossberg JT, Fuchs HA, Olsen NJ, Aune TM. Methotrexate increases expression of cell cycle checkpoint genes via JNK activation. Arthritis Rheum. Wiley Subscription Services, Inc., A Wiley Company; 2012;64:1780–9.

702. Karin M, Greten FR. NF-kappaB: linking inflammation and immunity to cancer development and progression. Nat. Rev. Immunol. 2005;5:749–59.

703. Ma S, Liu M, Xu Z, Li Y, Guo H, Ge Y, et al. A double feedback loop mediated by microRNA-23a/27a/24-2 regulates M1 versus M2 macrophage polarization and thus regulates cancer progression. Oncotarget. 2016.

704. Hu X, Herrero C, Li W-P, Antoniv TT, Falck-Pedersen E, Koch AE, et al. Sensitization of IFN-gamma Jak-STAT signaling during macrophage activation. Nat. Immunol. Nature Publishing Group; 2002;3:859–66.

705. Proudfoot NJ. Ending the message: poly(A) signals then and now. Genes Dev. 2011;25:1770–82.

706. Bronevetsky Y, Villarino AV, Eisley CJ, Barbeau R, Barczak AJ, Heinz GA, et al. T cell activation induces proteasomal degradation of Argonaute and rapid remodeling of the microRNA repertoire. J. Exp. Med. 2013;210:417–32.

707. Strauss-Ayali D, Conrad SM, Mosser DM. Monocyte subpopulations and their differentiation patterns during infection. Journal of Leukocyte Biology. 2007;82:244–52.

708. Ziegler-Heitbrock L. The CD14+ CD16+ blood monocytes: their role in infection and inflammation. Journal of Leukocyte Biology. 2007;81:584–92.

709. Cros J, Cagnard N, Woollard K, Patey N, Zhang S-Y, Senechal B, et al. Human CD14dim monocytes patrol and sense nucleic acids and viruses via TLR7 and TLR8 receptors. Immunity. 2010;33:375–86.

710. Belge K-U, Dayyani F, Horelt A, Siedlar M, Frankenberger M, Frankenberger B, et al. The proinflammatory CD14+CD16+DR++ monocytes are a major source of TNF. The Journal of Immunology. 2002;168:3536–42.

711. Naqvi AR, Fordham JB, Nares S. miR-24, miR-30b, and miR-142-3p Regulate Phagocytosis in Myeloid Inflammatory Cells. The Journal of Immunology. 2015;194:1916–27.

712. Gilicze AB, Wiener Z, Tóth S, Buzás E, Pállinger É, Falcone FH, et al. Myeloid-derived microRNAs, miR-223, miR27a, and miR-652, are dominant players in myeloid regulation. Biomed Res Int. Hindawi Publishing Corporation; 2014;2014:870267–9.

713. Atsumi T, Ishihara K, Kamimura D, Ikushima H, Ohtani T, Hirota S, et al. A point mutation of Tyr-759 in interleukin 6 family cytokine receptor subunit gp130 causes autoimmune arthritis. Journal of Experimental Medicine. 2002;196:979–90.

714. Jenkins BJ, Roberts AW, Greenhill CJ, Najdovska M, Lundgren-May T, Robb L, et al. Pathologic consequences of STAT3 hyperactivation by IL-6 and IL-11 during hematopoiesis and lymphopoiesis. Blood. 2007;109:2380–8.

715. Jones GW, McLeod L, Kennedy CL, Bozinovski S, Najdovska M, Jenkins BJ. Imbalanced gp130 signalling in ApoE-deficient mice protects against atherosclerosis. Atherosclerosis. 2015;238:321–8.

716. Clavel C, Ceccato L, Anquetil F, Serre G, Sebbag M. Among human macrophages polarised to different phenotypes, the M-CSF-oriented cells present the highest pro-inflammatory response to the rheumatoid arthritis-specific immune complexes containing ACPA. Ann. Rheum. Dis. BMJ Publishing Group Ltd and European League Against Rheumatism; 2016;:annrheumdis–2015–208887.

717. Wynn TA, Chawla A, Pollard JW. Macrophage biology in development, homeostasis and disease. Nature. Nature Research; 2013;496:445–55.

718. Sallusto F, Lanzavecchia A. Efficient presentation of soluble antigen by cultured human dendritic cells is maintained by granulocyte/macrophage colony-stimulating factor plus interleukin 4 and downregulated by tumor necrosis factor alpha. Journal of Experimental Medicine. 1994;179:1109–18.

719. Guschin D, Rogers N, Briscoe J, Witthuhn B, Watling D, Horn F, et al. A major role for the protein tyrosine kinase JAK1 in the JAK/STAT signal transduction pathway in response to interleukin-6. EMBO J. European Molecular Biology Organization; 1995;14:1421–9.

720. Tsuchiya S, Yamabe M, Yamaguchi Y, Kobayashi Y, Konno T, Tada K. Establishment and characterization of a human acute monocytic leukemia cell line (THP-1). Int. J. Cancer. 1980;26:171–6.

721. Tsuchiya S, Kobayashi Y, Goto Y, Okumura H, Nakae S, Konno T, et al. Induction of maturation in cultured human monocytic leukemia cells by a phorbol diester. Cancer Research. 1982;42:1530–6.

722. Schwende H, Fitzke E, Ambs P, Dieter P. Differences in the state of differentiation of THP-1 cells induced by phorbol ester and 1,25-dihydroxyvitamin D3. Journal of Leukocyte Biology. 1996;59:555–61.

723. Aldo PB, Craveiro V, Guller S, Mor G. Effect of culture conditions on the phenotype of THP-1 monocyte cell line. Am. J. Reprod. Immunol. 2013;70:80–6.

724. Gaffney EV, Dell'Aquila ML, Lingenfelter SE, Huffnagle GB, Wiest DL. Characterization of a colony-stimulating factor produced by the human monocytic leukemia cell line, THP-1. Journal of Leukocyte Biology. 1986;39:409–21.

725. Cousins RJ, Blanchard RK, Popp MP, Liu L, Cao J, Moore JB, et al. A global view of the selectivity of zinc deprivation and excess on genes expressed in human THP-1 mononuclear cells. Proceedings of the National Academy of Sciences. 2003;100:6952–7.

726. Burke B, Sumner S, Maitland N, Lewis CE. Macrophages in gene therapy: cellular delivery vehicles and in vivo targets. Journal of Leukocyte Biology. 2002;72:417–28.

727. Martinet W, Schrijvers DM, Kockx MM. Nucleofection as an efficient nonviral transfection method for human monocytic cells. Biotechnol. Lett. 2003;25:1025–9.

728. Schnoor M, Buers I, Sietmann A, Brodde MF, Hofnagel O, Robenek H, et al. Efficient non-viral transfection of THP-1 cells. J. Immunol. Methods. 2009;344:109–15.

729. Sneddon AA, McLeod E, Wahle KWJ, Arthur JR. Cytokine-induced monocyte adhesion to endothelial cells involves platelet-activating factor: Suppression by conjugated linoleic acid. Biochimica et Biophysica Acta (BBA) - Molecular and Cell Biology of Lipids. 2006;1761:793–801.

730. Sharif O, Bolshakov VN, Raines S, Newham P, Perkins ND. Transcriptional profiling of the LPS induced NF-kappaB response in macrophages. BMC Immunol. BioMed Central; 2007;8:1.

731. Kohro T, Tanaka T, Murakami T, Wada Y, Aburatani H, Hamakubo T, et al. A comparison of differences in the gene expression profiles of phorbol 12-myristate 13-acetate differentiated THP-1 cells and human monocyte-derived macrophage. J. Atheroscler. Thromb. 2004;11:88–97.

732. Mantovani A, Sica A, Sozzani S, Allavena P, Vecchi A, Locati M. The chemokine system in diverse forms of macrophage activation and polarization. Trends Immunol. 2004;25:677–86.

733. Spencer M, Yao-Borengasser A, Unal R, Rasouli N, Gurley CM, Zhu B, et al. Adipose tissue macrophages in insulin-resistant subjects are associated with collagen VI and fibrosis and demonstrate alternative activation. American Journal of Physiology - Endocrinology and Metabolism. American Physiological Society; 2010;299:E1016–27.

734. Goppelt-Struebe M, Reiser CO, Schneider N, Grell M. Modulation of tumor necrosis factor (TNF) receptor expression during monocytic differentiation by glucocorticoids. Inflamm. Res. 1996;45:503–7.

735. Yao Z, Spriggs MK, Derry JMJ, Strockbine L, Park LS, VandenBos T, et al. MOLECULAR CHARACTERIZATION OF THE HUMAN INTERLEUKIN (Il)-17 RECEPTOR. Cytokine. 1997;9:794–800.

736. Mao C, Merlin G, Aguet M. Differential regulation of the human IFN-gamma receptor expression in Raji and IM9 lymphoblastoid cells versus THP-1 monocytic cells by IFN-gamma and phorbol myristate acetate. The Journal of Immunology. 1990;144:4688–96.

737. Sanceau J, Wijdenes J, Revel M, Wietzerbin J. IL-6 and IL-6 receptor modulation by IFN-gamma and tumor necrosis factor-alpha in human monocytic cell line (THP-1). Priming effect of IFN-gamma. The Journal of Immunology. 1991;147:2630–7.

738. Inagaki Y, Yamagishi S-I, Amano S, Okamoto T, Koga K, Makita Z. Interferon-gamma-induced apoptosis and activation of THP-1 macrophages. Life Sci. 2002;71:2499–508.

739. Iyer A, Hatta M, Usman R, Luiten S, Oskam L, Faber W, et al. Serum levels of interferon-γ, tumour necrosis factor-α, soluble interleukin-6R and soluble cell activation markers for monitoring response to treatment of leprosy reactions. Clin. Exp. Immunol. 2007;150:210–6.

740. Peters M, Jacobs S, Ehlers M, Vollmer P, Müllberg J, Wolf E, et al. The function of the soluble interleukin 6 (IL-6) receptor in vivo: sensitization of human soluble IL-6 receptor transgenic mice towards IL-6 and prolongation of the plasma half-life of IL-6. Journal of Experimental Medicine. The Rockefeller University Press; 1996;183:1399–406.

741. Lissilaa R, Buatois V, Magistrelli G, Williams AS, Jones GW, Herren S, et al. Although IL-6 trans-signaling is sufficient to drive local immune responses,

classical IL-6 signaling is obligate for the induction of T cell-mediated autoimmunity. J Immunol. American Association of Immunologists; 2010;185:5512–21.

742. Liu B, Sun R, Luo H, Liu X, Jiang M, Yuan C, et al. Both intrinsic and extrinsic apoptotic pathways are involved in Toll-like receptor 4 (TLR4)-induced cell death in monocytic THP-1 cells. Immunobiology. 2016.

743. Fenizia C, Fiocchi M, Jones K, Parks RW, Ceribelli M, Chevalier SA, et al. Human T-cell leukemia/lymphoma virus type 1 p30, but not p12/p8, counteracts toll-like receptor 3 (TLR3) and TLR4 signaling in human monocytes and dendritic cells. J. Virol. American Society for Microbiology; 2014;88:393–402.

744. Todt JC, Freeman CM, Brown JP, Sonstein J, Ames TM, McCubbrey AL, et al. Smoking decreases the response of human lung macrophages to double-stranded RNA by reducing TLR3 expression. Respir. Res. BioMed Central; 2013;14:33.

745. Mistry P, Laird MHW, Schwarz RS, Greene S, Dyson T, Snyder GA, et al. Inhibition of TLR2 signaling by small molecule inhibitors targeting a pocket within the TLR2 TIR domain. Proc. Natl. Acad. Sci. U.S.A. National Acad Sciences; 2015;112:5455–60.

746. Fomsgaard A, Worsaae H, Bendtzen K. Detection of tumour necrosis factor from lipopolysaccharide-stimulated human mononuclear cells by enzyme-linked immunosorbent assay and cytotoxicity bioassay. Scand. J. Immunol. 1988;27:143–7.

747. Bendtzen K. Interleukin 1, interleukin 6 and tumor necrosis factor in infection, inflammation and immunity. Immunol. Lett. 1988;19:183–91.

748. Zhu Q, Sun W, Okano K, Chen Y, Zhang N, Maeda T, et al. Sponge transgenic mouse model reveals important roles for the microRNA-183 (miR-183)/96/182 cluster in postmitotic photoreceptors of the retina. Journal of Biological Chemistry. 2011;286:31749–60.

749. Jung J, Yeom C, Choi Y-S, Kim S, Lee E, Park MJ, et al. Simultaneous inhibition of multiple oncogenic miRNAs by a multi-potent microRNA sponge. Oncotarget. 2015;6:20370–87.

750. Kluiver J, Gibcus JH, Hettinga C, Adema A, Richter MKS, Halsema N, et al. Rapid generation of microRNA sponges for microRNA inhibition. Jeang KT, editor. PLoS ONE. 2012;7:e29275.

751. Haraguchi T, Ozaki Y, Iba H. Vectors expressing efficient RNA decoys achieve the long-term suppression of specific microRNA activity in mammalian cells. Nucleic Acids Res. 2009;37:e43–3.

752. Gentner B, Schira G, Giustacchini A, Amendola M, Brown BD, Ponzoni M, et al. Stable knockdown of microRNA in vivo by lentiviral vectors. Nat. Methods. 2009;6:63–6.

753. Qin JY, Zhang L, Clift KL, Hulur I, Xiang AP, Ren B-Z, et al. Systematic Comparison of Constitutive Promoters and the Doxycycline-Inducible Promoter. Hansen IA, editor. PLoS ONE. 2010;5:e10611.

754. Chen L, Zhang K, Shi Z, Zhang A, Jia Z, Wang G, et al. A lentivirus-mediated miR-23b sponge diminishes the malignant phenotype of glioma cells in vitro and in vivo. Oncol. Rep. 2014;31:1573–80.

755. Torres AG, Fabani MM, Vigorito E, Gait MJ. MicroRNA fate upon targeting with anti-miRNA oligonucleotides as revealed by an improved Northern-blot-based method for miRNA detection. RNA. 2011;17:933–43.

756. Lee JY, Kim S, Hwang DW, Jeong JM, Chung J-K, Lee MC, et al. Development of a dual-luciferase reporter system for in vivo visualization of MicroRNA biogenesis and posttranscriptional regulation. J. Nucl. Med. 2008;49:285–94.

757. Baccarini A, Chauhan H, Gardner TJ, Jayaprakash AD, Sachidanandam R, Brown BD. Kinetic analysis reveals the fate of a microRNA following target regulation in mammalian cells. Curr. Biol. 2011;21:369–76.

758. Marinov GK, Williams BA, McCue K, Schroth GP, Gertz J, Myers RM, et al. From single-cell to cell-pool transcriptomes: stochasticity in gene expression and RNA splicing. Genome Res. 2014;24:496–510.

759. Chanput W, Mes JJ, Wichers HJ. THP-1 cell line: an in vitro cell model for immune modulation approach. Int. Immunopharmacol. 2014;23:37–45.

760. Genin M, Clement F, Fattaccioli A, Raes M, Michiels C. M1 and M2 macrophages derived from THP-1 cells differentially modulate the response of cancer cells to etoposide. BMC Cancer. 2015;15:577.

761. Jones SA, Horiuchi S, Novick D, Yamamoto N, Fuller GM. Shedding of the soluble IL-6 receptor is triggered by Ca2+ mobilization, while basal release is predominantly the product of differential mRNA splicing in THP-1 cells. European Journal of Immunology. 1998;28:3514–22.

762. Gibson DG, Young L, Chuang R-Y, Venter JC, Hutchison CA, Smith HO. Enzymatic assembly of DNA molecules up to several hundred kilobases. Nat. Methods. 2009;6:343–5.

763. Lai X, Bhattacharya A, Schmitz U, Kunz M, Vera J, Wolkenhauer O. A systems' biology approach to study microRNA-mediated gene regulatory networks. Biomed Res Int. 2013;2013:703849–15.

764. Zhu L-H, Liu T, Tang H, Tian R-Q, Su C, Liu M, et al. MicroRNA-23a promotes the growth of gastric adenocarcinoma cell line MGC803 and downregulates interleukin-6 receptor. FEBS J. 2010;277:3726–34.

765. Su R, Dong L, Zou D, Zhao H, Ren Y, Li F, et al. microRNA-23a, -27a and -24 synergistically regulate JAK1/Stat3 cascade and serve as novel therapeutic targets in human acute erythroid leukemia. Oncogene. 2016;35:6001–14.

766. Balakrishnan I, Yang X, Brown J, Ramakrishnan A, Torok-Storb B, Kabos P, et al. Genome-Wide Analysis of miRNA-mRNA Interactions in Marrow Stromal Cells. Stem Cells. 2014;32:662–73.

767. Grimson A, Farh KK-H, Johnston WK, Garrett-Engele P, Lim LP, Bartel DP.

MicroRNA Targeting Specificity in Mammals: Determinants beyond Seed Pairing. Molecular Cell. 2007;27:91–105.

768. Saric T, Chang S-C, Hattori A, York IA, Markant S, Rock KL, et al. An IFN-γ–induced aminopeptidase in the ER, ERAP1, trims precursors to MHC class I–presented peptides. Nat. Immunol. 2002;3:1169–76.

769. Duncanson A, Donnelly Chair P, Easton D, Morris AP, Attwood AP, Boorman JP, et al. Association scan of 14,500 nonsynonymous SNPs in four diseases identifies autoimmunity variants. Nat. Genet. 2007;39:1329–37.

770. Weinblatt ME. Toxicity of low dose methotrexate in rheumatoid arthritis. J Rheumatol Suppl. 1985;12 Suppl 12:35–9.

771. Berkun Y. Methotrexate related adverse effects in patients with rheumatoid arthritis are associated with the A1298C polymorphism of the MTHFR gene. Ann. Rheum. Dis. 2004;63:1227–31.

772. Toffoli G, Russo A, Innocenti F, Corona G, Tumolo S, Sartor F, et al. Effect of methylenetetrahydrofolate reductase 677C?T polymorphism on toxicity and homocysteine plasma level after chronic methotrexate treatment of ovarian cancer patients. Int. J. Cancer. 2002;103:294–9.

773. Amelio I, Lena AM, Viticchie G, Shalom-Feuerstein R, Terrinoni A, Dinsdale D, et al. miR-24 triggers epidermal differentiation by controlling actin adhesion and cell migration. The Journal of Cell Biology. 2012;199:347–63.

774. Song GG, Bae S-C, Lee YH. Association of the MTHFR C677T and A1298C polymorphisms with methotrexate toxicity in rheumatoid arthritis: a meta-analysis. Clin. Rheumatol. Springer London; 2014;33:1715–24.

775. Berges C, Naujokat C, Tinapp S, Wieczorek H, Höh A, Sadeghi M, et al. A cell line model for the differentiation of human dendritic cells. Biochem. Biophys. Res. Commun. 2005;333:896–907.

776. Torres M, Ramachandra L, Rojas RE, Bobadilla K, Thomas J, Canaday DH, et al. Role of phagosomes and major histocompatibility complex class II (MHC-II) compartment in MHC-II antigen processing of Mycobacterium tuberculosis in human macrophages. Infect. Immun. 2006;74:1621–30.

777. Brown PM, Pratt AG, Isaacs JD. Mechanism of action of methotrexate in rheumatoid arthritis, and the search for biomarkers. Nat Rev Rheumatol. 2016;12:731–42.

778. Quemeneur L, Gerland LM, Flacher M, Ffrench M, Revillard JP, Genestier L. Differential Control of Cell Cycle, Proliferation, and Survival of Primary T Lymphocytes by Purine and Pyrimidine Nucleotides. The Journal of Immunology. 2003;170:4986–95.

779. Budzik GP, Colletti LM, Faltynek CR. Effects of methotrexate on nucleotide pools in normal human T cells and the CEM T cell line. Life Sci. 2000;66:2297–307.

780. FAIRBANKS LD, RüCKEMANN K, QIU Y, HAWRYLOWICZ CM, RICHARDS DF,

SWAMINATHAN R, et al. Methotrexate inhibits the first committed step of purine biosynthesis in mitogen-stimulated human T-lymphocytes: a metabolic basis for efficacy in rheumatoid arthritis? Biochemical Journal. 1999;342:143–52.

781. Whittle SL, Hughes RA. Folate supplementation and methotrexate treatment in rheumatoid arthritis: a review. Rheumatology. 2004;43:267–71.

782. SELHUB J, D'ANGELO A. Relationship Between Homocysteine and Thrombotic Disease. The American Journal of the Medical Sciences. 1998;316:129–41.

783. Haagsma CJ, van Riel PL, de Rooij DJ, Vree TB, Russel FJ, van't Hof MA, et al. Combination of methotrexate and sulphasalazine vs methotrexate alone: a randomized open clinical trial in rheumatoid arthritis patients resistant to sulphasalazine therapy. Br. J. Rheumatol. 1994;33:1049–55.

784. Stanley ER, Berg KL, Einstein DB, Lee PS, Yeung YG. The biology and action of colony stimulating factor-1. Stem Cells. 1994;12 Suppl 1:15–24–discussion25.

785. Garcia S, Hartkamp LM, Malvar-Fernandez B, van Es IE, Lin H, Wong J, et al. Colony-stimulating factor (CSF) 1 receptor blockade reduces inflammation in human and murine models of rheumatoid arthritis. Arthritis Res. Ther. BioMed Central; 2016;18:75.

786. Georganas C, Liu H, Perlman H, Hoffmann A, Thimmapaya B, Pope RM. Regulation of IL-6 and IL-8 expression in rheumatoid arthritis synovial fibroblasts: the dominant role for NF-kappa B but not C/EBP beta or c-Jun. The Journal of Immunology. 2000;165:7199–206.